Synthesis of Novel Inhibitors of 1-Deoxy-D-xylulose-5-phosphate Reductoisomerase as Potential Anti-malarial Lead Compounds

A thesis submitted in fulfillment of the requirements for the degree of

DOCTOR OF PHILOSOPHY

Of

Rhodes University

By

Marius Kudumo Mutorwa

B.Sc.Hons (Rhodes University)

November 2011

ABSTRACT

This research has focused on the development of novel substrate mimics as potential DXR inhibitors of 1-deoxy-D-xylulose-5-phosphate reductoisomerase (DXR), an essential enzyme in the mevalonate-independent pathway for the biosynthesis of isoprenoids in *Plasmodium falciparum*. DXR mediates the isomerisation and reduction of 1-deoxy-D-xylulose-5-phosphate (DOXP) into 2*C*-methyl-D-erithrytol 4-phosphate (MEP) and has been validated as an attractive target for the development of novel anti-malarial chemotherapeutic agents.

Reaction of various amines with specially prepared 4-phosphonated crotonic acid in the presence of the peptide coupling reagent, 1-ethyl-3-(3-dimethylaminopropyl)carbodiimide (EDC), has afforded a series of amido-phosphonate esters in moderate to good yields (48% - 73%) which, using a $RuCl_3/CeCl_3/NaIO_4$ catalyst system, have been dihydroxylated to furnish the dihydroxy-amido phosphonate ester pro-drugs; subsequent hydrolysis under microwave irradiation has afforded the corresponding phosphonic acids. A second series of potential inhibitors *viz.*, 3-substituted aniline-derived phosphonate esters, their corresponding phosphonic acids and mono-sodium salts, have also been successfully synthesised. In these compounds, the essential functional groups are separated by one, two, three or four methylene groups, Deprotonation of the 3-substituted aniline substrates, followed by reaction with the appropriate ω-chloroalkanoyl chloride produced the ω-chloroamide intermediates, which were subjected to the Michaelis-Arbuzov reaction to afford the diethyl phosphonate esters in moderate to good yields (48% - 74%). Microwave-assisted TMSBr-mediated cleavage of the phosphonate esters furnished the phosphonic acids, neutralisation of which afforded the mono-sodium salts.

Furan-derived phosphate esters and phosphonic acids have been prepared as conformationally-restricted DOXP analogues. Functionalization at C-5 of the trityl-protected furan was achieved using the Vilsmeier-Haack formylation and Friedel-Crafts acylation reactions and, following de-tritylation, phosphorylation and oximation, using hydroxylamine hydrochloride, the novel oxime derivatives have been isolated as a third series of potential DXR inhibitors in very good yields (87% - 96%). Finally, in order to exploit an additional binding pocket in the *Pf*DXR active site, a series of *N*-benzylated phosphoramidic derivatives were obtained in seven steps from the starting material, diethyl phosphoramidate. The

known inhibitors, fosmidomycin and its acetyl derivative FR900098, were also successfully synthesised as standards for STD-NMR binding and inhibition assays. In all, over 200 compounds (136 novel) have been prepared and appropriately characterised using 1-and 2-D NMR and IR spectroscopic analysis and, where necessary, HRMS or combustion analysis.

Saturation Transfer Difference (STD) protein-NMR experiments, undertaken using selected compounds, have revealed binding of most of the ligands examined to *Ec*DXR. Computer-simulated docking studies have also been used to explore the preferred ligand-binding conformations and interactions between the ligands and essential DXR active-site residues, while DXR-enzyme inhibition assays of selected synthesised ligands have revealed certain patterns of inhibitory activity.

AKNOWLEDGEMENTS

Foremost I would like to thank my supervisor, Professor Perry T. Kaye, for his dedication, guidance, unfailing advice and patience. I'm grateful to have had the privilege of working under your supervision and for your energy, always encouraging me to never give up throughout the course of my study. Thank you to my co-supervisor, Dr Rosa Klein, for her guidance and support in every aspect of this study; in the laboratory, in the analysis of data and in the writing-up stage.

To my parents, John and Agnes Mutorwa, thank you for your love, care, prayers, understanding and for the opportunity you have given me to pursue my studies. To my siblings, Nelson, Clemens and Wilhelmine, thank you for your love, support and always believing in me.

In addition, I wish to extend my gratitude and acknowledgement to:-

- Rhodes University Department of Chemistry academic and technical staff, for their meaningful inputs throughout the course of this research.
- Professor Mike Davies-Coleman for his guidance, advice and being a source of inspiration.
- Dr Kevin Lobb and Ms. Anne Conibear, for the guidance and patience, in teaching me computer modelling and STD-NMR techniques.
- Prof Greg Blatch and Dr Jess Goble (Department of Biochemistry, Rhodes University) and Miss Taryn Bodill (Rhodes University Centre for Chemico- and Biomedicinal Reseach) for their assistance and support, and work in purifying *Ec*DXR and conducting the bio-assays.
- University of Stellenbosh Central Analytical Facility for recording the HRMS data and Mr Francis Chindeka at the Nanotechnology Innovation Centre (NIC) for conducting the elemental analysis.
- Rhodes University for the financial assistance.
- My fellow colleagues in Lab F22, who over the years, have supported and encouraged me, and for providing a pleasant working environment.

I owe much thanks to all my friends in Grahamstown for the moral support, interest and encouragement. Special thanks to Eleph Gula-Ndebele, Asanda Chuma, Theodore Moyo, Laura Wener, Lulama Mciteka, Tina Dreier, Yung-Chaun Chen, Tunga Muganhiri, Zenzo Madubeko-sibanda and Mandla Gagayi.

DEDICATION

To my parents,

John and Agnes Mutorwa

and my siblings,

Nelson, Clemens and Wilhelmine

TABLE OF CONTENTS

1. INTRODUCTION

1.1. History of malaria

The interaction and evolution of malaria and humans can be traced back to ancient human civilizations, more than 5000 years ago.[1] The evidence of this affiliation or co-existence is authenticated within the manuscripts and writings of the Romans, Chinese, Indians, Greeks and Egyptians.[1] This includes the identification of malarial antigen molecules from skin and lung samples extracted from Egyptian mummies dating from the periods 3200 and 1304 *B.C*. Enlarged spleens, a phenomenon associated with malaria, have also been detected in mummies aged more than 3000 years old.[1] Documentation within the Chinese Classic of internal Medicine "Nei Ching", written around 2700 *B.C*, alludes to the characteristic symptoms observed in patients afflicted with malaria; specifically recurring fevers, enlarged spleens, headaches and chills.[1-2]

From the fifth century *B.C.* onwards, the identification and description of the disease along with its devastating effects are illustrated in the writings of several well-known philosophers and writers.[1] They include Homer (*ca.* 8th Century *B.C.*) Sophocles (496-406 *B.C.*), Hippocrates (460-370 *B.C.*), Plato (428-347 *B.C.*), Aristotle (384-322 *B.C.*) and Shakespeare (1564-1616).[1-3] During the Roman Empire and throughout the middle ages, malaria became more prevalent due to the growth in population worldwide and the increase of migration of people across nations. By the beginning of the 18th century, malarial infections were prominent and widespread across all continents.[1] Furthermore, the intermittent illness had acquired various descriptive names, such as jungle fever, swamp fever and marsh fever, as a result of its association with tropical and low-lying water environments. In Western Europe, specifically Italy, the term *mal'aria* (meaning bad air) was used to express the cause and pathogenicity of the parasite in malaria victims.[1,3]

Throughout the 19th century, particularly from the 1850's onwards, scientists and pathologists made numerous unsuccessful attempts to isolate, identify and culture the pathogenic organism responsible for malaria.[1] The discovery of the malaria-causing parasite in the blood of the human host was achieved through the work of a French surgeon, Charles Louis Alphonse Laveran, in 1880.[1] This finding was facilitated by previous work done by

Heinrich Meckel in 1847, who observed the discolouration of organs in patients suffering from intermittent fevers. The discolouration was due to the presence of the reddish-brown malaria pigment, hemozoin, and Laveran initially proposed that it was the transparent, flake-like or granular form hemozoin molecules that was the cause of the disease.[1,3] In addition to noticing the presence of hemozoin particles in the red blood cells of an infected person, Laveran also observed several forms of the mobile, flagellated male gametocytes as well as the spherical, motionless female gametocytes of the malaria parasite and subsequently proposed that the disease was caused by the single-celled protozoan organism *Plasmodium*, which he referred to as *Oscillaria malariae*.[1-3] Over the following decade, Laveran's observations were supported by detection of the parasite within human host red blood cells through experiments conducted by Marchiafava and Celli in 1884, Golgi in 1886, and MacCallum and Opie in 1897.[1-3] Following the successful identification of *Plasmodium* as the causative agent of malaria, scientists began to investigate and postulate modes of transmission of the parasite. Both Laveran and Manson suggested that mosquitoes were vectors of the disease.[1] Manson, who in 1878 had established the ability of mosquitoes to transmit the infectious microfilariae from the blood of patients suffering from elephantiasis, hypothesized that mosquitoes could be infected in a similar manner by the malaria pathogen as a result of its exflagellation morphology. Consequently, Manson influenced his apprentice and colleague, Ronald Ross, to perform experiments that would substantiate the mosquito transmission of malaria.[1]

Ross, a physician in the British Indian Medical Service, commenced his investigation on mosquitoes as possible vectors of the malaria parasite in India in 1895. Initially, he successfully disproved the hypothesis (postulated by Manson) that the parasites were transferred from the mosquitoes to a new human host through the ingestion of water contaminated with the eggs of infected mosquitoes.[1-2] Furthermore, he suggested that the transmission of the malaria plasmodia from mosquitoes to humans occurred through a bite or during feeding and concluded that the development of the human malaria parasite favoured a particular mosquito species, notably *Anopheles*.[2] On 20 August 1897, Ross ultimately confirmed the Anopheles mosquitoes as vectors of human malaria when he observed the development of the oocyst and the presence of the black granular malaria pigment, hemozoin, within the stomach of mosquitoes which had fed on a malaria-infected

patient.[1,3] A few years later, Ross demonstrated that malaria parasites infecting birds (*i.e.* sparrows and crows) developed into oocysts in the mosquito gut and subsequently migrated as sporozoites to the mosquito salivary glands from which they infected more birds during blood meals. He anticipated a similar transmission mechanism for human malaria, of which the experimental evidence was presented in 1898 by Grassi, Bignami and Bastianelli.[1,3] The Italian scientists reported the transmission of the malaria parasite *Plasmodium vivax (P. vivax)*, through the bite of the vector *Anopheles Claviger*, to a healthy volunteer. In addition, they also described the sporogonic cycle of *Plasmodium falciparum (P. falciparum)* and *Plasmodium malariae (P. malariae)* pathogens in anopheline mosquitoes.[1] In 1900, Grassi suggested a host tissue development phase for the malaria parasite, due to the difference in the structure of the nucleus in parasites initially observed in the host erythrocytes (trophozoites) and the parasites within the salivary glands of the mosquito vector.[1-3] The discovery of the *Plasmodium* malaria parasite in the tissues of both primate and human hosts was achieved in 1948 by H.E. Shortt and Garnham.[1,3] Upon infecting (either through a mosquito bite or intravenous injection of sporozoites from the mosquito salivary glands) rhesus monkeys with *Plasmodium cyanomolgi* and human volunteers with *P. vivax* parasites, respectively, Shortt and Garnham detected the maturation of the malaria parasites in the livers of both simian and human hosts. In subsequent work, they established the tissue phases for the human malarial parasite *P. falciparum* (in 1949), *P. ovale* (1954) and *P. malariae* (1959).[1,3] The latent tissue phase, referred to as hypnozoite, was observed and described by Krotoski and co-workers between 1980 and 1985.[1,3] This stage of the parasite's developmental cycle provided experimental evidence of the clinical relapse when humans afflicted with the disease lack the pathogen in their bloodstream and appear to be cured, but experience the disease's symptoms years later.[1,3]

Over the last half century, considerable efforts and advances have been made in the field of malarial research, particularly in understanding the biochemistry of the malaria vector and parasite, as well as in the discovery and design of drugs to prevent or cure malaria. These include:- the isolation of artemisinin from *Artemisia annua* in 1971 as a potential anti-malarial compound; the successful culturing of the pathogenic *P. falciparum* parasite within red blood cells by Trager; the development of several effective diagnostic test kits for the

detection of malaria parasite antigens; and the completion of the genome sequencing of the vector *Anopheles gambiae (A. gambiae)* and the parasite *P. falciparum* in 2002.[3-7]

1.2. Global impact of malaria

1.2.1. Epidemiology of malaria

Malaria is a vector-borne disease caused by protozoan parasites of the genus *plasmodium* and is regarded as the most deadly parasitic infection afflicting humans.[1] Four plasmodia species are traditionally considered to account for all malarial infections in humans; *Plasmodium ovale* (*P. ovale*), *Plasmodium vivax* (*P. vivax*), *Plasmodium malariae* (*P. malariae*) and *Plasmodium falciparum* (*P. falciparum*).[1] However, naturally acquired infections in humans have recently been reported for the parasite *Plasmodium knowlesi* (*P. knowlesi)*, which has been traditionally associated with monkeys.[8,9] *P. vivax* is geographically the most widespread of the parasites due to its ability to mature in mosquitoes at both low and high temperatures and under tropical climatic conditions.[2,9] In West Africa, *P. vivax* is absent as the majority of the population do not possess the Duffy antigen receptor, which the parasite requires for entry into the human host's red blood cells.[10] *P. falciparum* is however, the most virulent human malaria parasite causing the majority of severe clinical cases. *P. ovale* and *P. malariae* are less common both in terms of geographic distribution and human infectivity.[10] The female Anopheles mosquito is the vector responsible for the transmission of malaria.[2,10] There are *ca.* 70 *Anopheles* species differing in behavioural characteristics which are considered vectors of malaria. Variations in mosquito behaviour include host feeding preference (zoophilic or anthropophilic), biting habit (endophagic or exophagic) and resting behaviour (endophilic or exophilic).[2,10] *A. gambiae* and *A. funestus* are considered the most important malaria vector species in Africa and their behavioural patterns (anthropophilic, endophilic and endophagic), along with their high transmission efficiency and density, are factors which have been attributed to the enormous burden caused by malaria on the African continent. [6,11,12]

The distribution of malaria, however, is worldwide with the disease being endemic in 106 countries across all the continents except Antarctica and Australia. Of the 106 malaria endemic countries, 43 are on the African continent.[13] Recent estimates suggest that more

than 50 % of the world's population (3.3 billion) are living in malarious areas and are exposed to the disease.[14] Geographically, the disease is most prevalent within the tropical and sub-tropical regions (as depicted in figure 1).[1,14] Sub-Saharan Africa bears the greatest burden, accounting for approximately 90 % of all reported clinical cases with, 85 % of all malaria associated deaths occurring amongst children under 5 years old and pregnant women.[10,13-14] The severity of the disease in Africa is due to the fact that nearly all infections are caused by the most virulent malaria parasite, *P. falciparum*.[10]

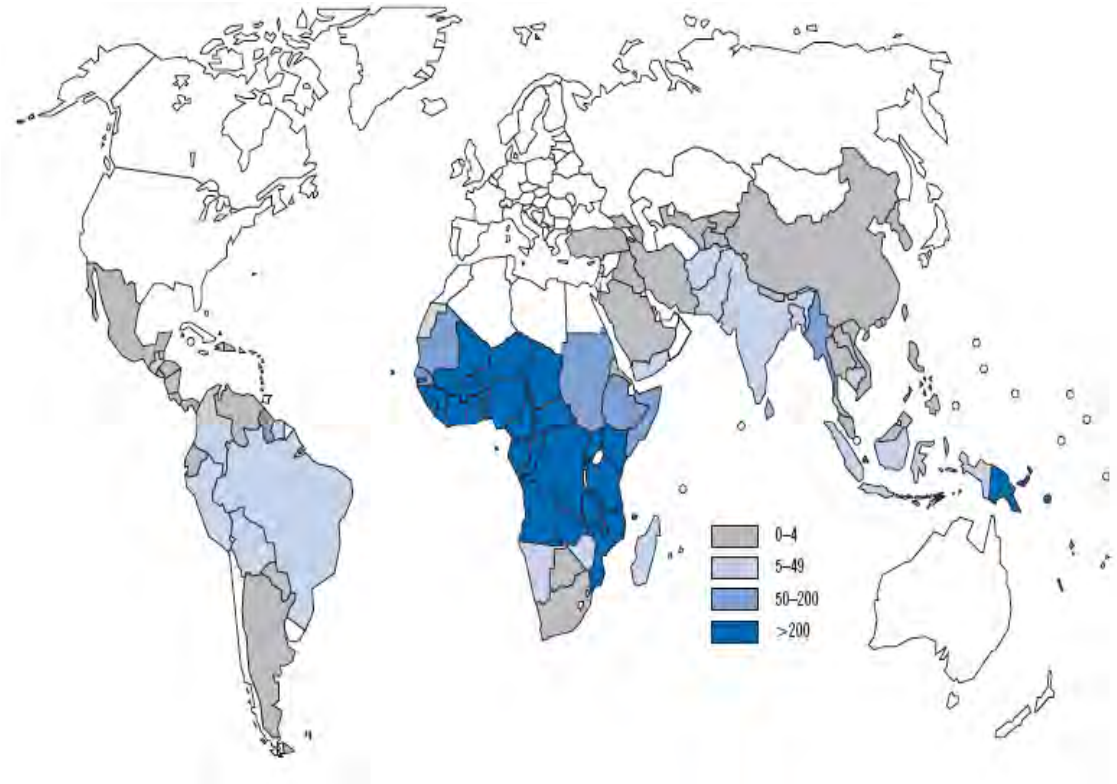

Figure 1. Estimated global malaria incidence per 1000 population.[14] (Reproduced with permission from the World Health Organisation).

The epidemiology of malaria is complex and the level of endemicity of the disease varies considerably within a given endemic region. Human activities at both a population and individual level have influenced the distribution pattern of malaria.[15-16] The promotion of economic and agricultural development and the movement of populations (including urbanization and tourism), have contributed directly and indirectly to an increase in malarial transmission intensity.[15-17] It is estimated that approximately 25 000 tourists and travellers from non-endemic countries are exposed to the disease annually upon visiting malaria endemic regions.[17]

The global impact and public health threat of malaria is staggering. According to the World Health Organization (WHO) world malaria report 2010, the disease was responsible for 225 million clinical episodes in 2009, of which 781 000 resulted in death.[13] Although efforts have been made to reduce the burden of malaria, the prevalence of the disease has remained high and in some cases increased.[10,13-14] Reports from Burkina Faso indicate a 3-fold increase in the number of malaria cases, whereas in Ethiopia, there is evidence suggesting a shift in parasite infection cases from predominantly *P. vivax* to *P. falciparum*.[18-19] Several factors are attributed to the increase in malaria prevalence worldwide. These include the emergence and spread of drug-resistant malaria parasites, particularly the virulent *P. falciparum*, towards chemotherapeutic drugs such as chloroquine.[9,16] Chloroquine-resistant parasites were originally reported in South America (Venezuela and Colombia) and South East Asia (Thailand and Cambodia) in the late 1950's, but are now widespread in all malaria endemic regions.[16] Moreover, insecticide-resistant mosquitoes (e.g. *A. gambiae* and *A. funestus*) have emerged recently.[20] Several studies on the interaction between malaria and HIV co-infection have suggested that the immune-suppression effect of HIV enhances malaria transmission by increasing susceptibility and *plasmodium* parasite density within the host, thus increasing the symptomatic malarial episodes, especially in pregnant women.[21-23] In addition, malaria adversely affects HIV-infected individuals by triggering CD4 cell activity and increasing viral loads, consequently accelerating the progression of HIV/AIDS.[22-23]

Most parasitic diseases, including malaria, commonly occur in poor or developing countries and are rarely encountered in the developed countries.[10] Consequently, the financial incentive (i.e. the generation of profits) for pharmaceutical companies in wealthy nations to discover and develop new anti-malarial drugs for the developing world populations is low and, as a result, progress in the discovery of new and effective anti-malarial drugs has been slow.[10] Other factors considered to contribute to the increase in the incidence of malaria include:- climatic instability; social unrest; failure in implementing effective malaria-control programmes; and weak public health service systems.[2,9,17] The past few years have witnessed increased efforts and commitment from international organizations towards controlling and ultimately eliminating malaria and its associated burdens. The Roll Back Malaria (RBM) partnership was established in 1998 to provide a coordinated global approach to fight malaria. RBM is an initiative whose vision is "a world free from the burden

of malaria" and its goals include reducing the global malaria morbidity and mortality cases reported in the year 2000:- i) by 50% by the end of 2010; and ii) by 75% or more by the year 2015.[13-14] The Global Malaria Action plan was launched by the RBM partnership in September 2008, to re-define the goals and accelerate the efforts required to reach these targets.[13] The fight against malaria is prioritised by the United Nations through the Millennium Development Goals (MDG's) and by African countries through the Abuja Declaration of 2000.[24-25] Other important organizations committed to overcoming malaria at a global level include:- the Malaria Vaccine Initiative; the Multilateral Initiative on Malaria (MIM); and the Global Fund to fight HIV/AIDS, Tuberculosis and Malaria.[26-28]

The complex life cycle of the *plasmodium* parasite has presented several approaches to malaria control and prevention, which are currently being exploited.[13,29] These control measures include:- i) the reduction of mosquito population densities through environmental management (by water treatment and the application of larvacides); ii) the use of chemo-prophylactic and therapeutic drugs for prevention and treatment purposes [e.g. Artemisinin Combination Therapy (ACT)]; iii) the use of Indoor Residual Spraying (IRS) within households with WHO-approved insecticides (e.g. DDT and pytheroids) to reduce and interrupt malaria transmission and; iv) the use of Insecticide-Treated Nets (ITNs) and long-lasting ITNs (LLITNs) as barriers for reducing the transmission of malaria infections.[29] With the high prevalence of malaria worldwide, the World Health Organisation (WHO) has endorsed the limited use of indoor residual spraying (IRS) with DDT as a method for malaria vector control until a less harmful alternative is obtained. IRS and ITNs vector-control methods are limited as they are heavily dependent on a single class of insecticides that require widespread usage, which increases the development of resistance by mosquito vectors.[13,29] Brooke and colleagues documented the emergence of pyrethroid-resistant *A. funestus* vectors.[30] Furthermore, the lifespans of ITNs and LLINTs are approximately 6 months and 3 years, respectively, thus requiring regular re-treatment and replacement, which is not financially viable in the long term.[9,29]

New malaria vector control strategies are being investigated. One such approach involves the infection of the *Anopheles* vectors with entomopathogenic fungi such as *Beauveria bassiana* and *Metarhizium anisopliae*.[31] Another vector control method being considered is the construction of transgenic mosquitoes, which are incapable of transmitting the

plasmodium parasite.[32] Research on the development of malaria vaccines is ongoing, but requires continued funding from public and private organizations and it seems unlikely that an effective vaccine will become available for at least another decade.[9,29,33]

1.3. Biology and life cycle of the malaria parasite

The malaria parasites are host-specific and the life cycle is accomplished in two hosts, the human and the *Anopheles* mosquito (Figure 3).[34] The parasite life cycle is complex with several asexual reproduction stages in the human host and sexual reproduction stages in the mosquito.

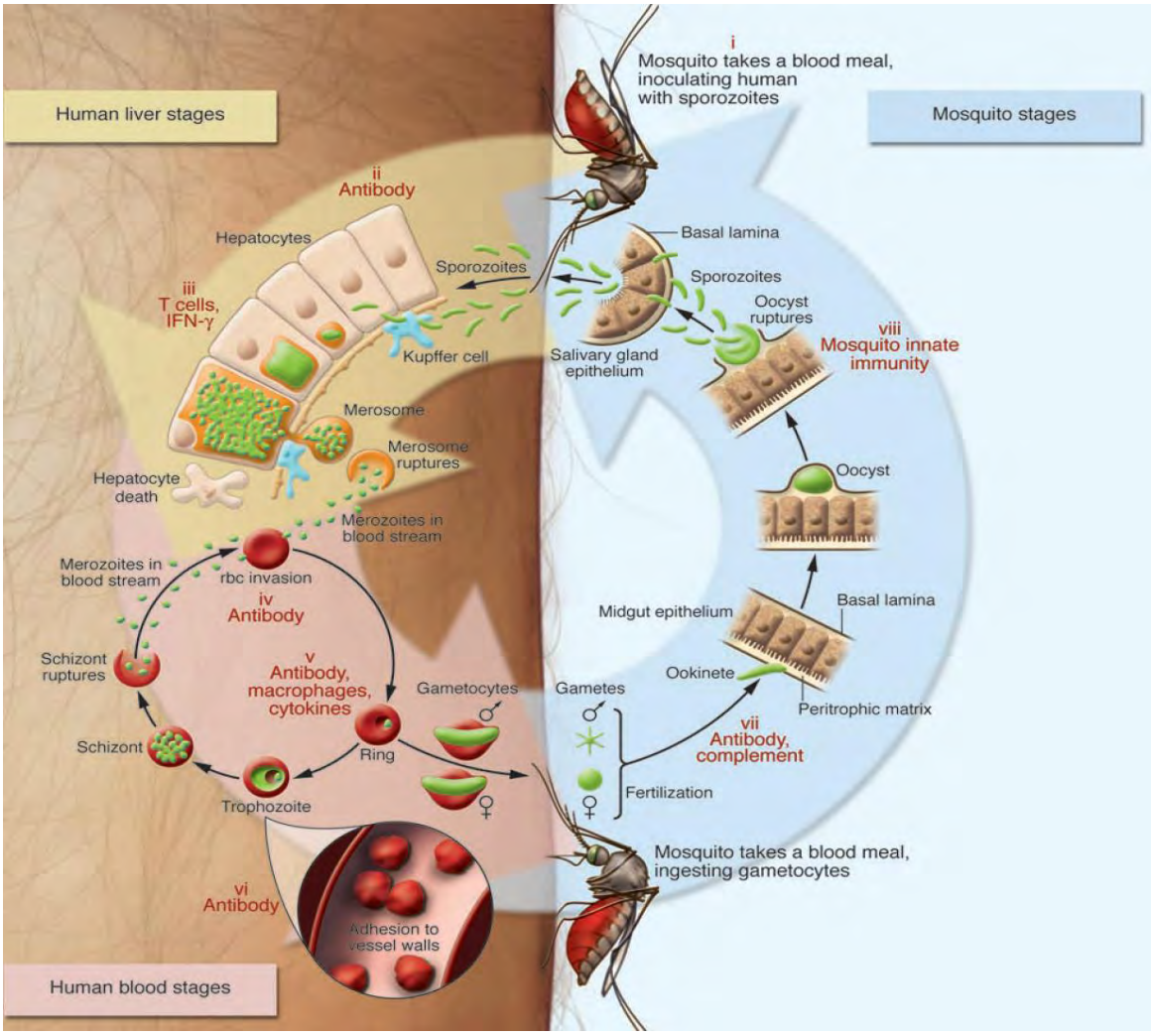

Figure 2. The life cycle of *Plasmodium* parasites in the human and mosquito.[34] (Reproduced with permission.)

Human malaria infections are initiated by the injection (through a bite during a blood-meal) of *plasmodium* sporozoites within the saliva of an infected mosquito into the host's bloodstream.[34] The circulating sporozoites enter the hepatocytes in the liver shortly after inoculation and start to divide mitotically – the pre-erythrocytic stage. Invasion into the hepatocytes is mediated by specific binding of the parasite circumsporozoite protein (CSP) and thrombospondin-related adhesive protein (TRAP) to heparin sulphate proteoglycans on the hepatocytes.[35] The intra-hepatocytic sporozoites divide asexually into pre-erythrocytic schizonts, each containing *ca*. 1 x 10^3 – 30 x 10^3 merozoites. Eventually, merozoites are released upon rupture of hepatocytes into the bloodstream and invade red blood cells (RBCs) to start the erythrocytic asexual phase. During invasion of RBCs, merozoites attach to RBC surface binding receptors (duffy glycoprotein for *P. vivax* and glycophorins for *P. falciparum*), undergo apical re-orientation, enter the erythrocytes through junctional movement and induce the formation of parasitophorous vacuoles.[10,36]

Inside the erythrocytes, merozoites differentiate into ring trophozoites that ingest haemoglobin and nutrients within the vacuole and mature into multi-nucleate schizonts. The mature schizonts differentiate into thousands of merozoites causing the RBCs to swell and rupture, releasing the merozoites into the bloodstream which subsequently attach and re-infect new RBCs, such that the erythrocytic cycle is repeated. These repeated cycles lead to exponential growth of infected RBCs and it is during the bursting of erythrocytes that the clinical symptoms of malaria appear in the infected person.[10,36] During the erythrocytic cycle, a proportion of merozoites follow a different developmental pathway and develop into male and female gametocytes, the sexual forms of the parasite.[36] The stimulus that triggers gametocytogenesis is not fully understood, but is likely to be the response of the host immune system to the infection. Gametocytes are ingested by a female *anopheles* mosquito during a blood-meal and develop in the midgut of the mosquito into male and female gametes. Fertilization occurs to form a zygote that develops into an ookinete. The ookinete migrates through the midgut epithelium and matures into an oocyst under the basal membrane. The oocyst undergoes maturation to generate sporozoites which, upon rupture, migrate through the hemocoel to the salivary glands from where they are injected and infect humans during the next blood-meal taken by the mosquito.[10,37]

1.3.1. Biological differences amongst malaria parasite species

There are species-specific biological differences within the *plasmodium* parasite generic life cycle. In *P. vivax* and *P. ovale*, a percentage of sporozoites invading the hepatic cells develop into hypnozoites (hypnozoite stage) which remain dormant in the liver.[10] The presence of hypnozoites may cause relapse of clinical malaria symptoms months to years after the initial infection. Several differences in the biology of *P. falciparum* account for its higher pathogenicity and ability to cause the most severe manifestation of malaria.[10] *P. falciparum* modifies the surfaces of infected RBCs causing them to adhere:- to the endothelium of capillaries (sequestration); to uninfected RBCs (rosetting); and to platelets (clumping). Adherence protects the parasite from the host's immune response mechanisms and from being removed from circulation into the spleen.[38] In addition, the *P. falciparum* genome contains the very large and diverse *var* gene family (*ca.* 60 genes) which encodes for the *P. falciparum* Erythrocyte Membrane Protein 1 (*pf*EMP1).[10] *pf*EMP1 mediates parasite binding to the various host receptors and, through a phenomenon known as antigenic variation, allows the parasite to evade host immune responses.[10,38] Several *var* genes encode for proteins that mediate adherence to Intercellular Adhesion Molecule 1 (ICAM-1) in the brain and adhesion to Chondroitin Sulphate A (CSA) in the placenta. Sequestration of parasites to these molecules is associated with cerebral malaria and the severe clinical manifestations observed in pregnant women.[38]

1.3.2. Clinical symptoms and diagnosis of malaria

The clinical symptoms of malaria occur during the erythrocytic life cycle phase of the parasite when RBCs rupture. Symptoms for uncomplicated malaria infections include fever, chills, headache, vomiting, diarrhoea, convulsions and muscular pains.[10,17] Severe malaria is a complex disorder that affects several tissues and organs, and complications include renal failure, hypoglycaemia, hepatic dysfunction, severe anaemia, cerebral malaria, respiratory distress and metabolic acidosis.[9-10] The standard method for diagnosing malaria involves light microscopy of thick and thin Giemsa-stained blood smears on glass microscope slides. Several advances have been made in the development of alternative diagnostic methods including:- fluorescence microscopy of parasite nuclei stained with acridine orange; rapid

dipstick immunoassays of various malaria antigens; and polymerase chain reaction (PCR) based assays.[9,17]

1.4. Current anti-malarial drugs: mechanism of action and resistance

Malaria is curable if it is diagnosed properly and treatment is provided promptly. The malaria chemotherapeutic drugs are generally classified into 3 groups, based on the *plasmodium* parasite life cycle phase they act on or interrupt, *viz*.,:- i) tissue schizonticides, which act against the development of liver stage parasites ii) blood schizonticides, which prevent parasite development at the intra-erythrocytic stage and iii) gametocides, which inhibit the maturation of sexual forms of the parasites.[39] The intra-erythrocytic phase of the parasite's life cycle is the most susceptible stage and is generally targeted by the available chemotherapeutic agents. Malaria chemotherapy currently relies on five classes of compounds, *viz*.,:- quinolines, artemisinins, anti-folates, hydroxynapthoquinones and antibiotics.[39]

1.4.1. Quinolines

Quinolines are heterocyclic aromatic compounds containing the quinoline nucleus **1**, which comprises a pyridine ring fused to a benzene ring; they are also referred to as 1-azanaphthalenes, benzopyridines or even, heterocyclic amines.[40] The nitrogen atom is located next to the benzene ring and the chemistry of quinolines reflects a preference for electrophilic aromatic substitution on the benzene ring and nucleophilic aromatic substitution on the pyridine ring. The quinoline ring system is found in many natural products such as alkaloids, particularly in those with pronounced biological activities.[41]

Many anti-malarial drugs (figure 3) are derivatives of quinine **2**, an alkaloid first isolated from the bark of the cinchona tree in Peru and used, in Western medicine, to treat patients suffering from malaria since the 18th century.[42-43] The structure of quinine **2** was elucidated by Paul Rabe in 1908, but its formal total synthesis was achieved by Woodward and Doering in 1944. The use of quinine for prophylaxis and treatment of uncomplicated malaria cases is limited due to its toxicity and adverse effects. However, it has excellent efficacy and is still used against highly drug-resistant parasites and to treat severe cases of malaria.[42-43] Since the 1940's, several quinoline anti-malarial analogues, based on quinine as a template, have

been synthesized. Some of these compounds exhibit better pharmacological profiles and include:- the 4-aminoquinolines (4-AQs) such as chloroquine **3** and amodiaquine **4**; aryl-amino alcohols such as mefloquine **5**, halofantrine **6** and lumefantrine **7**; and 8-aminoquinolines such as primaquine **8** and tafenoquine **9**.[42,44-45]

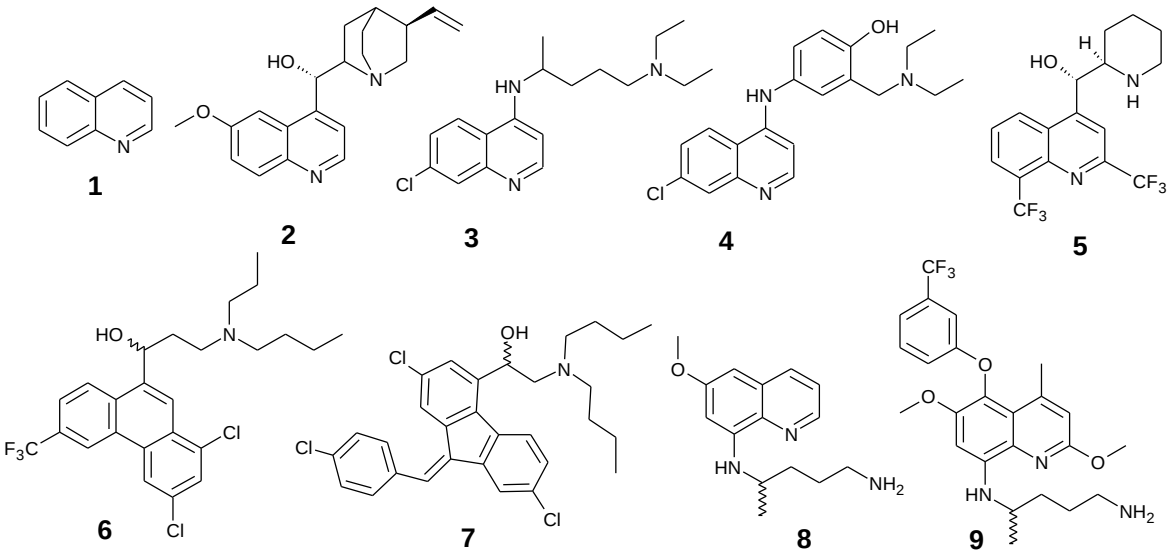

Figure 3: Structures of quinoline, quinine and selected anti-malarial drugs.

Chloroquine **3** [CQ; *N'*-(7-chloroquinolin-4-yl)-*N,N*-diethylpentane-1,4-diamine] has been used extensively for the treatment of malaria due to its low toxicity, low cost and excellent efficacy but, during the 1960's, resistant-parasites emerged.[45] *In vivo*, chloroquine **3** is metabolised by cytochrome P450 through a series of de-ethylation steps to yield the bis-desethyl compound **10**. Further oxidation produces the aldehyde **11** and then the carboxylic acid **12**, which is finally dealkylated to 4-aminoquinoline (4-AQ) **13** (Scheme 1).[44,46] CQ-resistant strains are presently widespread in most malaria-endemic regions.

Amodiaquine **4** is structurally related to CQ, containing a 4-hydroxy anilino group in the mannich side chain. Amodiaquine **4** is regarded suitable for prophylaxis use due to its long half-life. *In vivo*, amodiaquine **4** is rapidly dealkylated into its active derivative, *N*-desethylamodiaquine (*N*-DEAQ).[44,46] Although amodiaquine **4** is more active in parasite clearance than CQ and effective against CQ-resistant strains of *P. falciparum*, its clinical use has been limited by the development of hepatotoxicity and agranulocytosis in patients, along with the possibility of cross-resistance with CQ.[17,45]

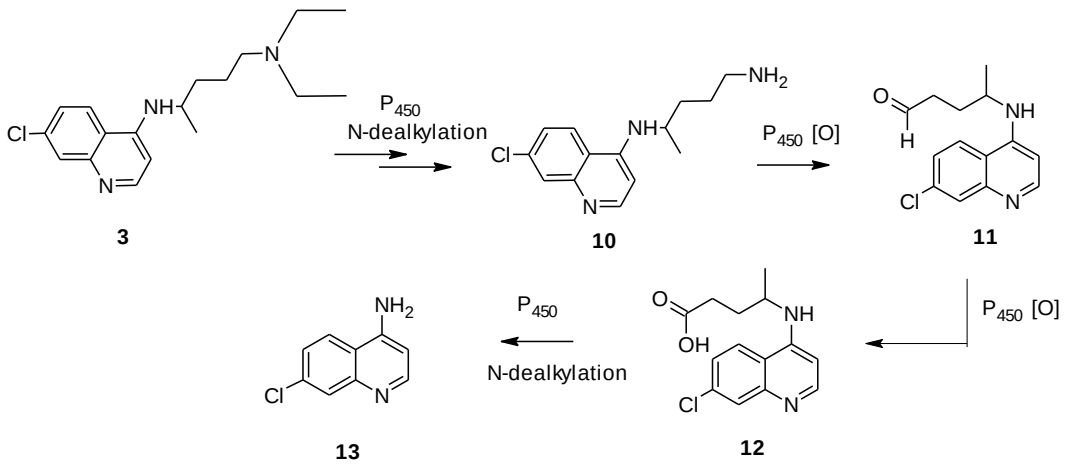

Scheme 1. Metabolic degradation of chloroquine **3** *in vivo* by cytochrome P450.

Mefloquine **5** and halofantrine **6** are therapeutic agents developed by the Walter Reed Army Institute and are active against CQ-resistant plasmodium parasites.[17] As with amodiaquine **4**, mefloquine's long half-life has made it useful as a prophylactic drug; however, when used for treatment of malaria, it is usually administered with artesunate (see p. 13).[17,45] Regrettably, its long half-life has led to the development of resistant *plasmodium* strains. In addition, the use of mefloquine **5** has been restricted due to frequently reported neuropsychiatric side effects, e.g. acute psychosis.[17] The use of halofantrine **6**, a substituted phenanthrene related to chloroquine **3**, as a therapeutic agent has been restricted by its erratic absorption profile and its association with cardiotoxicity effects, such as cardiac arrhythmias.[17] Lumefantrine **7**, which is structurally related compound to halofantrine **6**, was synthesized in China in the 1970's and has been shown to act synergistically with artemether (see p. 15) for the treatment of uncomplicated *P. falciparum* malaria. This course of therapy is relatively safe, but there are concerns about the therapeutic potential of lumefantrine **7** due to the possibility of cross resistance with chloroquine **3** and mefloquine **5**.[17,45]

Primaquine **8**, [(*R,S*)-*N*-(6-methoxyquinolin-8-yl)pentane-1,4-diamine], is an 8-aminoquinoline synthesized to target the maturation of parasite gametocytes (gametocytocidal activity), but is also active in the pre-erythrocytic stages (hypnozoites) of *P. falciparum, P. ovale* and *P. vivax*.[44-45] The drug is often referred to as an anti-relapse agent, as it interrupts the hypnozoite (dormant) stages, which leads to relapse in malaria infections. A disadvantage of primaquine **8** includes its short half-life as it is readily oxidised

to its carboxy derivative. Structural modifications of primaquine **8** directed the synthesis of the analogue tafenoquine **9**, which has a much longer half-life and improved anti-parasitic activities. However, both primaquine **8** and tafenoquine **9** exhibit toxicity effects, including gastrointestinal effects and haemolysis in G6PD deficient patients.[17,45]

1.4.1.1. Mechanism of action and resistance

Quinoline anti-malarial drugs generally have the same mechanism of action, arising from their accumulation within the food vacuole (FV) of the *plasmodium* parasite during the erythrocytic stage of the life cycle (Figure 4).[47-48] The catabolism of haemoglobin within the FV provides the parasite with a source of nutrients and amino acids which are essential for its biosynthetic pathways and growth. Toxic haem (ferriprotoporphyrin) moieties are generated as by-products during haemoglobin degradation, which are subsequently polymerized by the parasite to non-toxic haemozoin (malaria pigment) crystals. Quinoline-antimalarial drugs typically interrupt the haem-detoxification process, through the formation of drug-haemozoin complexes and/or binding of the drug to the growing face of the haemozoin crystals, causing the termination of growth.[45-47] The consequent accumulation of toxic haem molecules within the FV renders the parasites susceptible to oxidative stress, leading to death as shown in figure 4. Anti-parasitic functions may also include the inhibition of haemoglobin proteolysis, *i.e.* inhibition of aspartic and cysteine protease activity and the raising of the FV pH.[45,47]

The mechanism of resistance against quinoline anti-malarial drugs is not fully understood and is still being investigated. The general current consensus is that *plasmodium* parasites, particularly *P. falciparum*, develop resistance to these drugs through:- i) specific point mutations in the *pf*crt gene, which result in the reduced binding affinity of the drugs to haem molecules; and ii) mutations in the *pf*mdr *1* gene encoding for P-glycoprotein (Pgh-1), resulting in the amplification of the gene, leading to reduced drug accumulation in the FV and a decrease in drug concentrations *via* efflux from the FV.[45-48]

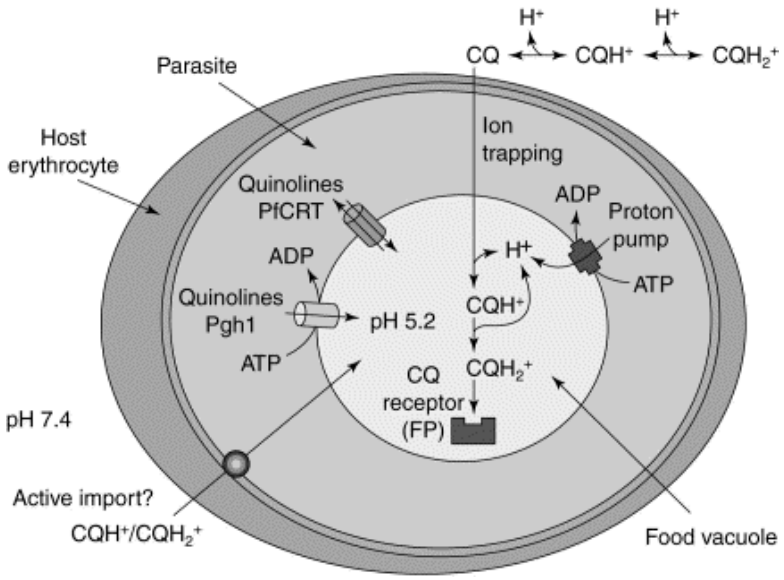

Figure 4: Proposed mode of action of CQ and related quinoline anti-malarials.[48] (Reproduced with permission.)

1.4.2. Artemisinin and its derivatives

Artemisinin (quinghaosu) **14** is a sesquiterpene trioxane lactone, isolated from the Chinese medicinal herbal plant, *Artemisia annua*, and has exceptional anti-plasmodial activity against drug-resistant parasite strains.[45] To improve the potency of artemisinin **14** and address drawbacks, such as poor solubility, short plasma half-life and limited bioavailability, simple chemical modifications of artemisinin **14** have resulted in the development of semi-synthetic analogues.[44-45] Reduction of artemisinin **14** afforded dihydroartemisinin (DHA) **15** which is roughly seven times more potent than artemisinin **14** *in vitro*, while alteration of the lactone carbonyl group at C-10 led to the development of artemisinin derivatives, such as artemether **16**, arteether **17** and sodium artesunate **18** (Figure 5).[44-45] Artemether **16** and arteether **17** are oil-soluble drugs which are administered *via* intramuscular injection, whilst artesunate **18** is water-soluble and is suitable for both oral and intravenous administration.[17,45] These analogues (**16-18**) are all rapidly hydrolysed *in vivo* to the hemiacetal **15**, which is then metabolized through glucuronidation.

Due to the short plasma half-lives of artemisinin drugs, high rates of recrudescent infections are frequently reported when they are administered as mono-therapeutic agents. To reduce recrudescence of infections and the development of resistant-parasites, the general recommendation is to combine artemisinin drugs is in combination with another effective,

long-acting, anti-malarial drug – an approach termed Artemisinin-based Combination Therapy (ACT).[9,49] Several ACT formulations are currently available, including:- artemether-lumefantrine; artesunate-amodiaquine and dihydroartemisinin-piperaquine. A major obstacle in the use of ACT's as first-line therapeutics, especially in poor, malaria-endemic countries, is their cost. Treatment with ACTs is approximately ten times more expensive than with mono-therapy treatments.[9]

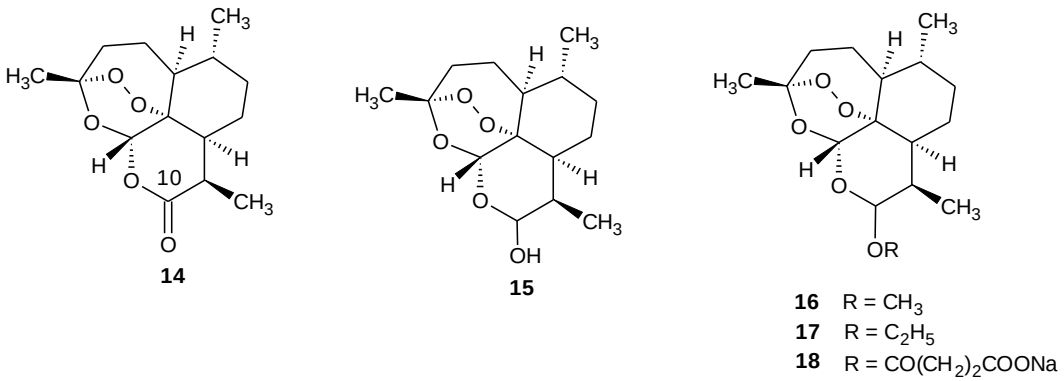

Figure 5. Artemisinin and its synthetic derivatives as anti-malarial agents.

1.4.2.1. Mechanism of action and resistance

Artemisinin **14** and its analogues are believed to be active against all the erythrocytic stages of the malaria parasite's life cycle. It has been suggested that the presence of the *endo*-peroxide bridge is essential for the anti-parasitic effect of the drugs.[43-45] The mechanism of action remains uncertain, but it has been suggested that it involves the reductive cleavage of the *endo*-peroxide moiety through interaction with intra-parasitic haem (iron-mediated) to generate free-radical species. These highly reactive radical species alkylate various parasite membranes including the endoplasmic reticulum, mitochondrial and plasma membranes, thus leading to their destruction (Figure 6).[43-45]

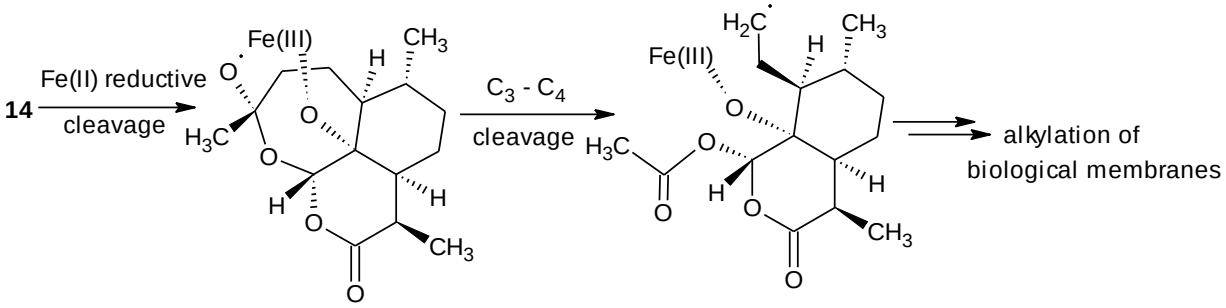

Figure 6. Proposed mode of action of artemisinin **14**.[45]

More recently, the *P. falciparum* sacro-endoplasmic reticulum Ca^{2+}-ATPase (pfATP6) has been identified as an important target for artemisinin and its analogues.[45] There are currently no reported clinical cases of parasite resistance to artemisinin derivatives, although there are reports of reduced efficacy of the drugs both *in vitro* and *in vivo* at the Thailand-Cambodia border.[9,45]

1.4.3. The Antifolates

The antifolate anti-malarial drugs affect the pre-erythrocytic and erythrocytic stages of the parasite life cycle, in particular, the folate biosynthetic pathway.[45] Several compounds that inhibit this pathway have been developed including pyrimethamine **19**, sulphadoxine **20** and proguanil **21,** shown in Figure 7. Proguanil **21** is converted *in vivo* to its active metabolite, the cyclic triazine cycloguanil **22**, by cytochrome P_{450}. Pyrimethamine **19** and sulphadoxine **20** are generally used in combination therapy with each other, as they exhibit synergistic activity due to the fact that they both act on enzymes in the same biosynthetic pathway.[45] The long half-lives of these drugs have resulted in their use as prophylactic agents for intermittent preventive therapy in pregnancy (IPTp) and infants (IPTi).[17]

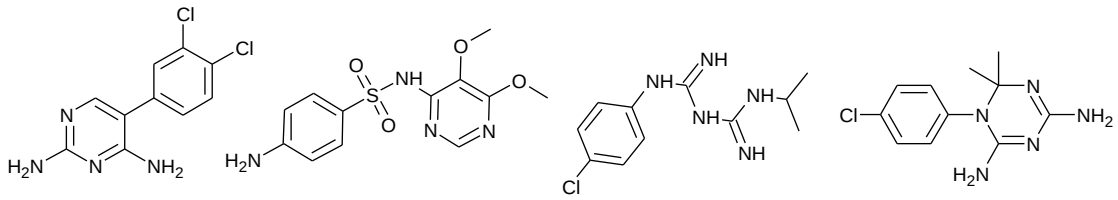

19 **20** **21** **22**

Figure 7. Current antifolate malaria chemotherapeutic drugs

1.4.3.1. Mechanism of action and resistance

The molecular targets of antifolates are well defined and, in contrast to other anti-malarial drugs, the mechanism of action has been comprehensively described.[44] Pyrimethamine **19** and proguanil **21** are competitive inhibitors of the enzyme, dihydrofolate reductase (DHFR), which catalyses the reduction of 7,8-dihydrofolate to tetrahydrofolate with concomitant oxidation of the NADPH co-factor.[45,50] The sulfonamide **20** competitively inhibits another enzyme within the pathway, dihydropteroate synthase (DHPS), which catalyses the formation of 7,8-dihydropteroate from 2-amino-4-hydroxy-6-hydroxymethyl-7,8-dihydro-

pteridine diphosphate and *p*-aminobenzoic acid (p-ABA). The inhibition of these two enzymes prevents formation of tetrahydrofolate co-factors, which are critical for the biosynthesis of pyrimidine and amino acids such as methionine and serine. The lack of pyrimidine inhibits DNA synthesis, whilst a deficiency in amino acids prevents parasite growth.[45,50] *Plasmodium* resistance towards antifolates has developed rapidly and is widespread. Mutations in the dhfr and dhps gene encoding for the DHFR and DHPS enzymes have resulted in structural modified enzymes, particularly in the enzyme active-sites, thus preventing the drugs from binding competitively.[45,50]

1.4.4. Hydroxynaphthoquinones

Atovaquone **23** {2-[trans-4-(4'-chlorophenyl)cyclohexyl]-3-hydroxy-1, 4-naphthaquinone} (Figure 8), was successfully developed by Glaxo Wellcome and is used in fixed-dose combination with proguanil **21** for chemo-prophylaxis and treatment of uncomplicated malaria infections.[17,25] When used as a mono-therapy agent, a high rate of recrudescence occurs. However, a synergistic effect and improved activity is achieved when used in combination with proguanil **21**.

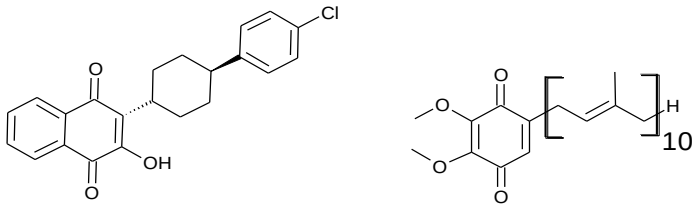

Figure 8. Ubiquinone **24** and its synthetic analogue atovaquone **23**.

1.4.4.1. Mechanism of action and resistance

The anti-malarial activity of atovaquone involves the interruption of mitochondrial electron transport and subsequent collapse of the mitochondrial membrane potential in the parasites. Atovaquone is a structural analogue of ubiquinone **24** (Figure 8), which binds competitively and inhibits the cytochrome bc_1 complex, thus interfering with electron transfer from ubiquinone to cytochrome C.[45,51] The collapse of the mitochondrial membrane potential has been associated with apoptosis. The mechanism of resistance in *Plasmodium* parasites towards atovaquone is attributed to point mutations within the cytochrome b

gene, which result in amino acid alterations in the catalytic site of the enzyme, thus reducing binding affinity of the drug.[51]

1.4.5. Antibiotics

Antibiotics which are currently being used as anti-malarial agents include clindamycin, azithromycin, ciprofloxacin and doxycycline (Figure 9). The anti-malarial activities of these compounds involve the inhibition of DNA replication (DNA gyrase, RNA polymerase) and inhibition of protein synthesis by interacting with the 23S ribosomal RNA unit in *plasmodium* species.[45]

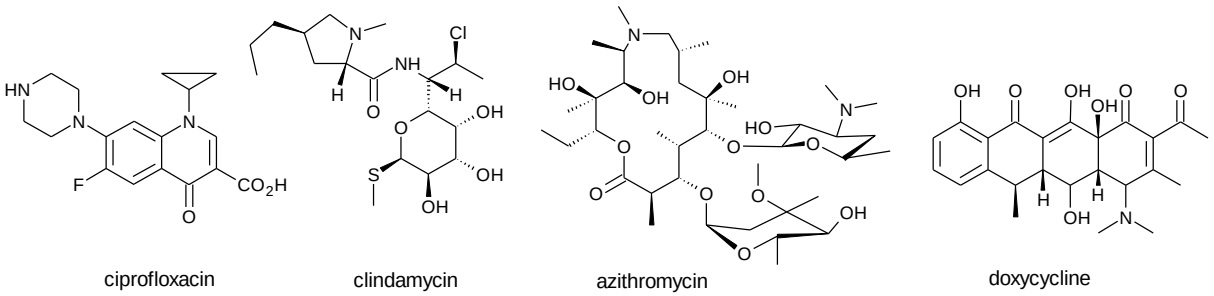

Figure 9. Anti-malarial antibiotics

1.5. Synthetic approaches to current anti-malarial drugs

1.5.1. Synthesis of 4-aminoquinolines, quinoline aryl-amino alcohols and 8-aminoquinolines.

Woodward and Doering achieved the first formal synthesis of quinine **2** in 1944, with a lack of stereocontrol at the four asymmetric centres in the molecule and hence, experienced difficulty in separating the isomers (Figure 10).[52-53]

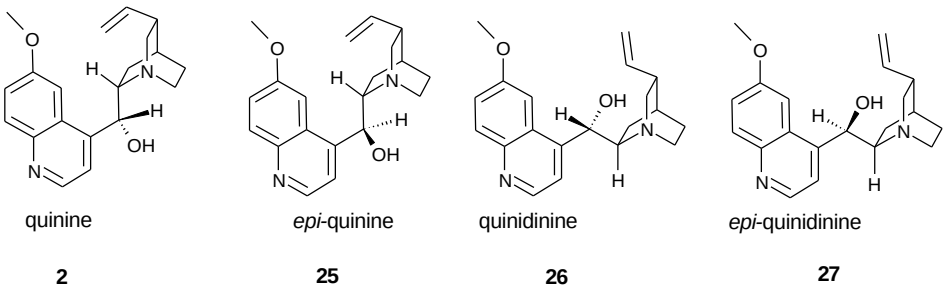

Figure 10. Quinine **2** and selected stereoisomers.

The first stereo-selective, total synthesis of quinine was reported by Stork and co-workers; the retrosynthetic strategy they adopted is summarised in Figure 11.[53]

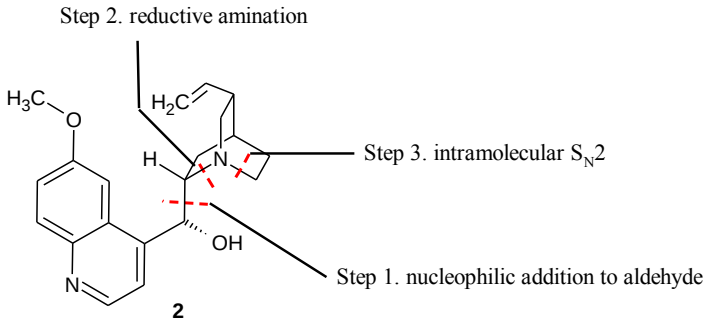

Figure 11. Stork's retrosynthetic approach to quinine **2**.[53]

The desired stereoselective synthesis of quinine **2** was achieved through the construction of the azido aldehyde **34** (Scheme 2), trisubstituted piperidine **39** (Scheme 3) and deoxyquinine **41** (Scheme 4) as key intermediates.[53] The synthesis of compound **34** involved a 7-step process starting from (*S*)-4-vinylbutyrolactone **28**. The vinyl lactone **28** was opened in the presence of diethylamine to give the primary alcohol *in situ*, which was protected as its *tert*-butylsilyl (TBS) derivative **29**. Alkylation of the TBS derivative **29** afforded the diethylamide **30**, which was deprotected with *p*-toluenesulfonic acid (PPTS) in EtOH to afford the *trans*-3,4-disubstituted butyrolactone **31**. Reduction of the lactone **31** using diisobutylaluminium hydride (DIBAL-H) led to the corresponding lactol, which was subjected to the Wittig reaction with methoxymethylene triphenylphosphorane to introduce an additional C-atom, thus furnishing the alcohol **32**. The alcohol **32** was efficiently transformed to the azide **33**, which was converted to the desired azido aldehyde **34** by hydrolysis in a two-phase system.[53]

The synthesis of the trisubstituted piperidine **39** (Scheme 3) involved the lithiation of 6-methoxy-4-methylquinoline **35** at C-6 and subsequent addition of the azide **34** *via* the carbonyl group to afford a mixture of the two epimers of secondary alcohol **36**. The mixture was exposed to Swern oxidation to obtain the corresponding azidoketone **37**, which was converted with triphenylphosphine in THF to the tetrahydropyridine **38**. Reduction of **35** with sodium borohydride in THF/MeOH mixture efficiently yielded the expected piperidine **39**.[53]

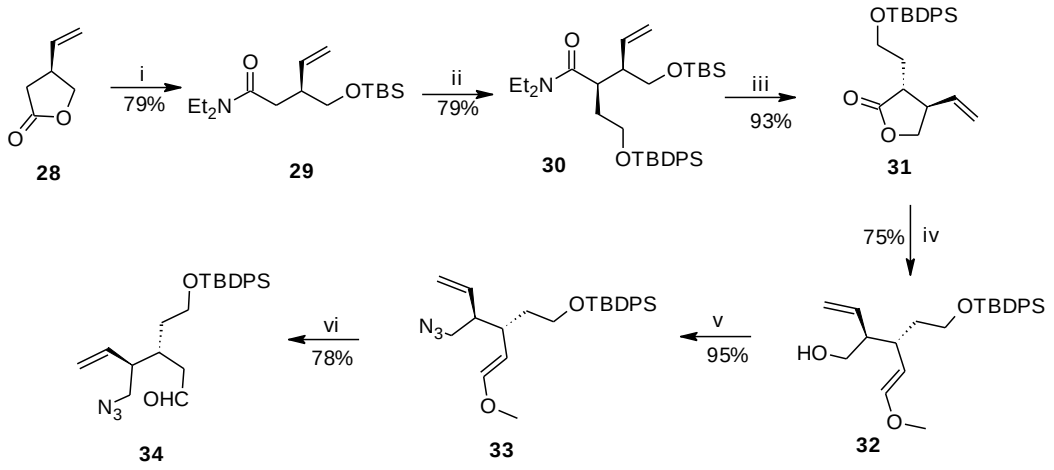

Scheme 2. Synthesis of the azido aldehyde **34**. *Reagents and conditions:* i) $Et_2NH/AlMe_3$, TBSCl/imidazole/DMF ii) LDA, -78°C, $ICH_2CH_2OTBDPS$ iii) PPTS, EtOH, 12h, xylenes, reflux 8-10 h; iv) DIBAL-H, -78°C, $Ph_3P{=}CHOMe$; v) Ph_3P/DEAD, $(PhO)_2P(O)N_3$; vi) 5N-HCl, THF/DCM.

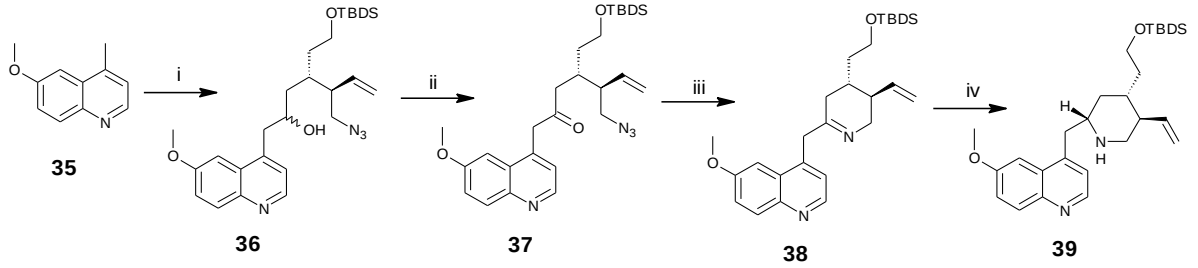

Scheme 3. Synthesis of the trisubstituted piperidine **39**. *Reagents and conditions:* i) LDA, THF, -78°C, **34** in THF, aq.$NaHCO_3$; ii) DMSO, $(ClCO)_2$, Et_3N; iii) Ph_3P, THF, reflux; iv) $NaBH_4$, MeOH/THF.

The completion of the synthesis of quinine **2** (Scheme 4) was achieved by deprotection of the silyl group of piperidine **39** to yield the alcohol **40**. The quinuclidine ring of deoxyquinine **41** was formed by mesylation of the alcohol **40** in the presence of pyridine and cyclization by refluxing in acetonitrile. Deoxyquinine **41** was then oxidised to yield quinine **2** .[53]

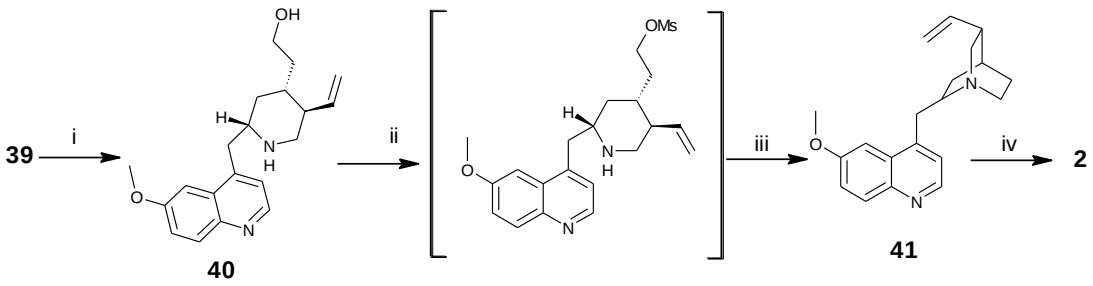

Scheme 4. Completion of the synthesis of quinine **2**. *Reagents and conditions*: i) HF/CH_3CN; ii) MsCl/Py, DCM; iii) CH_3CN, reflux; iv) NaH/DMSO, then O_2.

More recently, Jacobsen *et al*. [54] and Kobayashi *et al*. [55] have both published routes for the total, enantioselective synthesis of quinine **2** and its epimer quinidine **26**. The retrosynthetic strategy adopted by Jacobsen and co-workers is summarised in Figure 12.

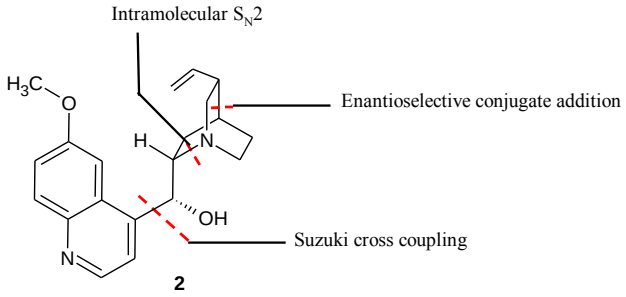

Figure 12. Jacobsen's retrosynthetic strategy to quinine and quinidinine.[54]

The cost-effective total synthesis of chloroquine **3** has been achieved by the Surrey and Hammer method (Scheme 5).[56-57] This involves the condensation of *m*-chloroaniline **42** with ethyl ethoxalylacetate **43** to yield the aniline derivative **44**, which undergoes pyrolytic cyclization to generate the carboxylate ester **45**. Subsequent hydrolysis produces the corresponding acid derivative **46**, thermal decarboxylation of which affords 4-hydroquinoline **47**. The chlorination of **47** is achieved with phosphorus oxychloride to yield 4,7-dichloroquinoline **48**, which is subjected to nucleophilic substitution with 4-diethylamino-1-methylbutylamine **49** to give chloroquine **3**.[56-57] More recently, Margolis *et al*.[58] have reported the synthesis of chloroquine **3** using a palladium catalyst system.

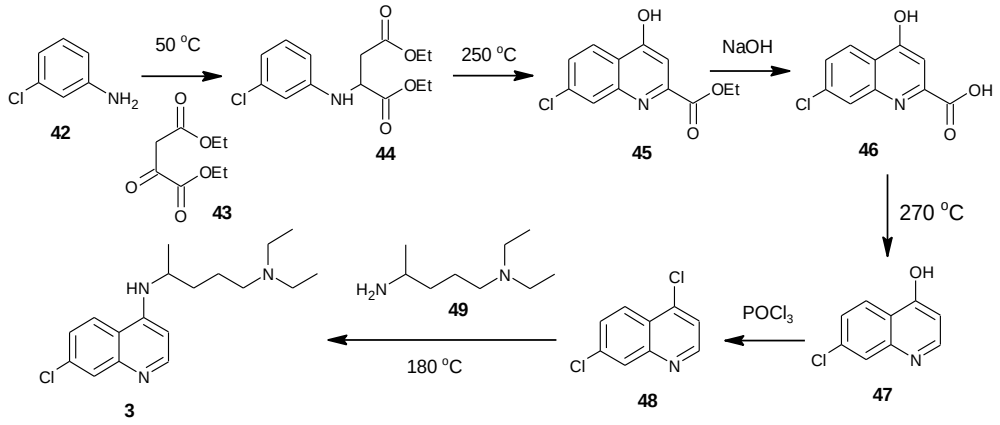

Scheme 5. Surrey and Hammer's total synthesis of chloroquine **3**.[56-57]

The four reaction step synthesis of mefloquine **5** has been described by Lutz *et al*.[59] (Scheme 6). The initial step involves the condensation of ethyl 4,4,4-trifluoroacetoacetate **50** and *o*-trifluoromethylaniline **51** with polyphosphoric acid (PPA) to obtain the 4-quinolone

52. Bromination using $POBr_3$ produces 4-bromoquinoline **53**, which is treated with BuLi, followed by CO_2, to yield the 4-quinolinecarboxylic acid **54**. The introduction of 2-pyridyllithium **55** yields the pyridyl ketone **56**, which is subjected to hydrogenation to afford mefloquine **5**.

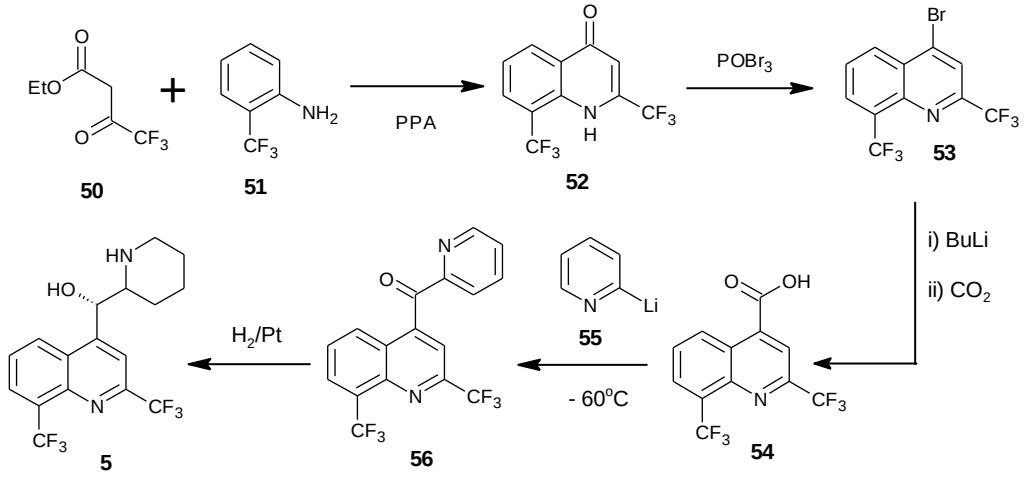

Scheme 6. Lutz's synthesis of mefloquine **5**.[59]

The large scale synthesis of primaquine **8** by Elderfield *et al*.,[60] is illustrated below (Scheme 7). This involves condensation of 1,4-dibromopentane **55** with potassium phthalimide **56** to obtain the phthalimido bromide **57**. Substitution of bromine by 6-methoxy-8-aminoquinoline **58** yields the phthalimido-quinoline intermediate **59**, which is subsequently reacted with hydrazine to remove the phthalimido moiety and afford primaquine **8**.

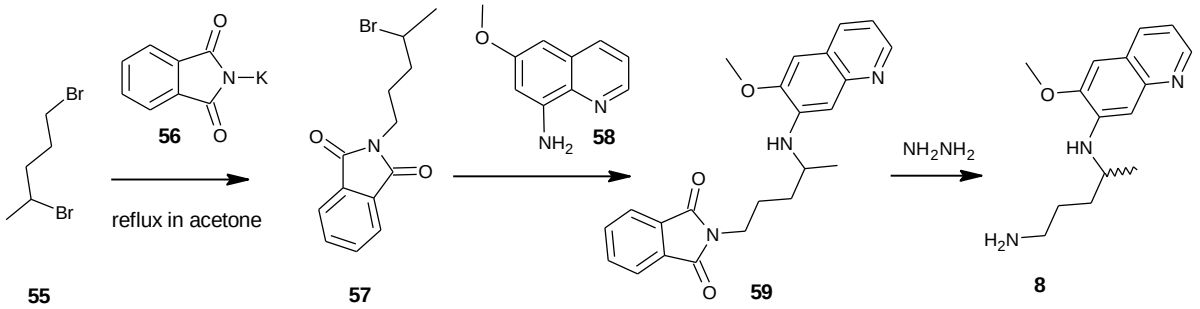

Scheme 7. Synthesis of primaquine **8** by Elderfield.[60]

1.5.2. Synthesis of Artemisinin and its derivatives

Over the last two decades, the total synthesis of the sesquiterpene endoperoxide lactone artemisinin **14** and its derivatives has been explored, since extraction from the herb *A.*

annua gives the compound in low yields.[61] Schmidt and Hofheinz developed the first complete synthetic route for artemisinin **14** from (-)-isopulegol.[62] Starting with (+)-isolimonene **60**, Ravindranathan *et al.* [63] completed the total stereoselective synthesis of artemisinin **14** *via* an intra-molecular Diels-Alder reaction, whilst Avery and co-workers detailed a 10-step stereoselective synthesis from (*R*)-(+)-pulegone.[64] Recently, Yadav and co-workers have described the complete synthesis of artemisinin **14** in fewer steps, with high stereoselectivity and high overall yield (Scheme 8).[65] The synthetic route involves regioselective exocyclic hydroboration of (+)-isolimonene **60** with dicyclohexyl borane **61** to afford the alcohol **62** in 82% yield.

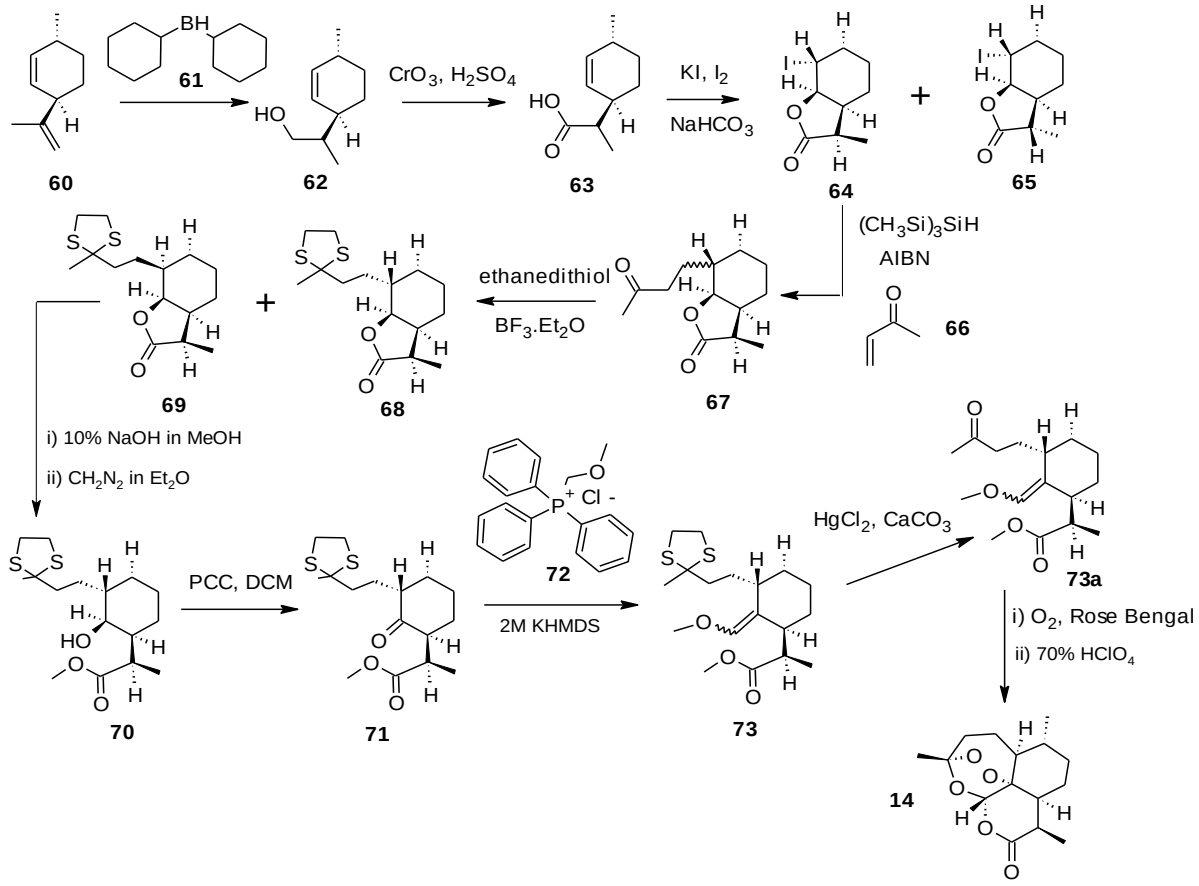

Scheme 8. Yadav's total stereoselective synthesis of artemisinin **14**.[65]

The alcohol **62** was oxidized using Jones reagent into its corresponding acid **63**, which was then subjected to iodolactonization with KI and I_2 in aq. $NaHCO_3$ to obtain the diastereomeric iodolactones **64** and **65**. Alkylation of iodolactone **64** was achieved *via* an intramolecular radical reaction using Chatgilialoglu's reagent and methyl vinyl ketone **66**, to form the alkylated lactone **67**. Treatment of the keto moiety of **67** with ethanedithiol in the

presence of $BF_3.Et_2O$ afforded the diastereomeric thioketal lactones **68** and **69** in overall quantitative yield. Subsequent hydrolysis and esterification of the thioketal lactone **69** in the presence of diazomethane yielded the ester **70**, which was oxidized with PCC to afford the keto derivative **71**. Transformation of the keto ester **71** to the corresponding methyl vinyl ether **73** was achieved *via* the Wittig reaction with the triphenylphosphonium salt **72** and 2M-KHMDS. In the presence of $HgCl_2.CaCO_3$, the thioketal **73** was deprotected to furnish the intermediate **73a**. Subsequent photo-oxidation using O_2 with Rose Bengal and acid hydrolysis afforded the artemisinin **14**.[65]

The transformation of artemisinin **14** into its derivative DHA **15** is conveniently achieved by reduction of the C-10 carbonyl group to the alcohol with sodium borohydride. In the presence of boron trifluoride-diethyl ether and the appropriate alcohol, DHA **15** is converted through an oxonium ion intermediate into the ester analogues **16**, **17** and **18** and anhydroartemisinin **74** (Scheme 9).[61,66]

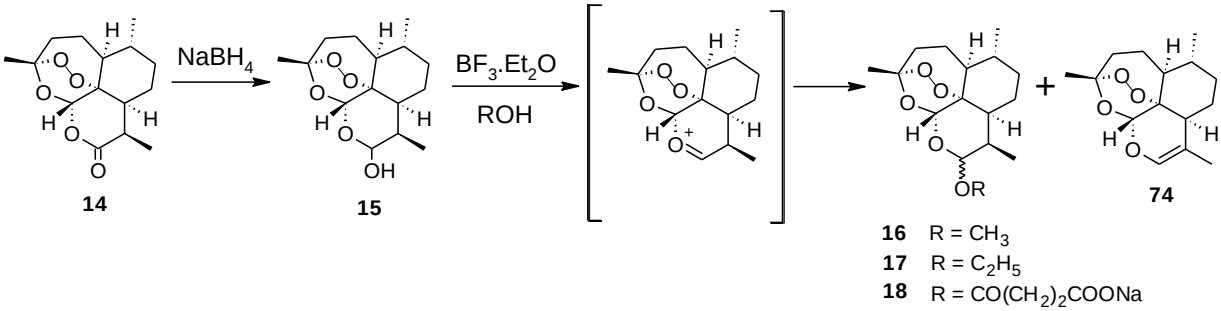

Scheme 9. Synthesis of DHA and artemisinin analogues.

1.6. Strategies for the discovery of new anti-malarial drugs

The need to develop new anti-malarial chemo-therapeutic and prophylactic agents has been increased by the emergence of *plasmodium* parasites which are resistant to the currently available drugs.[67] Approaches which are currently being pursued include:- i) the development of analogues of existing anti-malarial drugs through chemical modifications; ii) the discovery of biologically active natural products; and iii) the rational design of compounds which are active against new biological targets.[67-68]

1.6.1. Development of analogues of existing anti-malarial drugs

Chemical modification of existing anti-malarial therapeutics represents an effective and relatively inexpensive strategy.[44,67] In the quest to synthesize new quinoline anti-malarials with greater potency and better pharmacological profiles, structure-activity relationship (SAR) studies of chloroquine **3** have been carried out to identify the structural features that are necessary for anti-plasmodial activity, and these are summarised in Figure 13.[45-46]

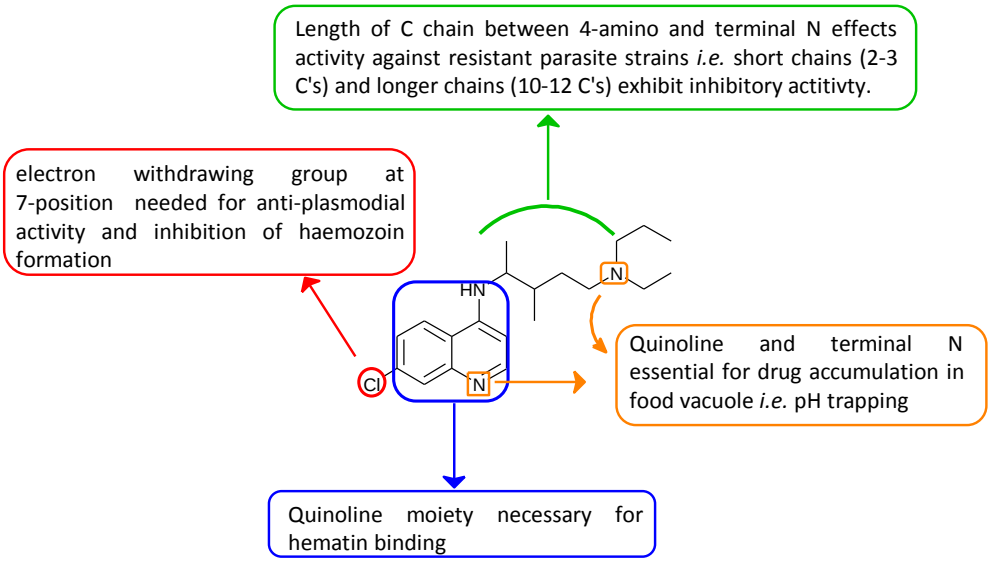

Figure 13. Structural features of chloroquine and their effect on anti-plasmodial activity.

Synthetic strategies in the design of new 4- and 8-AQs have focused on:- i) nucleophilic substitution of the quinoline nucleus; and ii) alteration of the length of the side chain and the nature of the terminal amino group on the side chain at C-4.[45-46,69] Solomon and co-workers recently modified the side chain amino group of 4-AQs in order to study the effect of introducing heterocyclic moieties on the biological activity; their approach is summarised in Scheme 10. In the presence of *N,N*-dicyclohexylcarbodiimide (DCC) as a dehydrating agent or in refluxing toluene alone, the desired thiazolidin-4-ones **78-86**, 5-methyl-thiazolidin-4-ones **87-95**, 1,3 thiazinan-4-ones **96-104** and 2,3-dihydrobenzo[*e*][1,3]thiazin-4-ones **105-113** were produced from the appropriate 4-AQ's **76a-c**, the aldehydes **75a-c** and the mercapto acids **77a-d**.[70] In another study, Wolf *et al.*[71] described the synthesis and biological activity of 4-amino-7-chloroquinolyl amides, sulfonamides, ureas and thioureas with the variation of the side-chain length. The condensation of dasyl chloride **114** and ethanolamine afforded the sulphonamide derivative **115**, which was treated with methanesulfonyl

chloride to obtain the mesylate **116**. The desired sulfonamides **118a-f** were formed by reacting the mesylate **116** with a series of quinoline-diamines **117 (**Scheme 11).

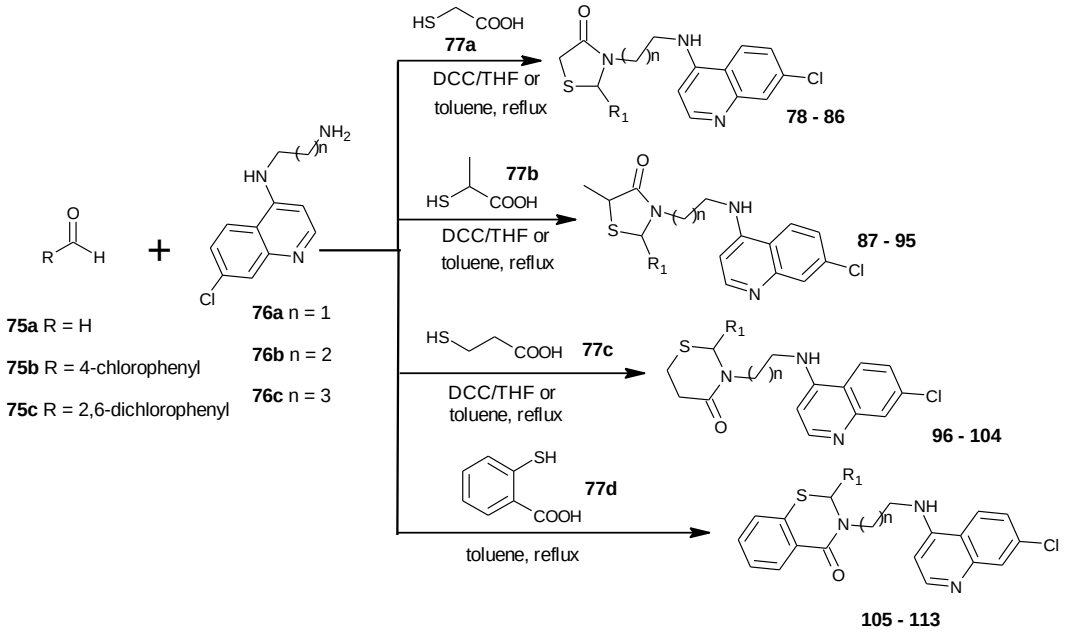

Scheme 10. Synthesis of heterocyclic derivatives as 4-AQ analogues.

The reaction of the diamine **119** with the appropriate isocyanate and isothiocyanate **120** furnished the corresponding ureas and thioureas **126a-f**. In addition, **119** was coupled with various acids **127** to afford the 7-chloro-4-aminoquinolyl-derived amides **128a-b**.

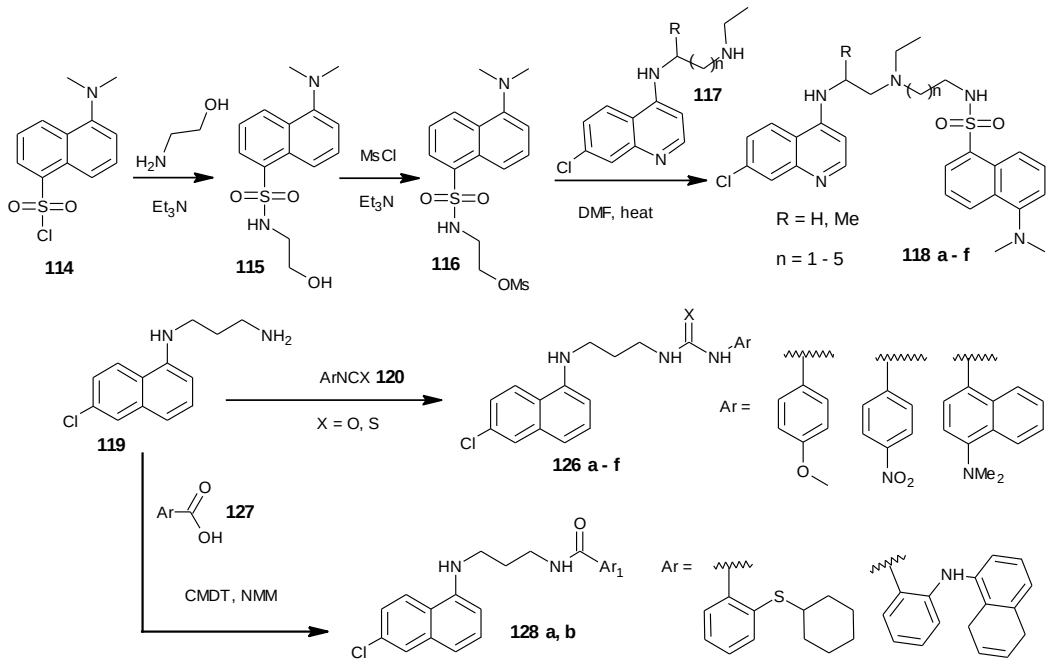

Scheme 11. Synthesis of novel 4-amino-7-chloroquinolyl amides, sulfonamides, ureas and thioureas.

In two related synthetic and anti-plasmodial activity studies, Chibale *et al.*[72-73] synthesized a series of α-acylamino amides and lactams, based on the 4-AQ pharmacophore with variation in the side chain length, using Ugi isocyanide multi-component reaction chemistry. The reaction of 4,7-dichloroquinoline **129** with selected alkyl diamines afforded the quinoline derivatives **130**, which were transformed into the Ugi adduct **134** in the presence of the aldehyde **131**, an isocyanide **132** and a carboxylic acid **133**. Using similar reaction conditions and resin-bound macroporous *p*-toluenesulfonic acid **137**, the anticipated lactams **138** were isolated in reasonable yields (Scheme 12).[73]

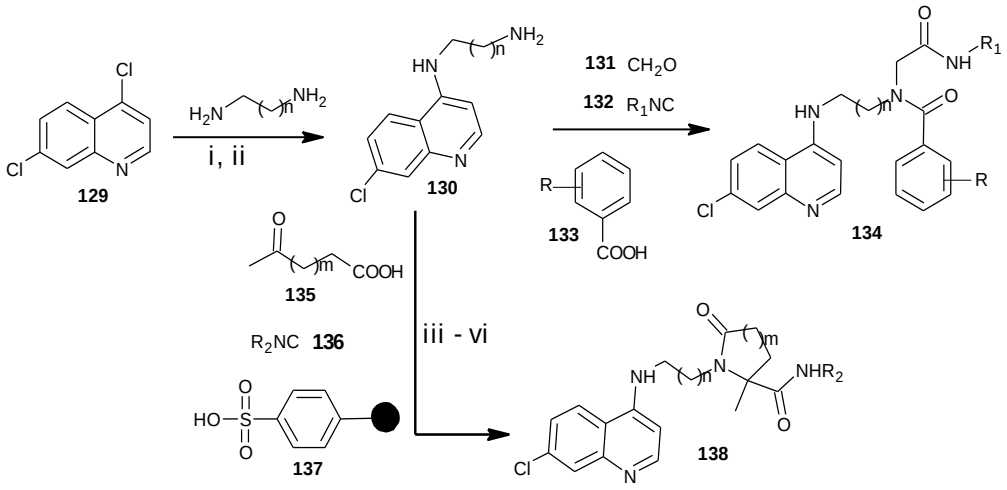

Scheme 12. Synthesis of α-acylamino amides and γ- and δ-lactams using Ugi isocyanide multi-component reaction chemistry. *Reagents and conditions:* i) 80°C, 1h ii) 135-140°C, 3h iii) MeOH, rt, 12-18h iv) **137**, 1h v) filter, wash vi) 3% NH_3/MeOH, filter, wash.

Novel compounds based on the modification of the quinoline ring system have also been explored. Guy *et al.*[74] reported the synthesis of 9-aminoacridine derivatives, which were screened for anti-malarial activity against chloroquine-resistant strains (Scheme 13). Treatment of the substituted salicylic acids **139** with methyl iodide and with trifluoromethanesulfonic anhydride furnished the triflates **140**, which were coupled with substituted anilines **141** using the Buchwald protocol to yield the diaryl amines **142**. The 9-chloroacridines **143** were generated by hydrolysis of the methyl esters **142**, followed by Friedel-Crafts cyclization with $POCl_3$. In a parallel synthesis, 1,3-diaminopropane **144** was mono-protected with the nosyl group to obtain **145**, which was treated with a series of carboxylic anhydrides **146**. The resulting amides were reduced *in situ* with borane-dimethylsulfide complex to afford the corresponding secondary amines **147**. Subsequent reductive amination reactions with the aldehydes **148**, followed by deprotection of the

nosyl group afforded the free amines **149**, which were coupled with the acridines **143** to generate the products **150**.[74]

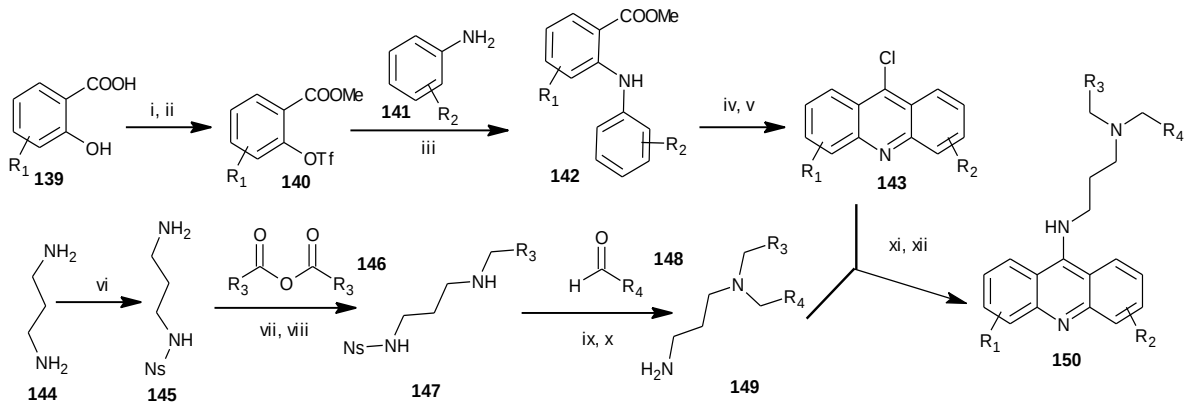

Scheme 13. Convergent synthesis of 9-aminoacridines from 9-chloroacridine and diaryl amines. *Reagents and conditions:* i) MeI, Cs_2CO_3, DMF ii) Tf_2O, Et_3N, DCM, -78 ^oC to rt iii) **141**, $Pd(OAc)_2$, BINAP, Cs_2CO_3, toluene iv) $Ba(OH)_2.8H_2O$, MeOH, 80 ^oC, overnight v) $POCl_3$, 120 ^oC, 1h vi) 2-nitrobenzenesulfonyl chloride, DCM,0 ^oC to rt, overnight vii) **146**, pyridine, THF viii) BH_3-dimethyl sulfide complex, THF, 60 ^oC, 30 min ix) **148**, sodium triacetoxyborohydride, THF, sonicated, 35 ^oC, 1h x) Benzenethiol, Cs_2CO_3, degassed CH_3CN, under argon xi) phenol, Cs_2CO_3, 3Å molecular sieves, DMSO, 100 ^oC, 2h xii) DMSO, 100 ^oC, 4h, methyl isocyanate polystyrene resin, overnight, rt.

Synthetic approaches to new 8-AQ derivatives have been reported. Thus, Gomes *et al.*[75] recently described the synthesis of 8-AQ derivatives containing the imidazolidin-4-one ring and examined their rate of hydrolysis under physiological conditions (Scheme 14). The synthesis involved coupling of primaquine **8** with *N*-Boc protected amino acid to give the *N*-Boc protected intermediate **152**, which upon deprotection, afforded the amino acid derivative **153**. Subsequent intramolecular cyclization of the intermediate **153** with an aldehyde or ketone furnished the desired product **154**.

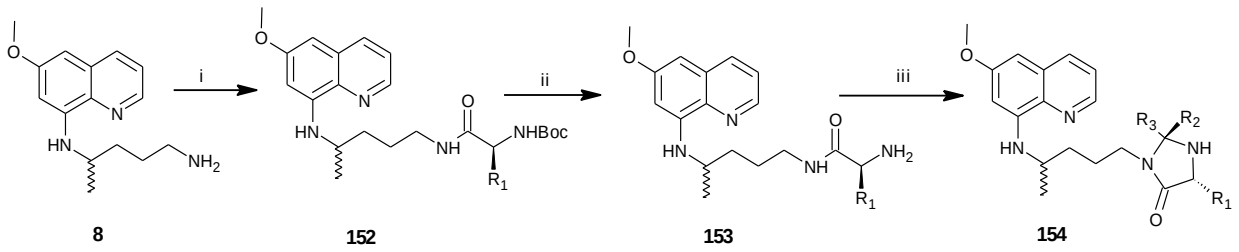

Scheme 14. Synthesis of imidazolidin-4-ones of primaquine analogues. *Reagents and conditions:* i) *N,N'*-dicyclohexylcarbodiimide (DCCI), HOBt, N^{α}-Boc-protected amino acid (BocAAOH); ii) TFA, Na_2CO_3 iii) Me_2CO or cyclic ketones or 3,4-$(MeO)_2$–C_6H_3CHO in MeOH, Et_3N, molecular sieves.

The discovery of ferrochloroquine (FQ) **155** as a potential anti-malarial drug has stimulated research into the design of metal-based aminoquinoline analogues.[76] Several organo-metallic compounds related to FQ have been successfully synthesized (Figure 14).[76-79]

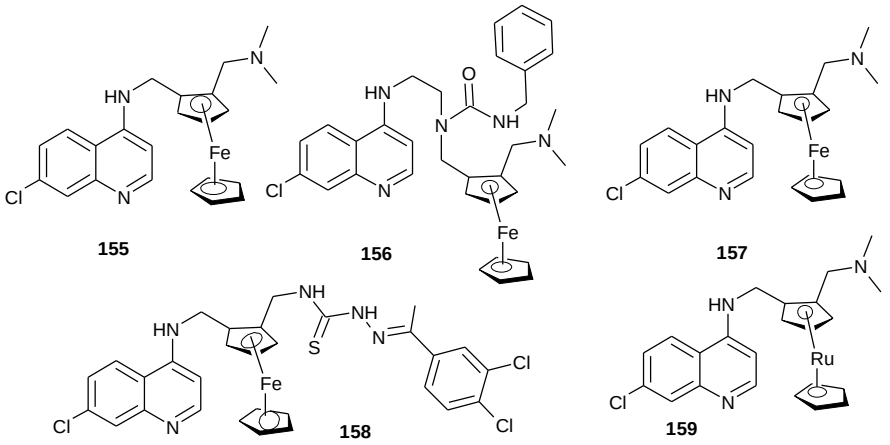

Figure 14. Metal-based 4-aminoquinoline anti-malarials.

The synthetic strategy for accessing the quinoline metal-complex **155** involves an S_NAr reaction between 4,7-dichloroquinoline **129** and the metallocene amine **160** in the presence of 1-methyl pyrrolidinone (NMP) and base.[77-78] Alternatively, compound **129** may be reacted with the diamine **161** to afford the substituted quinoline amine **162**, which upon treatment with the metallocenes **163** and **164** in the presence of sodium borohydride in methanol, gives the desired products **165** and **166** (Scheme 15).[78]

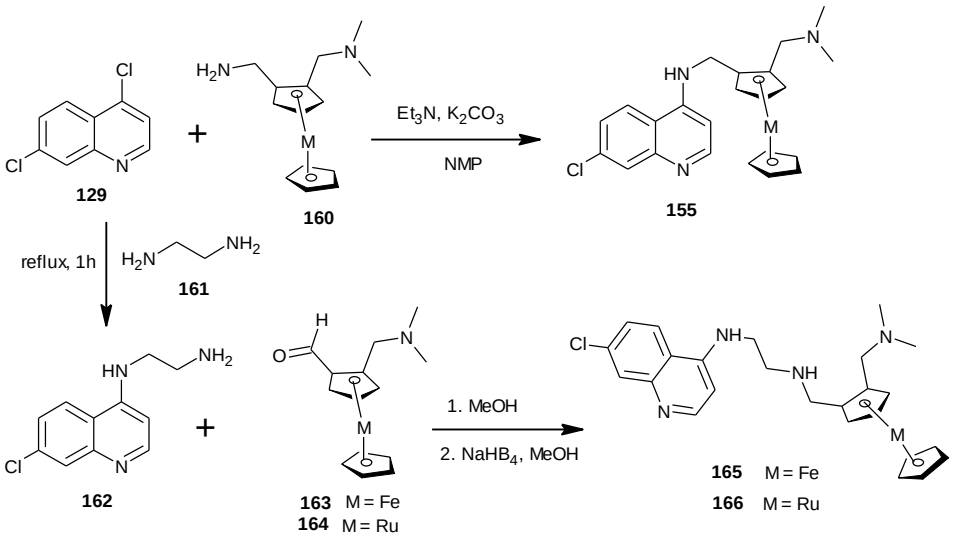

Scheme 15. Synthesis of ferrochloroquine derivatives as potential anti-malarials.

Research on the development of new artemisinin derivatives with improved potency has focused on replacement of the C-10 hydroxyl group in DHA **15** by groups that are not readily susceptible to reduction or hydrolysis.[44-45] Other structural modifications of the lactol ring system have involved derivatization at C-3, C-9, C-11 and C-13 respectively. In addition, compounds containing the peroxide moiety (1,2,4-trioxanes and tetraoxanes) have been used as synthetic scaffolds for the construction of potential novel inhibitors related to artemisinin **14**.[44,61] O'Neill *et al*.[80] anticipated that accumulation of the C-10 ether linked diamino artemisinin analogues, would increase in the parasite food vacuole, thus increasing their anti-plasmodial activity. Their approach involved coupling DHA **15** with 1,4-phenylenedimethanol **167** in the presence of boron trifluoride-diethyl ether ($BF_3.Et_2O$) to afford the alcohol **168**, which was treated with mesyl chloride to obtain the corresponding mesylate **169**. The desired diamino analogues **171** were isolated upon condensation of the mesylate **169** with the appropriate diamino nucleophiles **170** (Scheme 16).

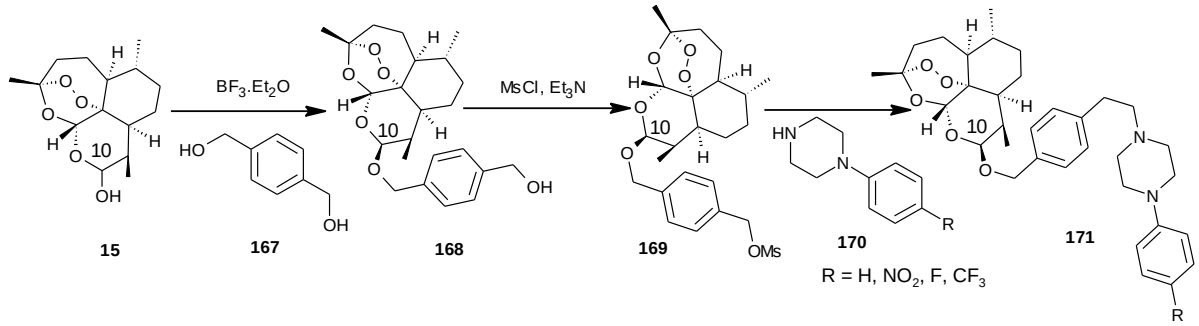

Scheme 16. Synthesis of C-10 ether linked diamino analogues of DHA **15**.

Chemical modification at the C-10 position was also investigated by Beué *et al.*[81] through the synthesis of artemisinin analogues containing a fluorine substituent at the hemiacetyl carbon (C-10) and the α-methylene carbon (C-11) of DHA. The reaction of DHA **15** with the alcohol **172** in the presence of $BF_3.Et_2O$ or TMSCl yielded the flurorinated artemisinin ether **173**. The fluorinated artemisinin alcohol **174** was produced by reacting artemisinin **14** with a molar equivalent of $TMSCF_3$ and *t*-$BAF.3H_2O$ at room temperature for 25 hours, shown in scheme 17. The poor bio-availability and short plasma half-lives of the current artemisinin drugs are due to the susceptibility to hydrolysis of the acetyl group *in vivo*.[45] Thus, the design of C-10 carba-analogues have been investigated by several research groups in the expectation that these compounds would be less prone to hydrolysis and exhibit long half-

lives. Such an approach, reported by O'Neill *et al.*,[82] involved the synthesis of fluorinated carba-analogues of artemisinin **14**, with either an ether or ester linkage (Scheme 18).

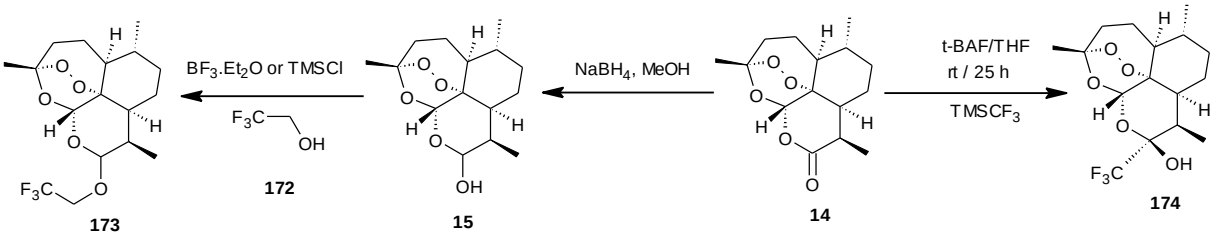

Scheme 17: synthesis of fluorine-substituted artemisinin derivatives.

DHA **15** was coupled with allyltrimethylsilane **175** to yield allyldeoxoartemisinin **176**. Ozonolysis and subsequent reduction with sodium borohydride of the alkene afforded the alcohol **177**, which was either deprotonated and reacted with appropriate substituted benzyl bromides **178** to obtain the ether products **179** or esterified with the corresponding substituted fluorinated acid chlorides **180** to yield the ester analogues **181**.

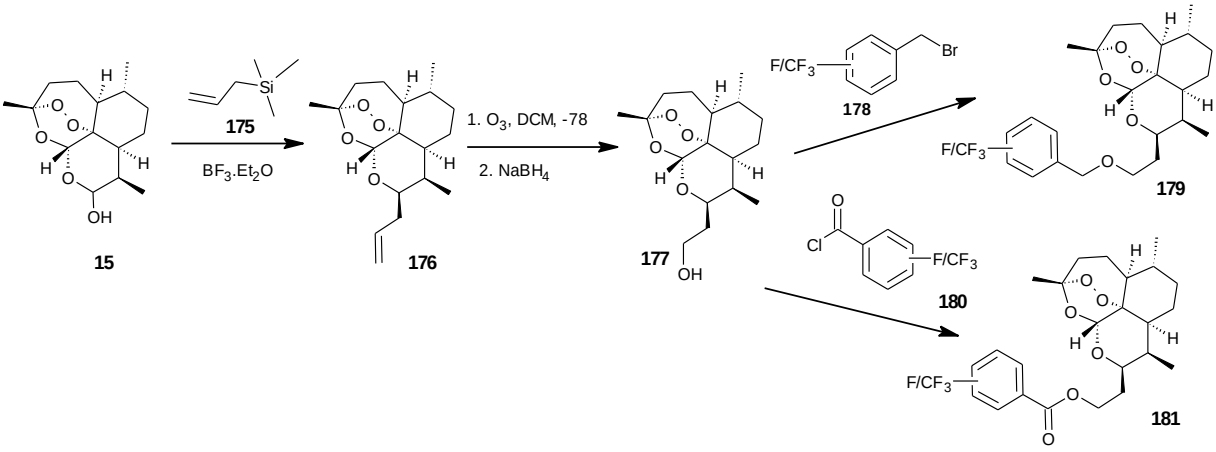

Scheme 18. Synthesis of C-10 carba-analogues of artemisinin **14**.

Yuthavong *et al*.[83] have reported the synthesis of artemisitene **185**, the oxidized form of DHA **15**. The regiospecific transformation of artemisinin **14** to **185** was achieved through a one-pot synthesis involving lithiation to yield the enolate **182**, formation of the phenylselenide bromide **183** and oxidation of which afforded the selenide species **184**. Subsequent elimination of selenoxide gave the desired product **185** as a single isomer (Scheme 19). Michael addition of Grignard reagents to artemisitene **185** furnished the

Michael adducts **187** and **188**, while, reaction of another molecule of artemisitene **185** with the enolate intermediate **186** afforded the dimer **189** (Scheme 20).[83]

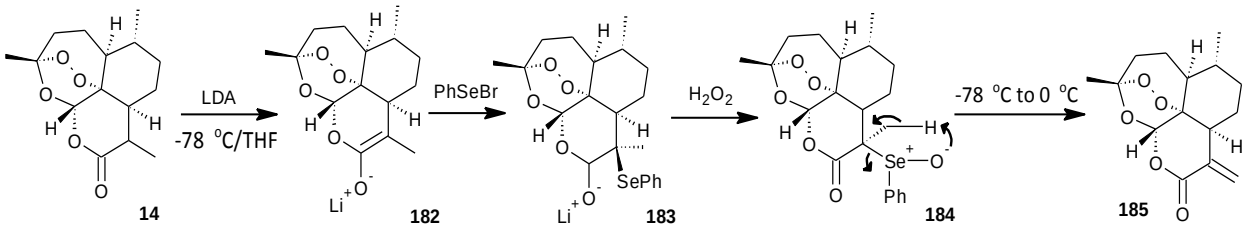

Scheme 19. Synthesis of artemisitene **185**.

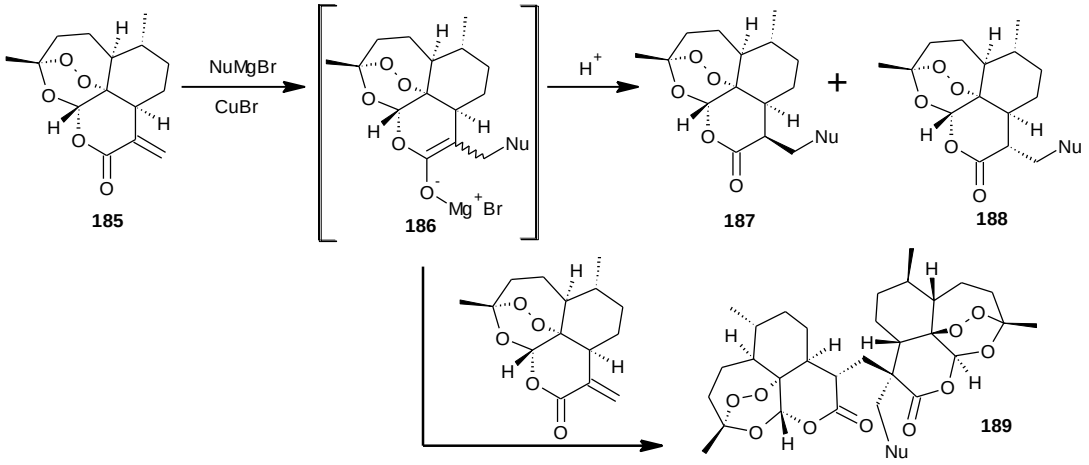

Scheme 20. Michael addition of nucleophiles to artemisitene **185** using Grignard reagents.

The design and synthesis of hybrid molecules as anti-malarial agents has recently been explored and offers a unique approach. These 'dual inhibitors' are envisaged to act against more than one target within the *plasmodium* parasite, thus making them potent against drug-resistant plasmodium strains.[84] Quite recently, N'Da and co-workers described the synthesis and biological activity of artemisinin-quinoline hybrid dimers,[85] and their synthetic strategy is outlined in Scheme 21. Initially, DHA **15** was treated with $BF_3.Et_2O$ and ethyl bromide **190** in DCM to obtain 2-(10β-dihydroartemisinoxy)ethyl bromide **191**, which was subsequently reacted with various aminoquinolines **192-197** in DMF at between 70 °C and 80 °C for 4 to 6 hours to yield the desired artemisinin-quinoline hybrids **198-203**.

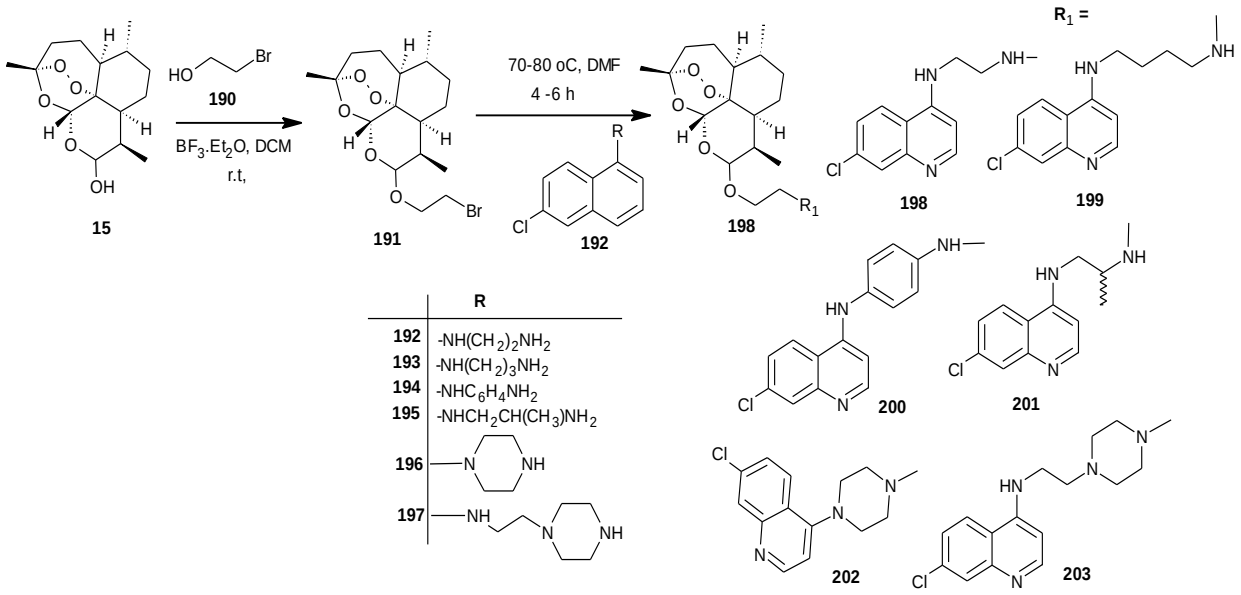

Scheme 21. Synthesis of artemisinin-quinoline hybrid molecules.

1.6.2. Natural products

Natural products derived from plants, bacteria and marine organisms are crucial sources for the discovery of lead compounds targeting various diseases and also offer novel scaffolds for the synthesis of analogues with improved potency and better pharmacokinetic profiles.[41,86] Importantly, the two classes of current anti-malarial chemo-therapeutic agents *i.e.* quinolines and artemisinins, originate from plants. Natural products with anti-malarial activity that have been isolated from various plants and organisms include:- i) alkaloids such as naphthylisoquinolines, indoles and manzamines; ii) terpenes including diterpenes and sesquiterpenes; iii) flavonoids; iv) chalcones; and v) coumarins.[86] Representative examples of compounds belonging to these classes are illustrated in Figure 15.

The extraction and purification of natural products is often challenging and, consequently, poor yields are frequently obtained. New synthetic methodologies for the construction of novel compounds are continually being reported.[86] The alkaloid febrifugine **210** and its stereoisomer, isofebrifugine **211**, are present in traditional Chinese medicines used to treat fevers associated with malaria. These isomers have been isolated from the root of *Dichroa febriguga* and exhibit potent anti-plasmodial activity, but toxic side effects have limited their use.[44,86] The synthesis of compounds **210** and **211** has been reported and chemical modifications have afforded potentially less toxic analogues. Scheme 22 outlines the asymmetric synthesis of the stereoisomers **210** and **211** reported by Takeuchi *et al*.[87]

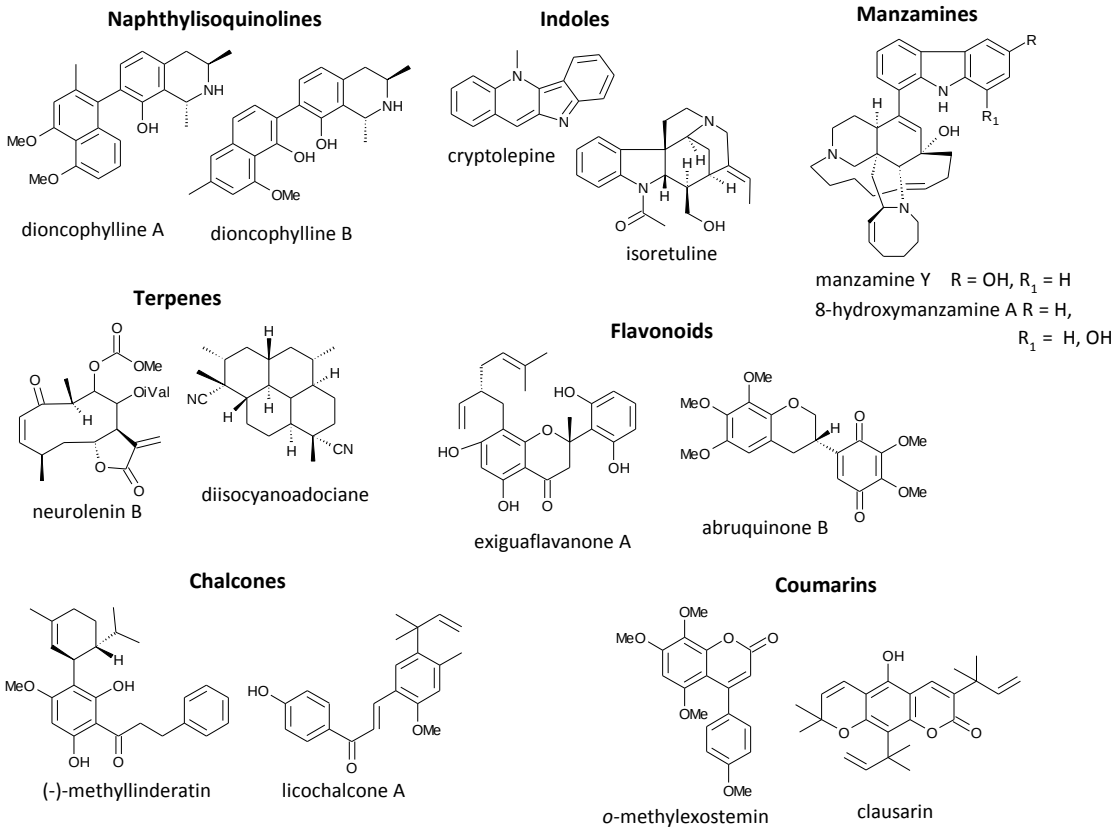

Figure 15. Anti-malarial natural products.

The approach involves reductive dynamic optical resolution of racemic-3-piperidones **204** using baker's yeast to obtain the chiral ketone **205** and alcohol **206**. The alcohol **206** is converted *via* intramolecular bromoetherification with NBS to give the cyclic ether **207**, dehydrobromination and bromoetherification of which affords a diastereomeric mixture of the methoxy intermediate **208**. The quinazolinone **209** is produced by deacetalization of intermediate **208** and subsequent coupling with 4(*3H*)-quinazolinone. Hydrogenolysis of **209** then affords isofebrifugine **d-210**, which is transformed upon heating to its isomer ***d*-211**.

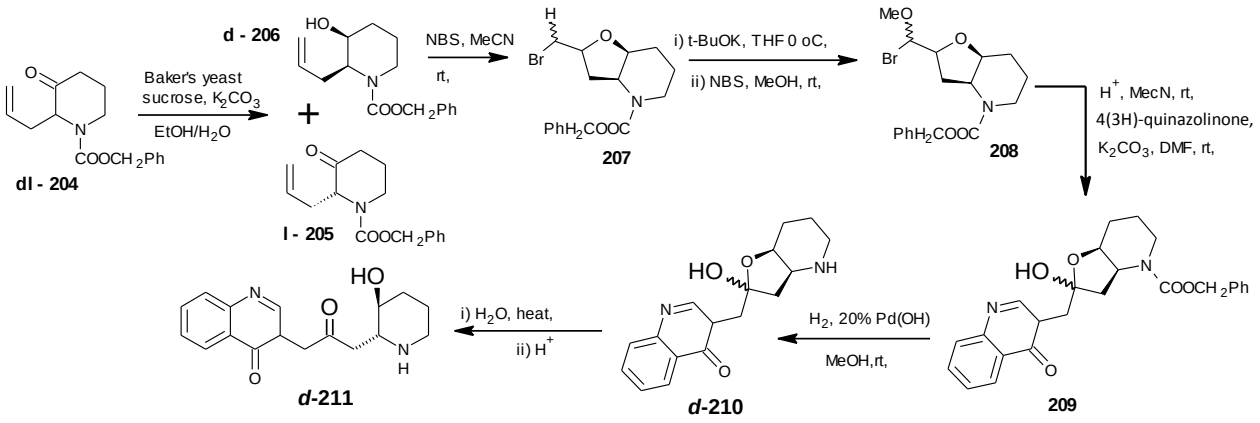

Scheme 22. Asymmetric synthesis of febrifugine and isofebrifugine.

In addition to isolating several novel naphthylisoquinoline alkaloids and exploring their anti-plasmodial activity, Bringmann *et al.*[88] synthesized a fluorescence-labelled analogue **219** of the natural product dioncophylline A **212**. The attachment of a fluorescent moiety allows for the detection of dioncophylline A in malaria parasite-infected host erythrocytes. Their synthetic approach is outlined in Scheme 23. Bromination and *O*- and *N*-benzyl protection of dioncophylline A **212** afforded the *N*,*O*-dibenzylated -5-bromodioncophylline A **213**, which was lithiated *in situ* and formylated with DMF to furnish the aldehyde **214**; subsequent deprotection produced the phenol **215**. Coupling of the sulfonyl amine **218** *via* reductive amination with compound **215** yielded the desired fluorescence-labelled analogue **219**.

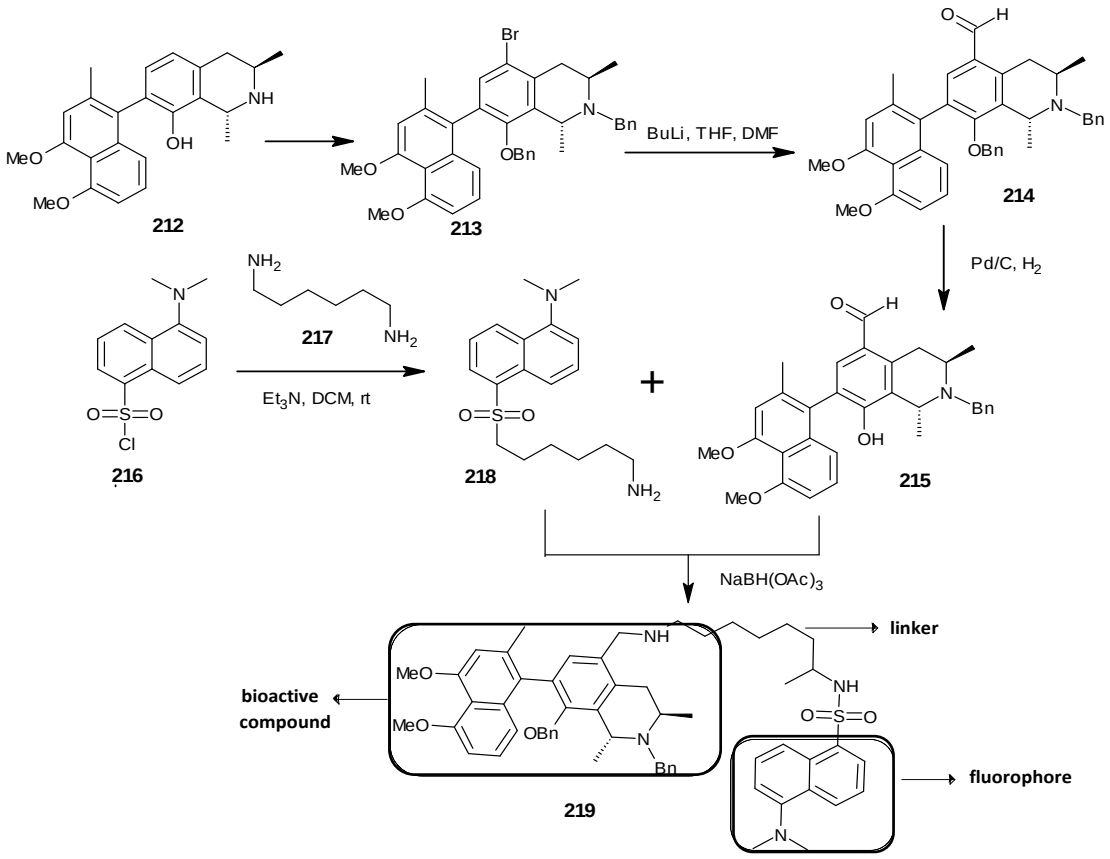

Scheme 23. Synthesis of fluorescence-labelled dioncophylline A analogue.

1.6.3. Rational drug design: inhibition of new biological targets

Advances in molecular biology and the development of sophisticated computational methods have led to the rational approach to drug design.[68] This innovative approach depends on the identification of pathogen enzymes as biological targets and the subsequent development of ligands that bind within the active-site and/or alter the biological function

of the target enzyme.[68] Knowledge of the 3D-structure of the target enzyme, including a detailed understanding of the ligand-receptor binding site, may be obtained using x-ray crystallography, NMR spectroscopy and computer-aided molecular modelling techniques. Other approaches which are often integrated into the rational drug design process include;- virtual screening, synthetic combinatorial chemistry, high-throughput screening, docking, quantitative structure-activity relationships (QSAR) and quantitative structure-property relationships (QSPR).[68] The rational design and optimization of potential inhibitors typically involves *in silico* binding affinity and *in vitro* biological activity studies as well as studies of the pharmacokinetic properties of the ligand of interest.[68] Biological pathways and enzymes in *plasmodium* species that have recently been targeted for the discovery of new anti-malarial drugs are summarised in Table 1.[67,89] One such target, which has been identified recently and which is the focus of this synthetic study, 1-deoxy-D-xylulose-5-phosphate reductoisomerase (DXR) – an enzyme which functions in the non-mevalonate pathway within the apicoplast organelle of *plasmodium* parasites.[67,89]

Table 1. *P. falciparum* targets for novel drug design.[89]

Target	Enzyme/process	Inhibitor
Membrane biosynthesis	Phospholipid synthesis (choline transporter)	G-25
Parasite proteases	Plasmepsins, falsipains	Leupeptin, pepstatin
Shikimate pathway	5-enolpyruvyl shikimate-3-phosphate synthase	Glyphosate
Apicoplast	DNA synthesis (DNA gyrase)	Quinolones
	Type II fatty acid biosynthesis (Fab H, Fab I)	Thiolactomycin, triclosan
Mitochondrial system	Cytochrome C oxidoreductase	Atavoquone
Redox system	Thioredoxin reductase	5,8-Dihydroxy-1,4-naphthoquinone
	Gamma-GCS	Buthionine sulfoximine
Pyrimidine metabolism	Thymidylate synthase	5-Fluoroorotate
Isoprenoid biosynthesis	1-deoxy-D-xylulose-5- phosphate reductoisomerase	Fosmidomycin
Cyclin-dependent protein kinase	Pfmrk	thiophene sulfonamide

1.7. 1-Deoxy-D-xylulose-5-phosphate reductoisomerase (DXR) as a target for anti-malarial drug design

1.7.1. Isoprenoid biosynthesis *via* the mevalonate-independent pathway

Isoprenoids are derived from the five-carbon isomeric isoprene units isopentenyl pyrophosphate (IPP) and dimethylallyl pyrophosphate (DMAPP), and form a large and structurally diverse class of natural products.[90] Currently, more than 30 000 isoprenoids have been discovered and these compounds are involved in carrying out various essential biological functions in all living organisms including:- i) electron transport processes (ubiquinone); ii) signal transduction (prenylated proteins); iii) growth regulation (steroid hormones and cytokinins) and; iv) membrane modulators (sterols).[91] The precursors for isoprenoid biosynthesis, IPP and DMAPP, are constructed *via* two different biosynthetic routes. In mammals, plants, fungi and some bacteria, the precursors are synthesized by the mevalonate (MVA) pathway, discovered in the 1950's and summarized in Figure 16.[90] This biosynthetic route involves Claisen condensation of two molecules of acetyl-CoA **220** to form acetoacetyl-CoA **221**, which further condenses with another molecule of acetyl-CoA producing 3-hydroxy-3-methylglutaryl-CoA (HMG-CoA) **222**. Two successive nicotinamide adenine dinucleotide phosphate (NADPH)-dependent reductions of HMG-CoA **222** produce MVA **223**, which is phosphorylated twice to yield mevalonic-5-diphosphate (MVA-PP) **225**. Subsequent decarboxylation of MVA-PP gives IPP **226**, which isomerizes *via* a 1,3-proton shift to give DMAPP **227**.[92]

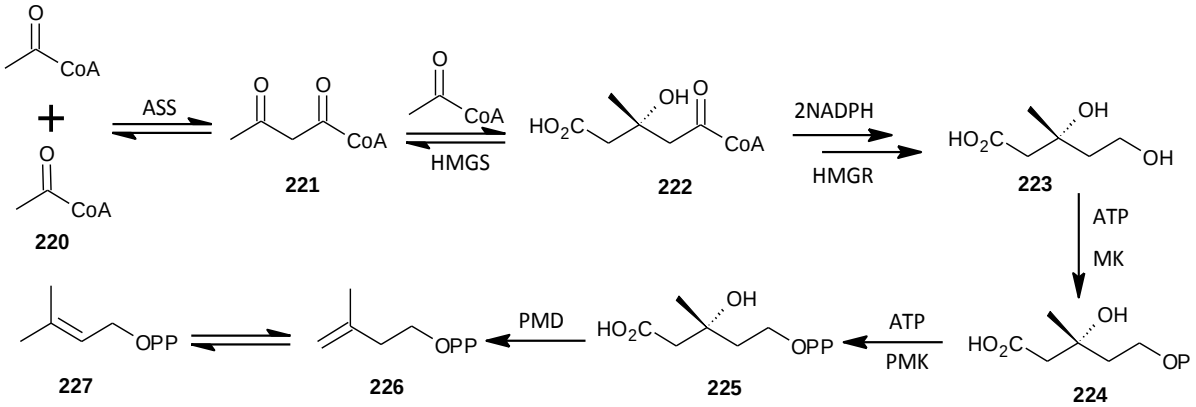

AAS = acetoacetyl-CoA synthase; HMGS = HMG-CoA synthase; HMGR = HMG-CoA reductase; MK = mevalonate kinase; PMK = phosphomevalonate kinase; PMD = mevalonate diphosphate decarboxylase

Figure 16. The mevalonate (MVA) pathway for isoprenoid biosynthesis.[92]

The second pathway, termed the non-mevalonate or DOXP/MEP pathway, was discovered in 1993 and occurs in most eubacteria as well as plastids of algae and higher plants.[91] Both pathways operate in higher plants, leading to cytosolic isoprenoids (sterols) *via* the MVA pathway and plastidic isoprenoids (carotenoids) are synthesized through the DOXP/MEP pathway. The DOXP/MEP pathway consists of the seven enzymatically catalysed steps summarized in Figure 17.[91,93]

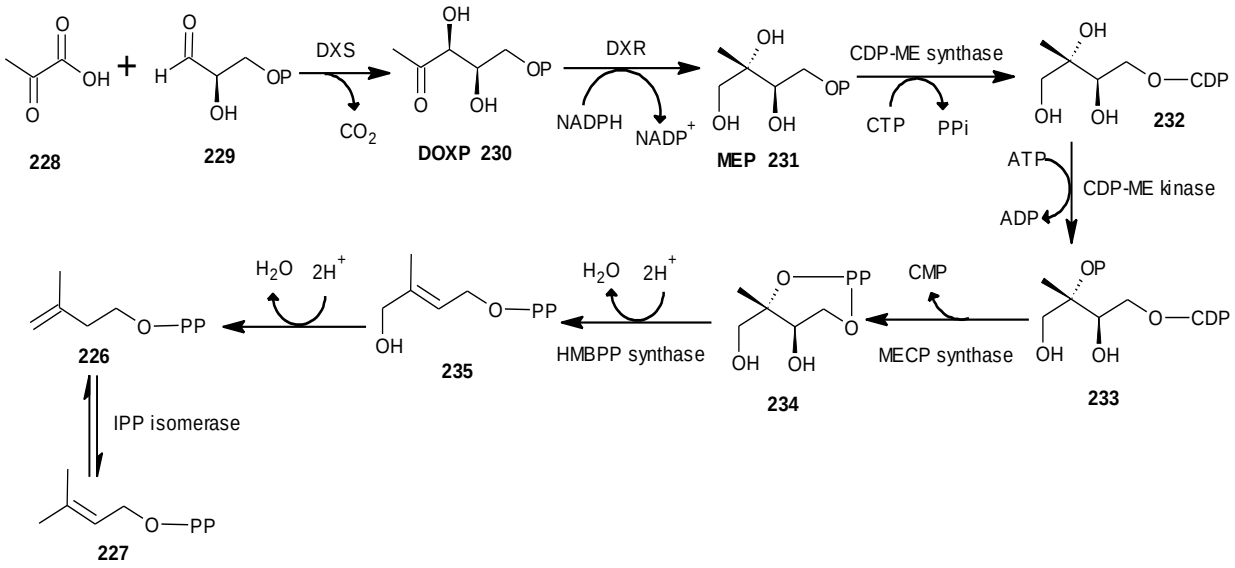

Figure 17. The reaction steps of the DOXP/MEP pathway.[93]

The initial step, catalysed by the thiamine diphosphate-dependent DXP synthase (DXS) involves the condensation of pyruvate **228** and glyceraldehyde-3-phosphate **229** to form 1-deoxy-D-xylulose 5-phosphate (DOXP) **230**. In the next step, DOXP reductoisomerase (DXR) catalyses the conversion of DOXP **230** into 2-C-methyl-D-erythritol 4-phosphate (MEP) **231** through an intramolecular rearrangement and NAPDH-dependent reduction step.[91] Subsequent cytidylylation of MEP **231** affords 4-diphosphocytidyl-2-C-methyl-D-erythritol (CDP-ME) **232**, which is phosphorylated at the C-2 hydroxyl group by CDP-ME kinase to yield 4-diphosphocytidyl-2-C-methyl-D-erythritol-2-phosphate (CDP-MEP) **233**. In the next step, CDP-MEP **233** is transformed through cyclization into 2-C-methyl-D-erythritol 2,4-cyclodiphosphate (MEcPP) **234** by MEcPP synthase.[91] The reduction and dehydration of MEcPP **234** by 1-hydroxy-2-methyl-2-(*E*)-butenyl-4-diphosphate (HMBPP) synthase affords HMBPP **235** which, upon further reduction and dehydration catalysed by HMBPP reductase,

produces IPP **226**, which is then isomerised by isopentenyl diphosphate (IPP) isomerise to DMAPP **277**.[91,93]

A large number of human bacterial pathogens such as *Escherichia coli*, *Mycobacterium tuberculosis*, *Helicobacter pylori* and the malaria *plasmodium* species, utilize the DOXP/MEP pathway exclusively for the biosynthesis of isoprenoids.[91,93] With regard to *P. falciparum*, enzymes within this pathway have thus been identified as targets for the rational design of novel anti-malarial drugs. Importantly, the absence of functionally equivalent enzymes in the human host has made the DOXP/MEP pathway an attractive target for therapeutic intervention.[93,94] A key enzyme in the pathway, 1-deoxy-D-xylulose-5-phosphate reductoisomerase (DXR), has been validated as a suitable target for a new class of anti-malarial drugs as its catalytic activity is specifically inhibited by the antibiotic fosmidomycin **236** and its acetyl derivative FR900098 **237** (Figure 18).[93,95]

fosmidomycin 236

FR900098 237

Figure 18. Inhibitors of the DXR enzyme.

1.7.2. Catalytic mechanism of DOXP reductoisomerase (DXR)

The catalytic mechanism for the conversion of 1-deoxy-D-xylulose-5-phosphate (DOXP) **230** to 2-*C*-methyl-D-erythritol-4-phosphate (MEP) **231** by 1-deoxy-D-xylulose-5-phosphate reductoisomerase (DXR) has been extensively studied in recent years.[91,96-97] This transformation is the committed step in the non-mevalonate pathway and involves the formation of the intermediate 2-*C*-methyl-D-erythrose-4-phosphate **238**, apparently *via* an intramolecular rearrangement followed by an NADPH-dependent reduction step. The presence of one of the divalent metal cations Co^{2+}, Mn^{2+} or Mg^{2+} is essential for enzyme function.[93,97] Although conclusive evidence is yet to the provided, three different mechanisms for the intramolecular rearrangement step **230 - 231** (Figure 17) have been proposed. These are: - i) retro-aldol/aldol rearrangement; ii) α-ketol rearrangement; and iii) 1,2-hydride/methyl shift type mechanism, as depicted in Figure 19.[97] The retro-aldol/aldol mechanism (Figure 19a) involves the deprotonation of the C-4 hydroxy group of DOXP **230**,

followed by C-3 and C-4 bond cleavage to give the enol/enolate of 3-hydroxyacetone **239** and glycoaldehyde-3-phosphate **240**. The recombination of these two moieties *via* an aldol addition reaction generates a new C-C bond between carbon atoms derived from C-2 and C-4 of **230** to furnish intermediate **238**.[93,97] The α-ketol rearrangement mechanism (Figure 19b) involves oxidation of the C-3 hydroxy group of DOXP **230** to the ketone, concomitant with migration of the 1-hydroxy-2-phosphoethyl moiety to the ketone C-2 to give the intermediate **238**.[97] Support for such a reaction mechanism is provided by acetohydroxy acid isomeroreductase catalysed reaction enzyme, involved in the biosynthetic pathway of the amino acids isoleucine, valine and leucine.[91,98] The third mechanism (Figure 19c) proposed by Argyrou *et al.*[97] involves a 1,2-hydride shift of the C-3 proton to the ketone C-2 carbonyl group of DOXP **230**, with a sequential 1,2-methyl shift to generate the intermediate **238**. Subsequent reduction of the intermediate **238** with NADPH yields MEP **231**.

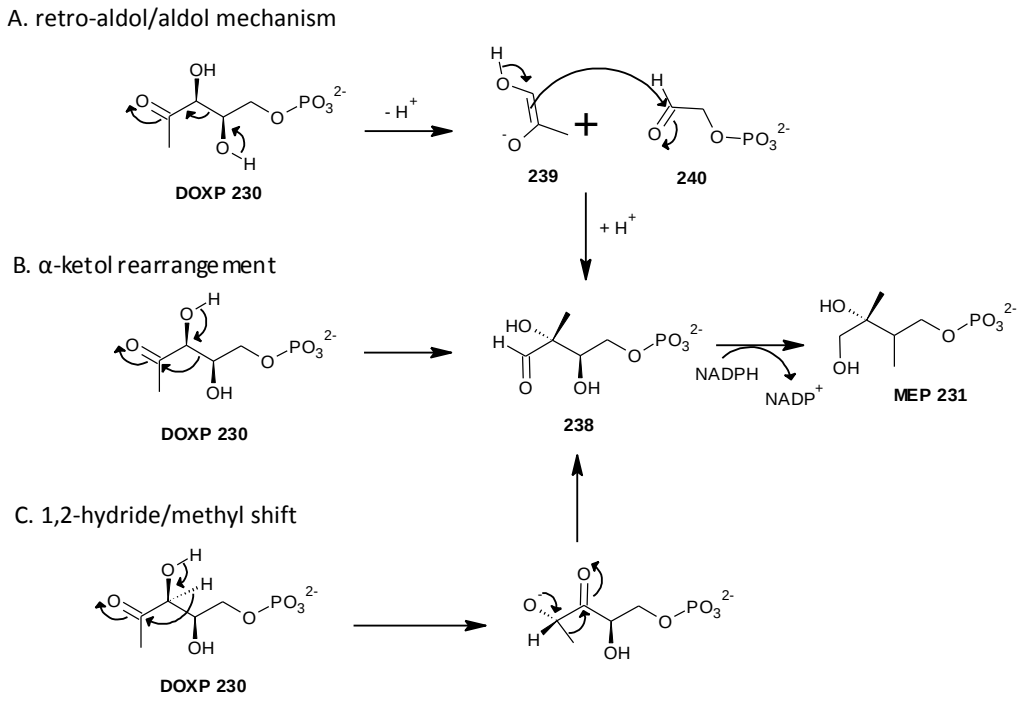

Figure 19. Proposed mechanisms for the DXR-catalysed conversion of DOXP **230** to MEP **231**.

The stereochemistry of the DXR catalysed rearrangement and NADPH-dependent reduction steps have been investigated using recombinant DXR enzymes from *Synechocystis*, *E. coli* and *M. tuberculosis*.[97,99-100] These studies indicated that the NADPH co-factor and the

migrating C-4 moiety are located on opposite faces of the metal-DOXP complex. The migration of the C-4 moiety to C-2 on the *re*-face of the intermediate **238** is followed by attack of the C-4 *pro-S* hyride from NADPH, as depicted in Figure 20. In addition, it was established that the C-1 *pro-S* hydrogen of MEP **231** is generated from the C-3 hydrogen of DOXP **230**, thus classifying DXR as a class B dehydrogenase enzyme.[99-100]

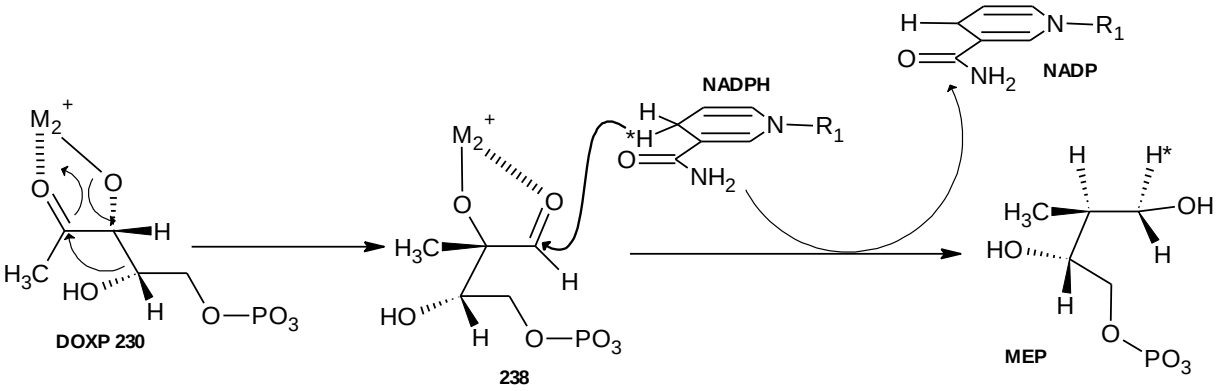

Figure 20. Stereochemical features of DXR-catalysed conversion of DOXP to MEP. H^* = NADPH pro-S hydrogen transferred to form MEP.[99-100]

1.7.3. Molecular structure of DXR

Various research groups have successfully solved and published X-ray crystallographic structures of the DXR enzyme from a variety of organisms, including:- *E. coli*, *M. tuberculosis, Z. mobilis* and, more recently, *T. maritima* and *Y. pestis*.[91,101-109] However, a well-defined crystal structure of *P. falciparum* DXR (*Pf*DXR) has yet to be published, although two homology models generated using comparative protein modelling, have been reported by Singh *et al.* and by Goble *et al.*, respectively.[110-111] The generation of these structures of the DXR enzyme has revealed important key features including:- i) the structure and conformational dynamics of DXR; ii) the ligand and metal binding residues of the catalytic site; and iii) kinetic parameters of DXR.

1.7.3.1. Structure and conformational dynamics of DXR

Analyses and evaluation of the architecture of *Ec*DXR from the published crystal structures reveal that DXR exists as an 86 kDa homo-dimer, with each monomeric unit comprising of three distinct domains arranged in a pronounced cleft-like or V-shaped structure, as

illustrated in Figure 21.[101-105] The three domains are:- i) an N-terminal binding domain (residues 1-150) consisting of several parallel-stranded β-sheets and α-helices that binds the NADPH co-factor; ii) a central or connective domain (residues 150-285) consisting of the active site and the flexible or catalytic loop; and iii) the C-terminal, four-helix bundle domain (residues 312-398), connected to the catalytic domain and providing structural support for the active site.[101,103,105] Structural analyses of the published apo-enzyme showed significant mobility of the catalytic and C-terminal domain of the three, protein conformers present in the asymmetric unit of the crystal.[101] In addition, the apparent flexibility seen for the catalytic loop suggests that DXR is structurally flexible and undergoes conformational change upon substrate binding, with the catalytic loop folding over the active site as a 'lid', thus shielding the active site from the solvent environment.[101,103-105] In the *Pf*DXR homology model structure, Goble *et al.*[111] established structural similarities between *Pf*DXR and EcDXR.

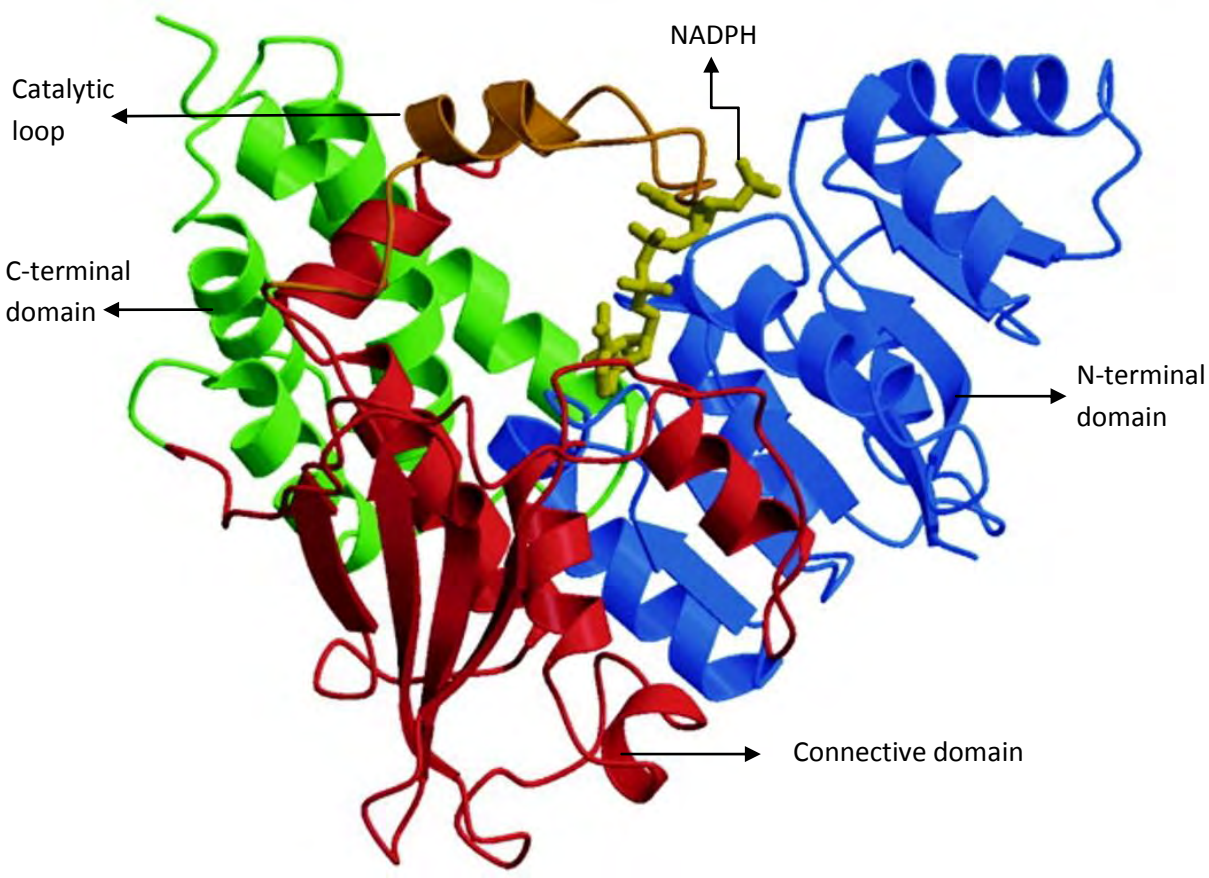

Figure 21. Ribbon representation of the *Ec*DXR monomer showing the three domains, the NADPH co-factor, the N-terminal domain (blue); the connective domain (red); the catalytic loop (ochre); C-terminal four-helix bundle domain; and NADPH (yellow). Adapted from the structure published by Reuter *et al.*[101]

1.7.3.2. DXR catalytic site: ligand-binding residues and binding of co-factors

X-ray crystal structures of DXR complexed with combinations of the substrate DOXP **230**, the inhibitor fosmidomycin **236** and the co-factors, NADPH and the metal cations (Mn^{2+}, Mg^{2+}), have permitted identification of the active-site residues involved in their binding.[102-105] These structures reveal that the DXR active-site is comprised of three regions:- i) the phosphonate binding pocket; ii) the divalent-metal cation binding site; and iii) a relatively narrow hydrophobic region accommodating the carbon backbone of the substrate or inhibitor.[103,105] A crystal structure of *Ec*DXR determined by Mac Sweeney *et al.*[105] reveals the phosphonate moiety of fosmidomycin **236** occupying the positively charged phosphonate binding pocket and interacting with active site residues Ser186, Gly187, Ser222, Met225, Asn227, Lys228 and Ile250 (Figure 22), with its carbon backbone of **236** aligned parallel to the Trp212 β-indole ring ca. 4 Å away; the hydroxamate moiety of the inhibitor adopts a planar configuration and interacts with the metal *via* a bidentate chelation.[105]

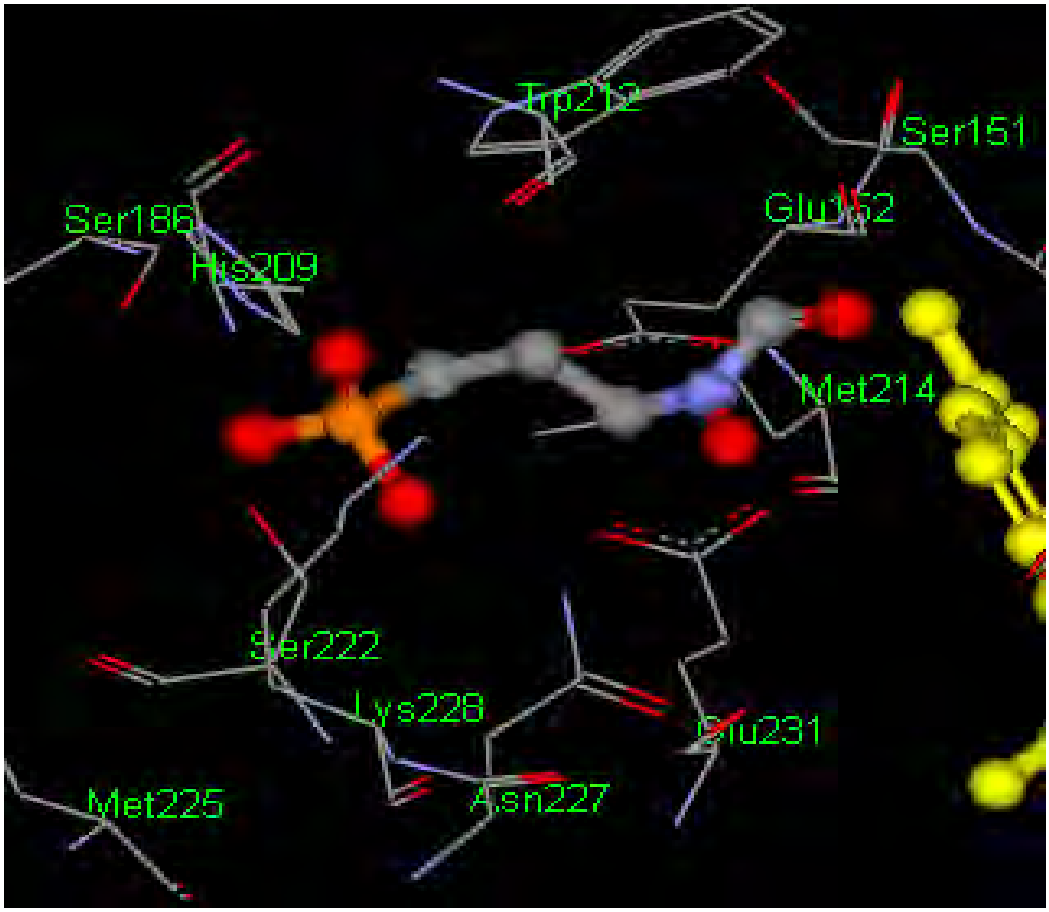

Figure 22. The *Ec*DXR active site with fosmidomycin **236** interacting with binding residues. Fosmidomycin is shown in ball and stick format (coloured by element), NADPH in ball and stick format (coloured yellow) and amino acid residues shown in wireframe format (coloured by element). Adapted from EcDXR PDB code 1Q0L[105]

The structure of *Ec*DXR complexed with DOXP **230** and NADPH reveal similar binding interactions, with the negatively-charged phosphonate moiety of DOXP interacting with residues Ser186, Ser222, Asn227 and Lys228.[105] The carbon backbone of the molecule again aligns parallel to the β-indole ring of Trp212 whilst:- the C-2 carbonyl oxygen interacts with Glu152 and Ser151; the C-3 hydroxyl group interacts with Lys125 and Glu231; and the C-4 hydroxyl group binds to Glu 152, Asn227 and Lys228, respectively. Also, NADPH is shown to interact with several residues in the N-terminal domain including Gly11, Ser12, Gly14, Ala35, Gly36 and Ala105.[105] Yajima *et al.*[103] observed that the binding of NADPH to *Ec*DXR structure results in stabilization of the active site, with a more ordered flexible loop region.[103] Structural analyses of *Ec*DXR complexed with fosmidomycin **230** and NADPH show the close binding proximity of the co-factor to the substrate **230**, as shown is Figure 23.[105]

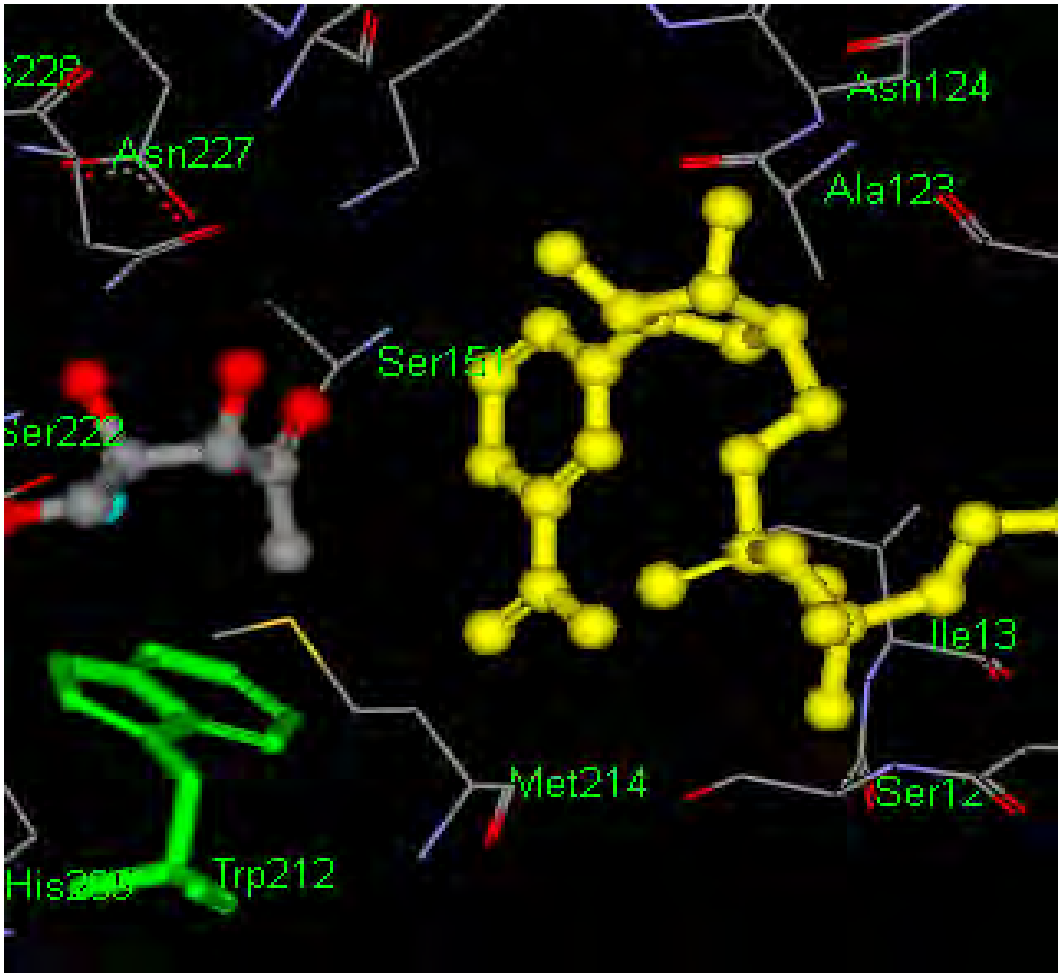

Figure 23. The *Ec*DXR active site with substrate DOXP **230** and NADPH interacting with specific binding residues. The close proximity of NADPH (shown in ball and stick format and coloured yellow) to DOXP (shown in ball and stick format and coloured by element) is essential for catalytic activity. Amino acid residue Trp212 is represented in stick format (coloured green). Adapted from *Ec*DXR PDB code 1Q0Q.[105]

The position of NADPH relative to the DOXP **230** in the active site is significant for the catalytic activity of DXR, as the C-4 *pro-S* hydrogen of NADPH is transferred to C-2 to form MEP.[99] NADPH is considered to interact with active-site residues before the substrate DOXP (or the inhibitor) binds and induces folding of the flexible loop over the active site. Several residues have been identified as essential for the correct positioning of DOXP **230** within the DXR catalytic site. These include residues His153, Gly185, Ser186, His209, Trp212, Met214,Glu231 and His257.[102,104,112] The two residues Ser186 and His209, which form part of the flexible loop, have been implicated in tight DXR-NADPH-ligand binding complexes, whilst Gly185 and Met214 are described as 'hinges' for the folding-mechanism of the catalytic loop.[105,113] The position of the divalent metal cation in *Mt*DXR was established by Henriksson *et al.*[107] and in *Ec*DXR by Steinbacher *et al*.[104] The metal cation is assumed to anchor the substrate in the desired conformation required for the rearrangement step and to stabilize the intermediate **238** through electrostatic interactions.[97,107] The C-2 carbonyl oxygen and C-3 hydroxyl group of DOXP **230** has been shown to coordinate to the metal cation; a water molecule and the active-site residues Asp150, Glu152 and Glu231 have also been identified as metal-chelating groups, resulting in the distorted octahedral coordination complex shown in Figure 24.[105,107] The interaction of fosmidomycin **236** with the metal cation is similar and involves a water molecule and the residues Asp151, Glu153 and Glu222 in *Mt*DXR, and residues Asp150, Glu152 and Glu231 in *Ec*DXR to form an octahedral coordination sphere (Figure 24).[103,105,107]

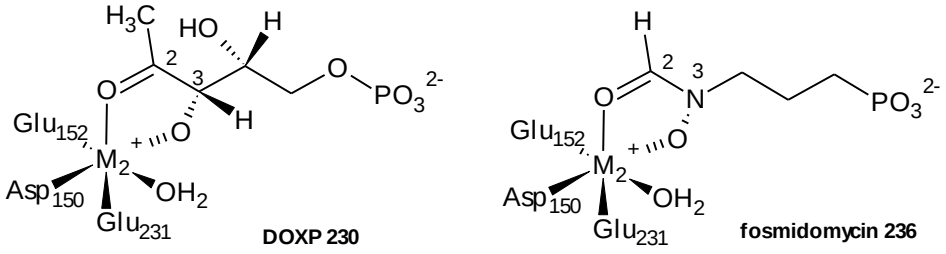

Figure 24. Chelation of the divalent metal cation by DOXP **230** and fosmidomycin **236**.[105,107]

1.7.3.3. Kinetic parameters of DXR

The kinetic parameters for DXR enzymes isolated from several organisms have been studied and quantified, and are summarised in Table 2.[114] The catalytic activity of DXR is optimal

within a pH range of 7 - 8.5 and temperature range of 50-60 ^{o}C. Studies have indicated DXR to have a preference for NADPH as oppose to NADH as co-factor and a higher affinity for Mg^{2+} over Mn^{2+} *in vivo*.[97,114] The Michaelis constant (K_m) describes the binding affinity of the substrate for the enzyme and quantifies the concentration of substrate at which the reaction occurs at half its maximum rate; whilst the catalytic constant (K_{cat}) measures the catalytic efficiency of the enzyme.[92]

Table 2. Kinetic parameters[a] for DXR from several organisms. [114]

DXR enzyme	K_m (µM)	K_{cat} (1/[S])
E. coli	3 – 250	29 – 38
Z. mobilis	300	14
S. coelicolor	190	19.2
M. tuberculosis	4 – 240	2.1 – 5.3
A. Thaliana	132	4.4
T. maritima	40 000	0.29

[a]Parameters determined with substrate DOXP, NADPH and divalent metals Mg^{2+}, Mn^{2+} or Co^{2+}

1.7.4. The design of DXR inhibitors: fosmidomycin and DOXP analogues

1-Deoxy-D-xylulose-5-phosphate reductoisomerase (DXR) is an attractive target for the rational design of new anti-malarial chemotherapeutic drugs due to the fact that:- i) the vital DOXP/MEP pathway for isoprenoid biosynthesis is present in *P. falciparum*, the most pathogenic species; and ii) neither DXR nor functionally homologous enzymes are present in humans, thus precluding undesirable side-effects during chemotherapy.[91,93] Also significant was the discovery of fosmidomycin **236**, an antibiotic isolated from *Streptomyces lavendulae*, as a specific and competitive inhibitor of DXR.[95,115] Jomaa *et al.*[116] established the anti-malarial activity of fosmidomycin **236** and its acetyl derivative FR900098 **237**, both of which inhibited the rodent malaria parasite *P. vinckei* in a dose-dependent manner. *In vivo* studies showed that fosmidomycin **236** was non-toxic and highly efficient in the treatment of patients with acute uncomplicated *P. falciparum* malaria, albeit with a high recrudescence rate. Unfortunately, the poor pharmacological properties exhibited by fosmidomycin **236** and FR900098 **237**, such as low bioavailability and short plasma half-life, due to its high hydrophilicity, have limited their use as therapeutic drugs.[91,95]

However, the potent and specific DXR inhibitory activity of compounds **236** and **237** has encouraged structure-activity relationship studies and synthetic approaches towards the design of analogues as potential DXR inhibitors. The availability of DXR crystal structures (discussed above) with bound substrate **230** and fosmidomycin **236**, have assisted in identifying the negatively charged hydroxamate functionality and phosphonate moiety as critical structural groups required for antimalarial activity.[103,105] The C-2 carbonyl oxygen and C-3 hydroxyl group in DOXP **230** and the hydroxamate functional group in fosmidomycin are involved in divalent-metal cation chelation; whilst the phosphonate moiety occupies the phosphonate binding site. In addition, Mac Sweeney *et al*.[105] observed that a defined distance (C-spacer) between these two polar functional groups is necessary for potent antimalarial activity. Synthetic strategies towards new DXR inhibitors have thus focused on:- i) the introduction of substituents in the C-backbone of DOXP **230** and fosmidomycin **236**; ii) functionalization of the phosphonate moiety; and iii) modification of the hydroxamate group.

In recent years, various fosmidomycin analogues based on modification of the phosphonate group (Figure 25), have been synthesised and evaluated for their anti-malarial activities. With the aim of improving the bioavailability, prodrugs of fosmidomycin **236** and FR900098 **237**, the phosphodiaryl **241**, acyloxyalkyl ester **242** and alkyoxycarbonyloxyethyl **243** analogues, showed a two-fold increase in anti-malarial efficacy in comparison to fosmidomycin **236** after oral administration in mice infected with *P. vinckei*, although the ester linkage is prone to hydrolysis *in vivo*.[117-119] In other studies, Yajima *et al.*[120] reported the synthesis of the bi-phosphonates **244** and **245** which exhibited inhibitory activity against *Ec*DXR with IC_{50} values of 4 and 7 µM respectively; and Woo *et al.*[121] designed fosmidomycin analogues by replacing the phosphonate group with a phosphate (**246-247**), carboxylate (**248**) and sulfamate (**249**) moiety. The biological activity of these novel compounds against recombinant *Synechocystis sp.* DXR showed that the phosphate **246** and its acetyl analogue **247** exhibited greater potency than fosmidomycin **236**, but subsequent cleavage by phosphatases resulted in inactivation.[121] Recently, a coordination-structure based approach was used by Song *et al.*[122] to develop the lipophilic DXR inhibitors **250** and with moderate (IC_{50} of 4.5 and 1.4 µM) anti-inhibitory activity.

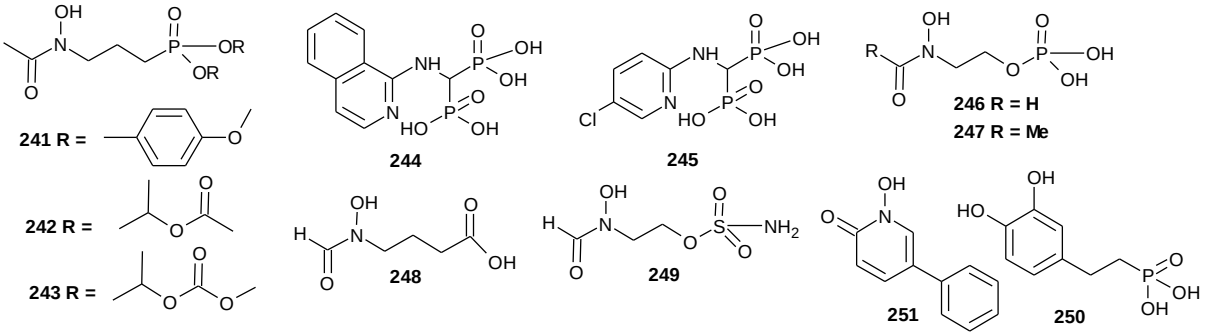

Figure 25. Fosmidomycin analogues, based on modification of the phosphonate moiety, as DXR inhibitors.

Analogues of fosmidomycin **236** and FR900098 **237**, in which the C-spacer between the phosphonate and hydroxamate moieties is functionalized, have been synthesised and their DXR activity evaluated (Figure 26). Van Calenbergh *et al.*[123-126] have synthesised:- i) α,β-unsaturated α-aryl-substituted analogues **252-254** of FR900098 **237**; ii) α-aryl-substituted fosmidomycin analogues **255-258**; iii) conformationally-restricted cyclopropyl analogues **259** and **260**; and, recently, iv) the α-halogenated analogue **261**.[123-126] *In vitro*, the anti-malarial activity of the analogues **255-258** and **261** analogues was comparable with that of fosmidomycin **236**; whilst analogues **252-254** and **259-260** exhibited low to zero anti-malarial activity.

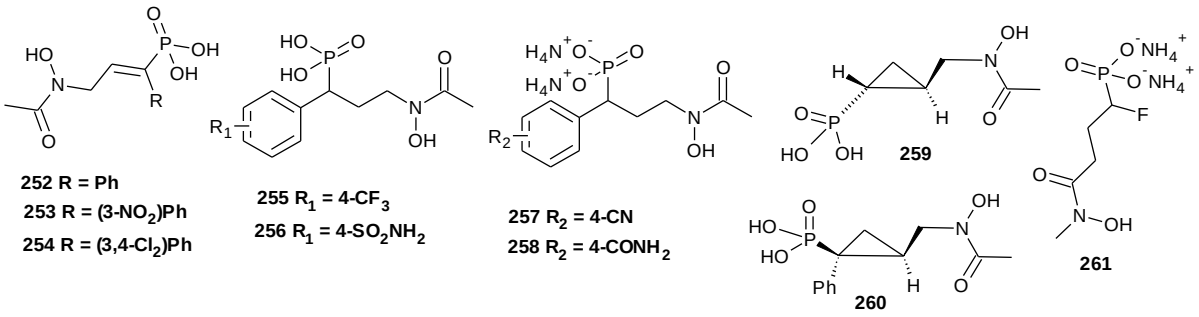

Figure 26. Fosmidomycin analogues, based on the functionalization of the C-spacer, as DXR inhibitors.

Structural studies of DXR have suggested that variation in the length of the C-spacer would decrease the binding affinity of potential inhibitors in the DXR active site, leading to reduced activity.[105] Interestingly, other studies have indicated the presence of a hydrophobic binding pocket beyond the phosphonate-moiety binding site and also a hydrophobic pocket within the active-site, located between the C-backbone α-position and the phosphonate binding

region.[127-129] These additional binding sites may be exploited and direct the synthesis of novel compounds with better DXR inhibitory activity. Structural modification of the metal-binding hydroxamate moiety has also been explored. Mercklé *et al.*[130] synthesised the cyclic analogue **262**, which showed DXR inhibitory activity in the μM range. The design of fosmidomycin analogues in which the hydroxamate functionality has been inverted or its orientation reversed to a hydroxamic acid group has also been investigated (Figure 27). Kuntz *et al.*[131] synthesised the hydroxamic analogues **263** and **264** which exhibited the same activity as fosmidomycin **236** against recombinant *Ec*DXR; while Kurz *et al.*[132-133] has reported the synthesis of carboxylic acid **265** and hydroxyurea **266** analogues of fosmidomycin **236**. Recently, Kurz *et al.*[134] reported the synthesis of α-phenyl substituted hydroxamic analogues and demonstrated the inhibitory activities of these analogues to be as potent as those of fosmidomycin **236** against recombinant *Pf*DXR and the multidrug-resistant K1 *P. falciparum* strain.[134]

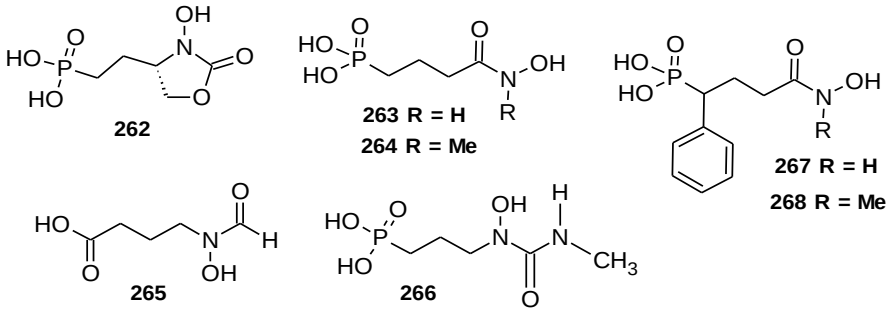

Figure 27. DXR inhibitors based on the modification of the hydroxamate moiety.

Various research groups have reported the synthesis of structural analogues of the substrate DOXP **230** as potential inhibitors of DXR (Figure 28). Hoeffler *et al.* synthesised DOXP analogues **269** and **270** with one of the hydroxyl groups absent at either the C-3 or C-4 position, and showed that these compounds acted as mixed-type inhibitors of *Ec*DXR.[135] Kinetic analyses of *Ec*DXR activity in the presence of these inhibitors indicated that the C-3 and C-4 hydroxyl groups are essential for catalytic transformation of DOXP **230** to MEP **231**, but not critical for inhibition activity. The analogues **271-273** inhibited *Ec*DXR at mM concentration, showing that compounds with neutral or negatively charged donor atoms can coordinate with the metal cation in the active site, whilst the ethyl DOXP analogue **274** and the trifluoromethyl analogue **275**, exhibited steric interactions upon chelation at the

metal-binding site.[136-137] The design of inhibitors which target the NADPH binding domain of DXR have also been explored. Link *et al.*[138] reported the synthesis of the 3',N^6-disubstituted adenosine NADPH analogue **276** (Figure 28), using a polymer-assisted solution-phase method. Biological evaluation of compound **276** revealed moderate anti-malarial activity (low mM) against *P. falciparum* strain Dd2 as well as *Ec*DXR inhibitory activity.[138] However, the study did not confirm the binding of the analogue **276** to the NADPH binding site and hence, the DXR inhibition observed could not be correlated with the anti-plasmodial activity.

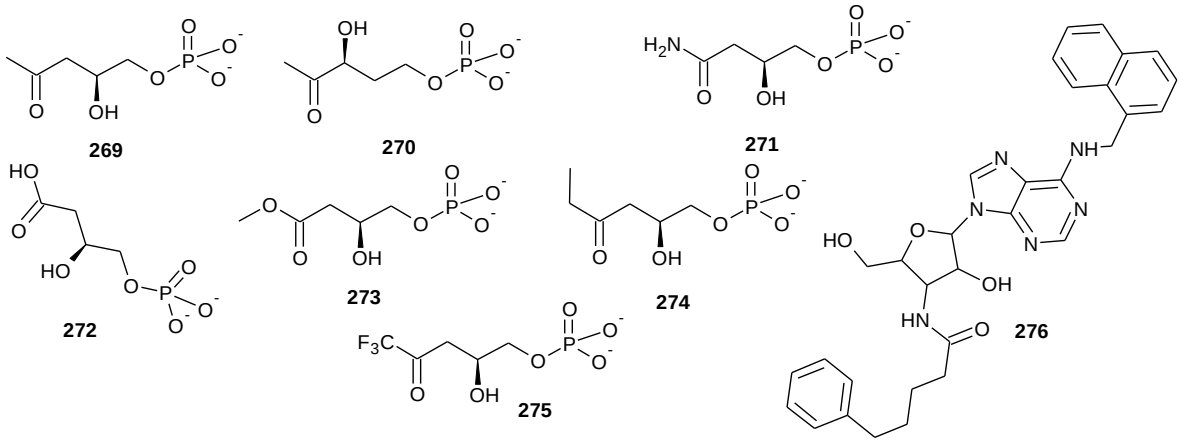

Figure 28. Structural analogues of DOXP and NADPH as DXR inhibitors.

1.8. Previous work in the group and aims of the present study

In an effort to develop novel adenosine triphosphate (ATP) analogues as potential glutamine synthetase (GS) inhibitors for the treatment of tuberculosis various compounds were prepared, including the anilide **277** (Figure 29).[139-141] Serendipitously, this compound was found to exhibit an explicit binding interaction with *Ec*DXR in Saturation Transfer Difference (STD) protein-NMR experiments. Furthermore, *Ec*DXR inhibition assay studies revealed that ligand **277** exhibited low-level inhibition of the enzyme, thus highlighting its potential as a lead compound in the design and synthesis of novel DXR inhibitors. In a cognate study in our group,[129,142] the heterocyclic phosphonate esters **278a-e** and **280a-e** and their corresponding phosphonic acid salts **279a-e** and **281a-e** (Figure 29) were synthesised. In these compounds the benzene ring in compound **277** has been replaced by various heterocyclic systems. The potential of these analogues to act as DXR inhibitors was evaluated *in silico* and *in vitro*. *Ec*DXR inhibition studies of these analogues, however,

revealed that they exhibited minimal to moderate inhibitory activity, whilst the presence of an additional binding pocket was observed during the *in silico* exploration of the DXR active site.[129,142] The presence of this additional binding pocket led to the *de novo* design of a new class of potential inhibitors.

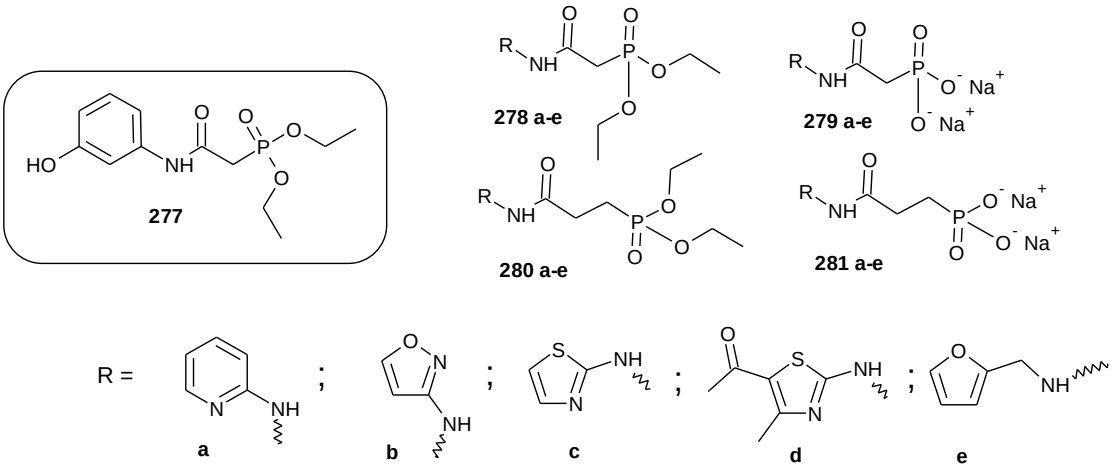

Figure 29. DXR inhibitors synthesised in our research group.

As indicated in the previous section, 1-deoxy-D-xylulose-5-phosphate reductoisomerase (DXR) is a key enzyme functioning in the biosynthesis of isoprenoid precursors in malaria-pathogenic *Plasmodium* species and has been validated as a target for anti-malarial chemotherapy.[93-95] Moreover, the antibiotic fosmidomycin **236** is a potent and selective DXR inhibitor of the virulent *P. falciparum* parasite.[95,115] With detailed knowledge of the DXR active-site architecture, the aim of this research has been to design and prepare novel compounds as potential DXR inhibitors. More specifically, the project has involved the following parallel phases.

1. The synthesis and characterization of:-
    i. dihydroxy-amido phosphonate esters and their corresponding phosphonic acids as DOXP and fosmidomycin analogues;
    ii. furan-derived phosphate esters and phosphonic acids as conformationally restricted DOXP analogues;
    iii. several series of 3-substituted aniline-derived phosphonate esters and their corresponding phosphonic acids as potential DXR inhibitors;

iv. *N*-substituted benzylphosphoramidic acid derivatives as fosmidomycin analogues; and

v. the known inhibitors fosmidomycin **236** and FR900098 **237** for use as standards in DXR binding and inhibition studies.

2. Biochemical and Microbiological studies, including:-
   i. the use of Saturation Transfer Difference (STD) protein-NMR experiments to detect the binding of selected synthesised compounds to *Ec*DXR; and
   ii. DXR-enzyme inhibition assays of selected ligands to examine their ability to inhibit *Ec*DXR *and Pf*DXR activity.
3. Molecular modelling, including simulated docking studies of selected ligands to establish preferred ligand-binding conformations, using the Cerius^2 LigandFit module and Autodock version 4.0.

2. DISCUSSION

With reference to the detailed aims and objectives, this discussion will focus on:- the synthesis of dihydroxy-amido phosphonate esters and phosphonic acid derivatives (**Section 2.1**), 3-substituted aniline scaffolds (**Section 2.2**), furan-derived phosphates (**Section 2.3**) and *N*-benzyl substituted phosphoramidic acid derivatives (**Section 2.4**) as novel DXR inhibitors; the synthesis of fosmidomycin and FR900098 as standards for biological studies (**Section 2.5**); STD-NMR binding studies (**Section 2.5**), enzyme inhibition assays (**Section 2.5**); and docking studies (**Section 2.6**) of selected synthesised compounds.

2.1. Synthesis of dihydroxy-amido phosphonate esters and phosphonic acid derivatives as novel DXR inhibitors

Structure-activity relationship (SAR) studies of the DXR enzyme with the natural substrate DOXP **230** and of known inhibitors fosmidomycin **236** and FR900098 **237** have led to the identification of structural groups which are considered critical for the inhibitory activity of DXR.[103,105] These include the hydroxamate functionality and the phosphonic acid group, illustrated in Figure 30. A distance of three carbon atoms between these two functional moieties appears to be essential for inhibition of DXR. Our strategy for the synthesis of the first series of novel DXR inhibitors thus involved:- i) mimicking the alkyl backbone of DOXP **230** to retain enzyme-ligand binding specificity; and ii) modifying the phosphonate and hydroxamate moieties to obtain analogues with improved inhibitory activity.

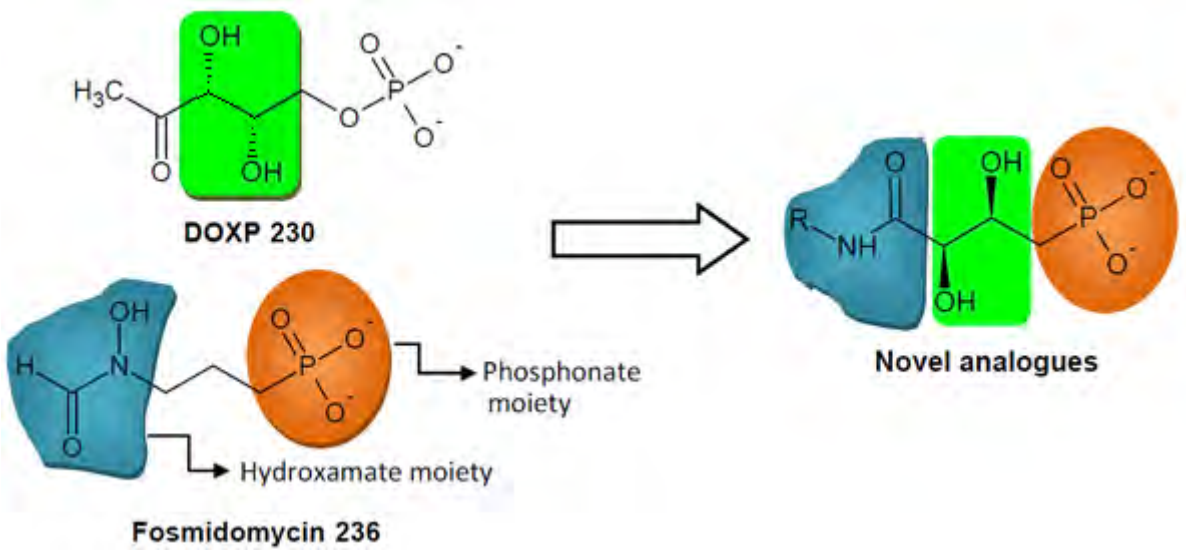

Figure 30. Design strategy for the construction of novel DXR inhibitors, showing essential structural features.

In the design and synthesis of the dihydroxy-amido phosphonate esters **292** and their corresponding phosphonic acid derivatives **293**, three synthetic routes were investigated, all of which commenced with ethyl (*E*)-crotonate; these are outlined in Scheme 24.

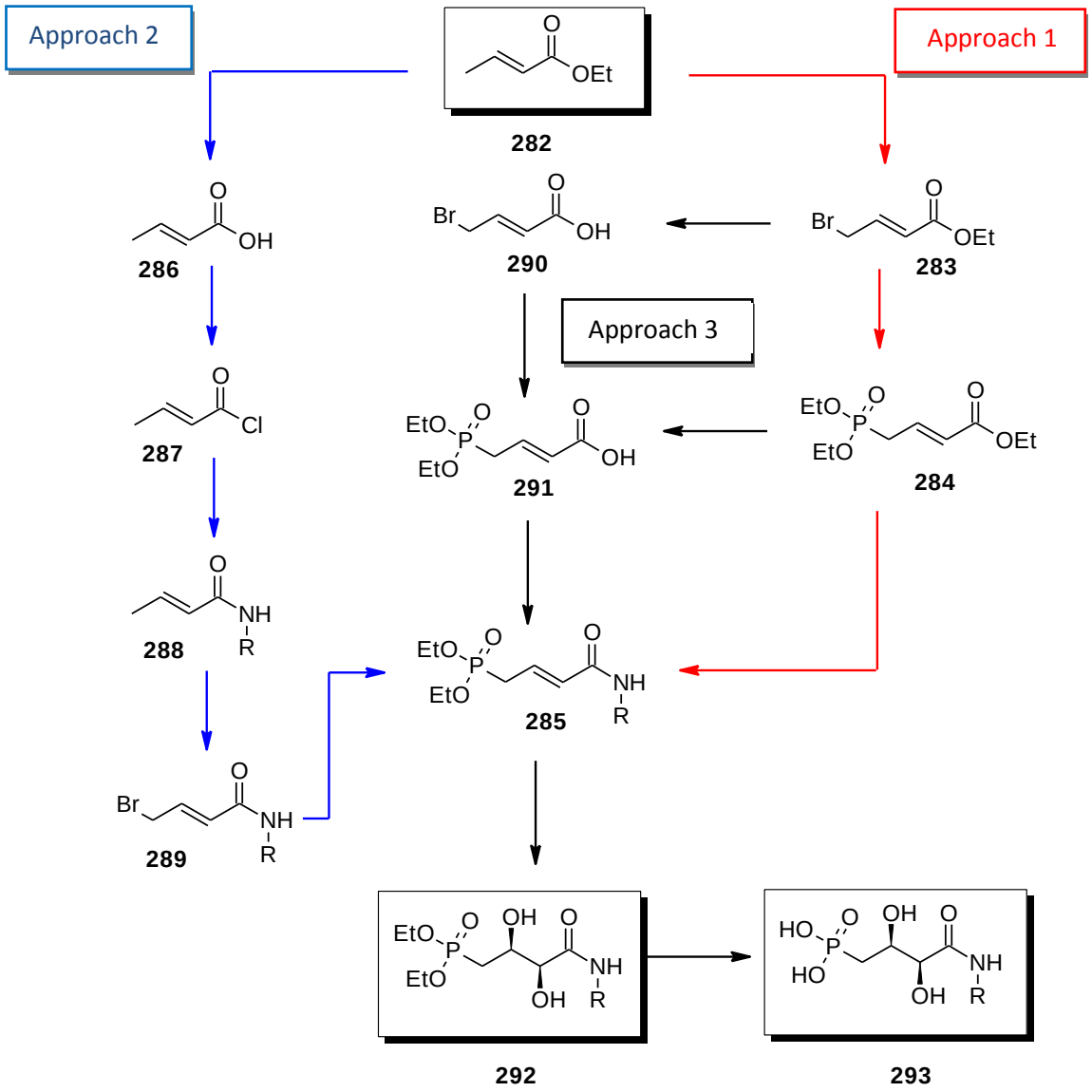

Scheme 24. Synthetic routes explored in the synthesis of the dihydroxy-amido phosphonate esters **292** and their corresponding acid derivatives **293**.

The initial step in Approach 1 (Scheme 24) involved bromination at the allylic position of commercially available ethyl (*E*)-crotonate **282**, in the presence of a stoichiometric quantity of *N*-bromosuccinimide (NBS) as a source of bromine and a catalytic quantity of benzoyl peroxide, to obtain ethyl 4-bromocrotonate **283** in 56% yield (Scheme 25).[143] This reaction is referred to as the Wohl-Ziegler bromination and involves a free-radical mechanistic

pathway, initiated by the non-ionic fission of the weak N-Br bond.[144] The use of NBS and carbon tetrachloride (CCl_4) in this method provides several advantages. Firstly, the poor solubility of NBS in CCl_4 ensures that the concentration of molecular bromine and hydrogen bromide (reagents generated *in situ*) are constantly kept low such that the bromination occurs exclusively at the allylic position and side reactions arising from addition across the double bond are prevented.[145] Secondly, the resulting by-product, succinimide, is insoluble in cold CCl_4 thus simplifying isolation of the product **283**.

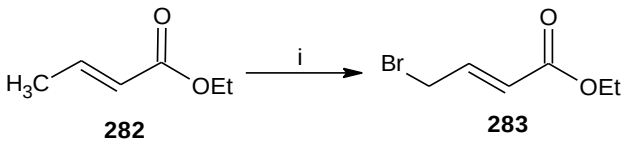

282 **283**

Scheme 25. Synthesis of compound **283** *via* Wohl-Ziegler bromination.[143]
Reagents and conditions: i) NBS, benzoyl peroxide, CCl_4, 3 h, reflux.

Figure 31 shows the ^{1}H NMR spectrum of compound **283**, indicating the two 4-methylene protons resonating as a doublet at 3.99 ppm. The 2- and 3-vinylic protons resonate as a doublet at 6.02 ppm and multiplet at 6.99 ppm, respectively whilst the 2'-methyl protons resonate as a triplet at 1.26 ppm and the 1'-methylene protons as a quartet at 4.18 ppm.

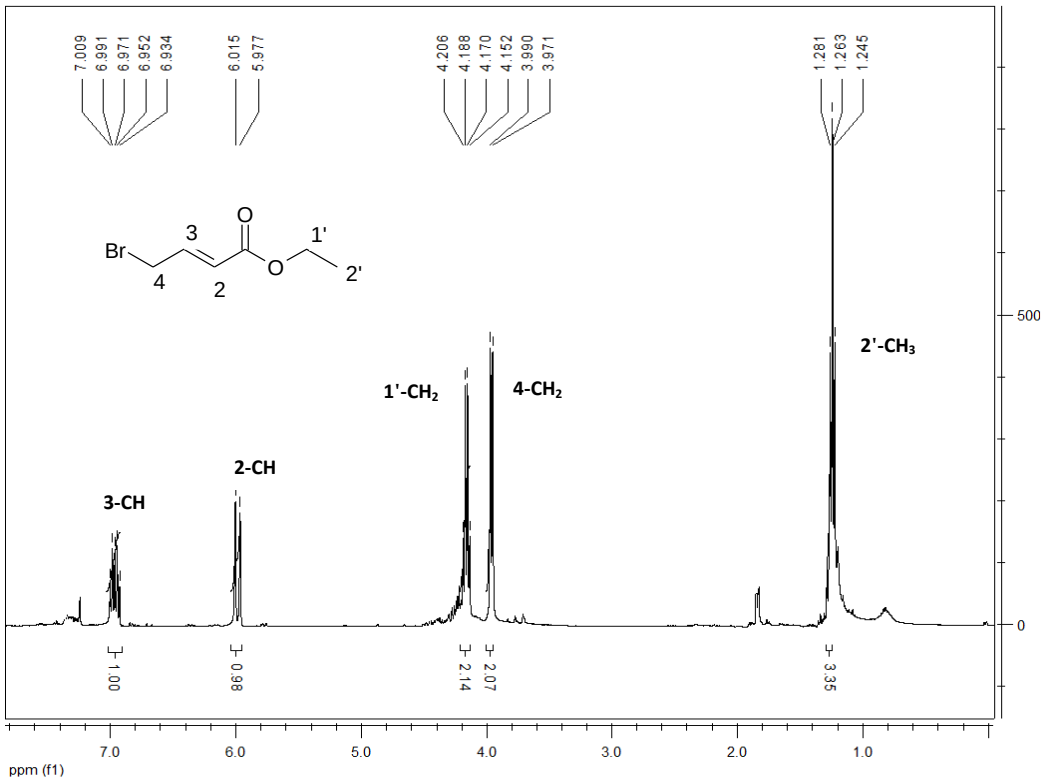

Figure 31. 400 MHz ^{1}H NMR spectrum of compound **283** in $CDCl_3$.

Synthetic inhibitors of the DXR enzyme are typically characterised by the presence of a phosphonate moiety, which occupies the hydrophilic phosphate binding pocket in the DXR catalytic site.[105,117-122] Several synthetic methods have been described, of which the Michaelis-Arbuzov reaction is one of the most versatile, for affording access to phosphonates, phosphinates and phosphine oxides.[146-148] Thus, by subjecting compound **283** to Michaelis-Arbuzov reaction conditions, the phosphonate ethyl ester **284** was obtained in reasonable yield (62%). The reaction involves the formation of an unstable trialkoxyphosphonium salt intermediate **294** by nucleophilic attack (S_N2) of triethyl phosphite on the electrophilic alkyl halide **283**.[147-148] Subsequent halide ion mediated de-alkylation of the intermediate **294** *via* another S_N2 reaction affords the desired phosphonate ethyl ester **284** and an alkyl halide **295** (Scheme 26).

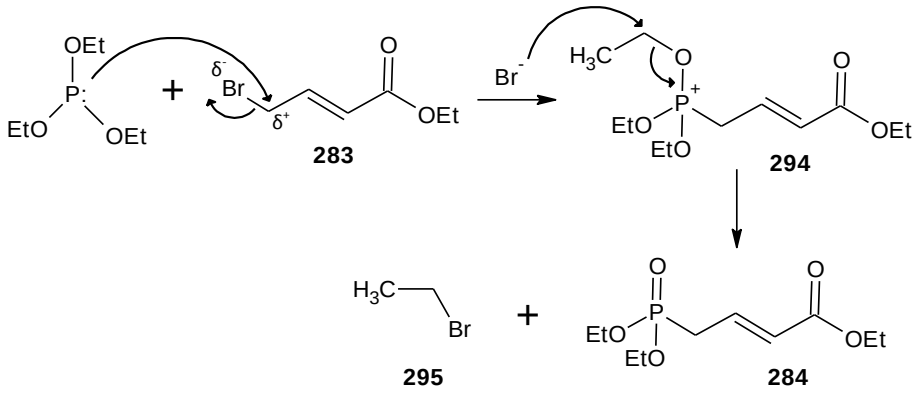

Scheme 26. Synthesis of phosphonate ethyl ester **284** *via* the Michaelis-Arbuzov reaction.

^1H, ^{13}C and ^{31}P NMR spectroscopic analysis confirmed the formation of the product **284**. The ^1H NMR spectrum (Figure 32) showed the presence of the 4-methylene proton signal as a double doublet at 2.70 ppm. The splitting of these methylene protons is due to the coupling to the adjacent ^{31}P nucleus with a characteristic coupling constant of *ca.* 23 Hz and coupling to the adjacent vinylic proton (J = 7.6 Hz). The overlapping multiplets at 4.10 ppm and 1.27 ppm are due to the 1' and 1''-methylene and 2' and 2''-methyl protons of the carboxylate and phosphonate ester ethyl groups, while the 2- and 3-vinylic protons resonate at 5.91 ppm and 6.85 ppm, respectively. Analysis of the ^{13}C NMR spectrum (Figure 33) clearly shows the characteristic splitting of the phosphonate methylene carbon (C-4) signal at *ca.* 29.9 ppm with a large coupling constant of 138 Hz, due to the coupling to the ^{31}P nucleus. The splitting of the signals corresponding to 1''- methylene and 2''-methyl carbons at 62.2 ppm and at 16.3 ppm, respectively, is also clearly evident, whilst the 2- and 3-vinylic carbon

signals appear at 125.8 ppm and 137.8 ppm, respectively; the C-1 carbonyl carbon signal is observed at 165.5 ppm. The ^{31}P NMR spectrum showed a characteristic singlet at *ca.* 25 ppm, confirming the presence of the phosphonate moiety.

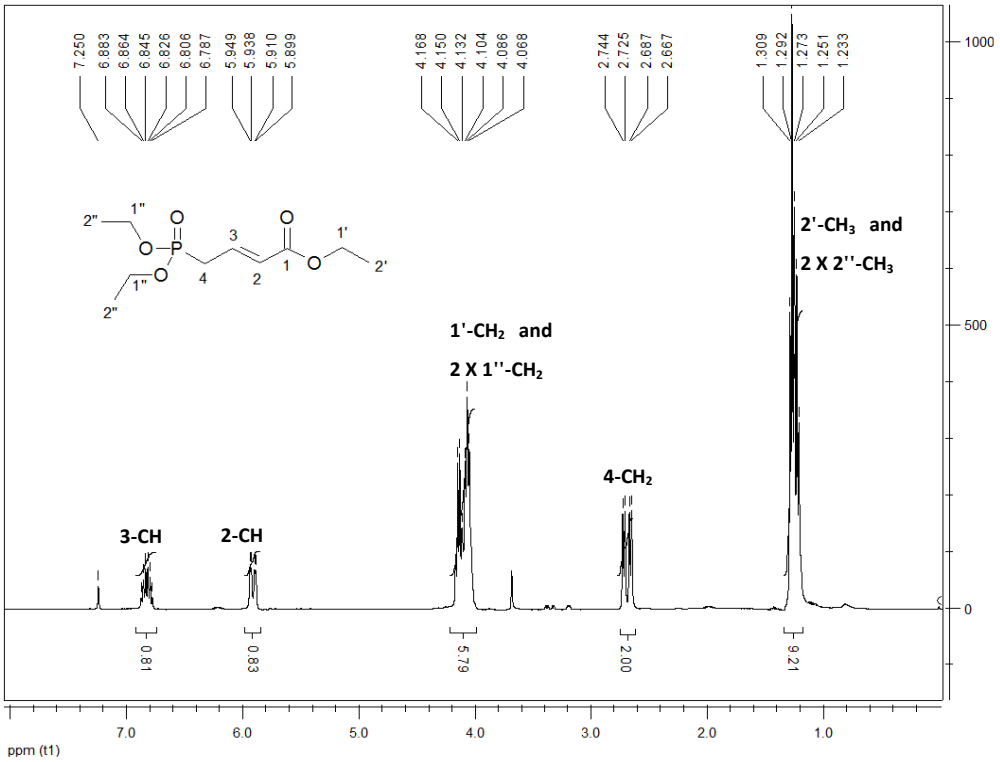

Figure 32. 400 MHz ^{1}H NMR spectrum of compound **284** in $CDCl_3$.

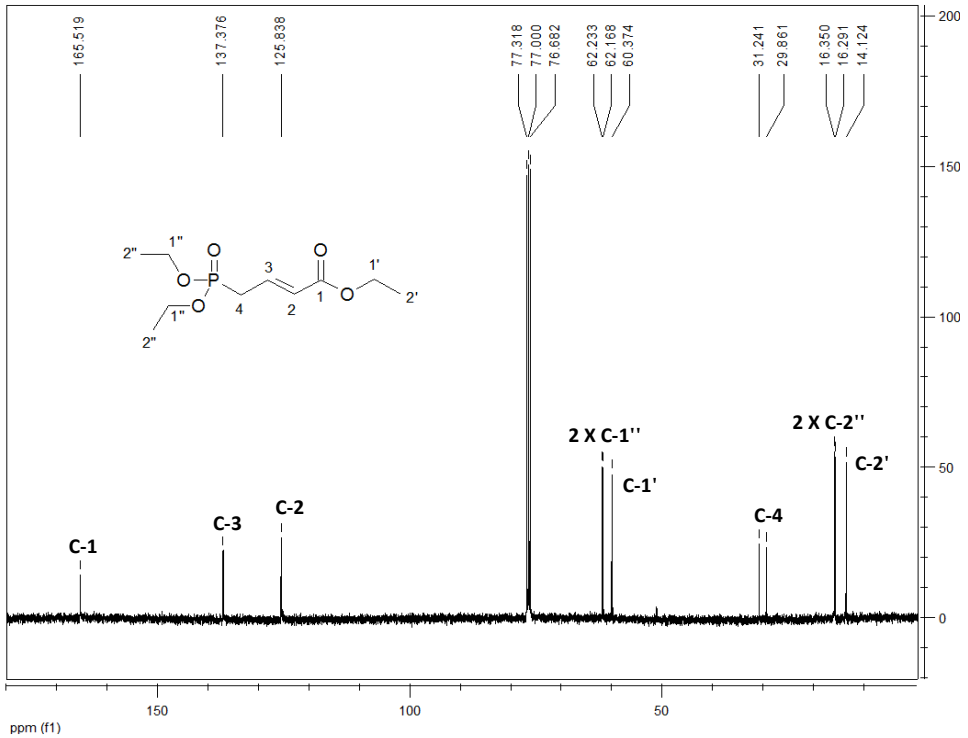

Figure 33. 400 MHz ^{13}C NMR spectrum of compound **284** in $CDCl_3$.

In our design of novel DXR inhibitors, emphasis was placed on the construction of ligands in which the hydroxamate group, present in the known inhibitors fosmidomycin **236** and FR900098 **237**, is 'rearranged' into an amide moiety. The amide oxygen and nitrogen atoms are expected to chelate to the hard divalent metal cation, thus increasing the binding affinity of the molecules in the DXR active site. Although various research groups are involved in the design of novel DXR inhibitors, very few inhibitors bearing the amide functional group have been synthesised or their biological activity reported. Recently, Kurz *et al.* reported the synthesis of DXR inhibitors with a reversed orientation of the hydroxamate group, which exhibited similar anti-plasmodial activity against *Pf*DXR as the known inhibitors fosmidomycin **236** and FR900098 **237**.[149] Furthermore, in our strategy, it was reasoned that by varying the substituents on the nitrogen atom, the hydrophobicity of the molecules could be tuned and additional binding interactions with the active site residues could be explored.

Various literature approaches were examined in an attempt to synthesize the phosphonated crotonamide derivatives **285a-g** directly from the phosphonated ethyl ester **284** (Scheme 27).[150-152]

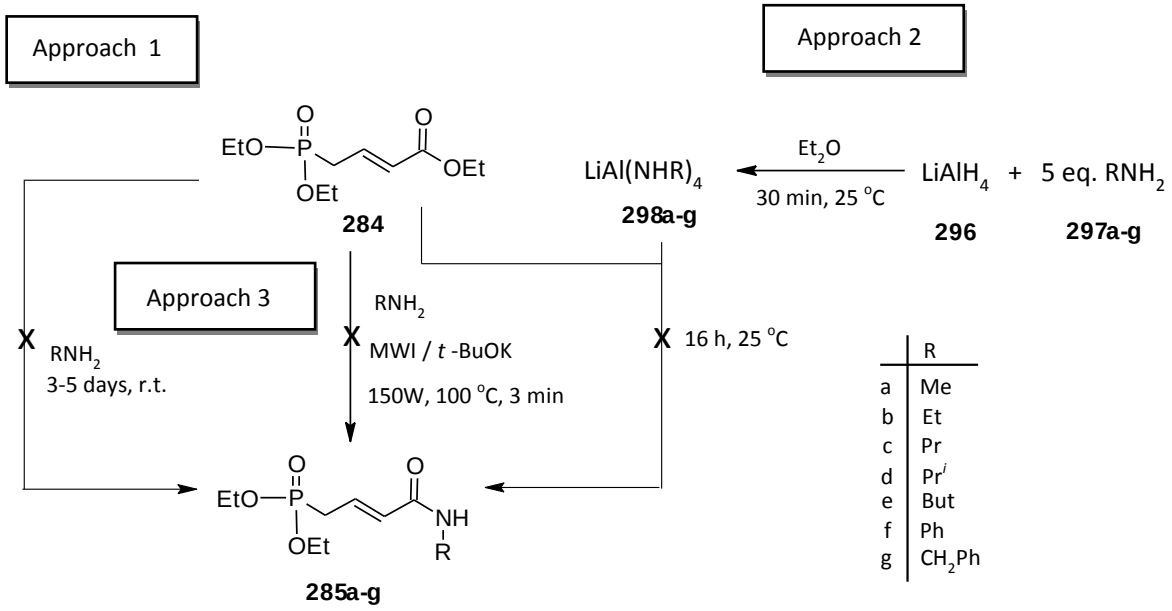

Scheme 27. Attempted synthesis of phosphono-crotonamide derivatives **285a-g** *via* various literature methods.[150-152]

Usually, the aminolysis of esters requires drastic reaction conditions, such as high temperatures and long reaction times. In addition, strong alkali metal catalysts are often used to achieve this transformation.[153-154] Driscoll *et al.*, however, reported the direct conversion of esters to the corresponding amides under fairly mild conditions, isolating the products in good yields.[150] We explored this method for the transformation of the phosphonated ethyl ester **284** to the phosphonated crotonamides **285a-g** (Scheme 27, Approach 1), but, although the reaction mixtures were stirred for several days and monitored by TLC, no products were observed and only the starting materials were recovered.

The next approach to be explored for the amidation of the phosphonated ethyl ester **284**, involved the use of a metal complex as a convenient source of the nucleophilic amine to achieve the transformation. Weinreb *et al.* reported the reaction of trimethylaluminum with various amines to produce the dimethylaluminum amides *in situ*, which upon treatment with a variety of carboxylic esters furnished the corresponding carboxamides in satisfactory yields (69 - 100%).[155] In a similar approach, Solladie-Cavallo reacted lithium aluminium hydride **296** with various amines **299a-d** (Scheme 28) to generate the lithium aluminum-amido complexes **300a-d** *in situ* with liberation of hydrogen.[151] Subsequent addition of the ester **301** to the metal-amido complexes **300a-d** and, ester **302** to metal-amido complex **300b**, afforded the desired carboxamides **303a-d** and **304b** in good yields, the former together with the diol **305**.

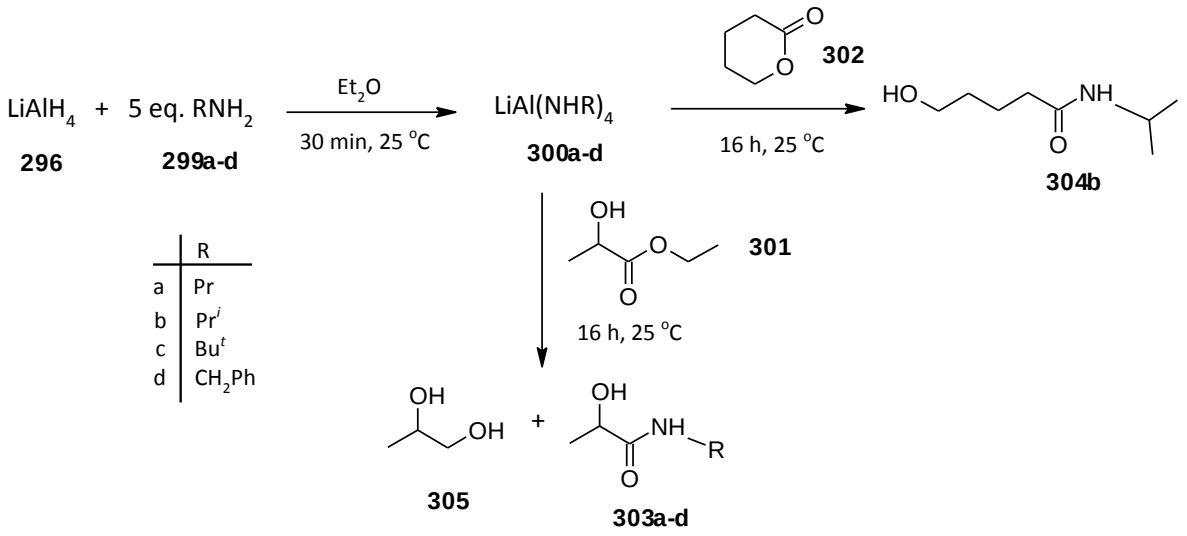

Scheme 28. Synthesis of amides from esters using lithium aluminium-amido complex **298**.[151]

We therefore attempted the conversion of compound **284** to the corresponding phosphonated crotonamide derivatives **285a-g** using Solladie-Cavallo's methodology[151] (Scheme 27, Approach 2). The reaction was monitored by TLC but only trace amounts of the products appeared to be formed. The conjugation in compound **284** presumably deactivates the acyl carbon to nucleophilic attack by the metal-amido complex. The molar ratio of the lithiumaluminum-amido complexes **300a-d** relative to compound **284** and the reaction time were then increased in an attempt to improve the yields, but this resulted in a mixture of products and Approach 2 was abandoned. Interestingly, competing reactions in the metal-amido complex catalysed conversion of esters to amides have also been described by Roskamp *et al.*, who used a mixed tin-amide complex generated *via* a metathesis reaction of tin chloride and bis(trimethylsilyl)amido-lithium.[156]

Hamelin *et al.* successfully synthesised a variety of carboxamides by reacting different esters and amines under solvent-free conditions in the presence of potassium *tert*-butoxide (*t*–BuOK) and microwave irradiation.[152] Based on this work, we subjected the phosphonated ethyl ester **284** and several amines to similar reaction conditions in the hope of isolating the desired phosphonated crotonamide derivatives **285a-g** (Scheme 27, Approach 3). However, after filtration and evaporation of the solvent *in vacuo*, only the starting materials were recovered. Increasing the reaction time and temperature resulted in formation of a black solid, reflecting the decomposition of the substrate **284** at the elevated temperature.

In the synthesis of various carboxylic acid derivatives, including amides, acid chlorides are often used as activated acyl intermediates.[157-158] Several reagents are commonly used for the conversion of carboxylic acids to their corresponding acid chlorides; these include phosphorous trichloride, thionyl chloride and oxalyl chloride.[158-160] Given the difficulties experienced in the direct conversion of the phosphonated ethyl ester **284** to the amide derivatives **285a-g**, we explored the generation of the more reactive acid chloride, using ethyl (*E*)-crotonate **282** as the model substrate (Scheme 24, Approach 2). Initially, compound **282** was saponified using potassium hydroxide in ethyl alcohol to obtain, after acidification and recrystallisation, crotonic acid **286** as white crystals. Compound **286** was characterised by ^{1}H NMR and IR spectroscopy, and converted to its corresponding acid chloride **287** using oxalyl chloride and a catalytic quantity of dimethylformamide (Scheme

29). The acid chloride **287** was purified by distillation and IR analysis showed the characteristic acyl chloride absorption band at 1757 cm^{-1}.

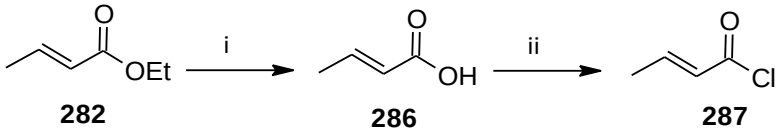

282 **286** **287**

Scheme 29. Conversion of ethyl (*E*)-crotonate **282** to its corresponding acid **286** and acid chloride **287**.
Reagents and conditions: i) KOH in EtOH, r.t., 24 h then H_3O^+ ii) $(COCl)_2$, DMF, 4 h, N_2.

With the crotonyl chloride **287** successfully formed, the crotonamides **288c-g** were synthesised in reasonable to good yields by treatment of the acid chloride **287** with a molar equivalent of each of the appropriate amines in the presence of triethylamine (Scheme 30). The synthesis of *N*-methylcrotonamide **288a** and *N*-ethylcrotonamide **288b**, however, required a different approach, as the amines used to obtain these amides were used as their hydrochloride salts. Proton sponge® [1,8-bis(dimethylamino)naphthalene],[161] was used as a strong non-nucleophilic base (pK_a = 12.34) to free the amines from their hydrochloride salt *in situ*, before treatment with the acid chloride **287** at 0 °C. Proton sponge has been successfully used in our group to promote nucleophilic substitution reactions of amine hydrochloride salts with coumarin substrates to furnish novel coumarin derivatives as potential HIV-1 protease inhibitors.[162] The crotonamides **288a-g** were all characterised by ^1H and ^{13}C NMR and IR spectroscopic analysis. Figure 34 shows the ^1H NMR spectrum of *N*-benzylcrotonamide **288g**.

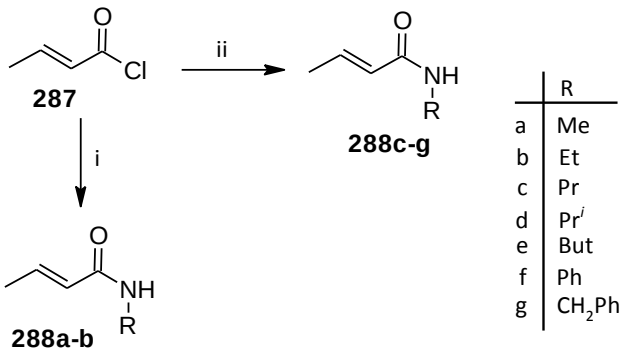

287 **288c-g** **288a-b**

	R
a	Me
b	Et
c	Pr
d	Pr^i
e	But
f	Ph
g	CH_2Ph

Scheme 30. Synthesis of crotonamides **288a-g** from crotonyl chloride **287.**

Reagents and conditions: i) RNH_2, Et_3N, 0 °C to r.t., 24 h ii) RNH_2.HCl, proton sponge, pyridine, 0 °C, 15 min, r.t., 24 h.

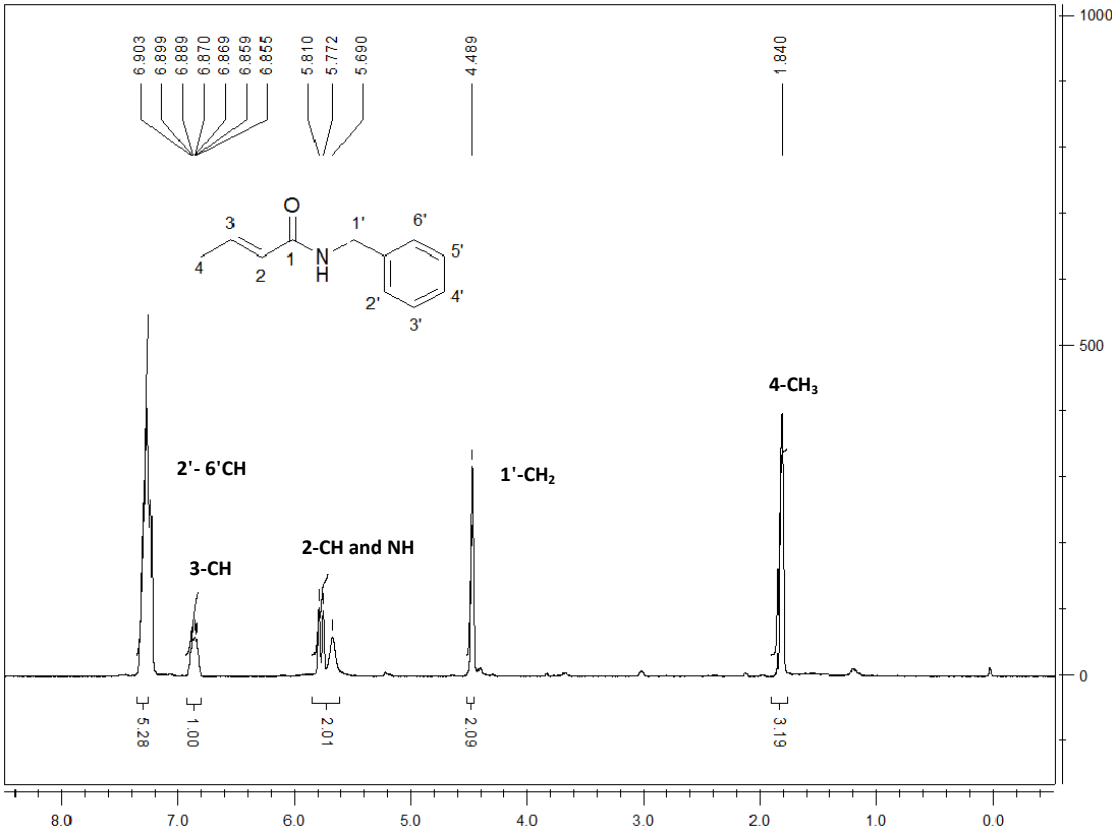

Figure 34. 400 MHZ ^{1}H NMR spectrum of *N*-benzylcrotonamide **288g** in $CDCl_3$.

The next step was expected to involve allylic bromination of the crotonamides **288a-g** using the Wohl-Ziegler method [143] to obtain the brominated crotonamides **289a-g** (Scheme 31). Attempted reaction of crotonamides **288a-g** in the presence of NBS and a catalytic quantity of azo*bis*(isobutyronitrile) (AIBN) in refluxing toluene was unsuccessful. Due to the sensitivity of this method to the solvent and temperature, different reaction conditions (Table 3) were investigated in an attempt to form compound **289f**. Even under these varied conditions, the desired product could not be isolated. Competing reactions could include conjugate addition of hydrogen bromide, generated *in situ*, to the alkene group of the crotonamide **288f**.

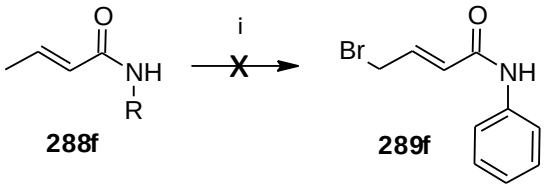

288f **289f**

Scheme 31. Attempted synthesis of brominated-crotonamides **289f** using Wohl-Ziegler reaction.

Reagents and conditions: i) NBS, benzoyl peroxide, CCl_4, 3 hours, reflux.

Table 3. Attempted bromination of crotonamide **288f** under various reaction conditions.

Compound 288f (equiv.)	NBS (equiv.)	Solvent	Temperature (^{o} C)	Catalyst	Time (h)
1	1.2	toluene	reflux	AIBN	3
1	1	toluene	r.t.	AIBN	3
1	0.5	toluene	r.t.	AIBN	12
1	1	benzene	reflux	benzoyl peroxide	3
1	1	CCl_4	reflux	benzoyl peroxide	6
1	0.5	CCl_4	r.t.	benzoyl peroxide	12
1	1	$C_2H_2Cl_4$	reflux	AIBN	3

A variety of coupling reagents have been developed for the formation of amide bonds directly from carboxylic acids and amines; these include *N*,*N*'-dicyclohexylcarbodiimide (DCC), *N*,*N*'-diisopropylcarbodiimide (DIC), 1,1'-carbonyldiimidazole (CDI) and 1-ethyl-3-(3-dimethylaminopropyl)carbodiimide (EDC).[163-166] With the success achieved in phosphonating compound **283** to afford the phosphonated ethyl ester **284**, but the failure to obtain the brominated crotonamides **289a-g**, the next strategy (Scheme 24, Approach 3), which involved direct coupling of γ-phosphonated crotonic acid **291** with amines, was explored.

The previously synthesised substrates **283** and **284** were efficiently transformed, using appropriate procedures, to furnish the γ-phosphonated carboxylic acid **291** (Scheme 32). Thus, hydrolysis of compound **283** afforded the brominated carboxylic acid **290** quantitatively; subsequent phosphonation using the Michaelis-Arbuzov [146] reaction gave the desired carboxylic acid **291**. Compound **291** was also obtained by hydrolysis of the phosphonated ethyl ester **284**.

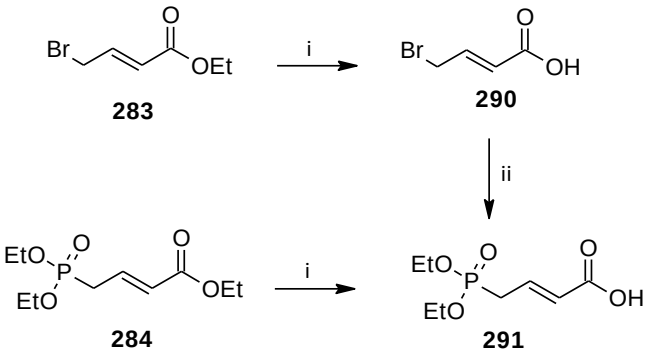

Scheme 32. Synthesis of the phosphonated carboxylic acid **291**.
Reagents and conditions: i) KOH in EtOH, r.t., 24 h then H_3O^+ ii) triethyl phosphite, 9 h, reflux, N_2.

Comparison of the ^{1}H NMR spectra of compound **284** (Figure 32) and compound **291** (Figure 35), clearly reveals the disappearance of the 1'-methylene and 2'-methyl protons of the carboxylate ester moiety, as the overlapping multiplets at 4.15 ppm and 1.33 ppm integrate for the 1''-methylene and 2''-methyl protons of the phosphonate ester ethyl groups alone. The 4-methylene protons resonate at 2.81 ppm as a double doublet due to coupling to the ^{31}P nucleus, while the broad signal at *ca.* 5.10 ppm is assigned to the carboxylic acid proton.

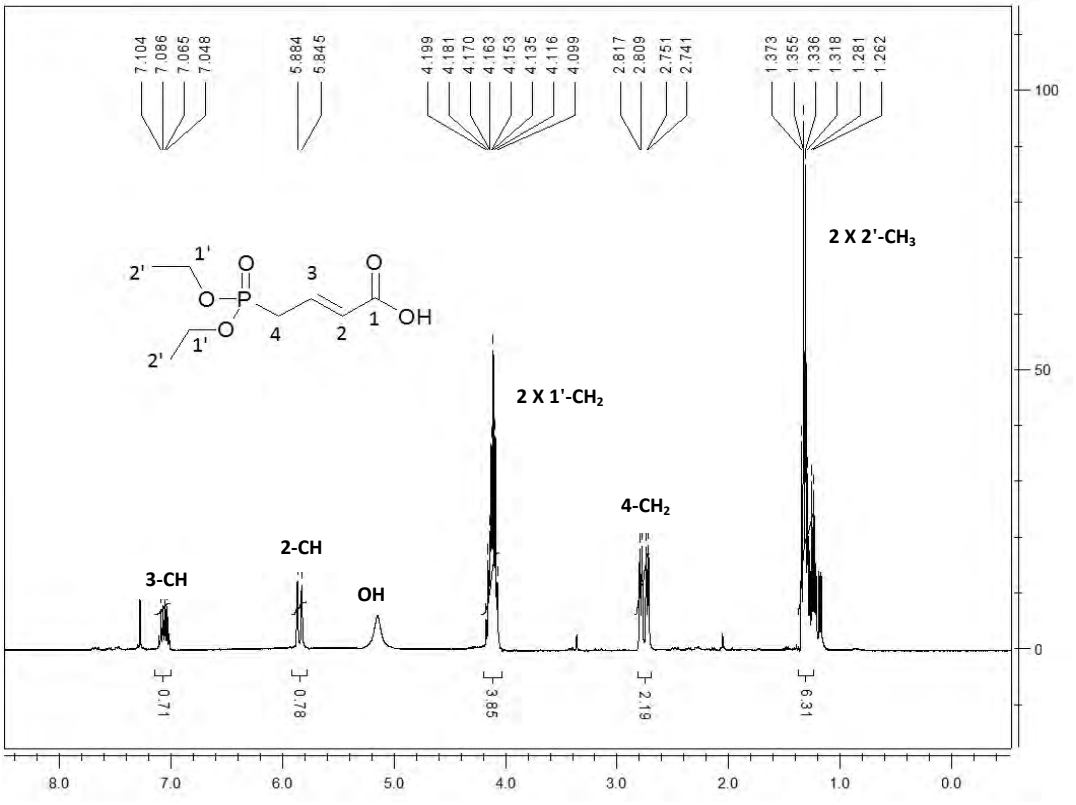

Figure 35. 400 MHZ ^{1}H NMR spectrum of phosphonated carboxylic acid **291** in $CDCl_3$.

Having synthesised compound **291** in reasonable yield, we decided to prepare the amido-phosphonate esters **285a-g** using EDC as the coupling reagent, in the presence of hydroxybenzotriazole (HOBt) and the appropriate primary amines (Scheme 33). The use of EDC-mediated coupling (as opposed to DIC- or DCC-mediated coupling) was motivated by the fact that EDC and its urea by-product are water soluble; hence, any excess reagent and by-product are easily separated from the desired products by aqueous extraction.[166]

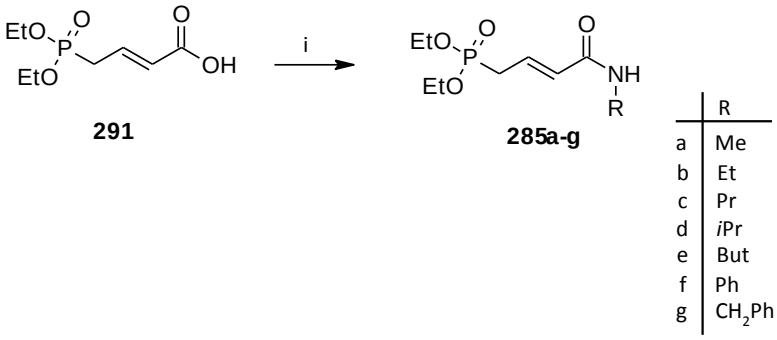

	R
a	Me
b	Et
c	Pr
d	*i*Pr
e	But
f	Ph
g	CH_2Ph

Scheme 33. Synthesis of amido-phosphonate esters **285a-g** using EDC-mediated coupling. *Reagents and conditions:* i) EDC, HOBt, RNH_2, DCM, 24 h, r.t., N_2.

The mechanism of the EDC-mediated coupling involves deprotonation of the carboxylic acid **291** by EDC **306** to produce the carboxylate anion **307** and the activated carbodiimide species **308** and then, the highly electrophilic *O*-acylisourea intermediate **309**. HOBt **310** is added to form the less reactive ester intermediate **311**, which undergoes a nucleophilic acyl substitution by amines, to furnish, in our case, the desired amide derivatives **285a-g** (Scheme 34). The HOBt suppresses competing reactions, including the formation of a stable *N*-acylurea by acyl migration and the formation of an acid anhydride in the presence of unreacted carboxylic acid.[166]

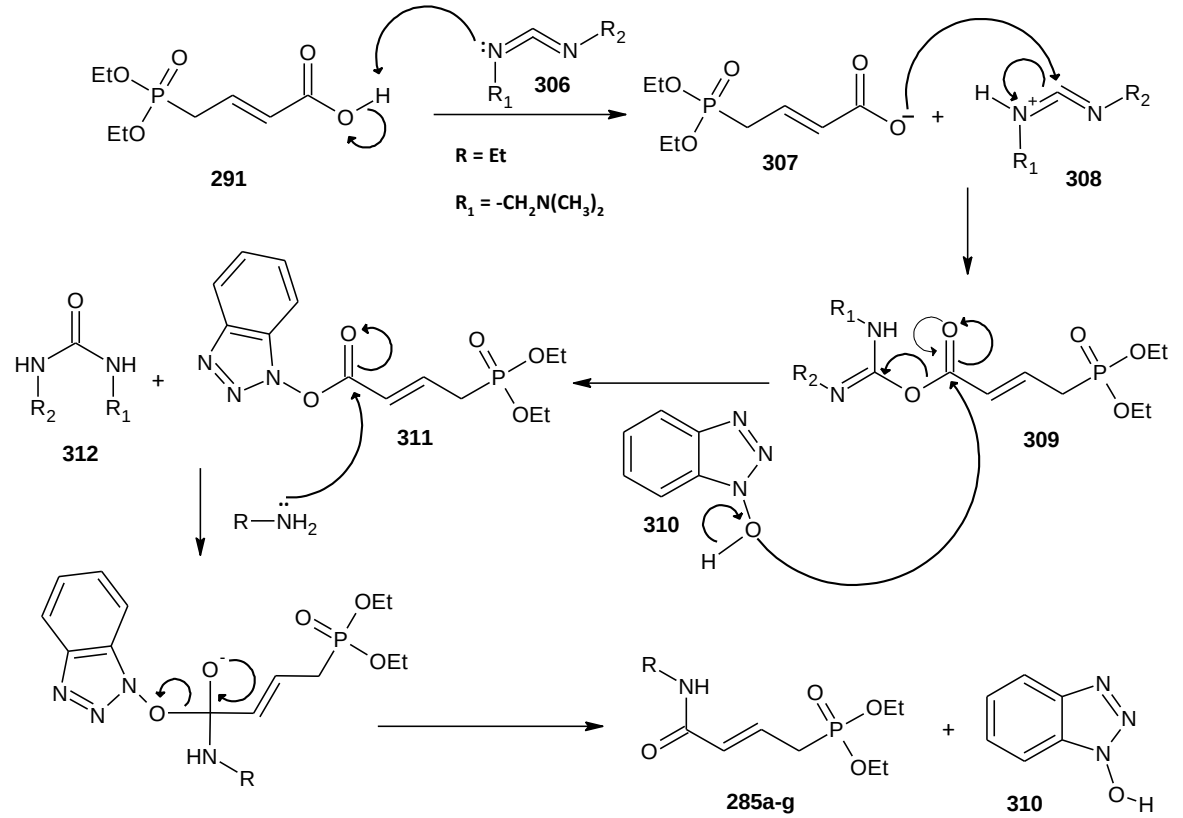

Scheme 34. Mechanism of the EDC-mediated coupling reaction of carboxylic acid **291** to form the amido-phosphonate esters **285a-g**.

The amido-phosphonate esters **285a-e** and **285g** are all new compounds, and were fully characterised by NMR spectroscopy and elemental analysis. The COSY spectrum of compound **285c** is illustrated in Figure 36, while Figure 37 shows the HSQC spectrum of compound **285g**. The couplings between the different protons present in compound **285c** are clearly evident in the COSY spectrum (Figure 36). The 3''-methylene protons (J = 7.2 Hz) couple with the 2''-methylene protons, which couple in turn, to the 1"-methylene protons. The complex splitting pattern observed for the 1'-methylene protons is due to coupling to the 2'-methyl protons and the ^{31}P nucleus. The 2-vinylic proton resonates as a double doublet (J = 13.6 and 1.6 Hz), indicative of coupling to the 3-vinylic proton and the allylic 4-methylene protons. In addition to coupling to the 2-vinylic proton, the 3-vinylic proton also exhibits coupling to the 4-methylene proton as well as long range coupling to the ^{31}P nucleus.

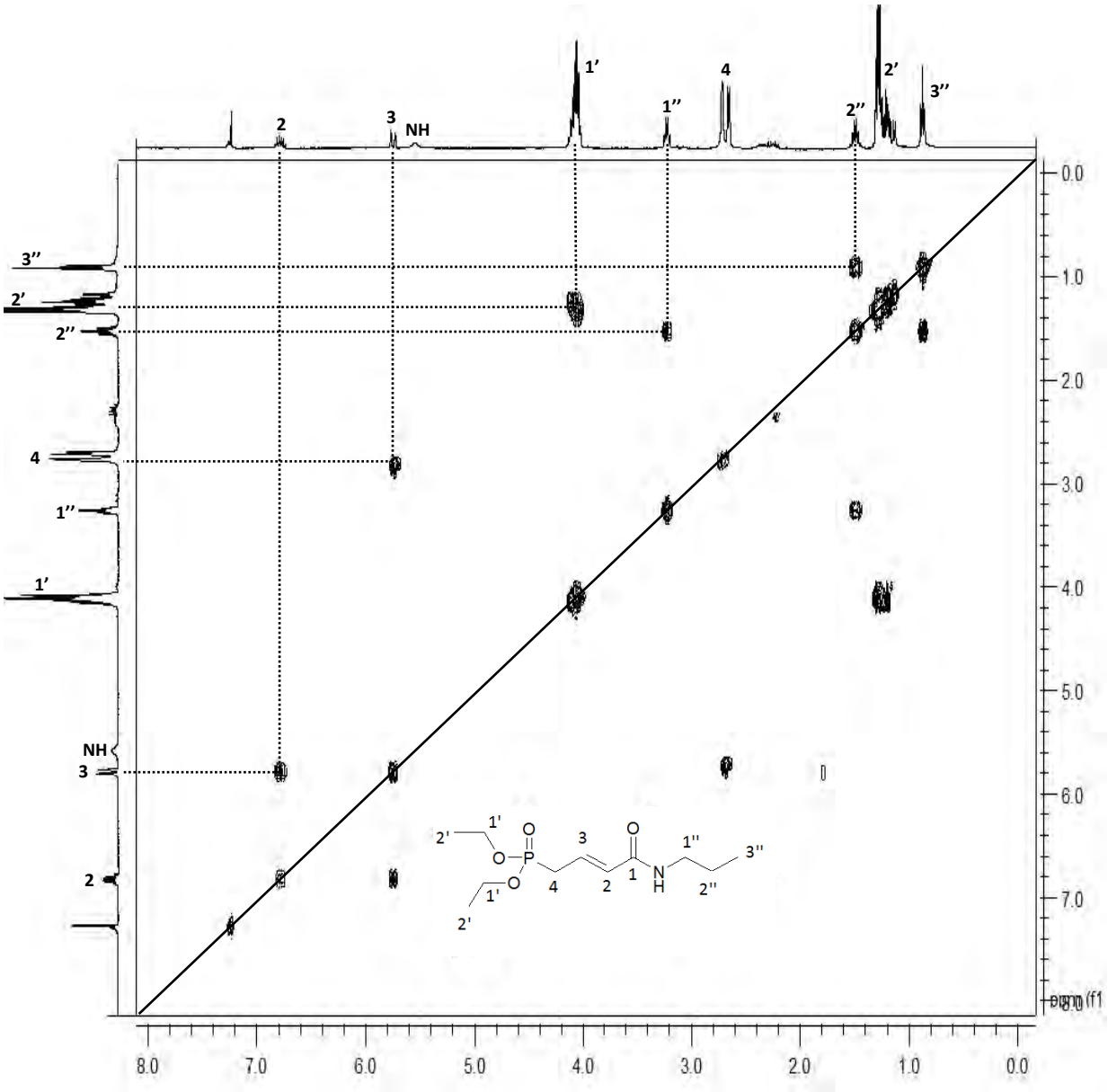

Figure 36. COSY spectrum of compound **285c** in $CDCl_3$.

The assignment of the carbon signals for compound **285g** was achieved by analysis of the HSQC spectrum (Figure 37). The 1'- methylene and 2'-methyl carbon signals corresponding to the phosphonate ethyl ester groups resonate at 63.6 ppm and 16.1 ppm, respectively. Both of these signals are split into doublets, with coupling constants of 6.7 and 5.8 Hz, due to coupling with the ^{31}P nucleus. The 4-methylene carbon signal at 35.4 ppm also appears as a doublet due to coupling with the adjacent ^{31}P nucleus, but with a much larger coupling constant of 143.9 Hz, while the 1''-methylene carbon signal resonates as a singlet at 43.5 ppm. The 2- and 3-vinylic carbon signals appear at 124.8 ppm and 138.3 ppm, respectively. The aromatic carbon signals are assigned as follows:- the signal at 127.5 ppm correlates to

C-5''; the signal at 127.8 ppm to C-3'' and C-7''; C-4'' and C-6'' correspond to the signal at 128.7 ppm and the signal at 140.3 ppm to the C-2'' quaternary carbon.

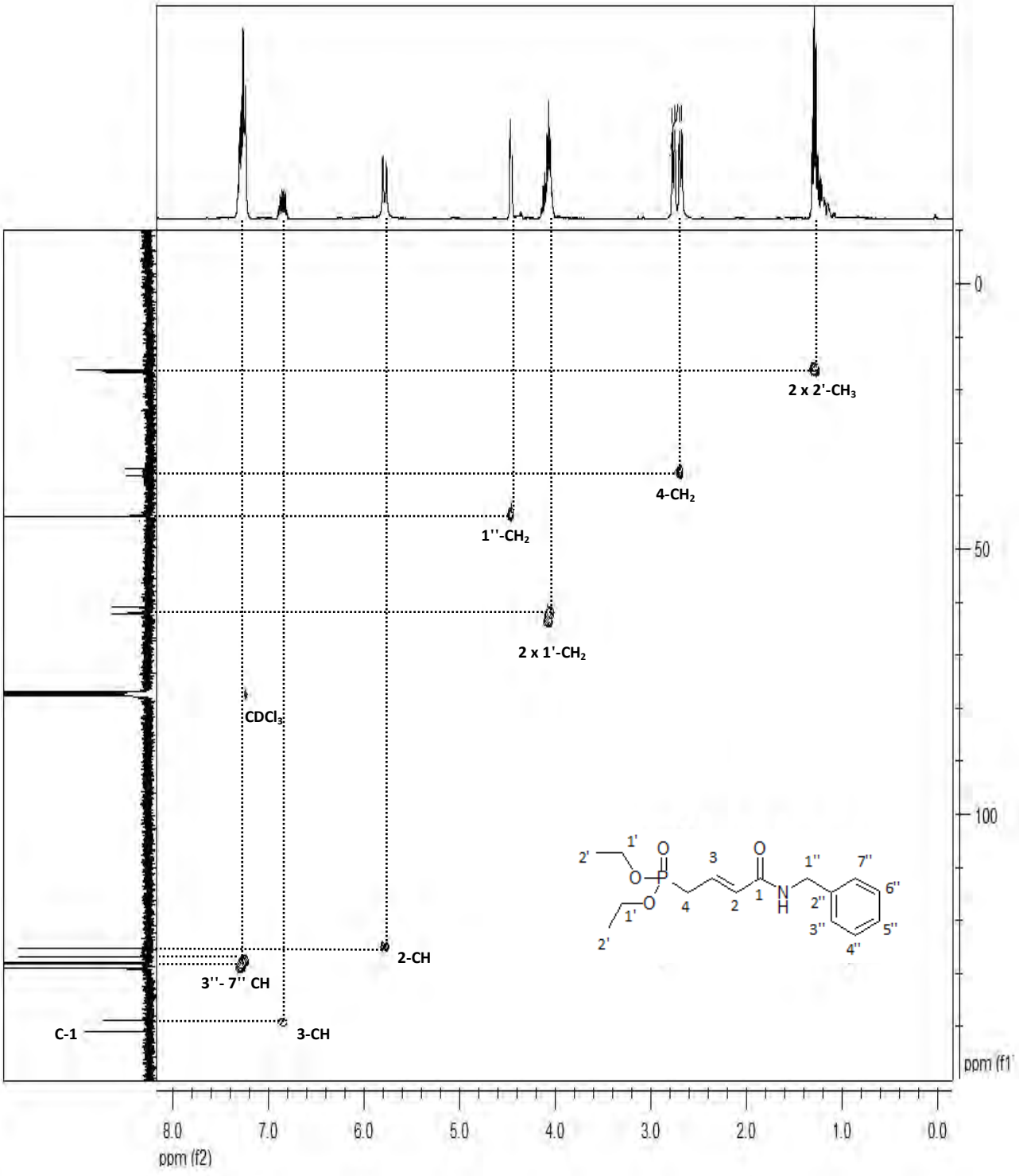

Figure 37. HSQC spectrum of compound **285g** in $CDCl_3$.

With the novel amido-phosphonate esters **285a-g** successfully prepared, attention could be given to the final synthetic step required to furnish the targeted dihydroxy-amido phosphonate esters **292**. This involved dihydroxylation of the alkene double bond. The hydroxyl groups were expected to hydrogen-bond with DXR active-site residues, such as Glu 152, Asn 227, Lys 228 and Glu 231.[105] Various methods can be used to accomplish dihydroxylation of alkenes. These include:- i) oxidation with $KMnO_4$ in an alkaline solution, in the presence of a phase transfer catalyst ii) osmium tetraoxide-mediated asymmetric dihydroxylation using a stoichiometric quantity of oxidant such as *tert*-butylhydroperoxide, H_2O_2 or *N*-methylmorpholine-*N*-oxide; and iii) the Prevost-Woodward reaction using iodine in the presence of an equivalent of silver acetate or silver benzoate.[167-169] Under anhydrous conditions (Prevost conditions), a vicinal diol with *anti* stereochemistry is formed, while in the presence of water (Woodward conditions), the *syn*-diol product is obtained.[169] However, over-oxidation of alkenes has been reported when using $KMnO_4$, while the toxicity and high cost associated with OsO_4 and, the cost of the expensive silver salts, limit the use of these reagents. In addition, these reactions depend on the nucleophilicity of the π-electron-rich alkene double bond whereas in our analogues **285a-g**, the double bond is deactivated towards electrophilic attack as a result of conjugation with the carbonyl group. Consequently, a different dihydroxylation approach was considered.

Plietker *et al.* have recently developed a $RuCl_3/CeCl_3/NaIO_4$ catalyst system for the dihydroxylation of deactivated alkenes, furnishing racemic *syn*-diol products in excellent yields.[170-171] This ruthenium-based catalytic system has also been successfully used in our group to synthesise dihydroxy coumarin derivatives as intermediates in the construction of potential HIV protease inhibitors.[162] Dihydroxylation of the phosphonated ester **284** (as a model substrate) using this catalytic system afforded the phosphonate diol **313** (Scheme 35), the structure of which was confirmed by NMR spectroscopy and elemental analysis. The mechanism of the reaction involves [3 + 2]–cycloaddition of ruthenium tetraoxide **314** (generated *in situ* from ruthenium trichloride) to the double bond in compound **284** to form the ruthenium(VI)-complex **315**, which is oxidised to the ruthenate ester **316**.[171] Subsequent protonation of the cyclic ruthenate ester **316** under acidic conditions leads to the highly electrophilic ruthenate complex **317**, which undergoes nucleophilic addition of water at the metal centre and cleavage of the ruthenium-oxygen bond, furnishing the desired *syn*-diol

313 and re-generation of the catalyst (Scheme 36). The acid-accelerated nucleophilic addition *via* protonation resembles the acid-catalysed hydrolysis of carboxylate esters.[172]

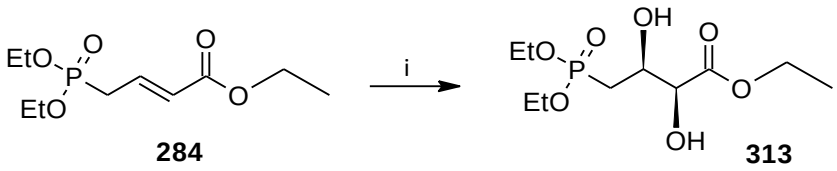

Scheme 35. Dihydroxylation of phosphonate ester **284** using the ruthenium-based catalyst system.
Reagents and conditions: i) $RuCl_3$ (0.25 mol %), $NaIO_4$ (1.5 eq.), $CeCl_3$ (10 mol %), EtOAc/CH_3CN/H_2O (3:3:1), 0 ^oC, 10 min.

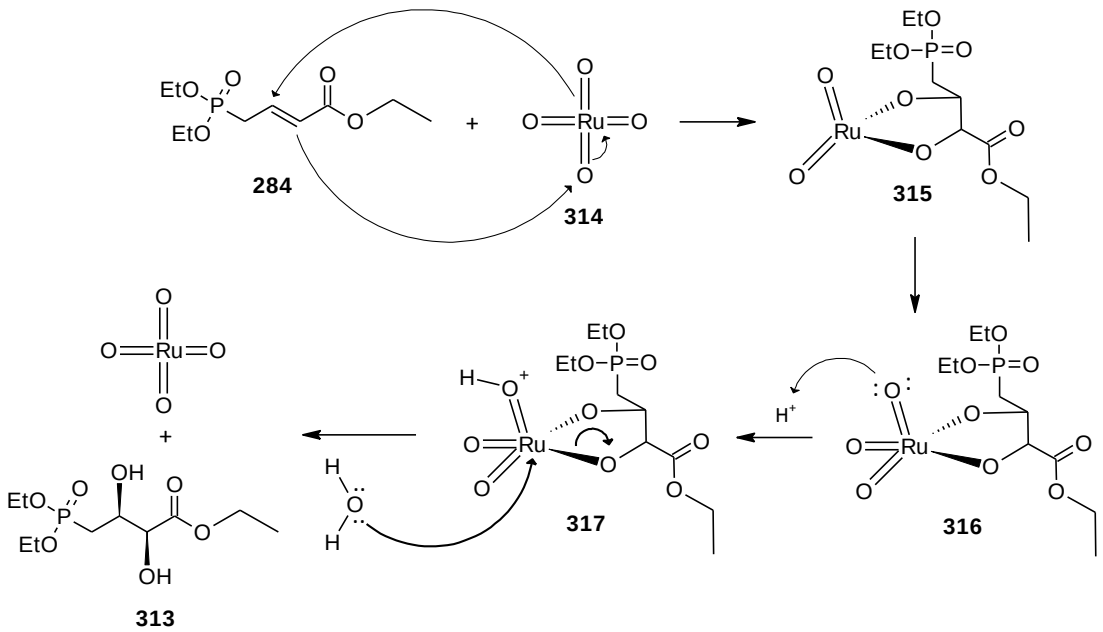

Scheme 36. Mechanism for the dihydroxylation of compound **284** using the ruthenium-based catalyst system.

The ^1H NMR spectrum (Figure 38) of compound **313** reveals the 1'-methylene and 2'-methyl proton signals of the phosphonate ethyl ester group overlapping with the signals for the ethoxy group at *ca.* 4.11 ppm and 1.28 ppm, respectively. The spectrum also confirmed the absence of the vinylic proton signals which had previously appeared between 6 and 7 ppm, supporting dihydroxylation of the double bond. The signals for the 2- and 3-methine protons appear at 4.35 and 4.33 ppm, respectively, while the pair of multiplets at 2.10 ppm and 2.3

ppm correspond to the diastereotopic methylene protons. The splitting pattern of these methylene protons reflects coupling to the adjacent ^{31}P and 3-H nuclei, as well as to each other.

While the overlap of signals in the ^{1}H NMR spectrum may preclude unambiguous characterisation of the product, the well resolved ^{13}C NMR spectrum (Figure 39) clearly supports identification of the product as the dihydroxy derivative **313**. Thus, the 1'-methylene and 2'-methyl carbon signals corresponding to the phosphonate ethyl ester group resonate as doublets, due to coupling with the ^{31}P nucleus, at 62.0 and 16.3 ppm, respectively. The signals at 14.0 ppm and 61.8 ppm correspond to the 1''-methylene and 2''-methyl carbons of the ethoxy group; the 4-methylene carbon resonates as a doublet (J = 139.1 Hz) at 29.2 ppm, while the 3- and 2-methine carbon signals appear at 67.7 ppm and 73.6 ppm, respectively. The C-1 carbonyl signal appears at 172.7 ppm.

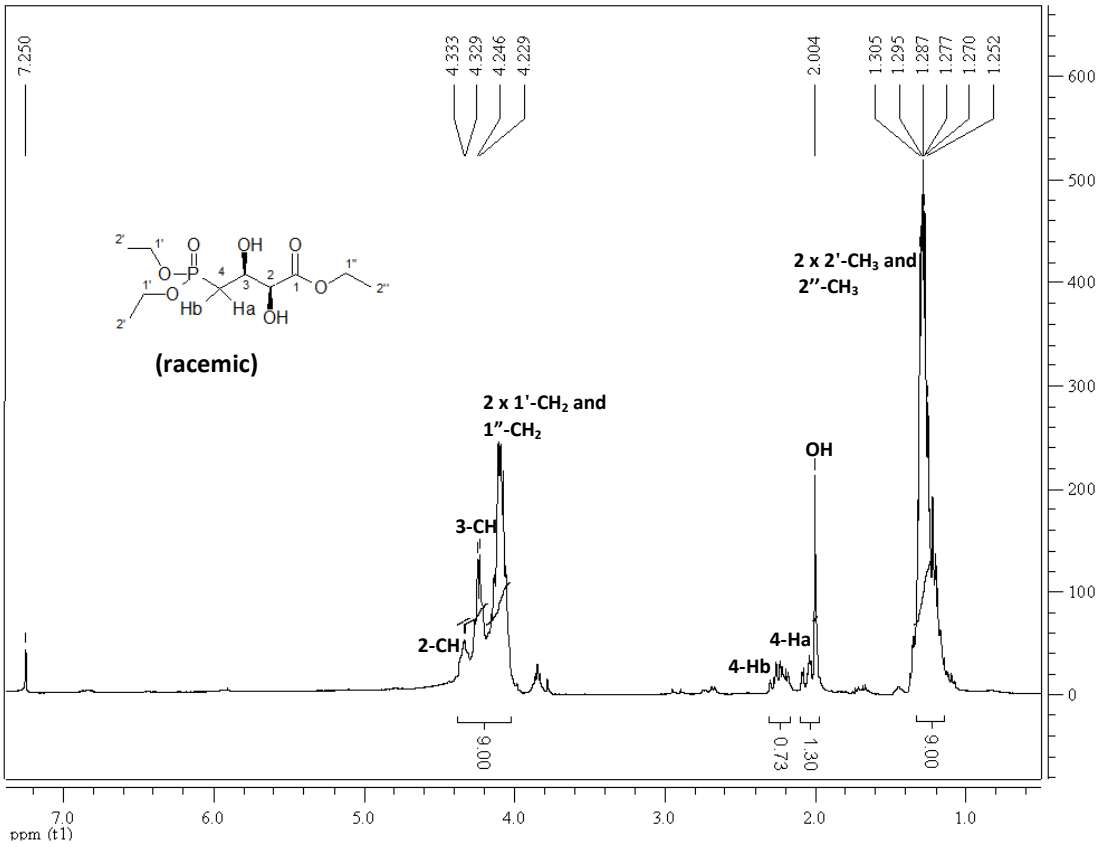

Figure 38. 400 MHZ ^{1}H NMR spectrum of compound **313** in $CDCl_3$.

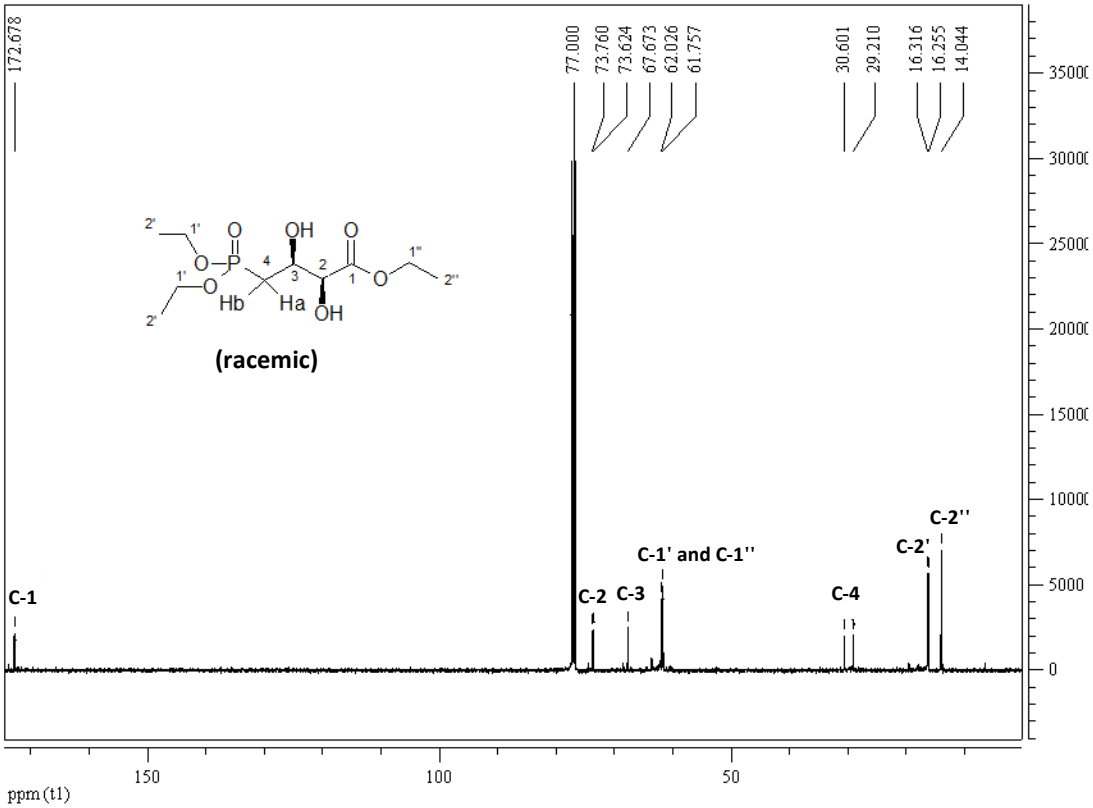

Figure 39. 100 MHz ^{13}C NMR spectrum of compound **313** in $CDCl_3$.

Given the successful dihydroxylation of the phosphonated ester **284**, using the ruthenium-based catalyst, the amide analogues **285a-g** were treated similarly to generate the dihydroxy-amido phosphonate esters **292a-g** in reasonable yields (47% - 53%, Scheme 47). These compounds were fully characterised by NMR spectroscopy, elemental analysis and IR spectroscopy; the ^{1}H and ^{13}C NMR spectra are illustrated in Figures 40 and 41.

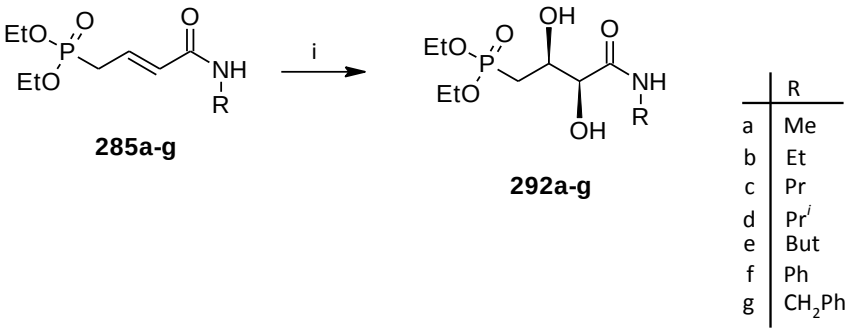

Scheme 47. Synthesis of dihydroxy-amido phosphonate esters **292a-g** using ruthenium-based catalyst system.

Reagents and conditions: i) $RuCl_3$ (0.25 mol %), $NaIO_4$ (1.5 eq.), $CeCl_3$ (10 mol %), $EtOAc/CH_3CN/H_2O$ (3/3/1), 0 ^{o}C, 10 min.

The ^{1}H NMR spectrum (Figure 40) of compound **292a** shows the 2'-methyl and 1'-methylene proton signals corresponding to the phosphonate ethyl ester group resonating at 1.20 ppm and 4.03 ppm, respectively. The 1'-methylene signal is split into a multiplet due to coupling to 2'-methyl protons and the ^{31}P nucleus. The signals corresponding to the diastereotopic 4-methylene protons resonate as a pair of multiplets as a result of geminal coupling to each other, as well as vicinal coupling to the 3-methine proton and coupling to the ^{31}P nucleus. The 3-methine proton signal is observed as a quartet (*J* = 7.2 Hz) at 3.46 ppm, while the 2-methine proton resonates as a doublet (*J* = 7.6 Hz) at 4.21 ppm, respectively. The signal corresponding to the 1''-methyl group is observed as a singlet at 2.70 ppm, while the signals for the hydroxyl and amide protons appear at 2.30 ppm and 10.29 ppm, respectively. IR spectroscopic analysis showed the hydroxyl group absorption band at 3241 cm^{-1} and amide carbonyl group absorption band at 1675 cm^{-1}.

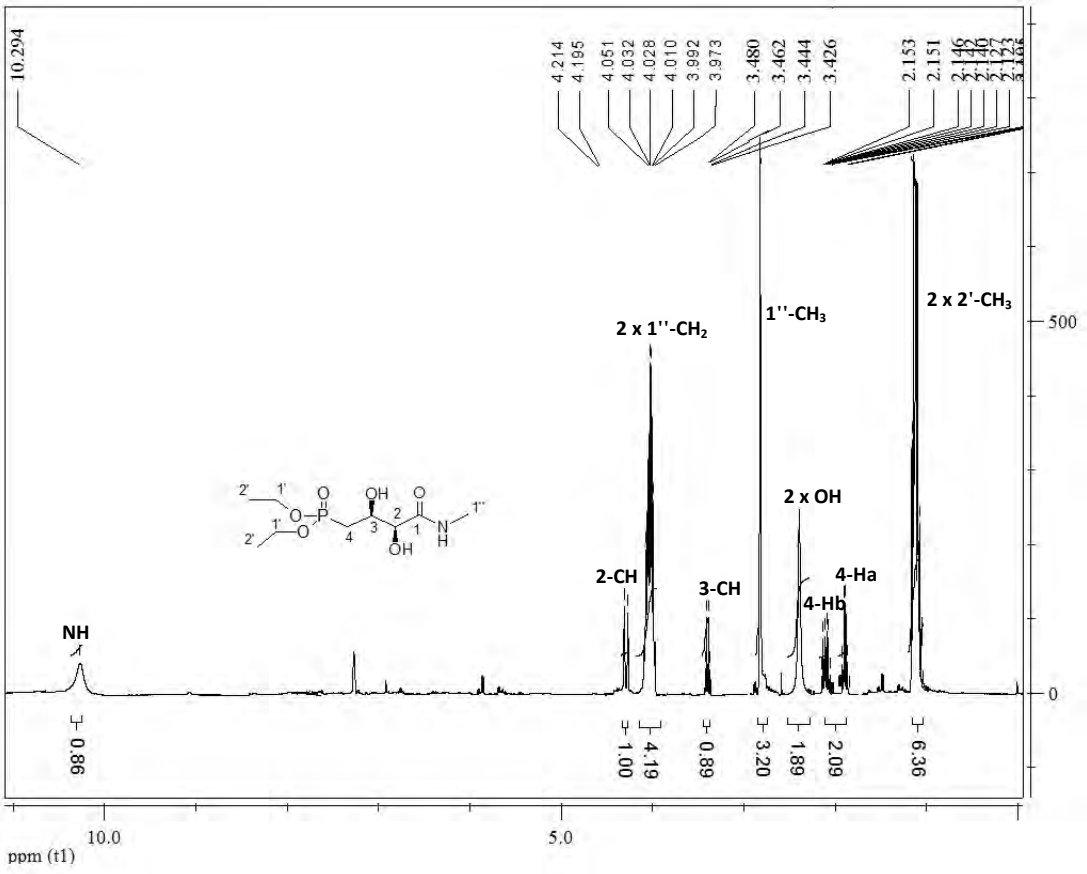

Figure 40. 400 MHz ^{1}H NMR spectrum of compound **292a** in $CDCl_3$.

In the ^{13}C spectrum of compound **392a** (Figure 41), the 1'-methylene and 2'-methyl signals corresponding to the phosphonate ethyl ester group resonate as doublets, due to coupling

to the adjacent ^{31}P nucleus, at 61.4 ppm and 16.3 ppm, respectively. The 4-methylene signal appears as a doublet (J = 141.2 Hz) at 29.2 ppm, while the 3- and 2-methine signals resonate at 58.7 ppm (J = 10.9 Hz) and 80.0 (J = 13.2 Hz) ppm, respectively. The signal at 168.6 ppm corresponds to the carbonyl carbon.

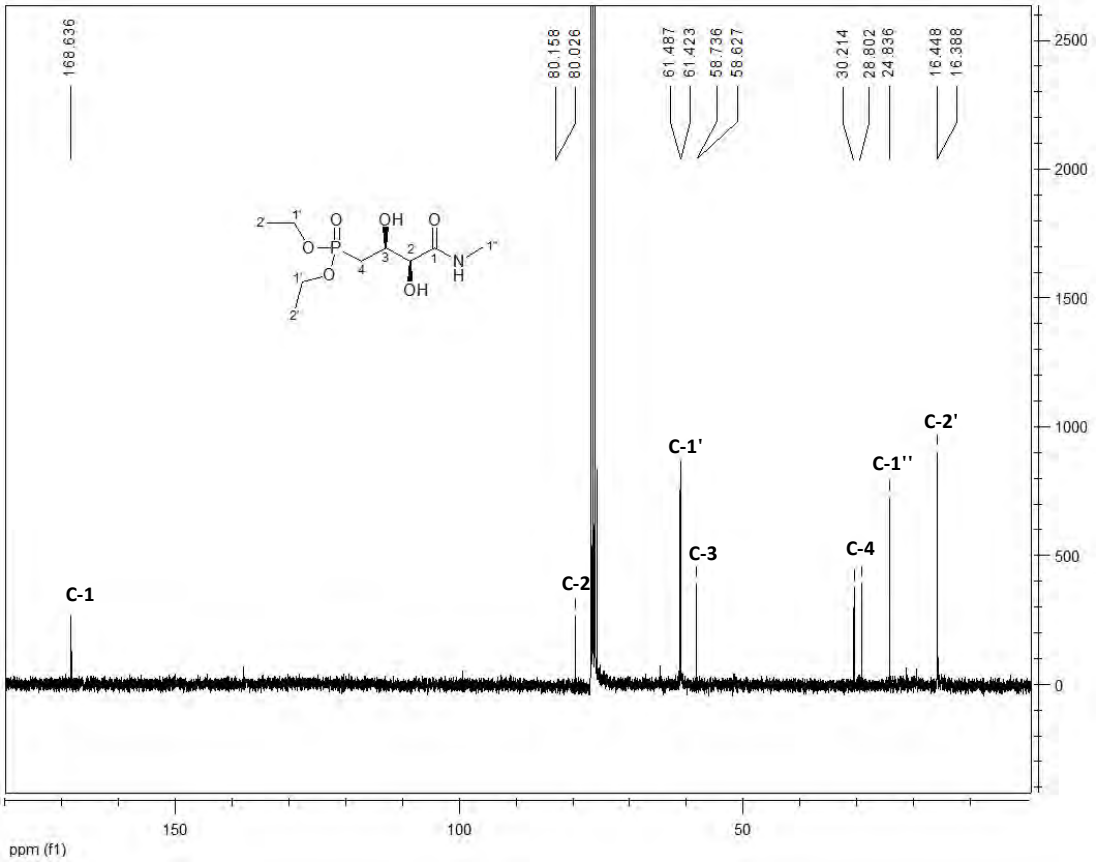

Figure 41. 100 MHz ^{13}C NMR spectrum of compound **392a** in $CDCl_3$.

The dihydroxy-amido phosphonate esters **292a-g** were expected to be sufficiently lipophilic to facilitate absorption across phospholipid membranes, and thus serve as ester pro-drug analogues of DOXP **230** and fosmidomycin **236**, being hydrolysed *in vivo* by plasma esterases.[117-118,173] Consequently, we considered it necessary to prepare the corresponding phosphonic acid derivatives **293a-g** as substrates for *in vitro* enzyme-binding and –inhibition assays. An established method for the cleavage of the ethoxy groups of phosphonate esters involves the use of trimethylsilyl bromide (TMSBr) at room temperature in dichloromethane, followed by hydrolysis.[174] This methodology has been successfully used in our group and a thorough kinetic study of the reaction has been reported.[129,142] Natarajan *et al.* have reported the microwave-assisted modification involving reaction of phosphonate esters in acetonitrile to obtain the corresponding phosphonic acids in excellent yields

(95%).[175] This modification[175] was therefore used and the phosphonate esters **292a-g** were treated with two equivalents of TMSBr in acetonitrile for ten minutes under microwave irradiation, followed by hydrolysis (Scheme 38), to furnish the dihydroxy-amido phosphonic acids **293a-g** in good yields (> 62%). The phosphonic acids **293a-g**, which are all new compounds, were fully characterised by spectroscopic (NMR and IR) and elemental analysis.

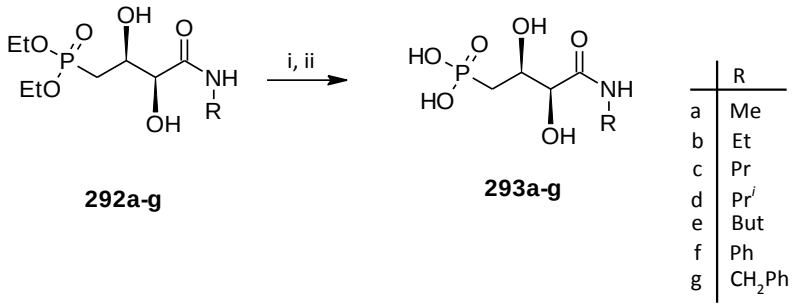

Scheme 38. Hydrolysis of dihydroxy-amido phosphonate esters **292a-g** using TMSBr.
Reagents and conditions: i) TMSBr, CH_3CN, 100 ^oC, 10 min ii) MeOH-H_2O(95:5 v/v), stir for 30 min, r.t.

The reaction involved the consecutive trans-esterification of each of the phosphonate ester groups of **292a-g** leading to the formation of the bis(trimethylsilyl) esters **318a-g**, which were hydrolysed readily to the phosphonic acids **293a-g** upon treatment with aqueous methanol (Scheme 39).

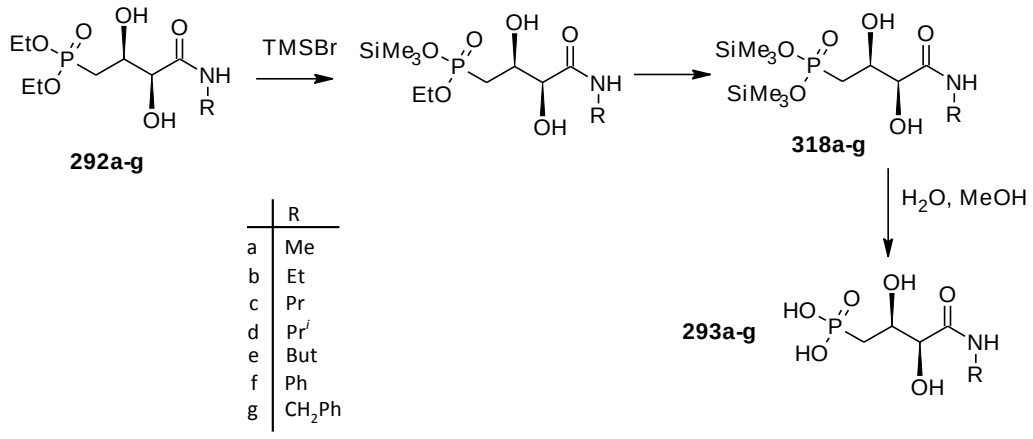

Scheme 39. Step-wise cleavage of phosphonate ethyl esters **292a-g** with TMSBr.

Comparison of the ^1H NMR spectra of the phosphonate ester **292d** and the phosphonic acid **293d** (Figure 42) clearly shows the disappearance of the signals corresponding to the 2'-

methyl and 1'-methylene phosphonate ethyl ester groups at 1.31 ppm and 4.10 ppm, respectively, and the emergence of a broad signal at 10.14 ppm corresponding to the phosphonic acid protons. Assignment of the hydroxyl signals in compound **293d** was assisted by analysis of the HMBC spectrum, which indicated correlation between the hydroxyl proton attached to C-2 and the C-1 carbonyl carbon signal. The IR spectrum reveals a broad hydroxyl group absorption band at *ca.* 3304 cm^{-1}. The assignment of all the protons in compound **293d** is illustrated in Figure 42 (bottom spectrum). In Figure 43, comparison of the ^{13}C NMR spectra of compounds **292b** and **293b** also indicate the successful cleavage of the phosphonate ethyl ester moeity in **292b** (top spectrum), as the signals corresponding to the ethyl groups, resonating at 16.1 ppm and 63.6 ppm, are absent in the spectrum of compound **293b** (bottom spectrum).

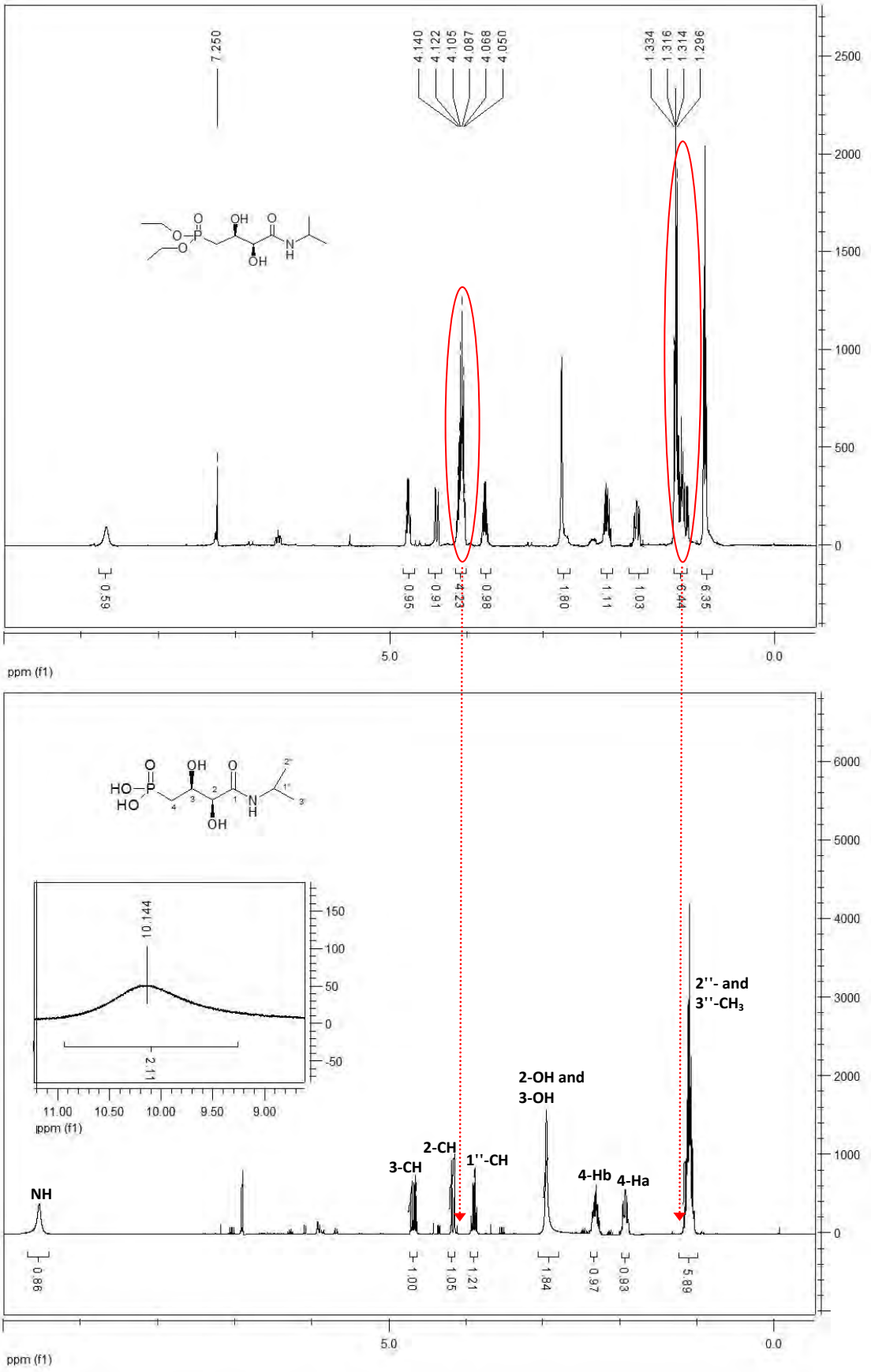

Figure 42. 400 MHz ^{1}H NMR spectra of phosphonate ester **292d** (top) and corresponding phosphonic acid **293d** (bottom) in $CDCl_3$, showing the disappearance of the phosphonate ethyl ester signals (circled) upon hydrolysis.

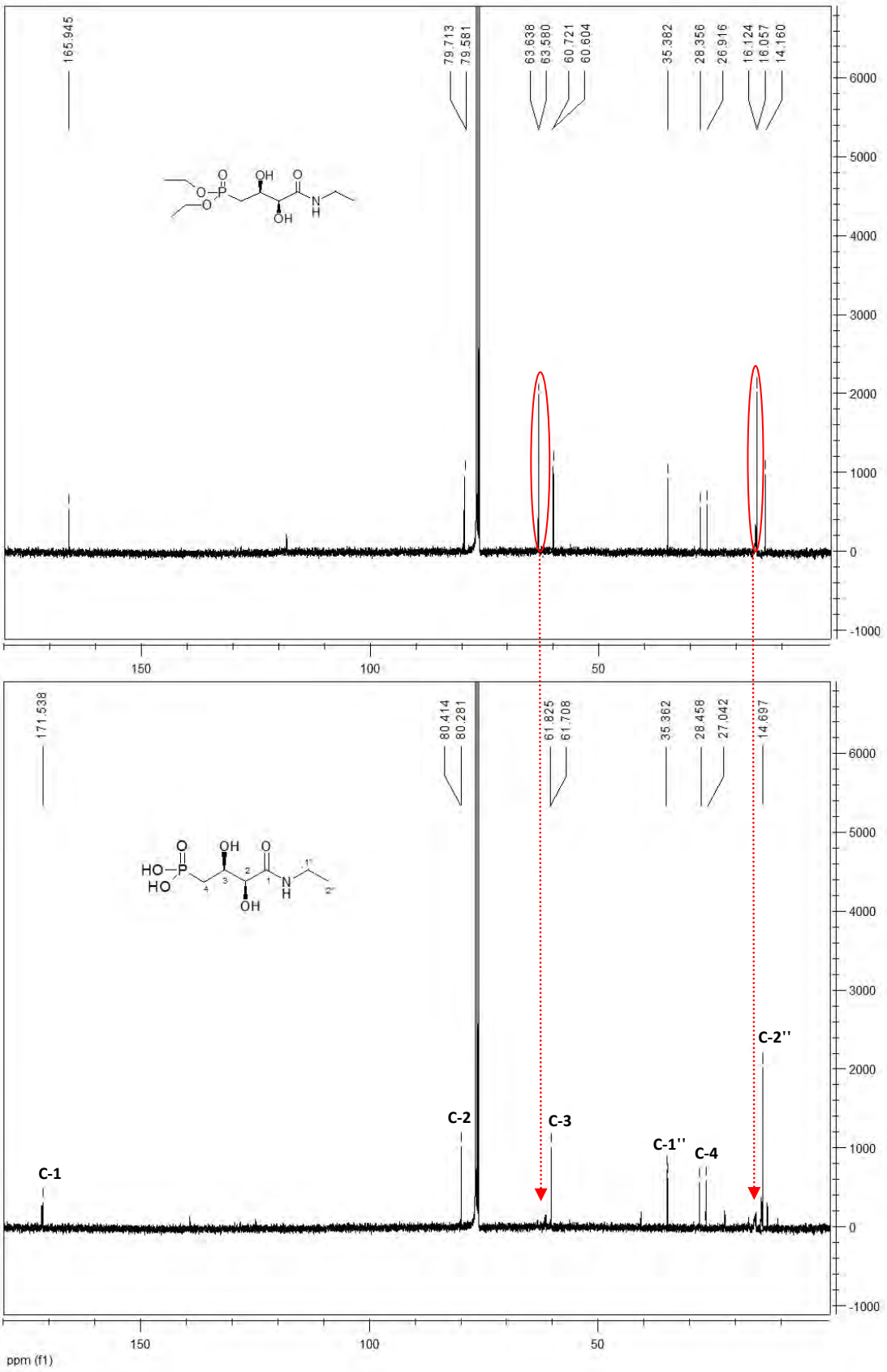

Figure 43. 100 MHz ^{13}C NMR spectra of phosphonate ester **292b** (top) and corresponding phosphonic acid **293b** (bottom) in $CDCl_3$, showing the disappearance of the phosphonate ethyl ester signals (circled) upon hydrolysis.

Thus, following the set-backs encountered with Approaches 1 and 2 (Scheme 24), the desired DOXP and fosmidomycin analogues **293a-g** were finally accessed *via* Approach 3 (Scheme 24) as outlined in Scheme 40; with the yields for the selected steps summarised in Table 4. A selection of the prepared dihydroxy-amido phosphonate esters **292a-g** and corresponding phosphonic acids **293a-g** were subjected to STD-NMR enzyme binding studies (Section 2.5), using *Ec*DXR.

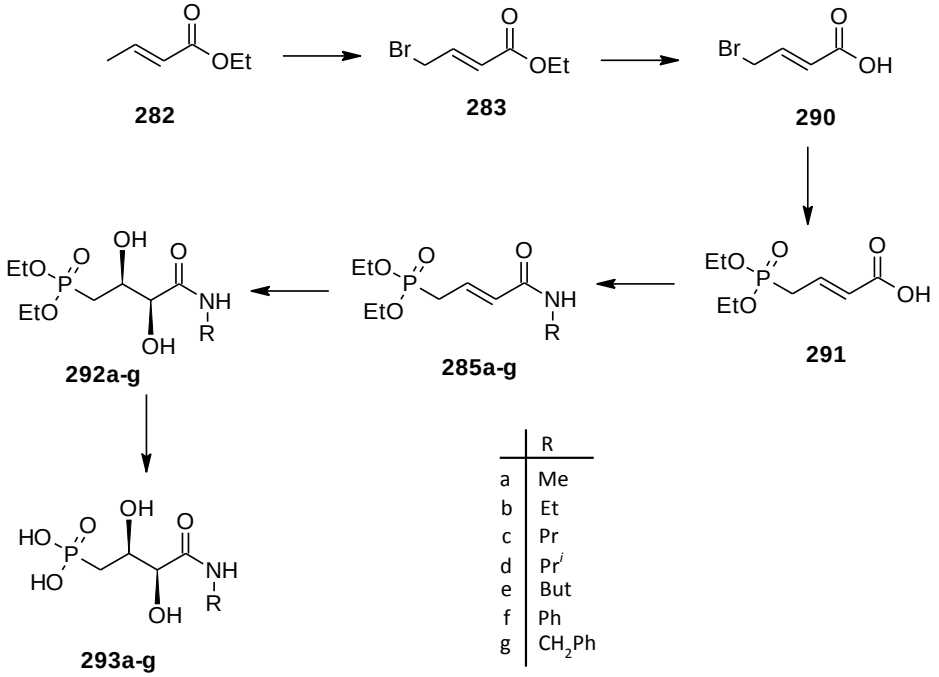

Scheme 40. Access to DOXP and fosmidomycin analogues **293a-g** *via* Approach 3.

Table 4. Yields (%) for selected steps in the preparation of the DOXP and fosmidomycin analogues **293a-g** (Scheme 43).

	R	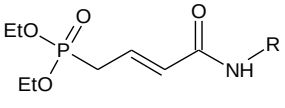		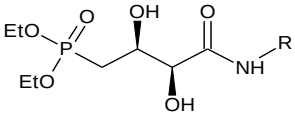		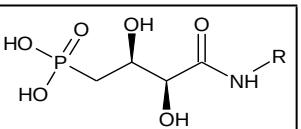	
a	Me	285a	54	292a	67	293a	80
b	Et	285b	48	292b	69	293b	77
c	Pr	285c	71	292c	67	293c	72
d	pr^i	285d	62	292d	71	293d	78
e	But	285e	65	292e	66	293e	73
f	Ph	285f	59	292f	62	293f	62
g	CH_2Ph	285g	73	292g	67	293g	74

2.2. Synthesis of 3-substituted aniline-derived phosphonate esters and phosphonic acids

As mentioned previously (section 1.8, p. 51), the anilide **277** was serendipitously discovered to exhibit binding interactions with *Ec*DXR in STD protein experiments, and shown to possess low-level inhibitory activity towards *Ec*DXR. Consequently, we have sought to prepare several series of analogues of compound **277**, with emphasis on the: - i) introduction of various meta-substituents on the benzene ring and; ii) alteration of the number of methylene groups between the amide functionality and the phosphonate group. The synthetic routes to the series of 3-substituted aniline-derived phosphonate esters (**321a-g**, **323a-g**, **325a-g** and **327a-g**) are outlined in Scheme 41. With regard to DXR structure-activity studies, the amide moiety was expected to serve as a metal-chelating group in the DXR active site and the phosphonate moiety to occupy its appropriate binding pocket. Moreover, the benzene ring should provide a degree of hydrophobicity and the anilide system a measure of conformational rigidity. The distance between the essential amide and phosphonate groups was varied, to establish the effects on DXR active-site binding and *in vitro* inhibitory activity.

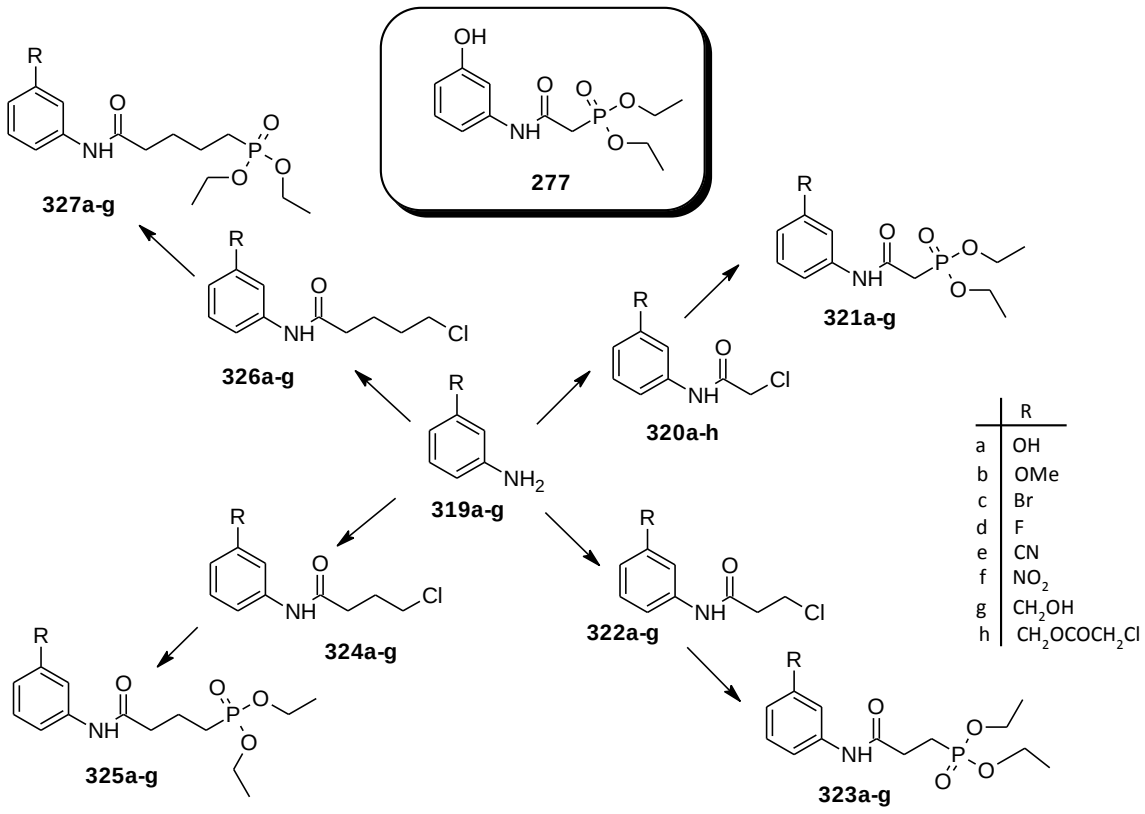

Scheme 41. Synthetic routes towards 3-substituted aniline-derived phosphonate esters.

2.2.1. Preparation of the chloroacetyl chloride-derived anilides 321a-g.

2.2.1.1. Reaction of 3-substituted anilines with chloroacetyl chloride.

The 3-substituted anilines **319a-g** were deprotonated with sodium hydride in THF, and then treated with chloroacetyl chloride (Scheme 42) to furnish the chloroacetamides **320a-g** in good yields (62% - 92%). The nucleophilicity of the primary amines **319a-g** is enhanced by deprotonation, and attack at the more electrophilic carbonyl carbon in chloroacetyl chloride leads to preferential nucleophilic acyl substitution.

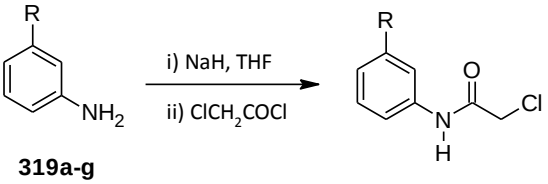

319a-g **320a-g**

	R
a	OH
b	OMe
c	Br
d	F
e	CN
f	NO_2
g	CH_2OH
h	CH_2OCOCH_2Cl

Scheme 42. Formation of chloroacetamides **320a-g.**

The structures of all of the chloroacetamides **320a-g** were confirmed by NMR and IR spectroscopic analysis. The ^{1}H NMR spectra all exhibit the presence of the characteristic chloromethylene singlet at *ca.* 4.3 ppm, as shown in Figure 44 for compound **320f**. Figures 45 and 46 show the DEPT 135 and ^{13}C NMR spectra of compound **320f**, respectively. Analysis of the DEPT 135 spectrum (Figure 45) clearly showed the chloromethylene signal at 43.4 ppm and allowed for the identification of the CH signals of the benzene ring and, identification of the carbonyl and quaternary carbon signals in the ^{13}C spectrum (Figure 46). The assignment of the benzene ring proton signals was assisted by analysis of the COSY spectrum, shown in Figure 47. The aromatic proton signals were assigned following the identification of the 2'-H singlet at 8.60 ppm and 5'-H triplet (J = 7.2 Hz) at 7.62 ppm; the 4'- and 6'-H protons both resonate at 7.95 ppm and couple with the 5'-H proton. Analysis of the HSQC and HMBC spectra confirmed the assignment of the aromatic proton and carbon signals.

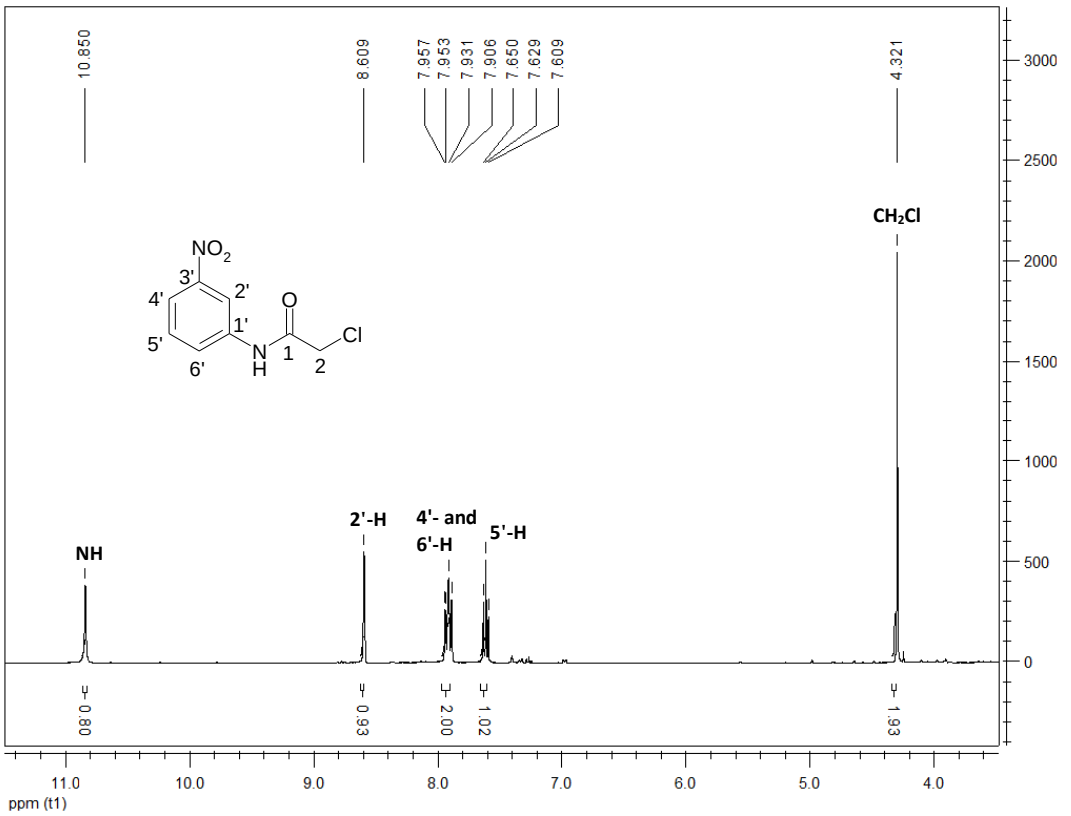

Figure 44. 400 MHZ ^{1}H NMR spectrum of compound **320f** in DMSO-d_6.

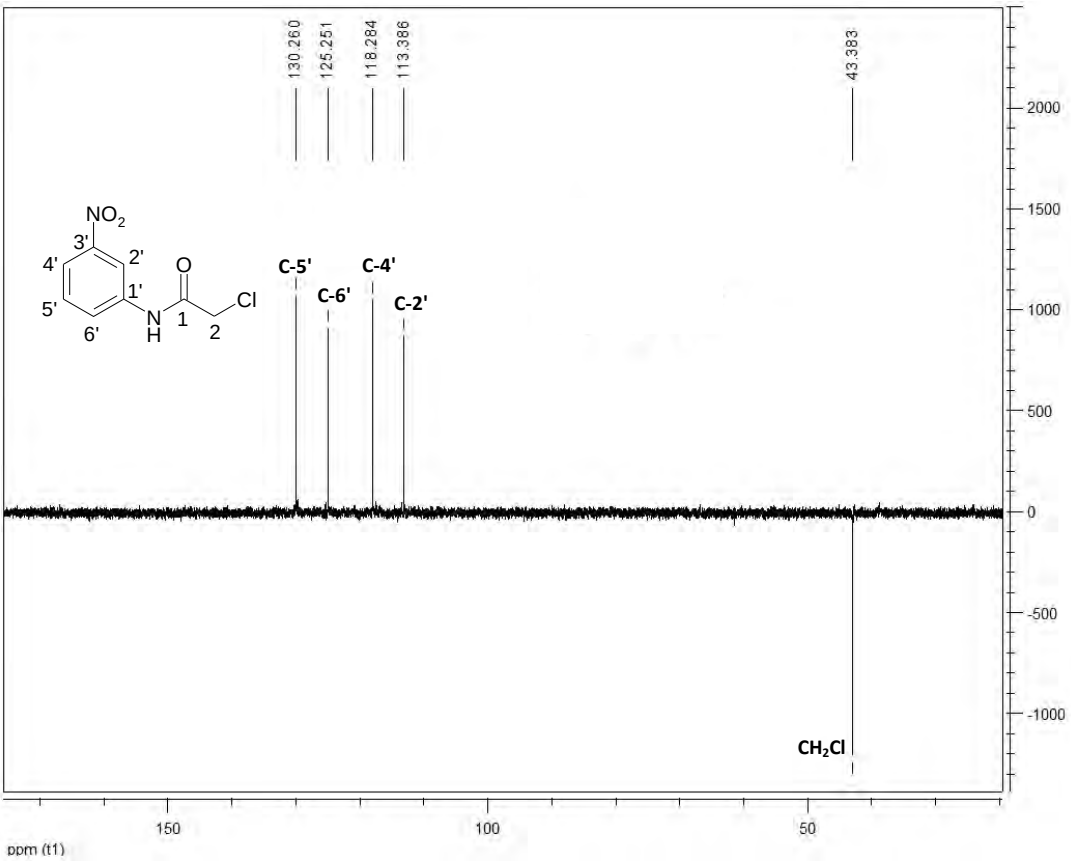

Figure 45. DEPT 135 NMR spectrum of compound **320f** in DMSO-d_6.

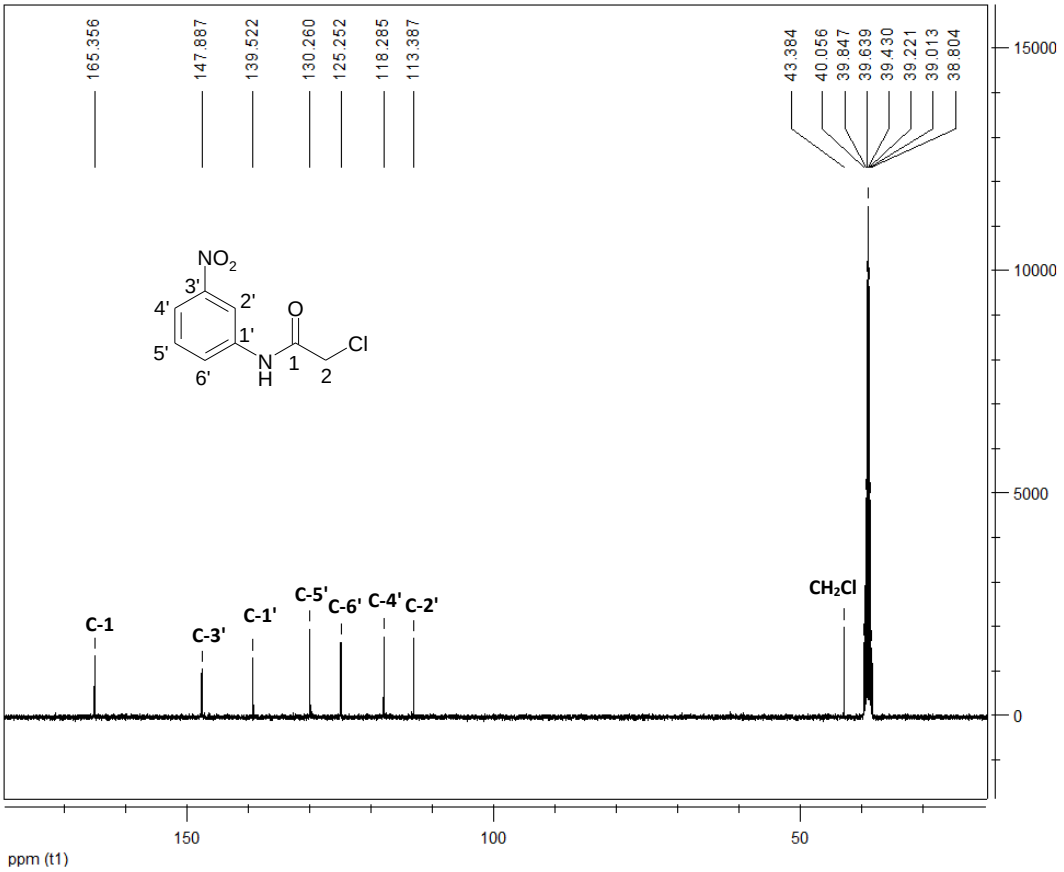

Figure 46. 100 MHz ^{13}C NMR spectrum of compound **320f** in DMSO-d_6.

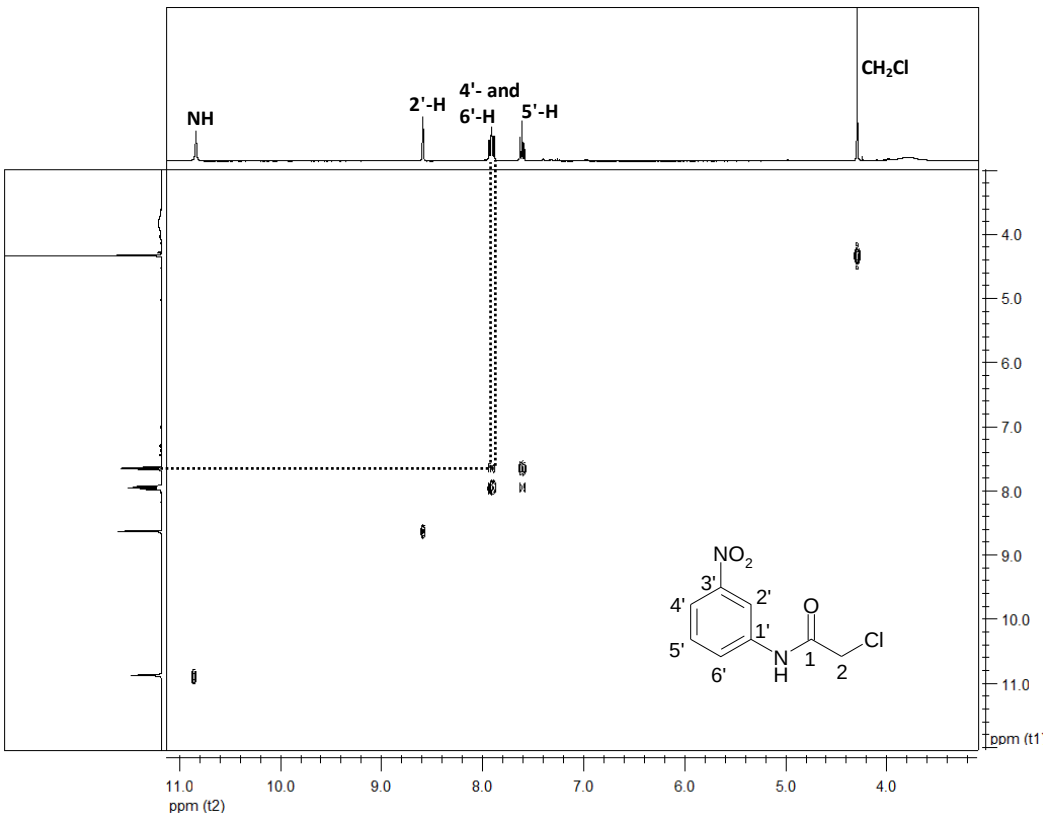

Figure 47. COSY NMR spectrum of compound **320f** in DMSO-d_6.

In addition to isolating compound **320g**, the *N,O-bis*-chloroacetylated product **320h** was also obtained in 11 % yield when 3-aminobenzyl alcohol **319g** was reacted with sodium hydride and chloroacetyl chloride. In the ^{1}H NMR spectrum of the bis-chloroacetylated product **320h** (Figure 48), the 2''- and 4'-chloromethylene protons resonate as a singlet at 4.19 ppm, while the 1'-methylene proton signal of the ester group appears at 4.32 ppm. The broad signal at 8.23 ppm corresponds to the amide proton. IR spectroscopic analysis revealed the presence of the amide carbonyl absorption band at 1673 cm^{-1} and the ester carbonyl absorption band at 1738 cm^{-1}.

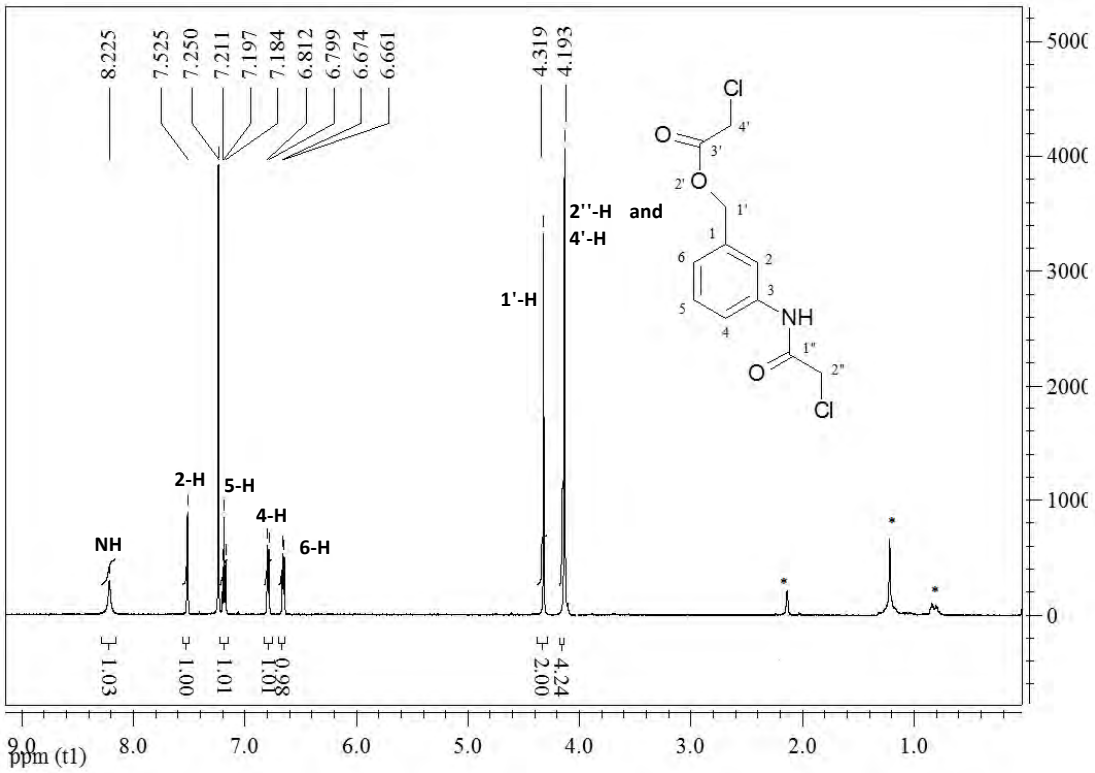

Figure 48. 400 MHZ ^{1}H NMR spectrum of compound **320h** in $CDCl_3$.
* mineral oil impurities from the storage of NaH.

2.2.1.2. Phosphonation of chloroacetamides via *Michaelis-Arbuzov reaction.*

Given the success in obtaining the chloroacetamides **320a-g**, the next step involved the introduction of the phosphonate ester group *via* the Michaelis-Arbuzov reaction.[146] Thus, the chloroacetamides **320a-g** were treated with triethyl phosphite under reflux for *ca.* 9 hours under inert atmosphere, to furnish the phosphonate esters **321a-g** in reasonable yields (48% - 72%). Compounds **321b-g** are all new and were fully characterised by NMR spectroscopy and high-resolution mass spectrometry. Figure 49 shows the ^{1}H NMR

spectrum of compound **321b**. The triplet at 1.34 ppm and the quintet at 4.17 ppm are characteristic of the phosphonate ethyl ester moiety, and hence, were observed for all of the phosphonate esters synthesised in the series. In addition, the disappearance of the chloromethylene singlet at 4.20 ppm and the emergence of the characteristic phosphonate 2'-methylene proton signal at 2.97 ppm, resonating as a doublet with large coupling constant (J = 20.8 Hz) due to ^{31}P nucleus coupling, clearly indicated the formation of the desired product. The singlet at 3.78 ppm corresponds to the methoxy methyl protons, while the amide proton resonates at 8.85 ppm.

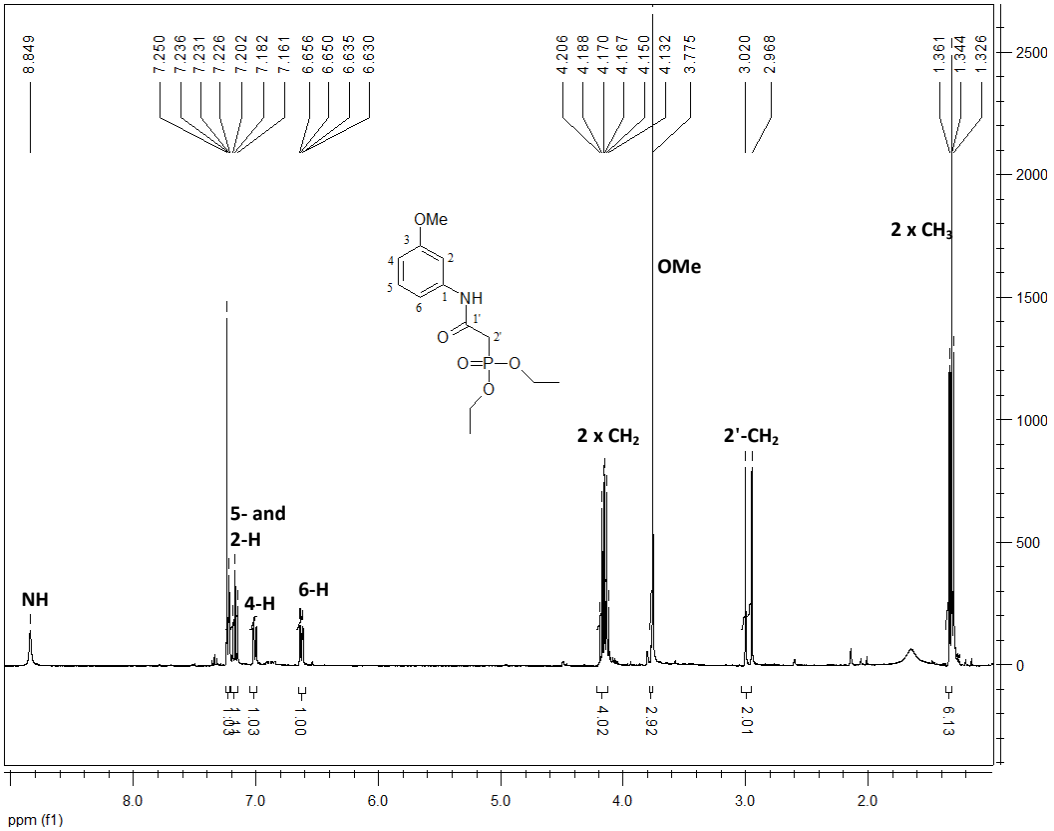

Figure 49. 400 MHZ ^{1}H NMR spectrum of compound **321b** in $CDCl_3$.

In the ^{1}H NMR spectrum for compound **321d** (Figure 50), the characteristic triplet and quintet signals corresponding to the phosphonate ethyl ester moiety are clearly seen at 1.35 ppm and 4.18 ppm; the 2'-methylene proton resonates at 2.99 ppm, with a large coupling constant of 20.8 Hz.

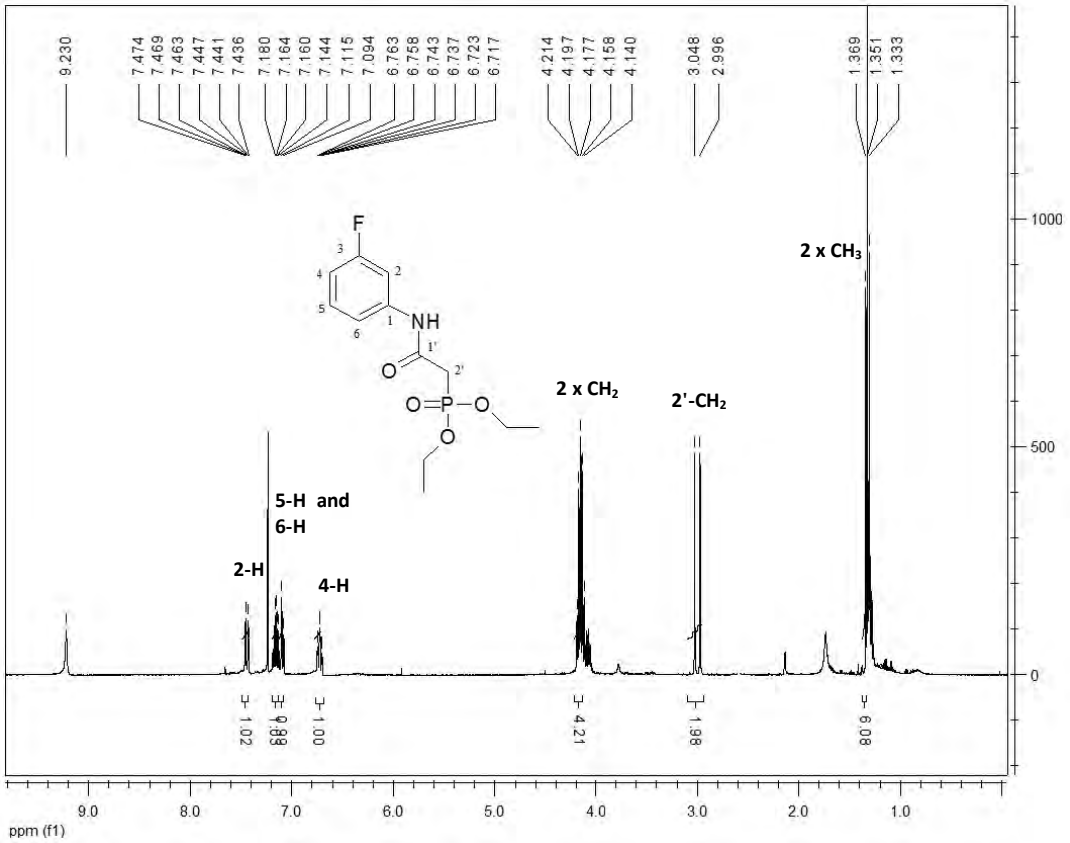

Figure 50. 400MHz ^{1}H NMR spectrum of compound **321d** in $CDCl_3$.

The complex coupling observed in the aromatic region of the ^{1}H NMR spectrum of the 3-fluoro analogue **321d** (Figure 50) between 6.60 ppm and 7.80 ppm is reproduced in Figure 51 and is worthy of further discussion. The 4-H nucleus resonates at 6.74 ppm as a triplet of doublets due to coupling to the ^{19}F nucleus (J = 2.0 Hz), in addition to coupling to both the 5-H (J = 6.0 Hz) and 2-H (J = 2.4 Hz) nuclei. The doublet at 7.09 ppm corresponds to 6-H, which couples to 5-H (J = 6.4 Hz), while the 5-H nucleus resonates at 7.16 ppm as a triplet of doublets, as a result of coupling to the 4- and 6-H (J = 6.4 Hz) and the ^{19}F nucleus (J = 1.6 Hz). Analysis of the COSY and HSQC data supported these assignments.

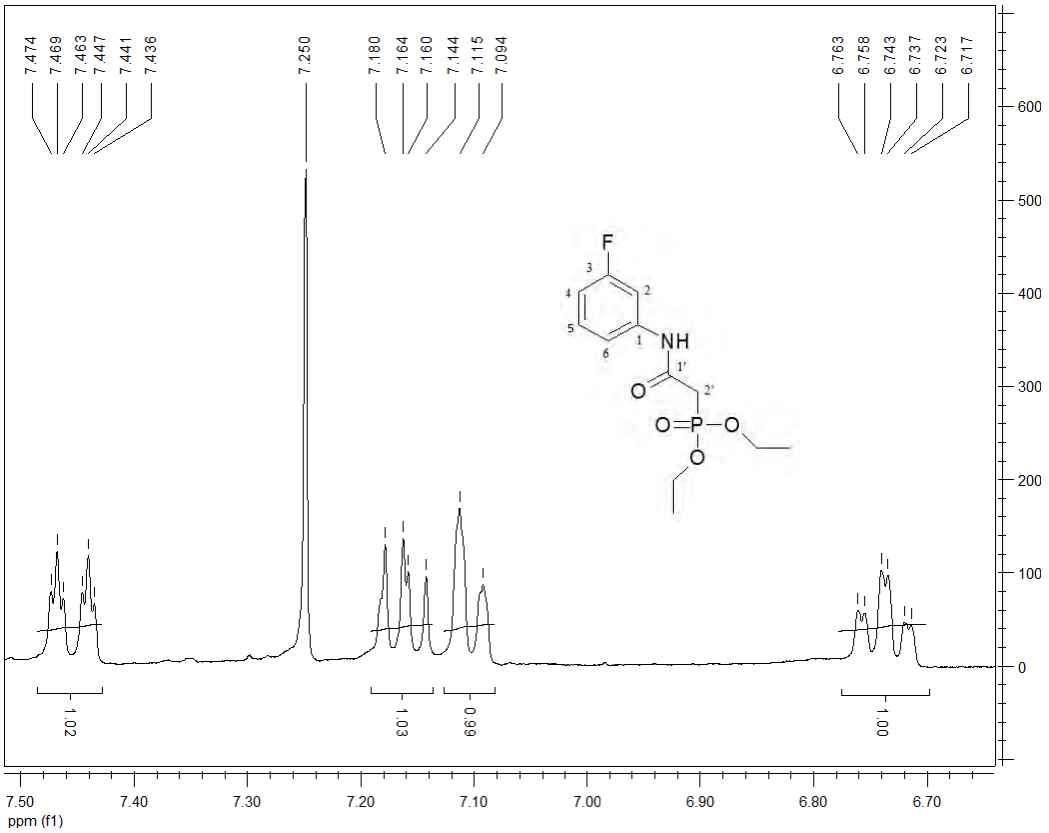

Figure 51. Expanded region of the 400 MHz ^{1}H NMR spectrum of compound **321d** in $CDCl_3$.

2.2.1.3. Hydrolysis of methyl phosphonate esters using TMSBr.

The next step involved the preparation of the phosphonic acid derivatives **328a-g** and the corresponding sodium phosphonate salts **329a-g** for the *in vitro* enzyme inhibition assays, since the phosphonate esters **321a-g** are expected to be hydrolysed *in vivo*. The cleavage of the phosphonate ethyl ester group was accomplished, as described previously, using TMSBr in acetonitrile under microwave irradiation,[175] followed by hydrolysis at room temperature (Scheme 43). The phosphonic acids **328a-g** were isolated in reasonable yields (42% - 67%) and subsequently converted, quantitatively, to their corresponding sodium phosphonate salts **329a-g** through treatment with 0.1M aqueous sodium hydroxide. All the products prepared in these reactions are new and were fully characterised by elemental and spectroscopic analysis.

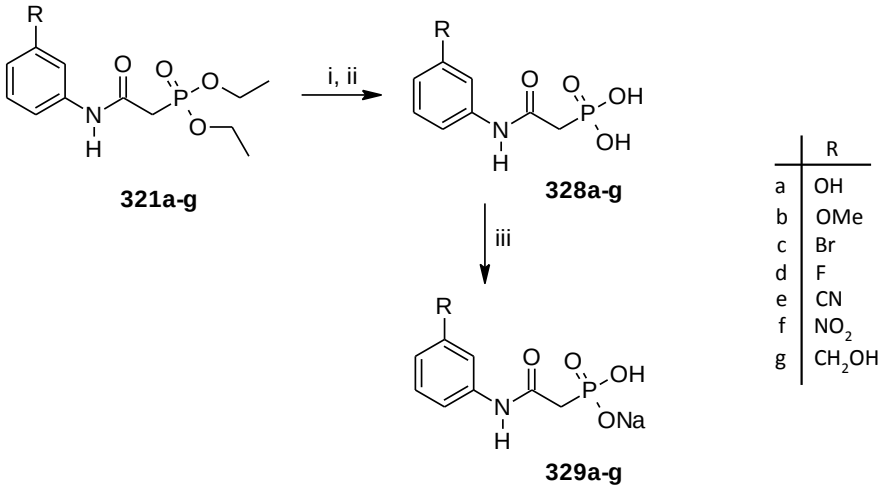

Scheme 43. Synthesis of phosphonic acid derivatives **328a-g** and corresponding mono-sodium salts **329a-g**.

Reagents and conditions: i) TMSBr, CH_3CN, microwave irradiation, 100 ^{o}C, 10 min ii) MeOH-H_2O (95:5 v/v), 30 min, r.t. iii) 1.1 mol NaOH, EtOH, 30 min, r.t.

Comparison of the ^{1}H NMR spectra of the phosphonate ester **321f** and the phosphonic acid **328f** (Figure 52) clearly shows the disappearance of the phosphonate ethyl ester signals following hydrolysis. As expected, the corresponding signals are also absent in the ^{13}C spectrum of the phosphonic acid. A selection of the synthesised 3-substituted aniline phosphonate esters **321a-g**, phosphonic acids **328a-g** and corresponding monosodium salts **329a-g** were subjected to *Ec*DXR-STD NMR binding studies and inhibition assays (Section 2.5).

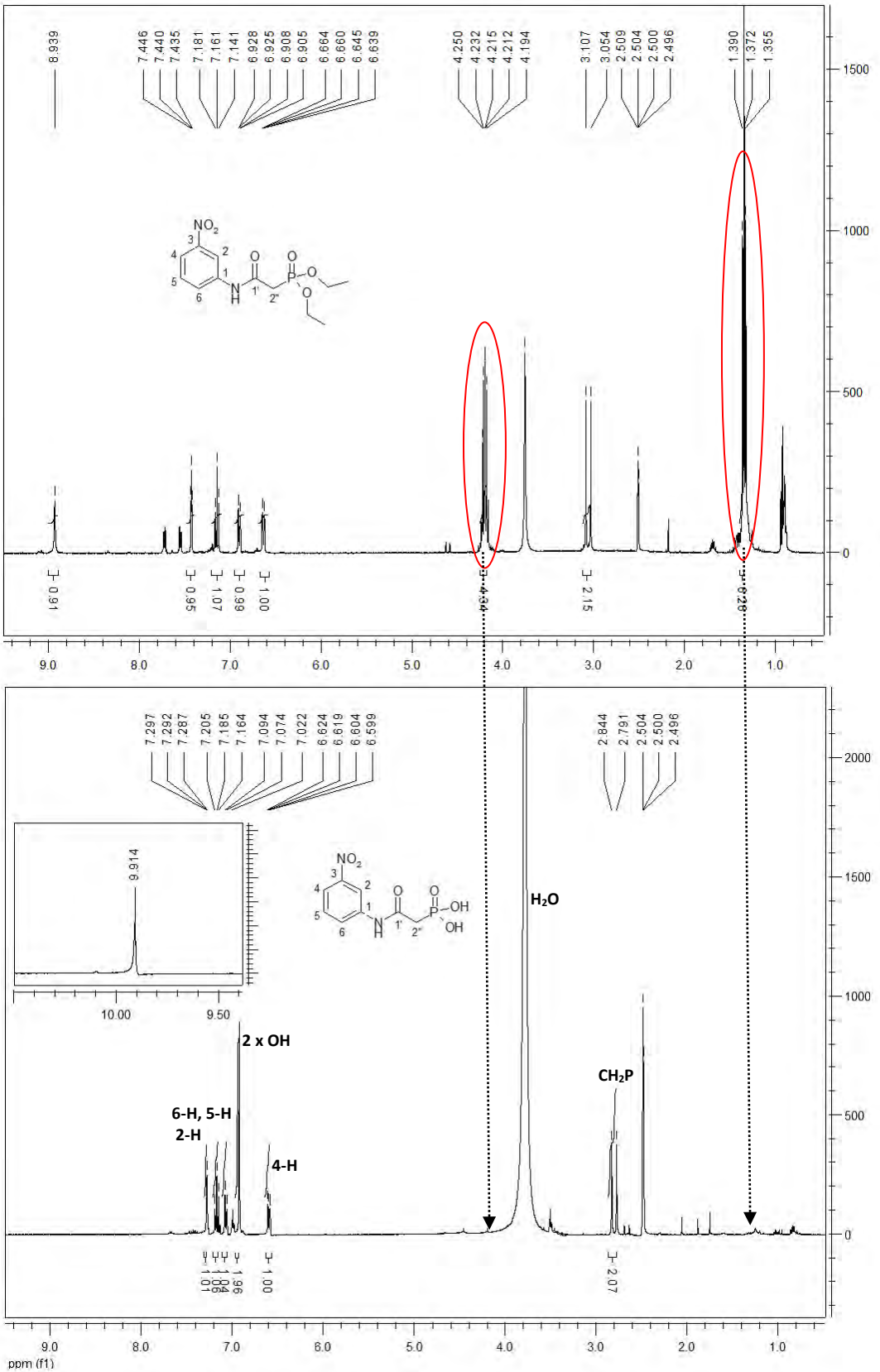

Figure 52. 400 MHz ^{1}H NMR spectra of phosphonate ester **321f** (top) and phosphonic acid **328f** (bottom) in DMSO-d_6, showing the disappearance of phosphonate ethyl ester signals (circled) upon hydrolysis.

2.2.2. Preparation of the ω-chloropropionyl chloride-derived anilides 322-327a-g.

An increase in inhibitory activity has been observed for several fosmidomycin analogues in which the distance between the phosphonate and hydroxamate moieties has been increased.[117,131] Consequently, attention was given to introducing additional methylene groups between the two essential functional groups by reacting the various 3-substituted anilines **319a-g** with 3-chloropropionyl chloride **330**, 4-chlorobutanoyl chloride **330a** and 5-chloropentanoyl chloride **332**, in place of chloroacetyl chloride which was successfully used to prepare compounds **321a-g** (scheme 41). The ω-chloroamide derivatives **322a-g**, **324a-g** and **326a-g** were isolated in good yields upon the deprotonation of the appropriate 3-substituted aniline substrates **319a-g** with sodium hydride, followed by reaction with the ω-chloroalkanoyl chlorides **330-330b**. The corresponding phosphonate esters **323a-g**, **325a-g** and **327a-g** were obtained in reasonable yields ranging from 48% to 74% using Michaelis-Arbuzov's reaction.[146] Microwave-assisted reaction of the phosphonate esters with TMSBr, [175] followed by hydrolysis, furnished the corresponding phosphonic acid derivatives **331a-g**, **333a-g** and **335a-g**, which were subsequently treated with 0.1M aqueous sodium hydroxide to furnish the sodium phosphonic acid salts **332a-g**, **334a-g** and **336a-g** (Scheme 44).

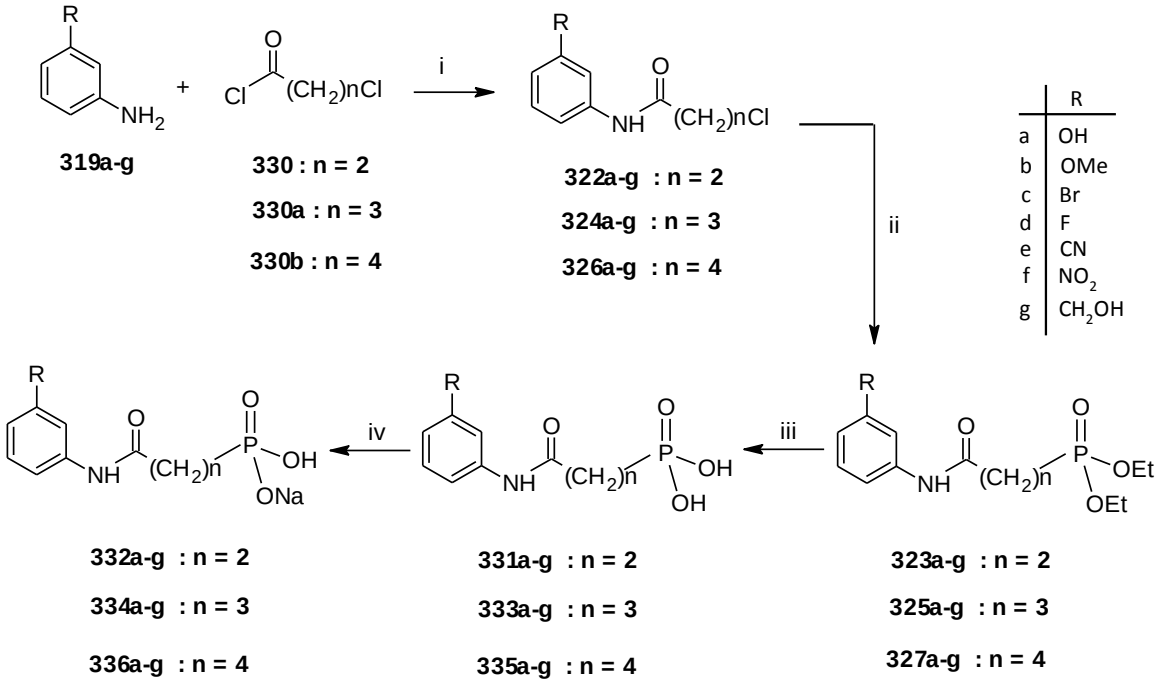

Scheme 44. Preparation of extended chain aniline-derived phosphonate esters and acids.
Reagents and conditions: i) NaH, THF, 6 h, N_2 ii) triethyl phosphite, 9 h, N_2 iii) TMSBr, CH_3CN, 100 ^oC, 10 min, MeOH-H_2O (95:5 v/v), 30 min, r.t., iv) 1.1 mol NaOH, EtOH, 30 min, r.t.

All of the compounds prepared as outlined in Scheme 44 were fully characterised. Their ^{1}H, ^{13}C and DEPT 135 NMR spectra all illustrate the effects of increasing the number of methylene groups. Comparison of the ^{1}H NMR spectra of the ω-chloro-*N*-alkylanilides **322b**, **324b** and **326b** (Figure 53), for example, clearly show the presence of a pair of triplet (*J* = 6.4 Hz) signals at 2.78 and 3.85 ppm integrating for two protons each, and thus, corresponding to the 3- and 2-methylene groups of compound **322b.** The presence of a quintet at 2.17 ppm and a pair of triplets at 2.53 ppm and 3.63 ppm in the ^{1}H NMR spectrum of compound **324b** confirmed the presence of the propylene linking group. The 3-methylene group couples to both the 2- and 4-methylene groups and thus resonates as a quintet (*J* = 6.8 Hz) signal at 2.17 ppm, while the triplets (*J* = 6.8 and 6.4 Hz) at 2.53 ppm and 3.63 ppm correspond to the 2-and 4-methylene groups, respectively. Analysis of the ^{1}H NMR spectrum of compound **326b** show a series of methylene signals integrating for eight protons, confirming the butylene linkage group between the phosphonate and amide functional moieties. The 3- and 4-methylene protons correspond to the triplet (*J* = 3.6 Hz) signal at 1.78 ppm, while the pair of triplets (*J* = 6.8 and 6.4 Hz) resonating at 2.29 ppm and 3.49 ppm represent the 2-and 5-methylene groups, respectively.

The singlet at *ca.* 3.80 ppm in each of the ^{1}H NMR spectra (Figure 53) of the products **322b**, **324b** and **326b** corresponds to the methoxy methyl protons. The signals resonating between 6.60 ppm and 7.28 ppm integrate for four protons and correspond to the aromatic protons and, were assigned as follows; the 4'-H and 6'-H nuclei resonate at *ca.* 6.62 ppm and 6.96 ppm as doublets (*J* = 8.4 and 8.0 Hz), while at the 5'-H nucleus resonates at *ca.* 7.16 ppm as a triplet (*J* = 8.4 Hz) as a result of coupling to the 4'-and 6'-H nuclei. In the ^{1}H NMR spectra for compound **322b** and **324b** (Figure 53), the amide proton resonates at *ca.* 7.50 ppm, whereas the same proton signal is observed at 8.12 ppm for compound **326b**.

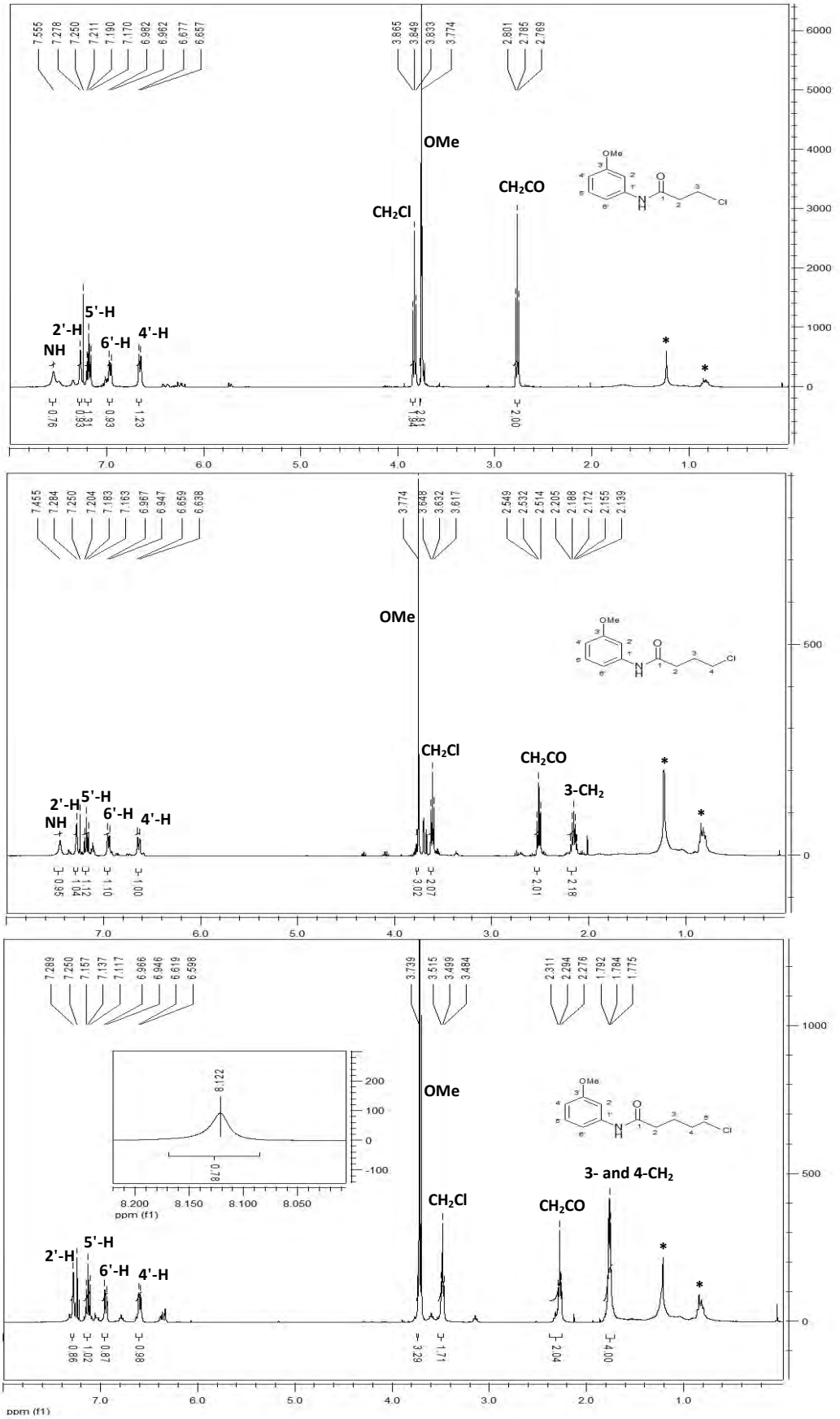

Figure 53. Comparative 400 MHz ^{1}H NMR spectra of compounds **322b**, **324b** and **326b** in $CDCl_3$, illustrating the increase in the number of methylene groups. *mineral oil impurities.

The ^{1}H and ^{13}C NMR signal assignments are supported by 2-D NMR data as illustrated for the set of spectra for the phosphonate ester **323b**, shown in Figures 54-59. ^{1}H NMR analysis (Figure 54) of the phosphonate ester **323b** showed the characteristic triplet and multiplet signals corresponding to the phosphonate ethyl ester moiety resonating at 1.31 and 4.10 ppm. The singlet at 3.78 ppm corresponds to the methoxy methyl protons while the amide proton resonates at 8.87 ppm. The complex splitting patterns seen for the 3- and 2-methylene signals resonating at 2.17 and 2.70 ppm, respectively, is as a result of coupling to each other and to the ^{31}P nucleus. Coupling between the 2- and 3-methylene protons and coupling of the phosphonate ethyl ester signals is clearly evident in the COSY spectrum (Figure 55). Comparison of the ^{1}H-^{1}H coupling constants and analysis of the COSY spectrum allowed for the assignment of the aromatic proton signals.

The DEPT 135 spectrum (Figure 56) clearly showed the signals of the 2-and 3-methylene nuclei resonating at 20.7 and 29.9 ppm and allowed for the identification of the quaternary aromatic carbon signals in the ^{13}C spectrum (Figure 57). The splitting (J= 142.5 Hz) of the signal at 20.7 ppm in the ^{13}C spectrum permitted assignment of this signal to the 3-methylene carbon adjacent to the ^{31}P nucleus, while the doublet (J = 3.3 Hz) at 29.9 ppm corresponds to the 2-methylene carbon. The 1'-methylene and 2'-methyl signals corresponding to the phosphonate ethyl ester group resonate as doublets, due to coupling to the adjacent ^{31}P nucleus, at 62.8 and 16.4 ppm, respectively. Analysis of the HSQC spectrum (Figure 58) confirmed the assignment of the aromatic carbon and protons signals and the methoxy carbon signal at 55.2 ppm. The HMBC spectrum (Figure 59) shows correlation of the C-2 carbon signal to the 3-methylene protons and, likewise, the C-3 carbon signal to the 2-methylene protons. Analysis of the HMBC spectrum confirmed the assignment of the aromatic proton and carbon signals and allowed assignment of the carbonyl carbon signal due to correlation with the 2- and 3- methylene protons.

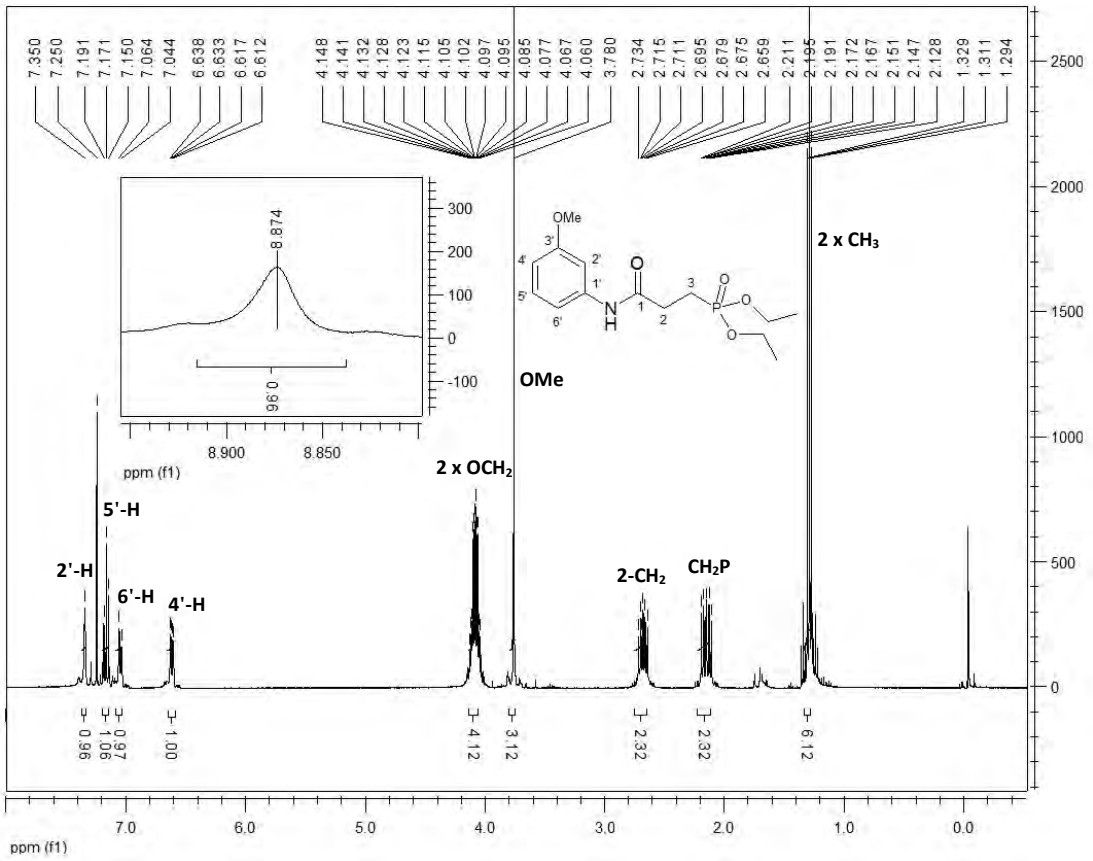

Figure 54. 400MHz ^{1}H NMR spectrum of compound **323b** in $CDCl_3$.

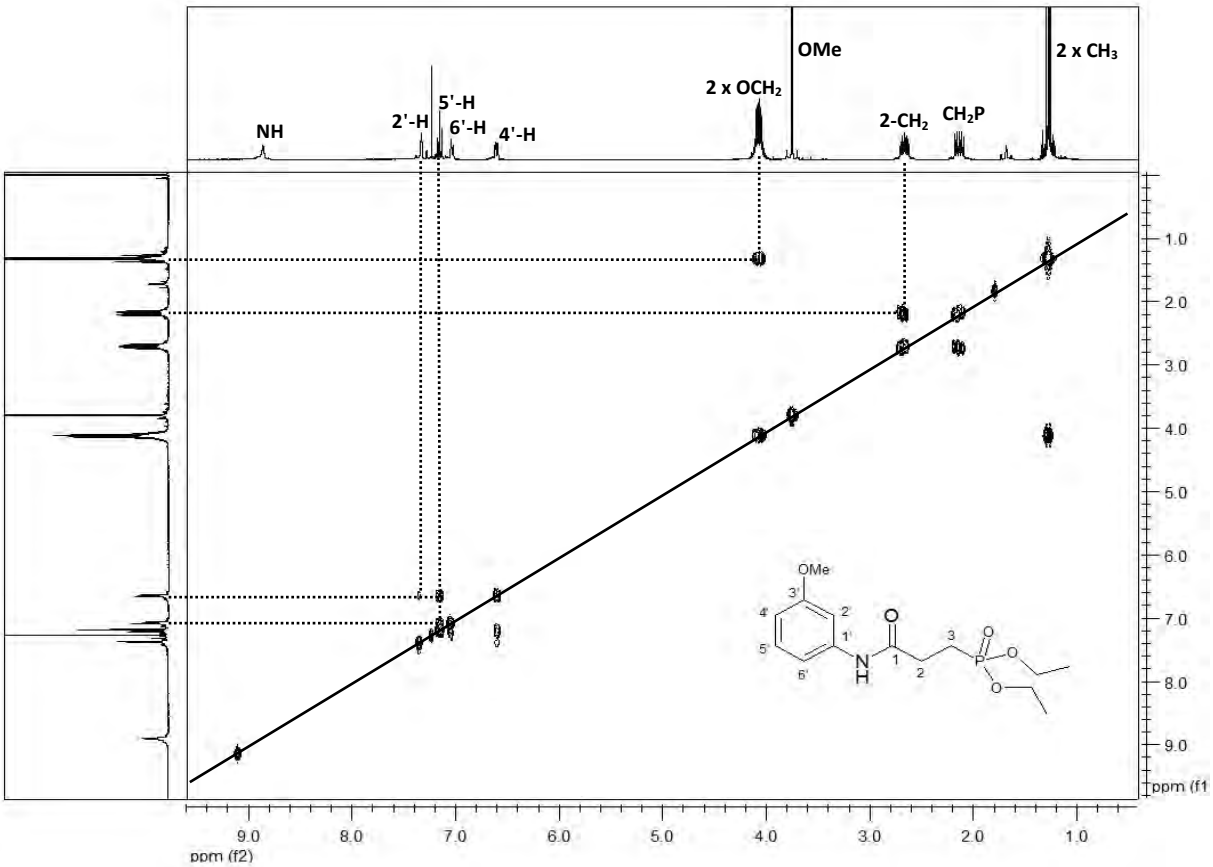

Figure 55. COSY NMR spectrum of compound **323** in $CDCl_3$.

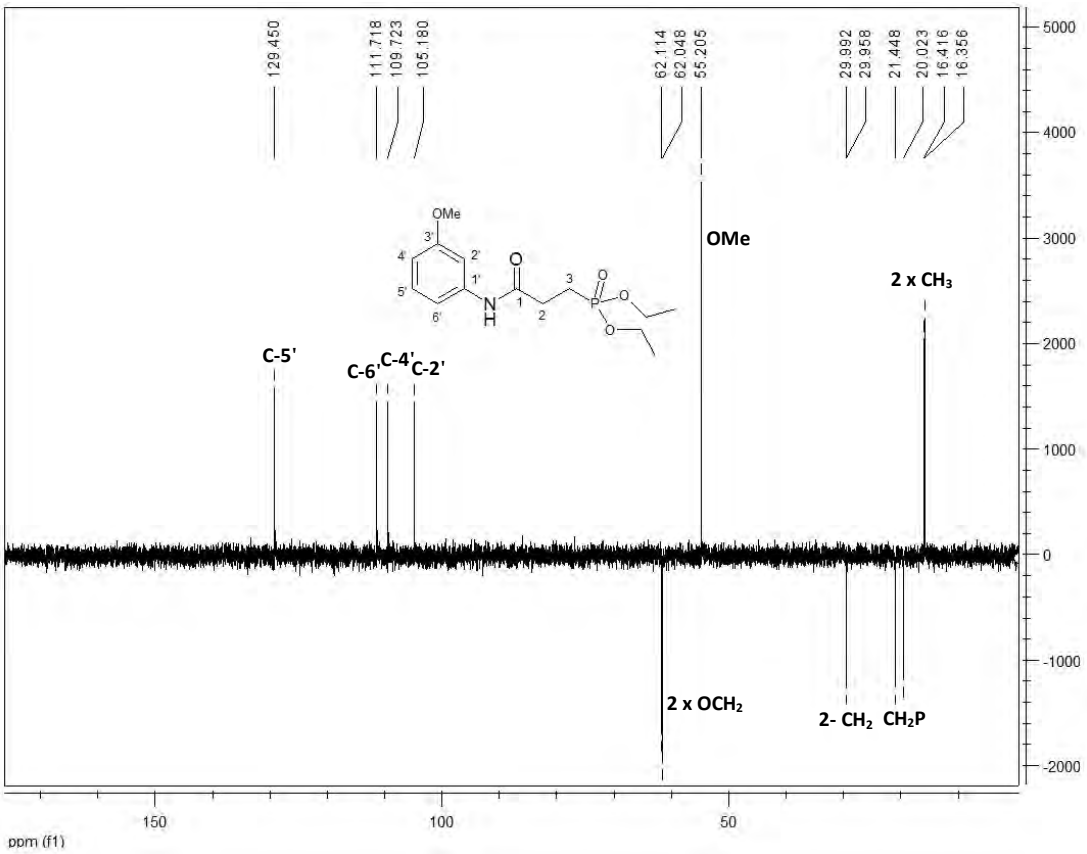

Figure 56. DEPT 135 NMR spectrum of compound **323b** in $CDCl_3$.

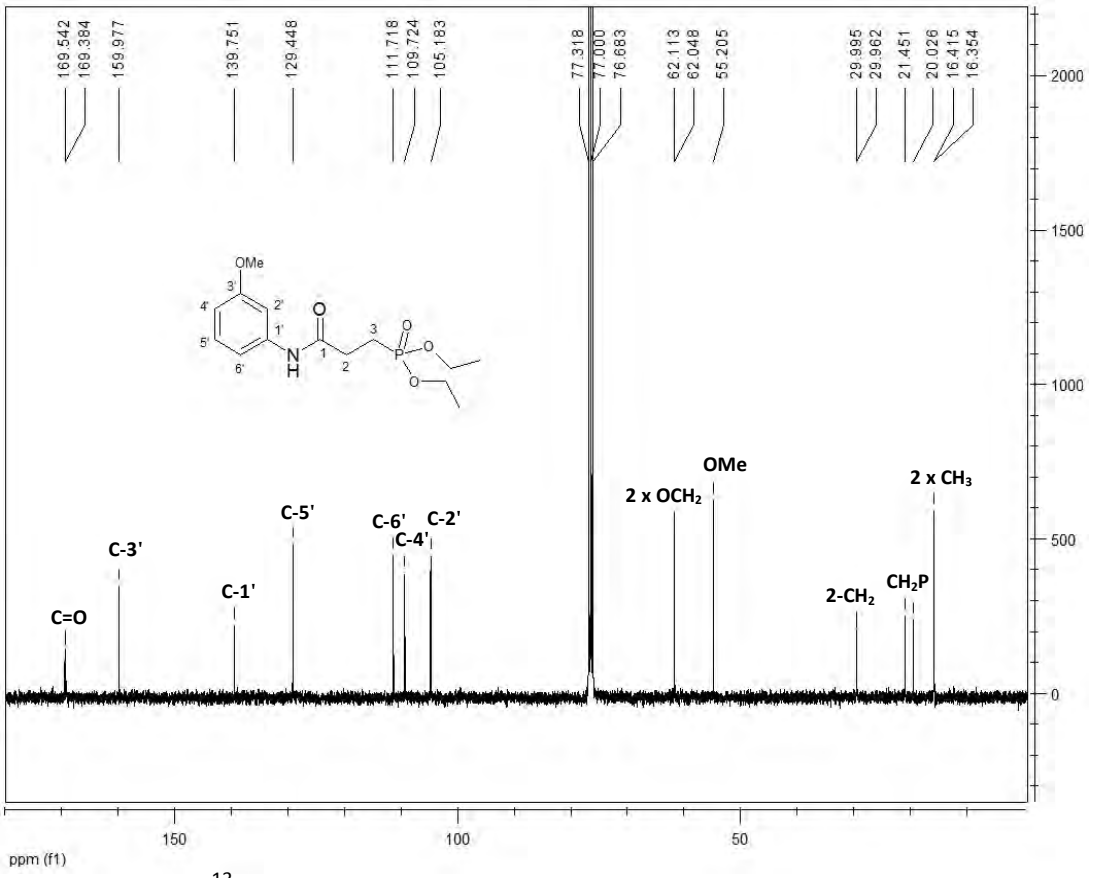

Figure 57. 100 MHz ^{13}C NMR spectrum of compound **323b** in $CDCl_3$.

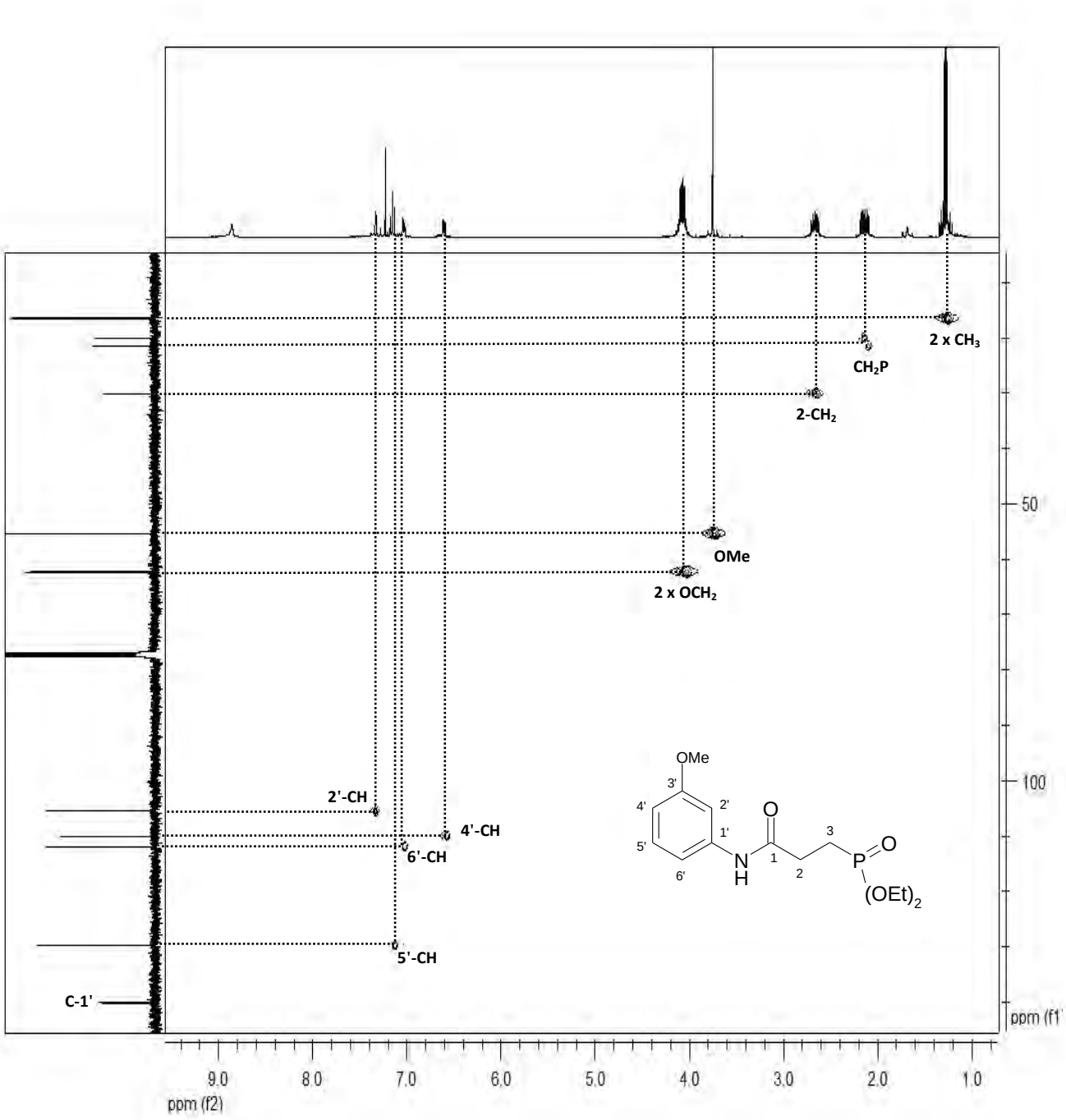

Figure 58. HSQC NMR spectrum of compound **323b** in $CDCl_3$.

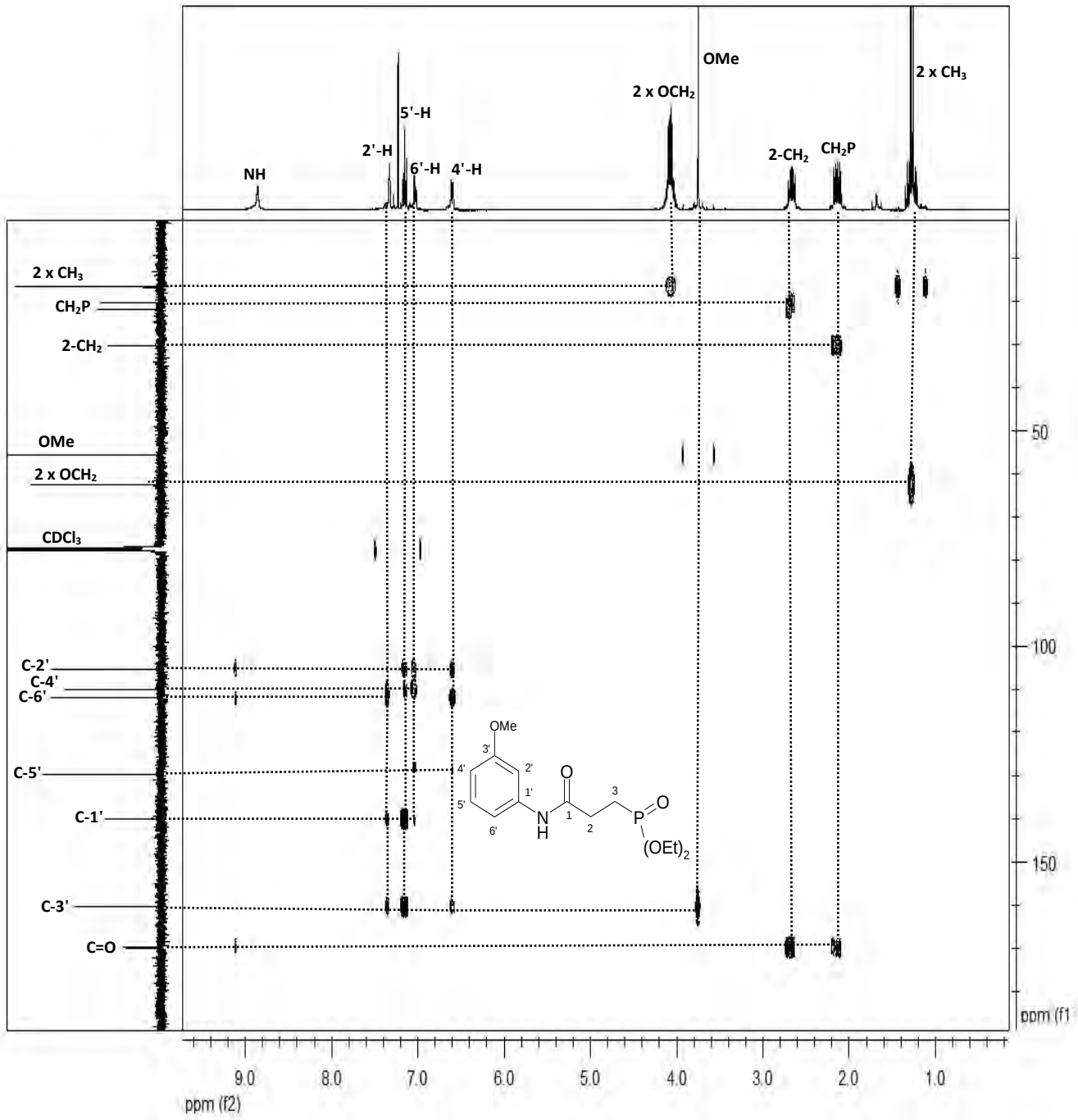

Figure 59. HMBC NMR spectrum of compound **323b** in $CDCl_3$.

Tables 5 and 6 summarise the percentage yields of the desired 3-substituted aniline-derived phosphonate esters **321a-g**, **323a-g**, **325a-g** and **327a-g**, and the corresponding phosphonic acid derivatives **328a-g**, **331a-g**, **333a-g** and **335a-g**, respectively. A selection of the prepared aniline-derived phosphonate esters and corresponding phosphonic acids were subjected to STD NMR enzyme binding studies and inhibition assays (Section 2.5), using *Ec*DXR.

Table 5. Yields (%) of phosphonate esters obtained from Michaelis-Arbuzov's reactions of ω-chloro-*N*-alkylanilides (Scheme 44).

	R	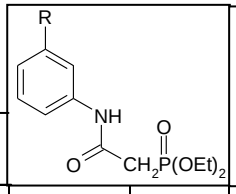		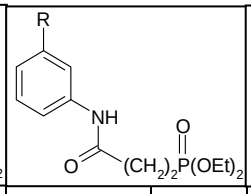		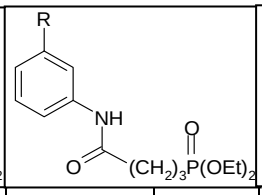		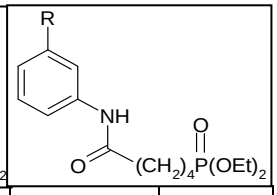	
a	OH	321a	66	323a	58	325a	65	327a	55
b	OMe	321b	65	323b	62	325b	66	327b	58
c	Br	321c	62	323c	53	325c	63	327c	60
d	F	321d	56	323d	48	325d	54	327d	57
e	CN	321e	48	323e	61	325e	61	327e	63
f	NO_2	321f	72	323f	67	325f	74	327f	66
g	CH_2OH	321g	65	323g	61	325g	66	327g	55

Table 6. Yields (%) of phosphonic acids obtained from hydrolysis of phosphonate esters (Scheme 44).

	R	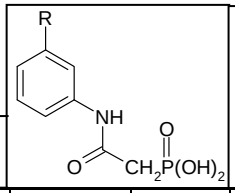		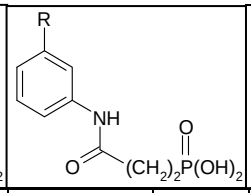		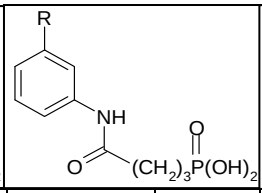		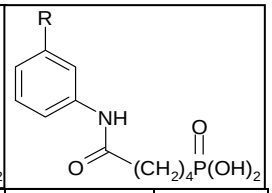	
a	OH	328a	63	331a	61	333a	63	335a	67
b	OMe	328b	62	331b	66	333b	61	335b	60
c	Br	328c	42	331c	58	333c	55	335c	60
d	F	328d	57	331d	68	333d	57	335d	63
e	CN	328e	59	331e	60	333e	61	335e	59
f	NO_2	328f	67	331f	71	333f	66	335f	69
g	CH_2OH	328g	48	331g	67	333g	60	335g	57

2.3. Synthesis of furan-derived phosphate analogues as conformationally restricted DOXP analogues

Much of the synthetic work towards the design of structural analogues of the natural substrate DOXP **230** as potential inhibitors of DXR has focused on:- i) removal of one of the hydroxyl groups at either the C-3 or C-4 position; ii) alteration of the length of the carbon spacer and; ii) modification of the phosphate moiety.[123-126] In addition, the construction of analogues of the antibiotic fosmidomycin **236** has involved modification of either the phosphonate or hydroxamate functional group, respectively.[117-121,130-133] Interestingly, very few studies have reported DOXP **230** or fosmidomycin **236** analogues in which the three carbon spacer has been structurally modified. Van Calenbergh *et al.*[125] have reported novel cyclopropyl analogues of fosmidomycin with restricted conformational mobility, by incorporating the C-1 and C-2 carbon atoms of the spacer in a three-membered ring. The inhibitory activity towards *Ec*DXR and *in vitro* growth inhibitory activity for *P. falciparum* of one such analogue **259**, was reported to be equally as potent as fosmidomycin **236**.[125] Analogues of the natural substrate DOXP **230** in which conformational mobility is restricted are yet to be reported. Consequently, we envisioned the design of the furan derivatives **337b-d** which contain phosphate and oxime moieties as confomationally restricted isosteres of the natural substrate DOXP **230** (Figure 60). In an earlier study in our group,[176] the capacity of the furan derivatives **337b-d** to adopt similar stable conformations to DOXP **230** was demonstrated, but synthetic access (Scheme 45) to these compounds could not be completed. The oxygen atom of the furan ring and oxime hydroxyl group of these novel analogues **337b-d** was expected to chelate to the divalent metal cation, thus anchoring the molecules in the active site of DXR.

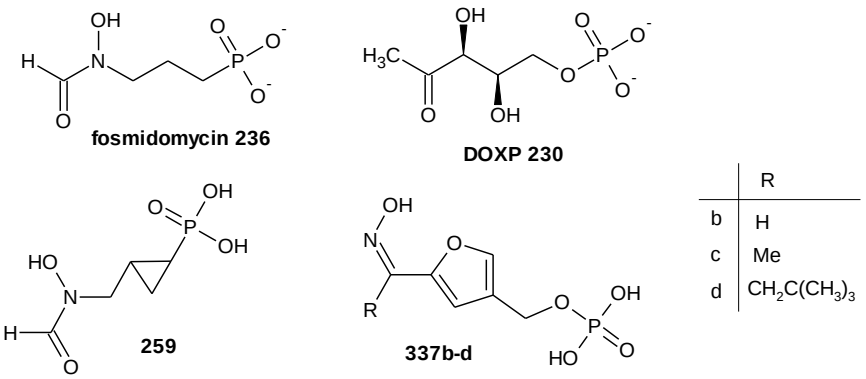

Figure 60. Design of conformationally-restricted fosmidomycin analogue **259** and novel DOXP analogues **337b-d.**

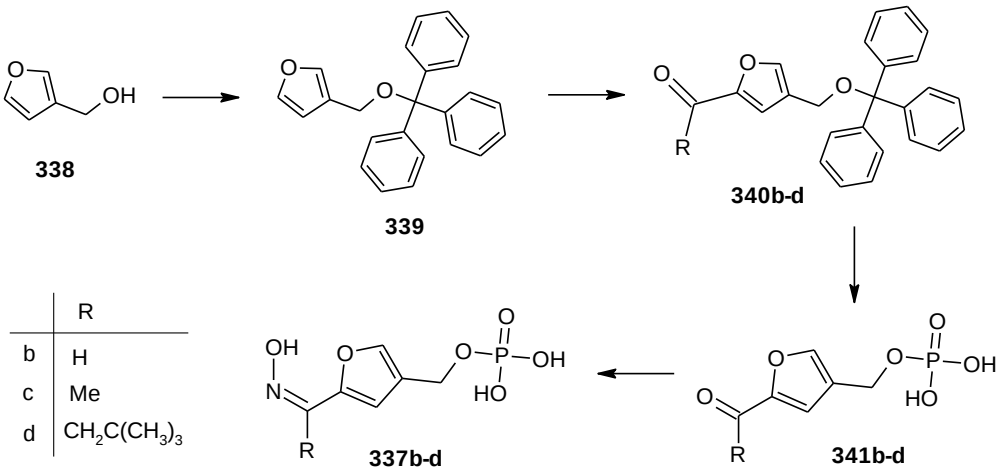

Scheme 45. Synthetic route towards conformationally-restricted DOXP analogues **337b-d**.

2.3.1. Protection of 3-furanmethanol *via* tritylation.

Functionalization of the readily available 3-furanmethanol **338** required initial protection of the hydroxyl group. This was achieved by treatment with triphenyl methyl chloride **342** in the presence of excess triethylamine and a catalytic amount of 4-dimethylaminopyridine (DMAP),[176] to obtain the trityl-protected furan **339** in 72 % yield (Scheme 46). Under the reaction conditions, the hydroxyl proton of 3-furanmethanol **338** is abstracted by the base to yield the deprotonated intermediate. Subsequent nucleophilic attack of the central carbon of the trityl halide **342** by the intermediate furnishes the desired trityl-protected furan **339**, while the hydrogen chloride generated is neutralised by unreacted base. The ^{1}H NMR spectrum (Figure 61) shows a singlet at 4.06 ppm corresponding to the 1'-methylene group, while the singlet at 6.42 ppm correlates to the 2-H nucleus. The multiplets between 7.26 and 7.53 ppm integrate for seventeen protons corresponding to the fifteen trityl group protons and the 4- and 5-H protons on the furan ring.

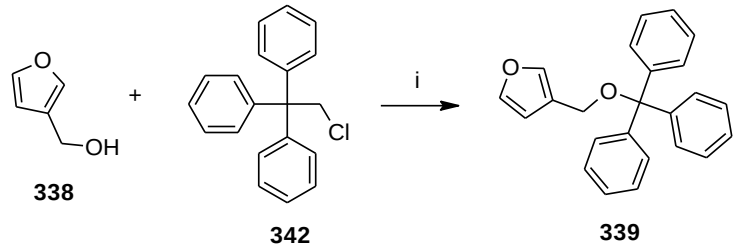

Scheme 46. Protection of 3-furanmethanol *via* tritylation.
Reagents and conditions: i) Et_3N, DMAP, THF, 80 ^{o}C, 15 h, N_2.

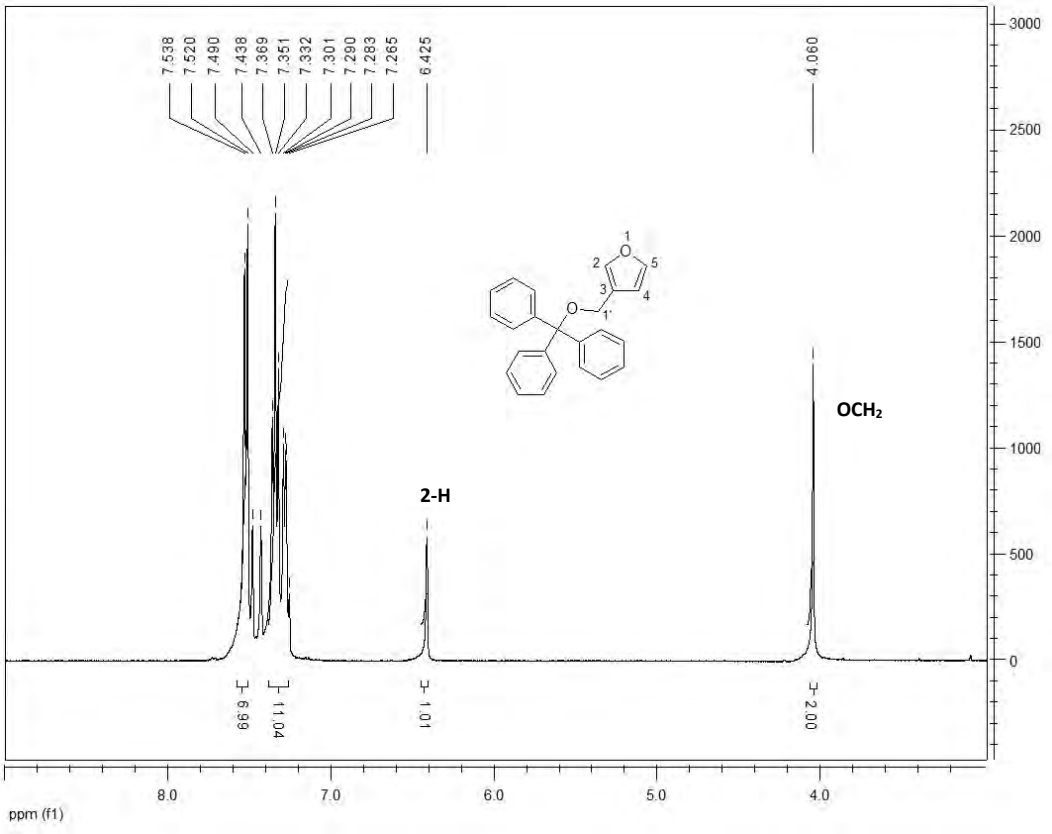

Figure 61. 400 MHz 1H NMR spectrum of 3-(trityloxymethyl) furan **339** in $CDCl_3$.

2.3.2. Functionalization of the 5-position of the furan ring.

The next step involved the functionalization of the furan ring by means of electrophilic substitution at C-5. The reactivity of the furan ring has been extensively studied and electrophilic substitution is known to occur exclusively at the α-positions (C-2 and C-5).[177-178] We planned to introduce the formyl and acetyl groups at C-5 as the known inhibitor fosmidomycin **236** possesses a formyl group, whilst the natural substrate DOXP **230** and the more potent inhibitor FR900098 **237** both contain an acetyl functional group. In addition, we hoped to exploit possible hydrophobic cavities beyond the metal-coordination site in the DXR-active site by introducing a *tert*-butylacetyl group. It is also possible that the carbonyl compounds **341b-d** (precursors to the planned oximes **337b-d**) might themselves act as DXR inhibitors.

Although the difference in reactivity between the 2- and 5-positions of the furan ring is expected to be small, we hoped that the presence of the bulky trityl group might provide steric hindrance to reaction at C-2 and thus direct substitution to C-5. Hence, 3-

(trityloxymethyl)furan **339** was lithiated using butylithium at -30 ^{o}C for four hours; subsequent treatment with electrophile, DMF, and stirring for a further four hours afforded a mixture shown by NMR analysis to contain the isomeric aldehydes **340a** and **340b**. The isomers were separated successfully using semi-preparative HPLC to obtain compound **340b** as the major product, in only 12 % yield (Scheme 47). In fact, this was the point at which the earlier synthetic attempt[176] foundered. Due to the poor yield and lack of selectivity for the desired aldehyde **340b**, a different method for the formylation of the 3-(trityloxymethyl)furan **339** was explored.

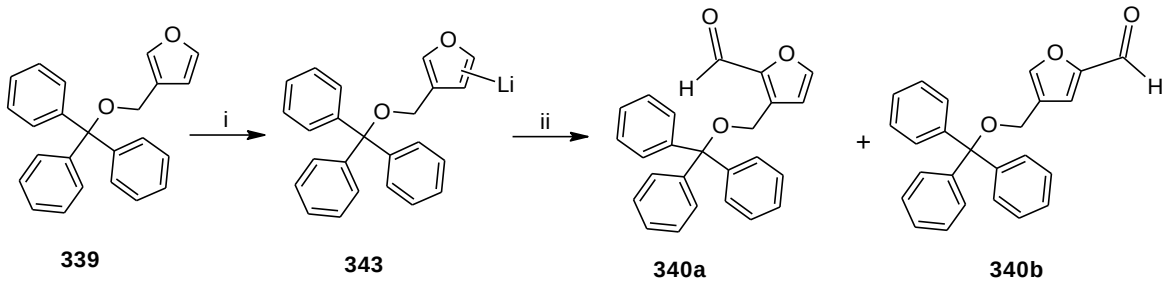

Scheme 47. Formylation of 3-(trityloxymethyl)furan **339** *via* lithiation.
Reagents and conditions: i) butyllithium, THF, -30 ^{o}C, 4 h, N_2 ii) DMF, -30 ^{o}C, 2 h, r.t., 2 h.

The Vilsmeier-Haack reaction[179-180] is widely used for the introduction of the formyl group in aromatic and heteroaromatic ring systems and was, therefore, considered. The Vilsmeier reagent was prepared from the reaction of phosphoryl chloride with DMF, and the protected furan **339** was formylated successfully to furnish the desired aldehyde **340b** in 64% yield with the isomeric aldehyde **340a** as the minor product (Scheme 48). The mechanism of the reaction is outlined in Scheme 49 and involves the reaction of $POCl_3$ and DMF to form the chloromethyleneiminium species **344**, which then reacts with the protected furan **339** in an electrophilic substitution process to produce the intermediate **345**. Aromatisation to form the iminium intermediate **346** followed by base-catalysed hydrolysis leads to the desired aldehyde **340b**.

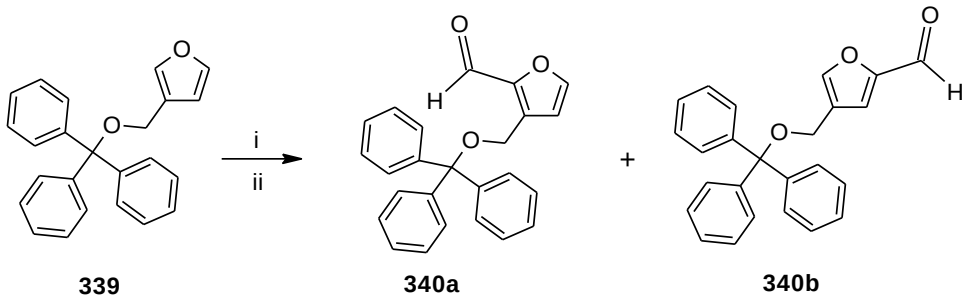

Scheme 48. Synthesis of aldehydes **340a** and **340b** *via* Vilsmeier-Haack formylation. *Reagents and Conditions*: i) $POCl_3$, DMF, 0 ^oC for 2 h, 65 ^oC for 1 h ii) H_2O/NaOH.

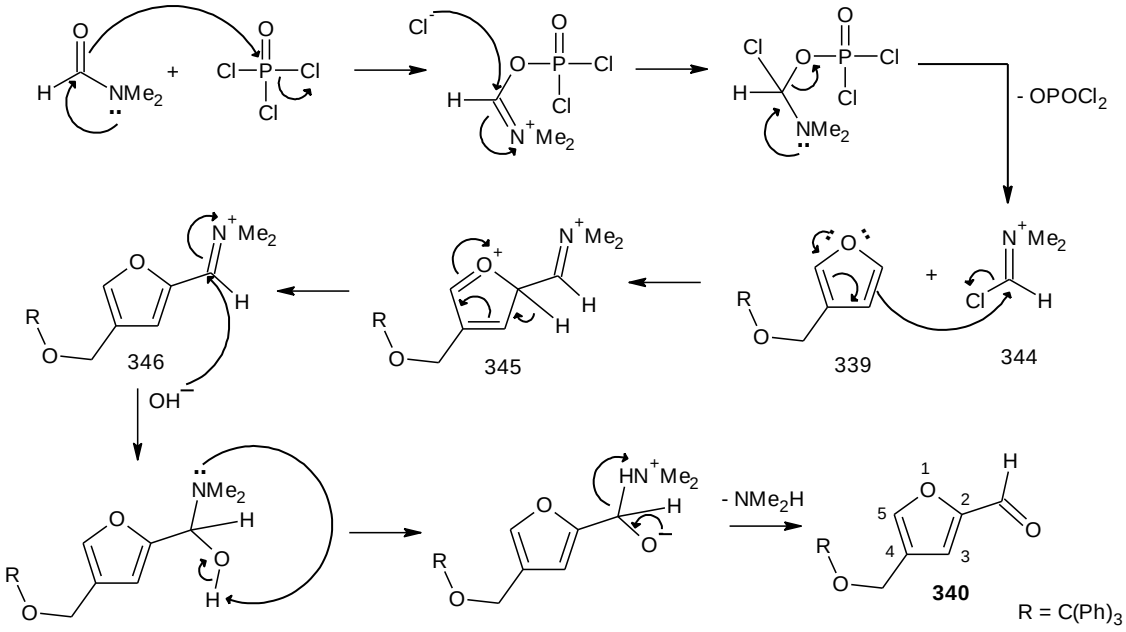

Scheme 49. Vilsmeier-Haack mechanism for the formation of aldehyde **340b**.

The structures of the isomeric aldehydes **340a** and **340b** were confirmed by NMR spectroscopic analysis. Figure 62 shows the comparative ^1H NMR spectra of aldehydes **340a** and **340b**, respectively. In the ^1H NMR spectrum of compound **340b** (top spectrum), the 5-H signal is clearly seen at 6.74 ppm; whereas in the ^1H NMR spectrum of aldehyde **340a** (bottom spectrum), the 5-H signal is not observed confirming successful formylation at this position. The signals resonating at 9.72 ppm (top spectrum) and 9.67 ppm (bottom spectrum) correspond to the aldehyde protons in compounds **340b** and **340a**, respectively. The 1'-methylene group signal resonates at 4.45 ppm for compound **340b**, whereas this signal is seen at 4.14 ppm for aldehyde **340a**. Figure 63 illustrates the comparative ^{13}C NMR spectra of aldehydes **340a** and **340b**, with the signals assigned as indicated.

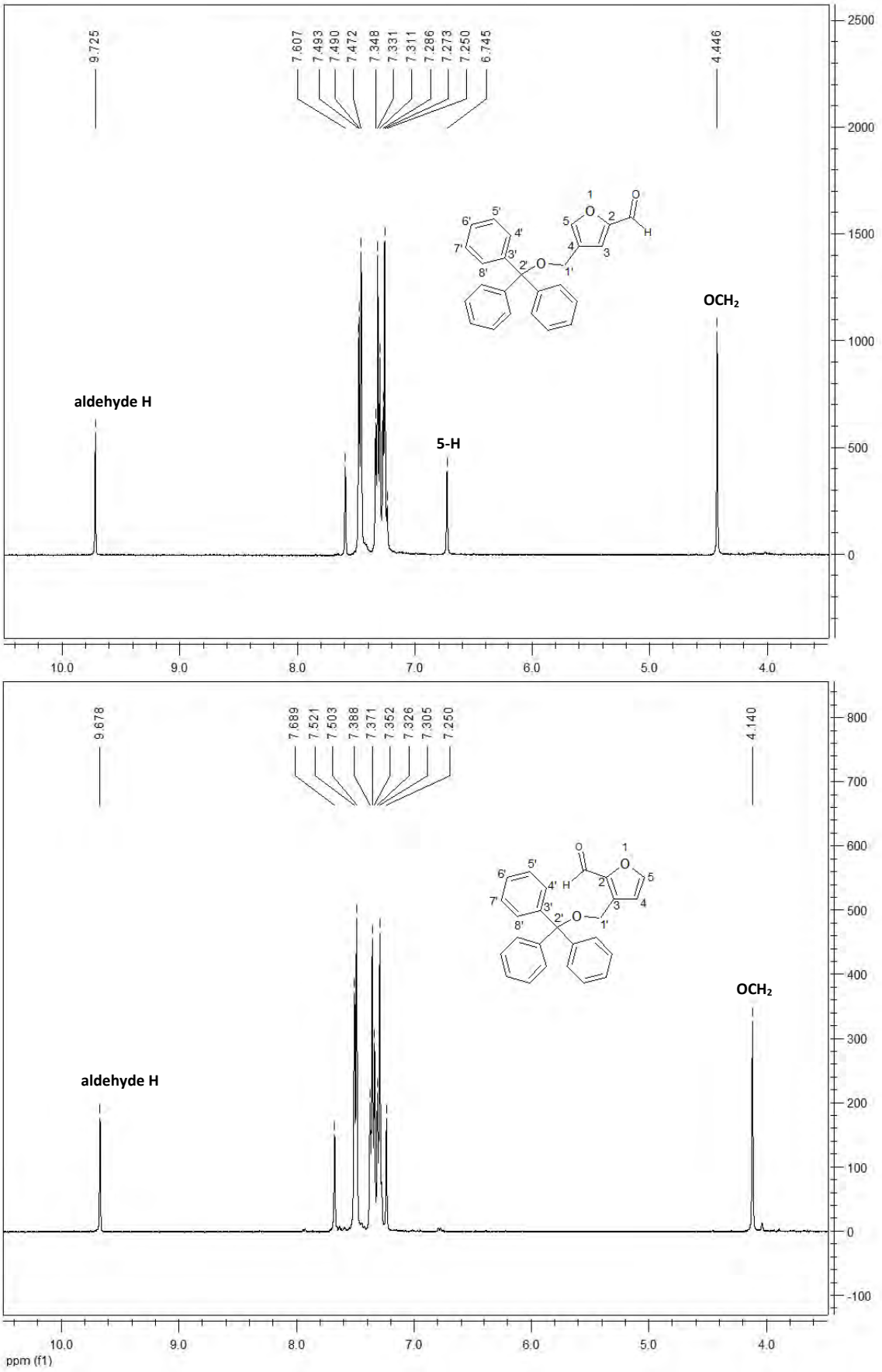

Figure 62. Comparative 400 MHz ^{1}H NMR spectra of aldehydes **340b** (top spectrum) and **340a** (bottom spectrum) in $CDCl_3$.

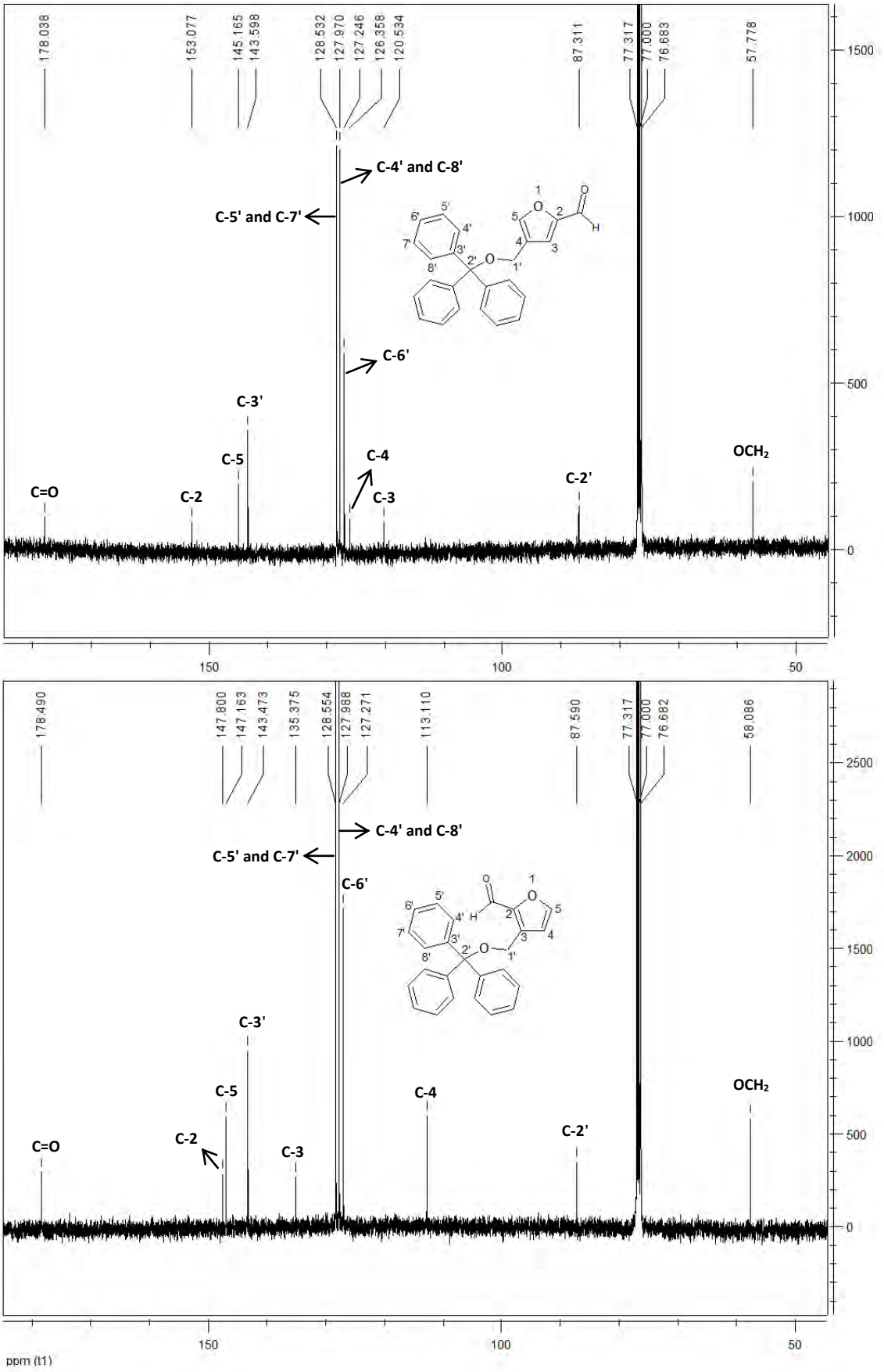

Figure 63. Comparative 400 MHz ^{13}C NMR spectra of aldehydes **340b** (top spectrum) and **340a** (bottom spectrum) in $CDCl_3$.

After the success of the Vilsmeier-Haack formylation, the introduction of the acetyl and *tert*-butylacetyl groups at C-5 of compound **339** was investigated. Friedel-Crafts acylation and alkylation reactions are well established methods used for electrophilic substitution in aromatic and heteroaromatic ring systems.[181-182] We exploited the broad scope of the Friedel-Crafts method in our effort to introduce the acetyl and *tert*-butylacetyl groups at C-5 of the furan ring in compound **339**. The reaction is usually carried out with aluminium trichloride ($AlCl_3$) as the Lewis acid catalyst, but $AlCl_3$ has been reported to induce the polymerisation of furan derivatives[183] and we decided to conduct the reactions with anhydrous tin tetrachloride ($SnCl_4$) and zinc chloride ($ZnCl_2$) as catalysts.[184-185] Other catalysts that have been successfully used, but were not considered, include iodine,[186] ferrous trichloride,[187] ortho-phosphoric acid[188] and the metal triflates.[189] For the acetylation of the furan derivative **339**, acetic anhydride was preferred as the acylating agent as opposed to acetyl chloride since a weaker acid is liberated in the course of the reaction and it has been reported to give better reaction yields.[190] The route to the furanyl ketones **340c** and **340d** is outlined in Scheme 50. Initially, acetic anhydride or *tert*-butylacetyl chloride was reacted with a catalytic quantity of $SnCl_4$ in DCM and this mixture was treated with the protected furan **339**. In another approach, a mixture of either acetic anhydride or *tert*-butylacetyl chloride and $ZnCl_2$ in DCM, was treated with the protected furan **339**. Subsequent aqueous work-up with K_2CO_3 of the reaction mixtures obtained using the two approaches furnished the desired ketones **340c** and **340d**. Table 7 summarises the reaction conditions and yields obtained for the ketones **340c** and **340d** using the different Lewis acid catalysts.

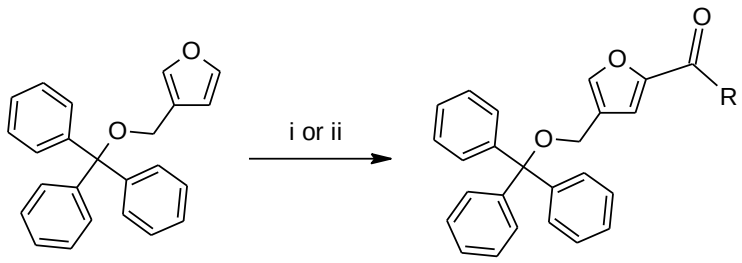

339

340c **R = Me**

340d **R = $CH_2C(CH_3)_3$**

Scheme 50. Synthesis of furanyl ketones **340c** and **340d** using Friedel-Crafts methodology. *Reagents and conditions:* i) acetic anhydride or *t*-butylacetyl chloride, $SnCl_4$, 0 ^oC for 1 h, 40 ^oC for 4 h, N_2 ii) acetic anhydride or *t*-butylacetyl chloride, $ZnCl_2$, 0 ^oC for 1 h, 40 ^oC for 8 h, N_2.

Table 7. Friedel-Crafts reaction of 3-(trityloxymethyl)furan **339** with acetic anhydride and *tert*-butylacetyl chloride in the presence of the Lewis acid catalysts, $SnCl_4$ and $ZnCl_2$.

Product	Catalyst	Temperature (^{o} C)[a]	Time (h)[a]	Yield (%)
340c	$SnCl_4$	0 ; 40	1 ; 4	64
340d	$ZnCl_2$	0 ; 40	1 ; 8	37
340c	$SnCl_4$	0 ; 40	1 ; 4	56
340d	$ZnCl_2$	0 ; 40	1 ; 8	33

[a] For two periods.

The furan system is more activated towards electrophilic attack at the α (2, 5)-positions than the phenyl rings of the trityl group and could be selectively acylated at lower temperatures. The Friedel-Crafts reactions were therefore carried out at 0 ^{o}C and then 40 ^{o}C, thus avoiding electrophilic substitution on the phenyl rings. Analysis of NMR spectra of the crude reaction mixtures indicated the formation of the ketones **340c** and **340d** as the major products; the unwanted isomers being limited to trace quantities due to the steric effect of the trityl group. The use of anhydrous $SnCl_4$ as catalyst produced the furanyl ketones **340c** and **340d** in a shorter time and in better yields (Table 7), possibly due to the tin metal coordinating more strongly with the carbonyl oxygen of the acylating reagent. The ketones **340c** and **340d** are new compounds and were fully characterised by NMR, IR and combustion analysis. Figure 64 shows the ^{1}H NMR spectrum of the 3-(trityloxymethyl)furanyl ketone **340c.** The singlet at 2.57 ppm corresponds to the acetyl methyl group, while the singlet at 4.42 ppm integrates for two protons and corresponds to the 1'-methylene protons. The overlapping signals between 7.14 and 7.33 ppm integrate for 17 protons and thus represent the fifteen protons of the trityl group and, the 3-H and 5-H nuclei of the furan ring. IR spectroscopic analysis revealed a carbonyl absorption band at 1675 cm^{-1}. Figure 65 illustrates the ^{13}C NMR spectrum of the 3-(trityloxymethyl)furanyl ketone **340d**, with the signals assigned as indicated.

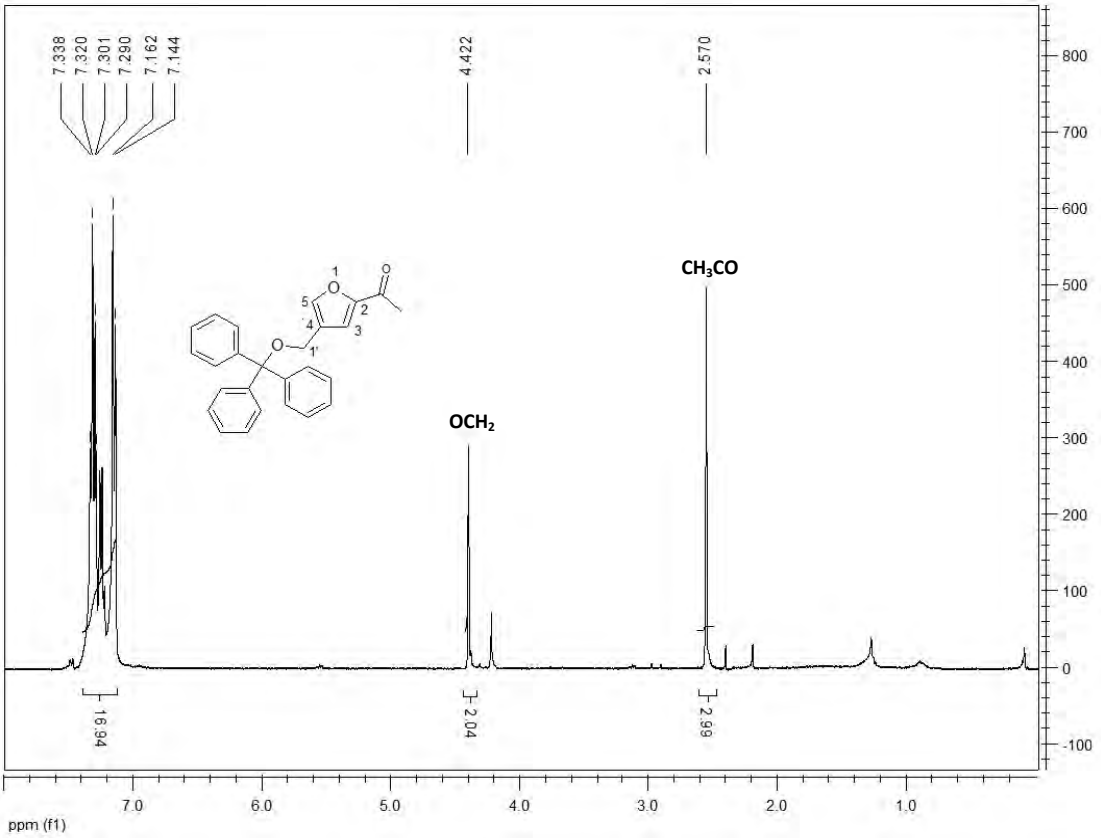

Figure 64. 400 MHz ^{1}H NMR spectrum of compound **340c** in $CDCl_3$.

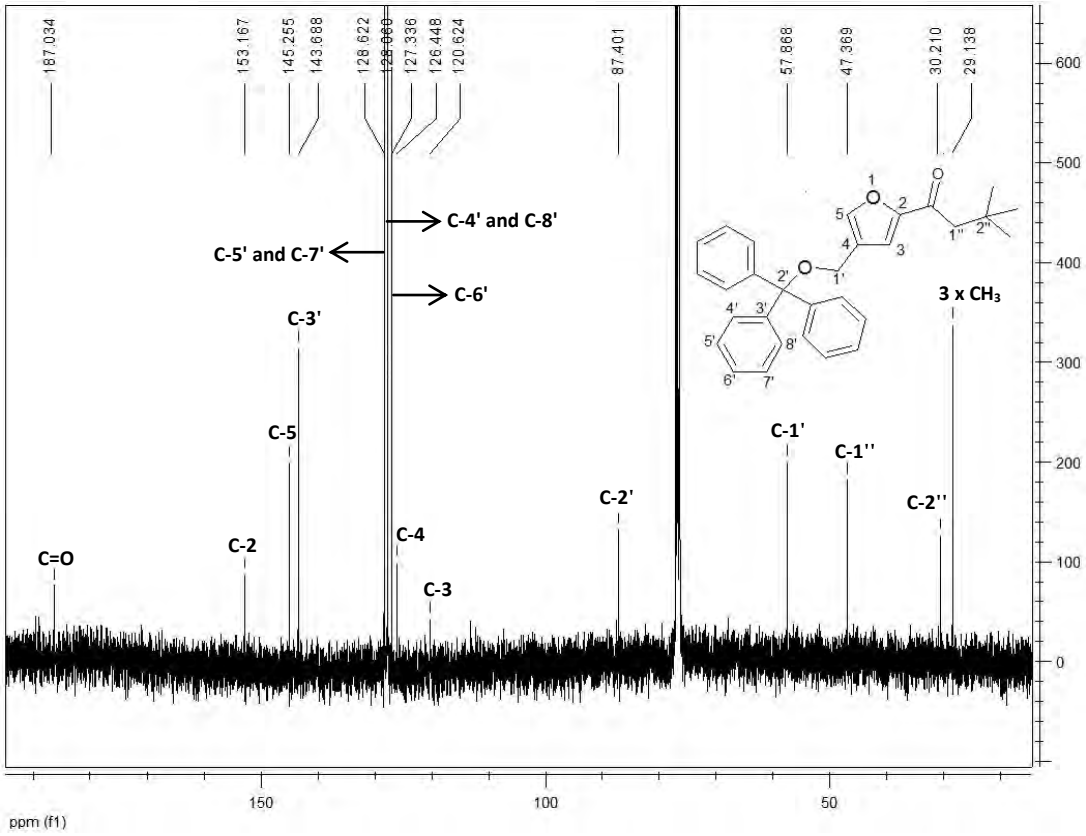

Figure 65. 100 MHz ^{13}C NMR spectrum of compound **340d** in $CDCl_3$.

2.3.3. De-tritylation and phosphorylation using mild acid hydrolysis.

Following the successful synthesis of compounds **340b-d**, the next step involved removal of the trityl protecting group and phosphorylation of the resulting alcohols. Various methods have been reported for the cleavage of the trityl moiety, including the use of boron trifluoride etherate in the presence of methanol,[191] catalytic hydrogenation[192] and treatment with diethylaluminium chloride.[193] Although these reagents[191-193] afford satisfactory yields, we decided to use mild acid hydrolysis conditions[194] to remove the trityl group. Thus, compounds **340b-d** were treated with formic acid in aqueous methanol for two hours at 50 ^{o}C. Removal of volatiles *in vacuo* gave the crude primary alcohols **347b-d**, which were used without further purification. The alcohols **347b-d** were phosphorylated to the corresponding phosphate esters **348b-d** using diethyl chlorophosphate in pyridine (Scheme 51). Compounds **340b-d** were also sequentially de-tritylated and phosphorylated using a mixture of H_3PO_4 and THF (1:1 v/v),[176] providing access to the dihydrogen phosphates **341b-d** in reasonable yields ranging from 58% to 65% (Scheme 51). Compounds **348b-d** and **341c-d** are all new compounds and were fully characterised by NMR, IR and combustion analysis.

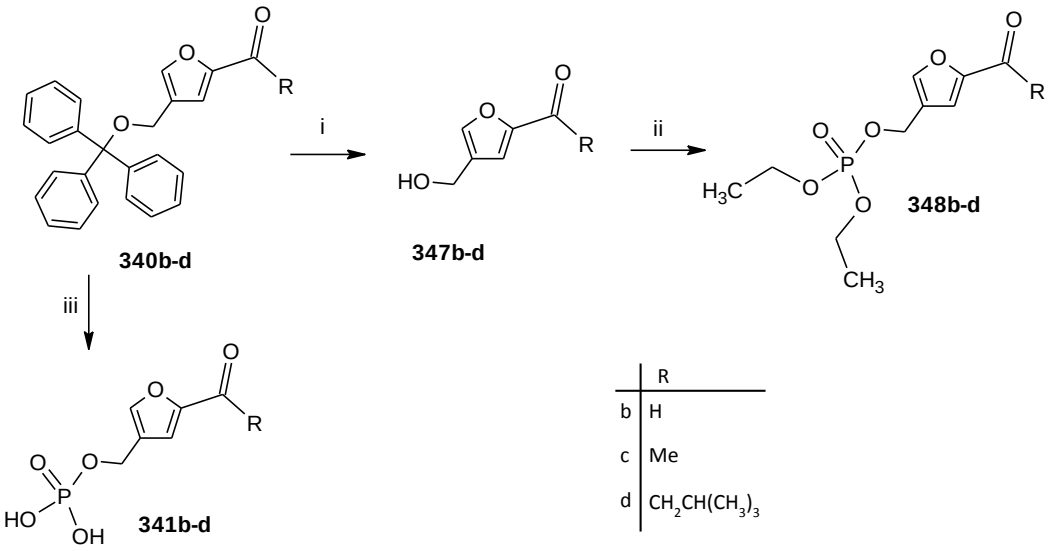

Scheme 51. Synthesis of phosphate esters **348b-d** and dihydrogen phosphate derivatives **341b-d**.
Reagents and conditions: i) HCOOH/THF/H_2O [(1:1:0.1 v/v/v)], 50 ^{o}C, 2 h ii) diethyl chlorophosphate, pyridine, 0 ^{o}C, 1 h, r.t., overnight; iii) H_3PO_4 / THF [(1:1 v/v)], 2 days, r.t.

Figures 66 and 67 illustrate the ^{1}H and ^{13}C NMR spectra of compound **348c**, respectively. The success of the phosphorylation reaction is clearly indicated in the ^{1}H NMR spectrum

(Figure 66) by the disappearance of the trityl group multiplet at *ca.* 7.20 ppm and the presence of the phosphate ethyl esters signals, the latter characterised by the methyl triplet at 1.30 ppm and the methylene signals as a multiplet at 4.06 ppm, due to coupling to the methyl protons and to the ^{31}P nucleus. In addition, coupling of the 1'-methylene protons to the ^{31}P nucleus is evident in the splitting of the signal at 5.05 ppm into a doublet (J = 1.6 Hz). The signal at 2.54 ppm corresponds to the acetyl methyl group, while the 3-H and 5-H nuclei of the furan ring resonate at 7.10 ppm and 7.12 ppm, respectively. Analysis of the ^{31}P NMR spectrum showed the presence of a ^{31}P signal at 0.8 ppm, while the IR spectrum showed the carbonyl and phosphate ester absorption bands at 1680 cm^{-1}and 1223 cm^{-1}, respectively.

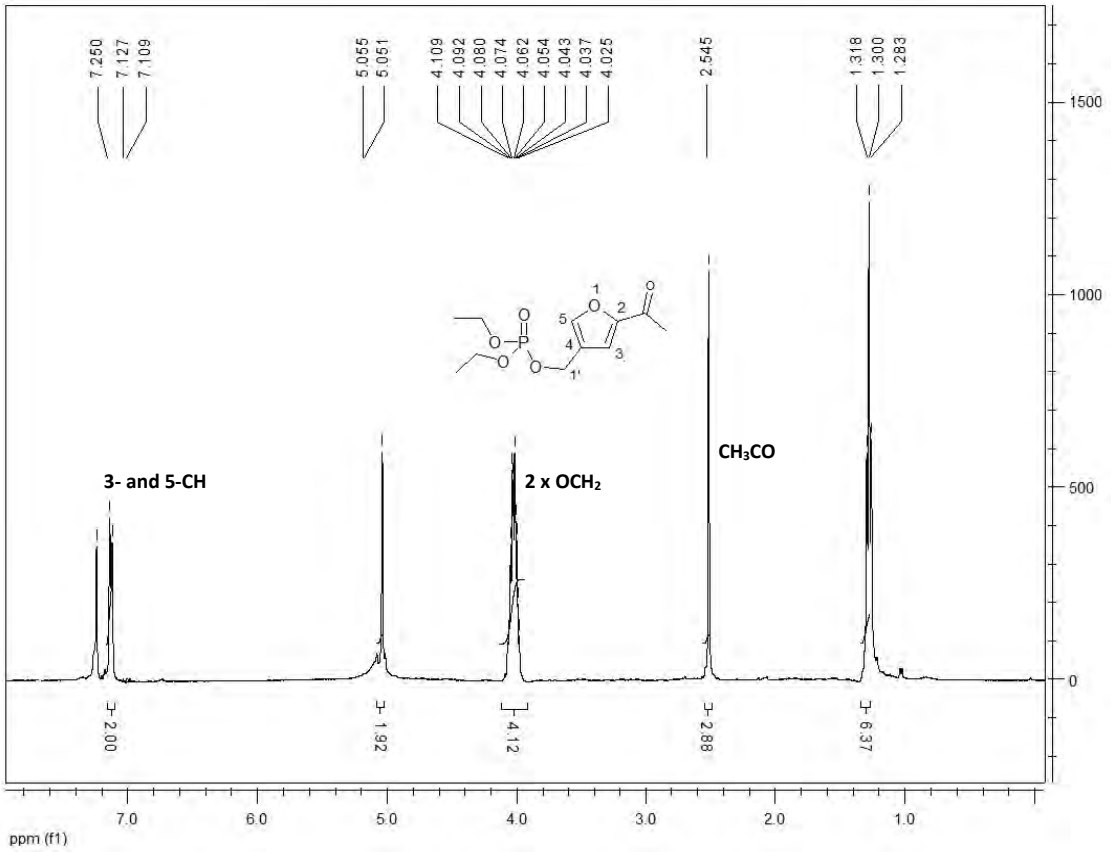

Figure 66. 400 MHz ^{1}H NMR spectrum of phosphate ester **348c** in $CDCl_3$.

In the ^{13}C spectrum (Figure 67) of compound **348c**, the phosphate ethyl ester signals at 16.3 ppm and 61.5 ppm are split (J = 6.0 and 6.5 Hz), reflecting coupling to the ^{31}P nucleus; the 1'-methylene carbon also resonates at 61.5 ppm. These assignments are supported by the DEPT135 and HSQC data.

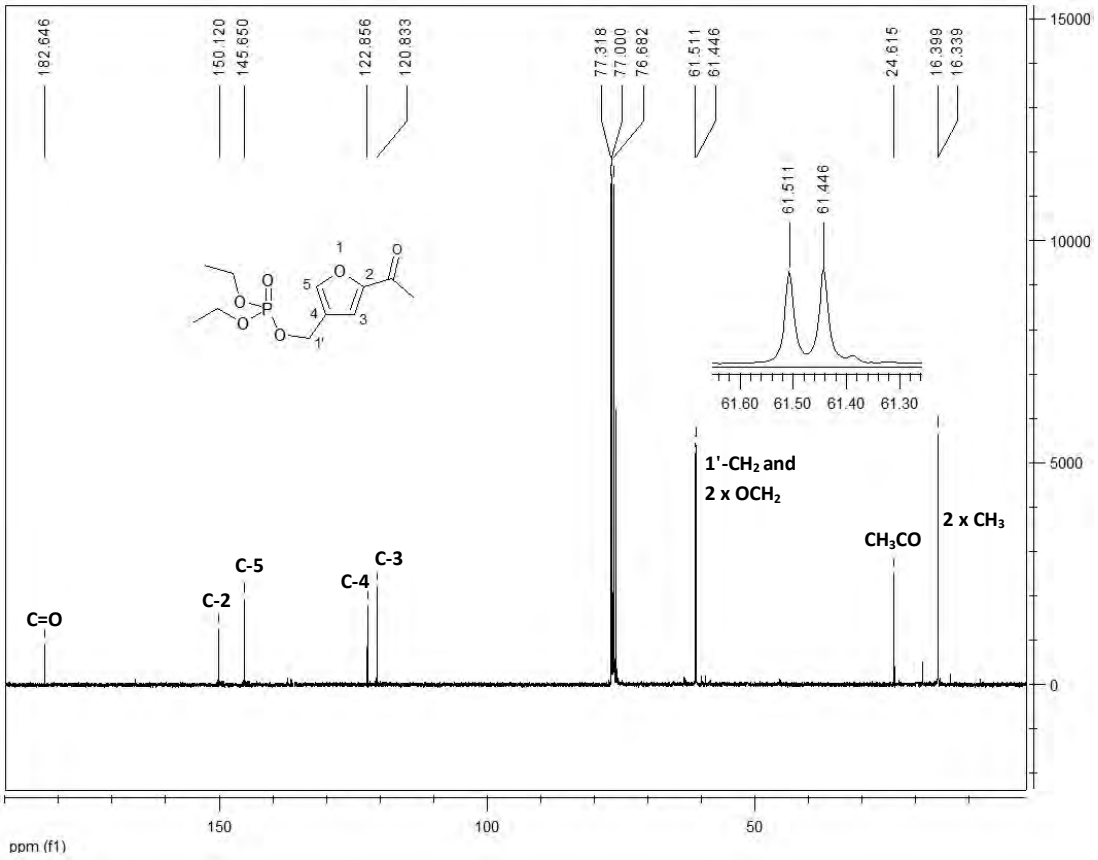

Figure 67. 100 MHz ^{13}C NMR spectrum of compound **348c** in $CDCl_3$.

Figures 68 and 69 illustrate the ^{1}H and ^{13}C NMR spectra of the dihydrogen phosphate derivatives **341b**, respectively. In the ^{1}H NMR spectrum (Figure 68) of compound **341b**, the presence of the phosphate group is indicated by the splitting of the 1'-methylene signal at 5.11 ppm by the nearby ^{31}P nucleus. The proton signals for the phosphate hydroxyl groups are not seen due to proton exchange with the D_2O solvent. Figure 69 illustrates the ^{13}C NMR spectrum of compound **341b**, with the 1'-methylene carbon resonating at 61.9 ppm and is split (J = 6.5 Hz) due to ^{31}P nucleus coupling; the remaining signals were assigned as indicated. Analysis of the ^{31}P NMR spectrum showed the presence of the ^{31}P signal at 0.8 ppm, while the IR spectrum showed the carbonyl group and phosphate ester absorption bands at 1675 cm^{-1} and 1219 cm^{-1}, respectively.

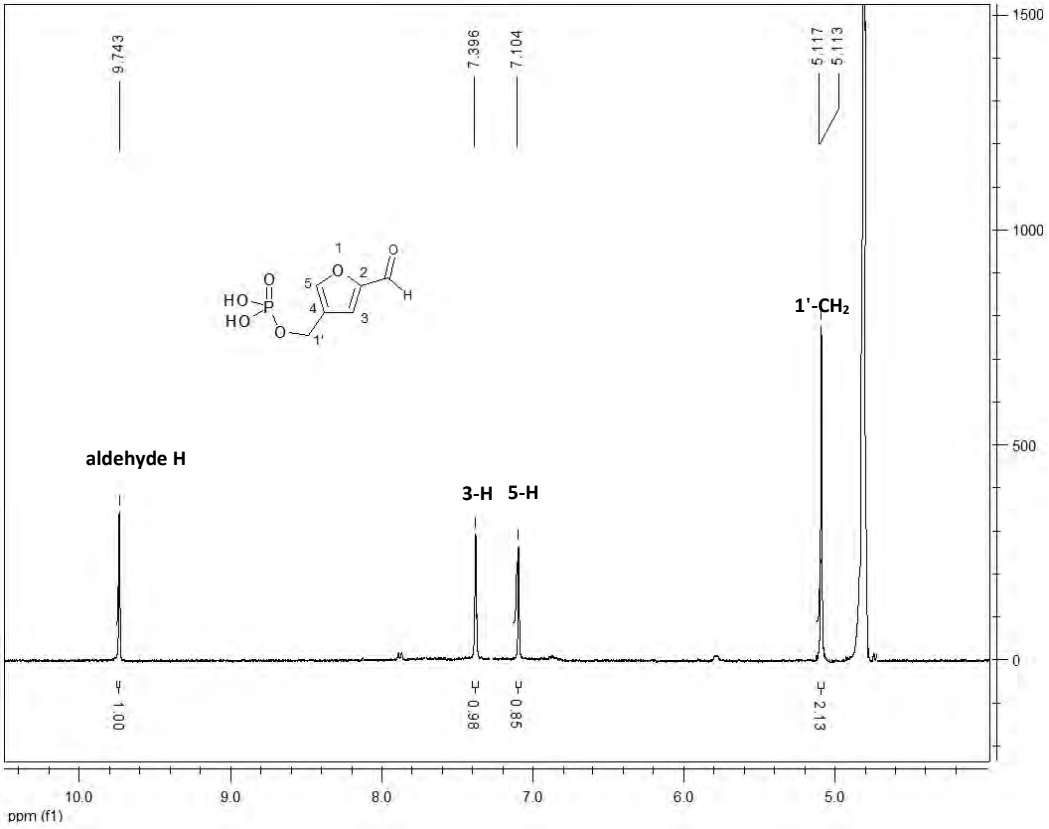

Figure 68. 400 MHz ^{1}H NMR spectrum of compound **341b** in D_2O.

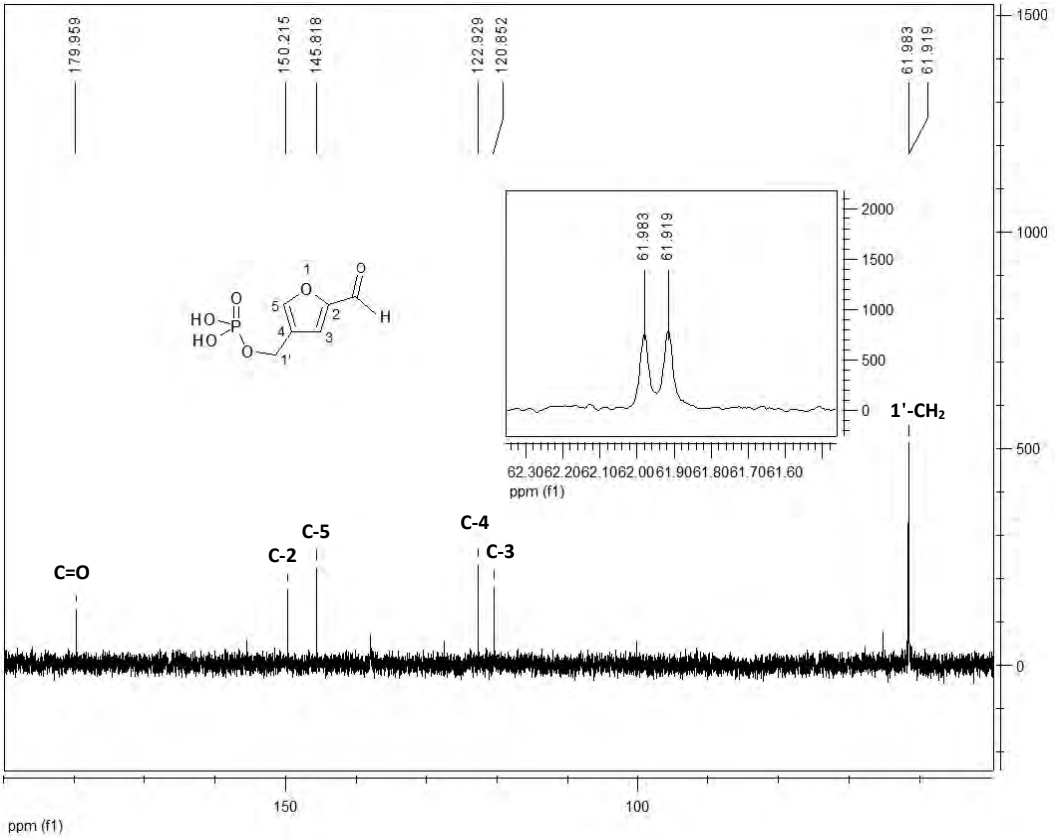

Figure 69. 100 MHz ^{13}C NMR spectrum of compound **341b** in D_2O.

2.3.4. Preparation of the phosphorylated furanyl oximes

Several methods have been reported for the transformation of carbonyl compounds to their corresponding oximes, including:- using ionic liquids,[195] grinding with hydroxylamine hydrochloride and sodium hydroxide pellets[196] and microwave irradiation with hydroxylamine hydrochloride impregnated on wet, basic Al_2O_3.[197] However, we decided to access the novel DOXP analogues **337b-d** using the classical method,[198] which involved treating compounds **348b-d** and **341b-d** with an ethanolic solution of hydroxylamine hydrochloride in the presence of a catalytic quantity of sodium acetate (Scheme 52). The phosphate esters **349b-d** were expected to act as pro-drugs of the diethyl dihydrogen derivatives **337b-d**. The diethyl esters **349b-d** were expected to exhibit better membrane permeability before being hydrolysed to active DXR inhibitors by esterases *in vivo*. The novel compounds **349b-d** and **337b-d** were isolated in good yields ranging from 87% to 96% and were fully characterised by spectroscopic methods (NMR and IR) and combustion analysis. A number of these compounds were subjected to *Ec*DXR-STD NMR binding analysis (Section 2.5).

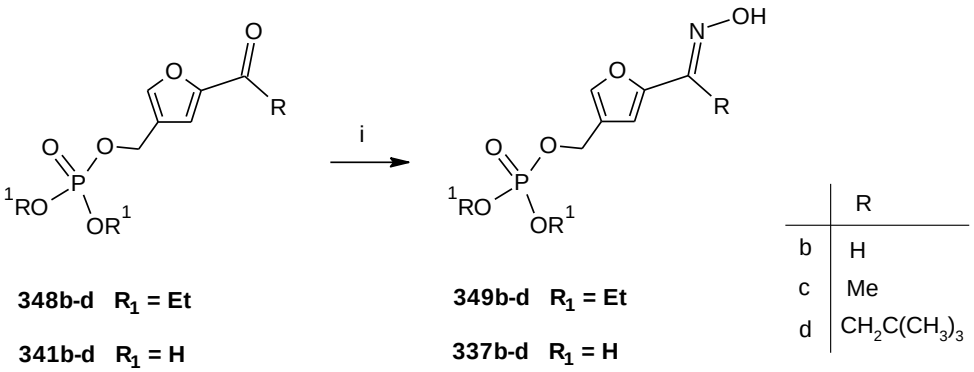

Scheme 52. Synthesis of phosphorylated oxime derivatives **349b-d and 337b-d**.
Reagents and conditions: i) $NH_2OH.HCl$, NaOAc, EtOH, reflux for 1 h.

Figure 70 illustrates the ^{13}C NMR spectrum of compound **349c**, showing the phosphate ethyl ester signals resonating at 16.2 ppm and 61.6 ppm and, significantly, the signal at 148.4 ppm corresponding to the oxime carbon. The remaining signals were assigned as indicated and analysis of the IR spectrum confirmed the presence of the C=N, hydroxyl and phosphate ester absorption bands at 1672, 3243 and 1225 cm^{-1}, respectively.

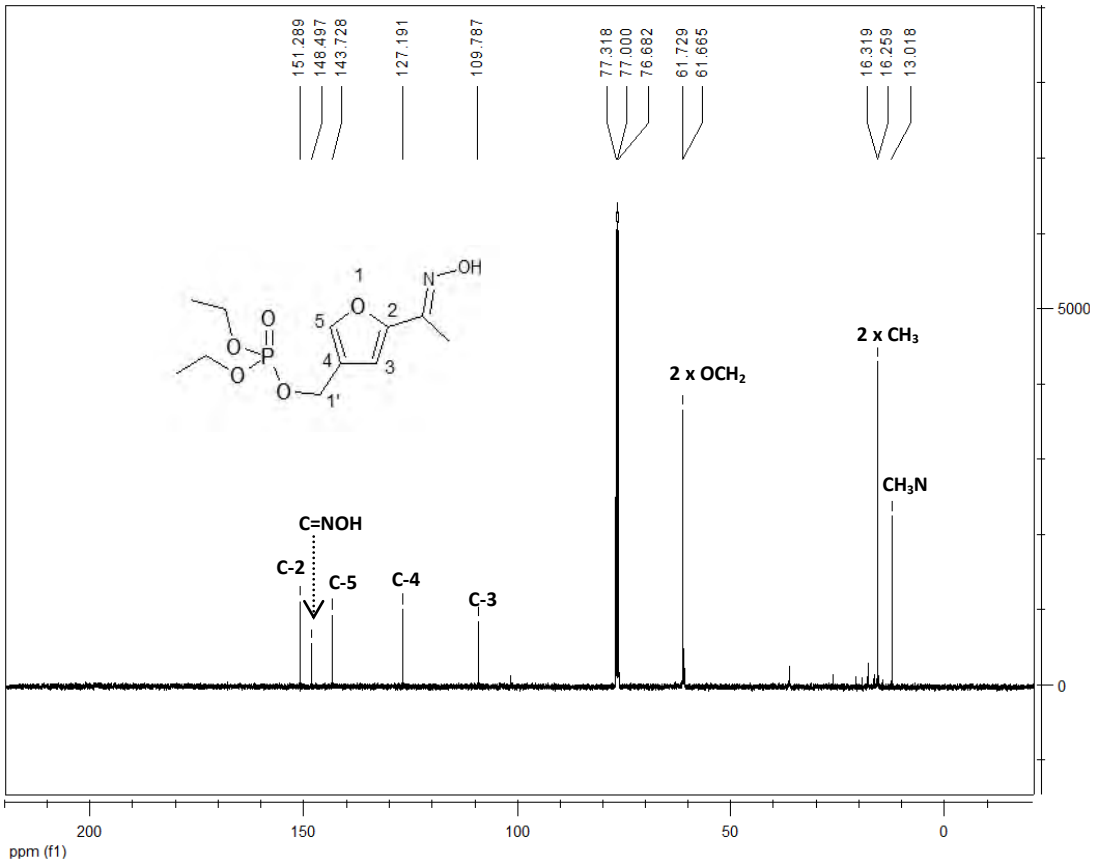

Figure 70. 100 MHz ^{13}C NMR spectrum of compound **349c** in $CDCl_3$.

In the ^{13}C NMR spectrum (Figure 71) of compound **337d**, the signal at 151.3 ppm correlates to the oxime carbon, while the absence of the ethyl ester signals confirmed hydrolysis to the dihydrogen product. The IR spectrum confirmed the presence of the C=N, hydroxyl and phosphate absorption bands at 1678, 3260 and 1235 cm^{-1}, respectively.

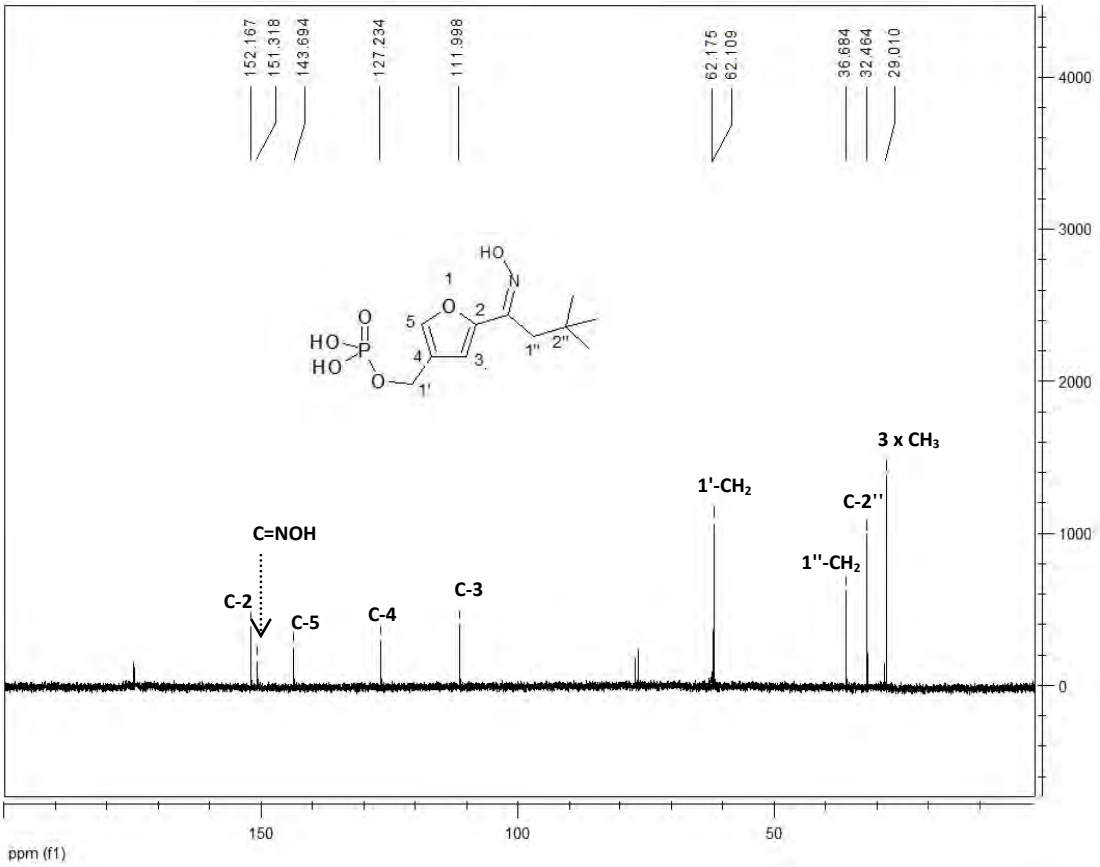

Figure 71. 100 MHz ^{13}C NMR spectrum of compound **337d** in D_2O.

2.4. Synthesis of *N*-benzyl substituted phosphoramidic acid derivatives based on a *de novo* design strategy.

Studies of several *Ec*DXR crystal structures with the known inhibitor fosmidomycin and natural substrate, DOXP, have identified the significant binding residues within the enzyme active and the essential structural features of the ligands which interact with the protein.[103,105] In addition to structure-activity relationship data reported in literature, a thorough analysis of the 3-D topology of both the active sites of *Ec*DXR and *Pf*DXR has been conducted in a previous study in our group.[129,142] This study revealed the presence of three additional pockets (I, II and III in Figure 72) adjacent to the phosphonate-binding region, which could be exploited in the design of novel inhibitors. The identification of these additional binding sites seems to provide an explanation for the increase in inhibitory activity observed for fosmidomycin analogues containing an aryl substituent on the carbon adjacent (α) to the phosphonate moiety – the α-aryl-substituent most likely occupies one of these pockets.[129,142] Studies by Song *et al.*[122] and Perruchon *et al.*[128] have also suggested the presence of a hydrophobic binding pocket near the phosphonate-binding region. Furthermore, analysis of the pocket in the homology model of the *Pf*DXR active site developed by Goble *et al.*, revealed the presence of an additional cysteine-267 residue (Figure 72), as opposed to the serine-253 residue in *Ec*DXR, and it was suggested that this difference could be exploited in the *de novo* design of specific *Pf*DXR inhibitors.[111,129]

Considering the information obtained from scrutinising the topology of the *Ec*DXR and *Pf*DXR active-sites and maintaining the essential phosphonate and hydroxamate functional groups present in fosmidomycin **236**, the novel ligands **350a-d** (Figure 73) were designed as specific inhibitors of *Pf*DXR.[129] A synthetic strategy was developed and initiated[129] but, due to limited time, the preparation of compounds **350a-d** could not be completed. Consequently, in the present study, attention was given to completing the synthesis of these novel fosmidomycin analogues. An α-benzyl group to occupy the additional binding pocket(s) (compounds **351a-d**) or capable of forming thioether or disulfide linkages with the cysteine-197 and -267 residues (compounds **351b-d**) was introduced, thus enhancing binding in the *Pf*DXR active site.

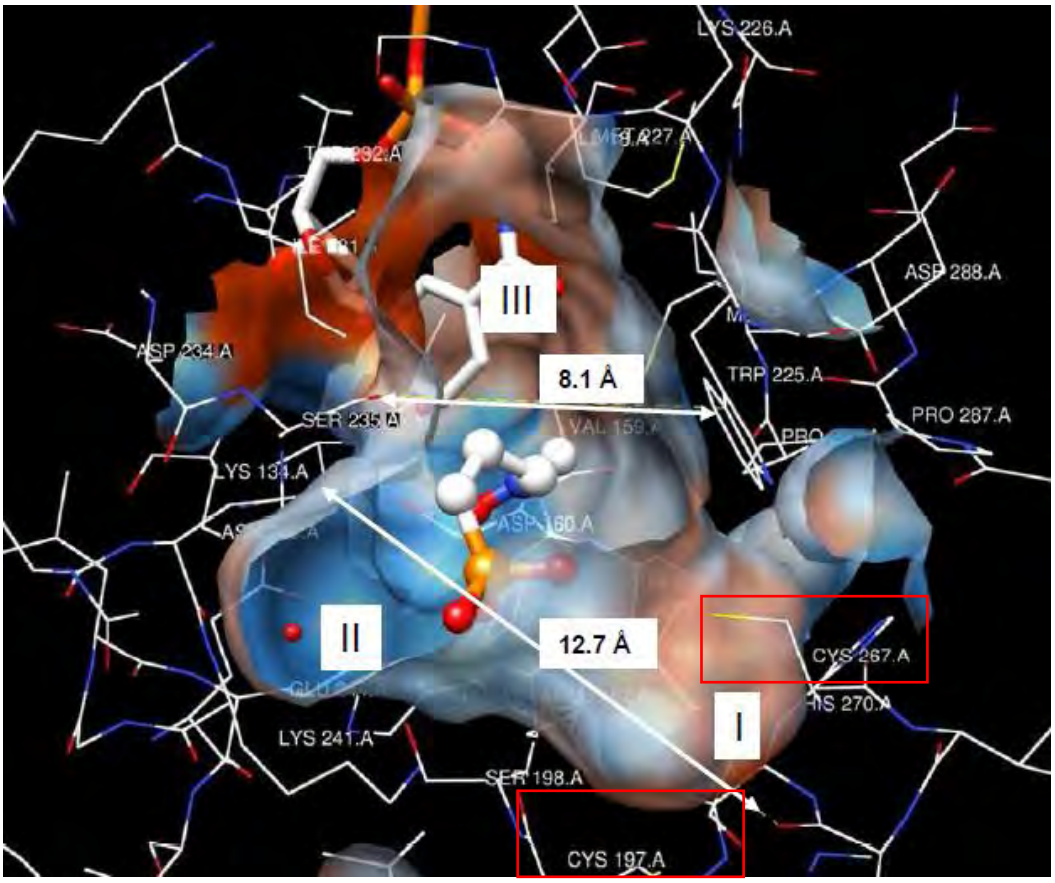

Figure 72. Active site of *Pf*DXR, showing the three additional binding pockets (I, II and III) close to the phosphonate-binding site and the position of the cysteine-197 and -267 residues. The surface zone at 8.0 Å from fosmidomycin **236** is shown with 30% transparency, coloured by hydrophobicity [polar (blue), non-polar (white), hydrophobic (orange)] and clipped in front. Protein residues less than 10 Å away from fosmidomycin **236** are shown in wireframe, coloured by atom type, and residues less than 8.0 Å away from fosmidomycin **236** are labelled. Fosmidomycin **236** is shown in ball-and-stick format, coloured by atom type, NADPH as sticks coloured by atom type and the crystal structure water molecules as red spheres.[129] (Reproduced with permission).

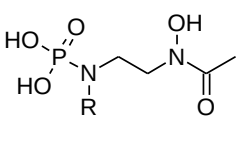

350a-d

	R
a	H
b	CH_2CH_2Br
c	CH_2CH_2Cl
d	CH_2CH_2SH

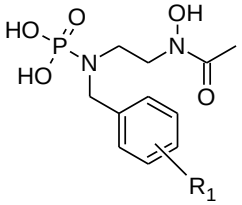

351a-d

	R_1
a	H
b	*p*-CH_2OH
c	*m*-NH_2
d	*m*-SH_2

Figure 73. Novel α- substituted analogues **350a-d** and **351a-d.**

The general synthetic strategy is outlined in Scheme 53 with the compounds prepared by Conibear[129] indicated in red. In the present study, the entire sequence was completed using, as the primary substrate, the diethyl phosphoramidate **352**.

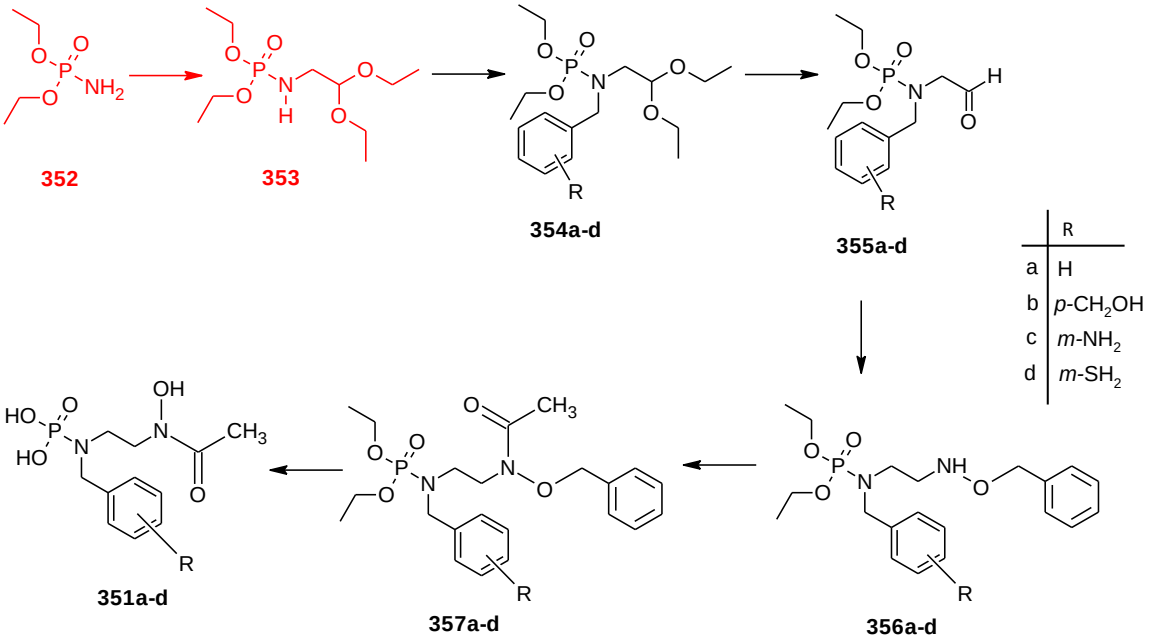

Scheme 53. Synthetic strategy towards the novel α-substituted analogues **351a-d.**

2.4.1. Synthesis of the diethyl phosphoramidate acetal 353 *via* silylation and alkylation.

The initial steps towards the construction of the *N*-benzyl substituted phosphoramidic acid derivatives **351a-d** is outlined in Scheme 54. Using a method reported by Zwierzak *et al.*[199], diethyl phosphoramidate **352** was treated with hexamethyldisilazane in refluxing benzene to obtain the silylated derivative **358** in essentially quantitative yield (98 %). The protected amine **358** was then deprotonated with sodium hydride and treated with bromoacetaldehyde diethylacetal in the presence of a catalytic quantity of tetrabutylammonium bromide (TBAB) to furnish the protected acetal **359**. Deprotection was effected by refluxing in ethanol for one hour, to afford the phosphoramidate acetal **353** in 93% yield.

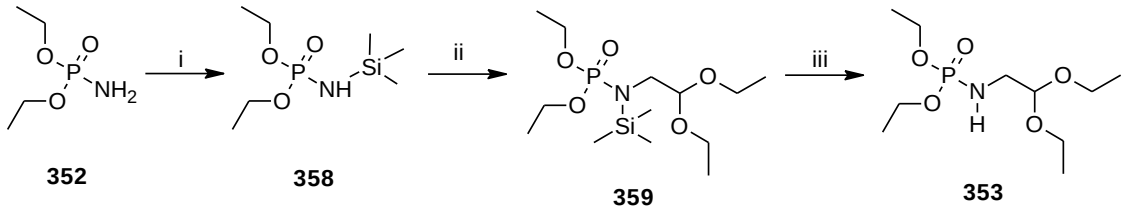

Scheme 54. Synthesis of phosphoramidate acetal **353.**
Reagents and conditions: i) hexamethyldisilazane (20% mol excess), benzene, 80 °C, 3 h ii) NaH, benzene, r.t., then bromoacetaldehyde diethylacetal, TBAB (10% mol), benzene, 80 °C, 4 h iii) EtOH, reflux, 1 h.

Figure 74 shows the ^{1}H NMR spectrum of compound **353**, with the triplet resonating at 1.15 ppm corresponding to the methyl groups of the diethyl acetal moiety, while the corresponding methylene protons resonate as a pair of quartets at 3.49 ppm and 3.62 ppm, respectively. The chemical non-equivalence of the geminal protons in both the methylene groups results in the splitting pattern observed. The signals at 1.24 ppm and 4.00 ppm correspond to the methyl and methylene protons of the diethyl phosphoramidate group, respectively. The doublet at 3.28 ppm corresponds to the 1-methylene protons, while the 2-methine proton resonates as a triplet at 4.58 ppm.

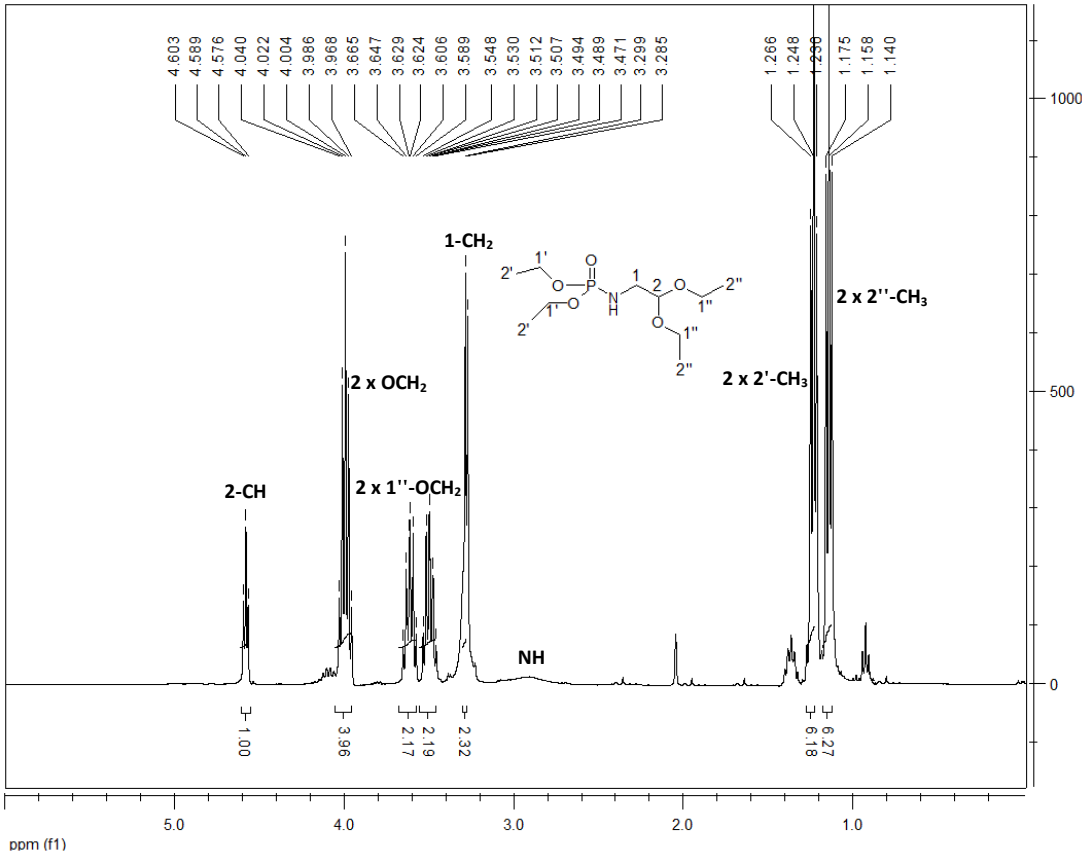

Figure 74. 400 MHz ^{1}H NMR spectrum of compound **353** in $CDCl_3$.

2.4.2. Synthesis of the *N*-substituted benzyl phosphoramidate acetals 354a-d.

The next step in the synthesis involved attachment of the various benzyl groups **360a-d** to the phosphoramidate nitrogen in compound **353**. Deprotonation of the NH group in compound **353** using sodium hydride, followed by treatment with the appropriate benzyl halides **360a-d** yielded the *N*-substituted benzyl phosphoramidate acetals **354a-d** in good yields ranging from 67 to 77% (Scheme 55). The benzyl substrates **360c-d** used for the construction of compounds **354c-d** were prepared as depicted in Scheme 56. The approach involved bromination of 3-aminobenzyl alcohol **361** using phosphorous tribromide to give the brominated derivative **360c**. Diazotization of compound **360c** followed by a reaction with sodium disulfide produced the disulfide compound **362**, which was reduced *in situ* with sodium borohydride in anhydrous THF to furnish the thiophenol **360d**.

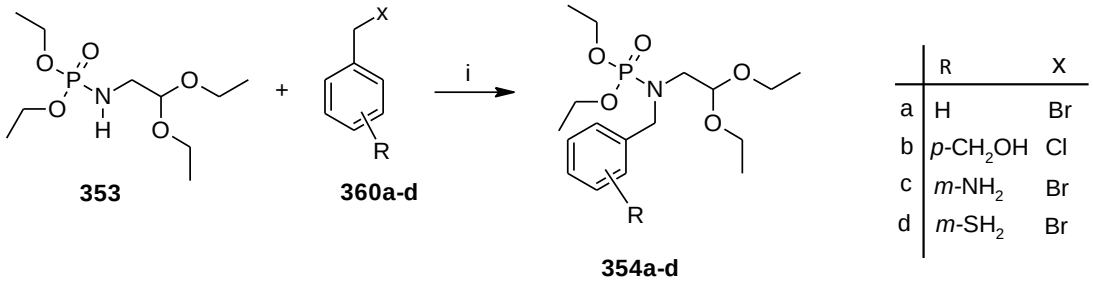

	R	X
a	H	Br
b	*p*-CH_2OH	Cl
c	*m*-NH_2	Br
d	*m*-SH_2	Br

Scheme 55. Synthesis of *N*-substituted benzyl phosphonate acetals **354a-d**.
Reagents and conditions: i) NaH, THF, r.t., 24 h, N_2.

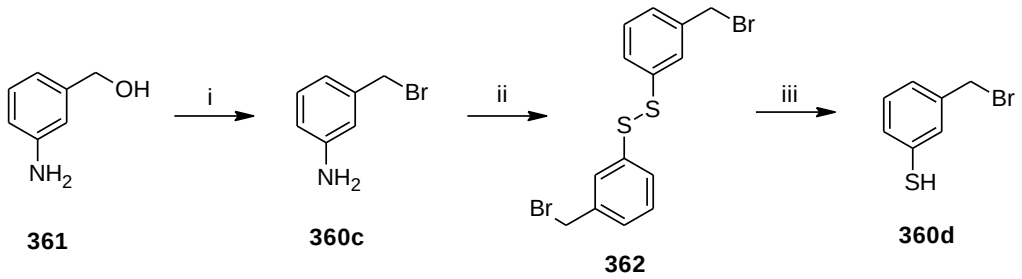

Scheme 56. Synthesis of benzyl substrates **360c** and **360d**.
Reagents and conditions: i) PBr_3, DCM, 0 ^oC, 1 h then r.t., 24 h ii) H_2O, HCl, $NaNO_2$, Na_2S_2, 0 ^oC, 1 h iii) $NaBH_4$, THF, 0 ^oC to r.t., 1 h.

Spectroscopic analysis (NMR and IR) and combustion analysis confirmed the formation of compounds **354a-d**. Figures 75 and 76 illustrate the ^1H and ^{13}C NMR spectra of compounds **354a** and **354d**, respectively. In Figure 75, the aromatic protons of the benzyl group are

clearly seen resonating between 7.28 ppm and 7.37 ppm, while the signal corresponding to the benzylic proton appears at 3.84 ppm. In the ^{13}C NMR spectrum of compound **354d** (Figure 76), the aromatic carbons are all accounted for, resonating between 124.7 ppm and 136.6 ppm, respectively. The benzylic carbon resonates at 68.9 ppm, while the signals corresponding to the phosphoramidate ethyl ester groups appear at 16.4 ppm and 62.7 ppm and are split due to coupling to the ^{31}P nucleus. Analysis of the ^{31}P NMR spectrum showed the presence of the ^{31}P signal at 24.2 ppm, while the IR spectrum revealed the presence of the SH and P=O absorption bands at 2571 cm^{-1} and 1260 cm^{-1}, respectively.

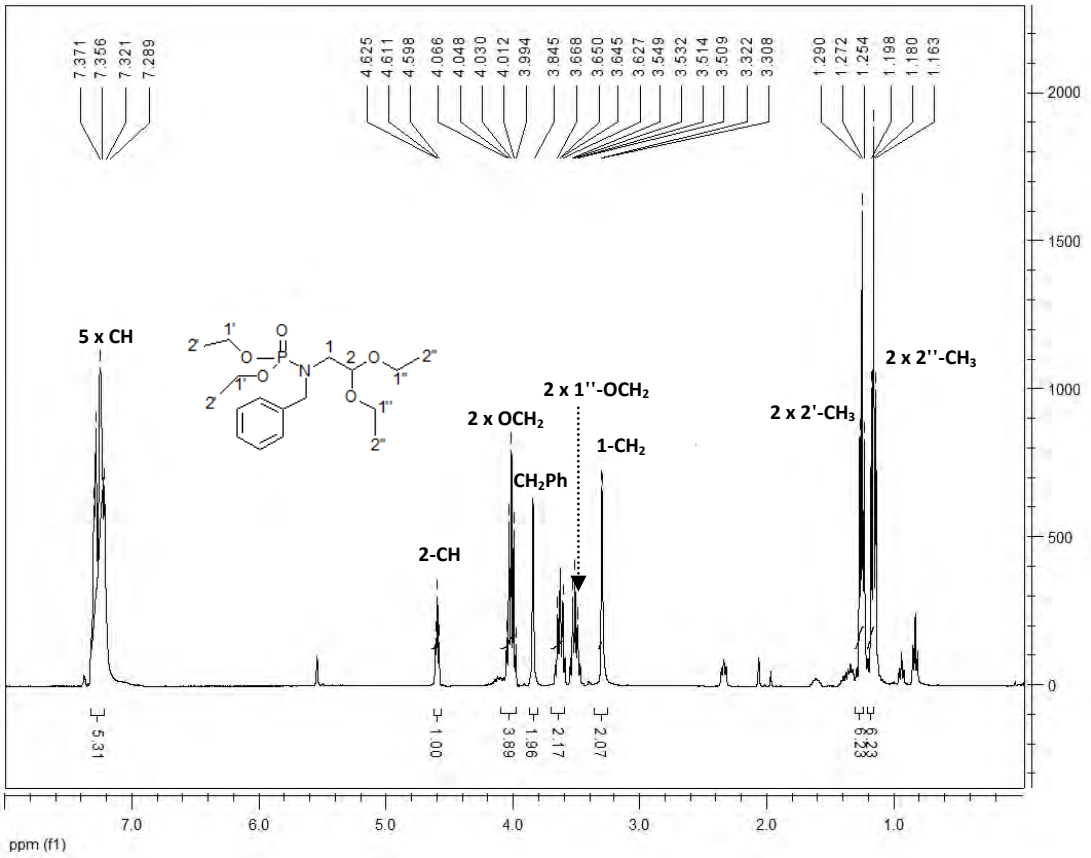

Figure 75. 400 MHz ^{1}H NMR spectrum of compound **354a** in $CDCl_3$.

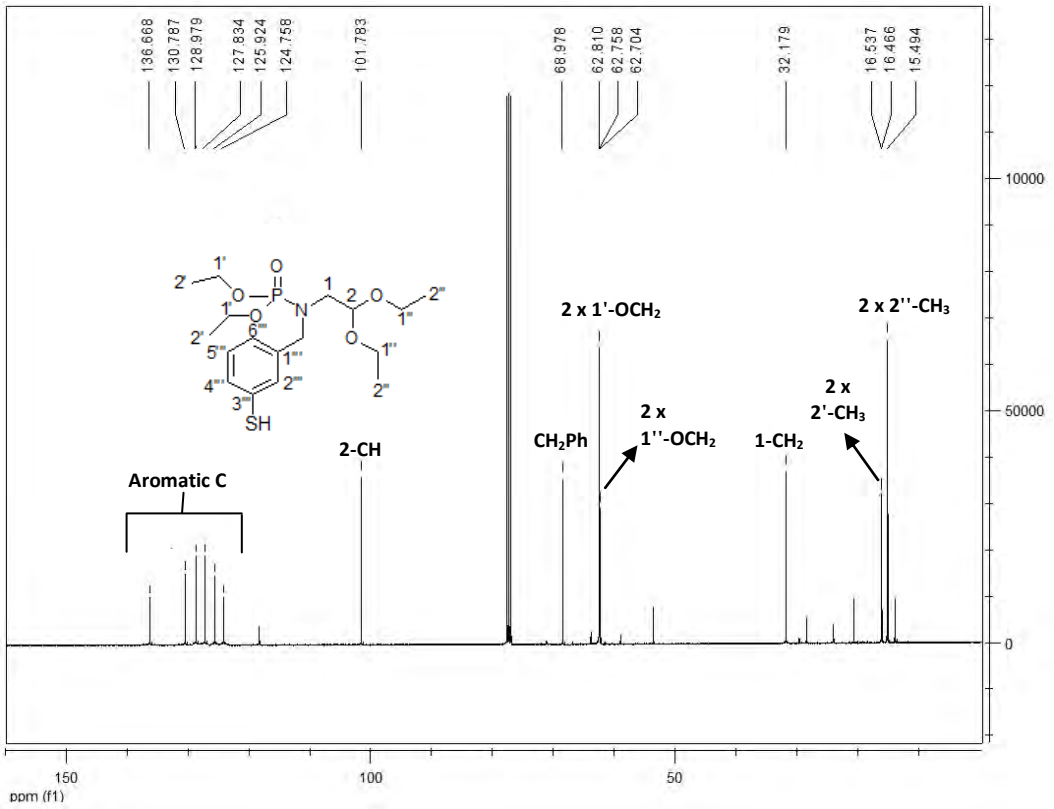

Figure 76. 100 MHz ^{13}C NMR spectrum of compound **354d** in $CDCl_3$.

2.4.3. Synthesis of *N*-benzyl substituted phosphoramidic acid derivatives 351a-d.

Since FR900098 **237**, the acetyl derivative of fosmidomycin **236**, is approximately twice as active *in vitro*, we decided to incorporate the acetyl functionality in our target compounds **351a-d**, which were accessed by adapting methodology reported by Schlitzer *et al*,[118-119] as outlined in Scheme 57. In addition to providing a point of attachment for the α-benzyl substituents, the presence of the nitrogen atom from the phosphoramidate group in compounds **351a-d** facilitated synthesis by avoiding chirality problems arising from the asymmetry of the sp^3 centre if the α-atom were carbon.

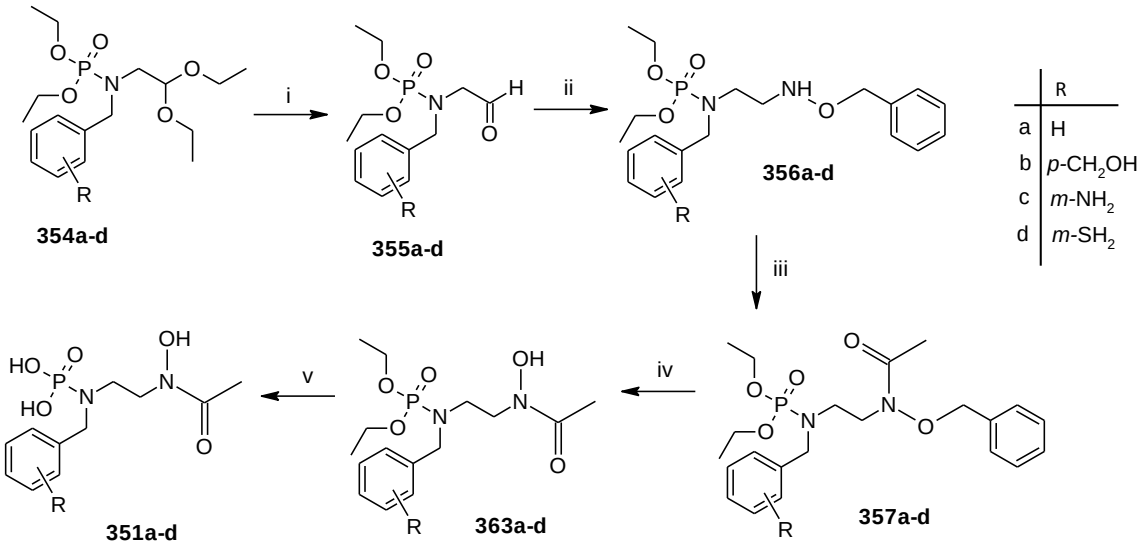

Scheme 57. Synthesis of *N*-benzyl-substituted phosphoramidic acid derivatives **351a-d.** *Reagents and conditions:* i) 2M-HCl, r.t., 24 h ii) *O*-benzylhydroxylamine in MeOH, 40 ^{o}C, 3 h and then $NaCNBH_3$, MeOH, HCl, r.t., 1 h iii) acetyl chloride, DCM, Et_3N, r.t., 24 h, N_2 iv) H_2, Pd/C, MeOH v) TMSBr, DCM, 0 ^{o}C, 1 h and then H_2O, r.t., overnight.

Thus, acid-catalysed hydrolysis of the acetal moiety afforded the corresponding aldehydes **355a-d** in good yields ranging from 88% to 92%. NMR spectroscopic analysis confirmed the formation of the aldehydes **355a-d**, as illustrated in the ^{1}H NMR spectrum of compound **355b** in Figure 77. Successful cleavage of the acetal moiety is clearly evident with the disappearance of the diethyl acetal signals and the emergence of the aldehydic proton signal at 9.81 ppm. The methylene protons adjacent to the aldehyde carbonyl resonate at 3.72 ppm, while the signal at 3.82 ppm corresponds to the methylene protons adjacent to both the nitrogen atom and benzene ring. The phosphonate ethyl ester signals resonate, characteristically, at 1.36 ppm and 4.13 ppm, while the signal at 4.82 ppm corresponds to the methylene protons adjacent to the hydroxyl group. The overlapping signals between 7.58 ppm and 7.67 ppm integrate for the four aromatic protons. The IR spectrum showed the absorption bands for the hydroxyl and carbonyl groups at 3261 cm^{-1} and 1738 cm^{-1}, respectively.

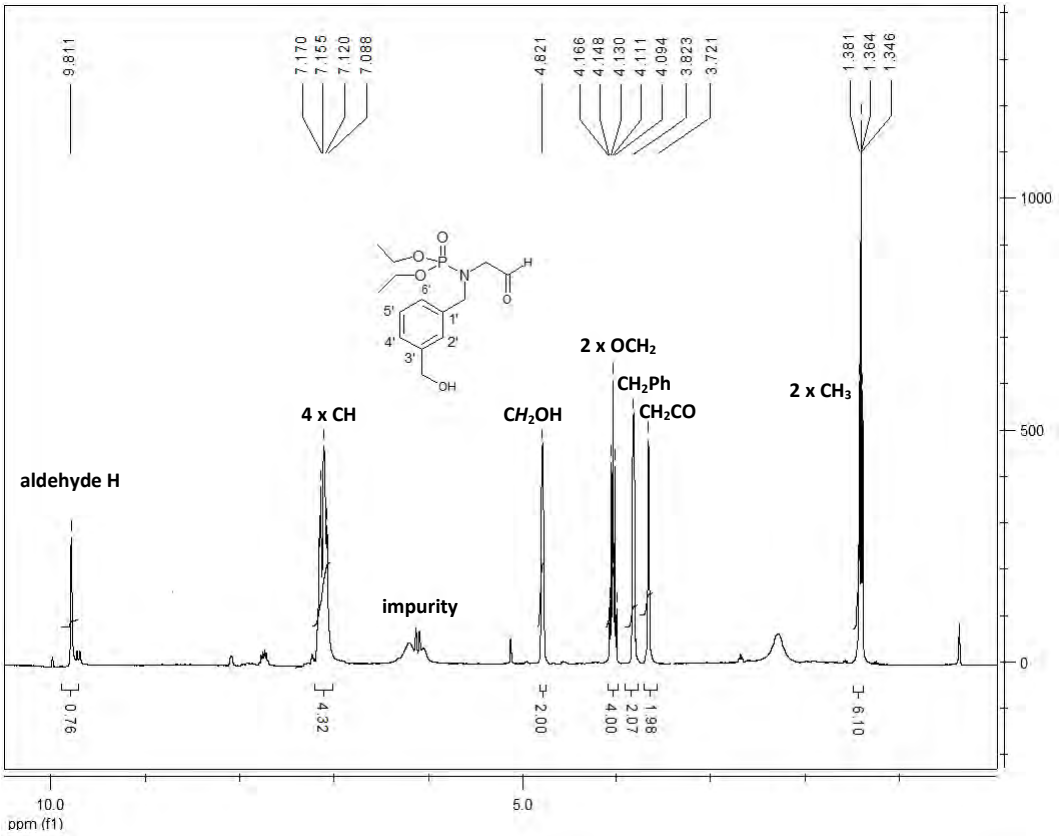

Figure 77. 400 MHz ^{1}H NMR spectrum of compound **355b** in $CDCl_3$.

The next step involved reductive amination of the aldehydes **355a-d** using *O*-benzylhydroxylamine, followed by sodium cyanoborohydride to furnish, *via* oxime intermediates, the *O*-benzyl-protected amines **356a-d** in reasonable yields (63% to 68%). Acetylation of compounds **356a-d** was achieved by using acetyl chloride in the presence of triethylamine, to obtain the *O*-benzyl-protected acetyl derivatives **357a-d**. Compounds **356a-d** and **357a-d** are all new and were fully characterised. Figures 78 and 79 illustrate the ^{1}H NMR spectra of compounds **356a** and **357c**, respectively. In Figure 79, the signals between 7.29 and 7.36 ppm integrate for the ten aromatic protons corresponding to the two benzyl groups and indicate the success of the reductive amination step. The vicinal 1- and 2-methylene protons couple with each other and resonate as a complex multiplet at *ca.* 2.90 ppm, while the two singlets at 3.82 and 4.73 ppm correspond to the 3- and 4-methylene groups attached to the benzene rings. In the ^{1}H NMR spectrum of compound **357c** (Figure 79), the success of the acetylation step was confirmed by the presence of the acetyl methyl singlet at 2.01 ppm. Significantly, introduction of the acetyl group deshields the 2-methylene protons, resulting in separation of the vicinal 1- and 2-methylene proton multiplets in the acetylated systems. Analysis of the COSY and HSQC spectra permitted

assignment of the aromatic protons signals in the anilino ring. The IR spectrum showed absorption bands for the NH_2 and carbonyl groups at 3387 cm^{-1} and 1692 cm^{-1}.

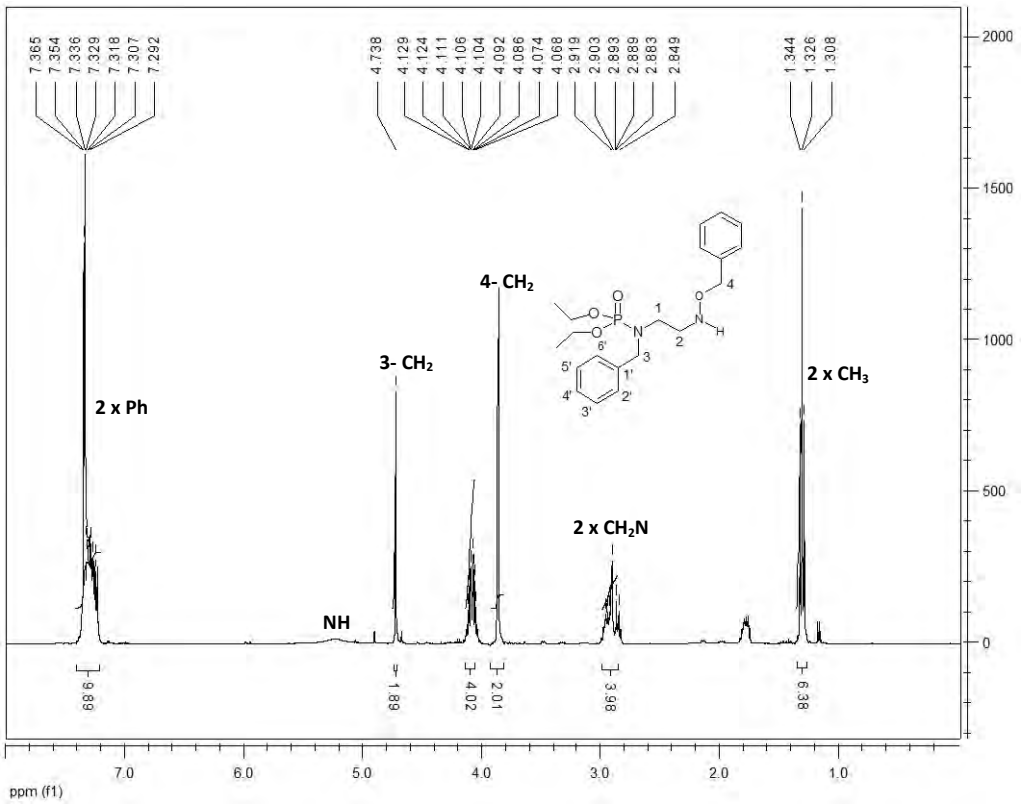

Figure 78. 400MHz ^{1}H NMR spectrum of compound **356a** in $CDCl_3$.

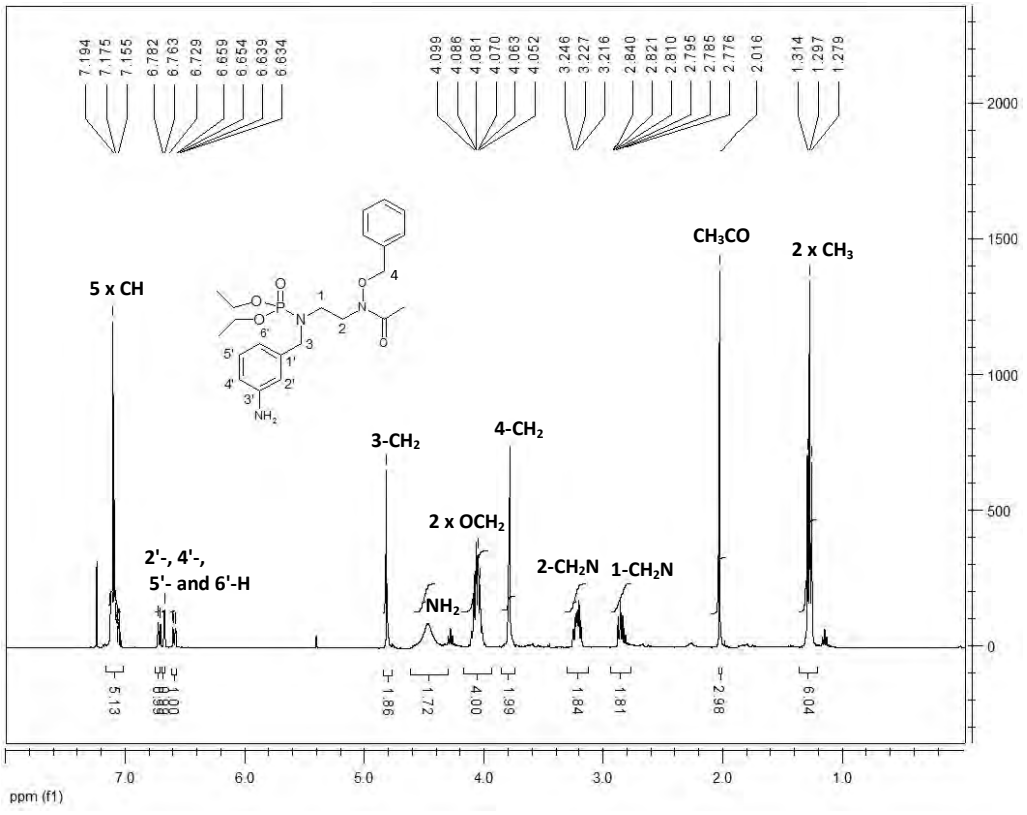

Figure 79. 400MHz ^{1}H NMR spectrum of compound **357c** in $CDCl_3$.

The final two steps in the synthesis (Scheme 57) of the target compounds **351a-d** involved the removal of the *O*-benzyl protecting group and hydrolysis of the diethyl ester groups of the phosphoramidate moiety. The *O*-benzyl protecting group was removed by catalytic hydrogenolysis using 10 % Pd/C in methanol to yield the hydroxamate derivatives **363a-d** which, following treatment with TMSBr and hydrolysis, furnished the corresponding phosphoramidic acids **351a-d**. The diethyl ester intermediates **363a-d** could serve as ester prodrugs of the phosphoramidic acids **351a-d**, exhibiting better lipophilicity prior to being hydrolysed by non-specific esterases *in vivo*. The novel products **363a-d** and **351a-d** were all fully characterised. Figure 80 illustrates comparative ^{13}C NMR spectra of the phosphoramidate ester **363d** and the phosphoramidic acid **351d**; and clearly reveals the success of the hydrolysis reaction with the disappearance of the ethyl ester signals. Analysis of the IR spectrum for compound **351d** showed the absorption band for the hydroxyl group at 3326 cm^{-1}, while the absorption bands for the mercapto and carbonyl groups were observed at 2575 cm^{-1} and 1687 cm^{-1}, respectively.

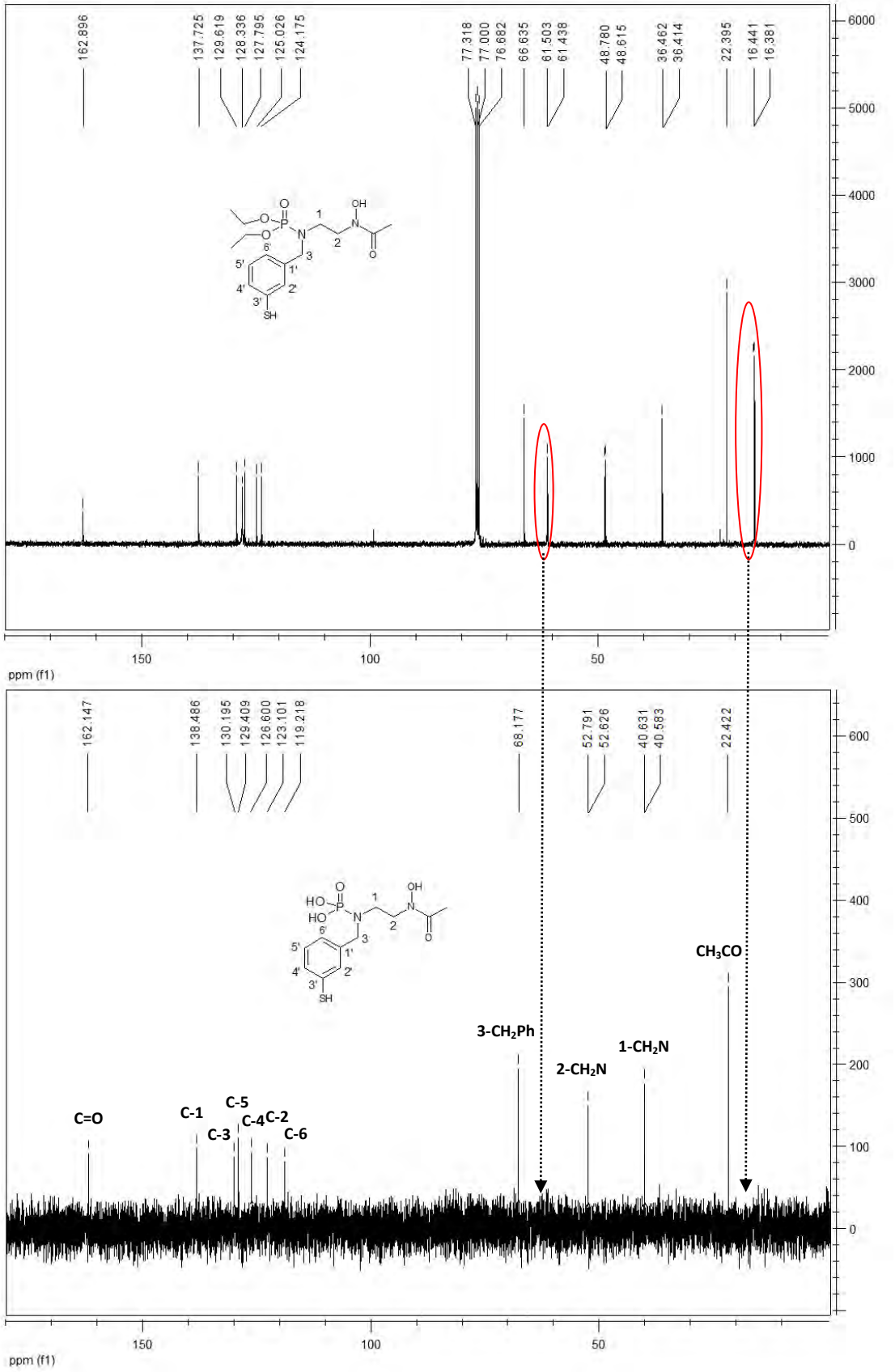

Figure 80. 100 MHz ^{13}C NMR spectra of compound **363d** (top, $CDCl_3$) and compound **351d** (bottom, D_2O), showing the disappearance of the ethyl ester signals (circled) upon hydrolysis.

2.5. Enzyme-binding and -Inhibition studies.

2.5.1. Synthesis of fosmidomycin and FR900098 as standards for biological studies.

Fosmidomycin **236** and its acetyl derivative, FR900098 **237**, have been identified as potent inhibitors of DXR and clinical studies have proven that these molecules exhibit strong anti-malarial activity *in vitro*.[116,200] One of the aims of this project has been to determine the biological activity of a selection of the synthesised novel compounds (Sections 2.1, 2.2, 2.3 and 2.4), against *Ec*DXR and *Pf*DXR *in vitro*. Consequently, we decided to synthesise fosmidomycin **236** and FR900098 **237** for use as standards in the STD NMR binding and the enzyme-inhibition studies. Much interest has been generated in the design of fosmidomycin-like molecules as DXR inhibitors, and various research groups have reported different synthetic routes to fosmidomycin **236** and FR900098 **237**.[118-119,201-202] We employed and adapted the method reported by Schlitzer *et al.*,[118-119] outlined in Scheme 58.

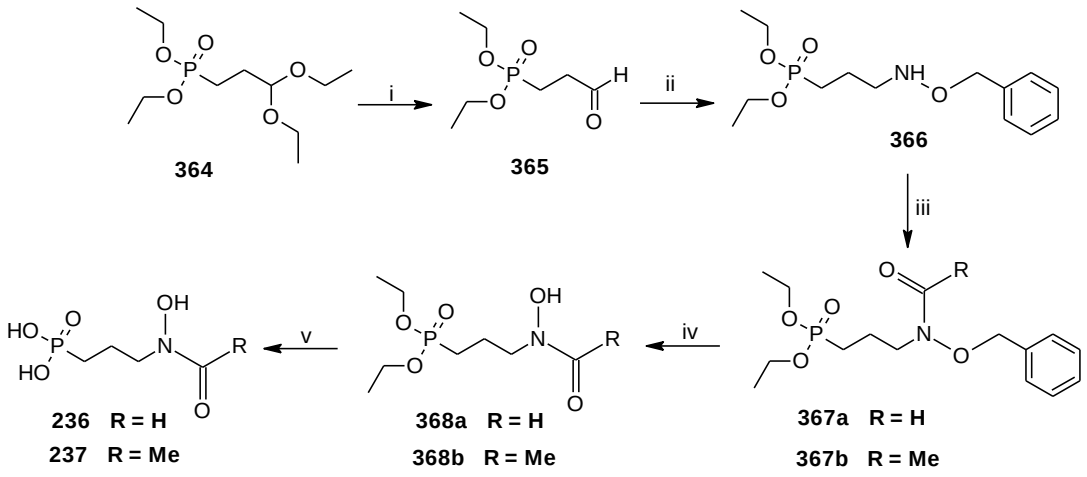

Scheme 58. Synthesis of known DXR inhibitors, fosmidomycin **236** and FR900098 **237**.[118]
Reagents and conditions: i) 2M-HCl, r.t., overnight; ii) *O*-benzylhydroxylamine, MeOH, 40 ^{o}C, 3 h and then $NaCNBH_3$, MeOH, HCl, r.t., 1 h; iii) formic acid, sodium formate, 80 ^{o}C, 2 h [203-204] or acetyl chloride, DCM, Et_3N, r.t., 24 h, N_2; iv) H_2, Pd/C, MeOH; v) TMSBr, DCM, 0 ^{o}C, 1 h and then H_2O, r.t., overnight.

The first step in the synthesis of inhibitors **236** and **237** involved acidic hydrolysis of the commercially available acetal **364** to give the corresponding aldehyde **365** in reasonable yield (68%). The aldehyde **365** was subsequently treated with *O*-benzylhydroxylamine to give the oxime, which was reduced *in situ* in the presence of sodium cyanoborohydride and

hydrochloric acid to furnish the *O*-benzyl-protected hydroxylamine **366**. Using a method adapted from Brahmachari *et al.*[203] and Majee *et al.*[204], compound **366** was successfully *N*-formylated by refluxing with formic acid and a catalytic quantity of sodium formate to obtain the intermediate **367a**. Also, compound **366** was acetylated with acetyl chloride in the presence of triethylamine to give the acetylated derivative **367b**.

Figures 81 and 82 illustrate the ^{1}H and ^{13}C NMR spectra of intermediates **367a** and **367b**, respectively. In the ^{1}H NMR spectrum (Figure 81) of intermediate **367a**, the success of the formylation reaction is indicated by the presence of the aldehyde signal at 8.13 ppm. The multiplets at 1.94 ppm and 1.74 ppm correspond to the 1- and 2-methylene groups, respectively, and are split due to coupling to each other and the adjacent ^{31}P nucleus, while the signal for the 3-methylene protons resonates as a triplet at 3.72 ppm. The phosphonate ethyl ester signals resonate at 1.32 ppm and 4.08 ppm, while the singlet at 4.83 ppm corresponds to the benzylic methylene protons. The signal at 7.39 ppm integrates for five protons and thus corresponds to the benzene ring protons. In the ^{13}C NMR spectrum (Figure 82) of compound **367b**, the methyl carbon of the acetyl group resonates at 19.7 ppm, while the carbonyl carbon signal appears at 162.9 ppm. The doublet at 23.5 ppm corresponds to the 1-methylene group, with a coupling constant of 141.2 Hz characteristic of coupling to an adjacent ^{31}P nucleus. The C-2 and C-3 methylene carbons resonate at 20.7 ppm and 52.3 ppm respectively, and are also split by coupling to ^{31}P nucleus coupling, as are the signals at 16.8 ppm and 61.9 ppm, which correspond to the phosphonate ethyl ester group; the acetyl carbonyl signal is evident at 163.0 ppm.

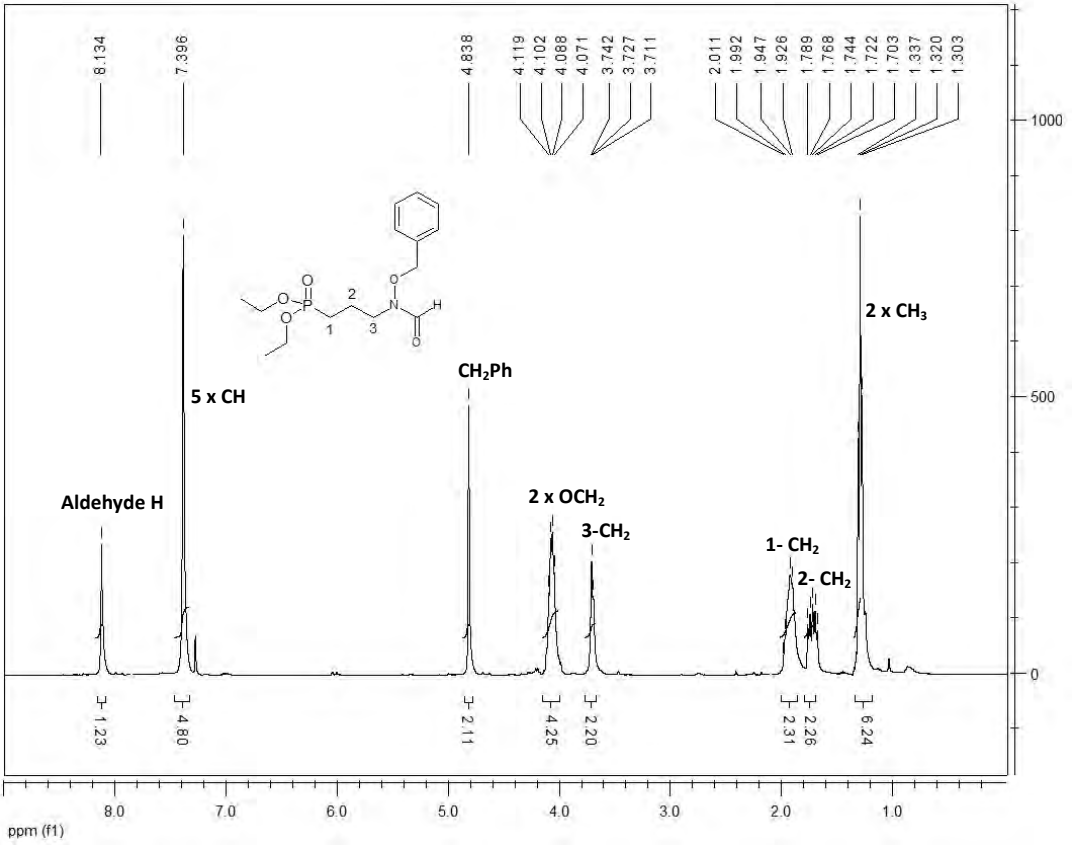

Figure 81. 400 MHz ^{1}H NMR spectrum of intermediate **367a** in $CDCl_3$.

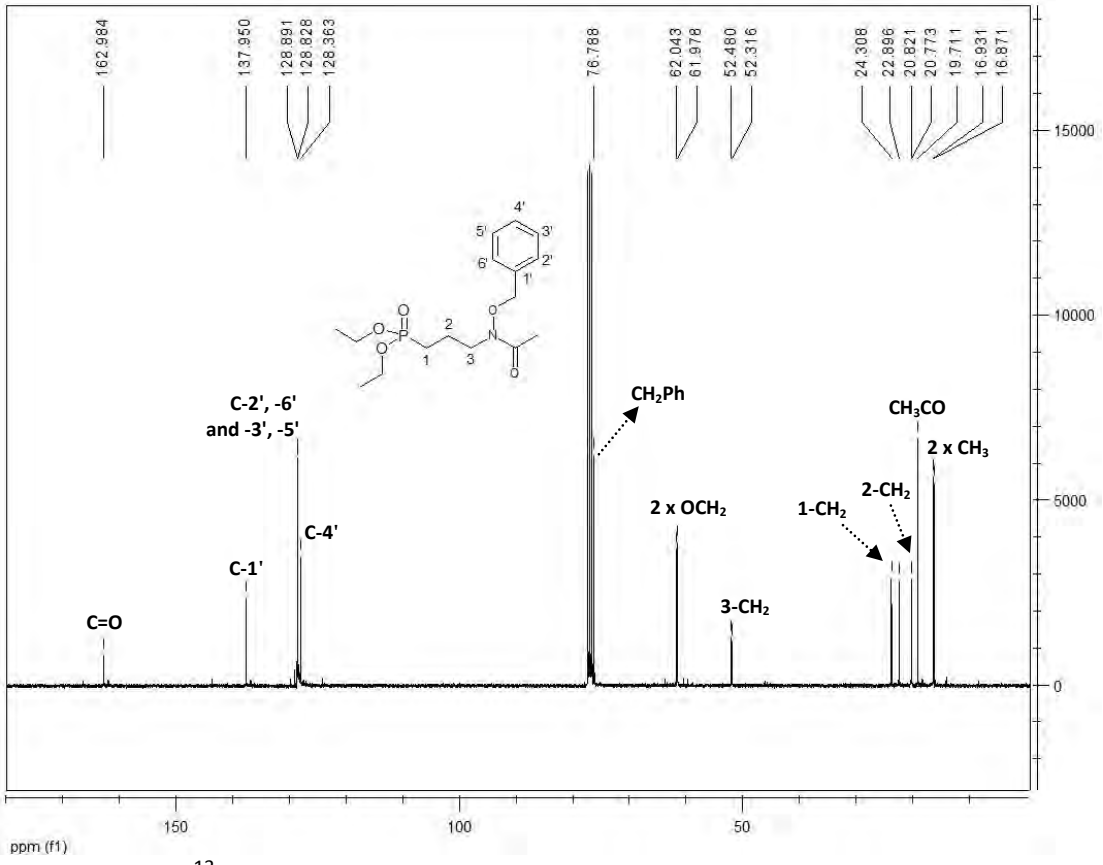

Figure 82. 100 MHz ^{13}C NMR spectrum of intermediate **367b** in $CDCl_3$.

The next step in the preparation of inhibitors **236** and **237** involved the removal of the benzyl protecting groups of intermediates **367a** and **367b** to yield the phosphonate ester derivatives **368a** and **368b**. Treatment of compounds **368a** and **368b** with TMSBr produced the silyl esters, *in situ* hydrolysis of which finally afforded fosmidomycin **236** and FR900098 **237**, respectively. While requiring HPLC purification prior to use as bioassay standards, both compounds were fully characterised with the ^{1}H and ^{13}C spectroscopic data corresponding to the published data. Figures 83 and 84 show the ^{13}C NMR spectra of fosmidomycin **236** and FR900098 **237** respectively, both of which reveal coupling of the ^{31}P nucleus with all three methylene groups. The carbonyl carbon of the formyl group resonates at 155.7 ppm in the ^{13}C spectrum of fosmidomycin **236**, while the acetyl group in FR900098 **237** is evidenced by the methyl signal at 20.0 ppm and the carbonyl signal at 162.8 ppm.

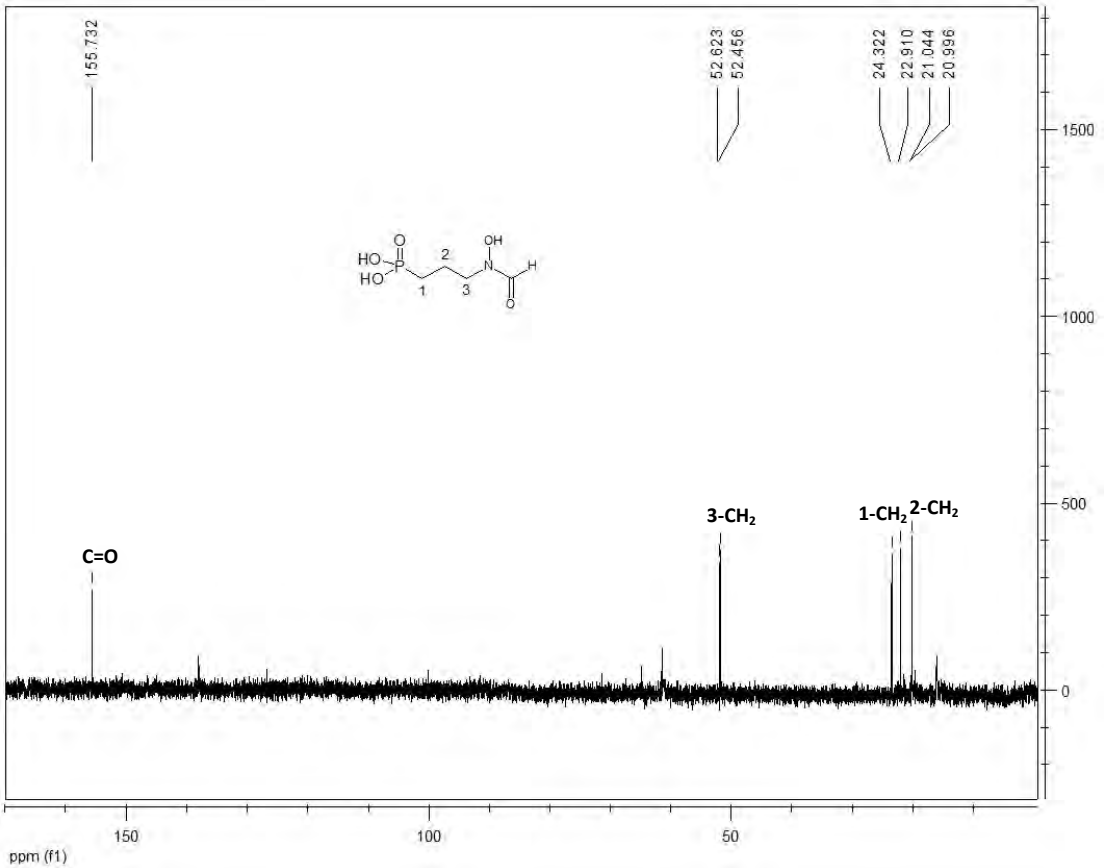

Figure 83. 100 ^{13}C NMR Spectrum of fosmidomycin **236** in D_2O.

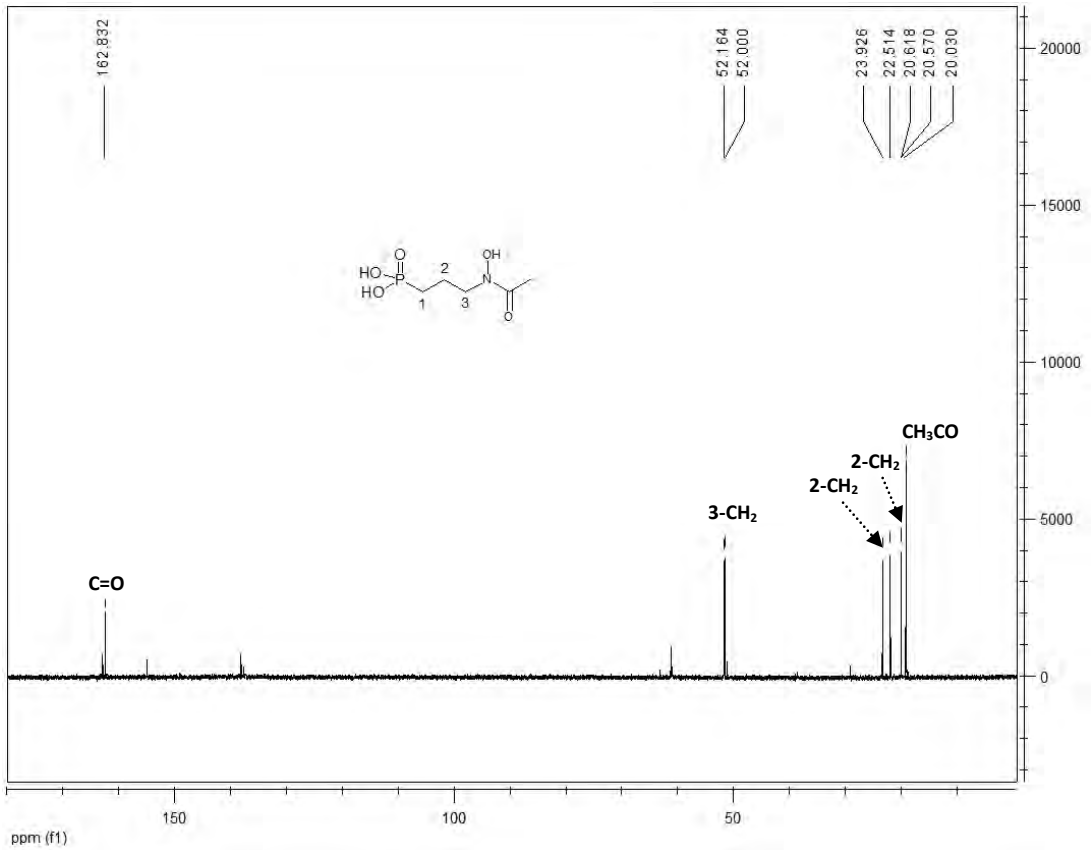

Figure 84. 100 MHz ^{13}C NMR spectrum of FR900098 **237** in D_2O.

2.5.2. Saturation transfer difference (STD) protein NMR binding studies.

The saturation transfer difference NMR experiment is a screening assay which may be used to determine binding interactions between a set of ligands and a target protein.[205-206] An STD spectrum is obtained by irradiating the protein at a frequency at which the ligands do not absorb. Intermolecular spin diffusion leads to the transfer of protein saturation to ligands which bind to the protein, and consequently, increase the signal intensities of these ligands; the non-binding ligands remain unaffected.[205-206] A reference spectrum is also acquired by irradiating the ligand-protein mixture at a frequency at which none of the species resonate (off-resonance irradiation), resulting in equal saturation of all the species. Subtraction of the reference spectrum from the saturated spectrum produces a difference spectrum, showing only the signals of the ligands interacting with the protein.[206] Sets of ligands can be studied simultaneously in a particular STD experiment, provided the ^{1}H NMR spectra of the individual ligands are sufficiently different.

STD experiments were conducted on a selection of the synthesised ligands (Section 2.1 - 2.4) to determine their binding to *Ec*DXR. The *Ec*DXR was expressed and purified, for the author, using standard protocols[115,142] and a fraction, 20 µM in *Ec*DXR, was used in each experiment. The *Ec*DXR in sodium phosphate buffer (pH 7.0) was freeze-dried and re-suspended in an equal volume of D_2O. The ligands were dissolved in the protein solution to give a protein:ligand molar ratio of 1:40. The STD experiments were carried out using parameters which had been optimized in a previous study in our group.[129] The saturating on-resonance and off-resonance pulses were set at frequencies of 0.73 ppm and 20 ppm, respectively, while cycling between the on- and off-resonance phases was used to reduce the effects of changes in temperature or magnetic field homogeneity.

The *Ec*DXR-STD experiments were carried out on the phosphonic acid derivatives as the corresponding phosphonate esters were expected to act as pro-drugs and require *in vivo* hydrolysis before binding. The ^{1}H NMR spectra of compounds **293a-d, 293f, 328a, 328e-f** and **331a-b**, and the corresponding STD difference spectra are illustrated as stacked plots in Figures 85 and 86. A spin-lock filter was not used in the experiments, resulting in the presence of the underlying protein spectrum in the difference spectrum. The results of the

*Ec*DXR-STD binding experiments conducted on the selected novel compounds are summarized in Table 8.

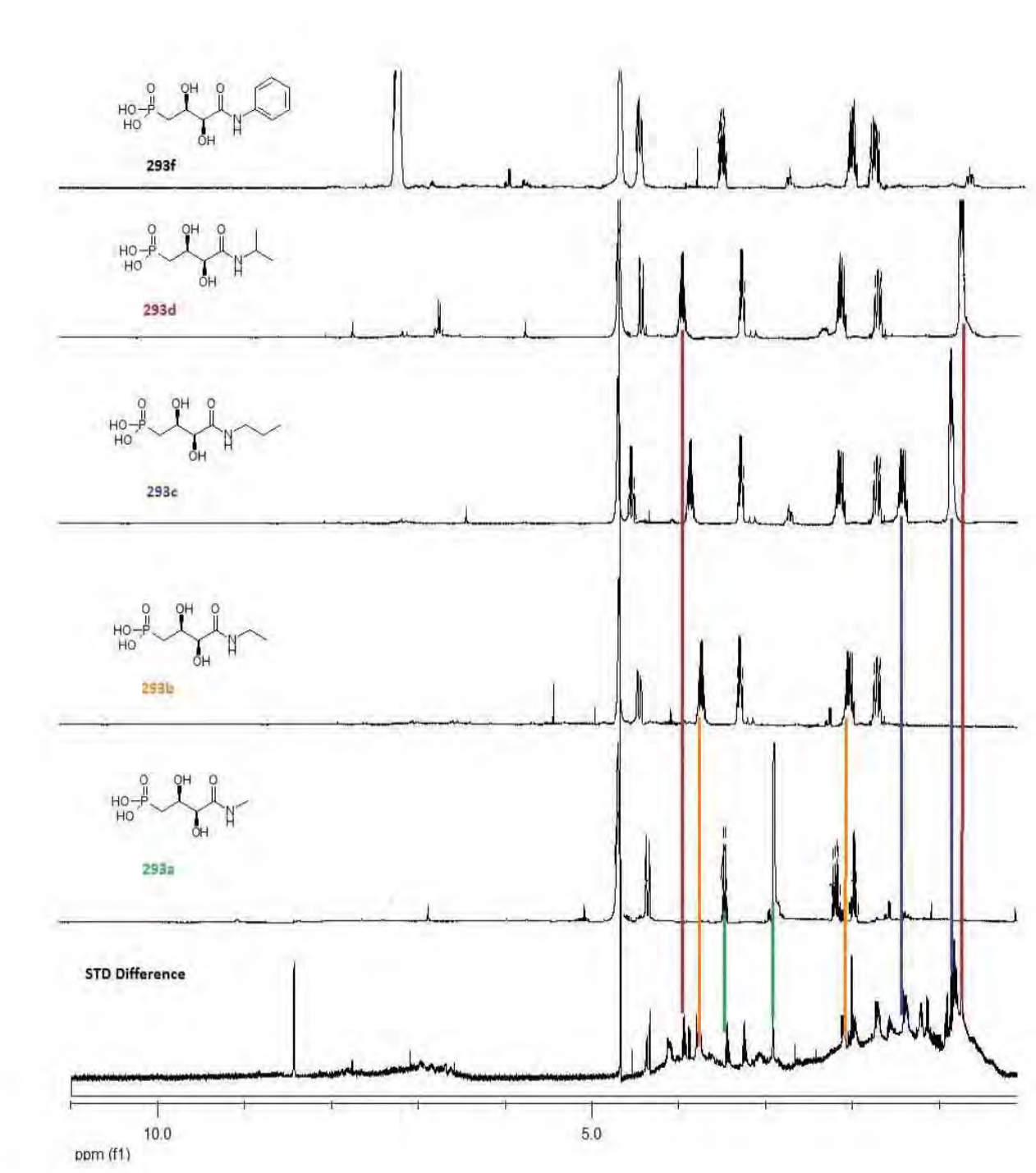

Figure 85. Stack-plot showing results from the *Ec*DXR STD experiment conducted in D_2O with compounds **293a-d** and **293f**. The correlations between individual ligand signals and signals in the difference spectrum are indicated by the coloured lines.

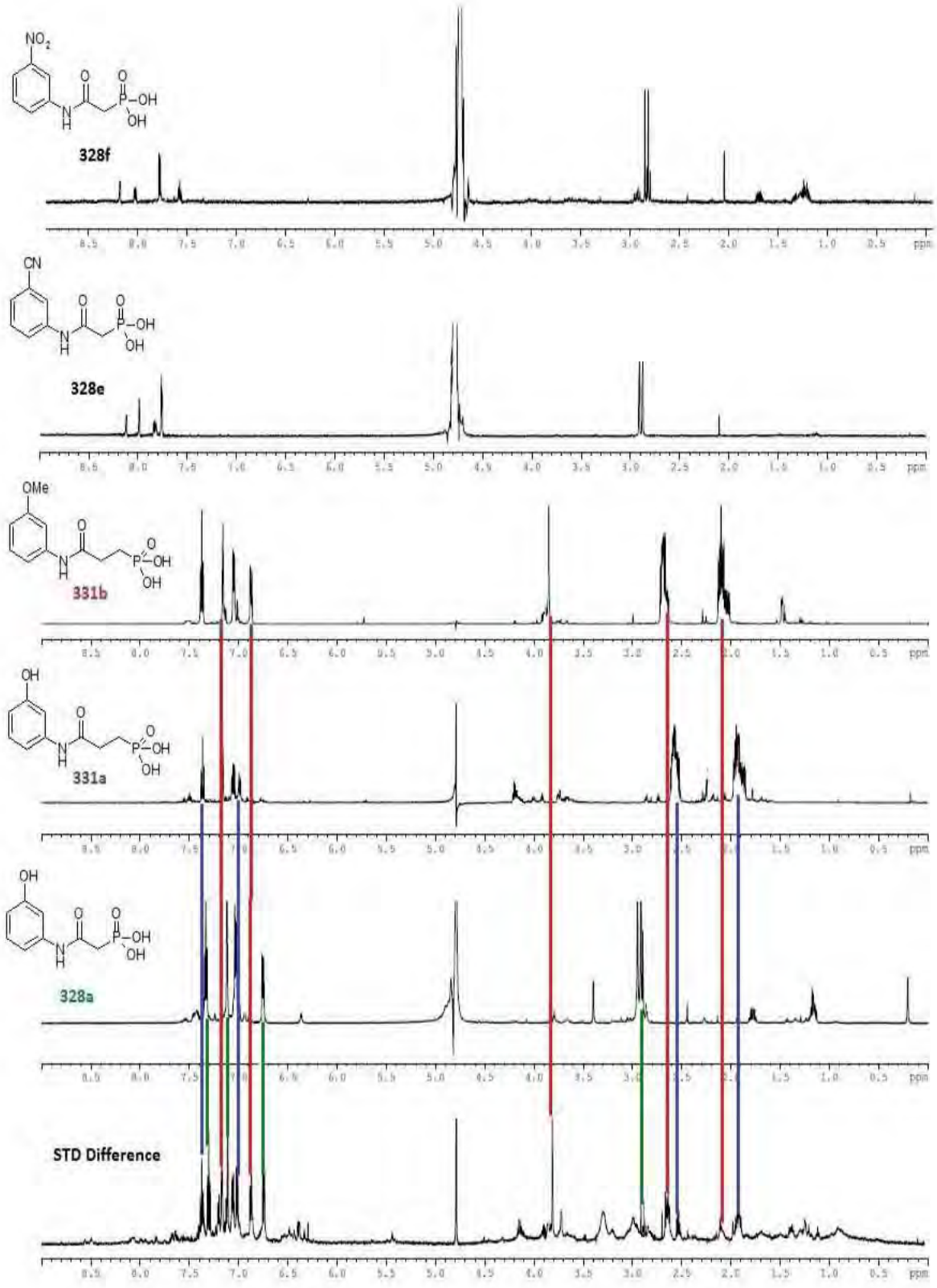

Figure 86. Stack-plot showing results from the *Ec*DXR STD experiment conducted in D_2O with compounds **328a**, **328e,f** and **331a,b**. The correlations between individual ligand signals and signals in the difference spectrum are indicated by the coloured lines.

Table 8. Results of *Ec*DXR STD binding experiments to screen selected ligands for binding to *Ec*DXR, with observed binding interactions indicated by a positive (+) sign.

*a) Dihydroxy-amido phosphonic acids **293a-g**.*

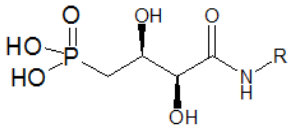

Compound	R	STD result
293a	Me	+
293b	Et	+
293c	Pr	-
293d	Pr^i	+
293e	Bu^t	-
293f	Ph	-
293g	CH_2Ph	-

*b) 3-Substituted aniline-derived phosphonic acids **328b,d-g**; **331a-d**; **333a,e,f**; **335a,c**.*

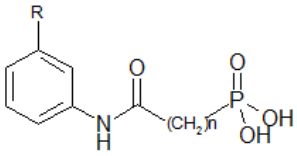

Compound	R	n	STD result
328b	OMe	1	+
328d	F	1	-
328e	CN	1	-
328f	NO_2	1	-
328g	CH_2OH	1	+
331a	OH	2	+
331b	OMe	2	+
331c	Br	2	+
331d	F	2	-
333a	OH	3	+
333e	CN	3	-
333f	NO_2	3	-
335a	OH	4	-
335c	Br	4	-

Table 8 Contd.

*c) Furan-derived phosphates **337b** and **337c**.*

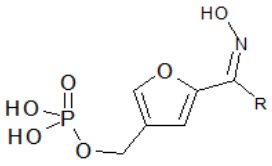

Compound	R	STD result
337b	H	+
337c	Me	+

d) N-*Benzyl-substituted phosphoramidic acids **351a** and **351d**.*

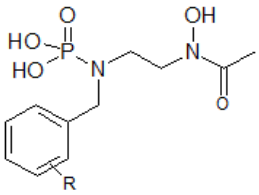

Compound	R	STD result
351a	H	+
351d	SH	+

The STD experimental data (Table 8) for the dihydroxy-amido phosphonic acid derivatives indicate that compounds **293a,b** and **d** bind to *Ec*DXR, whilst compounds **293c** and **e-g** do not. The binding interactions may be attributed to the fact that ligands **293a,b** and **d** are similar in size to the known inhibitors fosmidomycin **236** and FR900098 **237**, and are thus able to occupy the enzyme's active-site comfortably. Importantly, the presence of the hydroxyl groups at C-2 and C-3 are expected to provide additional hydrogen-bonding interactions with active-site residues. These conclusions are consistent with the molecular modelling results discussed in Section 2.6. Compounds **293c** and **e-g**, on the other hand, contain propyl, butyl, phenyl or benzyl groups attached to the amide nitrogen, and the steric bulk of these groups are presumed to prevent these analogues from fitting into the sterically restricted DXR-active site. It seems that the binding site can accommodate the branched *N*-isopropyl group in ligand **293d** but not the longer *N*-propyl group in **293c**. Access to the metal-binding region, which the amide moiety in compounds **293a-g** are expected to occupy, is constrained by the presence of the metal cation, the NADPH co-factor and the channel through which the ligand enters the active-site.[105,107] MacSweeney *et al.*[105] have suggested that inhibitors greater in length than fosmidomycin **236** could displace NADPH or bind to an open conformation of DXR, although a decrease in inhibitory activity

has been reported for inhibitors with an acyl chain extended beyond the hydroxamate group.[207]

STD experiments conducted with the 3-substituted aniline-derived phosphonic acids **328b,d-g** indicated binding of ligands **328b** and **328g**. From these results, it appears that the presence of a fluoro, nitro or cyano substituent on the phenyl ring has a negative effect on the binding affinity of compounds **328d-f**, possibly due to unfavourable electrostatic interactions. Interestingly, the *in silico* docking of compounds **328e** and **328f** in the active site of a modelled structure of *Pf*DXR in a collaborative study by Goble *et al.*,[208] indicated that these compounds do not fully occupy the active site and that they bind in a reverse orientation compared to fosmidomycin **236**. Further analysis of the STD results for the 3-aniline derived phosphonic acids (Table 8) revealed that:- i) the compounds containing an OH, OMe or CH_2OH substituent all showed positive binding to *Ec*DXR, except for **335a** (R = OH); ii) the extension of the carbon spacer to four methylene groups (n = 4) between the amide group and the phosphonic acid moiety appears to prevent compounds **335a** and **335c** from binding to *Ec*DXR, whereas analogues with fewer methylene groups (**331a,c**; **333a**) do appear to bind. These observations are consistent with those reported in literature, with the more active DXR inhibitors against DXR containing a hydroxyl group as part of the hydroxamate moiety and a three-carbon spacer between the phosphonate and metal binding groups being optimal. [105,122,125,131,134]

The positive binding data obtained for the furan analogues **337b,c** is encouraging and supports the *in silico* docking observations (Section 2.6, p.143) which indicate binding of the phosphonate group and metal-chelating group to their respective sites in the *Ec*DXR active-site. The restricted flexibility provided by the furan ring in compounds **337b,c** may well ensure that the inhibitors remain anchored in an ideal conformation within the active site. The *N*-benzyl substituted phosphoramidic acid analogues **351a** and **351d** were expected to show reasonable binding to *Ec*DXR, as these novel analogues were designed following a detailed study in our group[129] of the topology of the *Ec*DXR and *Pf*DXR catalytic sites. The *N*-benzyl α-substituent was expected to occupy one of the reported hydrophobic binding pockets,[122,128-129] thus increasing the compounds binding affinity to the enzyme. Furthermore, only α-phenyl substituted hydroxamic acid analogues of fosmidomycin **236**

have previously been shown to exhibit inhibitory activities as potent as those of fosmidomycin **236** and FR900098 **237**.[124-125,134]

The binding data obtained from the STD experiments have indicated that the technique is useful as an initial screen to identify potential DXR inhibitors, albeit with limitations. Although protein-ligand binding interactions were observed in the STD experiments, the possibility of the ligands binding non-specifically to regions other than the active-site cannot be excluded;[209] in its standard form, the STD experiment only provides qualitative data. However, it may be possible to optimize the experiment for a particular ligand and conduct the experiment in the presence of the slow, tight- binding inhibitor fosmidomycin in order to accurately determine whether the observed protein-ligand binding is active-site specific or allosteric and to calculate binding affinities.[129,209-210] Unfortunately, time constraints prevented further investigation.

2.5.3. Enzyme inhibition assays.

The mechanism for the catalytic conversion of DOXP **230** to MEP **231** by DXR involves an intramolecular rearrangement step followed by an NADPH-dependent reduction step.[91] A DXR-inhibition bioassay has been developed based on the spectrophotometric measurement of the conversion of NADPH to NADP, to determine the capacity of novel compounds to inhibit both *Ec*DXR and *Pf*DXR.[115,127] The compounds discussed in Section 2.2 were tested for *Ec*DXR inhibitory activity for the author[211] and for *Pf*DXR inhibitory activity in a collaborative study by Goble *et al*.[208] The novel compounds synthesized and discussed in Sections 2.1, 2.3 and 2.4 were not subjected to the inhibition bioassay due to time constraints and the limited availability of the *Ec*DXR and *Pf*DXR enzymes precluded bioassay of the other novel ligands prepared in this study. It is expected, however, that these assays will be conducted in due course.

To assess their inhibition potential, the selected ligands were tested at a concentration of 250 µM, as this represented the initial concentration at which none of the ligands gave complete inhibition of the enzyme. Considering that fosmidomycin **236** is a slow-tight binding inhibitor of DXR,[124] the synthesized ligands were pre-incubated with the enzyme and NADPH before the reaction was initiated with the addition of the substrate, DOXP **230**.

For each ligand, the bioassays were carried out in triplicate and the specific activity of the enzyme was determined by analyzing the linear portion of the graph generated by plotting average absorbance (at 340nm) against time (over 10 minutes). The specific activity of the enzyme in the experiment lacking a ligand was considered to be 100% (i.e. 0% inhibition), which allowed the inhibitory activities to be expressed as relative percentages. Fosmidomycin **236** was used as a positive control for DXR inhibition and exhibited 99.3% inhibition at 0.3 µM.

Table 9. Results for the inhibition[a] of recombinant *Ec*DXR at 250 µM for selected compounds.

		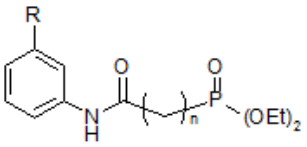		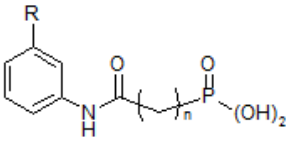		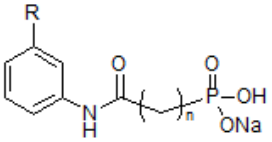	
R	**n**		**Inhibition (%)**		**Inhibition (%)**		**Inhibition (%)**
OH	1	321a	24.38	328a	43.94	329a	41.58
Br	1	321c	21.35	328c	26.46	329c	22.77
CN	1	321e	11.93	328e	20.01	329e	22.47
OH	2	323a	33.51	331a	49.23	332a	40.25
OMe	2	323b	14.11	331b	17.75	332b	12.13
CH_2OH	2	323g	17.92	331g	26.81	332g	34.95
OH	3	325a	0.81	333a	0.66	334a	0.96
Br	3	325c	-[b]	333c	-[b]	334c	-[b]
NO_2	3	325f	-[b]	333f	-[b]	334f	-[b]
OH	4	327a	-[b]	335a	-[b]	336a	-[b]
OMe	4	327b	-[b]	335b	-[b]	336b	-[b]
F	4	327d	-[b]	335d	-[b]	336d	-[b]

[a] Activity in the absence of compound set at 100 %.
[b] Negative % inhibition indicating activation of enzyme.

The inhibition assay data summarised in Table 9 shows that the inhibitory potency of all the compounds tested is much lower than that of fosmidomycin **236** and other inhibitors reported in literature. Nonetheless, several structure-activity relationship patterns were observed. Compounds **328a**, **329a**, **331a** and **332a** exhibited inhibitory activity against *Ec*DXR of more than 40% at 250 µM. Interestingly, all these compounds have the hydroxyl group attached at the *meta*-position of the benzene ring and the presence of this OH group

may well provide favourable electrostatic or hydrogen-bonding interactions within the enzyme's active site.

All of the phosphonate ester inhibitors, except compounds **323b** and **325a**, exhibited a lower percentage inhibition compared to their corresponding phosphonic acid derivatives. The catalytic site of *Ec*DXR is relatively polar in nature and is restricted by the phosphonate binding region on one side and the metal- and NADPH-binding site on the other.[103,110,127] Consequently, it is probable that the phosphonate ester ligands may be too hydrophobic and too bulky to be accommodated effectively in the active-site. Furthermore, Perruchon *et al.*[128] have emphasized the importance of a double negative charge on the phosphonate moiety. However, the phosphonate ester inhibitors could exhibit higher inhibition activity than the corresponding phosphonic acids *in* vivo, as their lipophilic nature could allow them to penetrate the parasite's membrane more readily, thus resulting in higher intra-parasitic drug concentrations.[118, 119, 212] The difference in percentage inhibition values between the phosphonic acids and their corresponding mono-sodium salts is relatively small.

It seems, from the data in Table 9, that the presence of two methylene groups between the amide group and the phosphonate moiety is advantageous but increasing the number to three or four decreases the inhibitory activity. This observation was expected, as analyses of the DXR active site have shown that the length of the cavity is restricted by the phosphonate-binding region at one end and the metal-and NADPH-binding site at the other.[105,110,127,129] Furthermore, fosmidomycin **236** analogues in which the length has been varied have shown a decrease in inhibitory activity and it has been suggested that the 3-carbon spacer between the hydroxamate- and phosphonate-binding groups in fosmidomycin **236** is ideal.[149,207] Compounds with one or two methylene spacers showed low to moderate inhibitory activity, whilst minimal or zero inhibition was observed for the compounds with three or four methylene spacers. These results are consistent with the docking studies (Section 2.6) from which it was apparent that three or four methylene groups extend beyond the active site and do not bind as efficiently as the ligands with one or two methylene groups.

2.6. Molecular modelling and simulated docking studies

Computer modelling studies were undertaken to explore the *Ec*DXR receptor-binding potential of selected compounds synthesised in this study. The Accelrys Cerius^2 module[213] was used to construct the selected compounds *in silico* as their mono-deprotonated species. Using Gaussian 03,[214] the structure for each compound was optimised geometrically and energy-minimised at the density functional theory (DFT) B3LYP/6–31G(d) level. Docking studies of the geometry optimised and energy-minimised ligands was carried out using Autodock version 4.0,[215] using the crystallographically-determined enzyme structure, *Ec*DXR 2EGH,[103] as the protein-receptor model. The X-ray crystal structure *Ec*DXR 2EGH, is complexed with fosmidomycin **236**, the divalent metal cation Mg^{2+} and the NADPH co-factor.[103]

To validate the reliability of the docking procedure, fosmidomycin **236** was removed from the receptor cavity, energy-minimised and re-docked into the protein. Simulated docking of the energy minimised ligands involved the removal of fosmidomycin **236** and the solvating water molecules from the active site of the 2EGH crystal structure, whilst the NADPH co-factor was retained. Using Autodock 4.0, Gasteiger charges were added and non-polar hydrogens were merged for the respective ligands and the protein model, while the active-site residues Ser185, Ser221, Asn226, Lys227 and Glu 230 were assigned as flexible. The AutoGrid 4.0 algorithm was employed to represent the active site with a grid box of dimensions 60 x 60 x 60 units (grid-point spacing of 0.375 Å) along the x-, y- and z-directions, and atom maps were calculated for all possible active-site residue-ligand interactions. *In silico* dockings were conducted using the Lamarckian algorithm with a population size of 150, allowing for a maximum of 27 000 generations and 2.5 x 10^6 energy evaluations. For each ligand docking experiment, ten possible docked-conformers were generated. The best docked-conformer for each of the ligands was selected upon analysis of:- i) the ligand binding affinity (Kcal.mol^{-1}); ii) the ligand efficiency relative to fosmidomycin and; iii) the number of hydrogen-bonding interactions. The binding affinity measures the strength of the non-covalent interactions between the ligand and the protein.[216-217] The ligand efficiency measures the binding free energy per atom of the ligand and provides an indication of the quality of fit of the ligand within the active site of the enzyme.[218-219] A

ligand is classified as having a good binding affinity and good ligand efficiency by the magnitude of the negative values, as illustrated for fosmidomycin **236** (Table 10). The docked conformations were visualised using the Accelrys Discovery Studio Visualizer 2.0[220] software package. The binding affinity and ligand efficiency values computed for the lowest energy docked conformations of fosmidomycin **236** and of selected ligands are summarised in Table 10.

Table 10. Binding affinity and ligand efficiency data of fosmidomycin and selected ligands docked into *Ec*DXR.

Compound[a]	Binding affinity (Kcal.mol^{-1})	Ligand efficiency
Fosmidomycin	-15.22	-1.38
293a	-12.77	-0.98
293b	-10.19	-0.57
293c	-7.96	-0.53
293d	-8.30	-0.55
293e	-6.73	-0.42
293f	-7.54	-0.54
293g	-6.27	-0.48
328a	-9.64	-0.64
328c	-9.33	-0.78
328f	-8.65	-0.51
331a	-8.56	-0.54
331e	-9.93	-0.58
331g	-8.46	-0.47
333a	-5.70	-0.34
333b	-6.19	-0.34
333g	-4.15	-0.23
335a	-4.46	-0.26
335d	-4.67	-0.27

[a] Modelled as mono-deprotonated species.

Table 10 contd.

Compound[a]	Binding affinity (Kcal.mol^{-1})	Ligand efficiency
335e	-5.98	-0.46
337b	-10.84	-0.77
337c	-10.20	-0.68
337d	-5.89	-0.31
351a	-9.39	-0.49
351b	-8.80	-0.42
351c	-9.84	-0.56
351d	-9.36	-0.47

[a] Modelled as mono-deprotonated species.

The ligand structures used for the docking studies were the mono-deprotonated phosphonic acid derivatives. The importance of the phosphonate moiety being negatively charged and involved in hydrogen-bonding interactions has been highlighted.[113,127-128] The corresponding phosphonate ester analogues were expected to act as pro-drugs, being hydrolysed *in vivo* before reaching the active-site. Furthermore, docking of *N*-heteroarylamino phosphonate ester derivatives in the *Ec*DXR active site, in a cognate study in our group, revealed that the phosphonate ester analogues are too bulky to fit in the active site.[129]

The active site of *Ec*DXR is considered to be restricted in length by the presence of the phosphonate binding-site at one end and the divalent metal cation and NADPH binding-region at the other.[105,107] Analysis of the binding affinity and ligand efficiency values, as well as the binding conformations of the dihydroxy-amido phosphonic acids **293e-g** and 3-substituted aniline-derived phosphonic acids **333a,b,g** and **335a,d,e**, indicate that these ligands all exhibit some binding interaction with active site residues, but appear to be too large to fit, completely, in the *Ec*DXR active site and thus extend beyond the catalytic cavity. Increasing the number of methylene groups (1 to 4) between the amide group and the phosphonate moiety resulted in decreases in the binding affinity and ligand efficiency values, reflecting the inability of the larger ligands (methylene group > 2) to occupy the EcDXR active site appropriately. These results are consistent with the *Ec*DXR STD-NMR binding data (Table 8) and the enzyme-inhibition assay data (Table 9) discussed in previous

sections. Figures 87 and 88 illustrate the docked conformations of ligands **293f** and **337e** in the *Ec*DXR active site, respectively. Interestingly, the benzene rings of both ligands **293f** and **335e** occupy a region adjacent to the NADPH-binding site towards the top of the active site and project towards the channel region through which the ligand enters the active site. The occupation of the active-site by larger ligands such as **293f** and **335e** may result in these ligands binding to the open conformation of DXR, which has been suggested by MacSweeney *et al*.[105] Moreover, Henriksson *et al.*[107] identified a hydrated cavity lined by the residues Thr175, Ser245 and His248 (in *Mt*DXR) and suggested that compounds larger than fosmidomycin **236** could extend into this cavity. The STD-NMR binding data (Table 8) and enzyme-inhibition data (Table 9), however, suggest that such arrangements prevent efficacious binding.

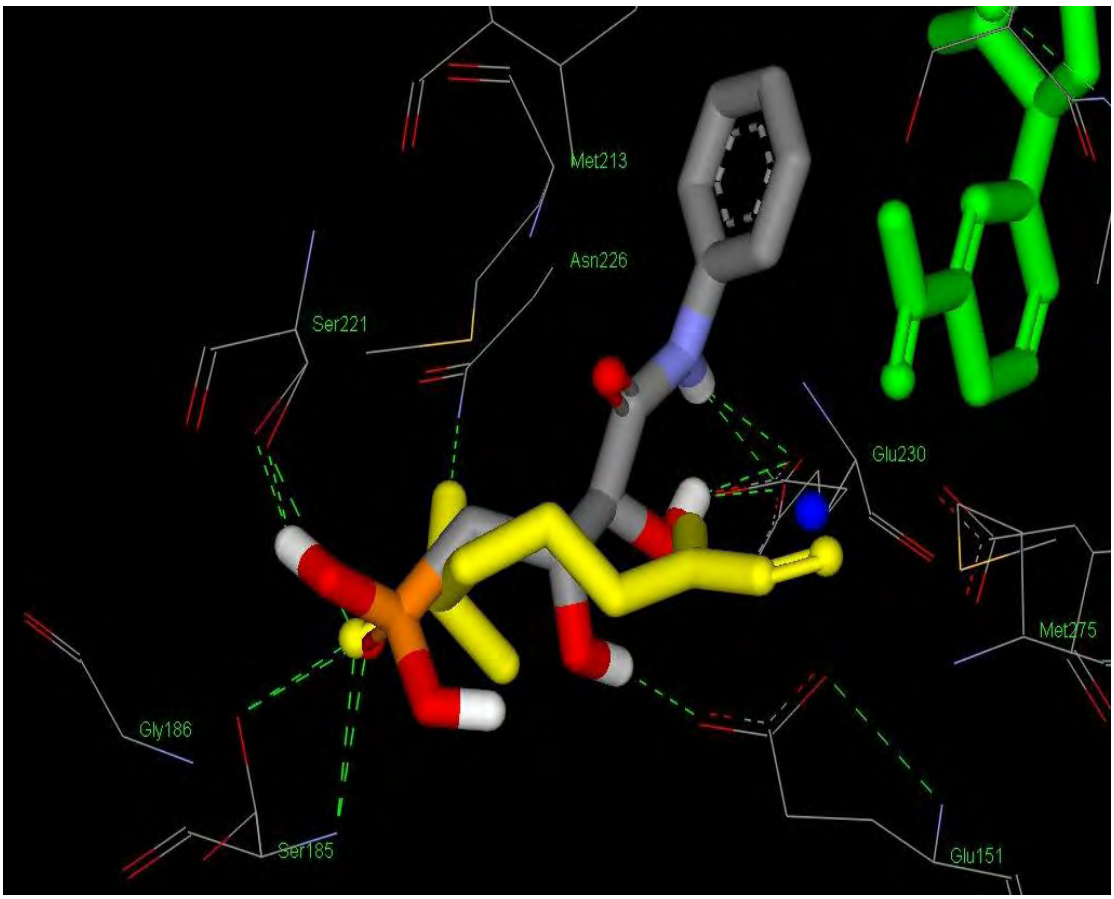

Figure 87. Docked conformation of the dihydroxy-amido phosphonic acid ligand **293f** in the *Ec*DXR active-site (2EGH), illustrating hydrogen-bonding of the ligand with active-site residues and the ligand extending beyond the metal binding site. The crystal structure conformation of fosmidomycin **236** is shown in stick format coloured yellow and highlights the docking alignment of ligand **293f**. Protein-active site residues are shown in wire-frame coloured by atom type, NADPH in stick coloured green, Mg^{2+} as a blue sphere and the ligand shown in stick format coloured by atom type. Hydrogen bonds are shown as green dashed lines.

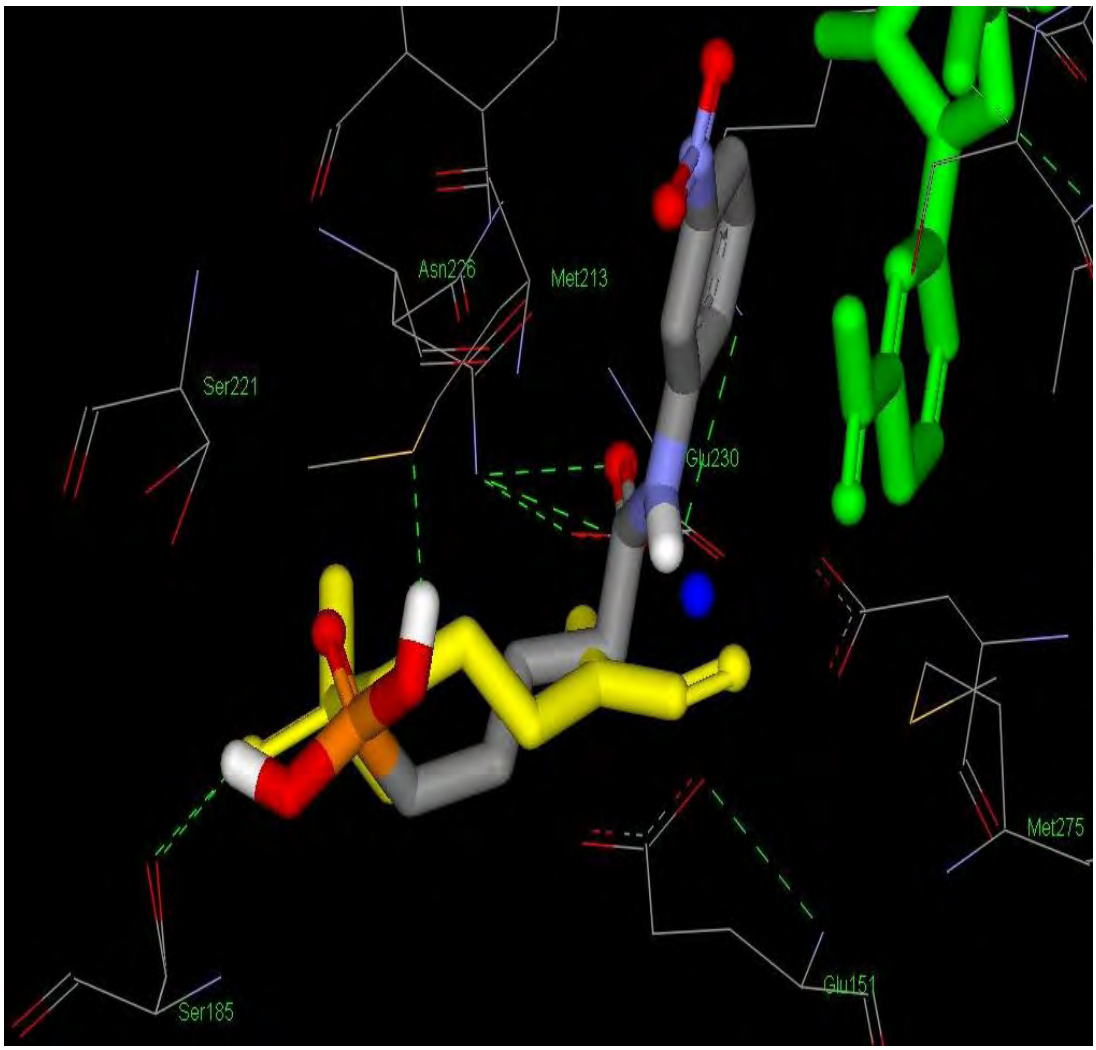

Figure 88. Docked conformation of the 3-substituted aniline-derived phosphonic acid ligand **335e** in the *Ec*DXR active-site (2EGH), illustrating hydrogen-bonding of the ligand with active-site residues and the ligand extending beyond the metal binding site. The crystal structure conformation of fosmidomycin **236** is shown in stick format coloured yellow and highlights the docking alignment of ligand **335e**. Protein active-site residues are shown in wire-frame coloured by atom type, NADPH in stick format coloured green, Mg^{2+} as a blue sphere and the ligand in sticks coloured by atom type. Hydrogen bonds are shown as green dashed lines.

The docking results (Table 10) show that ligands **293a,b** and **337b,c** exhibit the most favourable binding energy (relative to fosmidomycin), while ligands **293a**, **328c** and **337b** demonstrate ligand efficiency values better than -0.70. Examination of the docked conformation of ligand **293a** (Figure 89), suggests that the good binding affinity and ligand efficiency data observed for this ligand may be attributed to the close alignment with fosmidomycin. In addition, the carbonyl and NH groups of ligand **293a** exhibit hydrogen-bond with the active-site residues Lys 124, Glu151 and Asn226, while the phosphonic acid

group occupies the appropriate binding-region and interacts with the active-site residues Ser185 and Ser253. The positive STD-NMR binding data (Table 8) and enzyme-inhibition data (Table 9) obtained for compound **293a**, together with the favourable interactions observed in the *in silico* studies, presents ligand **293a** as a feasible, new lead-compound, targeting DXR in the development of novel anti-malarial drugs.

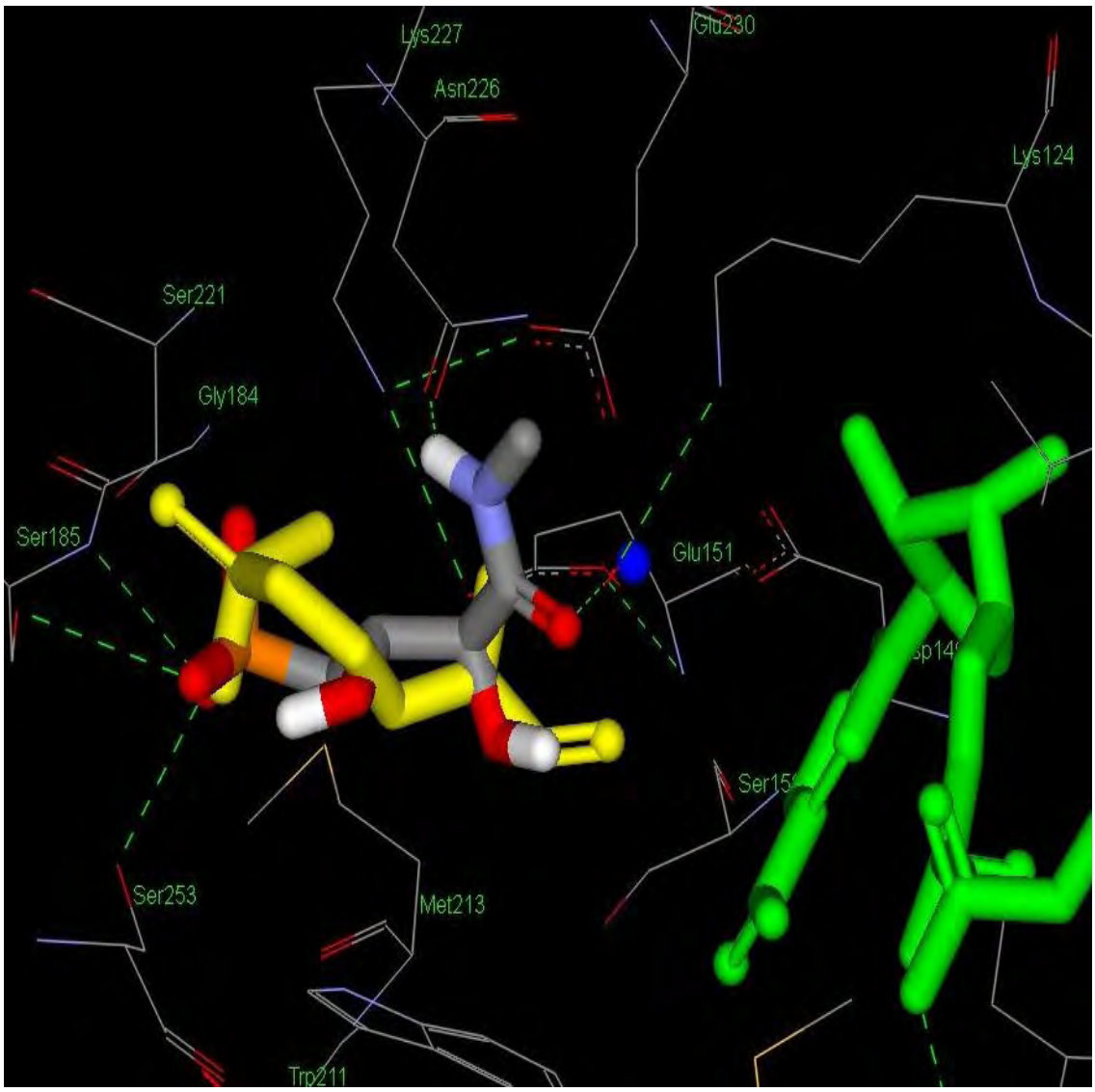

Figure 89. Docked conformation of the dihydroxy-amido phosphonic acid ligand **293a** in the *Ec*DXR active-site (2EGH), illustrating the close alignment of ligand **293a** with fosmidomycin and hydrogen-bonding of the ligand with active-site residues. The crystal structure conformation of fosmidomycin **236** is shown in stick format coloured yellow. Protein active-site residues are shown in wire-frame coloured by atom type, NADPH shown in stick format coloured green, Mg^{2+} as a blue sphere and the ligand in stick format coloured by atom type. Hydrogen bonds are shown as green dashed lines.

With regard to the conformationally-restricted furan-derived phosphate ligands **337b-d**, ligand **337b** exhibits the most favourable docked conformation within the active-site and exhibits hydrogen-bonding interactions with the residues, Lys 124, Glu151, Ser185, Ser221, Lys227 and Glu230 (Figure 90). Importantly, the presence of the furan-ring appears to restrict flexibility in the conformation of the linking group between the phosphonate-binding and metal-binding sites, while permitting hydrogen-bonding interactions between :- i) the furan-ring oxygen atom with Lys 124; and ii) the hydroxyl group of the oxime moiety with Lys 124. Analysis of the docked conformation of the analogue **337d** reveals that the ligand is too bulky to be accommodated in the active-site as the *tert*-butyl group extends well beyond the metal-binding site.

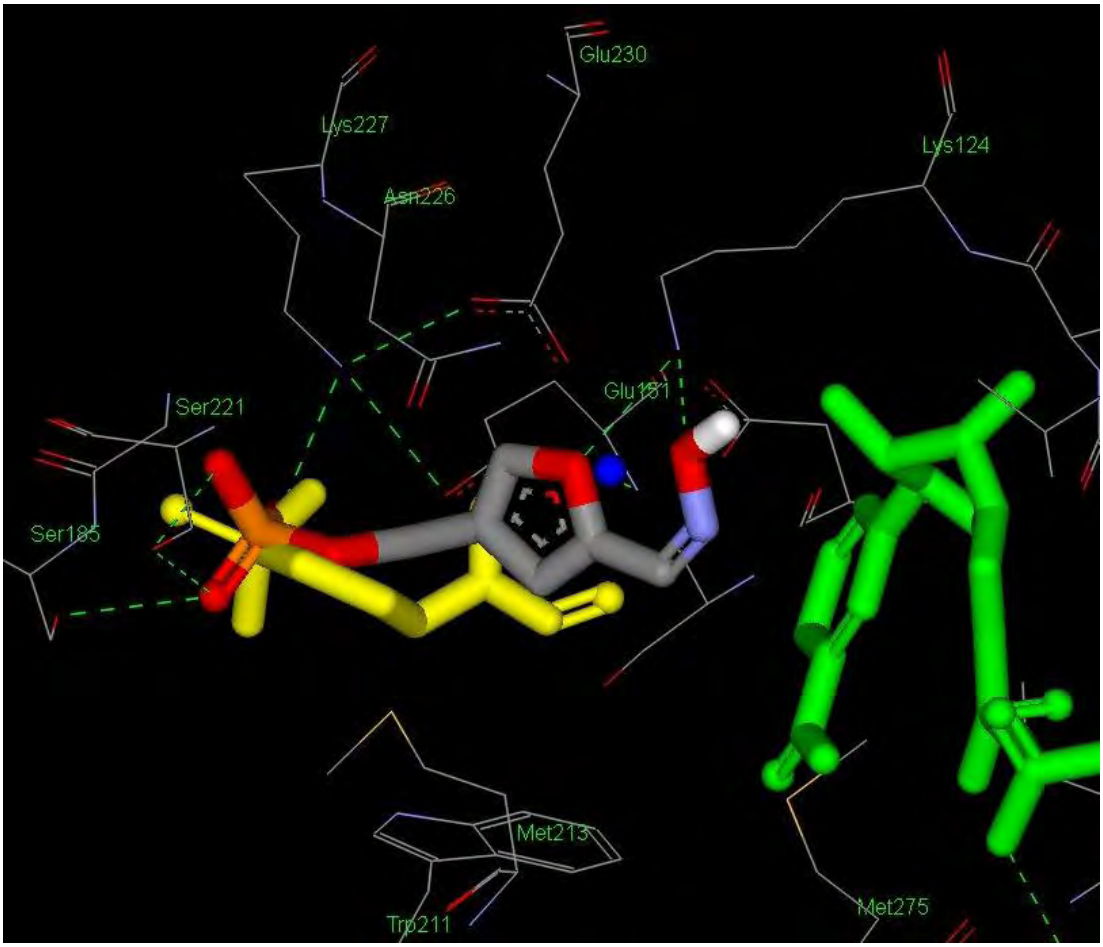

Figure 90. Docked conformation of the furan-derived phosphate ligand **337b** in the *Ec*DXR active-site (2EGH), illustrating hydrogen-bonding of the ligand with active-site residues. The crystal structure conformation of fosmidomycin **236** is shown in stick format coloured yellow and highlights the docking alignment of ligand **337b**. Protein active-site residues are shown in wire-frame coloured by atom type, NADPH in stick format coloured green, Mg^{2+} as a blue sphere and the ligand in stick format coloured by atom type. Hydrogen bonds are shown as green dashed lines.

Reasonable binding affinity data is observed for the 3-substituted aniline phosphonic acid dianionic ligands **328a**, **328c, 328f** and **331a, 331e, 331g**. Interestingly, docking orientations opposite to that of fosmidomycin **236** were exhibited by most of these ligands in the active site, as shown for ligand **328f** in Figure 91.

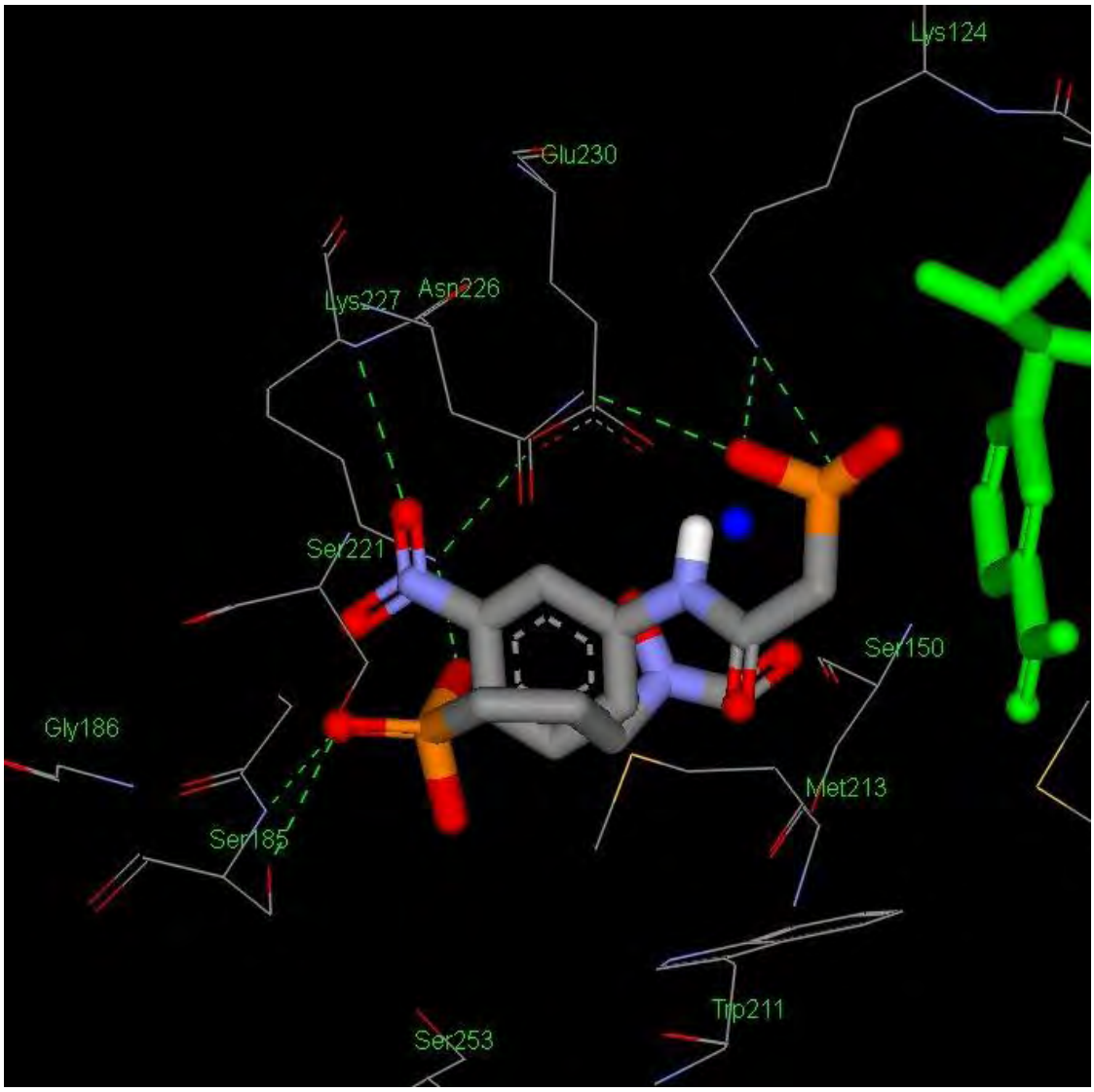

Figure 91. Docked conformation of the 3-substituted aniline-derived phosphonic acid ligand **328f** in the *Ec*DXR active-site (2EGH), illustrating 'reverse' binding of the ligand relative to fosmidomycin **236**. The crystal structure conformation of fosmidomycin **236** is shown in stick format coloured by atom type. Protein active-site residues are shown in wire-frame coloured by atom type, NADPH in stick format coloured green, Mg^{2+} as a blue sphere and the ligand shown in stick format coloured by atom type. Hydrogen bonds are shown as green dashed lines.

The 'reverse'-binding mode exhibited by these ligands has, in fact, also been reported for *N*-heterocyclic phosphonic acid analogues evaluated in a cognate study in our group, and is attributed to the favourable electrostatic attraction between the divalent metal cation and the phosphonic acid anion group of the ligand.[129,142] Furthermore, the authors have highlighted the fact that ligands exhibiting 'reverse' binding arrangements may still serve as DXR inhibitors as the binding interactions between the ligands and the enzyme are chemically feasible.[129,141] Yajima *et al.*[102] and Henriksson *et al*.[107] have reported that the DXR enzyme undergoes conformational changes itself upon binding of a ligand and co-factor; changes which may permit several plausible orientations of the ligand in the active site.

As previously discussed (Section 2.4, p. 141), the *N*-benzyl substituted phosphoramidic acid derivatives **351a-d** were designed and synthesised as specific inhibitors of *Pf*DXR. Thus*, in silico* docking of the ligands **351a-d** was explored using both *Ec*DXR (2EGH) and *Pf*DXR (the homology model developed by Goble *et al.*)[208] receptor cavities.[‡] Visual assessment of the dockings for the ligands **351a-d** in *Ec*DXR and *Pf*DXR revealed, as expected, that the ligands adopt binding orientations similar to that of fosmidomycin **236**, with the benzyl group adjacent to the phosphonate moiety occupying the hydrophobic pocket (pocket I in Figure 72) adjacent to the phosphonate-binding site. On docking in the *Pf*DXR receptor cavity, the phosphonate moiety of each of the ligands **351a-d** exhibits hydrogen-bonding interactions with the active-site residues, Ser 199 and Gly 201, while the carbonyl group interacts with residue Ser 235. In addition, the following interactions were observed between ligands **351a-d** and amino acid residues in the *Pf*DXR active-site:- i) Ser 161 acting as donor in hydrogen-bonding to the benzylic OH group in ligand **351b**; ii) Ile 269 and His 270 interacting with the 3-amino substituent in ligand **351c**; and iii) Cys 197 hydrogen-bonding with the phosphonate moiety in ligand **351d**. Figure 92 illustrates the binding conformation of ligand **351c** in the *Pf*DXR active-site with the benzyl ring occupying the pocket adjacent to the phosphonate-binding region.

[‡] Upon completion of this study, the *Pf*DXR crystal structure has been published by Tanaka *et al.*[208b]

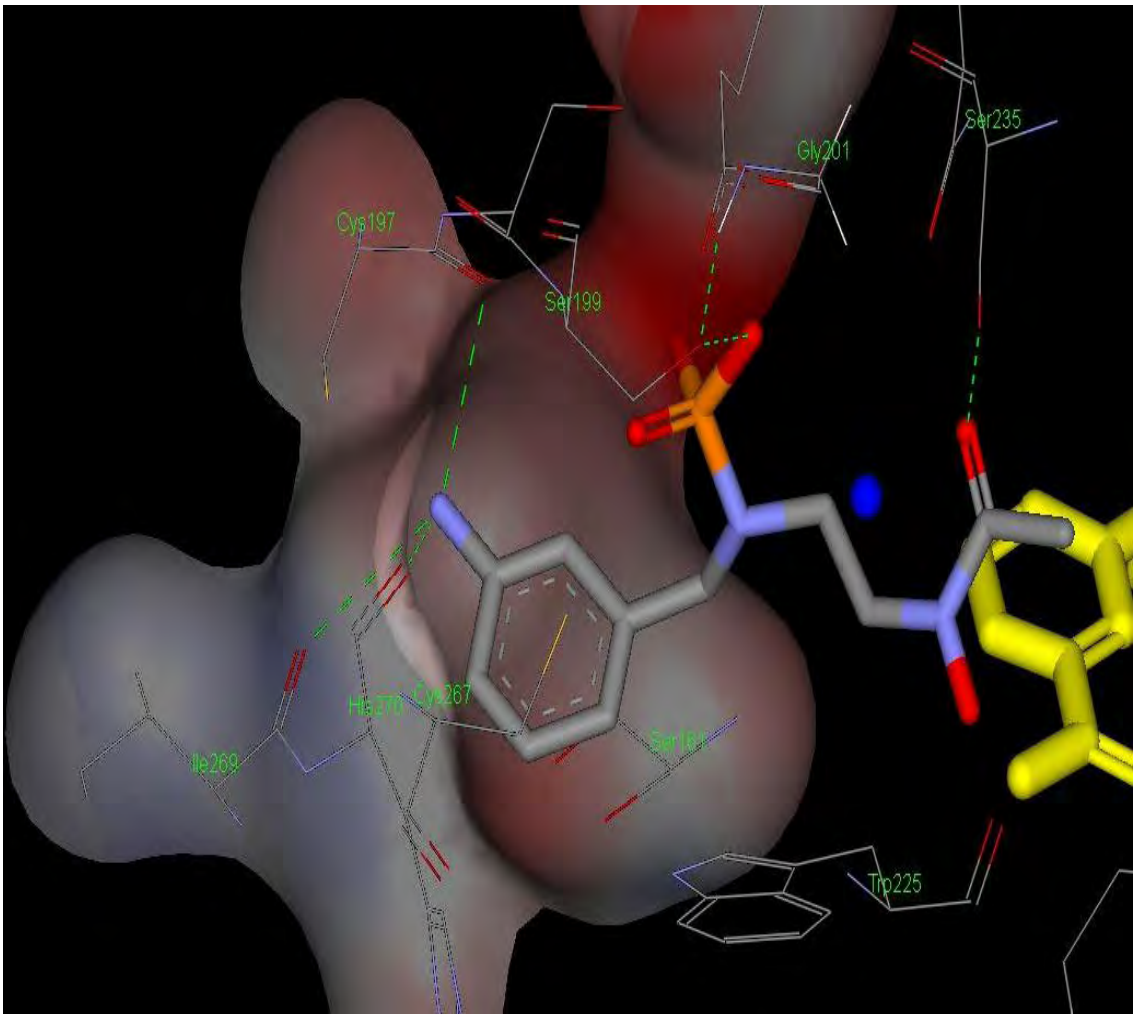

Figure 92. Docked conformation of the *N*-benzyl substituted phosphoramidic acid ligand **351c** in the *Pf*DXR active-site showing the benzyl ring occupying the pocket adjacent to the phosphonate-binding region. The surface zone at 4.1 Å from ligand **351c** is shown with 50% transparency, coloured by atom type and clipped in front. Protein active-site residues are shown in wire-frame coloured by atom type, NADPH in stick format coloured yellow, Mg^{2+} as a blue sphere and the ligand in stick format coloured by atom type. Hydrogen bonds are shown as green dashed lines.

The *in silico* screening tools used in this study have provided information regarding the ability of the various synthesised ligands to be accommodated in the DXR active-site and a measure of their potential to interact through hydrogen-bonding with active-site residues. From an analysis of the simulated-docking data, we have established that:- i) ligands **293a,b, 331a,g, 337b,c** and **351a-d** may be considered as feasible lead-compounds in the design and development of novel DXR inhibitors; and ii) the sterically restricted DXR active-site cannot adequately accommodate ligands possessing bulky substituents e.g. **293e-g**, nor could it

accommodate ligands containing three or four methylene carbon linkers between the essential phosphonate- and amide-binding groups as in compounds **333a,b,g**. In future, scrutiny of the topology and properties of the DXR active site, coupled with structural modifications of the synthesised compounds, may lead to the design of analogues with better binding and inhibition potential.

2.7. Conclusions

The various aims identified at the outset of the study have largely been achieved. Attention has been focused on synthesizing novel compounds that can act as inhibitors of DXR. In the design of these novel compounds, consideration has been given, *inter alia*, to the replacement of the phosphate group in the natural substrate DXP, by a phosphonate moiety, and the hydroxamate functionality, present in the established inhibitor, fosmidomycin, by an amide moiety.

Four general synthetic approaches (Scheme 24) have been explored in order to access the desired DXR inhibitors. In the first approach, the novel dihydroxy-amido phosphonate esters **292a-g** and their corresponding phosphonic acids **293a-g** were successfully prepared. EDC-mediated coupling of γ-phosphonated crotonic acid **291** with various amines afforded the amido-phosphonate esters **285a-g**, which were dihydroxylated using a $RuCl_3/CeCl_3/NaIO_4$ catalyst system to furnish the dihydroxy-amido phosphonate esters **292a-g** in good yields (> 62%). Subsequent hydrolysis using TMSBr and aqueous methanol gave the targeted phosphonic acids **293a-g**.

In the second approach, several series of 3-substituted aniline-derived phosphonate esters (**321a-g**, **323a-g**, **325a-g** and **327a-g**) and their corresponding phosphonic acids (**328a-g**, **331a-g**, **333a-g** and **335a-g**) and mono-sodium salts (**329a-g**, **332a-g**, **334a-g** and **336a-g**) have been successfully synthesised as fosmidomycin **236** analogues. The series differed in the number of methylene groups (1-4) separating the phosphonate and amide moieties. These compounds were prepared by deprotonating the 3-substituted aniline substrates **319a-g** with sodium hydride, followed by reaction with chloroacetyl chloride and the ω-chloroalkanoyl chlorides **330-330b** to give the ω-chloroamide intermediates **320a-g**, **322a-g**, **324a-g** and **326a-g** in generally good yields (> 59%). Subsequent phosphonation using the Michaelis-Arbuzov reaction afforded the diethyl phosphonate esters **321a-g**, **323a-g**, **325a-g** and **327a-g** in reasonable yields (48% - 74%). Microwave-assisted reaction of the phosphonate esters with TMSBr, followed by hydrolysis furnished the corresponding phosphonic acid derivatives **328a-g**, **331a-g**, **333a-g** and **335a-g**, and subsequent neutralisation with 0.1M aqueous sodium hydroxide furnished the mono-sodium phosphonic acid salts **329a-g**, **332a-g**, **334a-g** and **336a-g**.

Attention was then turned to developing the furan-derived phosphate analogues **349b-d** and **337b-d** as conformationally-restricted DOXP analogues. These novel analogues **337b-d** were accessed *via* trityl-protected 3-furanmethanol **349**, which was reacted with the specially prepared Vilsmeier reagent to furnish the desired formylated product **340b** in 64% yield. Friedel-Crafts acylation of the protected furan **349**, using $SnCl_4$ as the Lewis acid catalyst, afforded the furanyl ketones **340c** and **340d** in 64% and 56% yields, respectively. Deprotection and phosphorylation of compounds **340b-d** afforded the phosphate esters **348b-d** in 62-68% yields and, following hydrolysis, the dihydrogen phosphate derivatives **341b-d** were obtained in good yields (58% - 65%). Treatment of compounds **348b-d** and **341b-d** with an ethanolic solution of hydroxylamine hydrochloride in the presence of a catalytic quantity of sodium acetate, furnished the targeted phosphorylated oxime derivatives **349b-d** and **337b-d** in very good yields (87% - 96%).

Finally, based on a *de novo* design strategy, the *N*-benzyl substituted phosphoramidic derivatives **351a-d** have been successfully prepared from the primary substrate, diethyl phosphoramidate **352**. This approach involved silylation and alkylation of the substrate **352** to afford the phosphoramidate acetal **353**, which was reacted with appropriate benzyl substrates **360a-d** to give the *N*-benzyl substituted phosphoramidate acetals **354a-d**. Subsequent acid-catalysed hydrolysis of the acetal moiety gave the corresponding aldehydes **355a-d**, which were reduced and *O*-benzylated to afford the *O*-benzyl-protected amines **356a-d**. Acetylation and subsequent de-protection of the *O*-benzyl group gave the hydroxamate derivatives **363a-d** and, following hydrolysis, the desired phosphoramidic acids **351a-d** were obtained in moderate yields (37% - 44%). In addition to establishing synthetic methodologies for accessing the novel DXR inhibitors discussed in Sections 2.1 – 2.4, the known DXR inhibitor fosmidomycin **236** and its acetyl derivative, FR900098 **237**, have also been prepared, for use as bio-assay standards, by adapting methods reported in literature.[118-119,253] All of the prepared compounds have been fully characterised using 1- and 2-dimensional NMR spectroscopic methods and, where appropriate, elemental (HRMS or combustion) analysis.

Saturation Transfer Difference (STD) NMR experiments, conducted to explore the ability of synthesised ligands to bind to *Ec*DXR, have revealed that certain ligands (**293a,b,d, 328a,g, 331a-c, 333a, 337a,c** and **351a,d**) bind to the enzyme, whilst other ligands (**293c**,**e-g**, **328d-f**,

331d, **333e**,**f** and **335a**,**c**) do not. The positive STD results have been attributed to several factors, *viz* :-

i. ligands similar in size to fosmidomycin **236** being able to occupy the *Ec*DXR active-site comfortably;
ii. the presence of the hydroxyl groups at C-2 and C-3 in ligands **293a,b** and **293d** providing additional hydrogen-bonding interactions with active-site residues;
iii. the presence of a substituent containing an oxygen atom (*i.e.* OH, OMe and CH_2OH) in ligands **328a**,**g**, **331a-c** and **333a** providing favourable electrostatic interactions with active-site residues;
iv. the restriction in conformational flexibility provided by the furan ring in ligands **337a,c** ensuring that the ligands maintain an ideal conformation within the active site; and
v. the *N*-benzyl α-substituent in ligands **351a,d** occupying the hydrophobic binding pocket adjacent to the phosphonate binding site, thus increasing the binding affinity of the ligands to the enzyme.

*Ec*DXR inhibition assays were carried out, for the author,[211] on selected 3-substituted aniline-derived analogues to assess their inhibition potential. Some of the ligands (**328a**, **329a**, **331a** and **332a**) exhibited > 40% inhibition at a concentration of 250 μM, whilst a decrease in inhibitory activity was observed when the number of methylene groups between the amide group and the phosphonate moiety, in the aniline-derived phosphonate analogues, was increased beyond two. Furthermore, the phosphonate esters generally exhibited less effective inhibition than their corresponding phosphonic acid derivatives, whereas the phosphonic acids and their corresponding mono-sodium salts exhibited similar inhibition levels – not surprisingly given that the assays were conducted in a buffered medium.

Computer-simulated docking studies have been conducted, using *Ec*DXR (crystal structure 2EGH)[103] to explore the ability of selected synthesised ligands to fit within the DXR active-site and interact *via* hydrogen-bonding with active-site residues. Analysis of the docking results revealed that:- i) some of the ligands (**293a,b**, **328c**, **337b,c** and **351a-d**) exhibited good binding affinity values with a high degree of conformational alignment with bound

fosmidomycin **236**; ii) other ligands (**293e-g**, **333a,b,g, 335a,d,e** and **337d**) could not be accommodated within the active-site; iii) certain ligands (**328a,c,f** and **331a,e,g**) exhibited docking orientations opposite (*i.e.* reverse binding) to that of fosmidomycin **236**.

From the *Ec*DXR-STD binding, enzyme inhibition and simulated docking data, it seems that compounds **293a**, **293b**, **331a** and **331g** could serve as lead compounds for the development of new anti-malarial drugs.

The results of this study have provided a number of opportunities for future research; these include:-

i. optimisation of the STD NMR experiments to include fosmidomycin and FR900098 as highly competitive inhibitors and to access quantitative ligand binding affinity and ligand competition data;
ii. *Ec*DXR and *Pf*DXR inhibition bio-assays of the dihydroxy-amido phosphonic acid derivatives, furan derived-phosphate analogues and *N*-benzyl substituted phosphoramidic acid derivatives at different ligand concentrations to determine the IC_{50} values and inhibitory activity of the synthesised ligands;
iii. *P. falciparum* growth inhibition assays of novel compounds, to assess the anti-malarial activity and exploration of the toxicity of the inhibitors; and
iv. synthetic elaboration of ligands identified as potential lead compounds.

3. EXPERIMENTAL

3.1. General Procedures

Unless stated otherwise, the reagents were supplied by Sigma Aldrich or Fluka and used without further purification. Solvents were purified by drying and re-distillation, as described by Perrin and Armarego.[221] Reactions that required an inert atmosphere were conducted under nitrogen or argon gas. Thin layer chromatography was performed on Merck TLC silica gel 60 PF_{254} plates and viewed under UV light (254 nm) or developed with iodine vapour. Preparative layer chromatography was carried out using Merck silica gel 60 PF_{254} as the stationary phase. Flash chromatography was conducted using Merck silica gel 60 (particle size 0.040 – 0.063 mm) for normal-phase and Sep-Pak Vac 35cc C18 cartridges for reverse-phase. Normal-phase HPLC was carried out using a Whatman Partisil 10 semi-preparative column and reverse-phase HPLC using a Phenomenex C-18 LUNA semi-preparative column, with a Waters R401 refractive index detector.

Microwave-assisted reactions were conducted using a CEM-Discover microwave apparatus (model number 908010). NMR spectra were recorded on a Bruker AVANCE 400 MHz or Biospin 600 MHz spectrometers and were calibrated relative to the solvent signals (δ_H : 7.25 ppm for $CDCl_3$, 4.81 for D_2O and 2.50 ppm for DMSO-d_6; δ_C : 77.0 ppm for $CDCl_3$ and 39.4 ppm for DMSO-d_6; δ_P : 0 ppm for ^{31}P in H_3PO_4 as a standard.

Low-resolution mass spectra were acquired on a Finnigan MAT GCQ mass spectrometer at Rhodes University. High-resolution mass spectra were obtained at the University of Stellenbosch Central Analytical Facility using a Waters API Q-TOF Ultima spectrometer. Elemental analysis data were obtained using a Vario Elemental Microtube EL III analyzer. IR spectra were recorded on a Perkin-Elmer Spectrum 100 FT-IR spectrometer, as thin films or solid deposits between CsI discs, or as neat compounds on a diamond window.

Percentage yields of chromatographed products are based on the mass of crude material separated chromatographically. Melting points were measured using a Reichert hot-stage apparatus, and are uncorrected.

3.2. Dihydroxy-amido phosphonate esters and their corresponding phosphonic acids

Ethyl (*E*)-4-bromocrotonate 283 [222]

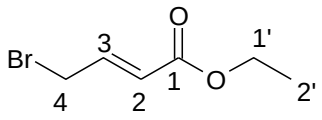

A mixture of ethyl crotonate (6.2 mL, 50 mmol) and NBS (8.89 g, 50 mmol) in carbon tetrachloride (20 mL) was refluxed at 120 ^{o}C for 3 hours, whilst stirring. The resulting mixture was cooled to 0 ^{o}C and the succinimide was filtered off. The organic layer was washed with water (10 mL), separated, and dried with anhydr. Na_2SO_4. Filtration and evaporation of the solvent afforded the crude product, which was purified by flash chromatography [on silica gel; elution with hexane-EtOAc (49:1)] to obtain ethyl (*E*)-4-bromocrotonate **283** as a yellow oil (5.39 g, 56 %); υ_{max} (thin film/cm^{-1}) 1648 (C=O); δ_H/ppm (400 MHz; $CDCl_3$) 1.26 (3H, t, *J* = 7.6 Hz, CH_3), 3.98 (2H, d, *J* = 7.6 Hz, CH_2Br), 4.18 (2H, q, *J* = 7.2 Hz, CH_2O), 6.02 (1H, d, *J* = 15.2 Hz, 2-H), 7.00 (1H, m, 3-H); δ_C/ppm (100 MHz; $CDCl_3$) 14.1 (C-2'), 29.1 (C-4), 60.7 (C-1'), 124.6 (C-2), 141.6 (C-3) and165.5 (C=O).

(*E*)-4-(Diethoxyphosphoryl)crotonate 284 [223]

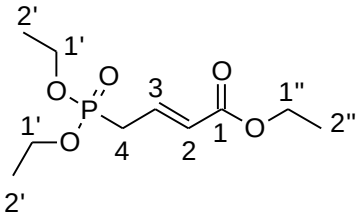

Triethyl phosphite (1.82 g, 10.8 mmol) was added slowly to a stirred solution of ethyl 4-bromocrotonate (1.03 g, 5.40 mmol) in toluene (10 mL) during a period of 1 hour, whilst the temperature of the mixture was maintained at 120 ^{o}C. After the addition, the mixture was stirred at the same temperature of a further 5 hours and then cooled to room temperature. The cooled mixture was then stirred with hexane (20 mL) for *ca.* 30 minutes followed by decantation of the hexane layer to remove the excess triethyl phosphite; this was repeated three times. The crude product was purified by flash chromatography [on silica gel; elution with hexane-EtOAc (3:1)], and subsequent evaporation of the solvent *in vacuo* afforded (*E*)-4-(diethyoxyphosphoryl)crotonate **284** as a yellow oil (1.00 g, 75 %); υ_{max} (thin film/cm^{-1})

1748 (C=O) and 1231 (P=O); δ_H/ppm (400 MHz; $CDCl_3$) 1.27 (9H, m, 3 x CH_3), 2.70 (2H, dd, *J* = 22.8 and 7.2 Hz, CH_2P), 4.12 (6H, m, 3 x OCH_2), 5.93 (1H, dd, *J* = 15.6 and 4.4 Hz, 2-H), 6.85 (1H, q, *J* = 7.6 Hz, 3-H); δ_C/ppm (100 MHz; $CDCl_3$) 14.1 (C-2'), 16.3 (2 x C-2''), 30.1 (C-4), 60.3 (C-1'), 62.2 (2 x C-1'), 125.8 (d, J_{P-C} = 11.0 Hz, C-2), 137.3 (d, J_{P-C} = 13.6 Hz, C-3) and 165.5 (C=O); δ_P/ppm (162 MHz; $CDCl_3$) 25.3 (P=O).

(*E*)-4-(Diethoxyphosphoryl)-*N*-methylbut-2-enamide 285a

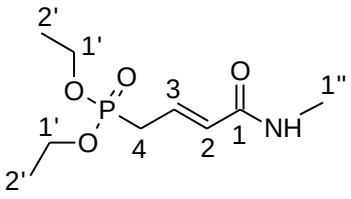

To a solution of EDC (0.65 g, 3.4 mmol) and HOBt (0.52 g, 3.4 mmol) in DCM (15 mL) under N_2, was added (*E*)-4-(diethoxyphosphoryl)but-2-enoic acid **291** (0.50 g, 2.3 mmol) and the mixture was stirred for 15 minutes. To the mixture, methylamine hydrochloride (0.46 g, 6.8 mmol) in DMF (5 mL) and triethylamine (0.74 mL, 3.4 mmol) was added and the resulting solution was stirred for 24 hours at room temperature. The solvent was evaporated *in vacuo* and the residue was dissolved in EtOAc (25 mL). The organic solution was washed sequentially with water (2 x 50 mL), 10 % *aq*. $NaHCO_3$ (2 × 50 mL) and brine (2 × 50 mL). The organic solution was dried with anhydr. $MgSO_4$, the solvent removed *in vacuo* and the residue chromatographed [preparative layer chromatography; elution with hexane-EtOAc (4:1)] to yield (E)-*4-(diethoxyphosphoryl)*-N-*methylbut-2-enamide* **285a** as a brown solid (0.36 g, 68 %), m.p. 104-106 °C (Found: C, 46.11; H, 7.67; N, 5.94 %. $C_9H_{18}NO_4P$ requires C, 45.96; H 7.71; N 5.95 %); υ/cm^{-1} 1701 (C=O) and 1218 (P=O); δ_H/ppm (400 MHz; $CDCl_3$) 1.27 (6H, t, *J* = 6.8 Hz, 2 x CH_3), 2.48 (2H, dd, *J* = 22.2 and 6.8 Hz, CH_2P), 2.71 (3H,s, 1''-CH_3), 4.17 (4H, m, 2 x OCH_2), 5.78 (1H, dd, *J* = 15.2 and 4.2 Hz, 2-H), 6.84 (1H, m, 3-H) and 7.62 (1H, s, NH); δ_C (100 MHz; $CDCl_3$) 16.2 (d, J_{P-C} = 5.9 Hz, 2 × CH_3), 26.4 (C-1''), 30.2 (d, J_{P-C} = 140.3 Hz, CH_2P), 61.3 (d, J_{P-C} = 6.5 Hz, 2 × OCH_2), 126.5 (d, J_{P-C} = 15.0 Hz, C-2), 137.5 (d, J_{P-C} = 14.7 Hz, C-3) and 163.1 (C=O).

(*E*)-4-(Diethoxyphosphoryl)-*N*-ethylbut-2-enamide 285b

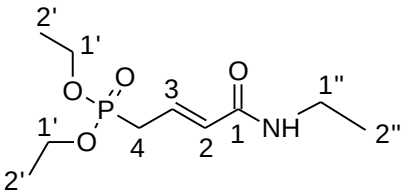

The procedure described for the synthesis of (*E*)-4-(diethoxyphosphoryl)-*N*-methylbut-2-enamide **285a** was employed, using EDC (0.65 g, 3.4 mmol), HOBt (0.52 g, 3.4 mmol) and (*E*)-4-(diethoxyphosphoryl)but-2-enoic acid **291** (0.50 g, 2.25 mmol) in DCM (15 mL) and, ethylamine hydrochloride (0.56 g, 6.8 mmol) and triethylamine (0.74 mL, 3.4 mmol) in DMF (5 mL). The crude product was chromatographed [preparative layer chromatography; elution with hexane-EtOAc (4:1)] to yield *(*E*)-4-(diethoxyphosphoryl)-*N-*ethylbut-2-enamide* **285b** as a yellow solid (0.40 g, 71 %), m.p. 91-93 °C (Found: C, 47.91; H, 8.87; N, 5.61 %. $C_{10}H_{22}NO_4P$ requires C, 47.80; H, 8.83; N, 5.57 %); υ/cm^{-1} 1683 (C=O) and 1226 (P=O); δ_H/ppm (400 MHz; $CDCl_3$) 1.14 (3H, t, *J* = 7.6 Hz, 2''-CH_3), 1.23 (6H, t, *J* = 7.2 Hz, 2 x CH_3), 2.50 (2H, dd, *J* = 22.4 and 7.6 Hz, CH_2P), 3.31 (2H,q, *J* = 7.2 Hz, 1''-CH_2), 4.18 (4H, m, 2 x OCH_2), 5.95 (1H, dd, *J* = 15.4 and 4.1 Hz, 2-H), 6.79 (1H, m, 3-H) and 8.99 (1H, s, NH); δ_C (100 MHz; $CDCl_3$) 14.2 (C-2''), 16.3 (d, J_{P-C} = 6.0 Hz, 2 × CH_3), 30.4 (d, J_{P-C} = 145.0 Hz, CH_2P), 36.8 (C-1''), 61.7 (d, J_{P-C} = 6.4 Hz, 2 × OCH_2), 125.0 (d, J_{P-C} = 13.5 Hz, C-2), 136.8 (d, J_{P-C} = 15.4 Hz, C-3) and 166.3 (C=O).

(*E*)-4-(Diethoxyphosphoryl)-*N*-propylbut-2-enamide 285c

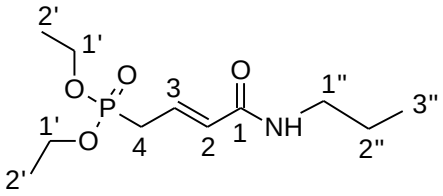

To a solution of EDC (0.65 g, 3.4 mmol) and HOBt (0.52 g, 3.4 mmol) in DCM (15 mL) under N_2, was added (*E*)-4-(diethoxyphosphoryl)but-2-enoic acid **291** (0.50 g, 2.3 mmol) and the mixture was stirred for 15 minutes. To the mixture, propylamine (0.57 mL, 6.8 mmol) was added and the resulting solution was stirred for 24 hours at room temperature. The solvent was evaporated *in vacuo* and the residue was dissolved in EtOAc (25 mL). The organic extract was washed sequentially with water (2 x 50 mL), 10 % *aq*. $NaHCO_3$ (2 × 50 mL) and

brine (2 × 50 mL). The organic solution was dried with anhydr. $MgSO_4$, the solvent removed *in vacuo* and the residue chromatographed [preparative layer chromatography; elution with hexane-EtOAc (4:1)] to yield *(E)-4-(diethoxyphosphoryl)-N-propylbut-2-enamide* **285c** as a yellow oil (0.39 g, 65 %) (Found: C, 49.75; H, 9.18; N, 5.31 %. $C_{11}H_{24}NO_4P$ requires C, 49.80; H, 9.12; N, 5.28 %); υ/cm^{-1} 1654 (C=O) and 1227 (P=O); δ_H/ppm (400 MHz; $CDCl_3$) 0.90 (3H, t, *J* = 7.6 Hz, 3''-CH_3), 1.32 (6H, t, *J* = 7.2 Hz, 2 x CH_3), 1.51 (2H, m, 2''-CH_2), 2.55 (2H, dd, *J* = 22.6 and 7.6 Hz, CH_2P), 3.25 (2H, t, *J* = 6.4 Hz, 1''-CH_2), 4.10 (4H, m, 2 x OCH_2), 5.58 (1H, s, NH), 5.76 (1H, dd, *J* = 15.2 and 2.6 Hz, 2-H) and 6.80 (1H, m, 3-H); δ_C (100 MHz; $CDCl_3$) 11.7 (C-3''), 16.4 (d, J_{P-C} = 6.0 Hz, 2 × CH_3), 23.2 (C-2''), 30.7 (d, J_{P-C} = 141.2 Hz, CH_2P), 42.6 (C-1''), 61.4 (d, J_{P-C} = 6.4 Hz, 2 × OCH_2), 123.5 (d, J_{P-C} = 13.0 Hz, C-2), 134.4 (d, J_{P-C} = 15.2 Hz, C-3) and 166.3 (C=O).

(*E*)-4-(Diethoxyphosphoryl)-*N*-isopropylbut-2-enamide 285d

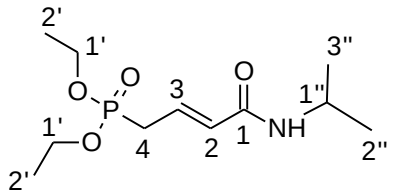

The procedure described for the synthesis of (*E*)-4-(diethoxyphosphoryl)-*N*-propylbut-2-enamide **285c** was employed, using EDC (0.65 g, 3.4 mmol), HOBt (0.52 g, 3.4 mmol), (*E*)-4-(diethoxyphosphoryl)but-2-enoic acid **291** (0.50 g, 2.3 mmol) and isopropylamine (0.58 mL, 6.8 mmol) in DCM (15 mL). The crude product was chromatographed [preparative layer chromatography; elution with hexane-EtOAc (4:1)] to yield *(*E*)-4-(diethoxyphosphoryl)-*N-*isopropylbut-2-enamide* **285d** as a yellow solid (0.44 g, 75 %), m.p. 82-84 °C (Found: C, 49.87; H, 9.20; N, 5.31 %. $C_{11}H_{24}NO_4P$ requires C, 49.80; H, 9.12; N, 5.28 %); υ/cm^{-1} 1662 (C=O) and 1229 (P=O); δ_H/ppm (400 MHz; $CDCl_3$) 1.15 (6H, d, *J* = 6.8 Hz, 2''- and 3''-CH_3), 1.31 (6H, t, *J* = 7.2 Hz, 2 x CH_3), 2.59 (2H, dd, *J* = 22.8 and 7.2 Hz, CH_2P), 3.99 (1H, m, 1''-H), 4.12 (4H, m, 2 x OCH_2), 5.22 (1H, s, NH), 5.77 (1H, dd, *J* = 15.2 and 4.2 Hz, 2-H) and 7.04 (1H, m, 3-H); δ_C (100 MHz; $CDCl_3$) 16.4 (d, J_{P-C} = 5.8 Hz, 2 × CH_3), 22.8 (C-2'' and C-3''), 27.6 (d, J_{P-C} = 144.0 Hz, CH_2P), 41.1 (C-1''), 63.6 (d, J_{P-C} = 5.8 Hz, 2 × OCH_2), 125.0 (d, J_{P-C} = 14.1 Hz, C-2), 139.4 (d, J_{P-C} = 14.3 Hz, C-3) and 165.9 (C=O).

(*E*)-4-(Diethoxyphosphoryl)-*N*-butylbut-2-enamide 285e

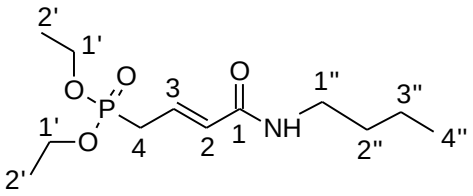

The procedure described for the synthesis of (*E*)-4-(diethoxyphosphoryl)-*N*-propylbut-2-enamide **285c** was employed, using EDC (0.65 g, 3.4 mmol), HOBt (0.52 g, 3.4 mmol), (*E*)-4-(diethoxyphosphoryl)but-2-enoic acid **291** (0.50 g, 2.3 mmol) and butylamine (0.65 mL, 6.8 mmol) in DCM (15 mL). The crude product was chromatographed [preparative layer chromatography; elution with hexane-EtOAc (4:1)] to yield *(*E*)-4-(diethoxyphosphoryl)-N-butylbut-2-enamide* **285e** as a brownish oil (0.39 g, 63 %) (Found: C, 51.83; H, 9.42; N, 5.07 %. $C_{12}H_{26}NO_4P$ requires C, 51.70; H, 9.38; N, 5.01 %); υ/cm^{-1} 1693 (C=O) and 1217 (P=O); δ_H/ppm (400 MHz; $CDCl_3$) 0.92 (3H, t, *J* = 7.6 Hz, 4''-CH_3), 1.20 (2H, m, 3''-CH_2), 1.30 (6H, t, *J* = 7.6 Hz, 2 x CH_3), 1.71 (2H, m, 2''-CH_2), 2.68 (2H, dd, *J* = 22.8 and 7.8 Hz, CH_2P), 3.20 (2H, m, 1''-CH_2), 4.11 (4H, m, 2 x OCH_2), 5.82 (1H, dd, *J* = 15.4 and 4.2 Hz, 2-H), 7.02 (1H, m, 3-H) and 5.58 (1H, s, NH); δ_C (100 MHz; $CDCl_3$) 13.8 (C-4''), 16.3 (d, J_{P-C} = 6.7 Hz, 2 × CH_3), 20.3 (C-3''), 27.9 (d, J_{P-C} = 144.0 Hz, CH_2P), 29.9 (C-2''), 41.4 (C-1''), 63.8 (d, J_{P-C} = 5.8 Hz, 2 × OCH_2), 125.3 (d, J_{P-C} = 14.1 Hz, C-2), 134.4 (d, J_{P-C} = 14.3 Hz, C-3) and 166.1 (C=O).

(*E*)-4-(Diethoxyphosphoryl)-*N*-phenylbut-2-enamide 285f

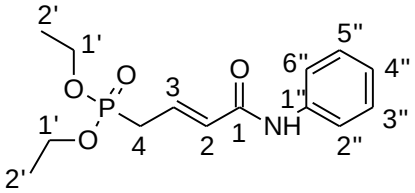

The procedure described for the synthesis of (*E*)-4-(diethoxyphosphoryl)-*N*-propylbut-2-enamide **285c** was employed, using EDC (0.65 g, 3.4 mmol), HOBt (0.52 g, 3.4 mmol), (*E*)-4-(diethoxyphosphoryl)but-2-enoic acid **291** (0.50 g, 2.3 mmol) and aniline (0.63 mL, 6.8 mmol) in DCM (15 mL). The crude product was chromatographed [preparative layer chromatography; elution with hexane-EtOAc (3:1)] to yield (*E*)-4-(diethoxyphosphoryl)-*N*-phenylbut-2-enamide **285f** as a brown solid (0.44 g, 66 %), m.p. 86-88 °C (Lit.[224] 88 °C); υ/cm^{-1} 1682 (C=O) and 1232 (P=O); δ_H/ppm (400 MHz; $CDCl_3$) 1.27 (6H, t, *J* = 7.6 Hz, 2 x CH_3),

2.30 (2H, dd, *J* = 22.8 and 7.6 Hz, CH_2P), 4.10 (4H, m, 2 x OCH_2), 5.80 (1H, dd, *J* = 15.4 and 4.4 Hz, 2-H), 6.99 (1H, m, 3-H), 7.02 (1H, t, *J* = 7.2 Hz, 4''-H), 7.39 (2H, t, *J* = 7.2 Hz, 3''-H and 5''-H), 7.57 (2H, d, *J* = 7.6 Hz, 2''-H and 6''-H) and 8.70 (1H, s, NH); δ_C (100 MHz; $CDCl_3$) 16.4 (d, J_{P-C} = 5.8 Hz, 2 × CH_3), 27.8 (d, J_{P-C} = 144.0 Hz, CH_2P), 63.6 (d, J_{P-C} = 5.8 Hz, 2 × OCH_2), 121.8 (C-2'' and C-6''), 124.5 (C-4''), 125.0 (d, J_{P-C} = 14.1 Hz, C-2), 129.2 (C-3'' and C-5''), 136.7 (C-1''), 139.3 (d, J_{P-C} = 14.3 Hz, C-3) and 165.9 (C=O).

(*E*)-4-(diethoxyphosphoryl)-*N*-benzylbut-2-enamide 285g

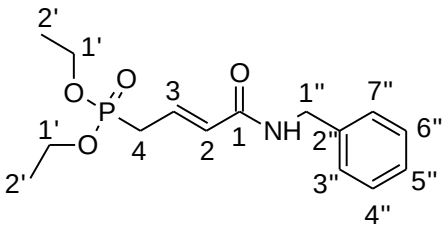

The procedure described for the synthesis of (*E*)-4-(diethoxyphosphoryl)-*N*-propylbut-2-enamide **285c** was employed, using EDC (0.65 g, 3.4 mmol), HOBt (0.52 g, 3.4 mmol), (*E*)-4-(diethoxyphosphoryl)but-2-enoic acid **291** (0.50 g, 2.3 mmol) and benzylamine (0.75 mL, 6.8 mmol) in DCM (15 mL). The crude product was chromatographed [preparative layer chromatography; elution with hexane-EtOAc (3:1)] to yield *(*E*)-4-(diethoxyphosphoryl)-N-benzylbut-2-enamide* **285g** as a yellow solid (0.49 g, 71 %), m.p. 95-97 °C (Found: C, 57.57; H, 7.69; N, 4.49 %. $C_{15}H_{24}NO_4P$ requires C, 57.50; H, 7.72; N, 4.47 %); υ/cm^{-1} 1692 (C=O) and 1239 (P=O); δ_H/ppm (400 MHz; $CDCl_3$) 1.27 (6H, m, 2 x CH_3), 2.72 (2H, dd, *J* = 22.8 and 7.6 Hz, CH_2P), 4.11 (4H, m, 2 x OCH_2), 4.48 (2H, s, 1''-CH_2), 5.80 (1H, dd, *J* = 15.2 and 1.2 Hz, 2-H), 6.89 (1H, m, 3-H), 7.31 (5H, m, 3''-H, 4''-H, 5''-H, 6''-H and 7''-H) and 8.19 (1H, s, NH); δ_C (100 MHz; $CDCl_3$) 16.4 (d, J_{P-C} = 5.9 Hz, 2 × CH_3), 27.6 (d, J_{P-C} = 143.9 Hz, CH_2P), 43.5 (1''-CH_2), 63.6 (d, J_{P-C} = 5.8 Hz, 2 × OCH_2), 124.8 (d, J_{P-C} = 13.8 Hz, C-2), 127.5 (C-5''), 127.8 (C-3'' and C-7''), 128.7 (C-4'' and C-6''), 138.3 (d, J_{P-C} = 13.6 Hz, C-3), 140.3 (C-2'') and 165.8 (C=O).

Crotonic acid 286

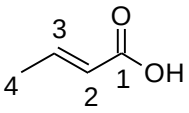

Ethyl (*E*)-crotonate **282** (10 mL, 81 mmol) was added to a 2M solution of potassium hydroxide in ethanol (8 mL, 0.1 mol) and the mixture was stirred at room temperature for

24 hours. After completion of the reaction, the ethanol was evaporated at reduced pressure and the residue was dissolved in water (100 mL), extracted with diethyl ether (2 x 50 mL), and the organic phase discarded. The aqueous phase was acidified (pH 2.5) with 2M HCl and extracted with diethyl ether (3 x 50 mL). The combined organic phases were washed with water (2 x 50 mL) and brine (2 x 50 mL), and dried (anhydr. Na_2SO_4). Evaporation of the solvent *in vacuo* gave crude product, which was washed with cold hexane to afford crotonic acid **286** as white crystals (6.69 g, 96 %), m.p. 72-74 °C (Lit.[225] 71-73 °C); υ/cm^{-1} 2891 (OH) and 1681 (C=O); δ_H/ppm (400 MHz; $CDCl_3$) 1.94 (3H, d, *J* = 6.8 Hz, CH_3), 5.88 (1H, d, *J* = 15.6 Hz, 2-H), 7.11 (1H, m, 3-H) and 10.18 (1H, s, OH); δ_C (100 MHz; $CDCl_3$) 18.8 (CH_3), 121.6 (C-2), 146.8 (C-3) and 169.3 (C=O).

Crotonyl chloride 287 [226]

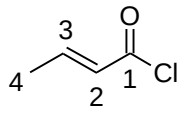

Oxalyl chloride (3.69 g, 29.1 mmol) was added dropwise to a pre-cooled (-2 °C), stirred solution of crotonic acid (5.00 g, 58.1 mmol) in DMF (20 mL) under N_2. The mixture was stirred for 1 hour, warmed to room temperature and stirred for an additional 3 hours. The reaction was quenched with water (5 mL) and extracted with DCM (3 x 50 mL). The combined organic phases were washed sequentially with water (100 mL), 10 % *aq.* $NaHCO_3$ (100 mL) and brine (100 mL), and dried (anhydr. $MgSO_4$). The solvent was removed under reduced pressure to afford the crude product as a yellow liquid, which was purified by distillation to yield crotonyl chloride **287** as a clear liquid (2.71 g, 89 %);[‡] υ/cm^{-1} 1757 (C=O); δ_H/ppm (400 MHz; $CDCl_3$) 1.93 (3H, d, *J* = 6.0 Hz, CH_3), 5.88 (1H, d, *J* = 15.6 Hz, 2-H) and 7.12 (1H, m, 3-H); δ_C (100 MHz; $CDCl_3$) 17.9 (CH_3), 125.4 (C-2), 150.8 (C-3) and 165.7 (C=O).

(*E*)-*N*-methylbut-2-enamide 288a

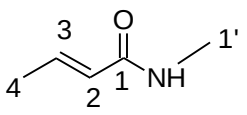

[‡] Product was stored under N_2 at 0 – 2 °C.

Methylamine hydrochloride (0.49 g, 7.2 mmol) and Proton Sponge® (2.05 g, 9.57 mmol) were dissolved in a mixture of pyridine (0.6 mL) and DCM (15 mL) at 0 ^{o}C under N_2. Crotonoyl chloride **287** (0.50 g, 4.8 mmol) was then added through a septum and the resulting mixture was stirred for 15 min. the reaction mixture was warmed to room temperature and stirred for 24 hours. The solvent was removed *in vacuo* and the residue extracted with EtOAc (100 mL). The organic extract was washed sequentially with satd. aq. $NaHCO_3$ (100 mL), water (100 mL) and brine (100 mL). The aqueous washings were extracted with EtOAc (2 x 100 mL) and the combined organic solutions were dried (anhydr. $MgSO_4$). Subsequent evaporation of the solvent *in vacuo* gave the crude product, which was recrystallised from EtOH to yield (*E*)-*N*-methylbut-2-enamide **288a** as white crystals (0.38 g, 81 %), m.p. 69-71 °C (Lit.[227-228] 67-69 °C); υ/cm^{-1} 1682 (C=O); δ_H/ppm (400 MHz; $CDCl_3$) 1.89 (3H, d, *J* = 6.0 Hz, 4-CH_3), 2.73 (3H, s, 1'-CH_3), 5.85 (1H, d, *J* = 15.6 Hz, 2-H), 7.12 (1H, m, 3-H) and 8.09 (1H, s, NH); δ_C (100 MHz; $CDCl_3$) 18.1 (C-4), 26.2 (C-1'), 124.4 (C-2), 142.8 (C-3) and 166.7 (C=O).

(*E*)-*N*-ethylbut-2-enamide 288b [229]

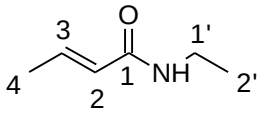

The procedure described for the synthesis of (*E*)-*N*-methylbut-2-enamide **288a** was employed, using ethylamine hydrochloride (0.59 g ,7.2 mmol), Proton Sponge® (2.05 g, 9.57 mmol) and crotonoyl chloride **287** (0.50 g, 4.8 mmol) in a mixture of DCM (15 mL) and pyridine (0.6 mL). Subsequent evaporation of the solvent *in vacuo* afforded (*E*)-*N*-ethylbut-2-enamide **288b** as a pale yellow oil (0.46 g, 85 %); υ/cm^{-1} 1673 (C=O); δ_H/ppm (400 MHz; $CDCl_3$) 1.12 (3H, t, *J* = 7.6 Hz, 2'-CH_3), 1.89 (3H, d, *J* = 6.0 Hz, 4-CH_3), 3.29 (2H, q, *J* = 7.6 Hz, 1'-CH_2), 5.88 (1H, d, *J* = 15.6 Hz, 2-H), 7.11 (1H, m, 3-H) and 8.24 (1H, s, NH); δ_C (100 MHz; $CDCl_3$) 14.6 (C-2'), 18.2 (CH_3), 36.3 (C-1'), 124.9 (C-2), 143.2 (C-3) and 166.5 (C=O).

(*E*)-*N*-propylbut-2-enamide 288c

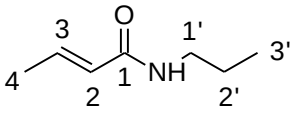

Crotonoyl chloride **287** (0.50 g, 4.78 mmol) was added dropwise to a pre-cooled (- 0 ^{o}C), stirred solution of propylamine (0.80 mL, 9.6 mmol) and triethylamine (0.79 mL, 5.7 mmol) in DCM (15 mL) under N_2. The resulting mixture was stirred for 30 min, warmed to room temperature and stirred for an additional 24 hours. The solvent was removed *in vacuo* and the residue extracted with $CHCl_3$ (50 mL). The organic extract was washed with water (2 x 50mL) and brine (2 x 50 mL). The aqueous washings were extracted with $CHCl_3$ (50 mL) and the combined organic solutions were dried (anhydr. $MgSO_4$). Subsequent evaporation of the solvent *in vacuo* gave the crude product, which was recrystallised from MeOH to yield (*E*)-*N*-propylbut-2-enamide **288c** as a brown solid (0.47 g, 77 %) m.p. 84-86 °C (Lit. 82-83 °C [227,230]); υ/cm^{-1} 1673 (C=O); δ_H/ppm (400 MHz; $CDCl_3$) 1.01 (3H, t, *J* = 7.2 Hz, 3'-CH_3), 1.53 (2H, m, 2'-CH_2) 1.84 (3H, d, *J* = 6.0 Hz, 4-CH_3), 3.24 (2H, m, 1'-CH_2), 5.91 (1H, d, *J* = 15.6 Hz, 2-H), 7.05 (1H, m, 3-H) and 8.41 (1H, s, NH); δ_C (100 MHz; $CDCl_3$) 11.4 (C-3'), 18.1 (C-4), 22.9 (C-2'), 42.4 (C-1'), 124.1 (C-2), 143.8 (C-3) and 166.3 (C=O).

(*E*)-*N*-isopropylbut-2-enamide 288d

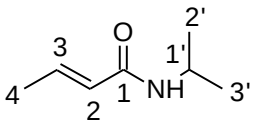

The procedure described for the synthesis of (*E*)-*N*-propylbut-2-enamide **288c** was employed, using isopropylamine (0.80 mL, 9.6 mmol), triethylamine (0.79 mL, 5.7 mmol) and crotonoyl chloride **287** (0.50 g, 4.8 mmol) in DCM (15 mL). Subsequent evaporation of the solvent *in vacuo* gave the crude product, which was recrystallised from MeOH to yield (*E*)-*N*-propylbut-2-enamide **288c** as pale yellow crystals (0.49 g, 82 %), m.p. 88-90 °C (Lit.[231] 89-90 °C); υ/cm^{-1} 1683 (C=O); δ_H/ppm (400 MHz; $CDCl_3$) 1.20 (6H, d, *J* = 7.0 Hz, 2'- and 3'-CH_3), 1.78 (3H, d, *J* = 6.0 Hz, 4-CH_3), 3.86 (1H, q, *J* = 6.8 Hz, 1'-H), 5.82 (1H, d, *J* = 15.2 Hz, 2-H), 7.02 (1H, m, 3-H) and 8.91 (1H, s, NH); δ_C (100 MHz; $CDCl_3$) 18.3 (C-4), 23.1 (C-2' and C-3'), 41.6 (C-1'), 124.2 (C-2), 143.1 (C-3) and 166.9 (C=O).

(*E*)-*N*-butylbut-2-enamide 288e [232]

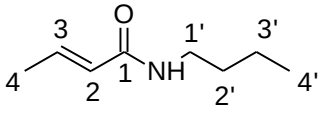

The procedure described for the synthesis of (*E*)-*N*-propylbut-2-enamide **288c** was employed, using butyllamine (0.91 mL , 9.6 mmol), triethylamine (0.79 mL, 5.8 mmol) and crotonoyl chloride **287** (0.50 g, 4.8 mmol) in DCM (15 mL). Subsequent evaporation of the solvent *in vacuo* afforded (*E*)-*N*-butylbut-2-enamide **288e** as a yellow oil (0.47 g, 69 %); υ/cm^{-1} 1658 (C=O); δ_H/ppm (400 MHz; $CDCl_3$) 0.96 (3H, t, *J* = 7.6 Hz, 4'-CH_3), 1.32 (2H, m, 3'-CH_2), 1.55 (2H, m, 2'-CH_2), 1.82 (3H, d, *J* = 6.1 Hz, 4-CH_3), 3.20 (2H, q, *J* = 7.2 Hz, 1'-CH_2), 5.87 (1H, d, *J* = 15.4 Hz, 2-H), 7.11 (1H, m, 3-H) and 8.22 (1H, s, NH); δ_C (100 MHz; $CDCl_3$) 13.9 (C-4'), 18.0 (C-4), 19.9 (C-3'), 31.8 (C-2'), 40.8 (C-1'), 124.6 (C-2), 144.1 (C-3) and 166.5 (C=O).

(*E*)-*N*-phenylbut-2-enamide 288f

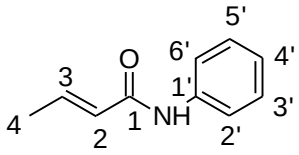

The procedure described for the synthesis of (*E*)-*N*-propylbut-2-enamide **288c** was employed, using aniline (0.89 mL , 9.6 mmol), triethylamine (0.79 mL, 5.7 mmol) and crotonoyl chloride **287** (0.50 g, 4.8 mmol) in DCM (15 mL). Subsequent evaporation of the solvent *in vacuo* gave the crude product, which was recrystallised from MeOH to yield (*E*)-*N*-phenylbut-2-enamide **288f** as light brown crystals (0.42 g, 65 %), m.p. 110-112 °C (Lit.[233-234] 110-111 °C); υ/cm^{-1} 1679 (C=O); δ_H/ppm (400 MHz; $CDCl_3$) 1.79 (3H, d, *J* = 6.4 Hz, 4-CH_3), 5.85 (1H, d, *J* = 15.6 Hz, 2-H), 7.07 (1H, m, 3-H) 7.12 (1H, t, *J* = 7.2 Hz, 4'-H), 7.29 (2H, t, *J* = 7.2 Hz, 3'-H and 5'-H), 7.60 (2H, d, *J* = 7.6 Hz, 2'-H and 6'-H) and 8.22 (1H, s, NH); δ_C (100 MHz; $CDCl_3$) 18.4 (C-4), 121.8 (C-2' and C-6'), 123.9 (C-2), 124.9 (C-4'), 128.9 (C-3' and C-5'), 136.7 (C-1'), 143.9 (C-3) and 166.9 (C=O).

(*E*)-*N*-benzylbut-2-enamide 288g

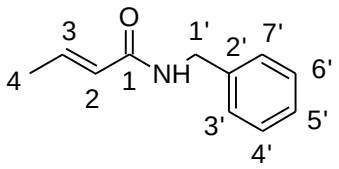

The procedure described for the synthesis of (*E*)-*N*-propylbut-2-enamide **288c** was employed, using benzylamine (1.05 mL , 9.6 mmol), triethylamine (0.79 mL, 5.7 mmol) and

crotonoyl chloride **287** (0.50 g, 4.8 mmol) in DCM (15 mL). Subsequent evaporation of the solvent *in vacuo* gave the crude product, which was recrystallised from MeOH to yield (*E*)-*N*-benzylbut-2-enamide **288g** as pale yellow crystals (0.41 g, 74 %), m.p. 110-112 °C (Lit.[235] 112-114 °C); υ/cm^{-1} 1684 (C=O); δ_H/ppm (400 MHz; $CDCl_3$) 1.77 (3H, d, *J* = 6.4 Hz, 4-CH_3), 5.86 (1H, d, *J* = 15.6 Hz, 2-H), 7.10 (1H, m, 3-H), 7.29 (5H, m, 3'-H, 4'-H, 5'-H, 6'-H and 7'-H) and 8.21 (1H, s, NH); δ_C (100 MHz; $CDCl_3$) 18.4 (C-4), 43.2 (1'-CH_2), 124.0 (C-2), 127.4 (C-5'), 128.0 (C-3' and C-7'), 128.8 (C-4' and C-6'), 140.3 (C-2'), 143.2 and 166.7 (C=O).

(*E*)-4-bromobut-2-enoic acid 290

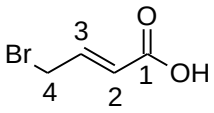

(*E*)-Ethyl 4-bromocrotonate **283** (1.20 g, 6.22 mmol) was added to a 2M solution of potassium hydroxide in ethanol (1.1 mL, 19 mmol) and the mixture was stirred at room temperature for 24 hours. After completion of the reaction, the ethanol was evaporated at reduced pressure and the residue was dissolved in water (100 mL), extracted with diethyl ether (2 x 50 mL), and the organic phase discarded. The aqueous phase was acidified (pH 2.5) with 2M-HCl and extracted with diethyl ether (3 x 50 mL). The combined organic phases were washed with water (2 x 50 mL) and brine (2 x 50 mL), and dried (Na_2SO_4). Evaporation of the solvent *in vacuo* gave crude product, which was washed with cold hexane to afford (*E*)-4-bromobut-2-enoic acid **290** as white crystals (1.01 g, 98 %), m.p. 72-74 °C (Lit.[236] 71-73 °C); υ/cm^{-1} 2891 (OH) and 1681 (C=O); δ_H/ppm (400 MHz; $CDCl_3$) 3.98 (2H, d, *J* = 7.6 Hz, CH_2Br), 6.00 (1H, d, *J* = 15.2 Hz, 2-H), 6.98 (1H, m, 3-H) and 8.83 (1H, s, OH); δ_C (100 MHz; $CDCl_3$) 35.2 (CH_2Br), 124.6 (C-2), 143.8 (C-3) and 169.7 (C=O).

(*E*)-4-(diethyloxyphosphoryl)but-2-enoic acid 291 [237]

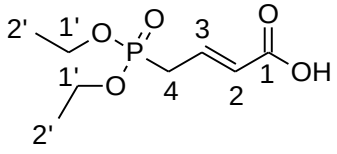

Method 1

(*E*)-4-(Diethoxyphosphoryl)crotonate **284** (2.00 g, 7.99 mmol) was added to a 2M solution of potassium hydroxide in ethanol (1.41 mL, 23.9 mmol) and the mixture was stirred at room temperature for 24 hours. After completion of the reaction, the ethanol was evaporated at reduced pressure and the residue was dissolved in water (100 mL), extracted with diethyl ether (2 x 50 mL), and the organic phase discarded. The aqueous phase was acidified (pH 2.5) with 2M-HCl and extracted with diethyl ether (3 x 50 mL). The combined organic phases were washed with water (2 x 50 mL) and brine (2 x 50 mL), and dried (anhydr. Na_2SO_4). The crude product was purified by flash chromatography [on silica gel; elution with hexane-EtOAc (4:1)], and subsequent evaporation of the solvent *in vacuo* afforded (*E*)-4-(diethyloxyphosphoryl)but-2-enoic acid **291** as a clear oil (1.72 g, 97 %); υ/cm^{-1} 2893 (OH), 1698 (C=O) and 1234 (P=O); δ_H/ppm (400 MHz; $CDCl_3$) 1.33 (6H, m, 2 x CH_3), 2.77 (2H, dd, *J* = 26.4 and 3.2 Hz, CH_2P), 4.16 (4H, m, 2 x OCH_2), 5.10 (1H, s, OH), 5.86 (1H, dd, *J* = 15.6 and 4.4 Hz, 2-H) and 7.07 (1H, m, 3-H); δ_C/ppm (100 MHz; $CDCl_3$) 16.2 (2 x C-2'), 30.3 (CH_2P), 62.3 (2 x C-1'), 125.7 (d, J_{P-C} = 11.0 Hz, C-2), 137.1 (d, J_{P-C} = 13.6 Hz, C-3) and 165.8 (C=O).

Method 2

Triethyl phosphite (3.07 g, 18.2 mmol) was added slowly to a stirred solution of (*E*)-4-bromobut-2-enoic acid **290** (1.50 g, 9.09 mmol) in toluene (15 mL) during a period of 1 hour, whilst the temperature of the mixture was maintained at 120 ^{o}C. After the addition, the mixture was stirred at the same temperature of a further 8 hours and then cooled to room temperature. The cooled mixture was stirred with hexane (20 mL) for *ca.* 30 minutes followed by decantation of the hexane layer to remove the excess triethyl phosphite; this was repeated three times. The crude product was purified by flash chromatography [on silica gel; elution with hexane-EtOAc (4:1)], and subsequent evaporation of the solvent *in vacuo* afforded (*E*)-4-(diethyloxyphosphoryl)but-2-enoic acid **291** as a clear oil (1.37 g, 68 %).

Diethyl [(2*S*, 3*S*)-2,3-dihydroxy-4-(methylamino)-4-oxobutyl]phosphonate 292a ‡

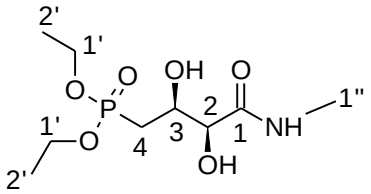

In a 100ml round-bottomed flask, a mixture of $NaIO_4$ (642 mg, 3 mmol) and $CeCl_3.H_2O$ (75 mg, 0.2 mmol) in H_2O (0.9 mL) was stirred and heated until a bright yellow suspension formed. The reaction mixture was then cooled to 0 °C, and EtOAc (3 mL), CH_3CN (6 mL) and a 0.1M aq. solution of $RuCl_3$ (50 µL, 0.01 mmol) were added successively. After stirring for 10 minutes, a solution of (*E*)-4-(diethoxyphosphoryl)-*N*-methylbut-2-enamide **285a** (240 mg, 1.0 mmol) in EtOAc (3 mL) was added, and the resulting heterogeneous mixture was stirred until the full consumption (followed by TLC) of the starting material. After completion of the reaction, anhydr. Na_2SO_4 (1 g) was added followed by EtOAc (25 mL). The solid was removed and the organic layer was washed with satd. aq. Na_2SO_3 (50 mL) and water (50 mL), dried (anhydr. Na_2SO_4), and the solvents were removed *in vacuo*. The crude product was chromatographed [preparative layer chromatography; elution with hexane-EtOAc-MeOH (1:1:1)] to yield **292a** as a yellow oil (65.9 mg, 49 %) (Found: C, 40.21; H, 7.53; N, 5.25 %. $C_9H_{20}NO_6P$ requires C, 40.15; H, 7.49; N, 5.20 %); υ/cm^{-1} 3241 (OH), 1675 (C=O) and 1231 (P=O); δ_H/ppm (400 MHz; $CDCl_3$) 1.26 (6H, t, *J* = 7.2 Hz, 2 x CH_3), 1.94 and 2.12 (2H, 2 x m, 4-CH_2P), 2.38 (2H, s, 2 x OH), 2.82 (3H, s, 1''-CH_3), 3.45 (1H, q, *J* = 7.2 Hz, 3-H), 4.04 (4H, m, 2 x OCH_2), 4.20 (1H, d, *J* = 7.6 Hz, 2-H) and 10.3 (1H, s, NH); δ_C (100 MHz; $CDCl_3$) 16.4 (d, J_{P-C} = 6.0 Hz, 2 × CH_3), 24.8 (1''-CH_3), 29.5 (d, J_{P-C} = 141.2 Hz, CH_2P), 58.3 (d, J_{P-C} = 10.9 Hz, C-3), 61.4 (d, J_{P-C} = 6.4 Hz, 2 x OCH_2), 80.1 (d, J_{P-C} = 13.2 Hz, C-2) and 168.6 (C=O).

Diethyl [(2*S*, 3*S*)-2,3-dihydroxy-4-(ethylamino)-4-oxobutyl]phosphonate 292b ‡

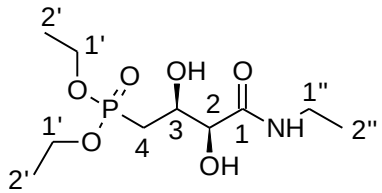

‡ Product isolated as a racemic mixture.

The procedure described for the synthesis of diethyl [(2*S*,3*S*)-2,3-dihydroxy-4-(methylamino)-4-oxobutyl]phosphonate **292a** was employed, using $NaIO_4$ (642 mg, 3 mmol), $CeCl_3.H_2O$ (75 mg, 0.2 mmol), $RuCl_3$ (50 µL, 0.01 mmol) and (*E*)-4-(diethoxyphosphoryl)-*N*-ethylbut-2-enamide **285b** (283 mg, 1.0 mmol). The crude product was chromatographed [preparative layer chromatography; elution with hexane-EtOAc-MeOH (1:1:1)] to yield *diethyl [(2S,3S)-2,3-dihydroxy-4-(ethylamino)-4-oxobutyl]phosphonate* **292b** as a clear oil (66.7 mg, 47 %) (Found: C, 42.44; H, 7.89; N, 5.01 %. $C_{10}H_{22}NO_6P$ requires C, 42.40; H, 7.83; N, 4.94 %); υ/cm^{-1} 3252 (OH), 1690 (C=O) and 1222 (P=O); δ_H/ppm (400 MHz; $CDCl_3$) 1.01 (3H, t, *J* = 7.6 Hz, 2''-CH_3), 1.32 (6H, t, *J* = 7.2 Hz, 2 x CH_3), 1.78 and 2.10 (2H, 2 x m, 4-CH_2P), 3.24 (2H, q, *J* = 7.6 Hz, 1''-CH_2), 4.10 (4H, m, 2 x OCH_2), 4.46 (1H, d, *J* = 7.6 Hz, 2-H), 4.68 (1H, q, *J* = 7.2 Hz, 3-H), 5.08 (2H, s, 2 x OH) and 8.72 (1H, s, NH); δ_C (100 MHz; $CDCl_3$) 14.2 (C-2''), 16.1 (d, J_{P-C} = 6.7 Hz, 2 × CH_3), 27.6 (d, J_{P-C} = 144.0 Hz, CH_2P), 35.4 (C-1''), 60.7 (d, J_{P-C} = 11.7 Hz, C-3), 63.6 (d, J_{P-C} = 5.8 Hz, 2 × OCH_2), 79.7 (d, J_{P-C} = 13.2 Hz, C-2) and 165.9 (C=O).

Diethyl [(2*S*, 3*S*)-2,3-dihydroxy-4-(propylamino)-4-oxobutyl]phosphonate 292c ‡

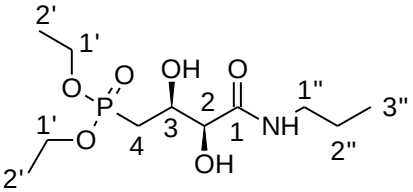

The procedure described for the synthesis of diethyl [(2*S*,3*S*)-2,3-dihydroxy-4-(methylamino)-4-oxobutyl]phosphonate **292a** was employed, using $NaIO_4$ (642 mg, 3 mmol), $CeCl_3.H_2O$ (75 mg, 0.2 mmol), $RuCl_3$ (50 µL, 0.01 mmol) and (*E*)-4-(diethoxyphosphoryl)-*N*-propylbut-2-enamide **285c** (263 mg, 1.0 mmol). The crude product was chromatographed [preparative layer chromatography; elution with hexane-EtOAc-MeOH (1:1.5:1)] to yield *diethyl [(2S,3S)-2,3-dihydroxy-4-(propylamino)-4-oxobutyl]phosphonate* **292c** as a yellow oil (75.8 mg, 51 %) (Found: C, 44.53; H, 8.20; N, 4.76 %. $C_{11}H_{24}NO_6P$ requires C, 44.44; H, 8.14; N, 4.71 %); υ/cm^{-1} 3130 (OH), 1692 (C=O) and 1239 (P=O); δ_H/ppm (400 MHz; $CDCl_3$) 0.99 (3H, t, *J* = 7.6 Hz, 3''-CH_3), 1.31 (6H, t, *J* = 7.2 Hz, 2 x CH_3), 1.54 (2H, m, 2''-CH_2), 1.80 and 2.08 (2H, 2 x m, 4-CH_2P), 3.28 (2H, q, *J* = 6.8 Hz, 1''-CH_2), 4.09 (4H, m, 2 x OCH_2), 4.43 (1H, d, *J* = 7.6 Hz, 2-H), 4.69 (1H, q, 7.6 Hz, 3-H), 7.75 (2H, s, 2 x OH) and 8.36 (1H, s, NH); δ_C (100 MHz;

‡ Product isolated as racemic mixture.

$CDCl_3$) 11.4 (C-3''), 16.5 (d, J_{P-C} = 5.8 Hz, 2 × CH_3), 23.0 (C-2''), 27.7 (d, J_{P-C} = 143.9 Hz, CH_2P), 41.2 (C-1''), 61.7 (d, J_{P-C} = 11.9 Hz, C-3), 63.7 (d, J_{P-C} = 5.8 Hz, 2 × OCH_2), 78.6 (d, J_{P-C} = 13.6 Hz, C-2) and 171.6 (C=O).

Diethyl [(2*S*, 3*S*)-2,3-dihydroxy-4-(isopropylamino)-4-oxobutyl]phosphonate 292d ‡

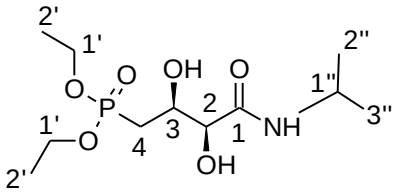

The procedure described for the synthesis of diethyl [(2*S*,3*S*)-2,3-dihydroxy-4-(methylamino)-4-oxobutyl]phosphonate **292a** was employed, using $NaIO_4$ (642 mg, 3 mmol), $CeCl_3.H_2O$ (75 mg, 0.2 mmol), $RuCl_3$ (50 µL, 0.01 mmol) and (*E*)-4-(diethoxyphosphoryl)-*N*-isopropylbut-2-enamide **285d** (263 mg, 1.0 mmol). The crude product was chromatographed [preparative layer chromatography; elution with hexane-EtOAc-MeOH (1:1:1)] to yield *diethyl [(2S,3S)-2,3-dihydroxy-4-(isopropylamino)-4-oxobutyl]phosphonate* **292d** as a clear oil (71.3 mg, 48 %) (Found: C, 44.48; H, 8.19; N, 4.75 %. $C_{11}H_{24}NO_6P$ requires C, 44.44; H, 8.14; N, 4.71 %); υ/cm^{-1} 3253 (OH), 1691 (C=O) and 1235 (P=O); δ_H/ppm (400 MHz; $CDCl_3$) 0.98 (6H, d, *J* = 6.8 Hz, 2''- and 3''-CH_3), 1.31 (6H, t, *J* = 7.2 Hz, 2 x CH_3), 1.79 and 2.12 (2H, 2 x m, 4-CH_2P), 2.78 (2H, s, 2 x OH), 3.84 (1H, q, *J* = 7.0 Hz, 1''-H), 4.11 (4H, m, 2 x OCH_2), 4.44 (1H, d, *J* = 7.6 Hz, 2-H), 4.85 (1H, q, *J* = 7.6 Hz, 3-H) and 8.71 (1H, s, NH); δ_C (100 MHz; $CDCl_3$) 16.1 (d, J_{P-C} = 6.7 Hz, 2 × CH_3), 22.9 (C-2'' and C-3''), 27.6 (d, J_{P-C} = 143.9 Hz, CH_2P), 41.1 (C-1''), 61.6 (d, J_{P-C} = 11.9 Hz, C-3), 63.6 (d, J_{P-C} = 5.8 Hz, 2 × OCH_2), 78.5 (d, J_{P-C} = 13.6 Hz, C-2) and 171.7 (C=O).

Diethyl [(2*S*, 3*S*)-2,3-dihydroxy-4-(butylamino)-4-oxobutyl]phosphonate 292e ‡

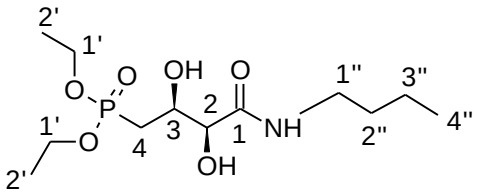

‡ Product isolated as racemic mixture.

The procedure described for the synthesis of diethyl [(2*S*,3*S*)-2,3-dihydroxy-4-(methylamino)-4-oxobutyl]phosphonate **292a** was employed, using $NaIO_4$ (642 mg, 3 mmol), $CeCl_3.H_2O$ (75 mg, 0.2 mmol), $RuCl_3$ (50 µL, 0.01 mmol) and (*E*)-4-(diethoxyphosphoryl)-*N*-butylbut-2-enamide **285e** (277 mg, 1.0 mmol). The crude product was chromatographed [preparative layer chromatography; elution with hexane-EtOAc-MeOH (1:1.5:1)] to yield *diethyl [(2S,3S)-2,3-dihydroxy-4-(butylamino)-4-oxobutyl]phosphonate* **292e** as a clear oil (73.2 mg, 47 %) (Found: C, 46.48; H, 8.51; N, 4.57 %. $C_{12}H_{26}NO_6P$ requires C, 46.30; H, 8.42; N, 4.50 %); υ/cm^{-1} 3122 (OH), 1704 (C=O) and 1226 (P=O); δ_H/ppm (400 MHz; $CDCl_3$) 1.12 (3H, t, *J* = 7.6 Hz, 4''-CH_3), 1.18 (6H, t, *J* = 7.6 Hz, 2 x CH_3), 1.52 (4H, m, 2''-CH_2 and 3''-CH_2), 1.81 and 2.11 (2H, 2 x m, 4-CH_2P), 3.22 (2H, q, *J* = 6.8 Hz, 1''-CH_2), 4.10 (4H, m, 2 x OCH_2), 4.50 (1H, d, *J* = 7.4 Hz, 2-H), 5.01 (1H, q, *J* = 7.2 Hz, 3-H), 7.67 (2H, s, 2 x OH) and 8.49 (1H, s, NH); δ_C (100 MHz; $CDCl_3$) 14.0 (C-4''), 16.2 (d, J_{P-C} = 5.9 Hz, 2 × CH_3), 20.0 (C-3''), 29.5 (d, J_{P-C} = 141.2 Hz, CH_2P), 31.9 (C-2''), 40.4 (C-1''), 60.1 (d, J_{P-C} = 11.2 Hz, C-3), 61.2 (d, J_{P-C} = 6.4 Hz, 2 × OCH_2), 79.8 (d, J_{P-C} = 13.2 Hz, C-2) and 169.9 (C=O).

Diethyl [(2*S*, 3*S*)-2,3-dihydroxy-4-(phenylamino)-4-oxobutyl]phosphonate 292f ‡

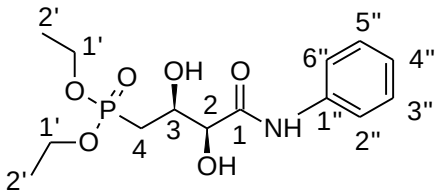

The procedure described for the synthesis of diethyl [(2*S*,3*S*)-2,3-dihydroxy-4-(methylamino)-4-oxobutyl]phosphonate **292a** was employed, using $NaIO_4$ (642 mg, 3 mmol), $CeCl_3.H_2O$ (75 mg, 0.2 mmol), $RuCl_3$ (50 µL, 0.01 mmol) and (*E*)-4-(diethoxyphosphoryl)-*N*-phenylbut-2-enamide **285f** (300 mg, 1.0 mmol). The crude product was chromatographed [preparative layer chromatography; elution with hexane-EtOAc-MeOH (1:1:1)] to yield *diethyl [(2S,3S)-2,3-dihydroxy-4-(phenylamino)-4-oxobutyl]phosphonate* **292f** as a brown oil (81.2 mg, 49 %) (Found: C, 50.78; H, 6.73; N, 4.29 %. $C_{14}H_{22}NO_6P$ requires C, 50.75; H, 6.69; N, 4.23 %); υ/cm^{-1} 3356 (OH), 1657 (C=O) and 1232 (P=O); δ_H/ppm (400 MHz; $CDCl_3$) 1.32 (6H, t, *J* = 7.6 Hz, 2 x CH_3), 1.78 and 2.03 (2H, 2 x m, 4-CH_2P), 4.13 (4H, m, 2 x OCH_2), 4.48 (1H, d, *J* = 7.1 Hz, 2-H), 5.04 (1H, q, *J* = 7.2 Hz, 3-H), 7.28 (5H, m, Ar-H), 8.02 (2H, s, 2 x OH)

‡ Product isolated as racemic mixture.

and 8.80 (1H, s, NH); δ_C (100 MHz; $CDCl_3$) 16.3 (d, J_{P-C} = 6.0 Hz, 2 × CH_3), 29.3 (d, J_{P-C} = 143.0 Hz, CH_2P), 60.0 (d, J_{P-C} = 11.5 Hz, C-3), 62.1 (d, J_{P-C} = 6.5 Hz, 2 × OCH_2), 79.5 (d, J_{P-C} = 13.6 Hz, C-2), 121.3 (C-2'' and C-6''), 124.1 (C-4''), 129.4 (C-3'' and C-5''), 137.6 (C-1'') and 169.6 (C=O).

Diethyl [(2*S*, 3*S*)-2,3-dihydroxy-4-(benzylamino)-4-oxobutyl]phosphonate 292g ‡

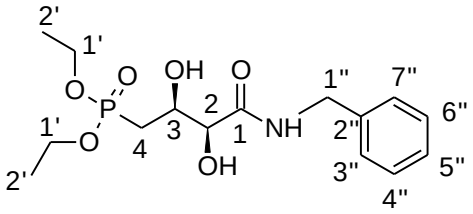

The procedure described for the synthesis of diethyl [(2*S*,3*S*)-2,3-dihydroxy-4-(methylamino)-4-oxobutyl]phosphonate **292a** was employed, using $NaIO_4$ (642 mg, 3 mmol), $CeCl_3.H_2O$ (75 mg, 0.2 mmol), $RuCl_3$ (50 µL, 0.01 mmol) and (*E*)-4-(diethoxyphosphoryl)-*N*-benzylbut-2-enamide **285g** (345 mg, 1.0 mmol). The crude product was chromatographed [preparative layer chromatography; elution with hexane-EtOAc-MeOH (1:1:1)] to yield *diethyl [(2S,3S)-2,3-dihydroxy-4-(benzylamino)-4-oxobutyl]phosphonate* **292g** as a yellow oil (91.5 mg, 53 %) (Found: C, 52.27; H, 6.96; N, 4.12 %. $C_{15}H_{24}NO_6P$ requires C, 52.17; H, 7.01; N, 4.06 %); υ/cm^{-1} 3180 (OH), 1688 (C=O) and 1228 (P=O); δ_H/ppm (400 MHz; $CDCl_3$) 1.33 (6H, t, *J* = 7.6 Hz, 2 x CH_3), 2.01 and 2.19 (2H, 2 x m, 4-CH_2P), 4.10 (4H, m, 2 x OCH_2), 4.29 (1H, d, *J* = 7.2 Hz, 2-H), 4.48 (2H, s, 1''-CH_2), 4.98 (1H, q, *J* = 7.2 Hz, 3-H), 7.31 (5H, m, Ar-H), 8.18 (2H, s, 2 x OH) and 8.82 (1H, s, NH); δ_C (100 MHz; $CDCl_3$) 16.6 (d, J_{P-C} = 6.8 Hz, 2 × CH_3), 28.1 (d, J_{P-C} = 143.9 Hz, CH_2P), 44.0 (1''-CH_2), 61.1 (d, J_{P-C} = 11.6 Hz, C-3), 62.2 (d, J_{P-C} = 6.4 Hz, 2 × OCH_2), 80.2 (d, J_{P-C} = 13.5 Hz, C-2), 127.9 (C-5''), 128.3 (C-3'' and C-7''), 129.1 (C-4'' and C-6''), 140.8 (C-2'') and 171.7 (C=O).

[(2*S*, 3*S*)-2,3-Dihydroxy-4-(methylamino)-4-oxobutyl]phosphonic acid 293a ‡

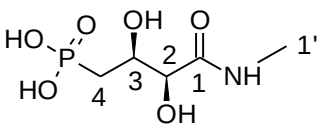

‡ Product isolated as racemic mixture.

Trimethylsilyl bromide (0.13 mL, 0.88 mmol) was added to diethyl [(2*S*,3*S*)-2,3-dihydroxy-4-(methylamino)-4-oxobutyl]phosphonate **292a** (0.12 g, 0.44 mmol) in CH_3CN (2 mL) and the mixture was heated in the microwave apparatus set to deliver 100 W of power, with a reaction temperature of 100 ^oC and reaction time of 10 min. After completion, the mixture was cooled to room temperature, treated with a 95:5 MeOH-H_2O mixture (1.5 mL) and stirred for 30 min. The solvent was removed *in vacuo* and the residue chromatographed [reverse-phase chromatography on C_{18} cellulose; elution with MeOH] to yield *[(2S, 3S)-2,3-dihydroxy-4-(methylamino)-4-oxobutyl]phosphonic acid* **293a** as a clear oil (60.9 mg, 65 %) (Found: C, 28.33; H, 5.71; N, 6.62 %. $C_5H_{12}NO_6P$ requires C, 28.18; H, 5.68; N, 6.57 %); υ/cm^{-1} 3184 (OH), 1683 (C=O) and 1244 (P=O); δ_H/ppm (400 MHz; D_2O) 1.91 and 2.18 (2H, 2 x m, 4-CH_2P), 2.81 (3H, s, 1'-CH_3), 4.38 (1H, d, *J* = 7.6 Hz, 2-H) and 4.71 (1H, q, *J* = 7.2 Hz, 3-H); δ_C (100 MHz; D_2O) 26.5 (1'-CH_3), 31.4 (d, J_{P-C} = 143.9 Hz, CH_2P), 59.8 (d, J_{P-C} = 11.2 Hz, C-3), 79.9 (d, J_{P-C} = 12.7 Hz, C-2) and 171.8 (C=O).

[(2*S*, 3*S*)-2,3-Dihydroxy-4-(ethylamino)-4-oxobutyl]phosphonic acid 293b ‡

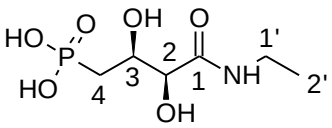

The procedure described for the synthesis of [(2*S*, 3*S*)-2,3-dihydroxy-4-(methylamino)-4-oxobutyl]phosphonic acid **293a** was employed, using trimethylsilyl bromide (0.12 mL, 0.85 mmol) and diethyl [(2*S*,3*S*)-2,3-dihydroxy-4-(ethylamino)-4-oxobutyl]phosphonate **292b** (0.12 g, 0.43 mmol) in CH_3CN (2 mL). The crude product was chromatographed [reverse-phase chromatography on C_{18} cellulose; elution with MeOH] to yield *[(2S, 3S)-2,3-dihydroxy-4-(ethylamino)-4-oxobutyl]phosphonic acid* **293b** as a clear oil (66.4 mg, 68 %) (Found: C, 31.57; H, 6.18; N, 6.11 %. $C_6H_{14}NO_6P$ requires C, 31.73; H, 6.21; N, 6.17 %); υ/cm^{-1} 3242 (OH), 1667 (C=O) and 1244 (P=O); δ_H/ppm (400 MHz; D_2O) 1.19 (3H, t, *J* = 7.6 Hz, 2'-CH_3), 1.77 and 2.02 (2H, 2 x m, 4-CH_2P), 3.23 (2H, q, *J* = 7.6 Hz, 1'-CH_2), 4.44 (1H, d, *J* = 7.6 Hz, 2-H) and 4.65 (1H, q, *J* = 7.2 Hz, 3-H); δ_C (100 MHz; D_2O) 14.7 (C-2'), 27.8 (d, J_{P-C} = 141.6 Hz, CH_2P), 35.4 (C-1'), 61.7 (d, J_{P-C} = 11.7 Hz, C-3), 80.3 (d, J_{P-C} = 13.3 Hz, C-2) and 171.5 (C=O).

‡ Product isolated as racemic mixture.

[(2*S*, 3*S*)-2,3-Dihydroxy-4-(propylamino)-4-oxobutyl]phosphonic acid 293c ‡

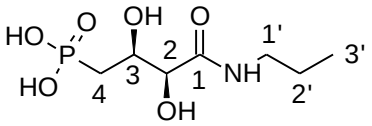

The procedure described for the synthesis of [(2*S*, 3*S*)-2,3-dihydroxy-4-(methylamino)-4-oxobutyl]phosphonic acid **293a** was employed, using trimethylsilyl bromide (0.11 mL, 0.80 mmol) and diethyl [(2*S*,3*S*)-2,3-dihydroxy-4-(propylamino)-4-oxobutyl]phosphonate **292c** (0.12 g, 0.40 mmol) in CH_3CN (2 mL). The crude product was chromatographed [reverse-phase chromatography on C_{18} cellulose; elution with MeOH] to yield *[(2S, 3S)-2,3-dihydroxy-4-(propylamino)-4-oxobutyl]phosphonic acid* **293c** as a yellow oil (64.6 mg, 67 %) (Found: C, 34.94; H, 6.63; N, 5.88 %. $C_7H_{16}NO_6P$ requires C, 34.86; H, 6.69; N, 5.81 %); υ/cm^{-1} 3245 (OH), 1652 (C=O) and 1262 (P=O); δ_H/ppm (400 MHz; D_2O) 1.01 (3H, t, *J* = 7.6 Hz, 3'-CH_3), 1.56 (2H, q, J = 7.2 Hz 2'-CH_2), 1.79 and 2.10 (2H, 2 x m, 4-CH_2P), 3.22 (2H, q, *J* = 6.8 Hz, 1'-CH_2), 4.44 (1H, d, *J* = 7.3 Hz, 2-H) and 4.89 (1H, q, 7.2 Hz, 3-H); δ_C (100 MHz; D_2O) 14.7 (C-3'), 22.5 (C-2'), 27.8 (d, J_{P-C} = 141.6 Hz, CH_2P), 41.2 (C-1''), 61.7 (d, J_{P-C} = 11.5 Hz, C-3), 80.1 (d, J_{P-C} = 13.8 Hz, C-2) and 171.5 (C=O).

[(2*S*, 3*S*)-2,3-Dihydroxy-4-(isopropylamino)-4-oxobutyl]phosphonic acid 293d ‡

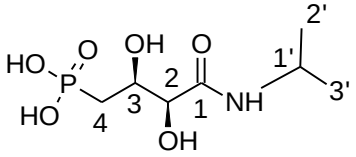

The procedure described for the synthesis of [(2*S*, 3*S*)-2,3-dihydroxy-4-(methylamino)-4-oxobutyl]phosphonic acid **293a** was employed, using trimethylsilyl bromide (0.11 mL, 0.80 mmol) and diethyl [(2*S*,3*S*)-2,3-dihydroxy-4-(isopropylamino)-4-oxobutyl]phosphonate **292d** (0.12 g, 0.40 mmol) in CH_3CN (2 mL). The crude product was chromatographed [reverse-phase chromatography on C_{18} cellulose; elution with MeOH] to yield *[(2S, 3S)-2,3-dihydroxy-4-(isopropylamino)-4-oxobutyl]phosphonic acid* **293d** as a yellow oil (61.7 mg, 64 %) (Found: C, 34.90; H, 6.72; N, 5.85 %. $C_7H_{16}NO_6P$ requires C, 34.86; H, 6.69; N, 5.81 %); υ/cm^{-1} 3090 (OH), 1687 (C=O) and 1240 (P=O); δ_H/ppm (400 MHz; D_2O) 1.12 (6H, d, *J* = 7.2 Hz, 2'- and 3'-

‡ Product isolated as racemic mixture.

CH_3), 1.89 and 2.20 (2H, 2 x m, 4-CH_2P), 3.88 (1H, q, *J* = 7.0 Hz, 1'-H), 4.23 (1H, d, *J* = 7.6 Hz, 2-H) and 4.71 (1H, q, *J* = 7.6 Hz, 3-H); δ_C (100 MHz; D_2O) 23.7 (C-2' and C-3'), 31.0 (d, J_{P-C} = 141.2 Hz, CH_2P), 41.4 (C-1'), 60.6 (d, J_{P-C} = 10.7 Hz, C-3), 81.8 (d, J_{P-C} = 13.9 Hz, C-2) and 169.4 (C=O).

[(2*S*, 3*S*)-2,3-Dihydroxy-4-(butylamino)-4-oxobutyl]phosphonic acid 293e ‡

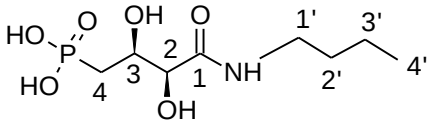

The procedure described for the synthesis of [(2*S*, 3*S*)-2,3-dihydroxy-4-(methylamino)-4-oxobutyl]phosphonic acid **293a** was employed, using trimethylsilyl bromide (0.11 mL, 0.77 mmol) and diethyl [(2*S*,3*S*)-2,3-dihydroxy-4-(butylamino)-4-oxobutyl]phosphonate **292e** (0.12 g, 0.38 mmol) in CH_3CN (3 mL). The crude product was chromatographed [reverse-phase chromatography on C_{18} cellulose; elution with MeOH:H_2O (1:0.5)] to yield *[(2S, 3S)-2,3-dihydroxy-4-(butylamino)-4-oxobutyl]phosphonic acid* **293e** as a clear oil (60.1 mg, 62 %) (Found: C, 37.70; H, 7.15; N, 5.54 %. $C_8H_{18}NO_6P$ requires C, 37.65; H, 7.11; N, 5.49 %); υ/cm^{-1} 3252 (OH), 1632 (C=O) and 1260 (P=O); δ_H/ppm (400 MHz; D_2O) 1.16 (3H, t, *J* = 7.2 Hz, 4'-CH_3), 1.50 (4H, m, 2'-CH_2 and 3'-CH_2), 1.80 and 2.01 (2H, 2 x m, 4-CH_2P), 3.23 (2H, q, *J* = 7.2 Hz, 1'-CH_2), 4.45 (1H, d, *J* = 7.2 Hz, 2-H) and 4.99 (1H, q, *J* = 6.9 Hz, 3-H); δ_C (100 MHz; D_2O) 14.1 (C-4'), 20.3 (C-3'), 30.6 (d, J_{P-C} = 138.0 Hz, CH_2P), 32.3 (C-2'), 40.6 (C-1'), 60.2 (d, J_{P-C} = 10.9 Hz, C-3), 79.0 (d, J_{P-C} = 11.6 Hz, C-2) and 169.6 (C=O).

[(2S, 3S)-2,3-Dihydroxy-4-(phenylamino)-4-oxobutyl]phosphonic acid 293f ‡

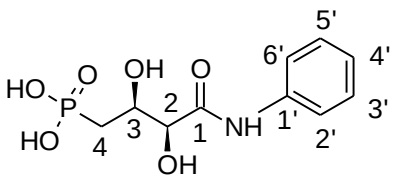

The procedure described for the synthesis of [(2*S*, 3*S*)-2,3-dihydroxy-4-(methylamino)-4-oxobutyl]phosphonic acid **293a** was employed, using trimethylsilyl bromide (0.10 mL, 0.72 mmol) and diethyl [(2*S*,3*S*)-2,3-dihydroxy-4-(phenylamino)-4-oxobutyl]phosphonate **292f**

‡ Product isolated as racemic mixture.

(0.12 g, 0.36 mmol) in CH_3CN (2 mL). The crude product was chromatographed [reverse-phase chromatography on C_{18} cellulose; elution with MeOH:H_2O (1:0.5)] to yield *[(2S, 3S)-2,3-dihydroxy-4-(phenylamino)-4-oxobutyl]phosphonic acid* **293f** as a yellow oil (61.4 mg, 62 %) (Found: C, 43.69; H, 5.15; N, 5.05 %. $C_{10}H_{14}NO_6P$ requires C, 43.64; H, 5.13; N, 5.09 %); υ/cm^{-1} 3070 (OH), 1685 (C=O) and 1264 (P=O); δ_H/ppm (400 MHz; D_2O) 1.93 and 2.18 (2H, 2 x m, 4-CH_2P), 4.45 (1H, d, *J* = 7.6 Hz, 2-H), 5.03 (1H, q, *J* = 7.6 Hz, 3-H) and 7.27 (5H, m, 2'-H, 3'-H, 4'-H, 5'-H and 6'-H); δ_C (100 MHz; D_2O) 29.3 (d, J_{P-C} = 141.2 Hz, CH_2P), 60.8 (d, J_{P-C} = 11.5 Hz, C-3), 80.2 (d, J_{P-C} = 13.9 Hz, C-2), 122.2 (C-2' and C-6'), 124.6 (C-4'), 129.3 (C-3' and C-5'), 138.2 (C-1') and 169.8 (C=O).

[(2*S*, 3*S*)-2,3-Dihydroxy-4-(benzylamino)-4-oxobutyl]phosphonic acid 293g ‡

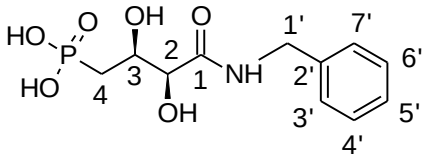

The procedure described for the synthesis of [(2*S*, 3*S*)-2,3-dihydroxy-4-(methylamino)-4-oxobutyl]phosphonic acid **293a** was employed, using trimethylsilyl bromide (0.10 mL, 0.70 mmol) and diethyl [(2*S*,3*S*)-2,3-dihydroxy-4-(benzylamino)-4-oxobutyl]phosphonate **292g** (0.12 g, 0.35 mmol) in CH_3CN (2 mL). The crude product was chromatographed [reverse-phase chromatography on C_{18} cellulose; elution with MeOH] to yield *[(2S, 3S)-2,3-dihydroxy-4-(benzylamino)-4-oxobutyl]phosphonic acid* **293g** as a yellow oil (62.1 mg, 62 %) (Found: C, 45.75; H, 5.63; N, 4.87 %. $C_{11}H_{16}NO_6P$ requires C, 45.68; H, 5.58; N, 4.84 %); υ/cm^{-1} 3076 (OH), 1666 (C=O) and 1252 (P=O); δ_H/ppm (400 MHz; D_2O) 1.88 and 2.10 (2H, 2 x m, 4-CH_2P), 4.28 (1H, d, *J* = 7.4 Hz, 2-H), 4.83 (2H, s, 1'-CH_2), 5.00 (1H, q, *J* = 7.2 Hz, 3-H) and 7.28 (5H, m, 3'-H, 4'-H, 5'-H, 6'-H and 7'-H); δ_C (100 MHz; D_2O) 27.6 (d, J_{P-C} = 145.9 Hz, CH_2P), 43.5 (1'-CH_2), 59.9 (d, J_{P-C} = 10.9 Hz, C-3), 79.8 (d, J_{P-C} = 14.6 Hz, C-2), 127.5 (C-5'), 127.8 (C-3' and C-7'), 128.7 (C-4' and C-6'), 140.3 (C-2') and 168.9 (C=O).

‡ Product isolated as racemic mixture.

Ethyl (2*S*, 3*S*)-4-(diethoxyphosphoryl)-2,3-dihydroxybutanoate 313 ‡

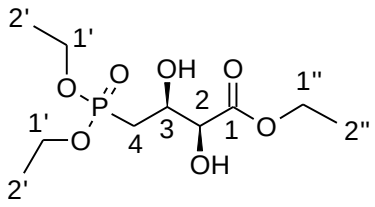

The procedure described for the synthesis of diethyl [(2*S*,3*S*)-2,3-dihydroxy-4-(methylamino)-4-oxobutyl]phosphonate **292a** was employed, using $NaIO_4$ (642 mg, 3 mmol), $CeCl_3.H_2O$ (75 mg, 0.2 mmol), $RuCl_3$ (50 µL, 0.01 mmol) and (*E*)-4-(diethoxyphosphoryl)-crotonate **284** (250 mg, 1.0 mmol). The crude product was chromatographed [preparative layer chromatography; elution with hexane-EtOAc-MeOH (1:1:1)] to yield *ethyl (2S, 3S)-4-(diethoxyphosphoryl)-2,3-dihydroxybutanoate* **313** as a yellow oil (0.11 g, 53 %) (Found: C, 42.29; H, 7.42 %. $C_{10}H_{21}NO_7P$ requires C, 42.25; H, 7.45 %); υ/cm^{-1} 3378 (OH), 1687 (C=O) and 1219 (P=O); δ_H/ppm (400 MHz; $CDCl_3$) 1.28 (9H, m, 3 x CH_3), 2.00 (2H, s, OH), 2.04 and 2.20 (2H, 2 x m, 4-CH_2P), 4.10 (6H, m, 2 x OCH_2 and 1''-CH_2), 4.33 - 4.38 (2H, m, 2- and 3-H); δ_C (100 MHz; $CDCl_3$) 14.0 (C-2''), 16.3 (d, J_{P-C} = 6.1 Hz, 2 × CH_3), 29.9 (d, J_{P-C} = 139.1 Hz, CH_2P), 61.8 (C-1''), 62.0 (d, J_{P-C} = 5.8 Hz, 2 × OCH_2), 67.7 (d, J_{P-C} = 11.6 Hz, C-3), 73.7 (d, J_{P-C} = 13.2 Hz, C-2) and 172.7 (C=O).

‡ Product isolated as racemic mixture.

3.3. 3-Substituted aniline-derived phosphonate esters and their corresponding phosphonic acids

3.3.1. Reaction of 3-substituted anilines with chloroacetyl chloride

2-Chloro-*N*-(3-hydroxyphenyl)acetamide 320a

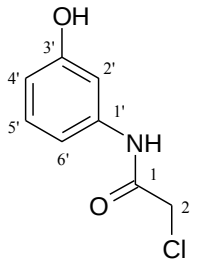

To a stirred solution of 3-aminophenol (3.01 g, 27.0 mmol) in THF (30 mL) under nitrogen was added NaH (60 % dispersion in mineral oil; 1.20 g, 48.0 mmol) in small portions to permit controlled evolution of hydrogen. Chloroacetyl chloride (2.20 mL, 28 mmol) was then added through a septum and the resulting solution was stirred for *ca.* 6 h. The solvent was evaporated *in vacuo* and the residue extracted with EtOAc (2 x 50 mL). The organic extract was washed sequentially with satd. aq. $NaHCO_3$ (2 × 100 mL), water (2 x 100 mL) and brine (2 × 100 mL). The aqueous washings were extracted with EtOAc and the combined organic solutions were dried (anhydr. $MgSO_4$). Evaporation of the solvent *in vacuo* afforded 2-chloro-*N*-(3-hydroxyphenyl)acetamide **320a** as a grey solid (4.78 g, 92 %), m.p. 132-134 °C (Lit.[141] 134.5-136 °C); υ_{max} (solid deposit/cm^{-1}) 3367 (OH) and 1648 (C=O); δ_H/ppm (400 MHz; $CDCl_3$) 4.22 (2H, s, 2-CH_2), 6.47 (1H, dd, *J* = 6.0 and 2.0 Hz, 6'-H), 6.94 (1H, dd, *J* = 6.0 and 0.8 Hz, 4'-H), 7.09 (1H, t, *J* = 8.0 Hz, 5'-H), 7.16 (1H, t, *J* = 2.0 Hz, 2'-H), 9.45 (1H, s, OH) and 10.16 (1H, s, NH); δ_C/ppm (100 MHz; $CDCl_3$) 43.6 (C-2), 106.3 (C-2'), 109.9 (C-6'), 110.9 (C-4'), 129.4 (C-5'), 139.4 (C-1'), 157.6 (C-3') and 164.4 (C=O).

2-Chloro-*N*-(3-methoxyphenyl)acetamide 320b

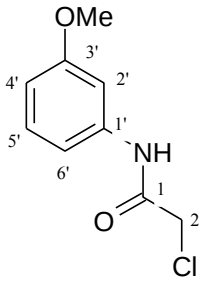

The procedure described for the synthesis of 2-chloro-*N*-(3-hydroxyphenyl)acetamide **320a** was employed, using 3-methoxyaniline (0.91 mL, 8.1 mmol), NaH (60 % dispersion in mineral oil; 0.36 g, 15 mmol) and chloroacetyl chloride (0.65 mL, 8.1 mmol) in THF (15 mL), to yield 2-chloro-*N*-(3-methoxyphenyl)acetamide **320b** as a light brown solid (1.35 g, 84 %), m.p 90-92 °C. (Lit.[141] 92-94 °C); υ_{max} (solid deposit/cm^{-1}) 1680 (C=O); δ_H/ppm (400 MHz; $CDCl_3$) 3.72 (3H, s, OCH_3), 4.08 (2H, s, 2-CH_2), 6.70 (1H, dd, *J* = 6.4 and 1.6 Hz, 6'-H), 6.83 (1H, dd, *J* = 6.8 and 0.8 Hz, 4'-H), 6.95 (1H, t, *J* = 8.0 Hz, 5'-H), 7.18 (1H, t, *J* = 1.8 Hz, 2'-H) and 8.20 (1H, s, NH); δ_C/ppm (100 MHz; $CDCl_3$) 42.8 (C-2), 55.3 (CH_3), 105.8 (C-2'), 110.9 (C-6'), 112.1 (C-4'), 129.7 (C-5'), 137.8 (C-1'), 160.1 (C-3') and 163.7 (C=O).

_N_-(3-Bromophenyl)-2-chloroacetamide 320c

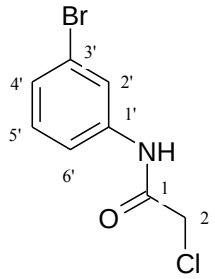

The procedure described for the synthesis of 2-chloro-*N*-(3-hydroxyphenyl)acetamide **320a** was employed, using 3-bromoaniline (0.63 mL, 5.8 mmol), NaH (60 % dispersion in mineral oil; 0.26 g, 11 mmol) and chloroacetyl chloride (0.41 mL, 5.8 mmol) in THF (15 mL), to yield *N*-(3-bromophenyl)-2-chloroacetamide **320c** as a brown solid (1.25 g, 87 %), m.p 100-102 °C (Lit.[141] 98-100 °C); υ_{max} (solid deposit/cm^{-1}) 1682 (C=O); δ_H/ppm (400 MHz; $CDCl_3$) 4.11 (2H, s, 2-CH_2), 7.12 (1H, t, *J* = 8.0 Hz, 5'-H), 7.21 (1H, d, *J* = 8.0 Hz, 4'-H), 7.40 (1H, d, *J* = 8.0 Hz, 6'-H), 7.72 (1H, s, 2'-H), and 8.19 (1H, s, NH); δ_C/ppm (100 MHz; $CDCl_3$) 42.7 (C-2), 118.5 (C-6'), 122.6 (C-3'), 122.9 (C-2'), 128.2 (C-4'), 130.3 (C-5'), 137.8 (C-1') and 163.8 (C=O).

2-Chloro-_N_-(3-fluorophenyl)acetamide 320d

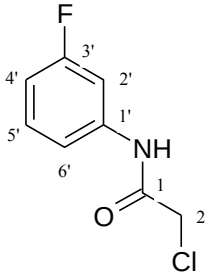

The procedure described for the synthesis of 2-chloro-*N*-(3-hydroxyphenyl)acetamide **320a** was employed, using 3-fluoroaniline (1.04 mL, 5.8 mmol), NaH (60 % dispersion in mineral oil; 0.26 g, 11 mmol) and chloroacetyl chloride (0.88 mL, 5.8 mmol) in THF (15 mL), to yield 2-chloro-*N*-(3-fluorophenyl)acetamide **320d** as a brown solid (1.52 g, 75 %), m.p 118-120 °C. (Lit.[141] 121-123 °C); υ_{max} (solid deposit/cm^{-1}) 1682 (C=O); δ_H/ppm (400 MHz; $CDCl_3$) 4.27 (2H, s, 2-CH_2), 6.92 (1H, td, *J* = 5.2, 2.0 and 0.8 Hz , 4'-H), 7.35 (2H, m, 5' and 6'-H), 7.57 (1H, dt, *J* = 7.2 and 2.4 Hz, 2'-H) and 10.54 (1H, s, NH); δ_C/ppm (100 MHz; $CDCl_3$) 43.4 (C-2), 105.9 (d, J_{F-C} = 26 Hz, C-2'), 110.1 (d, J_{F-C} = 21 Hz, C-4'), 115.0 (C-6'), 130.4 (C-5'), 140.0 (C-1'), 160.8 (d, J_{F-C} = 240.2 Hz, C-3') and 164.9 (C=O).

2-Chloro-*N*-(3-cyanophenyl)acetamide 320e

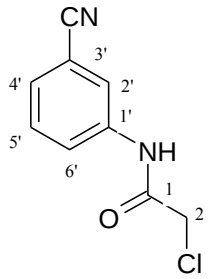

The procedure described for the synthesis of 2-chloro-*N*-(3-hydroxyphenyl)acetamide **320a** was employed, using 3-aminobenzonitrile (1.20 g, 10.1 mmol), NaH (60 % dispersion in mineral oil; 0.54 g, 23 mmol) and chloroacetyl chloride (1.04 mL, 10.1 mmol) in THF (15 mL), to yield *2-chloro*-N-*(3-cyanophenyl)acetamide* **320e** as a brown solid (1.57 g, 80 %), m.p 146-148 °C; (Found: $\mathbf{M}^+$, 194.02408 $C_9H_7ClN_2O$ requires: $\mathbf{M}^+$, 194.02432); υ_{max} (solid deposit/cm^{-1}) 2230 (C=N) and 1697 (C=O); δ_H/ppm (400 MHz; $CDCl_3$) 4.29 (2H, s, 2-CH_2), 7.55 (2H, d, *J* = 5.2 Hz , 4'-H and 6'-H), 7.82 (1H, m, 5'-H), 8.07 (1H, s, 2'-H), and 10.67 (1H, s, NH); δ_C/ppm (100 MHz; $CDCl_3$) 43.3 (C-2), 111.6 (C-3'), 118.5 (C=N), 121.9 (C-2'), 123.9 (C-5'), 127.3 (C-6'), 130.3 (C-4'), 139.1 (C-1') and 165.2 (C=O).

2-Chloro-*N*-(3-nitrophenyl)acetamide 320f

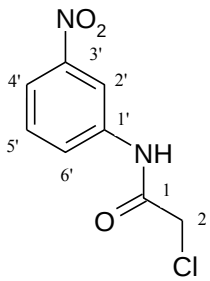

The procedure described for the synthesis of 2-chloro-*N*-(3-hydroxyphenyl)acetamide **320a** was employed, using 3-nitroaniline (1.01 g, 7.27 mmol), NaH (60 % dispersion in mineral oil; 0.33 g, 12.9 mmol) and chloroacetyl chloride (0.87 mL, 7.3 mmol) in THF (15 mL), to yield 2-chloro-*N*-(3-nitrophenyl)acetamide **320f** as a dark brown solid (1.37 g, 88 %), m.p 96-98 °C. (Lit.[241] 90-93 ^{o}C); υ_{max} (solid deposit/cm^{-1}) 1683 (C=O); δ_H/ppm (400 MHz; $CDCl_3$) 4.32 (2H, s, 2-CH_2), 7.62 (1H, t, *J* = 8.4 Hz, 5'-H), 7.93 (2H, m, 4'-H and 6'-H), 8.61 (1H, s, 2'-H), and 10.85 (1H, s, NH); δ_C/ppm (100 MHz; $CDCl_3$) 43.3 (C-2), 113.3 (C-2'), 118.2 (C-4'), 125.2 (C-6'), 130.2 (C-5'), 139.5 (C-1'), 147.8 (C-3') and 165.3 (C=O).

2-Chloro-*N*-[3-(hydroxymethyl)phenyl]acetamide 320g and 3-[(Chloroacetyl)amino]benzyl chloroacetate 320h

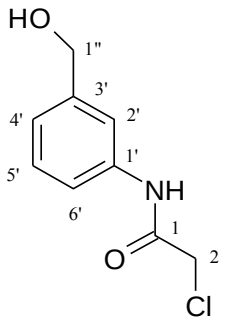

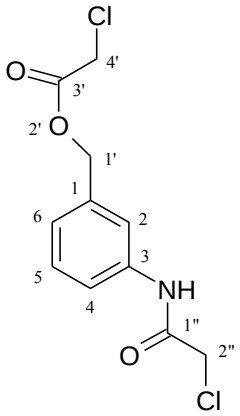

The procedure described for the synthesis of 2-chloro-*N*-(3-hydroxyphenyl)acetamide **320a** was employed, using 3-aminobenzyl alcohol (1.02 g, 8.12 mmol), NaH (60 % dispersion in mineral oil; 0.52 g, 21 mmol) and chloroacetyl chloride (0.67 mL, 8.1 mmol) in THF (15 mL). The solvent was evaporated *in vacuo* and flash chromatography gave two fractions.

i) *2-Chloro*-N-*[3-(hydroxymethyl)phenyl]acetamide* **320g** as a yellow solid (1.16 g, 62 %), m.p 91-93 °C; (Found: **M$^+$**, 201.03941 $C_9H_{10}ClNO_2$ requires: **M$^+$**, 201.03706); υ_{max} (solid deposit/cm^{-1}) 3349 (OH) and 1680 (C=O); δ_H/ppm (400 MHz; $CDCl_3$) 4.23 (2H, s, 2-CH_2), 4.47 (2H, s, 1''-CH_2), 5.21 (1H, s, OH), 7.01 (1H, d, *J* = 7.6 Hz, 4'-H), 7.26 (1H, t, *J* = 7.6 Hz, 5'-H), 7.45 (1H, d, *J* = 8.0 Hz, 6'-H), 7.55 (1H, s, 2'-H) and 10.26 (1H, s, NH) ; δ_C/ppm (100 MHz; $CDCl_3$) 43.5 (C-2), 62.6 (C-1''), 117.2 (C-2'), 117.5 (C-6'), 121.7 (C-4'), 128.4 (C-5'), 138.2 (C-1'), 143.3 (C-3') and 164.4 (C=O).

ii) 3-*[(Chloroacetyl)amino]benzyl chloroacetate* **320h** as a yellow solid (0.18 g, 11 %), m.p. 84-86°C; (Found: $\mathbf{M}^+$, 276.10711 $C_{11}H_{11}Cl_2NO_3$ requires: $\mathbf{M}^+$, 276.11594); υ_{max} (solid depsoit/cm^{-1}) 1738 (O-C=O) and 1676 (C=O); δ_H/ppm (400 MHz; $CDCl_3$) 4.20 (2H, s, 4'-CH_2), 4.29 (2H, s, 2''-CH_2), 5.30 (2H, s, 1'-CH_2), 7.28 (1H, d, *J* = 7.6 Hz, 6-H), 7.47 (1H, t, *J* = 7.9 Hz, 5-H), 7.62 (1H, d, *J* = 8.14 Hz, 4-H), 7.71 (1H, s, 2-H) and 8.30 (1H, s, NH); δ_C/ppm (100 MHz; $CDCl_3$) 42.1 (C-4'), 44.1 (C-2''), 68.7 (C-1'), 121.2 (C-2), 121.5 (C-4), 126.3 (C-6), 130.8 (C-5), 137.4 (C-3), 137.0 (C-1), 163.9 (C-1'') and 167.1 (C-3').

3.3.1.1. Synthesis of diethyl methylphosphonates using Michaelis-Arbuzov methodology

Diethyl [*N*-(3-hydroxyphenyl)carbamoyl]methylphosphonate 321a

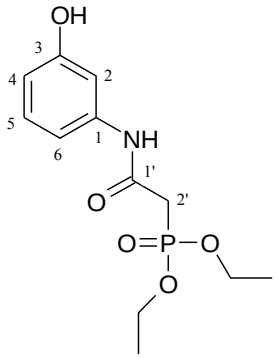

Triethyl phosphite (0.71 mL, 4.1 mmol) was added through a septum to 2-chloro-*N*-(3-hydroxyphenyl)acetamide **320a** (0.51 g, 2.8 mmol) under nitrogen in an oven-dried round-bottomed flask equipped with a reflux condenser, and the resulting mixture was refluxed for *ca.* 9 h during which time the reaction was monitored by TLC. The cooled mixture was then stirred with hexane (20 mL) for *ca.* 30 minutes followed by decantation of the hexane layer to remove the excess triethyl phosphite; this was repeated three times. The crude product was purified by flash chromatography [on silica gel; elution with hexane-EtOAc (3:1)], and subsequent evaporation of the solvent *in vacuo* afforded diethyl [*N*(3-hydroxyphenyl)carbamoyl)]methylphosphonate **321a** as a dark brown solid (0.52 g, 66 %), m.p. 116-118 °C (Lit.[141] 115-117 °C); υ_{max} (solid deposit/cm^{-1}) 3263 (OH), 1667 (C=O), 1230 (P=O) and 1024 (P−OEt); δ_H/ppm (400 MHz; $CDCl_3$) 1.32 (6H, t, *J* = 6.8 Hz, 2 × CH_3), 3.03 (2H, d, J_{P-H} = 21.1 Hz, CH_2P), 4.17 (4H, q, *J* = 7.2 Hz, 2 × OCH_2), 6.60 (1H, dd, *J* = 6.0 and 1.4 Hz, 4-H), 6.79 (1H, dd, *J* = 7.2 and 1.2 Hz, 6-H), 7.09 (1H, t, *J* = 8.0 Hz, 5-H), 7.46 (1H, t, *J* = 1.2 Hz, 2-

H), 7.99 (1H, s, OH) and 8.96 (1H, s, NH); δ_C (100 MHz; $CDCl_3$) 16.3 (d, J_{P-C} = 6.0 Hz, 2 × CH_3), 36.4 (d, J_{P-C} = 130.4 Hz, CH_2P), 63.3 (d, J_{P-C} = 6.6 Hz, 2 × OCH_2), 107.3 (C-2), 111.1 (C-4), 112.1 (C-6), 129.8 (C-5), 138.5 (C-1), 157.3 (C-3) and 162.7 (d, J_{P-C} = 4.1 Hz, C=O); δ_P/ppm (162 MHz; $CDCl_3$) 24.2 (P=O).

Diethyl [*N*-(3-methoxyphenyl)carbamoyl]methylphosphonate 321b

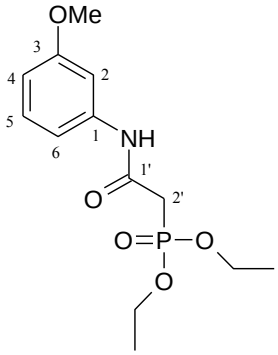

The procedure described for the synthesis of diethyl [*N*-(3-hydroxyphenyl)carbamoyl]methylphosphonate **321a** was employed, using 2-chloro-*N*-(3-methoxyphenyl)acetamide **320b** (0.55 g, 2.8 mmol) and triethyl phosphite (0.95 mL, 5.5 mmol). The crude product was purified by flash chromatography [on silica gel; elution with hexane-EtOAc (3:1)], and subsequent evaporation of the solvent *in vacuo* afforded *diethyl [*N*-(3-methoxyphenyl)carbamoyl]methylphosphonate* **321b** as a yellowish-brown solid (0.35 g, 65 %), m.p 88-90 °C. (Found: $\mathbf{M^+}$, 301.10976 $C_{13}H_{20}NO_5P$ requires: $\mathbf{M^+}$, 301.10791; υ_{max} (solid deposit/cm^{-1}) 1684 (C=O), 1239 (P=O) and 1050 (P−OEt); δ_H/ppm (400 MHz; $CDCl_3$) 1.34 (6H, t, *J* = 7.2 Hz, 2 × CH_3), 3.02 (2H, d, J_{P-H} = 20.8 Hz, CH_2P), 3.77 (3H, s, OCH_3) 4.17 (4H, q, *J* = 7.2 Hz, 2 × OCH_2), 6.63 (1H, dd, *J* = 6.0 and 2.0 Hz, 4-H), 7.01 (1H, dd, *J* = 6.4 and 1.2 Hz, 6-H), 7.18 (1H, t, *J* = 8.0 Hz, 5-H), 7.23 (1H, t, *J* = 1.2 Hz, 2-H) and 8.84 (1H, s, NH); δ_C (100 MHz; $CDCl_3$) 16.3 (d, J_{P-C} = 6.0 Hz, 2 × CH_3), 35.5 (d, J_{P-C} = 128.9 Hz, CH_2P), 55.3 (OCH_3) 63.0 (d, J_{P-C} = 6.6 Hz, 2 × CH_2P), 105.4 (C-2), 110.4 (C-4), 113.3 (C-6), 129.6 (C-5), 138.9 (C-1), 160.0 (C-3) and 162.0 (d, J_{P-C} = 3.3 Hz, C=O); δ_P/ppm (162 MHz; $CDCl_3$) 23.8 (P=O).

Diethyl [*N*-(3-bromophenyl)carbamoyl]methylphosphonate 321c

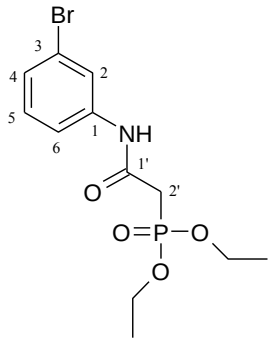

The procedure described for the synthesis of diethyl [*N*-(3-hydroxyphenyl)carbamoyl]methylphosphonate **321a** was employed, using 2-chloro-*N*-(3-bromophenyl)acetamide **320c** (0.67 g, 2.7 mmol) and triethyl phosphite (0.92 mL, 5.4 mmol). The crude product was purified by flash chromatography [on silica gel; elution with hexane-EtOAc (3:1)], and subsequent evaporation of the solvent *in vacuo* afforded *diethyl [*N*-(3-bromophenyl)carbamoyl]methylphosphonate* **321c** as a yellowish-brown solid (0.25 g, 62 %), m.p 73-75 °C; (Found: $\mathbf{M}^+$, 351.04263 $C_{12}H_{17}BrNO_4P$ requires: $\mathbf{M}^+$, 351.00581); υ_{max} (solid deposit/cm^{-1}) 1683 (C=O), 1238 (P=O) and 1050 (P−OEt); δ_H/ppm (400 MHz; $CDCl_3$) 1.33 (6H, t, J = 6.8 Hz, 2 × CH_3), 3.01 (2H, d, $J_{P–H}$ = 20.4 Hz, CH_2P), 4.11 (4H, q, J = 7.4 Hz, 2 × OCH_2), 7.00 (1H, t, J = 8.0 Hz, 5-H), 7.08 (1H, d, J = 8.0 Hz, 4-H), 7.39 (1H, d, J = 8.0 Hz, 6-H), 7.69 (1H, s, 2-H) and 7.75 (1H, s, NH); δ_C (100 MHz; $CDCl_3$) 16.3 (d, $J_{P–C}$ = 5.7 Hz, 2 × CH_3), 35.6 (d, $J_{P–C}$ = 129.1 Hz, CH_2P), 63.0 (d, $J_{P–C}$ = 6.6 Hz, 2 × OCH_2), 112.4 (C-6), 117.8 (C-3), 122.3 (C-2), 126.8 (C-4), 129.8 (C-5), 139.2 (C-1) and 162.2 (d, $J_{P–C}$ = 4.4 Hz, C=O); δ_P/ppm (162 MHz; $CDCl_3$) 24.1 (P=O).

Diethyl [*N*-(3-fluorophenyl)carbamoyl]methylphosphonate 321d

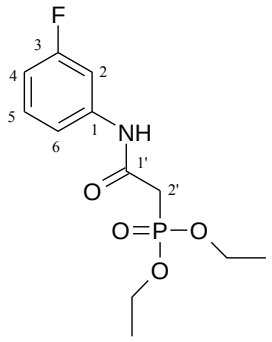

The procedure described for the synthesis of diethyl [*N*-(3-hydroxyphenyl)carbamoyl]methylphosphonate **321a** was employed, using 2-chloro-*N*-(3-

fluorophenyl)acetamide **320d** (0.50 g, 2.6 mmol) and triethyl phosphite (0.92 mL, 5.3 mmol). The crude product was purified by flash chromatography [on silica gel; elution with hexane-EtOAc (3:1)], and subsequent evaporation of the solvent *in vacuo* afforded *diethyl [*N-*(3-fluorophenyl)carbamoyl]methylphosphonate* **321d** as a brown solid (0.26 g, 56 %), m.p 83-85 °C; (Found: $\mathbf{M}^+$, 289.08671 $C_{12}H_{17}FNO_4P$ requires: $\mathbf{M}^+$, 289.08792); υ_{max} (solid deposit/cm^{-1}) 1680 (C=O), 1228 (P=O) and 1049 (P−OEt); δ_H/ppm (400 MHz; $CDCl_3$) 1.35 (6H, t, *J* = 7.2 Hz, 2 × CH_3), 3.04 (2H, d, J_{P-H} = 20.8 Hz, CH_2P), 4.17 (4H, q, *J* = 6.8 Hz, 2 × OCH_2), 6.74 (1H, ddd, *J* = 6.0, 2.4 and 2.0 Hz, 4-H), 7.09 (1H, d, *J*= 6.4, 6-H), 7.16 (1H, ddd, J = 2 x 6.4 Hz and 1.6 Hz, 5-H) 7.45 (1H, dt, *J* = 6.4 and 2.0 Hz, 2-H) and 9.23 (1H, s, NH); δ_C (100 MHz; $CDCl_3$) 16.3 (d, J_{P-C} = 6.0 Hz, 2 × CH_3), 35.5 (d, J_{P-C} = 127 Hz, CH_2P), 63.0 (d, J_{P-C} = 6.5 Hz, 2 × OCH_2), 107.0 (d, J_{F-C} = 26.3 Hz, C-2), 111.0 (d, J_{F-C} = 18.3 Hz, C-4), 114.9 (C-6), 129.8 (C-5), 139.8 (C-1), 162.1 (d, J_{F-C} = 243.2 Hz, C-3) and 164.0 (d, J_{P-C} = 4.4 Hz, C=O); δ_P/ppm (162 MHz; $CDCl_3$) 23.5 (P=O).

Diethyl [*N*-(3-cyanophenyl)carbamoyl]methylphosphonate 321e

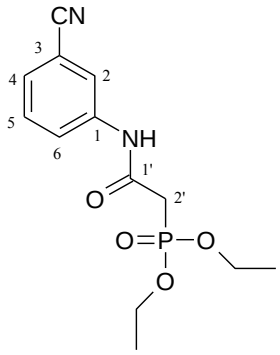

The procedure described for the synthesis of diethyl [*N*-(3-hydroxyphenyl)carbamoyl]methyl phosphonate **321a** was employed, using 2-chloro-*N*-(3-cyanophenyl)acetamide **320e** (0.50 g, 2.5 mmol) and triethyl phosphite (0.87 mL, 5.1 mmol). The crude product was purified by flash chromatography [on silica gel; elution with hexane-EtOAc (3:1)], and subsequent evaporation of the solvent *in vacuo* afforded *diethyl [*N-*(3-cyanophenyl)carbamoyl]methyl phosphonate* **321e** as a yellowish-brown solid (0.21 g, 48 %), m.p 117-119 °C; (Found: $\mathbf{M}^+$, 296.09070. $C_{13}H_{17}N_2O_4P$ requires: $\mathbf{M}^+$, 296.09259); υ_{max} (solid deposit/cm^{-1}) 2230 (C≡N), 1686 (C=O), 1217 (P=O) and 1050 (P−OEt); δ_H/ppm (400 MHz; $CDCl_3$) 1.37 (6H, t, *J* = 7.2 Hz, 2 × CH_3), 3.01 (2H, d, J_{P-H} = 20.8 Hz, CH_2P), 4.19 (4H, q, *J* =7.6 Hz, 2 × OCH_2), 7.44 (2H, m, 4-H and 6-H), 7.56 (1H, m, 5-H), 7.89 (1H, s, 2-H) and 9.88 (1H, s, NH); δ_C (100 MHz; $CDCl_3$) 16.3

(d, J_{P-C} = 6.0 Hz, 2 × CH_3), 36.9 (d, J_{P-C} = 129.3 Hz, CH_2P), 63.3 (d, J_{P-C} = 7.2 Hz, 2 × OCH_2), 112.6 (C-3), 118.4 (C≡N), 122.4 (C-2) 123.2 (C-5), 127.2 (C-6), 129.4 (C-4), 138.8 (C-1) and 162.5 (d, J_{P-C} = 4.4 Hz, C=O); δ_P/ppm (162 MHz; $CDCl_3$) 24.2 (P=O).

Diethyl [*N*-(3-nitrophenyl)carbamoyl]methylphosphonate 321f

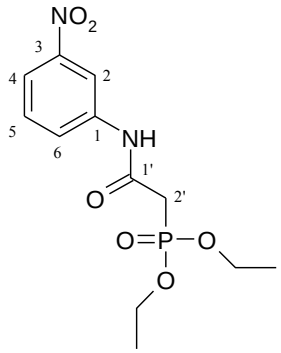

The procedure described for the synthesis of diethyl [*N*-(3-hydroxyphenyl)carbamoyl]methyl phosphonate **321a** was employed, using 2-chloro-*N*-(3-nitrophenyl)acetamide **320f** (0.40 g, 1.9 mmol) and triethyl phosphite (0.64 mL, 3.7 mmol). The crude product was purified by flash chromatography [on silica gel; elution with hexane-EtOAc (3:1)], and subsequent evaporation of the solvent *in vacuo* afforded *diethyl [*N*-(3-nitrophenyl)carbamoyl]methyl phosphonate* **321f** as a dark brown liquid (0.42 g, 72 %) (Found: $\mathbf{M}^+$, 316.082395 $C_{12}H_{17}N_2O_6P$ requires: $\mathbf{M}^+$, 316.08242); υ_{max} (thin film/cm^{-1}) 1684 (C=O), 1262 (P=O) and 1035 (P−OEt); δ_H/ppm (400 MHz; $CDCl_3$) 1.33 (6H, t, *J* = 7.2 Hz, 2 × CH_3), 3.06 (2H, d, J_{P-H} = 21.2 Hz, CH_2P), 4.17 (4H, q, *J* = 7.6 Hz, 2 × OCH_2), 6.60 (1H, dd, *J* = 6.0 and 2.0 Hz, 4-H), 6.88 (1H, dd, *J* = 6.4 and 2.0 Hz, 6-H),7.12 (1H, t, *J* = 8.4 Hz, 5-H), 8.29 (1H, t, *J* = 2.0 Hz, 2-H) and 8.90 (1H, s, NH); δ_C (100 MHz; $CDCl_3$) 16.3 (d, J_{P-C} = 6.2 Hz, 2 × CH_3), 35.6 (d, J_{P-C} = 128.2 Hz, CH_2P), 63.6 (d, J_{P-C} = 6.8 Hz, 2 × OCH_2), 114.1 (C-2), 118.5 (C-4), 124.8 (C-6), 124.9 (C-5), 129.5 (C-1), 139.1 (C-3) and 162.6 (d, J_{P-H} = 4.2 Hz, C=O); δ_P/ppm (162 MHz; $CDCl_3$) 24.6 (P=O).

Diethyl {*N*-[3-(hydroxymethyl)phenyl]carbamoyl}methylphosphonate 321g

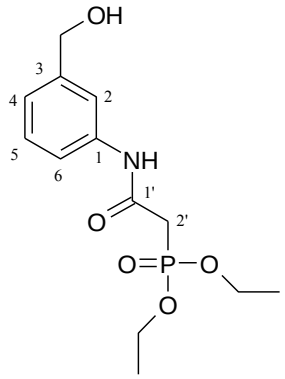

The procedure described for the synthesis of diethyl [*N*-(3-hydroxyphenyl)carbamoyl]methylphosphonate **321a** was employed, using 2-chloro-*N*-[3-(hydroxymethyl)phenyl]acetamide **320g** (0.30 g, 1.5 mmol) and triethyl phosphite (0.51 mL, 3.0 mmol). The crude product was purified by flash chromatography [on silica gel; elution with hexane-EtOAc (3:1)], and subsequent evaporation of the solvent *in vacuo* afforded *diethyl {*N-*[3-(hydroxymethyl)phenyl]carbamoyl}methylphosphonate* **321g** as a yellow oil (0.29 g, 65 %); (Found: $\mathbf{M}^+$, 301.108030. $C_{13}H_{20}NO_5P$ requires: $\mathbf{M}^+$, 301.10791); υ_{max} (thin film/cm^{-1}) 3274 (OH), 1684 (C=O), 1376 (P=O) and 1050 (P−OEt); δ_H/ppm (400 MHz; $CDCl_3$) 1.35 (6H, t, J = 6.8 Hz, 2 × CH_3), 2.03 (1H, s, OH), 3.01 (2H, d, $J_{P–H}$ = 21.2 Hz, CH_2P), 4.18 (4H, q, J = 7.2 Hz, 2 × OCH_2), 4.59 (2H, s, CH_2OH), 7.00 (1H, d, J = 7.6 Hz, 4-H), 7.20 (1H, t, J = 8.0 Hz, 5-H), 7.42 (1H, s, 2-H), 7.45 (1H, d, 8.0 Hz, 6-H) and 9.20 (1H, s, NH); δ_C (100 MHz; $CDCl_3$), 16.3 (d, $J_{P–C}$ = 5.8 Hz, 2 × CH_3), 36.7 (d, $J_{P–C}$ = 128.4 Hz, CH_2P), 63.0 (d, $J_{P–C}$ = 7.2 Hz, OCH_2), 64.7 (CH_2OH), 118.1 (C-2), 118.7 (C-6), 122.6 (C-4), 128.9 (C-5), 138.0 (C-1), 141.9 (C-3) and 163.5 (d, $J_{P–H}$ = 3.8 Hz, C=O); δ_P/ppm (162 MHz; $CDCl_3$) 24.2 (P=O).

3.3.1.2. Synthesis of methylphosphonic acids derivatives using TMSBr

[*N*-(3-Hydroxyphenyl)carbamoyl]methylphosphonic acid 328a

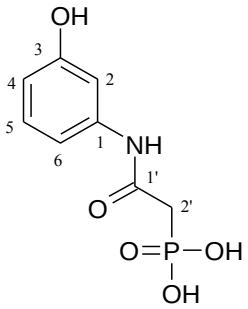

Trimethylsilyl bromide (0.23 mL, 1.7 mmol) was added to diethyl [*N*-(3-hydroxyphenyl)-carbamoyl]methylphosphonate **321a** (0.25 g, 0.87 mmol) in CH_3CN (3 mL) and the mixture was heated in the microwave apparatus set to deliver 100 W of power, with a reaction temperature of 60 ^oC and reaction time of 10 min. After completion, the mixture was cooled to room temperature, treated with a 95:5 MeOH-H_2O mixture and stirred for 30 min. The solvent was removed *in vacuo* and the residue chromatographed [preparative layer chromatography; elution with hexane-EtOAc-MeOH (1:1:1)] to yield *[*N-*(3-hydroxyphenyl)carbamoyl]methylphosphonic acid* **328a** as a yellow viscous liquid (0.22 g, 63 %); (Found: $\mathbf{M^+}$, 231.02110 $C_8H_{10}NO_5P$ requires: $\mathbf{M^+}$, 231.02966; υ/cm^{-1} 3264 (OH), 1674 (C=O) and 1241 (P=O); δ_H/ppm (400 MHz; DMSO-d_6) 2.82 (2H, d, $J_{P–H}$ = 21.2 Hz, CH_2P), 6.21 (2H, s, 2 × OH) 6.42 (1H, dd, *J* = 6.0 and 2.0 Hz, 6-H), 6.91 (1H, dd, *J* = 8.0 and 2.0 Hz, 4-H), 7.05 (1H, t, *J* = 8.0 Hz, 5-H), 7.12 (1H, t, *J* = 2.0 Hz, 2-H), 7.68 (1H, s, OH) and 9.06 (1H, s, NH); δ_C/ppm (100 MHz; DMSO-d_6) 35.5 (d, $J_{P–C}$ = 130.4 Hz, CH_2P), 108.1 (C-2), 114.7 (C-4), 117.6 (C-6), 130.9 (C-5), 138.8 (C-1), 146.9 (C-3) and 163.5 (d, $J_{P–C}$ = 3.8 Hz, C=O); δ_P/ppm (162 MHz; $CDCl_3$) 24.6 (P=O).

[*N*-(3-Methoxyphenyl)carbamoyl]methylphosphonic acid 328b

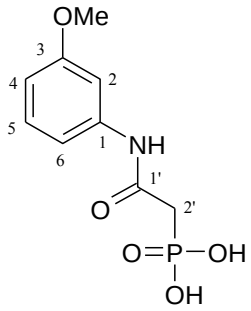

The procedure described for the synthesis of [*N*-(3-hydroxyphenyl)carbamoyl]methyl phosphonic acid **328a** was employed, using diethyl [*N*-(3-methoxyphenyl)carbamoyl]methyl phosphonate **321b** (0.25 g, 0.83 mmol) in CH_3CN (3 mL) and trimethylsilyl bromide (0.23 mL, 1.7 mmol). The solvent was removed *in vacuo* and the residue chromatographed [preparative layer chromatography; elution with hexane-EtOAc-MeOH (1:1:1)] to yield *[N-(3-methoxyphenyl)carbamoyl]methylphosphonic acid* **328b** as a grey viscous liquid (0.21 g, 62 %); (Found: $\mathbf{M^+}$, 245.03630 $C_9H_{12}NO_5P$ requires: $\mathbf{M^+}$, 245.04531; υ/cm^{-1} 3282 (OH), 1672 (C=O) and 1232 (P=O); δ_H/ppm (400 MHz; DMSO-d_6) 2.30 (1H, s, OH), 3.00 (2H, d, $J_{P–H}$ = 20.8 Hz, CH_2P), 3.82 (3H, s, OCH_3), 5.95 (1H, s, OH), 6.04 (1H, d, *J* = 7.6 Hz, OH), 6.20 (1H, dd, *J* =

6.4 and 2.4 Hz, 4-H), 6.65 (1H, dd, *J* = 5.6 and 2.4 Hz, 6-H), 7.19 (1H, t, *J* = 8.0 Hz, 5-H), 7.35 (1H, t, *J* = 2.0 Hz, 2-H) and 8.78 (1H, s, NH); δ_C/ppm (100 MHz; DMSO-d_6) 35.5 (d, J_{P-C} = 131.8 Hz, CH_2P), 55.3 (OCH_3), 105.4 (C-2), 110.4 (C-4), 112.0 (C-6), 129.6 (C-5), 138.9 (C-3), 160.1 (C-1) and 162.0 (d, J_{P-C} = 3.0 Hz, C=O); δ_P/ppm (162 MHz; $CDCl_3$) 24.0 (P=O).

[*N*-(3-Bromophenyl)carbamoyl]methylphosphonic acid 328c

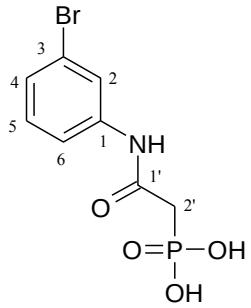

The procedure described for the synthesis of [*N*-(3-hydroxyphenyl)carbamoyl]methyl phosphonic acid **328a** was employed, using diethyl [*N*-(3-bromophenyl)carbamoyl]methyl phosphonate **321c** (0.11 g, 0.40 mmol) in CH_3CN (3 mL) and trimethylsilyl bromide (0.11 mL, 0.80 mmol). The solvent was removed *in vacuo* and the residue chromatographed [preparative layer chromatography; elution with hexane-EtOAc-MeOH (1:1:0.5)] to yield *[*N-*(3-bromophenyl)carbamoyl]methylphosphonic acid* **328c** as a yellow viscous liquid (0.067 g, 42 %); (Found: $\mathbf{M^+}$, 292.93953 $C_8H_9BrNO_4P$ requires: $\mathbf{M^+}$, 292.94526; υ/cm^{-1} 3289 (OH), 1668 (C=O) and 1218 (P=O); δ_H/ppm (400 MHz; DMSO-d_6) 2.79 (2H, d, J_{P-H} = 21.2 Hz, CH_2P), 3.71 (2H, s, 2 × OH), 6.60 (1H, dd, *J* = 6.0 and 2.0 Hz, 4-H), 7.07 (1H, dd, *J* = 8.0 and 2.0 Hz, 6-H), 7.19 (1H, t, *J* = 8.4 Hz, 5-H), 7.29 (1H, t, *J* = 2.0 Hz, 2-H) and 9.91 (1H, s, NH); δ_C/ppm (100 MHz; DMSO-d_6) 36.2 (d, J_{P-C} = 131.2 Hz, CH_2P), 112.6 (C-6), 118.0 (C-2), 122.5 (C-3), 127.0 (C-4), 130.2 (C-5), 139.5 (C-1) and 163.2 (d, J_{P-C} = 4.2 Hz, C=O); δ_P/ppm (162 MHz; $CDCl_3$) 24.1 (P=O).

[*N*-(3-Fluorophenyl)carbamoyl]methylphosphonic acid 328d

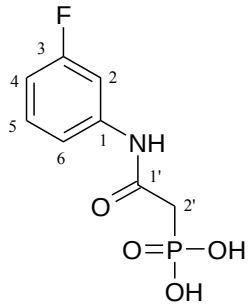

The procedure described for the synthesis of [*N*-(3-hydroxyphenyl)carbamoyl]methyl phosphonic acid **328a** was employed, using diethyl [*N*-(3-fluorophenyl)carbamoyl]methyl phosphonate **321d** (0.20 g, 0.69 mmol) in CH_3CN (3 mL) and trimethylsilyl bromide (0.19 mL, 1.4 mmol). The solvent was removed *in vacuo* and the residue chromatographed [preparative layer chromatography; elution with hexane-EtOAc-MeOH (1:1:1)] to yield *[*N-*(3-fluorophenyl)carbamoyl]methylphosphonic acid* **328d** as a yellow oil (0.13 g, 57 %); (Found: $\mathbf{M}^+$, 233.02363 $C_8H_9FNO_4P$ requires: $\mathbf{M}^+$, 233.02532; υ/cm^{-1} 3248 (OH), 1654 (C=O) and 1219 (P=O); δ_H/ppm (400 MHz; DMSO-d_6) 3.01 (2H, d, J_{P-H} = 21.3 Hz, CH_2P) 3.43 (2H, s, 2 x OH), 6.84 (1H, dd, *J* = 6.2 and 2.0 Hz, 4-H), 7.25 (2H, m, 5-H and 6-H), 7. 40 (1H, dt, *J* = 6.4 and 2.0 Hz, 2-H) and 9.28 (1H, s, NH); δ_C/ppm (100 MHz; DMSO-d_6) 35.4 (d, J_{P-C} = 131.4 Hz, CH_2P), 107.6 (d, J_{F-C} = 26.2 Hz, C-2), 111.5 (d, J_{F-C} = 18.1 Hz, C-4), 115.1 (C-6), 130.2 (C-5), 140.6 (C-1), 162.4 (d, J_{F-C} = 242.8 Hz, C-3) and 168.3 (d, J_{P-C} = 3.8 Hz, C=O); δ_P/ppm (162 MHz; $CDCl_3$) 24.8 (P=O).

[*N*-(3-Cyanophenyl)carbamoyl]methylphosphonic acid 328e

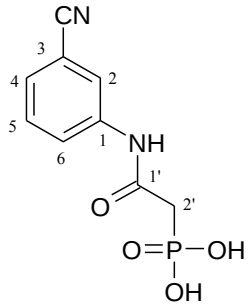

The procedure described for the synthesis of [*N*-(3-hydroxyphenyl)carbamoyl]methyl phosphonic acid **328a** was employed, using diethyl [*N*-(3-cyanophenyl)carbamoyl]methyl phosphonate **321e** (0.15 g, 0.51 mmol) in CH_3CN (3 mL) and trimethylsilyl bromide (0.13 mL, 1.0 mmol). The solvent was removed *in vacuo* and the residue chromatographed [preparative layer chromatography; elution with hexane-EtOAc-MeOH (1:1:0.5)] to yield *[*N-*(3-cyanophenyl)carbamoyl]methylphosphonic acid* **328e** as a light yellow viscous liquid (0.10 g, 59 %). (Found: $\mathbf{M}^+$, 240.02161 $C_9H_9N_2O_4P$ requires: $\mathbf{M}^+$, 240.02999; υ/cm^{-1} 3284 (OH), 2234 (C≡N), 1678 (C=O) and 1232 (P=O); δ_H/ppm (400 MHz; DMSO-d_6) 2.82 (2H, d, J_{P-H} = 21.2 Hz, CH_2P), 7.31 (2H, s, 2 × OH), 7.35 (1H, t, *J = 8*.0 Hz, 5-H), 7.51 (1H, dd, *J* = 7.2 and 2.0 Hz, 4-H), 7.73 (1H, dd, *J* = 6.4 and 1.2 Hz, 6-H), 8.02 (1H, t, *J* = 2.0 Hz, 2-H) and 8.09 (1H, s, NH); δ_C/ppm (100 MHz; DMSO-d_6) 36.8 (d, J_{P-C} = 130.8 Hz, CH_2P) 112.8 (C-3), 116.4 (C≡N),

125.5 (C-6) 126.8 (C-2), 128.2 (C-4), 129.6 (C-5), 138.9 (C-1) and 164.3 (d, J_{P-C} = 4.4 Hz, C=O); δ_P/ppm (162 MHz; $CDCl_3$) 24.8 (P=O).

[*N*-(3-Nitrophenyl)carbamoyl]methylphosphonic acid 328f

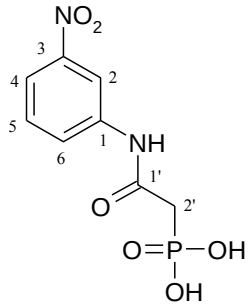

The procedure described for the synthesis of [*N*-(3-hydroxyphenyl)carbamoyl]methyl phosphonic acid **328a** was employed, using diethyl [*N*-(3-nitrophenyl)carbamoyl]methyl phosphonate **321f** (0.13 g, 0.40 mmol) in CH_3CN (3 mL) and trimethylsilyl bromide (0.11 mL, 0.80 mmol). The solvent was removed *in vacuo* and the residue chromatographed [preparative layer chromatography; elution with hexane-EtOAc-MeOH (1:1:1)] to yield *[*N-*(3-nitrophenyl)carbamoyl]methylphosphonic acid* **328f** as a brown viscous liquid (0.089 g, 67 %); (Found: $\mathbf{M}^+$, 260.01753 $C_8H_9N_2O_6P$ requires: $\mathbf{M}^+$, 260.01982; υ/cm^{-1} 3275 (OH), 1682 (C=O) and 1258 (P=O); δ_H/ppm (400 MHz; DMSO-d_6) 2.84 (2H, d, J_{P-H} = 21.2 Hz, CH_2P), 6.62 (1H, dd, *J* = 6.0 and 2.0 Hz, 4-H) 7.02 (2H, s, 2 x OH), 7.09 (1H, d, *J = 8*.0 Hz, 6-H), 7.21 (1H, t, *J* = 8.4, 5-H), 7.30 (1H, t, *J* = 2.0 Hz, 2-H) and 9.91 (1H, s, NH); δ_C/ppm (100 MHz; DMSO-d_6) 35.7 (d, J_{P-C} = 131.2 Hz, CH_2P), 114.6 (C-2), 118.9 (C-4), 125.2 (C-6), 125.8 (C-5), 129.6 (C-1), 139.1 (C-3) and 162.6 (d, J_{P-C} = 4.0 Hz, C=O); δ_P/ppm (162 MHz; $CDCl_3$) 24.2 (P=O).

***N*-[3-(Hydroxymethyl)phenylcarbamoyl]methylphosphonic acid 328g**

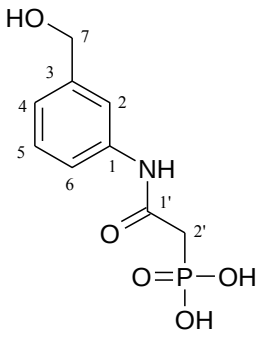

The procedure described for the synthesis of [*N*-(3-hydroxyphenyl)carbamoyl]methyl phosphonic acid **328a** was employed, using diethyl {*N*-[3-(hydroxymethyl)phenyl] carbamoyl}methyl phosphonate **321g** (0.12 g, 0.40 mmol) in CH_3CN (3 mL) and trimethylsilyl bromide (0.11 mL, 0.80 mmol). The solvent was removed *in vacuo* and the residue chromatographed [preparative layer chromatography; elution with hexane-EtOAc-MeOH (1:1:1)] to yield *N-[(3-(Hydroxymethyl)phenylcarbamoyl]methyl phosphonic acid* **328g** as a yellow viscous liquid (0.043 g, 48 %); (Found: $\mathbf{M}^+$, 245.03614 $C_9H_{12}NO_5P$ requires: $\mathbf{M}^+$, 245.03531; υ/cm^{-1} 3306 (OH), 1667 (C=O) and 1236 (P=O); δ_H/ppm (400 MHz; DMSO-d_6) 2.31 (1H, s, OH), 2.82 (2H, d, J_{P-H} = 21.2 Hz, CH_2P), 4.82 (2H, s, CH_2OH), 6.95 (2H, s, 2 x OH), 7.02 (1H, d, *J* = 7.4 Hz, 4-H), 7.25 (1H, t, *J* = 8.0 Hz, 5-H), 7.44 (2H, m, 2-H and 6-H) and 9.26 (1H, s, NH); δ_C (100 MHz; DMSO-d_6) 35.3 (d, J_{P-C} = 129.7 Hz, CH_2P), 64.9 (CH_2OH), 118.3 (C-2), 119.1 (C-6), 122.2 (C-4), 128.6 (C-5), 139.0 (C-1), 142.5 (C-3) and 166.3 (d, J_{P-C} = 4.4 Hz, C=O); δ_P/ppm (162 MHz; $CDCl_3$) 23.9 (P=O).

3.3.1.3. Synthesis of sodium hydrogen methylphosphonate derivatives

Sodium hydrogen [*N*-(3-hydroxyphenyl)carbamoyl]methylphosphonate 329a

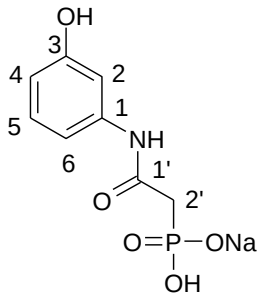

[N-(3-Hydroxyphenyl)carbamoyl]methylphosphonic acid **328a** (0.15 g, 0.65 mmol) was treated with a solution of NaOH (1.1 mol) in EtOH (0.6 mL) and the mixture was stirred for 30 min. The solvent was removed *in vacuo* and the residue chromatographed [reverse-phase column chromatography; elution with H_2O-MeOH (1:1)] to yield *sodium hydrogen [*N-*(3-hydroxyphenyl)carbamoyl]methylphosphonate* **329a** as a light brown semi-solid (98 mg, 98 %); υ/cm^{-1} 3208 (OH), 1677 (C=O), 1228 (P=O); δ_H/ppm (400 MHz; D_2O) 2.80 (2H, d, J_{P-H} = 22.4 Hz, CH_2P), 6.39 (1H, dd, *J* = 6.0 and 2.0 Hz, 6-H), 6.90 (1H, dd, *J* = 8.0 and 2 Hz, 4-H), 7.08 (1H, t, *J* = 8.0 Hz, 5-H) and 7.10 (1H, t, *J* = 1.2 Hz, 2-H); δ_C/ppm (100 MHz; D_2O) 36.2 (d, J_{P-C} =

139.1 Hz, CH_2P), 108.3 (C-2), 115.2 (C-4), 118.4 (C-6), 129.9 (C-5), 138.6 (C-1), 146.4 (C-3) and 164.1 (d, $J_{P–C}$ = 3.6 Hz, C=O).

Sodium hydrogen [*N*-(3-methoxyphenyl)carbamoyl]methylphosphonate 329b

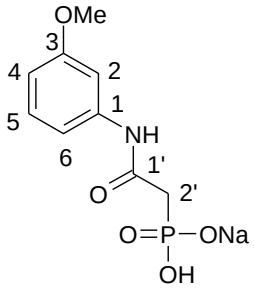

The procedure described for the synthesis of sodium hydrogen [*N*-(3-hydroxyphenyl)carbamoyl]methylphosphonate **329a** was employed, using [*N*-(3-methoxyphenyl)carbamoyl]methylphosphonic acid **328b** (0.15 g, 0.61 mmol) and a solution of NaOH (1.1 mol) in EtOH (0.58 mL). The solvent was removed *in vacuo* and the residue chromatographed [reverse-phase column chromatography; elution with H_2O-MeOH (1:1)] to yield *sodium hydrogen [*N*-(3-methoxyphenyl)carbamoyl]methylphosphonate* **329b** as a pale yellow semi-solid (0.11 g, 97 %); υ/cm^{-1} 1687 (C=O), 1221 (P=O); δ_H/ppm (400 MHz; D_2O) 2.79 (2H, d, $J_{P–H}$ = 20.9 Hz, CH_2P), 3.79 (3H, s, OCH_3), 6.19 (1H, dd, *J* = 6.2 and 2.4 Hz, 4-H), 6.66 (1H, dd, *J* = 6.2 and 2.4 Hz, 6-H), 7.20 (1H, t, *J* = 7.6 Hz, 5-H) and 7.31 (1H, t, *J* = 2.0 Hz, 2-H); δ_C/ppm (100 MHz; D_2O) 35.5 (d, $J_{P–C}$ = 143.8 Hz, CH_2P), 55.2 (OCH_3), 105.6 (C-2), 110.4 (C-4), 112.6 (C-6), 129.5 (C-5), 139.0 (C-3), 159.9 (C-1) and 162.4 (d, $J_{P–C}$ = 3.0 Hz, C=O).

Sodium hydrogen [*N*-(3-bromophenyl)carbamoyl]methylphosphonate 329c

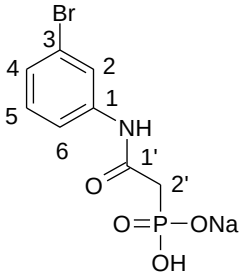

The procedure described for the synthesis of sodium hydrogen [*N*-(3-hydroxyphenyl)carbamoyl]methylphosphonate **329a** was employed, using [*N*-(3-bromophenyl)carbamoyl]methylphosphonic acid **328c** (0.15 g, 0.51 mmol) and a solution of

NaOH (1.1 mol) in EtOH (0.47 mL). The solvent was removed *in vacuo* and the residue chromatographed [reverse-phase column chromatography; elution with H_2O-MeOH (1:1)] to yield *sodium hydrogen [*N-*(3-bromophenyl)carbamoyl]methylphosphonate* **329c** as a brown semi-solid (0.10 g, 94 %); υ/cm^{-1} (OH), 1681 (C=O), 1219 (P=O); δ_H/ppm (400 MHz; D_2O) 2.80 (2H, d, J_{P-H} = 21.2 Hz, CH_2P), 5.99 (1H, dd, *J* = 6.0 and 2.0 Hz, 4-H), 7.10 (1H, dd, *J* = 8.0 and 2.0 Hz, 6-H), 7.20 (1H, t, *J* = 8.4 Hz, 5-H) and 7.28 (1H, t, *J* = 2.0 Hz, 2-H); δ_C/ppm (100 MHz; D_2O) 36.1 (d, J_{P-C} = 144.0 Hz, CH_2P), 112.47 (C-6), 118.4 (C-2), 122.6 (C-3), 126.8 (C-4), 129.8 (C-5), 139.3 (C-1) and 163.3 (d, J_{P-C} = 4.1 Hz, C=O).

Sodium hydrogen [*N*-(3-fluorophenyl)carbamoyl]methylphosphonate 329d

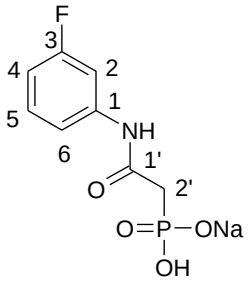

The procedure described for the synthesis of sodium hydrogen [*N*-(3-hydroxyphenyl)carbamoyl]methylphosphonate **329a** was employed, using [*N*-(3-fluorophenyl)carbamoyl]methylphosphonic acid **328d** (0.15 g, 0.64 mmol) and a solution of NaOH (1.1 mol) in EtOH (0.59 mL). The solvent was removed *in vacuo* and the residue chromatographed [reverse-phase column chromatography; elution with H_2O-MeOH (1:1)] to yield *sodium hydrogen [*N-*(3-fluorophenyl)carbamoyl]methylphosphonate* **329d** as a pale yellow semi-solid (96 mg, 97 %); υ/cm^{-1} 1668 (C=O), 1231 (P=O); δ_H/ppm (400 MHz; D_2O) 2.98 (2H, d, J_{P-H} = 21.4 Hz, CH_2P), 6.82 (1H, dd, *J* = 6.2 and 2.0 Hz, 4-H), 7.27 (2H, m, 5-H and 6-H) and 7. 38 (1H, dt, *J* = 6.4 and 2.0 Hz, 2-H); δ_C/ppm (100 MHz; D_2O) 35.3 (d, J_{P-C} = 138.4 Hz, CH_2P), 107.5 (d, J_{F-C} = 25.8 Hz, C-2), 112.1 (d, J_{F-C} = 18.5 Hz, C-4), 114.8 (C-6), 130.6 (C-5), 140.3 (C-1), 162.1 (d, J_{F-C} = 243.2 Hz, C-3) and 168.7 (d, J_{P-C} = 3.8 Hz, C=O).

Sodium hydrogen [*N*-(3-cyanophenyl)carbamoyl]methylphosphonate 329e

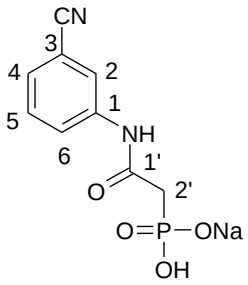

The procedure described for the synthesis of sodium hydrogen [*N*-(3-hydroxyphenyl)carbamoyl]methylphosphonate **329a** was employed, using [*N*-(3-cyanophenyl)carbamoyl]methylphosphonic acid **328e** (0.15 g, 0.64 mmol) and a solution of NaOH (1.1 mol) in EtOH (0.59 mL). The solvent was removed *in vacuo* and the residue chromatographed [reverse-phase column chromatography; elution with H_2O-MeOH (1:1)] to yield *sodium hydrogen [*N-*(3-cyanophenyl)carbamoyl]methylphosphonate* **329e** as a pale yellow semi-solid (96 mg, 97 %); υ/cm^{-1} 2228 (C≡N), 1679 (C=O), 1241 (P=O); δ_H/ppm (400 MHz; D_2O) 2.79 (2H, d, J_{P-H} = 21.4 Hz, CH_2P), 7.34 (1H, t, *J* = 8.0 Hz, 5-H), 7.52 (1H, dd, *J* = 7.2 and 2.0 Hz, 4-H), 7.73 (1H, dd, *J* = 6.4 and 1.6 Hz, 6-H) and 8.01 (1H, t, *J* = 2.0 Hz, 2-H); δ_C/ppm (100 MHz; D_2O) 36.6 (d, J_{P-C} = 130.8 Hz, CH_2P) 112.7 (C-3), 116.3 (C≡N), 125.7 (C-6), 126.5 (C-2), 128.3 (C-4), 129.9 (C-5), 139.1 (C-1) and 164.5 (d, J_{P-C} = 4.4 Hz, C=O).

Sodium hydrogen [*N*-(3-nitrophenyl)carbamoyl]methylphosphonate 329f

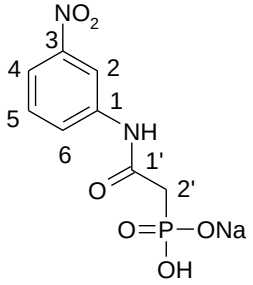

The procedure described for the synthesis of sodium hydrogen [*N*-(3-hydroxyphenyl)carbamoyl]methylphosphonate **329a** was employed, using [*N*-(3-nitrophenyl)carbamoyl]methylphosphonic acid **328f** (0.15 g, 0.58 mmol) and a solution of NaOH (1.1 mol) in EtOH (0.50 mL). The solvent was removed *in vacuo* and the residue chromatographed [reverse-phase column chromatography; elution with H_2O-MeOH (1:1)] to yield *sodium hydrogen [*N-*(3-nitrophenyl)carbamoyl]methylphosphonate* **329f** as a yellow

semi-solid (91 mg, 93 %); υ/cm^{-1} 1679 (C=O), 1241 (P=O); δ_H/ppm (400 MHz; D_2O) 2.83 (2H, d, J_{P-H} = 21.2 Hz, CH_2P), 6.60 (1H, dd, *J* = 6.0 and 2.0 Hz, 4-H), 7.10 (1H, dd, *J* = 7.6 and 2.0 Hz, 6-H), 7.22 (1H, t, *J* = 7.9 Hz, 5-H) and 7.28 (1H, t, *J* = 2.0 Hz, 2-H); δ_C/ppm (100 MHz; D_2O) 35.7 (d, J_{P-C} = 142.0 Hz, CH_2P), 114.3 (C-2), 118.5 (C-4), 125.4 (C-6), 126.2 (C-5), 129.6 (C-1), 139.3 (C-3) and 163.0 (d, J_{P-C} = 3.8 Hz, C=O).

Sodium hydrogen {*N*-[3-(hydroxymethyl)phenyl]carbamoyl}methylphosphonate 329g

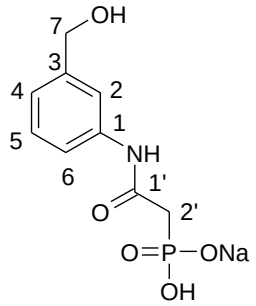

The procedure described for the synthesis of sodium hydrogen [*N*-(3-hydroxyphenyl)carbamoyl]methylphosphonate **329a** was employed, using [*N*-(3-(hydroxymethyl)phenylcarbamoyl]methylphosphonic acid **328g** (0.15 g, 0.61 mmol) and 1.1 mol NaOH in EtOH (0.56 mL). The solvent was removed *in vacuo* and the residue chromatographed [reverse-phase column chromatography; elution with H_2O-MeOH (1:1)] to yield *sodium hydrogen {*N-*[3-(hydroxymethyl)phenyl]carbamoyl}methylphosphonate* **329g** as a light yellow solid (86 mg, 94 %); υ/cm^{-1} 1687 (C=O), 1232 (P=O); δ_H/ppm (400 MHz; D_2O) 2.80 (2H, d, J_{P-H} = 21.2 Hz, CH_2P), 4.83 (2H, s, C*H*$_2$OH), 6.99 (1H, d, *J* = 7.6 Hz, 4-H), 7.28 (1H, t, *J* = 7.8 Hz, 5-H), 7.42 (2H, d, *J* = 7.6 Hz, 6-H) and 7.44 (1H, s, 2-H); δ_C (100 MHz; D_2O) 34.8 (d, J_{P-C} = 142.8 Hz, CH_2P), 64.6 (CH_2OH), 118.7 (C-2), 119.3 (C-6), 122.4 (C-4), 128.7 (C-5), 139.2 (C-1), 142.6 (C-3) and 166.5 (d, J_{P-C} = 4.2 Hz, C=O).

3.3.2. Reaction of 3-substituted anilines with 3-chloropropanoyl chloride

3-Chloro-*N*-(3-hydroxyphenyl)propanamide 322a

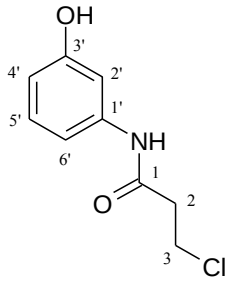

To a stirred solution of 3-aminophenol (1.50 g, 14.0 mmol) in THF (30 mL) under nitrogen was added NaH (60 % dispersion in mineral oil; 0.60 g, 24 mmol) in small portions to permit controlled evolution of hydrogen. 3-Chloropropionyl chloride (1.31 mL, 14.0 mmol) was then added through a septum and the resulting solution was stirred for *ca.* 6 h. The solvent was evaporated *in vacuo* and the residue dissolved in EtOAc (2 x 50 mL). The organic solution was washed sequentially with satd. aq. $NaHCO_3$ (2 × 100 mL), water (2 x 100 mL) and brine (2 × 100 mL). The aqueous washings were extracted with EtOAc and the combined organic solutions were dried (anhydr. $MgSO_4$). Evaporation of the solvent *in vacuo* afforded 3-chloro-*N*-(3-hydroxyphenyl)propanamide as a brown solid (2.25 g, 80 %) m.p. 119-121 °C (Lit.[238]); υ_{max} (solid deposit/cm^{-1}) 3362 (OH) and 1658 (C=O); δ_H/ppm (400 MHz; $CDCl_3$) 2.74 (2H, t, *J* 6.4 Hz, CH_2CO), 3.82 (2H, t, *J* = 6.4 Hz, CH_2Cl), 5.74 (1H, t, *J* = 9.2 Hz, 5-H), 5.99 (1H, dd, *J* = 9.2 and 1.2 Hz, 4-H), 6.57 (1H, dd, *J* = 6.0 and 1.2 Hz, 6-H), 7.13 (1H, t, *J* = 1.2 Hz, 2-H), 7.50 (1H, s, OH) and 7.69 (1H, s, NH); δ_C/ppm (100 MHz; $CDCl_3$) 42.6 (CH_2CO), 44.1 (CH_2Cl), 106.3 (C-2'), 109.9 (C-4'), 110.9 (C-6'), 129.4 (C-5'), 139.4 (C-1'), 157.6 (C-3') and 164.4 (C=O).

3-Chloro-*N*-(3-methoxyphenyl)propanamide 322b

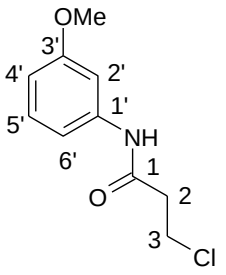

The procedure described for the synthesis of 3-chloro-*N*-(3-hydroxyphenyl)propanamide **322a** was employed, using 3-methoxyaniline (0.91 mL, 8.1 mmol), NaH (60 % dispersion in

mineral oil; 0.36 g, 15 mmol) and 3-chloropropionyl chloride (0.76 mL, 8.1 mmol) in THF (15 mL), to yield 3-chloro-*N*-(3-methoxyphenyl)propanamide **322b** as a yellow solid (1.49 g, 86 %), m.p 92-94 °C (Lit.[239] 90-92 °C); υ_{max} (solid deposit/cm^{-1}) 1681 (C=O); δ_H/ppm (400 MHz; $CDCl_3$) 2.79 (2H, t, *J* = 6.4 Hz, CH_2CO), 3.77 (3H, s, OCH_3), 3.85 (2H, t, *J* = 6.4 Hz, CH_2Cl), 6.66 (1H, d, *J* = 8.0 Hz, 4'-H), 6.97 (1H, d, *J* = 8.0 Hz, 6'-H), 7.19 (1H, t, *J* = 8.0 Hz, 5'-H), 7.28 (1H, s, 2'-H) and 7.56 (1H, s, NH); δ_C/ppm (100 MHz; $CDCl_3$) 36.7 (CH_2CO), 44.5 (CH_2Cl), 55.3 (OCH_3), 105.5 (C-2'), 110.3 (C-6'), 111.9 (C-4'), 129.7 (C-5'), 135.3 (C-1'), 160.2 (C-3') and 171.1 (C=O).

_N_-(3-Bromophenyl) 3-chloropropanamide 322c

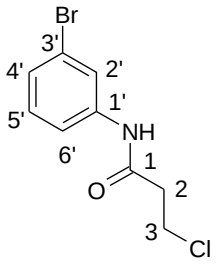

The procedure described for the synthesis of 3-chloro-*N*-(3-hydroxyphenyl)propanamide **322a** was employed, using 3-bromoaniline (0.63 mL, 5.8 mmol), NaH (60 % dispersion in mineral oil; 0.26 g, 10.8 mmol) and 3-chloropropionyl chloride (0.54 mL, 5.8 mmol) in THF (15 mL), to yield *N*-(3-bromophenyl)3-chloropropanamide **322c** as a dark brown solid (1.23 g, 81 %), m.p 106-108 °C (Lit.[240]); υ_{max} (solid deposit/cm^{-1}) 1658 (C=O); δ_H/ppm (400 MHz; $CDCl_3$) 2.80 (2H, t, *J* = 6.4 Hz, CH_2CO), 3.86 (2H, t, *J* = 6.4 Hz, CH_2Cl), 7.17 (1H, t, *J* = 8.0 Hz, 5'-H), 7.24 (1H, d, *J* = 7.6 Hz, 4'-H), 7.41 (1H, d, *J* = 8.0 Hz, 6'-H), 7.45 (1H, s, 2'-H), and 7.77 (1H, s, NH); δ_C/ppm (100 MHz; $CDCl_3$) 36.6 (CH_2CO), 44.2 (CH_2Cl), 118.7 (C-6'), 122.5 (C-3'), 123.1 (C-2'), 128.0 (C-4'), 130.3 (C-5'), 137.9 (C-1') and 164.2 (C=O).

3-Chloro-_N_-(3-fluorophenyl)propanamide 322d

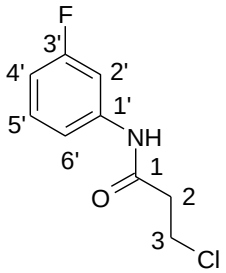

The procedure described for the synthesis of 3-chloro-*N*-(3-hydroxyphenyl)propanamide **322a** was employed, using 3-fluoroaniline (1.05 mL, 5.80 mmol), NaH (60 % dispersion in

mineral oil; 0.26 g, 11 mmol) and 3-chloropropionyl chloride (0.54 mL, 5.8 mmol) in THF (15 mL), to yield 3-chloro-*N*-(3-fluorophenyl)propanamide **322c** as a light yellow solid (1.04 g, 89 %), m.p 87-89 °C (Lit.[241]); υ_{max} (solid deposit/cm^{-1}) 1681 (C=O); δ_H/ppm (400 MHz; $CDCl_3$) 2.56 (2H, t, *J* = 6.4 Hz, CH_2CO), 3.65 (2H, t, *J* = 6.4 Hz, CH_2Cl), 6.80 (1H, td, *J* = 6.0, 2.0 and 0.8 Hz, 4'-H), 7.12 (1H, d, *J* = 8.0 Hz, 6'-H), 7.24 (1H, dt, *J* = 7.2 and 1.6 Hz, 5'-H), 7.47 (1H, td, *J* = 6.4, 2.4 and 0.8 Hz, 2'-H) and 7.49 (1H, s, NH); δ_C/ppm (100 MHz; $CDCl_3$) 34.1 (CH_2CO), 44.3 (CH_2Cl), 107.3 (d, J_{F-C} = 26.4 Hz, C-2'), 111.0 (d, J_{F-C} = 21.4 Hz, C-4'), 114.9 (C-6'), 130.1 (d, J_{F-C} = 9.3 Hz, C-5'), 139.1 (d, J_{F-C} = 11.0 Hz, C-1'), 163.0 (d, J_{F-C} = 243.5 Hz, C-3') and 170.1 (C=O).

3-Chloro-*N*-(3-cyanophenyl)propanamide 322e

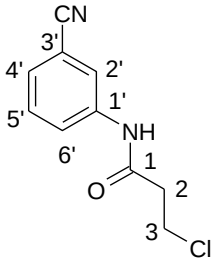

The procedure described for the synthesis of 3-chloro-*N*-(3-hydroxyphenyl)propanamide **322a** was employed, using 3-aminobenzonitrile (1.20 g, 10.1 mmol), NaH (60 % dispersion in mineral oil; 0.54 g, 23 mmol) and 3-chloropropionyl chloride (0.94 mL, 10 mmol) in THF (15 mL), to yield 3-chloro-*N*-(3-cyanophenyl)propanamide **322e** as a yellow solid (1.04 g, 89 %), m.p 108-110 °C (Lit.[242] 97-98 °C); υ_{max} (solid deposit/cm^{-1}) 2232 (C≡N), 1658 (C=O); δ_H/ppm (400 MHz; $CDCl_3$) 2.84 (2H, t, *J* = 6.0 Hz, CH_2CO), 3.87 (2H, t, *J* = 6.0 Hz, CH_2Cl), 7.42 (2H, m, 4'-H and 6'-H), 7.75 (1H, dt, *J* = 7.6 and 2.0 Hz, 5'-H), 7.89 (1H, s, NH) and 7.95 (1H, t, *J* = 2.0 Hz, 2'-H); δ_C/ppm (100 MHz; $CDCl_3$) 34.3 (CH_2CO), 44.2 (CH_2Cl), 113.2 (C-3'), 118.9 (C=N), 122.7 (C-2'), 124.3 (C-5'), 129.6 (C-6'), 131.2 (C-4'), 138.8 (C-1') and 168.7 (C=O).

3-Chloro-*N*-(3-nitrophenyl)propanamide 322f

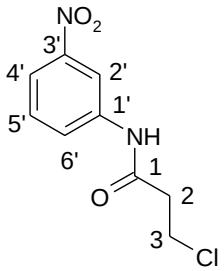

The procedure described for the synthesis of 3-chloro-*N*-(3-hydroxyphenyl)propanamide **322a** was employed, using 3-nitroaniline (1.01 g, 7.27 mmol), NaH (60 % dispersion in mineral oil; 0.33 g, 13 mmol) and 3-chloropropionyl chloride (0.49 mL, 7.3 mmol) in THF (15 mL), to yield 3-chloro-*N*-(3-nitrophenyl)propanamide **322f** as a dark yellow solid (1.56 g, 94 %), m.p 94-96 °C (Lit.[239] 95-97 ^{o}C); υ_{max} (solid deposit/cm^{-1}) 1687 (C=O); δ_H/ppm (400 MHz; $CDCl_3$) 2.88 (2H, t, *J* = 6.4 Hz, CH_2CO), 3.89 (2H, t, *J* = 6.4 Hz, CH_2Cl), 7.48 (1H, t, *J* = 8.0 Hz, 5'-H), 7.94 (2H, dd, *J* = 7.6 and 1.2 Hz, 4'-H and 6'-H), 8.06 (1H, s, NH) and 8.40 (1H, t, *J* = 2.0 Hz, 2'-H); δ_C/ppm (100 MHz; $CDCl_3$) 39.5 (CH_2CO), 40.4 (CH_2Cl), 114.7 (C-2'), 119.2 (C-4'), 125.7 (C-6'), 129.9 (C-5'), 138.5 (C-1'), 148.5 (C-3') and 168.3 (C=O).

3-Chloro-*N*-[3-(hydroxymethyl)phenyl]propanamide 322g

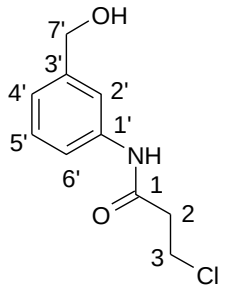

The procedure described for the synthesis of 3-chloro-*N*-(3-hydroxyphenyl)propanamide **322a** was employed, using 3-aminobenzyl alcohol (1.02 g, 8.12 mmol), NaH (60 % dispersion in mineral oil; 0.52 g, 21 mmol) and 3-chloropropionyl chloride (0.55 mL, 8.1 mmol) in THF (15 mL), to yield 3-chloro-*N*-[3-(hydroxymethyl)phenyl]propanamide **322g** as a grey solid (1.53 g, 88 %), m.p 101-103°C (Lit.[239] 97-99 ^{o}C); υ_{max} (solid deposit/cm^{-1}) 1674 (C=O); δ_H/ppm (400 MHz; $CDCl_3$) 2.85 (2H, t, *J* = 6.4 Hz, CH_2CO), 3.88 (2H, t, *J* = 6.4 Hz, CH_2Cl), 4.63 (2H, s, 7'-CH_2), 5.11 (1H, s, OH), 7.09 (1H, t, *J* = 6.4 Hz, 5'-H), 7.47 (1H, d, *J* = 6.8 Hz, 4'-H), 7.54 (1H, d, *J* = 6.8 Hz, 6'-H), 7.62 (1H, s, 2'-H) and 7.72 (1H, s, NH); δ_C/ppm (100 MHz; $CDCl_3$) 38.9 (CH_2CO), 40.4 (CH_2Cl), 66.4 (CH_2OH), 119.3 (C-2'), 119.9 (C-6'), 124.3 (C-4'), 129.3 (C-5'), 137.7 (C-1'), 142.0 (C-3') and 167.9 (C=O).

3.3.2.1. Synthesis of diethyl ethylphosphonates using Michaelis-Arbuzov methodology

Diethyl [*N*-(3-hydroxyphenyl)carbamoyl]ethylphosphonate 323a

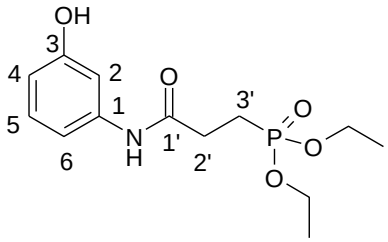

Triethyl phosphite (0.86 mL, 5.0 mmol) was added through a septum to 3-chloro-*N*-(3-hydroxyphenyl)propanamide **322a** (0.50 g, 2.5 mmol) under nitrogen in an oven-dried round-bottomed flask equipped with a reflux condenser, and the resulting mixture was refluxed for *ca.* 9 h during which time the reaction was monitored by TLC. The cooled mixture was then stirred with hexane (20 mL) for *ca.* 30 minutes followed by decantation of the hexane layer to remove the excess triethyl phosphite; this was repeated three times. The crude product was purified by flash chromatography [on silica gel; elution with hexane-EtOAc (3:1)], and subsequent evaporation of the solvent *in vacuo* afforded *diethyl [*N*(3-hydroxyphenyl)carbamoyl)]ethylphosphonate* **323a** as a dark brown oil (0.29 g, 58 %); (Found: $\mathbf{M}^+$, 301.11247 $C_{13}H_{20}NO_5P$ requires: $\mathbf{M}^+$, 301.10791); υ/cm^{-1} 3261 (OH), 1671 (C=O), 1232 (P=O) and 1024 (P−OEt); δ_H/ppm (400 MHz; $CDCl_3$) 1.29 (6H, t, J = 6.8 Hz, 2 × CH_3), 2.13 (2H, m, CH_2P), 2.68 (2H, m, CH_2CO), 4.06 (4H, m, 2 × OCH_2), 6.60 (1H, d, J = 8.4 Hz, 4-H), 6.91 (1H, d, J = 7.6 Hz, 6-H), 7.08 (1H, t, J = 8.0 Hz, 5-H), 7.36 (1H, s, 2-H), 8.44 (1H, s, OH) and 8.92 (1H, s, NH); δ_C (100 MHz; $CDCl_3$) 16.2 (d, J_{P-C} = 6.0 Hz, 2 × CH_3), 20.8 (d, J_{P-C} = 142.5 Hz, CH_2P), 27.6 (d, J_{P-C} = 3.7 Hz, CH_2CO), 62.2 (d, J_{P-C} = 6.6 Hz, 2 × OCH_2), 107.2 (C-2), 111.1 (C-4), 111.7 (C-6), 129.4 (C-5), 139.1 (C-1), 157.4 (C-3) and 169.5 (d, J_{P-C} = 15.6 Hz, C=O); δ_P/ppm (162 MHz; $CDCl_3$) 24.1 (P=O).

Diethyl [*N*-(3-methoxyphenyl)carbamoyl]ethylphosphonate 323b

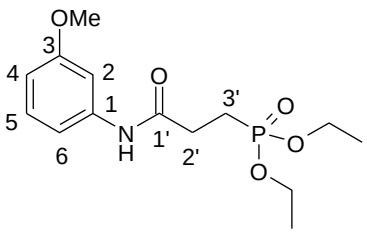

The procedure described for the synthesis of diethyl [*N*-(3-hydroxyphenyl)carbamoyl]ethylphosphonate **323a** was employed, using 3-chloro-*N*-(3-methoxyphenyl)propanamide **322b** (0.50 g, 2.3 mmol) and triethyl phosphite (0.81 mL, 4.7 mmol). The crude product was purified by flash chromatography [on silica gel; elution with hexane-EtOAc (3:1)], and subsequent evaporation of the solvent *in vacuo* afforded *diethyl [*N*-(3-methoxyphenyl)carbamoyl]ethylphosphonate* **323b** as a yellow oil (0.32 g, 62 %); (Found: $\mathbf{M}^+$, 315.12861 $C_{14}H_{22}NO_5P$ requires: $\mathbf{M}^+$, 315.12356); υ/cm^{-1} 1679 (C=O), 1231 (P=O) and 1049 (P−OEt); δ_H/ppm (400 MHz; $CDCl_3$) 1.31 (6H, t, *J* = 6.8 Hz, 2 × CH_3), 2.15 (2H, m, CH_2P), 2.71 (2H, m, CH_2CO), 3.78 (3H, s, OCH_3), 4.12 (4H, m, 2 × OCH_2), 6.62 (1H, dd, *J* = 6.4 and 2.0 Hz, 4-H), 7.05 (1H, d, *J* = 8.0 Hz, 6-H), 7.17 (1H, t, *J* = 8.4 Hz, 5-H), 7.35 (1H, t, *J* = 2.0 Hz, 2-H) and 8.87 (1H, s, NH); δ_C (100 MHz; $CDCl_3$) 16.3 (d, J_{P-C} = 6.0 Hz, 2 × CH_3), 20.7 (d, J_{P-C} = 142.5 Hz, CH_2P), 29.9 (d, J_{P-C} = 3.4 Hz, CH_2CO), 55.2 (OCH_3), 62.1 (d, J_{P-C} = 6.6 Hz, 2 × OCH_2), 105.2 (C-2), 109.7 (C-4), 111.7 (C-6), 129.4 (C-5), 139.8 (C-1), 160.0 (C-3) and 169.4 (d, J_{P-C} = 15.8 Hz, C=O); δ_P/ppm (162 MHz; $CDCl_3$) 23.8 (P=O).

Diethyl [*N*-(3-bromophenyl)carbamoyl]ethylphosphonate 323c

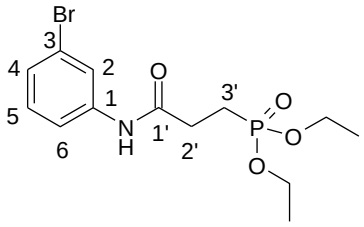

The procedure described for the synthesis of diethyl [*N*-(3-hydroxyphenyl)carbamoyl]ethylphosphonate **323a** was employed, using *N*-(3-bromophenyl)3-chloropropanamide **322c** (0.50 g, 1.9 mmol) and triethyl phosphite (0.65 mL, 3.8 mmol). The crude product was purified by flash chromatography [on silica gel; elution with hexane-EtOAc (3:1)], and subsequent evaporation of the solvent *in vacuo* afforded *diethyl [*N*-(3-bromophenyl)carbamoyl]ethylphosphonate* **323c** as a yellowish-brown oil (0.27 g, 53 %); (Found: $\mathbf{M}^+$, 363.02473 $C_{13}H_{19}BrNO_4P$ requires: $\mathbf{M}^+$, 363.02351); υ/cm^{-1} 1680 (C=O), 1240 (P=O) and 1037 (P−OEt); δ_H/ppm (400 MHz; $CDCl_3$) 1.37 (6H, t, *J* = 6.8 Hz, 2 × CH_3), 2.21 (2H, m, CH_2P), 2.73 (2H, m, CH_2CO), 4.16 (4H, m, 2 × OCH_2), 7.18 (1H, t, *J* = 7.6 Hz, 5-H), 7.23 (1H, d, *J* = 8.4 Hz, 4-H), 7.61 (1H, d, *J* = 7.6 Hz, 6-H), 7.84 (1H, s, 2-H) and 9.30 (1H, s, NH); δ_C (100 MHz; $CDCl_3$) 16.4 (d, J_{P-C} = 6.0 Hz, 2 × CH_3), 20.6 (d, J_{P-C} = 142.5 Hz, CH_2P),

29.9 (d, J_{P-C} = 3.3 Hz, CH_2CO), 62.2 (d, J_{P-C} = 6.6 Hz, 2 × OCH_2), 115.3 (C-6), 117.9 (C-3), 122.3 (C-2), 126.6 (C-4), 130.1 (C-5), 140.0 (C-1) and 169.5 (d, J_{P-C} = 15.1 Hz, C=O); δ_P/ppm (162 MHz; $CDCl_3$) 24.1 (P=O).

Diethyl [*N*-(3-fluorophenyl)carbamoyl]ethylphosphonate 323d

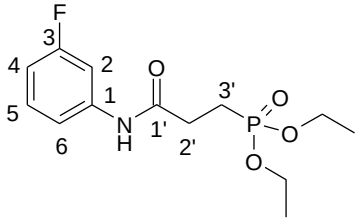

The procedure described for the synthesis of diethyl [*N*-(3-hydroxyphenyl)carbamoyl]ethylphosphonate **323a** was employed, using 3-chloro-*N*-(3-fluorophenyl)propanamide **322d** (0.50 g, 2.5 mmol) and triethyl phosphite (0.85 mL, 4.9 mmol). The crude product was purified by flash chromatography [on silica gel; elution with hexane-EtOAc (3:1)], and subsequent evaporation of the solvent *in vacuo* afforded *diethyl [*N*-(3-fluorophenyl)carbamoyl]ethylphosphonate* **323d** as a light yellow oil (0.24 g, 48 %); (Found: $\mathbf{M}^+$, 303.10843 $C_{13}H_{19}FNO_5P$ requires: $\mathbf{M}^+$, 303.10357); υ/cm^{-1} 1675 (C=O), 1234 (P=O) and 1037 (P−OEt); δ_H/ppm (400 MHz; $CDCl_3$) 1.31 (6H, t, *J* = 7.2 Hz, 2 × CH_3), 2.17 (2H, m, CH_2P), 2.70 (2H, m, CH_2CO), 4.11 (4H, m, 2 × OCH_2), 6.81 (1H, td, *J* = 6.0, 2.0 and 1.6 Hz, 4-H), 7.16 (1H, dd, *J* = 6.4 and 2.0 Hz, 6-H), 7.24 (1H, td, *J* = 6.4 and 1.6 Hz, 5-H) 7.49 (1H, dt, *J* = 6.4, 2.0 and 1.6 Hz, 2-H) and 7.76 (1H, s, NH); δ_C (100 MHz; $CDCl_3$) 16.3 (d, J_{P-C} = 6.2 Hz, 2 × CH_3), 20.7 (d, J_{P-C} = 142.3 Hz, CH_2P), 30.1 (d, J_{P-C} = 4.0 Hz, CH_2CO), 62.2 (d, J_{P-C} = 6.6 Hz, 2 × OCH_2), 107.4 (d, J_{F-C} = 26.2 Hz, C-2), 111.2 (d, J_{F-C} = 21.2 Hz, C-4), 115.1 (d, J_{F-C} = 2.9 Hz, C-6), 130.1 (d, J_{F-C} = 9.3 Hz, C-5), 139.0 (d, J_{F-C} = 10.9 Hz, C-1), 162.9 (d, J_{F-C} = 243.3 Hz, C-3) and 167.9 (C=O); δ_P/ppm (162 MHz; $CDCl_3$) 23.4 (P=O).

Diethyl [*N*-(3-cyanophenyl)carbamoyl]ethylphosphonate 323e

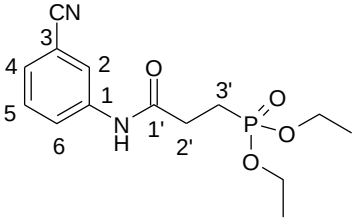

The procedure described for the synthesis of diethyl [*N*-(3-hydroxyphenyl)carbamoyl]ethyl phosphonate **323a** was employed, using 3-chloro-*N*-(3-cyanophenyl)propanamide **322e** (0.50 g, 2.4 mmol) and triethyl phosphite (0.82 mL, 4.8 mmol). The crude product was purified by flash chromatography [on silica gel; elution with hexane-EtOAc (3:1)], and subsequent evaporation of the solvent *in vacuo* afforded *diethyl [*N-*(3-cyanophenyl)carbamoyl]ethylphosphonate* **323e** as a yellow oil (0.30 g, 61 %); (Found: **M**$^+$, 311.11061 $C_{14}H_{19}N_2O_4P$ requires: **M**$^+$, 311.11160); υ/cm^{-1} 2232 (C≡N), 1657 (C=O), 1230 (P=O) and 1042 (P−OEt); δ_H/ppm (400 MHz; $CDCl_3$) 1.34 (6H, t, *J* = 7.2 Hz, 2 × CH_3), 2.17 (2H, m, CH_2P), 2.73 (2H, m, CH_2CO), 4.13 (4H, m, 2 × OCH_2), 7.34 (2H, m, 4-H and 6-H), 7.86 (1H, t, *J* = 8.0 Hz, 5-H), 7.96 (1H, t, *J* = 1.6 Hz, 2-H) and 9.62 (1H, s, NH); δ_C (100 MHz; $CDCl_3$) 16.4 (d, J_{P-C} = 6.1 Hz, 2 × CH_3), 20.7 (d, J_{P-C} = 142.3 Hz, CH_2P), 29.9 (d, J_{P-C} = 3.4 Hz, CH_2CO), 62.4 (d, J_{P-C} = 6.6 Hz, 2 × OCH_2), 112.7 (C-3), 118.7 (C≡N), 122.6 (C-2) 123.6 (C-5), 127.1 (C-6), 129.7 (C-4), 139.5 (C-1) and 169.9 (C=O); δ_P/ppm (162 MHz; $CDCl_3$) 24.0 (P=O).

Diethyl [*N*-(3-nitrophenyl)carbamoyl]ethylphosphonate 323f

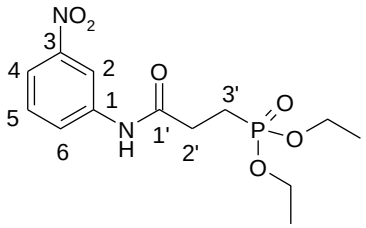

The procedure described for the synthesis of diethyl [*N*-(3-hydroxyphenyl)carbamoyl]ethyl phosphonate **323a** was employed, using 3-chloro-*N*-(3-nitrophenyl)propanamide **322f** (0.50 g, 2.2 mmol) and triethyl phosphite (0.76 mL, 4.4 mmol). The crude product was purified by flash chromatography [on silica gel; elution with hexane-EtOAc (3:1)], and subsequent evaporation of the solvent *in vacuo* afforded *diethyl[*N-*(3-nitrophenyl)carbamoyl]ethyl phosphonate* **323f** as a dark brown oil (0.33 g, 67 %); (Found: **M**$^+$, 330.10042 $C_{13}H_{19}N_2O_6P$ requires: **M**$^+$, 330.09807); υ/cm^{-1} 1679 (C=O), 1219 (P=O) and 1034 (P−OEt); δ_H/ppm (400 MHz; $CDCl_3$) 1.35 (6H, t, *J* = 7.2 Hz, 2 × CH_3), 2.18 (2H, m, CH_2P), 2.77 (2H, m, CH_2CO), 4.15 (4H, m, 2 × OCH_2), 7.45 (1H, t, *J* = 8.4 Hz, 5-H), 7.90 (1H, dd, *J* = 8.0 and 1.6 Hz, 4-H), 8.13 (1H, dd, *J* = 8.4 and 1.6 Hz, 6-H), 8.40 (1H, t, *J* = 2.0 Hz, 2-H) and 9.92 (1H, s, NH); δ_C (100 MHz; $CDCl_3$) 16.4 (d, J_{P-C} = 6.1 Hz, 2 × CH_3), 20.8 (d, J_{P-C} = 142.9 Hz, CH_2P), 29.7 (d, J_{P-C} = 3.1 Hz,

CH_2CO), 62.4 (d, $J_{P–C}$ = 6.6 Hz, 2 × OCH_2), 114.1 (C-2), 118.1 (C-4), 125.1 (C-6), 129.7 (C-5), 140.1 (C-1), 148.3 (C-3) and 169.9 (C=O); δ_P/ppm (162 MHz; $CDCl_3$) 24.4 (P=O).

Diethyl {*N*-[3-(hydroxymethyl)phenyl]carbamoyl}ethylphosphonate 323g

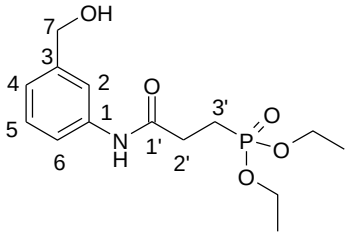

The procedure described for the synthesis of diethyl [*N*-(3-hydroxyphenyl)carbamoyl]ethylphosphonate **323a** was employed, using 3-chloro-*N*-[3-(hydroxymethyl)phenyl]propanamide **322g** (0.50 g, 2.3 mmol) and triethyl phosphite (0.80 mL, 4.7 mmol). The crude product was purified by flash chromatography [on silica gel; elution with hexane-EtOAc (3:1)], and subsequent evaporation of the solvent *in vacuo* afforded *diethyl {*N-*[3-(hydroxymethyl)phenyl]carbamoyl}ethylphosphonate* **323g** as a yellow oil (0.30 g, 61 %); (Found: $\mathbf{M}^+$, 315.12725 $C_{14}H_{22}NO_5P$ requires: $\mathbf{M}^+$, 315.12356); υ/cm^{-1} 3268 (OH), 1667 (C=O), 1232 (P=O) and 1041 (P−OEt); δ_H/ppm (400 MHz; $CDCl_3$) 1.33 (6H, t, *J* = 6.8 Hz, 2 × CH_3), 2.17 (2H, m, CH_2P), 2.78 (2H, m, CH_2CO), 4.12 (4H, m, 2 × OCH_2), 4.46 (1H, s, OH), 5.00 (2H, s, C*H*$_2$OH), 7.08 (1H, d, *J* = 7.6 Hz, 4-H), 7.28 (1H, t, *J* = 8.0 Hz, 5-H), 7.46 (1H, d, *J* = 8.0 Hz, 6-H), 7.58 (1H, s, 2-H) and 8.02 (1H, s, NH); δ_C (100 MHz; $CDCl_3$) 16.3 (d, $J_{P–C}$ = 6.0 Hz, 2 × CH_3), 20.7 (d, $J_{P–C}$ = 142.5 Hz, CH_2P), 29.9 (d, $J_{P–C}$ = 3.1 Hz, CH_2CO), 62.1 (d, $J_{P–C}$ = 6.6 Hz, OCH_2), 63.4 (CH_2OH), 118.2 (C-2), 119.1 (C-6), 122.4 (C-4), 129.4 (C-5), 139.1 (C-1), 139.6 (C-3) and 169.6 (C=O); δ_P/ppm (162 MHz; $CDCl_3$) 24.0 (P=O).

3.3.2.2. Synthesis of ethylphosphonic acid derivatives using TMSBr

[*N*-(3-Hydroxyphenyl)carbamoyl]ethylphosphonic acid 331a

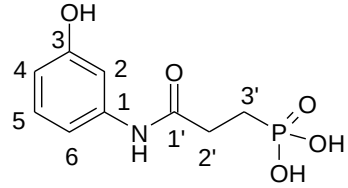

Trimethylsilyl bromide (0.22 mL, 1.7 mmol) was added to diethyl [*N*-(3-hydroxyphenyl)-carbamoyl]ethylphosphonate **323a** (0.25 g, 0.83 mmol) in CH_3CN (3 mL) and the mixture was

heated in the microwave apparatus set to deliver 100 W of power, with a reaction temperature of 60 ^{o}C and reaction time of 10 min. After completion, the mixture was cooled to room temperature, treated with a 95:5 MeOH-H_2O mixture and stirred for 30 min. The solvent was removed *in vacuo* and the residue chromatographed [preparative layer chromatography; elution with hexane-EtOAc-MeOH (1:1:1)] to yield *[*N*-(3-hydroxyphenyl)carbamoyl]ethylphosphonic acid* **331a** as a brown viscous liquid (0.12 g, 61 %); (Found: C, 44.27; H, 4.98; N, 5.73 %. $C_9H_{12}NO_5P$ requires C, 44.09; H, 4.93; N, 5.71 %); υ/cm^{-1} 3212 (OH), 1682 (C=O) and 1230 (P=O); δ_H/ppm (400 MHz; DMSO-d_6) 2.12 (2H, m, CH_2P), 2.70 (2H, m, CH_2CO), 5.71 (2H, s, 2 x OH), 6.61 (1H, d, *J* = 8.2 Hz, 4-H), 6.89 (1H, d, *J* = 7.6 Hz, 6-H), 7.11 (1H, t, *J* = 8.2 Hz, 5-H), 7.38 (1H, s, 2-H), 7.52 (1H, s, OH) and 8.82 (1H, s, NH); δ_C/ppm (100 MHz; DMSO-d_6) 20.7 (d, J_{P-C} = 142.5 Hz, CH_2P), 27.7 (d, J_{P-C} = 3.7 Hz, CH_2CO), 107.1 (C-2), 111.0 (C-4), 111.8 (C-6), 129.8 (C-5), 139.5 (C-1), 158.1 (C-3) and 169.3 (d, J_{P-C} = 15.4 Hz, C=O).

[*N*-(3-Methoxyphenyl)carbamoyl]ethylphosphonic acid 331b

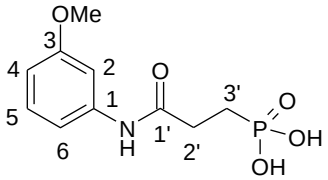

The procedure described for the synthesis of [*N*-(3-hydroxyphenyl)carbamoyl]ethyl phosphonic acid **331a** was employed, using diethyl [*N*-(3-methoxyphenyl)carbamoyl]ethyl phosphonate **323b** (0.25 g, 0.79 mmol) in CH_3CN (3 mL) and trimethylsilyl bromide (0.21 mL, 1.6 mmol). The solvent was removed *in vacuo* and the residue chromatographed [preparative layer chromatography; elution with hexane-EtOAc-MeOH (1:1:1)] to yield *[N-(3-methoxyphenyl)carbamoyl]ethylphosphonic acid* **331b** as a yellow viscous liquid (0.14 g, 66 %); (Found: C, 46.39; H, 5.49; N, 5.48 %. $C_{10}H_{14}NO_5P$ requires C, 46.34; H, 5.44; N, 5.40 %); υ/cm^{-1} 3210 (OH), 1670 (C=O) and 1228 (P=O); δ_H/ppm (400 MHz; DMSO-d_6) 2.14 (2H, m, CH_2P), 2.73 (2H, m, CH_2CO), 3.79 (3H, s, OCH_3), 5.93 (2H, s, 2 x OH), 6.60 (1H, dd, *J* = 6.4 and 2.0 Hz, 4-H), 7.08 (1H, d, *J* = 7.9 Hz, 6-H), 7.18 (1H, t, *J* = 8.2 Hz, 5-H), 7.37 (1H, t, *J* = 8.2 Hz, 2-H) and 8.83 (1H, s, NH); δ_C/ppm (100 MHz; DMSO-d_6) 20.7 (d, J_{P-C} = 142.3 Hz, CH_2P), 29.8 (d, J_{P-C} = 3.1 Hz, CH_2CO), 55.3 (OCH_3), 105.4 (C-2), 109.7 (C-4), 111.8 (C-6), 129.7 (C-5), 139.5 (C-1), 159.8 (C-3) and 169.2 (d, J_{P-C} = 15.6 Hz, C=O).

[*N*-(3-Bromophenyl)carbamoyl]ethylphosphonic acid 331c

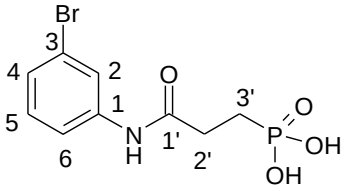

The procedure described for the synthesis of [*N*-(3-hydroxyphenyl)carbamoyl]ethyl phosphonic acid **331a** was employed, using diethyl [*N*-(3-bromophenyl)carbamoyl]ethyl phosphonate **323c** (0.25 g, 0.69 mmol) in CH_3CN (3 mL) and trimethylsilyl bromide (0.19 mL, 1.4 mmol). The solvent was removed *in vacuo* and the residue chromatographed [preparative layer chromatography; elution with hexane-EtOAc-MeOH (1:1:1)] to yield *[*N-*(3-bromophenyl)carbamoyl]ethylphosphonic acid* **331c** as a brown gum (0.18 g, 58 %); (Found: C, 35.15; H, 3.71; N, 4.51 %. $C_9H_{11}BrNO_4P$ requires C, 35.09; H, 3.60; N, 4.55 %); υ/cm^{-1} 3189 (OH), 1672 (C=O) and 1219 (P=O); δ_H/ppm (400 MHz; DMSO-d_6) 2.21 (2H, m, CH_2P), 2.73 (2H, m, CH_2CO), 5.21 (2H, s, 2 x OH), 7.20 (1H, t, *J* = 7.6 Hz, 5-H), 7.24 (1H, d, *J* = 8.0 Hz, 4-H), 7.59 (1H, d, *J* = 7.6 Hz, 6-H), 7.82 (1H, s, 2-H) and 8.87 (1H, s, NH); δ_C/ppm (100 MHz; DMSO-d_6) 20.8 (d, J_{P-C} = 142.5 Hz, CH_2P), 29.8 (d, J_{P-C} = 3.2 Hz, CH_2CO), 115.1 (C-6), 117.9 (C-3), 122.5 (C-2), 126.8 (C-4), 129.8 (C-5), 140.2 (C-1) and 169.7 (d, J_{P-C} = 15.2 Hz, C=O).

[*N*-(3-Fluorophenyl)carbamoyl]ethylphosphonic acid 331d

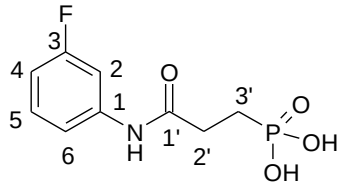

The procedure described for the synthesis of [*N*-(3-hydroxyphenyl)carbamoyl]ethyl phosphonic acid **331a** was employed, using diethyl [*N*-(3-fluorophenyl)carbamoyl]ethyl phosphonate **323d** (0.25 g, 0.82 mmol) in CH_3CN (3 mL) and trimethylsilyl bromide (0.22 mL, 1.6 mmol). The solvent was removed *in vacuo* and the residue chromatographed [preparative layer chromatography; elution with hexane-EtOAc-MeOH (1:1:1)] to yield *[*N-*(3-fluorophenyl)carbamoyl]ethylphosphonic acid* **331d** as a yellow viscous liquid (0.17 g, 68 %); (Found: C, 43.82; H, 4.56; N, 5.73 %. $C_9H_{11}FNO_4P$ requires C, 43.74; H, 4.49; N, 5.67 %); υ/cm^{-1} 3228 (OH), 1689 (C=O) and 1236 (P=O); δ_H/ppm (400 MHz; DMSO-d_6) 2.13 (2H, m,

CH_2P), 2.73 (2H, m, CH_2CO), 4.95 (2H, s, 2 x OH), 6.79 (1H, td, *J* = 6.0, 2.0 and 1.6 Hz, 4-H), 7.17 (1H, d, *J*= 6.2 Hz, 6-H), 7.27 (1H, ddd, *J* = 6.4, 6.0 and 1.6 Hz, 5-H) 7.46 (1H, dt, *J* = 6.4 and 1.6 Hz, 2-H) and 8.21 (1H, s, NH); δ_C/ppm (100 MHz; DMSO-d_6) 20.7 (d, J_{P-C} = 142.5 Hz, CH_2P), 29.9 (d, J_{P-C} = 3.8 Hz, CH_2CO), 107.7 (d, J_{F-C} = 26.2 Hz, C-2), 111.3 (d, J_{F-C} = 21.2 Hz, C-4), 115.3 (d, J_{F-C} = 2.8 Hz, C-6), 130.5 (d, J_{F-C} = 9.2 Hz, C-5), 139.3 (d, J_{F-C} = 11 Hz, C-1), 163.4 (d, J_{F-C} = 243.1 Hz, C-3) and 168.1 (C=O).

[*N*-(3-Cyanophenyl)carbamoyl]ethylphosphonic acid 331e

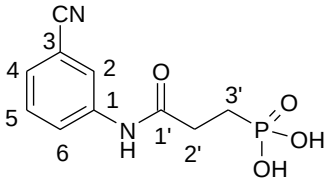

The procedure described for the synthesis of [*N*-(3-hydroxyphenyl)carbamoyl]ethyl phosphonic acid **331a** was employed, using diethyl [*N*-(3-cyanophenyl)carbamoyl]ethyl phosphonate **323e** (0.25 g, 0.81 mmol) in CH_3CN (3 mL) and trimethylsilyl bromide (0.22 mL, 1.6 mmol). The solvent was removed *in vacuo* and the residue chromatographed [preparative layer chromatography; elution with hexane-EtOAc-MeOH (1:1:1)] to yield *[N-(3-cyanophenyl)carbamoyl]ethylphosphonic acid* **331e** as a light yellow viscous liquid (0.12 g, 60 %); (Found: C, 47.19; H, 4.32; N, 11.12 %. $C_{10}H_{11}N_2O_4P$ requires C, 47.25; H, 4.36; N, 11.02 %); (0.10 g, 59 %); υ/cm^{-1} 3284 (OH), 2238 (C≡N), 1678 (C=O) and 1232 (P=O); δ_H/ppm (400 MHz; DMSO-d_6) 1.56 (2H, s, 2 x OH), 2.15 (2H, m, CH_2P), 2.72 (2H, m, CH_2CO), 7.33 (2H, m, 4-H and 6-H), 7.83 (1H, t, *J* = 8.0 Hz, 5-H), 7.96 (1H, t, *J* = 1.6 Hz, 2-H), and 9.03 (1H, s, NH); δ_C/ppm (100 MHz; DMSO-d_6) 20.7 (d, J_{P-C} = 142.5 Hz, CH_2P), 30.3 (d, J_{P-C} = 3.2 Hz, CH_2CO), 113.0 (C-3), 118.9 (C≡N), 122.9 (C-2) 124.1 (C-5), 127.3 (C-6), 129.8 (C-4), 139.8 (C-1) and 170.0 (C=O).

[*N*-(3-Nitrophenyl)carbamoyl]ethylphosphonic acid 331f

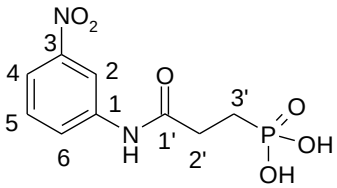

The procedure described for the synthesis of [*N*-(3-hydroxyphenyl)carbamoyl]ethyl phosphonic acid **331a** was employed, using diethyl [*N*-(3-nitrophenyl)carbamoyl]ethyl phosphonate **323f** (0.25 g, 0.76 mmol) in CH_3CN (3 mL) and trimethylsilyl bromide (0.14 mL, 1.5 mmol). The solvent was removed *in vacuo* and the residue chromatographed [preparative layer chromatography; elution with hexane-EtOAc-MeOH (1:1:0.5)] to yield *[*N*-(3-nitrophenyl)carbamoyl]ethylphosphonic acid* **331f** as a dark yellow gum (0.19 g, 71 %); (Found: C, 39.52; H, 4.10; N, 10.29 %. $C_9H_{11}N_2O_6P$ requires C, 39.43; H, 4.04; N, 10.22 %); υ/cm^{-1} 3229 (OH), 1664 (C=O) and 1239 (P=O); δ_H/ppm (400 MHz; DMSO-d_6) 2.12 (2H, m, CH_2P), 2.70 (2H, m, CH_2CO), 4.45 (2H, s, 2 x OH), 7.34 (1H, t, *J* = 8.2 Hz, 5-H), 7.78 (1H, dd, *J* = 8.0 and 1.6 Hz, 4-H), 8.10 (1H, dd, *J* = 8.0 and 1.6 Hz, 6-H), 8.30 (1H, t, *J* = 2.0 Hz, 2-H) and 9.62 (1H, s, NH); δ_C/ppm (100 MHz; DMSO-d_6) 20.8 (d, J_{P-C} = 142.9 Hz, CH_2P), 30.2 (d, J_{P-C} = 3.3 Hz, CH_2CO), 114.5 (C-2), 118.3 (C-4), 125.4 (C-6), 129.8 (C-5), 140.2 (C-1), 148.6 (C-3) and 170.2 (C=O).

_N_-[3-(Hydroxymethyl)phenylcarbamoyl]ethylphosphonic acid 331g

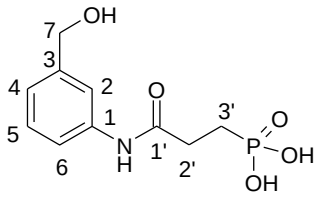

The procedure described for the synthesis of [*N*-(3-hydroxyphenyl)carbamoyl]ethyl phosphonic acid **331a** was employed, using diethyl {*N*-[3-(hydroxymethyl) phenyl]carbamoyl}ethylphosphonate **323g** (0.25 g, 0.79 mmol) in CH_3CN (3 mL) and trimethylsilyl bromide (0.21 mL, 1.6 mmol). The solvent was removed *in vacuo* and the residue chromatographed [preparative layer chromatography; elution with hexane-EtOAc-MeOH (1:1:1)] to yield *N-[3-(hydroxymethyl)phenylcarbamoyl]ethyl phosphonic acid* **331g** as a yellow viscous oil (0.14 g, 67 %); (Found: C, 46.41; H, 5.51; N, 5.38 %. $C_{10}H_{14}NO_5P$ requires C, 46.34; H, 5.44; N, 5.40 %); υ/cm^{-1} 3267 (OH), 1687 (C=O) and 1232 (P=O); δ_H/ppm (400 MHz; DMSO-d_6) 2.15 (2H, m, CH_2P), 2.77 (2H, m, CH_2CO), 4.51 (1H, s, OH), 5.14 (2H, s, CH_2OH), 7.12 (1H, d, *J* = 7.6 Hz, 4-H), 7.31 (1H, t, *J* = 8.0 Hz, 5-H), 7.51 (1H, d, 8.0 Hz, 6-H), 7.62 (1H, s, 2-H), 7.80 (2H, s, 2 x OH) and 8.06 (1H, s, NH); δ_C/ppm (100 MHz; DMSO-d_6) 20.8

(d, J_{P-C} = 142.5 Hz, CH_2P), 29.9 (d, J_{P-C} = 3.2 Hz, CH_2CO), 63.7 (CH_2OH), 118.6 (C-2), 119.4 (C-6), 122.5 (C-4), 129.8 (C-5), 139.0 (C-1), 139.8 (C-3) and 170.1 (C=O).

3.3.2.3. Synthesis of sodium hydrogen ethylphosphonate derivatives

Sodium hydrogen [*N*-(3-hydroxyphenyl)carbamoyl]ethylphosphonate 332a

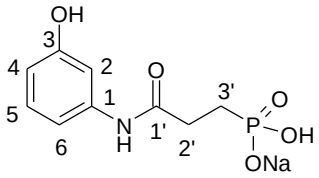

[N-(3-Hydroxyphenyl)carbamoyl]ethylphosphonic acid **331a** (0.15 g, 0.61 mmol) was treated with a solution of NaOH (1.1 mol) in EtOH (0.58 mL) and the mixture was stirred for 30 min. The solvent was removed *in vacuo* and the residue chromatographed [reverse-phase column chromatography; elution with H_2O-MeOH (1:1)] to yield *sodium hydrogen [*N*-(3-hydroxyphenyl)carbamoyl]ethylphosphonate* **332a** as a grey semi-solid (0.12 g, 89 %); υ/cm^{-1} 3267 (OH), 1671 (C=O) and 1231 (P=O); δ_H/ppm (400 MHz; D_2O) 2.13 (2H, m, CH_2P), 2.73 (2H, m, CH_2CO), 6.59 (1H, d, *J* = 8.2 Hz, 4-H), 6.90 (1H, d, *J* = 7.6 Hz, 6-H), 7.12 (1H, t, *J* = 8.2 Hz, 5-H) and 7.35 (1H, s, 2-H); δ_C/ppm (100 MHz; D_2O) 20.6 (d, J_{P-C} = 142.6 Hz, CH_2P), 28.0 (d, J_{P-C} = 3.6 Hz, CH_2CO), 107.2 (C-2), 110.8 (C-4), 111.7 (C-6), 129.5 (C-5), 139.8 (C-1), 158.2 (C-3) and 169.5 (d, J_{P-C} = 15.2 Hz, C=O).

Sodium hydrogen [*N*-(3-methoxyphenyl)carbamoyl]ethylphosphonate 332b

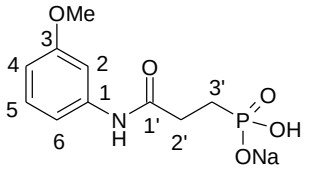

The procedure described for the synthesis of sodium hydrogen [*N*-(3-hydroxyphenyl)carbamoyl]ethylphosphonate **332a** was employed, using [*N*-(3-methoxyphenyl)carbamoyl]ethylphosphonic acid **331b** (0.15 g, 0.58 mmol) and a solution of NaOH (1.1 mol) in EtOH (0.55 mL). The solvent was removed *in vacuo* and the residue chromatographed [reverse-phase column chromatography; elution with H_2O-MeOH (1:1)] to yield *sodium hydrogen [*N*-(3-methoxyphenyl)carbamoyl]ethylphosphonate* **332b** as a pale yellow semi-solid (0.12 g, 91 %); υ/cm^{-1} 3184 (OH), 1677 (C=O) and 1232 (P=O); δ_H/ppm (400

MHz; D_2O) 2.13 (2H, m, CH_2P), 2.75 (2H, m, CH_2CO), 3.78 (3H, s, OCH_3), 6.62 (1H, dd, *J* = 6.3 and 2.0 Hz, 4-H), 7.11 (1H, d, *J* = 8.0 Hz, 6-H), 7.19 (1H, t, *J* = 8.0 Hz, 5-H) and 7.32 (1H, t, *J* = 2.0 H, 2-H); δ_C/ppm (100 MHz; D_2O) 20.8 (d, J_{P-C} = 142.2 Hz, CH_2P), 29.9 (d, J_{P-C} = 3.2 Hz, CH_2CO), 55.1 (OCH_3), 105.7 (C-2), 110.1 (C-4), 111.6 (C-6), 129.8 (C-5), 139.4 (C-1), 159.6 (C-3) and 169.5 (d, J_{P-C} = 15.6 Hz, C=O).

Sodium hydrogen [*N*-(3-bromophenyl)carbamoyl]ethylphosphonate 332c

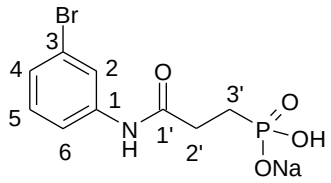

The procedure described for the synthesis of sodium hydrogen [*N*-(3-hydroxyphenyl)carbamoyl]ethylphosphonate **332a** was employed, using [*N*-(3-bromophenyl)carbamoyl]ethylphosphonic acid **331c** (0.15 g, 0.49 mmol) and a solution of NaOH (1.1 mol) in EtOH (0.46 mL). The solvent was removed *in vacuo* and the residue chromatographed [reverse-phase column chromatography; elution with H_2O-MeOH (1:1)] to yield *sodium hydrogen [*N*-(3-bromophenyl)carbamoyl]ethylphosphonate* **332c** as a brown semi-solid (0.11 g, 87 %); υ/cm^{-1} 3079 (OH), 1692 (C=O) and 1215 (P=O); δ_H/ppm (400 MHz; D_2O) 2.19 (2H, m, CH_2P), 2.71 (2H, m, CH_2CO), 7.22 (1H, t, *J* = 7.6 Hz, 5-H), 7.25 (1H, d, *J* = 8.0 Hz, 4-H), 7.56 (1H, d, *J* = 7.6 Hz, 6-H) and 7.81 (1H, s, 2-H); δ_C/ppm (100 MHz; D_2O) 20.8 (d, J_{P-C} = 142.5 Hz, CH_2P), 29.8 (d, J_{P-C} = 3.1 Hz, CH_2CO), 115.2 (C-6), 117.5 (C-3), 123.2 (C-2), 126.5 (C-4), 130.2 (C-5), 139.8 (C-1) and 170.0 (d, J_{P-C} = 15.2 Hz, C=O).

Sodium hydrogen [*N*-(3-fluorophenyl)carbamoyl]ethylphosphonate 332d

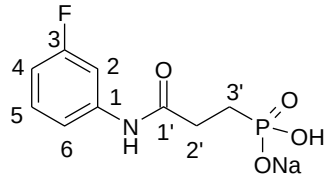

The procedure described for the synthesis of sodium hydrogen [*N*-(3-hydroxyphenyl)carbamoyl]ethylphosphonate **332a** was employed, using [*N*-(3-fluorophenyl)carbamoyl]ethylphosphonic acid **331d** (0.15 g, 0.61 mmol) and a solution of NaOH (1.1 mol) in EtOH (0.58 mL). The solvent was removed *in vacuo* and the residue

chromatographed [reverse-phase column chromatography; elution with H_2O-MeOH (1:1)] to yield *sodium hydrogen [*N-*(3-fluorophenyl)carbamoyl]ethylphosphonate* **332d** as a pale yellow semi-solid (0.14 g, 94 %); υ/cm^{-1} 3150 (OH), 1682 (C=O) and 1233 (P=O); δ_H/ppm (400 MHz; D_2O) 2.15 (2H, m, CH_2P), 2.65 (2H, m, CH_2CO), 6.80 (1H, td, *J* = 6.0, 2.0 and 1.6 Hz, 4-H), 7.15 (1H, dd, *J*= 6.2 and 2.0 Hz, 6-H), 7.25 (1H, ddd, *J* = 6.4, 2.0 and 1.6 Hz, 5-H) and 7.42 (1H, dt, *J* = 6.4 and 2.0 Hz, 2-H); δ_C/ppm (100 MHz; D_2O) 20.8 (d, J_{P-C} = 142.1 Hz, CH_2P), 30.0 (d, J_{P-C} = 3.6 Hz, CH_2CO), 107.8 (d, J_{F-C} = 26.2 Hz, C-2), 111.7 (d, J_{F-C} = 21.2 Hz, C-4), 115.1 (d, J_{F-C} = 2.6 Hz, C-6), 130.2 (d, J_{F-C} = 9.2 Hz, C-5), 139.8 (d, J_{F-C} = 10.8 Hz, C-1), 163.7 (d, J_{F-C} = 242.8 Hz, C-3) and 167.7 (C=O).

Sodium hydrogen [*N*-(3-cyanophenyl)carbamoyl]ethylphosphonate 332e

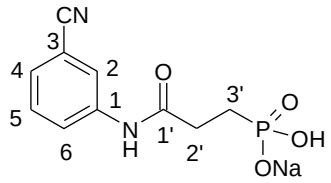

The procedure described for the synthesis of sodium hydrogen [*N*-(3-hydroxyphenyl)carbamoyl]ethylphosphonate **332a** was employed, using [*N*-(3-cyanophenyl)carbamoyl]ethylphosphonic acid **331e** (0.15 g, 0.59 mmol) and a solution of NaOH (1.1 mol) in EtOH (0.56 mL). The solvent was removed *in vacuo* and the residue chromatographed [reverse-phase column chromatography; elution with H_2O-MeOH (1:1)] to yield *sodium hydrogen [N-(3-cyanophenyl)carbamoyl]ethylphosphonate* **332e** as a pale yellow semi-solid (0.13 g, 96 %); υ/cm^{-1} 2236 (C≡N), 1655 (C=O) and 1214 (P=O); δ_H/ppm (400 MHz; D_2O) 2.12 (2H, m, CH_2P), 2.80 (2H, m, CH_2CO), 7.27 (2H, m, 4-H and 6-H), 7.79 (1H, t, *J* = 8.0 Hz, 5-H) and 7.93 (1H, t, *J* = 1.6 Hz, 2-H); δ_C/ppm (100 MHz; D_2O) 20.8 (d, J_{P-C} = 142.4 Hz, CH_2P), 29.9 (d, J_{P-C} = 3.2 Hz, CH_2CO), 112.6 (C-3), 118.2 (C≡N), 122.4 (C-2) 124.3 (C-5), 127.8 (C-6), 129.8 (C-4), 139.6 (C-1) and 169.9 (C=O).

Sodium hydrogen [*N*-(3-nitrophenyl)carbamoyl]ethylphosphonate 332f

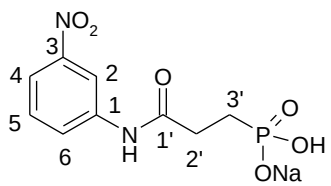

The procedure described for the synthesis of sodium hydrogen [*N*-(3-hydroxyphenyl)carbamoyl]ethylphosphonate **332a** was employed, using [*N*-(3-nitrophenyl)carbamoyl]ethylphosphonic acid **331f** (0.15 g, 0.55 mmol) and a solution of NaOH (1.1 mol) in EtOH (0.52 mL). The solvent was removed *in vacuo* and the residue chromatographed [reverse-phase column chromatography; elution with H_2O-MeOH (1:1)] to yield *sodium hydrogen [*N-*(3-nitrophenyl)carbamoyl]ethylphosphonate* **332f** as a yellow semi-solid (0.12 g, 91 %); υ/cm^{-1} 3143 (OH), 1670 (C=O) and 1218 (P=O); δ_H/ppm (400 MHz; D_2O) 2.17 (2H, m, CH_2P), 2.79 (2H, m, CH_2CO), 7.41 (1H, t, *J* = 8.4 Hz, 5-H), 7.85 (1H, dd, *J* = 8.2 and 1.6 Hz, 4-H), 8.12 (1H, dd, *J* = 8.0 and 1.6 Hz, 6-H) and 8.40 (1H, t, *J* = 2.0 Hz, 2-H); δ_C/ppm (100 MHz; D_2O) 20.9 (d, J_{P-C} = 142.8 Hz, CH_2P), 30.1 (d, J_{P-C} = 3.2 Hz, CH_2CO), 114.2 (C-2), 117.8 (C-4), 125.5 (C-6), 129.9 (C-5), 140.1 (C-1), 148.0 (C-3) and 170.2 (C=O).

Sodium hydrogen {*N*-[3-(hydroxymethyl)phenyl]carbamoyl}ethylphosphonate 332g

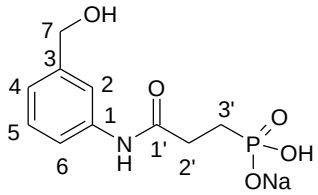

The procedure described for the synthesis of sodium hydrogen [*N*-(3-hydroxyphenyl)carbamoyl]ethylphosphonate **332a** was employed, using [*N*-(3-(hydroxymethyl)phenylcarbamoyl]ethylphosphonic acid **331g** (0.15 g, 0.58 mmol) and a solution of NaOH (1.1 mol) in EtOH (0.55 mL). The solvent was removed *in vacuo* and the residue chromatographed [reverse-phase column chromatography; elution with H_2O-MeOH (1:1)] to yield *sodium hydrogen {*N-*[3-(hydroxymethyl)phenyl]carbamoyl}ethylphosphonate* **332g** as a light yellow semi-solid (0.12 g, 89 %); υ/cm^{-1} 3198 (OH), 1653 (C=O) and 1230 (P=O); δ_H/ppm (400 MHz; D_2O) 2.18 (2H, m, CH_2P), 2.80 (2H, m, CH_2CO), 4.86 (2H, s, CH_2OH), 7.08 (1H, d, *J* = 7.6 Hz, 4-H), 7.28 (1H, t, *J* = 8.0 Hz, 5-H), 7.44 (1H, d, 8.0 Hz, 6-H) and 7.58 (1H, s, 2-H); δ_C/ppm (100 MHz; D_2O) 20.7 (d, J_{P-C} = 142.3 Hz, CH_2P), 29.8 (d, J_{P-C} = 3.2 Hz, CH_2CO), 63.5 (CH_2OH), 118.2 (C-2), 119.7 (C-6), 123.4 (C-4), 130.4 (C-5), 139.6 (C-1), 139.5 (C-3) and 169.5 (C=O).

3.3.3. Reaction of 3-substituted anilines with 4-chlorobutanoyl chloride

4-Chloro-*N*-(3-hydroxyphenyl)butanamide 324a

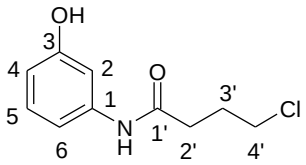

To a stirred solution of 3-aminophenol (1.50 g, 14.0 mmol) in THF (30 mL) under nitrogen was added NaH (60 % dispersion in mineral oil; 0.60 g, 24 mmol) in small portions to permit controlled evolution of hydrogen. 4-Chlorobutanoyl chloride (1.18 mL, 14.0 mmol) was then added through a septum and the resulting solution was stirred for *ca.* 6 h. The solvent was evaporated *in vacuo* and the residue dissolved in EtOAc (2 x 50 mL). The organic solution was washed sequentially with satd. aq. $NaHCO_3$ (2 × 100 mL), water (2 x 100 mL) and brine (2 × 100 mL). The aqueous washings were extracted with EtOAc and the combined organic solutions were dried (anhydr. $MgSO_4$). Evaporation of the solvent *in vacuo* afforded *4-chloro*-N-*(3-hydroxyphenyl)butanamide* **324a** as a brown solid (2.15 g, 71 %) m.p. 88-90 °C; (Found: $\mathbf{M^+}$, 213.05711 $C_{10}H_{12}ClNO_2$ requires: $\mathbf{M^+}$, 213.05566); υ/cm^{-1} 3176 (OH) and 1662 (C=O); δ_H/ppm (400 MHz; $CDCl_3$) 2.17 (2H, m, 3'-CH_2), 2.73 (2H, t, *J* = 6.8 Hz, CH_2CO), 3.59 (2H, t, *J* = 6.4 Hz, CH_2Cl), 6.45 (1H, dd, *J* = 6.0 and 2.0 Hz, 4-H), 6.51 (1H, dd, *J* = 6.0 and 2.4 Hz, 6-H), 6.97 (1H, t, *J* = 8.0 Hz, 5-H), 7.48 (1H, t, *J* = 1.2 Hz, 2-H), 7.65 (1H, s, OH) and 7.69 (1H, s, NH); δ_C/ppm (100 MHz; $CDCl_3$) 26.8 (C-3), 33.1 (CH_2CO), 44.2 (CH_2Cl), 106.4 (C-2), 109.4 (C-4), 111.2 (C-6), 129.7 (C-5), 139.8 (C-1), 158.2 (C-3) and 166.7 (C=O).

4-Chloro-*N*-(3-methoxyphenyl)butanamide 324b

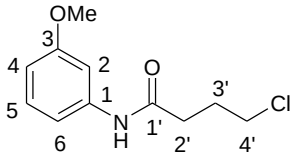

The procedure described for the synthesis of 4-chloro-*N*-(3-hydroxyphenyl)butanamide **324a** was employed, using 3-methoxyaniline (0.91 mL, 8.1 mmol), NaH (60 % dispersion in mineral oil; 0.36 g, 15 mmol) and 4-chlorobutanoyl chloride (0.68 mL, 8.1 mmol) in THF (15 mL), to yield 4-chloro-*N*-(3-methoxyphenyl)butanamide **324b** as a yellow solid (1.38 g, 75 %) m.p 56-58°C (Lit.[243] 50-54 °C); υ/cm^{-1} 1687 (C=O); δ_H/ppm (400 MHz; $CDCl_3$) 2.17 (2H, m, 3'-

CH_2), 2.54 (2H, t, *J* = 6.8 Hz, CH_2CO), 3.65 (2H, t, *J* = 6.0 Hz, CH_2Cl), 3.79 (3H, s, OCH_3), 6.65 (1H, dd, *J* = 6.4 and 1.6 Hz, 4-H), 6.95 (1H, d, *J* = 7.6 Hz, 6-H), 7.19 (1H, t, *J* = 8.0 Hz, 5-H), 7.29 (1H, s, NH) and 7.32 (1H, t, *J* = 2.0 Hz, 2-H); δ_C/ppm (100 MHz; $CDCl_3$) 26.7 (C-3'), 36.7 (CH_2CO), 44.4 (CH_2Cl), 55.2 (OCH_3), 105.2 (C-2), 110.7 (C-6), 111.8 (C-4), 129.8 (C-5), 135.2 (C-1), 160.2 (C-3) and 171.2 (C=O).

_N_-(3-Bromophenyl) 4-chlorobutanamide 324c

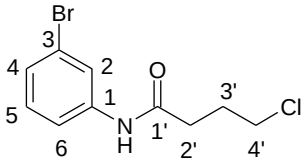

The procedure described for the synthesis of 4-chloro-*N*-(3-hydroxyphenyl)butanamide **324a** was employed, using 3-bromoaniline (0.63 mL, 5.8 mmol), NaH (60 % dispersion in mineral oil; 0.26 g, 11 mmol) and 4-chlorobutanoyl chloride (0.48 mL, 5.8 mmol) in THF (15 mL), to yield *N-(3-bromophenyl)4-chlorobutanamide* **324c** as a brown solid (1.15 g, 72 %), m.p 85-87 °C; (Found: $\mathbf{M}^+$, 275.00328 $C_{10}H_{11}BrClNO$ requires: $\mathbf{M}^+$, 274.97125); υ/cm^{-1} 1691 (C=O); δ_H/ppm (400 MHz; $CDCl_3$) 2.18 (2H, m, 3'-CH_2), 2.55 (2H, t, *J* = 6.8 Hz, CH_2CO), 3.64 (2H, t, *J* = 6.4 Hz, CH_2Cl), 7.16 (1H, t, *J* = 8.0 Hz, 5-H), 7.22 (1H, d, *J* = 8.0 Hz, 4-H), 7.37 (1H, d, *J* = 8.0 Hz, 6-H), 7.40 (1H, s, 2-H), and 7.77 (1H, s, NH); δ_C/ppm (100 MHz; $CDCl_3$) 26.8 (C-3'), 33.4 (CH_2CO), 44.6 (CH_2Cl), 118.5 (C-6), 122.2 (C-3), 123.6 (C-2), 127.8 (C-4), 129.9 (C-5), 137.8 (C-1) and 164.1 (C=O).

4-Chloro-_N_-(3-fluorophenyl)butanamide 324d

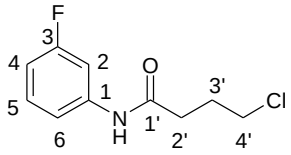

The procedure described for the synthesis of 4-chloro-*N*-(3-hydroxyphenyl)butanamide **324a** was employed, using 3-fluoroaniline (1.05 mL, 5.8 mmol), NaH (60 % dispersion in mineral oil; 0.26 g, 11 mmol) and 4-chlorobutanoyl chloride (0.48 mL, 5.8 mmol) in THF (15 mL), to yield 4-chloro-*N*-(3-fluorophenyl)butanamide **324d** as a yellow solid (0.84 g, 68 %), m.p 62.64 °C (Lit.[244] 55-56 ^oC); υ/cm^{-1} 1681 (C=O); δ_H/ppm (400 MHz; $CDCl_3$) 2.18 (2H, m, 3'-CH_2), 2.55 (2H, t, *J* = 7.2 Hz, CH_2CO), 3.64 (2H, t, *J* = 6.0 Hz, CH_2Cl), 6.78 (1H, ddd, *J* = 6.4, 2.4 and 1.2 Hz, 4-H), 7.12 (1H, dd, *J* = 8.4 and 2.0 Hz, 6-H), 7.25 (1H, dt, *J* = 6.8 and 1.6 Hz, 5-H),

7.48 (1H, td, *J* = 6.4, 2.0 and 1.2 Hz, 2-H) and 9.41 (1H, s, NH); δ_C/ppm (100 MHz; $CDCl_3$) 26.8 (C-3'), 33.6 (CH_2CO), 44.2 (CH_2Cl), 107.4 (d, J_{F-C} = 26.2 Hz, C-2), 111.2 (d, J_{F-C} = 21.2 Hz, C-4), 114.8 (C-6), 130.0 (d, J_{F-C} = 9.5 Hz, C-5), 139.3 (d, J_{F-C} = 10.8 Hz, C-1), 162.9 (d, J_{F-C} = 242.8 Hz, C-3) and 169.9 (C=O).

4-Chloro-*N*-(3-cyanophenyl)butanamide 324e

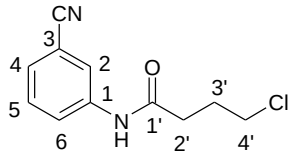

The procedure described for the synthesis of 4-chloro-*N*-(3-hydroxyphenyl)butanamide **324a** was employed, using 3-aminobenzonitrile (1.20 g, 10.1 mmol), NaH (60 % dispersion in mineral oil; 0.54 g, 23 mmol) and 4-chlorobutanoyl chloride (0.84 mL, 10 mmol) in THF (15 mL), to yield 4-chloro-*N*-(3-cyanophenyl)butanamide **324e** as a yellow solid (2.00 g, 89 %), m.p 84-86 °C (Lit.[244] 87-88 °C); υ/cm^{-1} 2230 (C≡N), 1663 (C=O); δ_H/ppm (400 MHz; $CDCl_3$) 2.18 (2H, m, 3'-CH_2), 2.59 (2H, t, *J* = 7.2 Hz, CH_2CO), 3.65 (2H, t, *J* = 6.4 Hz, CH_2Cl), 7.39 (2H, m, 4-H and 6-H), 7.62 (1H, s, NH), 7.70 (1H, t, *J* = 7.6 Hz, 5-H) and 7.94 (1H, t, *J* = 2.0 Hz, 2-H); δ_C/ppm (100 MHz; $CDCl_3$) 27.6 (C-3'), 34.0 (CH_2CO), 44.3 (CH_2Cl), 112.9 (C-3), 118.5 (C=N), 122.6 (C-2), 123.8 (C-5), 127.7 (C-6), 129.9 (C-4), 138.6 (C-1) and 170.4 (C=O).

4-Chloro-*N*-(3-nitrophenyl)butanamide 324f

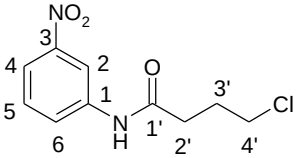

The procedure described for the synthesis of 4-chloro-*N*-(3-hydroxyphenyl)butanamide **324a** was employed, using 3-nitroaniline (1.01 g, 7.27 mmol), NaH (60 % dispersion in mineral oil; 0.33 g, 13 mmol) and 4-chlorobutanoyl chloride (0.61 mL, 7.3 mmol) in THF (15 mL), to yield 4-chloro-*N*-(3-nitrophenyl)butanamide **324f** as a dark yellow solid (1.55 g, 88 %), m.p 78-80 °C (Lit.[245] 82 °C); (Found: $\mathbf{M}^+$, 242.04819 $C_{10}H_{11}ClN_2O_3$ requires: $\mathbf{M}^+$, 242.04582); υ/cm^{-1} 1675 (C=O); δ_H/ppm (400 MHz; $CDCl_3$) 2.21 (2H, m, 3'-CH_2), 2.66 (2H, t, *J* = 8.0 Hz, CH_2CO), 3.92 (2H, t, *J* = 6.8 Hz, CH_2Cl), 7.52 (1H, t, *J* = 8.4 Hz, 5-H), 7.98 (1H, dd, *J* = 6.8 and 1.2 Hz, 4-H), 8.20 (1H, dd, *J* = 6.8 and 1.2 Hz, 6-H), 8.34 (1H, t, *J* = 2.0 Hz, 2-H) and

8.55 (1H, s, NH); δ_C/ppm (100 MHz; $CDCl_3$) 17.8 (C-3'), 32.6 (CH_2CO), 48.5 (CH_2Cl), 113.7 (C-2), 118.8 (C-4), 125.4 (C-6), 129.6 (C-5), 140.4 (C-1), 148.5 (C-3) and 174.6 (C=O).

4-Chloro-*N*-[3-(hydroxymethyl)phenyl]butanamide 324g

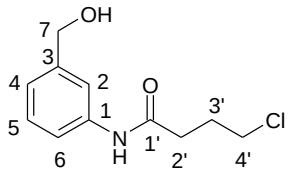

The procedure described for the synthesis of 4-chloro-*N*-(3-hydroxyphenyl)butanamide **324a** was employed, using 3-aminobenzylalcohol (1.02 g, 8.12 mmol), NaH (60 % dispersion in mineral oil; 0.52 g, 21 mmol) and 4-chlorobutanoyl chloride (0.68 mL, 8.1 mmol) in THF (15 mL), to yield *4-chloro*-N-*[3-(hydroxymethyl)phenyl]butanamide* **324g** as a light yellow solid (1.35 g, 73 %), m.p 80-82 °C; (Found: $\mathbf{M^+}$, 227.07341 $C_{11}H_{14}ClNO_2$ requires: $\mathbf{M^+}$, 227.07131); υ/cm^{-1} 1678 (C=O); δ_H/ppm (400 MHz; $CDCl_3$) 2.16 (2H, m, 3'-CH_2), 2.52 (2H, t, *J* = 7.6 Hz, CH_2CO), 3.62 (2H, t, *J* = 6.4 Hz, CH_2Cl), 4.62 (2H, s, 7-CH_2), 7.02 (1H, d, *J* = 7.2 Hz, 4-H), 7.27 (1H, t, *J* = 8.0 Hz, 5-H), 7.46 (1H, d, *J* = 8.4 Hz, 6-H), 7.56 (1H, s, 2-H), 7.62 (1H, s, OH) and 10.3 (1H, s, NH); δ_C/ppm (100 MHz; $CDCl_3$) 26.8 (C-3'), 33.6 (CH_2CO), 43.5 (CH_2Cl), 62.7 (CH_2OH), 117.3 (C-2), 117.6 (C-6), 121.7 (C-4), 128.4 (C-5), 138.3 (C-1), 143.3 (C-3) and 164.5 (C=O).

3.3.3.1. Synthesis of diethyl propylphosphonates using Michaelis-Arbuzov methodology

Diethyl [*N*-(3-hydroxyphenyl)carbamoyl]propylphosphonate 325a

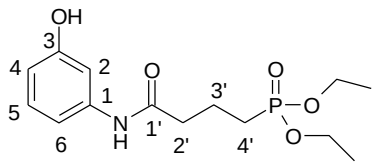

Triethyl phosphite (0.81 mL, 4.6 mmol) was added through a septum to 4-chloro-*N*-(3-hydroxyphenyl)butanamide **324a** (0.50 g, 2.3 mmol) under nitrogen in an oven-dried round-bottomed flask equipped with a reflux condenser, and the resulting mixture was refluxed for *ca.* 9 h during which time the reaction was monitored by TLC. The cooled mixture was then stirred with hexane (20 mL) for *ca.* 30 minutes followed by decantation of the hexane layer

to remove the excess triethyl phosphite; this was repeated three times. The crude product was purified by flash chromatography [on silica gel; elution with hexane-EtOAc (4:1)], and subsequent evaporation of the solvent *in vacuo* afforded *diethyl [*N*(3-hydroxyphenyl)carbamoyl)]propylphosphonate* **325a** as yellow oil (0.31 g, 65 %); (Found: **M**$^{+}$, 315.12483 $C_{14}H_{22}NO_5P$ requires: **M**$^{+}$, 315.12356); υ/cm^{-1} 3308 (OH), 1678 (C=O), 1224 (P=O) and 1012 (P−OEt); δ_H/ppm (400 MHz; $CDCl_3$) 1.31 (6H, t, *J* = 7.2 Hz, 2 × CH_3), 2.16 (4H, m, 3'-CH_2 and CH_2P), 2.68 (2H, m, CH_2CO), 4.09 (4H, m, 2 × OCH_2), 6.60 (1H, d, *J* = 8.0 Hz, 4-H), 6.91 (1H, d, *J* = 7.6 Hz, 6-H), 7.10 (1H, t, *J* = 8.0 Hz, 5-H), 7.36 (1H, s, 2-H), 8.44 (1H, s, OH) and 8.92 (1H, s, NH); δ_C (100 MHz; $CDCl_3$) 16.3 (d, J_{P-C} = 6.0 Hz, 2 × CH_3), 18.3 (d, J_{P-C} = 15.2 Hz, C-3'), 26.8 (d, J_{P-C} = 136.2 Hz, CH_2P), 36.5 (d, J_{P-C} = 3.2 Hz, CH_2CO), 62.3 (d, J_{P-C} = 6.5 Hz, 2 × OCH_2), 107.5 (C-2), 111.3 (C-4), 112.3 (C-6), 129.1 (C-5), 138.9 (C-1), 157.7 (C-3) and 166.3 (C=O).

Diethyl [*N*-(3-methoxyphenyl)carbamoyl]propylphosphonate 325b

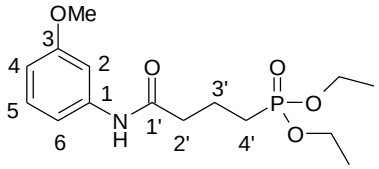

The procedure described for the synthesis of diethyl [*N*-(3-hydroxyphenyl)carbamoyl]propylphosphonate **325a** was employed, using 4-chloro-*N*-(3-methoxyphenyl)butanamide **324b** (0.50 g, 2.2 mmol) and triethyl phosphite (0.76 mL, 4.3 mmol). The crude product was purified by flash chromatography [on silica gel; elution with hexane-EtOAc (4:1)], and subsequent evaporation of the solvent *in vacuo* afforded *diethyl [*N*-(3-methoxyphenyl)carbamoyl]propylphosphonate* **325b** as a clear oil (0.32 g, 66 %); (Found: **M**$^{+}$, 329.14251 $C_{15}H_{24}NO_5P$ requires: **M**$^{+}$, 329.13921). υ/cm^{-1} 1678 (C=O), 1251 (P=O) and 1039 (P−OEt); δ_H/ppm (400 MHz; $CDCl_3$) 1.32 (6H, t, *J* = 6.8 Hz, 2 × CH_3), 2.17 (2H, m, CH_2P), 2.70 (2H, m, 3'-CH_2), 3.08 (2H, t, *J* = 4.8 Hz, CH_2CO), 3.77 (3H, s, OCH_3), 4.10 (4H, m, 2 × OCH_2), 6.62 (1H, d, *J* = 6.4 Hz, 4-H), 7.06 (1H, d, *J* = 8.0 Hz, 6-H), 7.16 (1H, t, *J* = 8.4 Hz, 5-H), 7.35 (1H, s, 2-H) and 9.00 (1H, s, NH); δ_C (100 MHz; $CDCl_3$) 16.3 (d, J_{P-C} = 6.5 Hz, 2 × CH_3), 18.1 (d, J_{P-C} = 15.6 Hz, C-3'), 26.7 (d, J_{P-C} = 142.1 Hz, CH_2P), 36.3 (d, J_{P-C} = 3.1 Hz, CH_2CO), 55.3 (OCH_3), 62.4 (d, J_{P-C} = 6.6 Hz, 2 × OCH_2), 105.3 (C-2), 109.5 (C-4), 112.1 (C-6), 129.8 (C-5), 139.8 (C-1), 159.7 (C-3) and 169.4 (C=O).

Diethyl [*N*-(3-bromophenyl)carbamoyl]propylphosphonate 325c

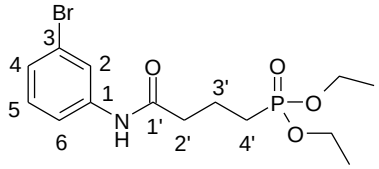

The procedure described for the synthesis of diethyl [*N*-(3-hydroxyphenyl)carbamoyl]propylphosphonate **325a** was employed, using 4-chloro-*N*-(3-bromophenyl)butanamide **324c** (0.50 g, 1.8 mmol) and triethyl phosphite (0.62 mL, 3.6 mmol). The crude product was purified by flash chromatography [on silica gel; elution with hexane-EtOAc (3:1)], and subsequent evaporation of the solvent *in vacuo* afforded *diethyl [*N*-(3-bromophenyl)carbamoyl]propylphosphonate* **325c** as a brown oil (0.30 g, 63 %); (Found: $\mathbf{M}^+$, 377.04215 $C_{14}H_{21}BrNO_4P$ requires: $\mathbf{M}^+$, 377.03916. υ/cm^{-1} 1681 (C=O), 1232 (P=O) and 1019 (P−OEt); δ_H/ppm (400 MHz; $CDCl_3$) 1.32 (6H, t, *J* = 6.8 Hz, 2 × CH_3), 1.80 (2H, m, CH_2P), 2.17 (2H, m, 3'-CH_2), 2.71 (2H, t, *J* = 7.6 Hz, CH_2CO), 4.11 (4H, m, 2 × OCH_2), 6.79 (1H, t, *J* = 7.6 Hz, 5-H), 7.23 (2H, m, 4-H and 6-H), 7.48 (1H, t, *J* = 7.6 Hz, 5-H), 7.61 (1H, s, 2-H) and 8.88 (1H, s, NH); δ_C (100 MHz; $CDCl_3$) 16.4 (d, J_{P-C} = 6.1 Hz, 2 × CH_3), 18.2 (d, J_{P-C} = 15.1 Hz, C-3'), 27.2 (d, J_{P-C} = 142.2 Hz, CH_2P), 36.7 (d, J_{P-C} = 3.2 Hz, CH_2CO), 62.4 (d, J_{P-C} = 6.0 Hz, 2 × OCH_2), 118.1 (C-6), 122.6 (C-3), 123.1 (C-2), 126.7 (C-4), 130.0 (C-5), 139.8 (C-1) and 168.8 (C=O).

Diethyl [*N*-(3-fluorophenyl)carbamoyl]propylphosphonate 325d

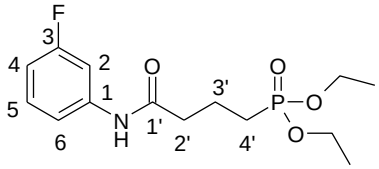

The procedure described for the synthesis of diethyl [*N*-(3-hydroxyphenyl)carbamoyl]propylphosphonate **325a** was employed, using 4-chloro-*N*-(3-fluorophenyl)butanamide **324d** (0.50 g, 2.3 mmol) and triethyl phosphite (0.80 mL, 4.6 mmol). The crude product was purified by flash chromatography [on silica gel; elution with hexane-EtOAc (3:1)], and subsequent evaporation of the solvent *in vacuo* afforded *diethyl [*N*-(3-fluorophenyl)carbamoyl]propylphosphonate* **325d** as a clear oil (0.25 g, 54 %); (Found: $\mathbf{M}^+$, 317.12162 $C_{14}H_{21}FNO_4P$ requires: $\mathbf{M}^+$, 317.11922); υ/cm^{-1} 1684 (C=O), 1233 (P=O) and

1021 (P−OEt); δ_H/ppm (400 MHz; $CDCl_3$) 1.29 (6H, t, *J* = 7.2 Hz, 2 × CH_3), 1.79 (2H, m, CH_2P), 2.18 (2H, m, 3'-CH_2), 2.71 (2H, t, *J* = 6.8 Hz, CH_2CO), 4.10 (4H, m, 2 × OCH_2), 6.79 (1H, dd, *J* = 6.4, 2.4 and 1.6 Hz, 4-H), 7.17 (1H, dd, *J* = 6.4 and 2.0 Hz, 6-H), 7.23 (1H, td, *J* = 6.4, 2.8 and 1.6 Hz, 5-H) 7.52 (1H, dt, *J* = 2.4 and 1.6 Hz, 2-H) and 8.21 (1H, s, NH); δ_C (100 MHz; $CDCl_3$) 16.3 (d, J_{P-C} = 6.1 Hz, 2 × CH_3), 17.9 (d, J_{P-C} = 15.6 Hz, C-3'), 26.8 (d, J_{P-C} = 143.9 Hz, CH_2P), 36.5 (d, J_{P-C} = 3.2 Hz, CH_2CO), 62.4 (d, J_{P-C} = 6.6 Hz, 2 × OCH_2), 107.6 (d, J_{F-C} = 26.2 Hz, C-2), 111.3 (d, J_{F-C} = 21.2 Hz, C-4), 115.4 (d, J_{F-C} = 2.8 Hz, C-6), 130.1 (d, J_{F-C} = 9.0 Hz, C-5), 138.9 (d, J_{F-C} = 10.8 Hz, C-1), 162.7 (d, J_{F-C} = 242.7 Hz, C-3) and 164.5 (C=O).

Diethyl [*N*-(3-cyanophenyl)carbamoyl]propylphosphonate 325e

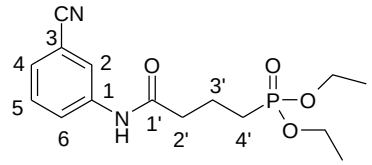

The procedure described for the synthesis of diethyl [*N*-(3-hydroxyphenyl)carbamoyl]propyl phosphonate **325a** was employed, using 4-chloro-*N*-(3-cyanophenyl)butanamide **324e** (0.50 g, 2.3 mmol) and triethyl phosphite (0.77 mL, 4.5 mmol). The crude product was purified by flash chromatography [on silica gel; elution with hexane-EtOAc (3:1)], and subsequent evaporation of the solvent *in vacuo* afforded *diethyl [*N*-(3-cyanophenyl) carbamoyl]propylphosphonate* **325e** as a clear oil (0.28 g, 61 %). (Found: $\mathbf{M}^+$, 324.12408 $C_{15}H_{21}N_2O_4P$ requires: $\mathbf{M}^+$, 324.12389); υ/cm^{-1} 2218 (C≡N), 1652 (C=O), 1219 (P=O) and 1046 (P−OEt); δ_H/ppm (400 MHz; $CDCl_3$) 1.33 (6H, t, *J* = 7.2 Hz, 2 × CH_3), 1.81 (2H, m, CH_2P), 2.18 (2H, m, 3'-CH_2), 2.73 (2H, t, *J* = 7.2 Hz, CH_2CO), 4.12 (4H, m, 2 × OCH_2), 7.35 (2H, m, 4-H and 6-H), 7.83 (1H, t, *J* = 8.4 Hz, 5-H), 7.95 (1H, t, *J* = 1.6 Hz, 2-H), and 9.83 (1H, s, NH); δ_C (100 MHz; $CDCl_3$) 16.4 (d, J_{P-C} = 6.1 Hz, 2 × CH_3), 18.2 (d, J_{P-C} = 15.6 Hz, C-3'), 26.8 (d, J_{P-C} = 144.0 Hz, CH_2P), 36.8 (d, J_{P-C} = 3.4 Hz, CH_2CO), 62.4 (d, J_{P-C} = 6.6 Hz, 2 × OCH_2), 112.8 (C-3), 118.6 (C≡N), 122.5 (C-2) 124.1 (C-5), 127.3 (C-6), 129.8 (C-4), 139.4 (C-1) and 172.2 (C=O).

Diethyl [*N*-(3-nitrophenyl)carbamoyl]propylphosphonate 325f

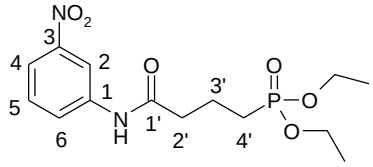

The procedure described for the synthesis of diethyl [*N*-(3-hydroxyphenyl)carbamoyl]propyl phosphonate **325a** was employed, using 4-chloro-*N*-(3-nitrophenyl)butanamide **324f** (0.50 g, 2.1 mmol) and triethyl phosphite (0.72 mL, 4.1 mmol). The crude product was purified by flash chromatography [on silica gel; elution with hexane-EtOAc (3:1)], and subsequent evaporation of the solvent *in vacuo* afforded *diethyl[*N-*(3-nitrophenyl)carbamoyl]propyl phosphonate* **325f** as a yellow oil (0.35 g, 74 %); (Found: $\mathbf{M}^+$, 344.11837 $C_{14}H_{21}N_2O_6P$ requires: $\mathbf{M}^+$, 344.11372); υ/cm^{-1} 1683 (C=O), 1218 (P=O) and 1028 (P−OEt); δ_H/ppm (400 MHz; $CDCl_3$) 1.34 (6H, t, *J* = 7.2 Hz, 2 × CH_3), 1.80 (2H, m, CH_2P), 2.19 (2H, m, 3'-CH_2), 2.75 (2H, t, *J* = 7.6 Hz, CH_2CO), 4.16 (4H, m, 2 × OCH_2), 7.46 (1H, t, *J* = 8.4 Hz, 5-H), 7.91 (1H, dd, *J* = 8.0 and 1.6 Hz, 4-H), 8.15 (1H, dd, *J* = 8.4 and 1.6 Hz, 6-H), 8.39 (1H, t, *J* = 2.0 Hz, 2-H) and 9.24 (1H, s, NH); δ_C (100 MHz; $CDCl_3$) 16.8 (d, J_{P-C} = 5.9 Hz, 2 × CH_3), 18.2 (d, J_{P-C} = 15.6 Hz, C-3'), 33.7 (d, J_{P-C} = 131.4 Hz, CH_2P), 48.9 (d, J_{P-C} = 2.8 Hz, CH_2CO), 62.0 (d, J_{P-C} = 6.5 Hz, 2 × OCH_2), 114.2 (C-2), 119.2 (C-4), 125.8 (C-6), 130.1 (C-5), 140.9 (C-1), 148.9 (C-3) and 175.1 (C=O).

Diethyl {*N*-[3-(hydroxymethyl)phenyl]carbamoyl}propylphosphonate 325g

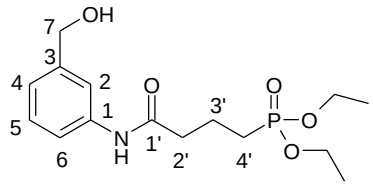

The procedure described for the synthesis of diethyl [*N*-(3-hydroxyphenyl)carbamoyl]propylphosphonate **325a** was employed, using 4-chloro-*N*-[3-(hydroxymethyl)phenyl]butanamide **324g** (0.50 g, 2.2 mmol) and triethyl phosphite (0.75 mL, 4.4 mmol). The crude product was purified by flash chromatography [on silica gel; elution with hexane-EtOAc (4:1)], and subsequent evaporation of the solvent *in vacuo* afforded *diethyl {*N-*[3-(hydroxymethyl)phenyl]carbamoyl}propylphosphonate* **325g** as a clear oil (0.31 g, 66 %); (Found: $\mathbf{M}^+$, 329.14287 $C_{15}H_{24}NO_5P$ requires: $\mathbf{M}^+$, 329.13921); υ/cm^{-1} 3173 (OH), 1676 (C=O), 1236 (P=O) and 1048 (P−OEt); δ_H/ppm (400 MHz; $CDCl_3$) 1.32 (6H, t, *J* = 6.8 Hz, 2 × CH_3), 1.79 (2H, m, CH_2P), 2.17 (2H, m, 3'-CH_2), 2.77 (2H, t, *J* = 6.8 Hz, CH_2CO), 4.12 (4H, m, 2 × OCH_2), 4.48 (2H, s, CH_2OH), 5.08 (1H, s, OH), 7.10 (1H, d, *J* = 7.6 Hz, 4-H), 7.27 (1H, t, *J* = 8.0 Hz, 5-H), 7.45 (1H, d, *J* = 8.0 Hz, 6-H), 7.53 (1H, s, 2-H) and 8.61 (1H, s, NH); δ_C

(100 MHz; $CDCl_3$) 16.3 (d, $J_{P–C}$ = 6.1 Hz, 2 × CH_3), 18.2 (d, $J_{P–C}$ = 15.2 Hz, C-3'), 26.8 (d, $J_{P–C}$ = 138.9 Hz, CH_2P), 36.8 (d, $J_{P–C}$ = 3.1 Hz, CH_2CO), 62.2 (d, $J_{P–C}$ = 6.5 Hz, OCH_2), 63.4 (CH_2OH), 118.1 (C-2), 118.9 (C-6), 122.8 (C-4), 129.4 (C-5), 138.9 (C-1), 139.8 (C-3) and 172.3 (C=O).

3.3.3.2. Synthesis of propylphosphonic acids derivatives using TMSBr

[*N*-(3-Hydroxyphenyl)carbamoyl]propylphosphonic acid 333a

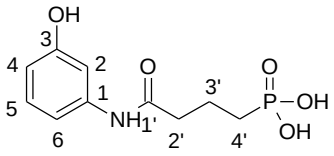

Trimethylsilyl bromide (0.21 mL, 1.6 mmol) was added to diethyl [*N*-(3-hydroxyphenyl)-carbamoyl]propylphosphonate **325a** (0.25 g, 0.79 mmol) in CH_3CN (3 mL) and the mixture was heated in the microwave apparatus set to deliver 100 W of power, with a reaction temperature of 60 ^oC and reaction time of 10 min. After completion, the mixture was cooled to room temperature, treated with a 95:5 MeOH-H_2O mixture and stirred for 30 min. The solvent was removed *in vacuo* and the residue chromatographed [preparative layer chromatography; elution with hexane-EtOAc-MeOH (1:1.5:1)] to yield *[*N-*(3-hydroxyphenyl)carbamoyl]propylphosphonic acid* **333a** as a yellow oil (0.10 g, 63 %); (Found: C, 46.47; H, 5.60; N, 5.47 %. $C_{10}H_{14}NO_5P$ requires C, 46.34; H, 5.44; N, 5.40 %); υ/cm^{-1} 3073 (OH), 1681 (C=O) and 1228 (P=O); δ_H/ppm (400 MHz; DMSO-d_6) 2.17 (4H, m, 3'-CH_2 and CH_2P), 2.70 (2H, m, CH_2CO), 3.27 (2H, s, OH), 6.62 (1H, d, *J* = 8.0 Hz, 4-H), 6.87 (1H, d, *J* = 7.6 Hz, 6-H), 7.12 (1H, t, *J* = 8.0 Hz, 5-H), 7.35 (1H, s, 2-H) and 8.34 (1H, s, NH); δ_C/ppm (100 MHz; DMSO-d_6) 18.0 (d, $J_{P–C}$ = 15.6 Hz, C-3'), 27.2 (d, $J_{P–C}$ = 141.7 Hz, CH_2P), 36.2 (d, $J_{P–C}$ = 3.3 Hz, CH_2CO), 108.2 (C-2), 111.8 (C-4), 112.5 (C-6), 130.2 (C-5), 139.8 (C-1), 158.4 (C-3) and 165.7 (C=O).

[*N*-(3-Methoxyphenyl)carbamoyl]propylphosphonic acid 333b

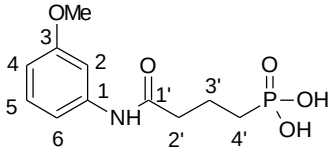

The procedure described for the synthesis of [*N*-(3-hydroxyphenyl)carbamoyl]propyl phosphonic acid **333a** was employed, using diethyl [*N*-(3-methoxyphenyl)carbamoyl]propyl phosphonate **325b** (0.25 g, 0.76 mmol) in CH_3CN (3 mL) and trimethylsilyl bromide (0.20 mL, 1.5 mmol). The solvent was removed *in vacuo* and the residue chromatographed [preparative layer chromatography; elution with hexane-EtOAc-MeOH (1:1:1)] to yield *[N-(3-methoxyphenyl)carbamoyl]propylphosphonic acid* **333b** as a yellow oil (0.11 g, 61 %); (Found: C, 48.51; H, 6.01; N, 5.20 %. $C_{10}H_{16}NO_5P$ requires C, 48.36; H, 5.90; N, 5.13 %); υ/cm^{-1}, 1678 (C=O) and 1232 (P=O); δ_H/ppm (400 MHz; DMSO-d_6) 1.93 (2H, m, CH_2P), 2.17 (2H, m, 3'-CH_2), 2.81 (2H, t, *J* = 7.2 Hz, CH_2CO), 3.78 (3H, s, OCH_3), 5.71 (2H, s, 2 x OH), 6.62 (1H, d, *J* = 6.8 Hz, 4-H), 7.10 (1H, d, *J* = 8.0 Hz, 6-H), 7.17 (1H, t, *J* = 8.4 Hz, 5-H), 7.31 (1H, s, 2-H) and 8.72 (1H, s, NH); δ_C/ppm (100 MHz; DMSO-d_6) 18.3 (d, J_{P-C} = 15.6 Hz, C-3'), 29.2 (d, J_{P-C} = 142.8 Hz, CH_2P), 36.8 (d, J_{P-C} = 3.2 Hz, CH_2CO), 55.1 (OCH_3), 104.8 (C-2), 110.2 (C-4), 112.4 (C-6), 129.5 (C-5), 139.7 (C-1), 159.2 (C-3) and 172.3 (C=O).

[*N*-(3-Bromophenyl)carbamoyl]propylphosphonic acid 333c

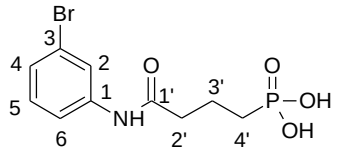

The procedure described for the synthesis of [*N*-(3-hydroxyphenyl)carbamoyl]propyl phosphonic acid **333a** was employed, using diethyl [*N*-(3-bromophenyl)carbamoyl]propyl phosphonate **325c** (0.25 g, 0.66 mmol) in CH_3CN (3 mL) and trimethylsilyl bromide (0.18 mL, 1.3 mmol). The solvent was removed *in vacuo* and the residue chromatographed [preparative layer chromatography; elution with hexane-EtOAc-MeOH (1:1:1)] to yield *[*N-*(3-bromophenyl)carbamoyl]propylphosphonic acid* **333c** as a light brown oil (0.098 g, 55 %); (Found: C, 37.35; H, 4.13; N, 4.30 %. $C_{10}H_{13}BrNO_4P$ requires C, 37.29; H, 4.07; N, 4.35 %); υ/cm^{-1} 3127 (OH), 1685 (C=O) and 1224 (P=O); δ_H/ppm (400 MHz; DMSO-d_6) 1.78 (2H, m, CH_2P), 2.17 (2H, m, 3'-CH_2), 2.68 (2H, t, *J* = 7.2 Hz, CH_2CO), 5.99 (2H, s, 2 x OH), 6.80 (1H, t, *J* = 7.6 Hz, 5-H), 7.24 (1H, d, *J* = 6.4 Hz, 4-H), 7.45 (1H, d, *J* = 6.8 Hz, 6-H), 7.71 (1H, s, 2-H) and 9.41 (1H, s, NH); δ_C/ppm (400 MHz; DMSO-d_6) 17.8 (d, J_{P-C} = 15.4 Hz, C-3'), 26.7 (d, J_{P-C} = 144.0 Hz, CH_2P), 36.4 (d, J_{P-C} = 3.4 Hz, CH_2CO), 115.8 (C-6), 118.4 (C-3), 122.2 (C-2), 127.6 (C-4), 129.8 (C-5), 137.8 (C-1) and 167.9 (C=O).

[*N*-(3-Fluorophenyl)carbamoyl]propylphosphonic acid 333d

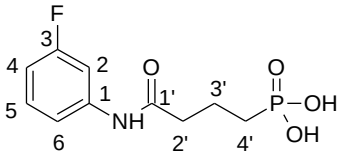

The procedure described for the synthesis of [*N*-(3-hydroxyphenyl)carbamoyl]propyl phosphonic acid **333a** was employed, using diethyl [*N*-(3-fluorophenyl)carbamoyl]propyl phosphonate **325d** (0.25 g, 0.79 mmol) in CH_3CN (3 mL) and trimethylsilyl bromide (0.21 mL, 1.6 mmol). The solvent was removed *in vacuo* and the residue chromatographed [preparative layer chromatography; elution with hexane-EtOAc-MeOH (1:1:1)] to yield *[*N-*(3-fluorophenyl)carbamoyl]propylphosphonic acid* **333d** as a clear oil (0.10 g, 57 %); (Found: C, 46.19; H, 5.09; N, 5.41 %. $C_{10}H_{13}FNO_4P$ requires C, 45.99; H, 5.02; N, 5.36 %); υ/cm^{-1}, 1656 (C=O) and 1215 (P=O); δ_H/ppm (400 MHz; DMSO-d_6) 1.78 (2H, m, CH_2P), 2.17 (2H, m, 3'-CH_2), 2.70 (2H, t, *J* = 6.4 Hz, CH_2CO), 4.82 (2H, s, 2 x OH), 6.77 (1H, ddd, *J* = 6.8, 2.0 and 1.6 Hz, 4-H), 7.17 (1H, dd, *J* = 6.4 and 2.4 Hz, 6-H), 7.25 (1H, td, *J* = 6.4, 2.8 and 1.6 Hz, 5-H) 7.50 (1H, dt, *J* = 6.8, 2.4 and 1.6 Hz, 2-H) and 8.87 (1H, s, NH); δ_C/ppm (100 MHz; DMSO-d_6) 18.3 (d, $J_{P–C}$ = 15.2 Hz, C-3'), 27.0 (d, $J_{P–C}$ = 144.0 Hz, CH_2P), 36.6 (d, $J_{P–C}$ = 3.1 Hz, CH_2CO), 107.6 (d, $J_{F–C}$ = 26.2 Hz, C-2), 112.4 (d, $J_{F–C}$ = 21.2 Hz, C-4), 115.7 (d, $J_{F–C}$ = 2.7 Hz, C-6), 129.8 (d, $J_{F–C}$ = 9.1 Hz, C-5), 139.5 (d, $J_{F–C}$ = 11.0 Hz, C-1), 164.2 (d, $J_{F–C}$ = 243.2 Hz, C-3) and 164.8 (C=O).

[*N*-(3-Cyanophenyl)carbamoyl]propylphosphonic acid 333e

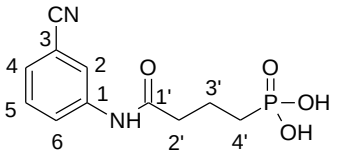

The procedure described for the synthesis of [*N*-(3-hydroxyphenyl)carbamoyl]propyl phosphonic acid **333a** was employed, using diethyl [*N*-(3-cyanophenyl)carbamoyl]propyl phosphonate **325e** (0.25 g, 0.77 mmol) in CH_3CN (3 mL) and trimethylsilyl bromide (0.21 mL, 1.5 mmol). The solvent was removed *in vacuo* and the residue chromatographed [preparative layer chromatography; elution with hexane-EtOAc-MeOH (1:1:1)] to yield *[*N-*(3-cyanophenyl)carbamoyl]propylphosphonic acid* **333e** as a clear oil (0.11 g, 61 %); (Found: C, 49.37; H, 4.93; N, 10.39 %. $C_{11}H_{13}N_2O_4P$ requires C, 49.26; H, 4.86; N, 10.44 %); (0.10 g, 59

%); υ/cm^{-1} 3310 (OH), 2227 (C≡N), 1667 (C=O) and 1226 (P=O); δ_H/ppm (400 MHz; DMSO-d_6) 1.78 (2H, m, CH_2P), 2.15 (2H, m, 3'-CH_2), 2.75 (2H, t, *J* = 7.6 Hz, CH_2CO), 5.87 (2H, s, 2 x OH), 7.33 (2H, m, 4-H and 6-H), 7.80 (1H, t, *J* = 8.0 Hz, 5-H), 7.98 (1H, t, *J* = 1.6 Hz, 2-H), and 8.97 (1H, s, NH); δ_C/ppm (400 MHz; DMSO-d_6) 17.8 (d, J_{P-C} = 15.6 Hz, C-3'), 27.1 (d, J_{P-C} = 142.7 Hz, CH_2P), 36.3 (d, J_{P-C} = 3.2 Hz, CH_2CO), 112.5 (C-3), 118.5 (C≡N), 123.2 (C-2) 124.6 (C-5), 127.8 (C-6), 129.5 (C-4), 139.1 (C-1) and 173.5 (C=O).

[*N*-(3-Nitrophenyl)carbamoyl]propylphosphonic acid 333f

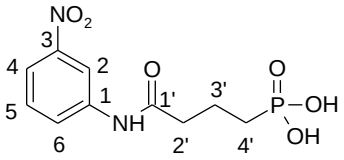

The procedure described for the synthesis of [*N*-(3-hydroxyphenyl)carbamoyl]propyl phosphonic acid **333a** was employed, using diethyl [*N*-(3-nitrophenyl)carbamoyl]propyl phosphonate **325f** (0.25 g, 0.73 mmol) in CH_3CN (3 mL) and trimethylsilyl bromide (0.13 mL, 1.5 mmol). The solvent was removed *in vacuo* and the residue chromatographed [preparative layer chromatography; elution with hexane-EtOAc-MeOH (1:1:0.5)] to yield *[*N-*(3-nitrophenyl)carbamoyl]propylphosphonic acid* **333f** as a yellow oil (0.12 g, 66 %); (Found: C, 41.55; H, 4.63; N, 9.64 %. $C_{10}H_{13}N_2O_6P$ requires C, 41.68; H, 4.55; N, 9.72 %); υ/cm^{-1} 3229 (OH), 1664 (C=O) and 1239 (P=O); δ_H/ppm (400 MHz; DMSO-d_6) 1.75 (2H, m, CH_2P), 2.18 (2H, m, 3'-CH_2), 2.78 (2H, t, *J* = 7.6 Hz, CH_2CO), 4.76 (2H, s, 2 x OH), 7.48 (1H, t, *J* = 8.0 Hz, 5-H), 7.87 (1H, dd, *J* = 8.0 and 1.6 Hz, 4-H), 8.17 (1H, dd, *J* = 8.4 and 1.6 Hz, 6-H), 8.41 (1H, t, *J* = 2.0 Hz, 2-H) and 9.34 (1H, s, NH); δ_C/ppm (400 MHz; DMSO-d_6) 18.0 (d, J_{P-C} = 15.4 Hz, C-3'), 33.8 (d, J_{P-C} = 135.7 Hz, CH_2P), 48.3 (d, J_{P-C} = 3.2 Hz, CH_2CO), 114.8 (C-2), 118.7 (C-4), 126.3 (C-6), 129.7 (C-5), 141.2 (C-1), 148.3 (C-3) and 173.5 (C=O).

***N*-[3-(Hydroxymethyl)phenylcarbamoyl]propylphosphonic acid 333g**

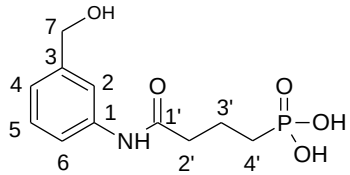

The procedure described for the synthesis of [*N*-(3-hydroxyphenyl)carbamoyl]propyl phosphonic acid **333a** was employed, using diethyl {*N*-[3-(hydroxymethyl) phenyl]carbamoyl}propylphosphonate **325g** (0.25 g, 0.79 mmol) in CH_3CN (3 mL) and trimethylsilyl bromide (0.21 mL, 1.6 mmol). The solvent was removed *in vacuo* and the residue chromatographed [preparative layer chromatography; elution with hexane-EtOAc-MeOH (1:1:1.5)] to yield N-*[3-(hydroxymethyl)phenylcarbamoyl]propylphosphonic acid* **333g** as a clear oil (0.11 g, 60 %); (Found: C, 46.52; H, 5.61; N, 5.27 %. $C_{11}H_{16}NO_5P$ requires C, 46.34; H, 5.44; N, 5.40 %); υ/cm^{-1} 3267 (OH), 1687 (C=O) and 1232 (P=O); δ_H/ppm (400 MHz; DMSO-d_6) 1.77 (2H, m, CH_2P), 2.16 (2H, m, 3'-CH_2), 2.77 (2H, t, *J* = 7.2 Hz, CH_2CO), 3.68 (2H, s, 2 x OH), 4.46 (2H, s, CH_2OH), 5.77 (1H, s, OH), 7.12 (1H, d, *J* = 7.6 Hz, 4-H), 7.25 (1H, t, *J* = 8.0 Hz, 5-H), 7.48 (1H, d, *J* = 8.0 Hz, 6-H), 7.63 (1H, s, 2-H) and 8.78 (1H, s, NH); δ_C/ppm (400 MHz; DMSO-d_6) 19.9 (d, J_{P-C} = 15.6 Hz, C-3'), 25.2 (d, J_{P-C} = 143.5 Hz, CH_2P), 37.0 (d, J_{P-C} = 3.3 Hz, CH_2CO), 67.7 (CH_2OH), 118.2 (C-2), 120.6 (C-6), 122.3 (C-4), 129.1 (C-5), 138.5 (C-1), 141.2 (C-3) and 171.2 (C=O).

3.3.3.3. Synthesis of sodium hydrogen propylphosphonate derivatives

Sodium hydrogen [*N*-(3-hydroxyphenyl)carbamoyl]propylphosphonate 334a

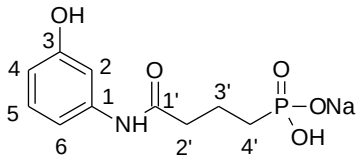

[N-(3-Hydroxyphenyl)carbamoyl]propylphosphonic acid **333a** (0.15 g, 0.58 mmol) was treated with a solution of NaOH (1.1 mol) in EtOH (0.55 mL) and the mixture was stirred for 30 min. The solvent was removed *in vacuo* and the residue chromatographed [reverse-phase column chromatography; elution with H_2O-MeOH (1:1)] to yield *sodium hydrogen [*N-*(3-hydroxyphenyl)carbamoyl]propylphosphonate* **334a** as a pale yellow semi-solid (0.098 g, 94 %); υ/cm^{-1} 3317 (OH), 1682 (C=O) and 1215 (P=O); δ_H/ppm (400 MHz; D_2O) 1.90 (2H, m, CH_2P), 2.16 (2H, m, 3'-CH_2), 2.73 (2H, m, CH_2CO), 6.62 (1H, d, *J* = 7.9 Hz, 4-H), 6.85 (1H, d, *J* = 7.6 Hz, 6-H), 7.11 (1H, t, *J* = 8.0 Hz, 5-H) and 7.33 (1H, s, 2-H); δ_C/ppm(100 MHz; D_2O) 17.7 (d, J_{P-C} = 15.4 Hz, C-3'), 27.0 (d, J_{P-C} = 143.7 Hz, CH_2P), 37.3 (d, J_{P-C} = 3.4 Hz, CH_2CO), 108.5 (C-2), 112.1 (C-4), 112.4 (C-6), 129.8 (C-5), 138.2 (C-1), 158.1 (C-3) and 166.3 (C=O).

Sodium hydrogen [*N*-(3-methoxyphenyl)carbamoyl]propylphosphonate 334b

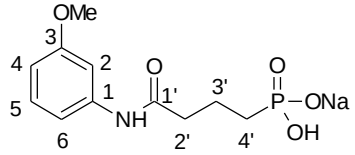

The procedure described for the synthesis of sodium hydrogen [*N*-(3-hydroxyphenyl)carbamoyl]propylphosphonate **334a** was employed, using [*N*-(3-methoxyphenyl)carbamoyl]propylphosphonic acid **333b** (0.15 g, 0.55 mmol) and a solution of NaOH (1.1 mol) in EtOH (0.52 mL). The solvent was removed *in vacuo* and the residue chromatographed [reverse-phase column chromatography; elution with H_2O-MeOH (1:1)] to yield *sodium hydrogen [*N-*(3-methoxyphenyl)carbamoyl]propylphosphonate* **334b** as a light brown semi-solid (0.096 g, 92 %); υ/cm^{-1} 3148 (OH), 1680 (C=O) and 1219 (P=O); δ_H/ppm (400 MHz; D_2O) 1.87 (2H, m, CH_2P), 2.16 (2H, m, 3'-CH_2), 2.78 (2H, t, *J* = 7.2 Hz, CH_2CO), 3.78 (3H, s, OCH_3), 6.60 (1H, d, *J* = 6.8 Hz, 4-H), 7.13 (1H, d, *J* = 8.0 Hz, 6-H), 7.20 (1H, t, *J* = 8.4 Hz, 5-H) and 7.29 (1H, s, 2-H); δ_C/ppm (100 MHz; D_2O) 18.0 (d, J_{P-C} = 15.2 Hz, C-3'), 30.3 (d, J_{P-C} = 142.5 Hz, CH_2P), 36.4 (d, J_{P-C} = 2.8 Hz, CH_2CO), 55.4 (OCH_3), 105.2 (C-2), 109.7 (C-4), 112.7 (C-6), 129.8 (C-5), 140.0 (C-1), 159.1 (C-3) and 172.6 (C=O).

Sodium hydrogen [*N*-(3-bromophenyl)carbamoyl]propylphosphonate 334c

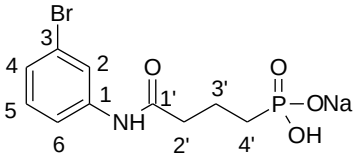

The procedure described for the synthesis of sodium hydrogen [*N*-(3-hydroxyphenyl)carbamoyl]propylphosphonate **334a** was employed, using [*N*-(3-bromophenyl)carbamoyl]propylphosphonic acid **333c** (0.15 g, 0.47 mmol) and a solution of NaOH (1.1 mol) in EtOH (0.44 mL). The solvent was removed *in vacuo* and the residue chromatographed [reverse-phase column chromatography; elution with H_2O-MeOH (1:1)] to yield *sodium hydrogen [*N-*(3-bromophenyl)carbamoyl]propylphosphonate* **334c** as a red-brown semi-solid (0.097 g, 89 %); υ/cm^{-1} 3209 (OH), 1648 (C=O) and 1221 (P=O); δ_H/ppm (400 MHz; D_2O) 1.80 (2H, m, CH_2P), 2.16 (2H, m, 3'-CH_2), 2.71 (2H, t, *J* = 7.2 Hz, CH_2CO), 6.79 (1H, t, *J* = 7.6 Hz, 5-H), 7.24 (1H, t, *J* = 7.6 Hz, 4-H), 7.42 (1H, dd, *J* = 6.8 and 2.0 Hz, 6-H) and 7.80 (1H, t, *J* = 2.0 Hz, 2-H); δ_C/ppm (100 MHz; D_2O) 17.9 (d, J_{P-C} = 15.6 Hz, C-3'), 26.3 (d, J_{P-C}

= 143.8 Hz, CH_2P), 37.0 (d, J_{P-C} = 3.2 Hz, CH_2CO), 115.5 (C-6), 118.6 (C-3), 122.8 (C-2), 127.6 (C-4), 129.7 (C-5), 138.2 (C-1) and 165.7 (C=O).

Sodium hydrogen [*N*-(3-fluorophenyl)carbamoyl]propylphosphonate 334d

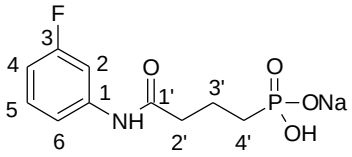

The procedure described for the synthesis of sodium hydrogen [*N*-(3-hydroxyphenyl)carbamoyl]propylphosphonate **334a** was employed, using [*N*-(3-fluorophenyl)carbamoyl]propylphosphonic acid **333d** (0.15 g, 0.57 mmol) and a solution of NaOH (1.1 mol) in EtOH (0.55 mL). The solvent was removed *in vacuo* and the residue chromatographed [reverse-phase column chromatography; elution with H_2O-MeOH (1:1)] to yield *sodium hydrogen [*N-*(3-fluorophenyl)carbamoyl]propylphosphonate* **334d** as a cream semi-solid (0.11 g, 96 %); υ/cm^{-1} 1684 (C=O) and 1231 (P=O); δ_H/ppm (400 MHz; D_2O) 1.80 (2H, m, CH_2P), 2.15 (2H, m, 3'-CH_2), 2.71 (2H, t, *J* = 6.4 Hz, CH_2CO), 6.78 (1H, ddd, *J* = 6.8, 2.4 and 1.6 Hz, 4-H), 7.16 (1H, dd, *J* = 6.4 and 1.6 Hz, 6-H), 7.24 (1H, td, *J* = 6.4, 2.8 and 1.6 Hz, 5-H) and 7.50 (1H, dt, *J* = 6.8, 2.4 and 1.6 Hz, 2-H); δ_C/ppm (100 MHz; D_2O) 17.8 (d, J_{P-C} = 15.6 Hz, C-3'), 26.5 (d, J_{P-C} = 142.0 Hz, CH_2P), 36.4 (d, J_{P-C} = 3.2 Hz, CH_2CO), 107.7 (d, J_{F-C} = 26.3 Hz, C-2), 112.6 (d, J_{F-C} = 21.2 Hz, C-4), 116.2 (d, J_{F-C} = 2.7 Hz, C-6), 129.5 (d, J_{F-C} = 8.8 Hz, C-5), 139.5 (d, J_{F-C} = 11.2 Hz, C-1), 164.0 (d, J_{F-C} = 243.1 Hz, C-3) and 168.7 (C=O).

Sodium hydrogen [*N*-(3-cyanophenyl)carbamoyl]propylphosphonate 334e

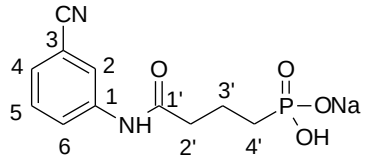

The procedure described for the synthesis of sodium hydrogen [*N*-(3-hydroxyphenyl)carbamoyl]propylphosphonate **334a** was employed, using [*N*-(3-cyanophenyl)carbamoyl]propylphosphonic acid **333e** (0.15 g, 0.56 mmol) and a solution of NaOH (1.1 mol) in EtOH (0.53 mL). The solvent was removed *in vacuo* and the residue chromatographed [reverse-phase column chromatography; elution with H_2O-MeOH (1:1)] to yield *sodium hydrogen [*N-*(3-cyanophenyl)carbamoyl]propylphosphonate* **334e** as a pale

yellow semi-solid (0.12 g, 96 %); υ/cm^{-1} 2231 (C≡N), 1678 (C=O) and 1219 (P=O); δ_H/ppm (400 MHz; D_2O) 1.77 (2H, m, CH_2P), 2.17 (2H, m, 3'-CH_2), 2.72 (2H, t, *J* = 7.2 Hz, CH_2CO), 7.35 (2H, m, 4-H and 6-H), 7.79 (1H, t, *J* = 8.0 Hz, 5-H) and 8.01 (1H, t, *J* = 1.6 Hz, 2-H); δ_C/ppm (100 MHz; D_2O) 18.1 (d, J_{P-C} = 15.3 Hz, C-3'), 26.8 (d, J_{P-C} = 143.2 Hz, CH_2P), 36.7 (d, J_{P-C} = 3.3 Hz, CH_2CO), 112.4 (C-3), 118.2 (C≡N), 122.8 (C-2) 124.5 (C-5), 127.8 (C-6), 129.8 (C-4), 138.7 (C-1) and 173.7 (C=O).

Sodium hydrogen [*N*-(3-nitrophenyl)carbamoyl]propylphosphonate 334f

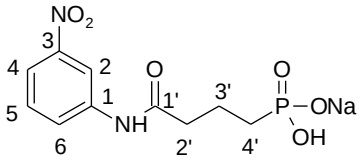

The procedure described for the synthesis of sodium hydrogen [*N*-(3-hydroxyphenyl)carbamoyl]propylphosphonate **334a** was employed, using [*N*-(3-nitrophenyl)carbamoyl]propylphosphonic acid **333f** (0.15 g, 0.52 mmol) and a solution of NaOH (1.1 mol) in EtOH (0.49 mL). The solvent was removed *in vacuo* and the residue chromatographed [reverse-phase column chromatography; elution with H_2O-MeOH (1:1)] to yield *sodium hydrogen [*N*-(3-nitrophenyl)carbamoyl]propylphosphonate* **334f** as a yellow semi-solid (0.12 g, 96 %); υ/cm^{-1} 3150 (OH), 1684 (C=O) and 1230 (P=O); δ_H/ppm (400 MHz; D_2O) 1.78 (2H, m, CH_2P), 2.16 (2H, m, 3'-CH_2), 2.77 (2H, t, *J* = 7.6 Hz, CH_2CO), 7.51 (1H, t, *J* = 8.0 Hz, 5-H), 7.88 (1H, dd, *J* = 8.0 and 1.6 Hz, 4-H), 8.20 (1H, dd, *J* = 8.4 and 1.6 Hz, 6-H) and 8.38 (1H, t, *J* = 2.0 Hz, 2-H); δ_C/ppm (100 MHz; D_2O) 18.4 (d, J_{P-C} = 15.6 Hz, C-3'), 32.9 (d, J_{P-C} = 140.8 Hz, CH_2P), 46.7 (d, J_{P-C} = 3.1 Hz, CH_2CO), 114.5 (C-2), 119.2 (C-4), 126.8 (C-6), 129.7 (C-5), 140.8 (C-1), 148.5 (C-3) and 170.1 (C=O).

Sodium hydrogen {*N*-[3-(hydroxymethyl)phenyl]carbamoyl}propylphosphonate 334g

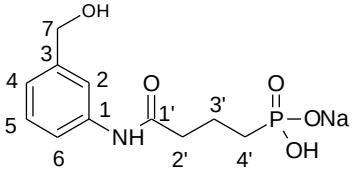

The procedure described for the synthesis of sodium hydrogen [*N*-(3-hydroxyphenyl)carbamoyl]propylphosphonate **334a** was employed, using [*N*-(3-(hydroxymethyl)phenylcarbamoyl]propylphosphonic acid **333g** (0.15 g, 0.55 mmol) and a

solution of NaOH (1.1 mol) in EtOH (0.52 mL). The solvent was removed *in vacuo* and the residue chromatographed [reverse-phase column chromatography; elution with H_2O-MeOH (1:1)] to yield *sodium hydrogen {*N-*[3-(hydroxymethyl)phenyl]carbamoyl}propylphosphonate* **334g** as a pale yellow semi-solid (0.092 g, 85 %); υ/cm^{-1} 1675 (C=O) and 1231 (P=O); δ_H/ppm (400 MHz; D_2O) 1.80 (2H, m, CH_2P), 2.18 (2H, m, 3'-CH_2), 2.77 (2H, t, *J* = 7.2 Hz, CH_2CO), 4.47 (2H, s, C*H*$_2$OH), 7.10 (1H, d, *J* = 7.6 Hz, 4-H), 7.23 (1H, t, *J* = 8.0 Hz, 5-H), 7.46 (1H, d, *J* = 8.0 Hz, 6-H) and 7.56 (1H, s, 2-H); δ_C/ppm (100 MHz; D_2O) 18.0 (d, $J_{P–C}$ = 15.5 Hz, C-3'), 26.7 (d, $J_{P–C}$ = 143.8 Hz, CH_2P), 36.5 (d, $J_{P–C}$ = 3.4 Hz, CH_2CO), 64.2 (CH_2OH), 118.2 (C-2), 118.8 (C-6), 122.6 (C-4), 129.8 (C-5), 138.2 (C-1), 139.8 (C-3) and 166.5 (C=O).

3.3.4. Reaction of 3-substituted anilines with 5-chloropentanoyl chloride

5-Chloro-*N*-(3-hydroxyphenyl)pentanamide 326a

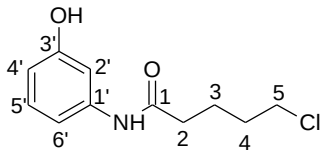

To a stirred solution of 3-aminophenol (1.50 g, 14.0 mmol) in THF (30 mL) under nitrogen was added NaH (60 % dispersion in mineral oil; 0.60 g, 24 mmol) in small portions to permit controlled evolution of hydrogen. 5-Chloropentanoyl chloride (1.67 mL, 14.0 mmol) was then added through a septum and the resulting solution was stirred for *ca.* 6 h. The solvent was evaporated *in vacuo* and the residue dissolved in EtOAc (2 x 50 mL). The organic solution was washed sequentially with satd. aq. $NaHCO_3$ (2 × 100 mL), water (2 x 100 mL) and brine (2 × 100 mL). The aqueous washings were extracted with EtOAc and the combined organic solutions were dried (anhydr. $MgSO_4$). Evaporation of the solvent *in vacuo* afforded *5-chloro*-N-*(3-hydroxyphenyl)pentanamide* **326a** as a brown gum (2.42 g, 76 %); (Found: $\mathbf{M^+}$, 227.07866 $C_{11}H_{14}ClNO_2$ requires: $\mathbf{M^+}$, 227.07131); υ_{max} (solid deposit/cm^{-1}) 1672 (C=O); δ_H/ppm (400 MHz; $CDCl_3$) 1.88 (4H, m, 3-CH_2 and 4-CH_2), 2.41 (2H, t, *J* = 6.8 Hz, CH_2CO), 3.57 (2H, t, *J* = 6.0 Hz, CH_2Cl), 6.80 (1H, d, *J* = 7.2 Hz, 4'-H), 7.18 (1H, d, *J* = 8.0 Hz, 6'-H), 7.25 (1H, t, *J* = 8.0 Hz, 5'-H), 7.28 (1H, s, OH), 7.42 (1H, s, 2'-H) and 7.46 (1H, s, NH); δ_C/ppm (100 MHz; $CDCl_3$) 22.2 (C-4), 31.8 (C-3), 33.5 (CH_2CO), 44.3 (CH_2Cl), 113.3 (C-2'), 116.9 (C-4'), 117.1 (C-6'), 129.5 (C-5'), 139.0 (C-1'), 151.0 (C-3') and 171.7 (C=O).

5-Chloro-*N*-(3-methoxyphenyl)pentanamide 326b [246]

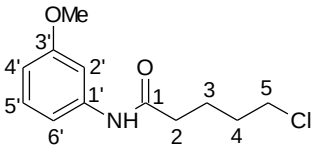

The procedure described for the synthesis of 5-chloro-*N*-(3-hydroxyphenyl)pentanamide **326a** was employed, using 3-methoxyaniline (0.91 mL, 8.1 mmol), NaH (60 % dispersion in mineral oil; 0.36 g, 15 mmol) and 5-chloropentanoyl chloride (0.97 mL, 8.1 mmol) in THF (15 mL), to yield 5-chloro-*N*-(3-methoxyphenyl)pentanamide **326b** as a yellow gum (1.41 g, 72 %); υ_{max} (solid deposit/cm^{-1}) 1682 (C=O); δ_H/ppm (400 MHz; $CDCl_3$) 1.78 (4H, m, 3-CH_2 and 4-CH_2), 2.29 (2H, t, *J* = 6.8 Hz, CH_2CO), 3.50 (2H, t, *J* = 6.0 Hz, CH_2Cl), 3.74 (3H, s, OCH_3), 6.60 (1H, dd, *J* = 6.4 and 1.6 Hz, 4'-H), 6.95 (1H, d, *J* = 7.6 Hz, 6'-H), 7.14 (1H, t, *J* = 8.0 Hz, 5'-H), 7.29 (1H, t, *J* = 2.0 Hz, 2'-H) and 8.12 (1H, s, NH); δ_C/ppm (100 MHz; $CDCl_3$) 22.8 (C-4), 31.8 (C-3), 36.7 (CH_2CO), 44.5 (CH_2Cl), 55.3 (OCH_3), 105.6 (C-2'), 110.2 (C-6'), 111.8 (C-4'), 129.7 (C-5'), 130.0 (C-1'), 160.2 (C-3') and 170.5 (C=O).

***N*-(3-Bromophenyl) 5-chloropentanamide 326c** [247]

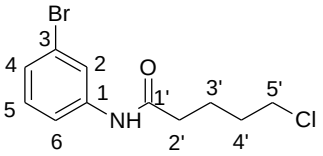

The procedure described for the synthesis of 4-chloro-*N*-(3-hydroxyphenyl)pentanamide **326a** was employed, using 3-bromoaniline (0.63 mL, 5.80 mmol), NaH (60 % dispersion in mineral oil; 0.26 g, 10.8 mmol) and 5-chloropentanoyl chloride (0.69 mL, 5.80 mmol) in THF (15 mL), to yield *N*-(3-bromophenyl) 5-chloropentanamide **326c** as a brown gum (1.10 g, 65 %); υ_{max} (solid deposit/cm^{-1}) 1676 (C=O); δ_H/ppm (400 MHz; $CDCl_3$) 1.80 (4H, m, 3-CH_2 and 4-CH_2), 2.32 (2H, t, *J* = 6.8 Hz, CH_2CO), 3.51 (2H, t, *J* = 6.8 Hz, CH_2Cl), 7.11 (1H, t, *J* = 8.0 Hz, 5-H), 7.17 (1H, d, *J* = 8.0 Hz, 4-H), 7.37 (1H, d, *J* = 8.0 Hz, 6-H), 7.74 (1H, s, 2-H) and 8.18 (1H, s, NH); δ_C/ppm (100 MHz; $CDCl_3$) 22.2 (C-4'), 31.8 (C-3'), 33.5 (CH_2CO), 44.3 (CH_2Cl), 113.8 (C-6), 117.4 (C-3), 117.7 (C-2), 128.3 (C-4), 130.4 (C-5), 139.4 (C-1) and 172.2 (C=O).

5-Chloro-*N*-(3-fluorophenyl)pentanamide 326d [247]

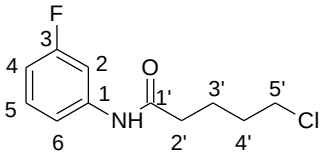

The procedure described for the synthesis of 5-chloro-*N*-(3-hydroxyphenyl)pentanamide **326a** was employed, using 3-fluoroaniline (1.05 mL, 5.80 mmol), NaH (60 % dispersion in mineral oil; 0.26 g, 11 mmol) and 5-chloropentanoyl chloride (0.69 mL, 5.8 mmol) in THF (15 mL), to yield 5-chloro-N-(3-fluorophenyl)pentanamide **326d** as a light brown gum (0.96 g, 72 %); υ_{max} (solid deposit/cm^{-1}) 1669 (C=O); δ_H/ppm (400 MHz; $CDCl_3$) 1.93 (4H, m, 3'-CH_2 and 4'-CH_2), 2.55 (2H, t, *J* = 6.8 Hz, CH_2CO), 3.63 (2H, t, *J* = 6.8 Hz, CH_2Cl), 6.93 (1H, ddd, *J* = 6.4, 2.4 and 0.8 Hz, 4-H), 6.99 (1H, dt, *J* = 6.4 and 1.6 Hz, 5-H), 7.03 (1H, dd, *J* = 6.8 and 0.8 Hz, 6-H), 7.31 (1H, td, *J* = 6.4, 2.0 and 1.2 Hz, 2-H) and 8.23 (1H, s, NH); δ_C/ppm (100 MHz; $CDCl_3$) 22.8 (C-4'), 32.5 (C-3'), 36.2 (CH_2CO), 44.2 (CH_2Cl), 107.8 (d, J_{F-C} = 26.2 Hz, C-2), 111.1 (d, J_{F-C} = 21.4 Hz, C-4), 114.6 (d, J_{F-C} = 3.8 Hz, C-6), 129.8 (d, J_{F-C} = 10.2 Hz, C-5), 139.7 (d, J_{F-C} = 11.3 Hz, C-1), 163.6 (d, J_{F-C} = 241.8 Hz, C-3) and 173.2 (C=O).

5-Chloro-*N*-(3-cyanophenyl)pentanamide 326e

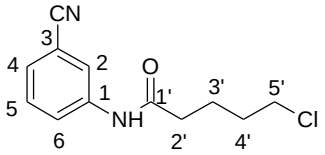

The procedure described for the synthesis of 5-chloro-*N*-(3-hydroxyphenyl)pentanamide **326a** was employed, using 3-aminobenzonitrile (1.20 g, 10.1 mmol), NaH (60 % dispersion in mineral oil; 0.54 g, 23 mmol) and 5-chloropentanoyl chloride (1.20 mL, 10.1 mmol) in THF (15 mL), to yield *5-chloro*-N-*(3-cyanophenyl)pentanamide* **326e** as a yellow viscous oil (2.00 g, 84 %); (Found: $\mathbf{M^+}$, 236.07431 $C_{12}H_{13}ClN_2O$ requires: $\mathbf{M^+}$, 236.07164); υ_{max} (thin film/cm^{-1}) 2223 (C≡N), 1689 (C=O); δ_H/ppm (400 MHz; $CDCl_3$) 1.88 (4H, m, 3'-CH_2 and 4'-CH_2), 2.43 (2H, t, *J* = 6.8 Hz, CH_2CO), 3.57 (2H, t, *J* = 6.2 Hz, CH_2Cl), 7.39 (2H, m, 4-H and 6-H), 7.54 (1H, s, NH), 7.72 (1H, t, *J* = 7.2 Hz, 5-H) and 7.93 (1H, s, 2-H); δ_C/ppm (100 MHz; $CDCl_3$) 22.6 (C-4'), 31.8 (C-3'), 36.5 (CH_2CO), 44.5 (CH_2Cl), 112.9 (C-3), 118.5 (C=N), 122.8 (C-2), 123.8 (C-5), 127.6 (C-6), 129.9 (C-4), 138.7 (C-1) and 171.0 (C=O).

5-Chloro-*N*-(3-nitrophenyl)pentanamide 326f

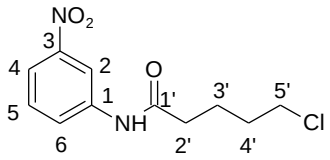

The procedure described for the synthesis of 5-chloro-*N*-(3-hydroxyphenyl)pentanamide **326a** was employed, using 3-nitroaniline (1.01 g, 7.27 mmol), NaH (60 % dispersion in mineral oil; 0.33 g, 13 mmol) and 5-chloropentanoyl chloride (0.87 mL, 7.3 mmol) in THF (15 mL), to yield *5-chloro*-N-*(3-nitrophenyl)pentanamide* **326f** as a dark yellow viscous oil (1.60 g, 86 %); (Found: $\mathbf{M}^+$, 256.06328 $C_{11}H_{13}ClN_2O_3$ requires: $\mathbf{M}^+$, 256.06147); υ_{max} (solid deposit/cm^{-1}) 1685 (C=O); δ_H/ppm (400 MHz; $CDCl_3$) 1.85 (4H, m, 3'-CH_2 and 4'-CH_2), 2.46 (2H, t, *J* = 6.8 Hz, CH_2CO), 3.53 (2H, t, *J* = 6.4 Hz, CH_2Cl), 7.43 (1H, t, *J* = 8.4 Hz, 5-H), 7.90 (2H, m, 4-H and 6-H), 8.34 (1H, s, NH) and 8.40 (1H, t, *J* = 2.0 Hz, 2-H); δ_C/ppm (100 MHz; $CDCl_3$) 22.5 (C-4'), 31.6 (C-3'), 36.4 (CH_2CO), 44.4 (CH_2Cl), 113.3 (C-2), 118.7 (C-4), 125.7 (C-6), 129.9 (C-5), 139.8 (C-1), 148.6 (C-3) and 173.3 (C=O).

5-Chloro-*N*-[3-(hydroxymethyl)phenyl]pentanamide 326g

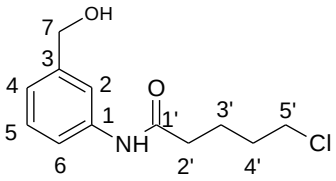

The procedure described for the synthesis of 5-chloro-*N*-(3-hydroxyphenyl)pentanamide **326a** was employed, using 3-aminobenzylalcohol (1.02 g, 8.12 mmol), NaH (60 % dispersion in mineral oil; 0.52 g, 21 mmol) and 5-chloropentanoyl chloride (0.97 mL, 8.1 mmol) in THF (15 mL), to yield *5-chloro*-N-*[3-(hydroxymethyl)phenyl]pentanamide* **326g** as a brown gum (1.51 g, 77 %); (Found: $\mathbf{M}^+$, 241.09015 $C_{12}H_{16}ClNO_2$ requires: $\mathbf{M}^+$, 241.08696); υ_{max} (solid deposit/cm^{-1}) 1684 (C=O); δ_H/ppm (400 MHz; $CDCl_3$) 2.12 (4H, m, 3'-CH_2 and 4'-CH_2), 2.49 (2H, t, *J* = 6.8 Hz, CH_2CO), 3.59 (2H, t, *J* = 6.4 Hz, CH_2Cl), 4.58 (2H, s, 7-CH_2), 7.02 (1H, d, *J* = 7.6 Hz, 4-H), 7.11 (1H, d, *J* = 7.6 Hz, 6-H), 7.23 (1H, t, *J* = 7.6 Hz, 5-H), 7.59 (1H, s, 2-H), 7.76 (1H, s, OH) and 8.00 (1H, s, NH); δ_C/ppm (100 MHz; $CDCl_3$) 22.7 (C-4'), 32.1 (C-3'), 36.8 (CH_2CO), 44.6 (CH_2Cl), 63.1 (CH_2OH), 117.1 (C-2), 117.8 (C-6), 122.3 (C-4), 128.6 (C-5), 138.6 (C-1), 142.9 (C-3) and 168.9 (C=O).

3.3.4.1. Synthesis of diethyl butylphosphonates *via* Michaelis-Arbuzov methodology

Diethyl [*N*-(3-hydroxyphenyl)carbamoyl]butylphosphonate 327a

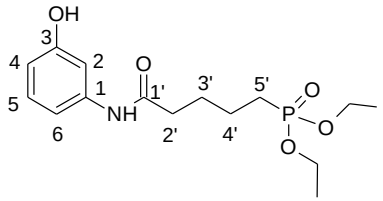

Triethyl phosphite (0.76 mL, 4.4 mmol) was added through a septum to 5-chloro-*N*-(3-hydroxyphenyl)pentanamide **326a** (0.50 g, 2.2 mmol) under nitrogen in an oven-dried round-bottomed flask equipped with a reflux condenser, and the resulting mixture was refluxed for *ca.* 9 h during which time the reaction was monitored by TLC. The cooled mixture was then stirred with hexane (20 mL) for *ca.* 30 minutes followed by decantation of the hexane layer to remove the excess triethyl phosphite; this was repeated three times. The crude product was purified by flash chromatography [on silica gel; elution with hexane-EtOAc (4:1)], and subsequent evaporation of the solvent *in vacuo* afforded *diethyl [*N*(3-hydroxyphenyl)carbamoyl)]butylphosphonate* **327a** as clear oil (0.22 g, 55 %); (Found: $\mathbf{M}^+$, 329.14287 $C_{15}H_{24}NO_5P$ requires: $\mathbf{M}^+$, 329.13921); υ/cm^{-1} 3128 (OH), 1672 (C=O), 1219 (P=O) and 1018 (P−OEt); δ_H/ppm (400 MHz; $CDCl_3$) 1.19 (2H, m, 4'-CH_2), 1.30 (6H, t, *J* = 7.2 Hz, 2 × CH_3), 1.77 (2H, m, CH_2P), 1.98 (2H, m, 3'-CH_2), 2.38 (2H, t, *J* = 6.4 Hz, CH_2CO), 4.12 (4H, m, 2 × OCH_2), 6.63 (1H, d, *J* = 7.2 Hz, 4-H), 6.87 (1H, d, *J* = 7.6 Hz, 6-H), 7.12 (1H, t, *J* = 7.6 Hz, 5-H), 7.40 (1H, s, 2-H), 7.64 (1H, s, OH) and 8.46 (1H, s, NH); δ_C (100 MHz; $CDCl_3$) 16.3 (d, $J_{P–C}$ = 6.0 Hz, 2 × CH_3), 21.9 (d, $J_{P–C}$ = 15.2 Hz, C-4'), 23.6 (d, $J_{P–C}$ = 141.2 Hz, CH_2P), 26.6 (d, $J_{P–C}$ = 4.8 Hz, C-3'), 36.5 (d, $J_{P–C}$ = 3.2 Hz, CH_2CO), 62.1 (d, $J_{P–C}$ = 6.5 Hz, 2 × OCH_2), 107.7 (C-2), 111.8 (C-4), 112.6 (C-6), 129.1 (C-5), 138.7 (C-1), 158.2 (C-3) and 164.8 (C=O).

Diethyl [*N*-(3-methoxyphenyl)carbamoyl]butylphosphonate 327b

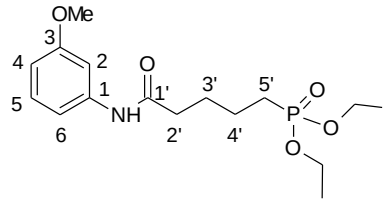

The procedure described for the synthesis of diethyl [*N*-(3-hydroxyphenyl)carbamoyl]-butylphosphonate **327a** was employed, using 5-chloro-*N*-(3-methoxyphenyl)pentanamide

326b (0.50 g, 2.1 mmol) and triethyl phosphite (0.72 mL, 4.1 mmol). The crude product was purified by flash chromatography [on silica gel; elution with hexane-EtOAc (3:1)], and subsequent evaporation of the solvent *in vacuo* afforded *diethyl [*N-*(3-methoxyphenyl)carbamoyl]butylphosphonate* **327b** as a brown oil (0.32 g, 66 %); (Found: $\mathbf{M}^+$, 343.15836 $C_{16}H_{26}NO_5P$ requires: $\mathbf{M}^+$, 343.15486); υ/cm^{-1} 1681 (C=O), 1237 (P=O) and 1038 (P−OEt); δ_H/ppm (400 MHz; $CDCl_3$) 1.28 (2H, m, 4'-CH_2), 1.31 (6H, t, *J* = 6.8 Hz, 2 × CH_3), 2.06 (4H, m, 3'-CH_2 and CH_2P), 2.39 (2H, t, *J* = 6.4 Hz, CH_2CO), 3.80 (3H, OCH_3), 4.13 (4H, m, 2 × OCH_2), 6.65 (1H, d, *J* = 8.4 Hz, 4-H), 6.93 (1H, d, *J* = 7.2 Hz, 6-H), 7.10 (1H, s, 2-H), 7.20 (1H, t, *J* = 8.0 Hz, 5-H) and 7.30 (1H, s, NH); δ_C (100 MHz; $CDCl_3$) 16.2 (d, J_{P-C} = 6.6 Hz, 2 × CH_3), 22.2 (d, J_{P-C} = 15.2 Hz, C-4'), 23.4 (d, J_{P-C} = 141.2 Hz, CH_2P), 26.7 (d, J_{P-C} = 4.7 Hz, C-3'), 36.5 (d, J_{P-C} = 4.2 Hz, CH_2CO), 55.2 (OCH_3), 62.4 (d, J_{P-C} = 6.5 Hz, 2 × OCH_2), 105.5 (C-2), 109.5 (C-4), 112.4 (C-6), 129.9 (C-5), 139.5 (C-1), 160.2 (C-3) and 167.3 (C=O).

Diethyl [*N*-(3-bromophenyl)carbamoylbutylphosphonate 327c

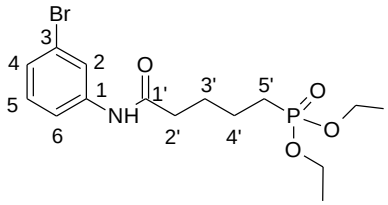

The procedure described for the synthesis of diethyl [*N*-(3-hydroxyphenyl)carbamoyl] butylphosphonate **327a** was employed, using 5-chloro-*N*-(3-bromophenyl)pentanamide **326c** (0.50 g, 1.7 mmol) and triethyl phosphite (0.58 mL, 3.4 mmol). The crude product was purified by flash chromatography [on silica gel; elution with hexane-EtOAc (3:1)], and subsequent evaporation of the solvent *in vacuo* afforded *diethyl [*N-*(3-bromophenyl)carbamoyl]butylphosphonate* **327c** as a brown oil (0.30 g, 63 %); (Found: $\mathbf{M}^+$, 391.05517 $C_{15}H_{23}BrNO_4P$ requires: $\mathbf{M}^+$, 391.05481; υ/cm^{-1} 1685 (C=O), 1221 (P=O) and 1029 (P−OEt); δ_H/ppm (400 MHz; $CDCl_3$) 1.17 (2H, m, 4'-CH_2), 1.27 (6H, t, *J* = 6.8 Hz, 2 × CH_3), 1.79 (2H, m, CH_2P), 1.99 (2H, m, 3'-CH_2), 2.37 (2H, t, *J* = 6.4 Hz, CH_2CO), 4.12 (4H, m, 2 × OCH_2), 6.78 (1H, t, *J* = 7.6 Hz, 5-H), 7.25 (1H, d, *J* = 7.6 Hz, 4-H), 7.31 (1H, d, *J* = 7.2 Hz, 6-H), 7.48 (1H, s, 2-H) and 8.36 (1H, s, NH); δ_C (100 MHz; $CDCl_3$) 16.3 (d, J_{P-C} = 6.6 Hz, 2 × CH_3), 22.1 (d, J_{P-C} = 15.6 Hz, C-4'), 23.3 (d, J_{P-C} = 141.4 Hz, CH_2P), 26.4 (d, J_{P-C} = 4.8 Hz, C-3'), 36.4 (d, J_{P-C} = 3.8 Hz, CH_2CO), 62.8 (d, J_{P-C} = 6.5 Hz, 2 × OCH_2), 115.6 (C-6), 118.3 (C-3), 122.6 (C-2), 126.4 (C-4), 129.7 (C-5), 139.7 (C-1) and 168.1 (C=O).

Diethyl [*N*-(3-fluorophenyl)carbamoyl]butylphosphonate 327d

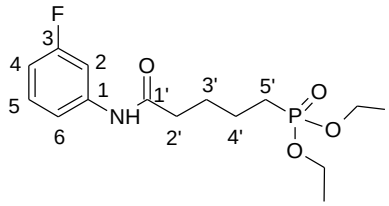

The procedure described for the synthesis of diethyl [*N*-(3-hydroxyphenyl)carbamoyl]butylphosphonate **327a** was employed, using 5-chloro-*N*-(3-fluorophenyl)pentanamide **326d** (0.50 g, 2.2 mmol) and triethyl phosphite (0.75 mL, 4.4 mmol). The crude product was purified by flash chromatography [on silica gel; elution with hexane-EtOAc (3:1)], and subsequent evaporation of the solvent *in vacuo* afforded *diethyl [*N-*(3-fluorophenyl)carbamoyl]butylphosphonate* **327d** as a clear oil (0.25 g, 54 %); (Found: **M**$^+$, 331.13529 $C_{15}H_{23}FNO_4P$ requires: **M**$^+$, 331.13487); υ/cm^{-1} 1653 (C=O), 1231 (P=O) and 1023 (P−OEt); δ_H/ppm (400 MHz; $CDCl_3$) 1.22 (2H, m, 4'-CH_2), 1.31 (6H, t, *J* = 7.2 Hz, 2 × CH_3), 1.91 (2H, m, CH_2P), 2.10 (2H, m, 3'-CH_2), 2.38 (2H, t, *J* = 6.4 Hz, CH_2CO), 4.12 (4H, m, 2 × OCH_2), 6.81 (1H, ddd, *J* = 6.4, 2.4 and 1.6 Hz, 4-H), 7.17 (1H, d, *J* = 6.4 Hz, 6-H), 7.25 (1H, td, *J* = 6.8, 2.8 and 1.2 Hz, 5-H) 7.43 (1H, dt, *J* = 6.4 and 2.4 Hz, 2-H) and 7.98 (1H, s, NH); δ_C (100 MHz; $CDCl_3$) 16.4 (d, J_{P-C} = 6.6 Hz, 2 × CH_3), 22.0 (d, J_{P-C} = 15.6 Hz, C-4'), 23.6 (d, J_{P-C} = 140.8 Hz, CH_2P), 26.4 (d, J_{P-C} = 4.5 Hz, C-3'), 36.4 (d, J_{P-C} = 4.2 Hz, CH_2CO), 63.1 (d, J_{P-C} = 6.7 Hz, 2 × OCH_2), 108.2 (d, J_{F-C} = 25.7 Hz, C-2), 111.4 (d, J_{F-C} = 20.8 Hz, C-4), 115.6 (d, J_{F-C} = 3.1 Hz, C-6), 129.9 (d, J_{F-C} = 8.7 Hz, C-5), 138.7 (d, J_{F-C} = 11.3 Hz, C-1), 163.2 (d, J_{F-C} = 241.2 Hz, C-3) and 168.3 (C=O).

Diethyl [*N*-(3-cyanophenyl)carbamoyl]butylphosphonate 327e

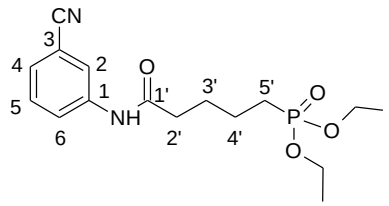

The procedure described for the synthesis of diethyl [*N*-(3-hydroxyphenyl)carbamoyl]butyl-phosphonate **327a** was employed, using 5-chloro-*N*-(3-cyanophenyl)pentanamide **326e** (0.50 g, 2.1 mmol) and triethyl phosphite (0.72 mL, 4.2 mmol). The crude product was purified by flash chromatography [on silica gel; elution with hexane-EtOAc (3:1)], and subsequent evaporation of the solvent *in vacuo* afforded *diethyl [*N-*(3-*

cyanophenyl)carbamoyl]butylphosphonate **327e** as a clear oil (0.28 g, 61 %); (Found: $\mathbf{M}^+$, 338.14137 $C_{156}H_{23}N_2O_4P$ requires: $\mathbf{M}^+$, 338.13954); υ/cm^{-1} 2238 (C≡N), 1667 (C=O), 1218 (P=O) and 1046 (P−OEt); δ_H/ppm (400 MHz; $CDCl_3$) 1.19 (2H, m, 4'-CH_2), 1.34 (6H, t, *J* = 7.2 Hz, 2 × CH_3), 1.70 (2H, m, CH_2P), 1.92 (2H, m, 3'-CH_2), 2.43 (2H, t, *J* = 6.8 Hz, CH_2CO), 4.14 (4H, m, 2 × OCH_2), 7.38 (2H, t, *J* = 7.2 Hz, 5-H), 7.64 (1H, d, *J* = 5.8 Hz, 4-H), 7.72 (1H, d, *J* = 7.6 Hz, 6-H) 7.93 (1H, s, 2-H) and 9.79 (1H, s, NH); δ_C (100 MHz; $CDCl_3$) 16.3 (d, $J_{P–C}$ = 6.5 Hz, 2 × CH_3), 22.4 (d, $J_{P–C}$ = 15.6 Hz, C-4'), 23.5 (d, $J_{P–C}$ = 142.0 Hz, CH_2P), 26.3 (d, $J_{P–C}$ = 4.8 Hz, C-3'), 37.1 (d, $J_{P–C}$ = 3.9 Hz, CH_2CO), 62.6 (d, $J_{P–C}$ = 6.7 Hz, 2 × OCH_2), 112.6 (C-3), 118.8 (C≡N), 122.6 (C-2), 124.6 (C-5), 127.2 (C-6), 129.8 (C-4), 139.8 (C-1) and 173.5 (C=O).

Diethyl [*N*-(3-nitrophenyl)carbamoyl]butylphosphonate 327f

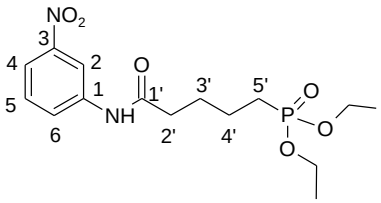

The procedure described for the synthesis of diethyl [*N*-(3-hydroxyphenyl)carbamoyl]butyl phosphonate **326a** was employed, using 5-chloro-*N*-(3-nitrophenyl)pentanamide **326f** (0.50 g, 2.0 mmol) and triethyl phosphite (0.68 mL, 3.9 mmol). The crude product was purified by flash chromatography [on silica gel; elution with hexane-EtOAc (3:1)], and subsequent evaporation of the solvent *in vacuo* afforded *diethyl [*N*-(3-nitrophenyl)carbamoyl]butyl phosphonate* **327f** as a yellow oil (0.35 g, 74 %); (Found: $\mathbf{M}^+$, 358.13018 $C_{15}H_{23}N_2O_6P$ requires: $\mathbf{M}^+$, 358.12937); υ/cm^{-1} 1683 (C=O), 1218 (P=O) and 1028 (P−OEt); δ_H/ppm (400 MHz; $CDCl_3$) 1.16 (2H, m, 4'-CH_2), 1.30 (6H, t, *J* = 7.6 Hz, 2 × CH_3), 1.79 (4H, m, 3'-CH_2 and CH_2P), 2.46 (2H, t, *J* = 6.8 Hz, CH_2CO), 4.07 (4H, m, 2 × OCH_2), 7.47 (1H, s, 2-H), 7.49 (1H, t, *J* = 8.4 Hz, 5-H), 7.96 (2H, m, 4-H and 6-H) and 8.36 (1H, s, NH); δ_C (100 MHz; $CDCl_3$) 16.5 (d, $J_{P–C}$ = 6.4 Hz, 2 × CH_3), 22.1 (d, $J_{P–C}$ = 15.6 Hz, C-4'), 23.4 (d, $J_{P–C}$ = 141.2 Hz, CH_2P), 26.6 (d, $J_{P–C}$ = 4.8 Hz, C-3'), 36.4 (d, $J_{P–C}$ = 4.5 Hz, CH_2CO), 62.4 (d, $J_{P–C}$ = 6.5 Hz, 2 × OCH_2), 113.8 (C-2), 119.1 (C-4), 124.9 (C-6), 129.8 (C-5), 140.7 (C-1), 149.1 (C-3) and 173.4 (C=O).

Diethyl {*N*-[3-(hydroxymethyl)phenyl]carbamoyl}butylphosphonate 327g

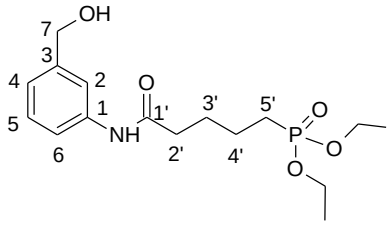

The procedure described for the synthesis of diethyl [*N*-(3-hydroxyphenyl)carbamoyl]-butylphosphonate **327a** was employed, using 5-chloro-*N*-[3-(hydroxymethyl)phenyl]-pentanamide **326g** (0.50 g, 2.1 mmol) and triethyl phosphite (0.72 mL, 4.1 mmol). The crude product was purified by flash chromatography [on silica gel; elution with hexane-EtOAc (4:1)], and subsequent evaporation of the solvent *in vacuo* afforded *diethyl {*N-*[3-(hydroxymethyl)phenyl]carbamoyl}butylphosphonate* **327g** as a clear oil (0.31 g, 66 %); (Found: $\mathbf{M}^+$, 343.15504 $C_{16}H_{26}NO_5P$ requires: $\mathbf{M}^+$, 343.15486); υ/cm^{-1} 3173 (OH), 1676 (C=O), 1236 (P=O) and 1048 (P−OEt); δ_H/ppm (400 MHz; $CDCl_3$) 1.20 (2H, m, 4'-CH_2), 1.31 (6H, t, *J* = 7.6 Hz, 2 × CH_3), 1.85 (4H, m, 3'-CH_2 and CH_2P), 2.43 (2H, t, *J* = 6.8 Hz, CH_2CO), 4.11 (4H, m, 2 × OCH_2), 4.53 (2H, s, CH_2OH), 5.62 (1H, s, OH), 7.12 (1H, d, *J* = 7.2 Hz, 4-H), 7.23 (1H, t, *J* = 8.0 Hz, 5-H), 7.43 (1H, d, *J* = 8.0 Hz, 6-H), 7.50 (1H, s, 2-H) and 8.13 (1H, s, NH); δ_C (100 MHz; $CDCl_3$) 16.3 (d, J_{P-C} = 6.5 Hz, 2 × CH_3), 21.8 (d, J_{P-C} = 15.3 Hz, C-4'), 23.8 (d, J_{P-C} = 143.8 Hz, CH_2P), 26.3 (d, J_{P-C} = 4.8 Hz, C-3'), 36.4 (d, J_{P-C} = 3.8 Hz, CH_2CO), 62.8 (d, J_{P-C} = 6.5 Hz, 2 × OCH_2), 64.7 (CH_2OH), 118.2 (C-2), 118.7 (C-6), 123.2 (C-4), 129.8 (C-5), 138.7 (C-1), 140.7 (C-3) and 173.5 (C=O).

3.3.4.2. Synthesis of butylphosphonic acids derivatives using TMSBr

[*N*-(3-Hydroxyphenyl)carbamoyl]butylphosphonic acid 335a

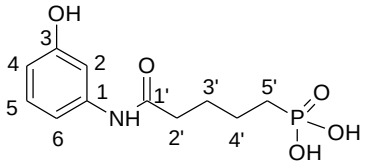

Trimethylsilyl bromide (0.20 mL, 1.6 mmol) was added to diethyl [*N*-(3-hydroxyphenyl) carbamoyl]butylphosphonate **327a** (0.25 g, 0.75 mmol) in CH_3CN (3 mL) and the mixture was heated in the microwave apparatus set to deliver 100 W of power, with a reaction temperature of 60 ^oC and reaction time of 10 min. After completion, the mixture was cooled

to room temperature, treated with a 95:5 MeOH-H_2O mixture and stirred for 30 min. The solvent was removed *in vacuo* and the residue chromatographed [preparative layer chromatography; elution with hexane-EtOAc-MeOH (1:1:1)] to yield *[*N-*(3-hydroxyphenyl)carbamoyl]butylphosphonic acid* **335a** as a yellow oil (0.11 g, 67 %); (Found: C, 48.51; H, 5.82; N, 5.08 %. $C_{11}H_{16}NO_5P$ requires C, 48.36; H, 5.90; N, 5.13 %); υ/cm^{-1} 3376 (OH), 1687 (C=O) and 1235 (P=O); δ_H/ppm (400 MHz; $CDCl_3$) 1.25 (2H, m, 4'-CH_2), 2.06 (4H, m, CH_2P), 2.39 (2H, t, *J* = 6.4 Hz, CH_2CO), 6.05 (2H, s, 2 x OH), 6.65 (1H, d, *J* = 7.2 Hz, 4-H), 6.93 (1H, d, *J* = 7.6 Hz, 6-H), 7.10 (1H, s, OH), 7.18 (1H, t, *J* = 7.6 Hz, 5-H), 7.30 (1H, s, 2-H) and 8.28 (1H, s, NH); δ_C/ppm (100 MHz; $CDCl_3$) 21.3 (d, J_{P-C} = 15.2 Hz, C-4'), 23.6 (d, J_{P-C} = 143.5 Hz, CH_2P), 26.4 (d, J_{P-C} = 4.8 Hz, C-3'), 36.2 (d, J_{P-C} = 3.3 Hz, CH_2CO), 107.9 (C-2), 112.3 (C-4), 112.8 (C-6), 128.7 (C-5), 138.7 (C-1), 158.3 (C-3) and 164.1 (C=O).

[*N*-(3-Methoxyphenyl)carbamoylbutylphosphonic acid 335b

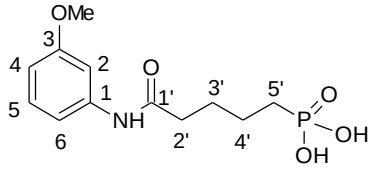

The procedure described for the synthesis of [*N*-(3-hydroxyphenyl)carbamoyl]butyl phosphonic acid **335a** was employed, using diethyl [*N*-(3-methoxyphenyl)carbamoyl]butyl phosphonate **327b** (0.25 g, 0.73 mmol) in CH_3CN (3 mL) and trimethylsilyl bromide (0.19 mL, 1.5 mmol). The solvent was removed *in vacuo* and the residue chromatographed [preparative layer chromatography; elution with hexane-EtOAc-MeOH (1:1:1)] to yield *[*N-*(3-methoxyphenyl)carbamoyl]butylphosphonic acid* **335b** as a yellow oil (0.097 g, 60 %); (Found: C, 50.27; H, 6.38; N, 4.82 %. $C_{12}H_{18}NO_5P$ requires C, 50.18; H, 6.32; N, 4.88 %); υ/cm^{-1} 3152 (OH), 1679 (C=O) and 1231 (P=O); δ_H/ppm (400 MHz; $CDCl_3$) 1.29 (2H, m, 4'-CH_2), 2.03 (4H, m, 3'-CH_2 and CH_2P), 2.42 (2H, t, *J* = 6.4 Hz, CH_2CO), 3.79 (3H, OCH_3), 4.89 (2H, s, 2 × OH), 6.60 (1H, d, *J* = 8.4 Hz, 4-H), 7.01 (1H, d, *J* = 7.2 Hz, 6-H), 7.12 (1H, s, 2-H), 7.23 (1H, t, *J* = 8.0 Hz, 5-H) and 7.83 (1H, s, NH); δ_C/ppm (100 MHz; $CDCl_3$) 21.9 (d, J_{P-C} = 15.6 Hz, C-4'), 23.6 (d, J_{P-C} = 141.2 Hz, CH_2P), 26.2 (d, J_{P-C} = 4.3 Hz, C-3'), 36.3 (d, J_{P-C} = 4.5 Hz, CH_2CO), 55.3 (OCH_3), 106.2 (C-2), 109.4 (C-4), 112.7 (C-6), 129.8 (C-5), 139.8 (C-1), 159.9 (C-3) and 169.2 (C=O).

[*N*-(3-Bromophenyl)carbamoyl]butylphosphonic acid 335c

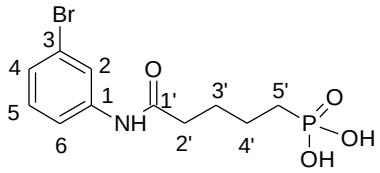

The procedure described for the synthesis of [*N*-(3-hydroxyphenyl)carbamoyl]butyl phosphonic acid **335a** was employed, using diethyl [*N*-(3-bromophenyl)carbamoyl]butyl phosphonate **325c** (0.25 g, 0.63 mmol) in CH_3CN (3 mL) and trimethylsilyl bromide (0.17 mL, 1.3 mmol). The solvent was removed *in vacuo* and the residue chromatographed [preparative layer chromatography; elution with hexane-EtOAc-MeOH (1:1:1)] to yield *[*N-*(3-bromophenyl)carbamoyl]butylphosphonic acid* **335c** as a brown oil (0.099 g, 60 %); (Found: C, 39.54; H, 4.59; N, 4.25 %. $C_{11}H_{15}BrNO_4P$ requires C, 39.31; H, 4.50; N, 4.17 %); υ/cm^{-1} 3163 (OH), 1680 (C=O) and 1219 (P=O); δ_H/ppm (400 MHz;$CDCl_3$) 1.25 (2H, m, 4'-CH_2), 1.77 (2H, m, CH_2P), 2.00 (2H, m, 3'-CH_2), 2.38 (2H, t, *J* = 6.4 Hz, CH_2CO), 5.77 (2H, x, 2 × OH), 6.80 (1H, dd, *J* = 5.2 and 2.0 Hz, 4-H), 7.05 (1H, t, *J* = 2.0 Hz, 2-H), 7.09 (1H, dd, *J* = 5.6 and 0.8 Hz, 6-H), 7.23 (1H, t, *J* = 8.0 Hz, 5-H) and 7.48 (1H, s, NH); δ_C/ppm (400 MHz; $CDCl_3$) 21.7 (d, J_{P-C} = 15.6 Hz, C-4'), 23.5 (d, J_{P-C} = 144.5 Hz, CH_2P), 26.7 (d, J_{P-C} = 5.2 Hz, C-3'), 36.1 (d, J_{P-C} = 4.1 Hz, CH_2CO), 115.8 (C-6), 118.2 (C-3), 122.5 (C-2), 126.8 (C-4), 129.8 (C-5), 138.9 (C-1) and 170.4 (C=O).

[*N*-(3-Fluorophenyl)carbamoyl]butylphosphonic acid 335d

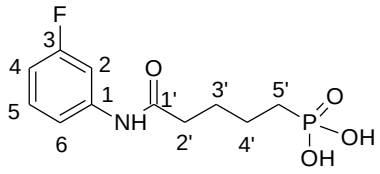

The procedure described for the synthesis of [*N*-(3-hydroxyphenyl)carbamoyl]butyl phosphonic acid **335a** was employed, using diethyl [*N*-(3-fluorophenyl)carbamoyl]butyl phosphonate **327d** (0.25 g, 0.73 mmol) in CH_3CN (3 mL) and trimethylsilyl bromide (0.20 mL, 1.5 mmol). The solvent was removed *in vacuo* and the residue chromatographed [preparative layer chromatography; elution with hexane-EtOAc-MeOH (1:1:1)] to yield *[*N-*(3-fluorophenyl)carbamoyl]butylphosphonic acid* **335d** as a yellow oil (0.10 g, 63 %); (Found: C, 48.12; H, 5.60; N, 6.87 %. $C_{11}H_{15}FNO_4P$ requires C, 48.01; H, 5.49; N, 6.90 %); υ/cm^{-1} 3019

(OH), 1664 (C=O) and 1216 (P=O); δ_H/ppm (400 MHz; $CDCl_3$) 1.23 (2H, m, 4'-CH_2), 1.90 (2H, m, CH_2P), 2.03 (2H, m, 3'-CH_2), 2.43 (2H, t, *J* = 6.4 Hz, CH_2CO), 3.65 (2H, s, 2 × OH), 6.83 (1H, ddd, *J* = 6.4, 2.4 and 1.6 Hz, 4-H), 6.90 (1H, dd, *J* = 6.4 and 0.8 Hz, 6-H), 6.92 (1H, td, *J* = 6.8, 2.4 and 1.2 Hz, 5-H) 7.54 (1H, dt, *J* = 6.4 and 2.4 Hz, 2-H) and 9.01 (1H, s, NH); δ_C/ppm (100 MHz; $CDCl_3$) 20.7 (d, J_{P-C} = 15.6 Hz, C-4'), 22.9 (d, J_{P-C} = 142.0 Hz, CH_2P), 26.8 (d, J_{P-C} = 4.4 Hz, C-3'), 36.4 (d, J_{P-C} = 3.9 Hz, CH_2CO), 108.5 (d, J_{F-C} = 26.3 Hz, C-2), 111.1 (d, J_{F-C} = 21.2 Hz, C-4), 115.7 (d, J_{F-C} = 3.3 Hz, C-6), 129.8 (d, J_{F-C} = 8.8 Hz, C-5), 138.7 (d, J_{F-C} = 10.8 Hz, C-1), 164.3 (d, J_{F-C} = 243.2 Hz, C-3) and 167.6 (C=O).

[*N*-(3-Cyanophenyl)carbamoyl]butylphosphonic acid 335e

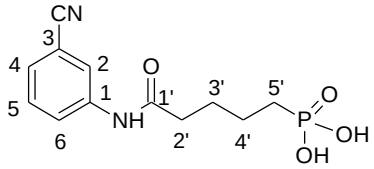

The procedure described for the synthesis of [*N*-(3-hydroxyphenyl)carbamoyl]butyl phosphonic acid **335a** was employed, using diethyl [*N*-(3-cyanophenyl)carbamoyl]butyl phosphonate **327e** (0.25 g, 0.74 mmol) in CH_3CN (3 mL) and trimethylsilyl bromide (0.20 mL, 1.5 mmol). The solvent was removed *in vacuo* and the residue chromatographed [preparative layer chromatography; elution with hexane-EtOAc-MeOH (1:1:1)] to yield *[*N-*(3-cyanophenyl)carbamoyl]butylphosphonic acid* **335e** as a clear oil (0.096 g, 59 %); (Found: C, 51.21; H, 5.45; N, 9.98 %. $C_{12}H_{15}N_2O_4P$ requires C, 51.07; H, 5.36; N, 9.93 %); (0.10 g, 59 %); υ/cm^{-1} 3235 (OH), 2234 (C≡N), 1684 (C=O) and 1232 (P=O); δ_H/ppm (400 MHz; $CDCl_3$) 1.24 (2H, m, 4'-CH_2), 1.73 (2H, m, CH_2P), 1.89 (2H, m, 3'-CH_2), 2.41 (2H, t, *J* = 6.8 Hz, CH_2CO), 7.18 (2H, s, 2 x OH), 7.35 (2H, t, *J* = 7.2 Hz, 5-H), 7.50 (1H, d, *J* = 6.2 Hz, 4-H), 7.69 (1H, d, *J* = 7.6 Hz, 6-H), 7.89 (1H, s, 2-H) and 9.78 (1H, s, NH); δ_C/ppm (400 MHz; $CDCl_3$) 21.8 (d, J_{P-C} = 15.6 Hz, C-4'), 23.5 (d, J_{P-C} = 143.5 Hz, CH_2P), 26.9 (d, J_{P-C} = 4.8 Hz, C-3'), 36.6 (d, J_{P-C} = 3.8 Hz, CH_2CO), 112.5 (C-3), 118.4 (C≡N), 122.6 (C-2), 124.2 (C-5), 127.4 (C-6), 129.7 (C-4), 139.2 (C-1) and 169.4 (C=O).

[*N*-(3-Nitrophenyl)carbamoyl]butylphosphonic acid 335f

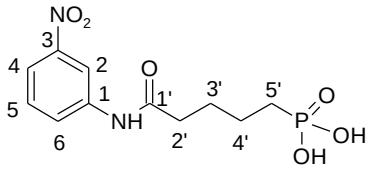

The procedure described for the synthesis of [*N*-(3-hydroxyphenyl)carbamoyl]butyl phosphonic acid **335a** was employed, using diethyl [*N*-(3-nitrophenyl)carbamoyl]butyl phosphonate **327f** (0.25 g, 0.70 mmol) in CH_3CN (3 mL) and trimethylsilyl bromide (0.18 mL, 1.4 mmol). The solvent was removed *in vacuo* and the residue chromatographed [preparative layer chromatography; elution with hexane-EtOAc-MeOH (1:1:1)] to yield *[*N-*(3-nitrophenyl)carbamoyl]butylphosphonic acid* **335f** as a yellow oil (0.12 g, 69 %); (Found: C, 43.79; H, 5.09; N, 9.35 %. $C_{11}H_{15}N_2O_6P$ requires C, 43.72; H, 5.00; N, 9.27 %); υ/cm^{-1} 3267 (OH), 1659 (C=O) and 1235 (P=O); δ_H/ppm (400 MHz; $CDCl_3$) 1.20 (2H, m, 4'-CH_2), 1.81 (4H, m, 3'-CH_2 and CH_2P), 2.44 (2H, t, *J* = 6.8 Hz, CH_2CO), 5.89 (2H, s, 2 × OH), 7.48 (1H, s, 2-H), 7.52 (1H, t, *J* = 8.4 Hz, 5-H), 7.95 (2H, m, 4-H and 6-H) and 8.89 (1H, s, NH); δ_C/ppm (400 MHz; $CDCl_3$) 21.8 (d, J_{P-C} = 15.8 Hz, C-4'), 24.1 (d, J_{P-C} = 143.5 Hz, CH_2P), 26.7 (d, J_{P-C} = 4.2 Hz, C-3'), 36.9 (d, J_{P-C} = 4.6 Hz, CH_2CO), 114.2 (C-2), 118.8 (C-4), 124.5 (C-6), 129.6 (C-5), 139.8 (C-1), 148.4 (C-3) and 169.7 (C=O).

4-{[3-(Hydroxymethyl)phenyl]carbamoyl}butylphosphonic acid 335g

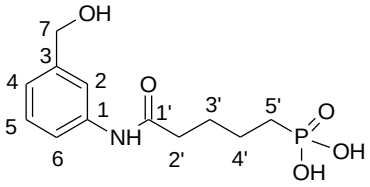

The procedure described for the synthesis of [*N*-(3-hydroxyphenyl)carbamoyl]butyl phosphonic acid **335a** was employed, using diethyl {*N*-[3-(hydroxymethyl) phenyl]carbamoyl}butylphosphonate **327g** (0.25 g, 0.76 mmol) in CH_3CN (3 mL) and trimethylsilyl bromide (0.20 mL, 1.5 mmol). The solvent was removed *in vacuo* and the residue chromatographed [preparative layer chromatography; elution with hexane-EtOAc-MeOH (1:1:1.5)] to yield *{*N-*[3-(hydroxymethyl)phenyl]carbamoyl}butylphosphonic acid* **335g** as a yellow oil (0.094 g, 57 %); (Found: C, 50.24; H, 6.39; N, 4.95 %. $C_{12}H_{18}NO_5P$ requires C, 50.18; H, 6.32; N, 4.88 %); υ/cm^{-1} 3276 (OH), 1682 (C=O) and 1234 (P=O); δ_H/ppm (400 MHz;

$CDCl_3$) 1.24 (2H, m, 4'-CH_2), 1.87 (4H, m, 3'-CH_2 and CH_2P), 2.39 (2H, t, *J* = 6.8 Hz, CH_2CO), 3.22 (2H, s, 2 x OH), 5.08 (2H, s, CH_2OH), 7.11 (1H, d, *J* = 7.2 Hz, 4-H), 7.19 (1H, s, 2-H), 7.23 (1H, t, *J* = 8.0 Hz, 5-H), 7.60 (1H, d, *J* = 8.0 Hz, 6-H), 7.75 (1H, s, OH) and 8.15 (1H, s, NH); δ_C/ppm (400 MHz; $CDCl_3$) 21.8 (d, J_{P-C} = 15.6 Hz, C-4'), 23.6 (d, J_{P-C} = 142.0 Hz, CH_2P), 26.7 (d, J_{P-C} = 4.8 Hz, C-3'), 35.8 (d, J_{P-C} = 3.8 Hz, CH_2CO), 64.3 (CH_2OH), 118.1 (C-2), 118.8 (C-6), 123.6 (C-4), 129.8 (C-5), 138.9 (C-1), 141.3 (C-3) and 169.8 (C=O).

3.3.4.3. Synthesis of sodium hydrogen butylphosphonate derivatives

Sodium hydrogen [*N*-(3-hydroxyphenyl)carbamoyl]butylphosphonate 336a

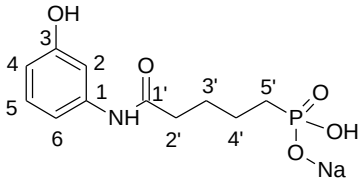

[*N*-(3-Hydroxyphenyl)carbamoyl]butylphosphonic acid **335a** (0.15 g, 0.55 mmol) was treated with a solution of NaOH (1.1 mol) in EtOH (0.52 mL) and the mixture was stirred for 30 min. The solvent was removed *in vacuo* and the residue chromatographed [reverse-phase column chromatography; elution with H_2O-MeOH (1:1)] to yield *sodium hydrogen [*N*-(3-hydroxyphenyl)carbamoyl]butylphosphonate* **336a** as a grey semi-solid (0.094 g, 91 %); (Found: C, 44.85; H, 5.23; N, 4.79 %. $C_{11}H_{15}NNaO_5P$ requires C, 44.75; H, 5.12; N, 4.74 %); υ/cm^{-1} 3265 (OH), 1653 (C=O) and 1219 (P=O); δ_H/ppm (400 MHz; D_2O) 1.21 (2H, m, 4'-CH_2), 1.79 (2H, m, CH_2P), 2.03 (2H, m, 3'-CH_2), 2.41 (2H, t, *J* = 6.4 Hz, CH_2CO), 6.63 (1H, d, *J* = 7.2 Hz, 4-H), 6.95 (1H, d, *J* = 7.6 Hz, 6-H), 7.12 (1H, t, *J* = 7.6 Hz, 5-H) and 7.40 (1H, s, 2-H); δ_C/ppm(100 MHz; D_2O) 22.5 (d, J_{P-C} = 15.6 Hz, C-4'), 23.6 (d, J_{P-C} = 143.5 Hz, CH_2P), 26.7 (d, J_{P-C} = 4.8 Hz, C-3'), 35.9 (d, J_{P-C} = 3.4 Hz, CH_2CO), 108.0 (C-2), 112.1 (C-4), 112.8 (C-6), 128.2 (C-5), 138.3 (C-1), 158.5 (C-3) and 168.1 (C=O).

Sodium hydrogen [*N*-(3-methoxyphenyl)carbamoyl]butylphosphonate 336b

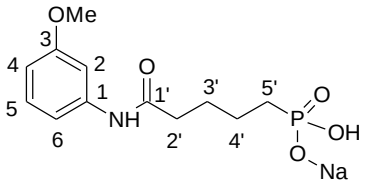

The procedure described for the synthesis of sodium hydrogen [*N*-(3-hydroxyphenyl)carbamoyl]butylphosphonate **336a** was employed, using [*N*-(3-methoxyphenyl)carbamoyl]butylphosphonic acid **335b** (0.15 g, 0.52 mmol) and a solution of NaOH (1.1 mol) in EtOH (0.49 mL). The solvent was removed *in vacuo* and the residue chromatographed [reverse-phase column chromatography; elution with H_2O-MeOH (1:1)] to yield *sodium hydrogen [*N*-(3-methoxyphenyl)carbamoyl]butylphosphonate* **336b** as a yellow semi-solid (0.098 g, 94 %); (Found: C, 46.73; H, 5.62; N, 4.57 %. $C_{12}H_{17}NNaO_5P$ requires C, 46.61; H, 5.54; N, 4.53 %); υ/cm^{-1} 3317 (OH), 1678 (C=O) and 1232 (P=O); δ_H/ppm (400 MHz; D_2O) 1.25 (2H, m, 4'-CH_2), 1.98 (4H, m, 3'-CH_2 and CH_2P), 2.44 (2H, t, *J* = 6.4 Hz, CH_2CO), 3.78 (3H, OCH_3), 6.61 (1H, d, *J* = 8.0 Hz, 4-H), 7.02 (1H, d, *J* = 7.2 Hz, 6-H), 7.11 (1H, s, 2-H) and 7.23 (1H, t, *J* = 7.6 Hz, 5-H); δ_C/ppm (100 MHz; D_2O) 22.8 (d, J_{P-C} = 15.6 Hz, C-4'), 24.1 (d, J_{P-C} = 141.8 Hz, CH_2P), 26.7 (d, J_{P-C} = 4.4 Hz, C-3'), 36.3 (d, J_{P-C} = 4.3 Hz, CH_2CO), 54.7 (OCH_3), 106.5 (C-2), 110.2 (C-4), 112.5 (C-6), 129.9 (C-5), 140.0 (C-1), 159.7 (C-3) and 167.3 (C=O).

Sodium hydrogen [*N*-(3-bromophenyl)carbamoyl]butylphosphonate 336c

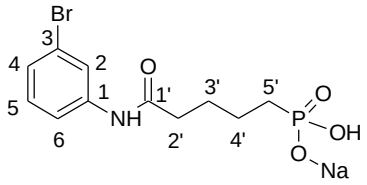

The procedure described for the synthesis of sodium hydrogen [*N*-(3-hydroxyphenyl)carbamoyl]butylphosphonate **336a** was employed, using [*N*-(3-bromophenyl)carbamoyl]butylphosphonic acid **335c** (0.15 g, 0.44 mmol) and a solution of NaOH (1.1 mol) in EtOH (0.41 mL). The solvent was removed *in vacuo* and the residue chromatographed [reverse-phase column chromatography; elution with H_2O-MeOH (1:1)] to yield *sodium hydrogen [*N*-(3-bromophenyl)carbamoyl]butylphosphonate* **336c** as a pale yellow semi-solid (0.098 g, 94 %); (Found: C, 37.01; H, 4.17; N, 3.88 %. $C_{11}H_{14}BrNNaO_4P$ requires C, 36.89; H, 3.94; N, 3.91 %); υ/cm^{-1} 3271 (OH), 1666 (C=O) and 1230 (P=O); δ_H/ppm (400 MHz; D_2O) 1.27 (2H, m, 4'-CH_2), 1.80 (2H, m, CH_2P), 1.98 (2H, m, 3'-CH_2), 2.41 (2H, t, *J* = 6.2 Hz, CH_2CO), 6.78 (1H, t, *J* = 7.6 Hz, 5-H), 7.21 (1H, d, *J* = 7.6 Hz, 4-H), 7.29 (1H, d, *J* = 7.2 Hz, 6-H) and 7.43 (1H, s, 2-H); δ_C/ppm (100 MHz; D_2O) 22.3 (d, J_{P-C} = 15.4 Hz, C-4'), 24.2 (d, J_{P-C} = 144.1 Hz, CH_2P), 26.5 (d, J_{P-C} = 5.6 Hz, C-3'), 36.6 (d, J_{P-C} = 4.2 Hz, CH_2CO), 115.5 (C-6), 118.3 (C-3), 123.4 (C-2), 126.5 (C-4), 129.7 (C-5), 138.8 (C-1) and 167.4 (C=O).

Sodium hydrogen [*N*-(3-fluorophenyl)carbamoyl]butylphosphonate 336d

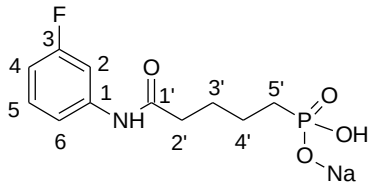

The procedure described for the synthesis of sodium hydrogen [*N*-(3-hydroxyphenyl)carbamoyl]butylphosphonate **336a** was employed, using [*N*-(3-fluorophenyl)carbamoyl]butylphosphonic acid **335d** (0.15 g, 0.54 mmol) and a solution of NaOH (1.1 mol) in EtOH (0.52 mL). The solvent was removed *in vacuo* and the residue chromatographed [reverse-phase column chromatography; elution with H_2O-MeOH (1:1)] to yield *sodium hydrogen [*N-*(3-fluorophenyl)carbamoyl]butylphosphonate* **336d** as a grey semi-solid (0.010 g, 96 %); (Found: C, 44.53; H, 4.70; N, 4.80 %. $C_{11}H_{14}FNNaO_4P$ requires C, 44.45; H, 4.75; N, 4.71 %); υ/cm^{-1} 3416 (OH), 1683 (C=O) and 1239 (P=O); δ_H/ppm (400 MHz; D_2O) 1.28 (2H, m, 4'-CH_2), 1.92 (2H, m, CH_2P), 1.99 (2H, m, 3'-CH_2), 2.36 (2H, t, *J* = 6.4 Hz, CH_2CO), 6.80 (1H, ddd, *J* = 6.8, 2.4 and 1.6 Hz, 4-H), 7.20 (1H, dd, *J* = 6.2 and 0.8 Hz, 6-H), 7.26 (1H, td, *J* = 6.8, 2.4 and 1.6 Hz, 5-H) and 7.40 (1H, dt, *J* = 6.4 and 2.4 Hz, 2-H); δ_C/ppm (100 MHz; D_2O) 22.2 (d, J_{P-C} = 15.6 Hz, C-4'), 23.1 (d, J_{P-C} = 142.0 Hz, CH_2P), 26.5 (d, J_{P-C} = 3.8 Hz, C-3'), 36.8 (d, J_{P-C} = 3.2 Hz, CH_2CO), 108.3 (d, J_{F-C} = 26.2 Hz, C-2), 111.5 (d, J_{F-C} = 20.8 Hz, C-4), 115.4 (d, J_{F-C} = 3.8 Hz, C-6), 129.7 (d, J_{F-C} = 10.2 Hz, C-5), 138.9 (d, J_{F-C} = 11.2 Hz, C-1), 163.6 (d, J_{F-C} = 241.7 Hz, C-3) and 172.1 (C=O).

Sodium hydrogen [*N*-(3-cyanophenyl)carbamoyl]butylphosphonate 336e

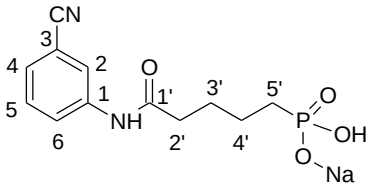

The procedure described for the synthesis of sodium hydrogen [*N*-(3-hydroxyphenyl)carbamoyl]butylphosphonate **336a** was employed, using [*N*-(3-cyanophenyl)carbamoyl]butylphosphonic acid **335e** (0.15 g, 0.53 mmol) and a solution of NaOH (1.1 mol) in EtOH (0.50 mL). The solvent was removed *in vacuo* and the residue chromatographed [reverse-phase column chromatography; elution with H_2O-MeOH (1:1)] to yield *sodium hydrogen [*N-*(3-cyanophenyl)carbamoyl]butylphosphonate* **336e** as a yellow

semi-solid (0.10 g, 94 %); (Found: C, 47.27; H, 4.73; N, 9.25 %. $C_{12}H_{14}N_2NaO_4P$ requires C, 47.38; H, 4.64; N, 9.21 %); (0.10 g, 59 %); υ/cm^{-1} 3849 (OH), 2225 (C≡N), 1678 (C=O) and 1219 (P=O); δ_H/ppm (400 MHz; D_2O) 1.23 (2H, m, 4'-CH_2), 1.77 (2H, m, CH_2P), 1.90 (2H, m, 3'-CH_2), 2.43 (2H, t, *J* = 6.8 Hz, CH_2CO), 7.37 (2H, t, *J* = 7.6 Hz, 5-H), 7.63 (1H, d, *J* = 6.8 Hz, 4-H), 7.69 (1H, d, *J* = 7.6 Hz, 6-H) and 7.87 (1H, s, 2-H); δ_C/ppm (100 MHz; D_2O) 22.3 (d, J_{P-C} = 15.8 Hz, C-4'), 22.6 (d, J_{P-C} = 143.6 Hz, CH_2P), 26.6 (d, J_{P-C} = 4.8 Hz, C-3'), 36.4 (d, J_{P-C} = 3.7 Hz, CH_2CO), 112.6 (C-3), 118.2 (C≡N), 122.6 (C-2), 124.8 (C-5), 127.5 (C-6), 129.6 (C-4), 138.8 (C-1) and 173.5 (C=O).

Sodium hydrogen [*N*-(3-nitrophenyl)carbamoyl]butylphosphonate 336f

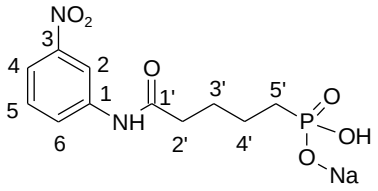

The procedure described for the synthesis of sodium hydrogen [*N*-(3-hydroxyphenyl)carbamoyl]butylphosphonate **336a** was employed, using [*N*-(3-nitrophenyl)carbamoyl]butylphosphonic acid **335f** (0.15 g, 0.49 mmol) and a solution of NaOH (1.1 mol) in EtOH (0.46 mL). The solvent was removed *in vacuo* and the residue chromatographed [reverse-phase column chromatography; elution with H_2O-MeOH (1:1)] to yield *sodium hydrogen [*N*-(3-nitrophenyl)carbamoyl]butylphosphonate* **336f** as a yellow semi-solid (0.099 g, 92 %); (Found: C, 40.89; H, 4.47; N, 8.57 %. $C_{11}H_{14}N_2NaO_6P$ requires C, 40.75; H, 4.35; N, 8.64 %); υ/cm^{-1} 3423 (OH), 1678 (C=O) and 1227 (P=O); δ_H/ppm (400 MHz; D_2O) 1.21 (2H, m, 4'-CH_2), 1.80 (4H, m, 3'-CH_2 and CH_2P), 2.32 (2H, t, *J* = 6.8 Hz, CH_2CO), 7.43 (1H, s, 2-H), 7.55 (1H, t, *J* = 8.0 Hz, 5-H) and 7.86 (2H, m, 4-H and 6-H); δ_C/ppm (100 MHz; D_2O) 23.4 (d, J_{P-C} = 15.6 Hz, C-4'), 24.2 (d, J_{P-C} = 142.9 Hz, CH_2P), 25.8 (d, J_{P-C} = 4.2 Hz, C-3'), 36.4 (d, J_{P-C} = 3.2 Hz, CH_2CO), 114.7 (C-2), 118.3 (C-4), 123.7 (C-6), 128.6 (C-5), 139.7 (C-1), 149.3 (C-3) and 168.6 (C=O).

Sodium hydrogen {*N*-[3-(hydroxymethyl)phenyl]carbamoyl}butylphosphonate 336g

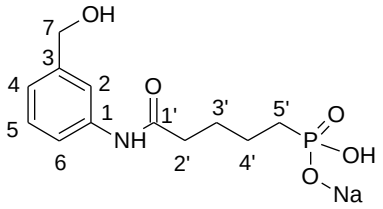

The procedure described for the synthesis of sodium hydrogen [*N*-(3-hydroxyphenyl)carbamoyl]butylphosphonate **336a** was employed, using {*N*-[(3-(hydroxymethyl)phenyl]carbamoyl}butylphosphonic acid **335g** (0.15 g, 0.52 mmol) and a solution of NaOH (1.1 mol) in EtOH (0.49 mL). The solvent was removed *in vacuo* and the residue chromatographed [reverse-phase column chromatography; elution with H_2O-MeOH (1:1)] to yield *sodium hydrogen {*N*-[3-(hydroxymethyl)phenyl]carbamoyl}butylphosphonate* **336g** as a white semi-solid (0.011 g, 96 %); (Found: C, 46.71; H, 5.58; N, 4.50 %. $C_{12}H_{17}NNaO_5P$ requires C, 46.61; H, 5.54; N, 4.53 %); υ/cm^{-1} 3384 (OH), 1682 (C=O) and 1234 (P=O); δ_H/ppm (400 MHz; D_2O) 1.27 (2H, m, 4'-CH_2), 1.84 (4H, m, 3'-CH_2 and CH_2P), 2.35 (2H, t, *J* = 6.8 Hz, CH_2CO), 4.62 (2H, s, C*H*$_2$OH), 7.17 (1H, d, *J* = 7.2 Hz, 4-H), 7.22 (1H, t, *J* = 8.0 Hz, 5-H), 7.38 (1H, d, *J* = 8.0 Hz, 6-H) and 7.42 (1H, s, 2-H); δ_C/ppm (100 MHz; D_2O) 22.0 (d, J_{P-C} = 15.6 Hz, C-4'), 23.7 (d, J_{P-C} = 143.7 Hz, CH_2P), 26.3 (d, J_{P-C} = 4.5 Hz, C-3'), 36.1 (d, J_{P-C} = 3.6 Hz, CH_2CO), 63.7 (CH_2OH), 118.0 (C-2), 118.8 (C-6), 124.3 (C-4), 129.9 (C-5), 139.4 (C-1), 140.9 (C-3) and 167.8 (C=O).

3.4. Furan-containing phosphoric acid derivatives

3-[(Trityloxy)methyl]furan 339 [176]

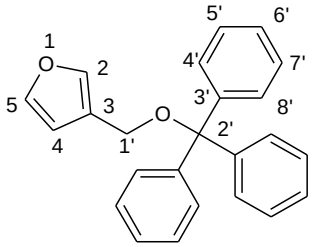

A solution of triphenylmethyl chloride **342** (6.00 g, 20.5 mmol), 3-furanmethanol **338** (2.00 g, 20.4 mmol), triethylamine (4.46 mL, 20.4 mmol) and DMAP (0.61 g, 5.0 mmol) in THF (30 mL) was stirred under N_2 at 80 ^oC for 15 hours. The solvent was evaporated *in vacuo* and the residue dissolved in EtOAc (100 mL). The organic phase was washed sequentially with water

(2 x 50 mL) and brine (2 x 50 mL). The aqueous washings were extracted with EtOAc and the organic layers were combined and dried (anhydr. $MgSO_4$). The solvent was evaporated *in vacuo* to afford 3-[(trityloxy)methyl]furan **339** as a yellow gum (4.98 g, 72 %); δ_H/ppm (400 MHz; $CDCl_3$) 4.06 (2H, s, OCH_2), 6.43 (1H, s, 2-H), 7.27 – 7.54 (17H, m, 4-H, 5-H and trityl group); δ_C/ppm (100 MHz; $CDCl_3$) 58.4 (OCH_2), 86.9 (C-2'), 109.9 (C-4), 123.1 (C-3), 127.0 (C-6'), 127.8 (C-4' and C-8'), 128.6 (C-5' and C-7'), 139.7 (C-3'), 143.0 (C-2) and 144.0 (C-5).

3-[(Trityloxy)methyl]furan-2-carbaldehyde 340a and 4-[(trityloxy)methyl]furan-2-carbaldehyde 340b [176]

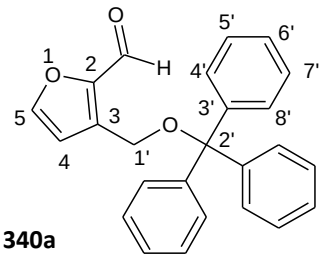

340a

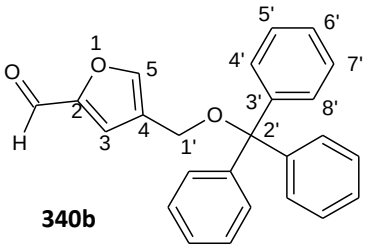

340b

Method 1

To a stirred solution of 3-[(trityloxy)methyl]furan **339** (2.00 g, 5.88 mmol) in THF (20 mL) under N_2 at *ca.* -30 ^oC, butyllithium (6.0 mL, 12 mml) was slowly added dropwise *via* a septum, ensuring that the temperature did not exceed -30 ^oC. The resulting mixture was stirred for 4 hours; DMF (1.38 mL) was then added and the mixture stirred for a further 2 hours. The reaction mixture was allowed to warm to room temperature and stirred for an additional 2 hours before being quenched with water (15 mL) and extracted with diethyl ether (2 x 50 mL). The organic extracts were washed sequentially with 10 % aq. $NaHCO_3$ (2 x 50 mL), brine (2 x 50 mL) and dried (anhydr. $MgSO_4$). The solvent was removed *in vacuo* to obtain the crude product as a yellow solid. The crude product was purified [normal-phase HPLC; elution with hexane-EtOAc (4:1)] to yield two products.

i. 3-[(Trityloxy)methyl]furan-2-carbaldehyde **340a** as a white solid (4 mg, 6 %); δ_H/ppm (400 MHz; $CDCl_3$) 4.14 (2H, s, OCH_2), 7.31 – 7.69 (17H, m, 4-H, 5-H and trityl group) and 9.68 (1H, s, CHO); δ_C/ppm (100 MHz; $CDCl_3$) 58.1 (OCH_2), 87.6 (C-2'), 113.1 (C-4), 127.3 (C-6'), 128.0 (C-4' and C-8'), 128.6 (C-5' and C-7'), 135.4 (C-3), 143.5 (C-3'), 147.2 (C-5), 147.8 (C-2) and 178.5 (C=O).

ii. 4-[(Trityloxy)methyl]furan-2-carbaldehyde **340b** as a pale yellow solid (12 mg, 12 %); δ_H/ppm (400 MHz; $CDCl_3$) 4.45 (2H, s, OCH_2), 6.75 (1H, s, 5-H), 7.26 – 7.49 (15H, m, trityl group), 7.61 (1H, s, 3-H) and 9.73 (1H, s, CHO); δ_C/ppm (100 MHz; $CDCl_3$) 57.8 (OCH_2), 87.3 (C-2'), 120.5 (C-3), 126.4 (C-4), 127.2 (C-6') 128 (C-4' and C-8'), 128.5 (C-5' and C-7'), 143.6 (C-3'), 145.2 (C-5), 153.1 (C-2) and 178.0 (C=O).

Method 2

The Vilsmeier reagent was prepared by adding phosphorus oxychloride (1.86 mL, 26.0 mmol) dropwise to DMF (20 mL) under nitrogen over a period of 30 min, maintaining the temperature below 5 ^oC. The mixture was stirred for 30 min, after which 3-[(trityloxy)methyl]furan **339** (2.00 g, 5.88 mmol) in DMF (5 mL) was added. The reaction mixture was stirred for 3 hours at room temperature and then heated at 80 ^oC for 1 hour. After cooling, the mixture was poured into ice-water (200 mL) and the pH adjusted to pH 10 with 0.1 M aq. NaOH. The solution was extracted with diethyl ether (4 x 50 mL), and the organic extracts were combined, washed with water and brine and the dried (anhydr. $MgSO_4$). The solvent was removed *in vacuo* to afford the crude product, which was recrystallised from MeOH to yield 4-[(trityloxy)methyl]furan-2-carbaldehyde **340b** as a pale yellow crystals (1.39 g, 64 %).

2-Acetyl-4-[(trityloxy)methyl]furan 340c and 2-acetyl-3-[(trityloxy)methyl]furan 369

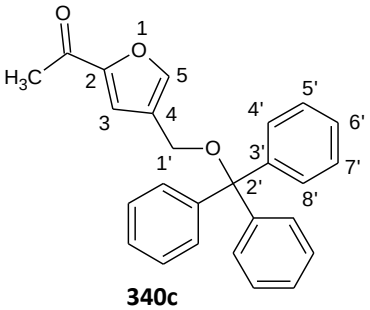

340c

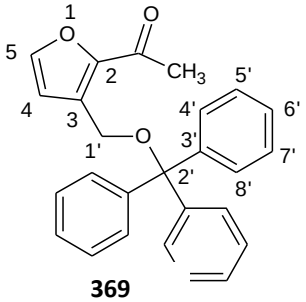

369

Method 1

Acetic anhydride (0.27 mL, 2.9 mmol) was added dropwise to a solution of $SnCl_4$ (0.12 mL, 0.49 mmol) in DCM (10 mL) under N_2 at 0 ^oC and the mixture was stirred for 15 min. 3-[(Trityloxy)methyl]furan **339** (1.00 g, 2.94 mmol) in DCM (10 mL) was added and the reaction mixture was stirred at 0 ^oC for 1 hour. The reaction mixture was then warmed to 40

^{o}C and stirred for 4 hours. After completion, the mixture was treated with saturated aq. $NaHCO_3$ (50 mL) and extracted with diethyl ether (2 x 50 mL). The organic extracts were combined, dried (anhydr. $MgSO_4$) and filtered. The solvent was removed under reduced pressure and the residue was purified [normal-phase HPLC; elution with hexane-EtOAc (3:1)] to yield two products.

i. *2-Acetyl-4-[(trityloxy)methyl]furan* **340c** as a yellow oil (47 mg, 64 %); (Found: C, 81.58; H, 5.76 %. $C_{26}H_{22}O_3$ requires C, 81.65; H, 5.80 %); υ/cm^{-1} 1675 (C=O); δ_H/ppm (400 MHz; $CDCl_3$) 2.57 (3H, s, CH_3CO), 4.42 (2H, s, OCH_2) and 7.14 – 7.34 (17H, m, 3-H, 5-H and trityl group); δ_C/ppm (100 MHz; $CDCl_3$) 24.2 (CH_3), 57.3 (OCH_2), 87.6 (C-2'), 120.4 (C-3), 126.4 (C-4), 127.4 (C-6') 127.9 (C-4' and C-8'), 128.4 (C-5' and C-7'), 143.5 (C-3'), 145.3 (C-5), 153.5 (C-2) and 181.3 (C=O).

ii. *2-Acetyl-3-[(trityloxy)methyl]furan* **369** as a yellow oil (2 mg, 2.4 %); (Found: C, 81.60; H, 5.82 %. $C_{26}H_{22}O_3$ requires C, 81.65; H, 5.80 %); υ/cm^{-1} 1682 (C=O); δ_H/ppm (400 MHz; $CDCl_3$) 2.59 (3H, s, CH_3CO), 4.45 (2H, s, OCH_2) and 7.12 – 7.28 (17H, m, 4-H, 5-H and trityl group); δ_C/ppm (100 MHz; $CDCl_3$) 24.8 (CH_3), 56.8 (OCH_2), 87.3 (C-2'), 112.8 (C-4), 126.7 (C-6'), 128.1 (C-4' and C-8'), 128.8 (C-5' and C-7'), 134.6 (C-3), 143.6 (C-3'), 147.3 (C-2), 148.2 (C-5) and 181.8 (C=O).

Method 2

Acetic anhydride (0.14 mL, 1.5 mmol) was added dropwise to a solution of 3-[(trityloxy)methyl]furan **339** (0.50 g, 1.5 mmol) and $ZnCl_2$ (0.10 g, 0.75 mmol) in DCM (10 mL) under N_2 at 0 ^{o}C and the mixture was stirred for 1 hour. The reaction mixture was then warmed to 40 ^{o}C and stirred for 8 hours. After completion, the mixture was treated with saturated aq. $NaHCO_3$ (20 mL) and extracted with diethyl ether (2 x 25 mL). The organic extracts were combined, dried (anhydr. $MgSO_4$) and filtered. The solvent was removed under reduced pressure and the residue was purified [normal-phase HPLC; elution with hexane-EtOAc (3:1)] to yield *2-acetyl-4-[(trityloxy)methyl]furan* **340c** as a yellow oil (28 mg, 37 %) and *2-acetyl-3-[(trityloxy)methyl]furan* **369** as a yellow oil (0.88 mg, 1.1 %).

2-(3,3-Dimethylbutanoyl)-4-[(trityloxy)methyl]furan 340d and 2-(3,3-dimethylbutanoyl)-3-[(trityloxy)methyl]furan 370

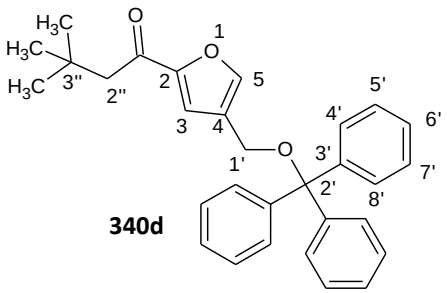

340d

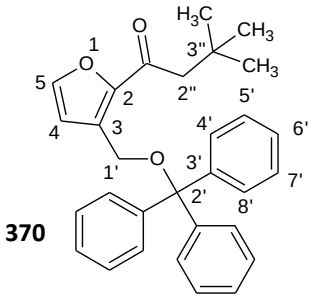

370

The procedure described for the synthesis of 2-acetyl-4-[(trityloxy)methyl]furan **340c** was employed, using 3-[(trityloxy)methyl]furan **339** (1.01 g, 2.94 mmol), *tert*-butylacetyl chloride (0.42 mL, 2.9 mmol) and $SnCl_4$ (0.12 mL, 0.49 mmol). The solvent was removed under reduced pressure and the residue was purified [normal-phase HPLC; elution with hexane-EtOAc (4:1)] to yield two products.

i. *2-(3,3-Dimethylbutanoyl)-4-[(trityloxy)methyl]furan* **340d** as a yellow oil (32 mg, 56 %); (Found: C, 82.30; H, 6.78 %. $C_{30}H_{30}O_3$ requires C, 82.16; H, 6.89 %); υ/cm^{-1} 1685 (C=O); δ_H/ppm (400 MHz; $CDCl_3$) 1.19 (9H, s, 3 x CH_3), 2.58 (2H, s, CH_2CO), 4.47 (2H, s, OCH_2) and 7.19 – 7.31 (17H, m, 3-H, 5-H and trityl group); δ_C/ppm (100 MHz; $CDCl_3$) 29.1 (3 x CH_3), 30.2 (C-3''), 47.4 (C-2''), 57.9 (OCH_2), 87.4 (C-2'), 120.6 (C-3), 126.4 (C-4), 127.3 (C-6') 128.0 (C-4' and C-8'), 128.6 (C-5' and C-7'), 143.7 (C-3'), 145.3 (C-5), 153.2 (C-2) and 187.0 (C=O).

ii. *2-(3,3-Dimethylbutanoyl)-3-[(trityloxy)methyl]furan* **370** as a yellow oil (1.6 mg, 2.9 %); (Found: C, 82.35; H, 6.83 %. $C_{30}H_{30}O_3$ requires C, 82.16; H, 6.89 %); υ/cm^{-1} 1691 (C=O); δ_H/ppm (400 MHz; $CDCl_3$) 1.21 (9H, s, 3 x CH_3), 2.56 (2H, s, CH_2CO), 4.52 (2H, s, OCH_2) and 7.14 – 7.21 (17H, m, 4-H, 5-H and trityl group); δ_C/ppm (100 MHz; $CDCl_3$) 29.5 (3 x CH_3), 31.3 (C-3''), 46.8 (C-2''), 58.2 (OCH_2), 87.3 (C-2'), 113.2 (C-4), 126.6 (C-6'), 127.8 (C-4' and C-8'), 128.9 (C-5' and C-7'), 132.8 (C-3), 143.8 (C-3'), 145.7 (C-5), 146.4 (C-2) and 186.4 (C=O).

4-(Hydroxymethyl)furan-2-carbaldehyde 347b [248]

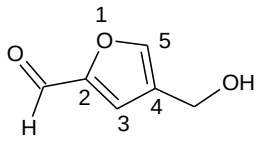

A suspension of 4-[(trityloxy)methyl]furan-2-carbaldehyde **340b** (0.25 g, 0.70 mmol) in HCOOH-THF-H_2O (1:1:0.1; 5 mL) was heated at 50 ^oC for 2 hours. The solvent was removed *in vacuo*, [co-evaporated with hexane (2 x 10 mL)] to yield 4-(hydroxymethyl)furan-2-carbaldehyde **347b** as a clear oil (0.20 g, 82 %), (Lit.[248]); υ/cm^{-1} 3347 (OH) and 1672 (C=O); δ_H/ppm (400 MHz; $CDCl_3$) 2.00 (1H, s, OH), 4.57 (2H, s, OCH_2), 6.46 (1H, s, 5-H), 7.42 (1H, s, 3-H) and 9.64 (1H, s, CHO); δ_C/ppm (100 MHz; $CDCl_3$) 58.2 (CH_2OH), 119.7 (C-3), 126.2 (C-4), 145.5 (C-5), 152.8 (C-2) and 182.5 (C=O).

2-Acetyl-1-[4-(Hydroxymethyl)furan 347c [249]

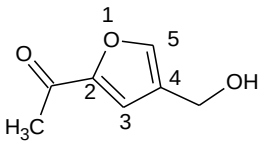

The procedure described for the synthesis of 4-(hydroxymethyl)furan-2-carbaldehyde **347b** was employed, using 2-acetyl-4-[(trityloxy)methyl]furan **340c** (0.25 g, 0.65 mmol) in HCOOH-THF-H_2O (1:1:0.1; 5 mL). The solvent was removed *in vacuo*, co-evaporated with hexane (2 x 10 mL) to yield 2-acetyl-1-[4-(Hydroxymethyl)furan **347c** as a colourless oil (0.21 g, 84 %); υ/cm^{-1} 3284 (OH) and 1687 (C=O); δ_H/ppm (400 MHz; $CDCl_3$) 2.56 (3H, s, CH_3CO), 3.20 (1H, s, OH), 4.52 (2H, s, OCH_2), 6.43 (1H, s, 5-H) and 7.36 (1H, s, 3-H); δ_C/ppm (100 MHz; $CDCl_3$) 24.6 (CH_3), 57.7 (OCH_2), 120.3 (C-3), 125.8 (C-4), 145.3 (C-5), 153.4 (C-2) and 178.9 (C=O).

2-(3,3-Dimethylbutanoyl)-1-[4-(hydroxymethyl)]furan 347d

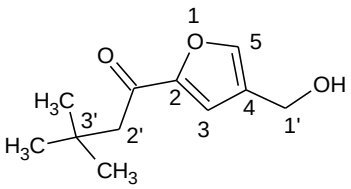

The procedure described for the synthesis of 4-(hydroxymethyl)furan-2-carbaldehyde **347b** was employed, using 2-(3,3-dimethylbutanoyl)-4-[(trityloxy)methyl]furan **340d** (0.25 g, 0.60 mmol) in HCOOH-THF-H_2O (1:1:0.1; 5 mL). The solvent was removed *in vacuo*, [co-

evaporated] with hexane (2 x 10 mL) to yield *2-(3,3-dimethylbutanoyl)-1-[4-(hydroxyl-methyl)]furan* **347d** as a colourless oil (0.20 g, 81 %); δ_H/ppm (400 MHz; $CDCl_3$) 1.19 (9H, s, 3 x CH_3), 2.12 (1H, s, OH), 2.54 (2H, s, CH_2CO), 4.52 (2H, s, OCH_2), 6.41 (1H, s, 5-H) and 7.39 (1H, s, 3-H); δ_C/ppm (100 MHz; $CDCl_3$) 28.6 (3 x CH_3), 32.6 (C-3'), 36.7 (C-2'), 58.6 (CH_2OH), 120.2 (C-3), 123.8 (C-4), 145.3 (C-5), 153.2 (C-2) and 184.7 (C=O).

Diethyl (2-formylfuran-4-yl)methyl phosphate 348b

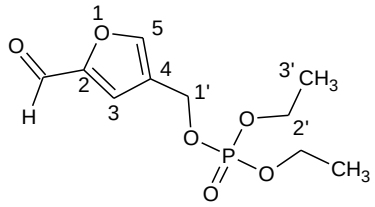

Diethyl chlorophosphate (0.52 g, 3.0 mmol) was added slowly to a stirred solution of 4-(hydroxymethyl)furan-2-carbaldehyde **347b** (0.20 g, 1.5 mmol) in pyridine (10 mL) at 0 ^oC. The reaction mixture was allowed to reach room temperature and the stirred for 24 hours. The solvent was removed *in vacuo* and the residue was dissolved in DCM (25 mL). The organic phase was washed with satd. aq. $NaHCO_3$ (2 x 50 mL), water (2 x 50 mL) and brine (2 x 50 mL), and dried (anhydr. $MgSO_4$). The solvent was evaporated *in vacuo* and the residue chromatographed [preparative layer chromatography; elution with hexane-EtOAc (4:1)] to yield *diethyl (2-formylfuran-4-yl)methyl phosphate* **348b** as a clear oil (0.14 g, 71 %); (Found: C, 45.90; H, 5.84 %. $C_{10}H_{15}O_6P$ requires C, 45.81; H, 5.77 %); υ/cm^{-1} 1677 (C=O) and 1227 (P=O); δ_H/ppm (400 MHz; $CDCl_3$) 1.29 (6H, m, 2 x CH_3), 4.10 (4H, m, 2 x CH_2CH_3), 4.87 (2H, d, J = 2.2 Hz, OCH_2), 6.45 (1H, s, 5-H), 7.39 (1H, s, 3-H) and 10.12 (1H, s, CHO); δ_C/ppm (100 MHz; $CDCl_3$) 16.3 (d, J_{F-C} = 6.1 Hz, 2 x CH_3), 60.8 (d, J_{P-C} = 6.4 Hz, OCH_2), 61.4 (d, J_{P-C} = 6.6 Hz, 2 x CH_2CH_3), 120.3 (C-3), 125.6 (C-4), 145.3 (C-5), 153.2 (C-2) and 181.7 (C=O).

(2-Acetylfuran-4-yl)methyl diethyl phosphate 348c

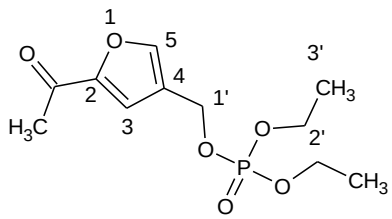

The procedure described for the synthesis of (2-formylfuran-4-yl)methyl diethyl phosphate **348b** was employed, using 2-acetyl-1-[4-(Hydroxymethyl)furan **347c** (0.20 g, 1.4 mmol) and

diethyl chlorophosphate (0.47 g, 2.8 mmol) in pyridine (10 mL). The solvent was evaporated *in vacuo* and the residue chromatographed [preparative layer chromatography; elution with hexane-EtOAc (4:1)] to yield *(2-acetylfuran-4-yl)methyl diethyl phosphate* **348c** as a yellow oil (0.15 g, 74 %); (Found: C, 48.01; H, 6.15 %. $C_{11}H_{17}O_6P$ requires C, 47.83; H, 6.20 %); υ/cm^{-1} 1680 (C=O) and 1223 (P=O); δ_H/ppm (400 MHz; $CDCl_3$) 1.30 (6H, t, *J* = 6.8 Hz, 2 x CH_2CH_3), 2.54 (3H, s, CH_3CO), 4.07 (4H, m, 2 x CH_2CH_3), 5.05 (2H, d, *J* = 1.6 Hz, OCH_2), 7.11 (1H, s, 5-H) and 7.13 (2H, s, 3-H); δ_C/ppm (100 MHz; $CDCl_3$) 16.3 (d, J_{P-C} = 6.0 Hz, 2 x CH_3), 24.6 (CH_3CO), 61.5 (d, J_{P-C} = 6.5 Hz, OCH_2 and 2 x CH_2CH_3), 120.8 (C-3), 122.9 (C-4), 145.7 (C-5), 150.1 (C-2) and 182.6 (C=O).

Diethyl [2-(3,3-dimethylbutanoyl)furan-4-yl]methyl phosphate 348d

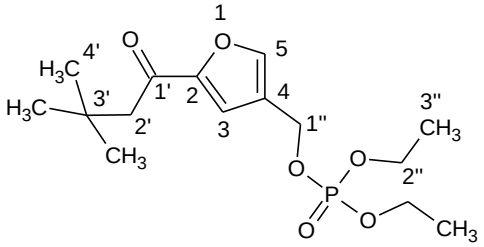

The procedure described for the synthesis of diethyl (2-formylfuran-4-yl)methyl phosphate **348b** was employed, using 2-(3,3-dimethylbutanoyl)-1-[4-(hydroxymethyl)]furan **347d** (0.20 g, 1.0 mmol) and diethyl chlorophosphate (0.39 g, 2.0 mmol) in pyridine (10 mL). The solvent was evaporated *in vacuo* and the residue chromatographed [preparative layer chromatography; elution with hexane-EtOAc (4:1)] to yield *diethyl [2-(3,3-dimethylbutanoyl)furan-4-yl]methyl phosphate* **348d** as a yellow oil (0.14 g, 71 %); (Found: C, 54.30; H, 7.60 %. $C_{15}H_{25}O_6P$ requires C, 54.21; H, 7.58 %); υ/cm^{-1} 1681 (C=O) and 1232 (P=O); δ_H/ppm (400 MHz; $CDCl_3$) 1.21 (9H, s, 3 x CH_3), 1.31 (6H, t, *J* = 6.8 Hz, 2 x CH_2CH_3), 2.56 (2H, s, CH_2CO), 4.08 (4H, m, 2 x CH_2CH_3), 5.09 (2H, d, *J* = 1.6 Hz, OCH_2), 6.47 (1H, s, 5-H) and 7.12 (1H, s, 3-H); δ_C/ppm (100 MHz; $CDCl_3$) 16.3 (d, J_{P-C} = 6.1 Hz, 2 x CH_2CH_3), 29.2 (3 x CH_3), 32.3 (C-3'), 36.8 (C-2'), 62.3 (d, J_{P-C} = 6.5 Hz, OCH_2 and 2 x CH_2CH_3), 120.5 (C-3), 124.2 (C-4), 145.7 (C-5), 153.4 (C-2) and 185.3 (C=O).

(2-Formylfuran-4-yl)methyl dihydrogen phosphate 341b

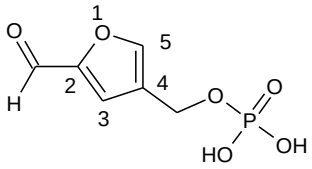

A solution of 4-[(trityloxy)methyl]furan-2-carbaldehyde **340b** (0.30 g, 0.84 mmol) and H_3PO_4:THF (1:1 v/v; 2.0 mL) was stirred at room temperature for *ca.* 2 days. The solvent was removed under reduced pressure and the residue dissolved in EtOAc (25 mL). The organic phase was washed with 10 % aq. $NaHCO_3$ (2 × 50 mL), and the aqueous layers were collected and acidified (pH 2.0) with 0.1M-HCl. The aqueous phase was extracted with EtOAc (3 x 25 mL) and the combined organic solutions were dried (anhydr. $MgSO_4$). The solvent was evaporated *in vacuo* and the residue chromatographed [preparative layer chromatography; elution with hexane-EtOAc-MeOH (1:1:1)] to yield *(2-formylfuran-4-yl)methyl dihydrogen phosphate* **341b** as a yellow oil (0.12 g, 65 %); (Found: C, 35.01; H, 3.49 %. $C_6H_7O_6P$ requires C, 34.97; H, 3.42 %); υ/cm^{-1} 1673 (C=O) and 1234 (P=O); δ_H/ppm (400 MHz; D_2O) 5.11 (2H, d, *J* = 1.6 Hz, OCH_2), 7.10 (1H, s, 5-H), 7.40 (1H, s, 3-H) and 9.74 (1H, s, CHO); δ_C/ppm (100 MHz; D_2O) 61.9 (d, J_{P-C} = 6.4 Hz, 2 × OCH_2), 120.9 (C-3), 123.0 (C-4), 145.8 (C-5), 150.2 (C-2) and 180.0 (C=O).

(2-Acetylfuran-4-yl)methyl dihydrogen phosphate 341 c

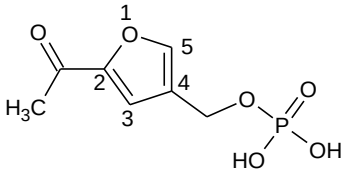

The procedure described for the synthesis of (2-Formylfuran-4-yl)methyl dihydrogen phosphate **341b** was employed, using 2-acetyl-4-[(trityloxy)methyl]furan **340c** (0.2 g, 0.52 mmol) and H_3PO_4:THF (1:1 v/v, 1.0 mL). The solvent was evaporated *in vacuo* and the residue chromatographed [preparative layer chromatography; elution with hexane-EtOAc-MeOH (1:1:1)] to yield *(2-acetylfuran-4-yl)methyl dihydrogen phosphate* **341c** as a colourless oil (0.12 g, 61 %); (Found: C, 38.27; H, 4.09 %. $C_7H_9O_6P$ requires C, 38.20; H, 4.12 %); υ/cm^{-1} 1687 (C=O) and 1241 (P=O); δ_H/ppm (400 MHz; D_2O) 2.61 (3H, s, CH_3CO), 5.07 (2H, d, *J* = 2.3

Hz, OCH_2), 7.12 (1H, s, 5-H) and 7.35 (1H, s, 3-H); δ_C/ppm (100 MHz; D_2O) 24.3 (CH_3), 62.3 (d, J_{P-C} = 6.5 Hz, OCH_2), 120.7 (C-3), 122.9 (C-4), 145.5 (C-5), 153.2 (C-2) and 182.3 (C=O).

[2-(3,3-Dimethylbutanoyl)furan-4-yl]methyl dihydrogen phosphate 341d

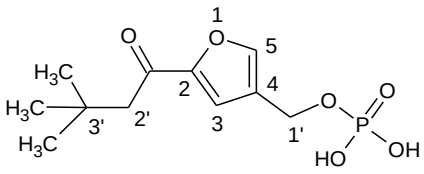

The procedure described for the synthesis of (2-Formylfuran-4-yl)methyl dihydrogen phosphate **341b** was employed, using 2-(3,3-dimethylbutanoyl)-4-[(trityloxy)methyl]furan **340d** (0.20 g, 0.46 mmol) and H_3PO_4:THF (1:1 v/v, 1.0 mL). The solvent was evaporated *in vacuo* and the residue chromatographed [preparative layer chromatography; elution with hexane-EtOAc-MeOH (1:1:0.5)] to yield *[2-(3,3-dimethylbutanoyl)furan-4-yl]methyl dihydrogen phosphate* **341d** as a colourless oil (0.10 g, 58 %); (Found: C, 47.91; H, 6.11 %. $C_{11}H_{17}O_6P$ requires C, 47.83; H, 6.20 %); υ/cm^{-1} 3307 (OH), 1687 (C=O) and 1231 (P=O); δ_H/ppm (400 MHz; D_2O) 1.21 (9H, s, 3 x CH_3), 2.55 (2H, s, CH_2CO), 5.02 (2H, d, *J* = 2.4 Hz, OCH_2), 7.15 (1H, s, 5-H) and 7.39 (1H, s, 3-H); δ_C/ppm (100 MHz; D_2O) 29.3 (3 x CH_3), 32.2 (C-3'), 36.8 (C-2'), 62.2 (d, J_{P-C} = 6.5 Hz, OCH_2), 120.4 (C-3), 123.7 (C-4), 145.5 (C-5), 152.8 (C-2) and 185.6 (C=O).

Diethyl {2-[(hydroxyimino)methyl]furan-4-yl}methyl phosphate 349b

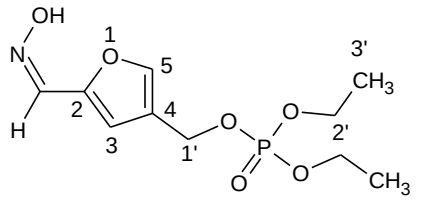

Diethyl (2-formylfuran-4-yl)methyl phosphate **348b** (0.11 g, 0.46 mmol), hydroxylamine hydrochloride (0.10 g, 1.5 mmol) and sodium acetate (0.020 g, 0.24 mmol) were dissolved in EtOH (8 mL) and the mixture was refluxed at 80 ^oC for 1 hour. After completion of the reaction, the solvent was removed under reduced pressure and the residue was dissolved in diethyl ether (20 mL). The organic layer was washed sequentially with water (20 mL) and brine (20 mL), and dried (anhydr. Na_2SO_4). The solvent was removed *in vacuo* and the residue chromatographed [preparative layer chromatography; elution with hexane-EtOAc

(4:1)] to yield *diethyl {2-[(hydroxyimino)methyl]furan-4-yl}methyl phosphate* **349b** as a colourless oil (97 mg, 87 %); (Found: C, 43.47; H, 5.69; N, 5.11 %. $C_{10}H_{16}NO_6P$ requires C, 43.33; H, 5.82; N, 5.05 %); υ/cm^{-1} 3271 (OH), 1651 (C=N) and 1218 (P=O); δ_H/ppm (400 MHz; $CDCl_3$) 1.28 (6H, m, 2 x CH_3), 4.08 (4H, m, 2 x C*H*$_2$CH$_3$), 5.05 (2H, d, *J* = 2.0 Hz, OCH_2), 6.44 (1H, s, 5-H), 7.41 (1H, s, 3-H), 8.17 (1H, s, OH) and 9.89 (1H, s, aldehydic proton); δ_C/ppm (100 MHz; $CDCl_3$) 16.2 (d, J_{P-C} = 6.5 Hz, 2 x CH_3), 59.8 (d, J_{P-C} = 6.4 Hz, OCH_2), 61.3 (d, J_{F-C} = 6.5 Hz, 2 x *C*H$_2$CH$_3$), 110.7 (C-3), 125.7 (C-4), 145.1 (C-5), 149. 6 (C=N) and 153.7 (C-2).

Diethyl {2-[1-(hydroxyimino)ethyl]furan-4-yl}methyl phosphate 349c

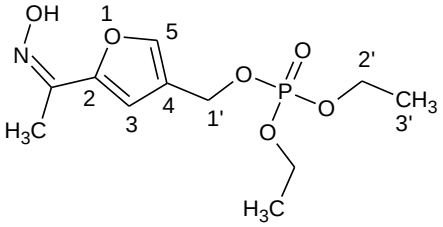

The procedure described for the synthesis of diethyl {2-[(hydroxyimino)methyl]furan-4-yl}methyl phosphate **349b** was employed, using (2-acetylfuran-4-yl)methyl diethyl phosphate **348c** (0.10 g, 0.40 mmol), hydroxylamine hydrochloride (0.10 g, 1.5 mmol) and sodium acetate (0.020, 0.24 mmol) in EtOH (8 mL). The solvent was removed *in vacuo* and the residue chromatographed [preparative layer chromatography; elution with hexane-EtOAc (4:1)] to yield *diethyl {2-[1-(hydroxyimino)ethyl]furan-4-yl}methyl phosphate* **349c** as a colourless oil (91 mg, 91 %); (Found: C, 45.27; H, 6.14; N, 4.88 %. $C_{11}H_{18}NO_6P$ requires C, 45.36; H, 6.23; N, 4.81 %); υ/cm^{-1} 3243 (OH), 1672 (C=N) and 1225 (P=O); δ_H/ppm (400 MHz; $CDCl_3$) 1.31 (6H, t, *J* = 7.2 Hz, 2 x CH_3), 2.53 (3H, s, C*H*$_3$C=N), 4.09 (4H, m, 2 x C*H*$_2$CH$_3$), 5.02 (2H, d, *J* = 2.0 Hz, OCH_2), 5.87 (1H, s, OH), 6.48 (1H, s, 5-H) and 7.11 (1H, s, 3-H); δ_C/ppm (100 MHz; $CDCl_3$) 13.0 (*C*H$_3$C=N) 16.3 (d, J_{P-C} = 6.0 Hz, 2 x CH_3), 61.7 (d, J_{P-C} = 6.4 Hz, OCH_2 and 2 x *C*H$_2$CH$_3$), 109.8 (C-3), 127.2 (C-4), 143.7 (C-5), 148.5 (C=N) and 151.3 (C-2).

Diethyl {2-[1-(hydroxyimino)-3,3-dimethylbutyl]furan-4-yl}methyl phosphate 349d

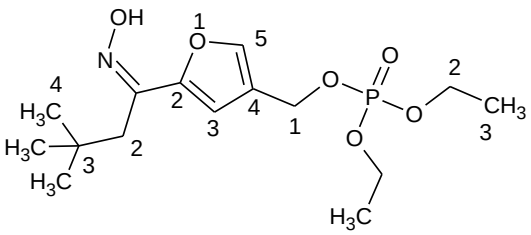

The procedure described for the synthesis of diethyl {2-[(hydroxyimino)methyl]furan-4-yl}methyl phosphate **349b** was employed, using diethyl [2-(3,3-dimethylbutanoyl)furan-4-yl]methyl phosphate **348d** (0.10 g, 0.75 mmol), hydroxylamine hydrochloride (0.10 g, 1.5 mmol) and sodium acetate (0.020, 0.24 mmol) in EtOH (8 mL). The solvent was removed *in vacuo* and the residue chromatographed [preparative layer chromatography; elution with hexane-EtOAc (4:1)] to yield *diethyl {2-[1-(hydroxyimino)-3,3-dimethylbutyl]furan-4-yl}methyl phosphate* **349d** as a colourless oil (92 mg, 92 %); (Found: C, 51.79; H, 7.49; N, 3.97 %. $C_{15}H_{26}NO_6P$ requires C, 51.87; H, 7.54; N, 4.03 %); υ/cm^{-1} 3281 (OH) 1663 (C=N) and 1218 (P=O); δ_H/ppm (400 MHz; $CDCl_3$) 1.15 (9H, s, 3 x CH_3), 1.26 (6H, t, *J* = 6.8 Hz, 2 x CH_2CH_3), 2.55 (2H, CH_2C=N), 4.03 (4H, m, 2 x CH_2CH_3), 4.98 (2H, d, *J* = 1.6 Hz, OCH_2), 5.67 (1H, s, OH), 6.50 (1H, s, 5-H) and 7.12 (1H, s, 3-H); δ_C/ppm (100 MHz; $CDCl_3$) 16.2 (d, J_{P-C} = 6.0 Hz, 2 x CH_2CH_3), 28.6 (3 x CH_3), 32.4 (C-3'), 36.6 (C-2'), 62.0 (OCH_2), 62.1 (d, J_{P-C} = 6.7 Hz, 2 x CH_2CH_3), 110.3 (C-3), 127.6 (C-4), 143.3 (C-5), 149.8 (C=N) and 153.4 (C-2).

{2-[(Hydroxyimino)methyl]furan-4-yl}methyl dihydrogen phosphate 337b

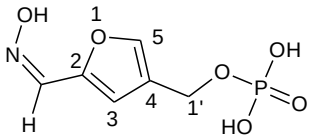

(2-Formylfuran-4-yl)methyl dihydrogen phosphate **341b** (0.10 g, 0.48 mmol), hydroxylamine hydrochloride (0.10 g, 1.5 mmol) and sodium acetate (0.020 g, 0.24 mmol) were dissolved in EtOH (8 mL) and the mixture was refluxed at 80 ^{o}C for 1 hour. After completion of the reaction, the solvent was removed under reduced pressure and the residue was dissolved in diethyl ether (20 mL). The organic solution was washed sequentially with water (20 mL) and brine (20 mL), and dried (anhydr. Na_2SO_4). The solvent was removed *in vacuo* and the residue chromatographed [preparative layer chromatography; elution with hexane-EtOAc-MeOH (1:1:1)] to yield *{2-[(hydroxyimino)methyl]furan-4-yl}methyl dihydrogen phosphate* **337b** as a colourless oil (88 mg, 88 %); (Found: C, 32.71; H, 3.72; N, 6.30 %. $C_6H_8NO_6P$ requires C, 32.59; H, 3.65; N, 6.33 %); υ/cm^{-1} 3245 (OH), 1657 (CH=N) and 1232 (P=O); δ_H/ppm (400 MHz; DMSO-d_6) 3.57 (2H, s, 2 x OH), 5.11 (2H, d, *J* = 2.0 Hz, OCH_2), 5.89 (1H, s, CH=N), 7.10 (1H, s, 5-H), 7.37 (1H, s, 3-H) and 9.41 (1H, s, NOH); δ_C/ppm (100 MHz; DMSO-

d_6) 62.2 (d, $J_{P–C}$ = 5.9 Hz, OCH_2), 110.1 (C-3), 127.0 (C-4), 143.2 (C-5), 150.7 (C=NOH) and 151.8 (C-2).

{2-[1-(Hydroxyimino)ethyl]furan-4-yl}methyl dihydrogen phosphate 337c

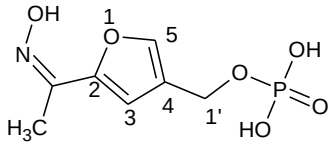

The procedure described for the synthesis of {2-[(hydroxyimino)methyl]furan-4-yl}methyl dihydrogen phosphate **337b** was employed, using (2-acetylfuran-4-yl)methyl dihydrogen phosphate **341c** (0.10 g, 0.44 mmol), hydroxylamine hydrochloride (0.10 g, 1.5 mmol) and sodium acetate (0.020, 0.24 mmol) in EtOH (8 mL). The solvent was removed *in vacuo* and the residue chromatographed [preparative layer chromatography; elution with hexane-EtOAc-MeOH (1:1:1)] to yield *{2-[1-(Hydroxyimino)ethyl]furan-4-yl}methyl dihydrogen phosphate* **337c** as a colourless oil (91 mg, 91 %); (Found: C, 35.84; H, 4.31; N, 5.32 %. $C_7H_{10}NO_6P$ requires C, 35.76; H, 4.29; N, 5.29 %); υ/cm^{-1} 3253 (OH), 1648 (HC=N) and 1228 (P=O); δ_H/ppm (400 MHz; DMSO-d_6) 2.37 (3H, s, CH_3), 3.90 (2H, s, 2 x OH), 5.11 (2H, d, *J* = 2.0 Hz, OCH_2), 7.12 (1H, s, 5-H), 7.32 (1H, s, 3-H) and 8.93 (1H, s, NOH); δ_C/ppm (100 MHz; DMSO-d_6) 13.2 (CH_3), 62.5 (d, $J_{P–C}$ = 6.3 Hz, OCH_2), 110.2 (C-3), 127.1 (C-4), 143.7 (C-5), 150.8 (C=NOH) and 153.3 (C-2).

{2-[1-(Hydroxyimino)-3,3-dimethylbutyl]furan-4-yl}methyl dihydrogen phosphate 337d

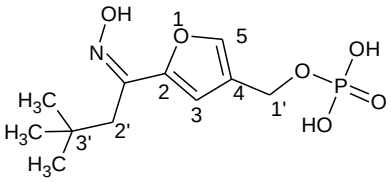

The procedure described for the synthesis of 2-[(hydroxyimino)methyl]furan-4-yl}methyl dihydrogen phosphate **337b** was employed, using [2-(3,3-dimethylbutanoyl)furan-4-yl]methyl dihydrogen phosphate **341d** (0.10 g, 0.36 mmol), hydroxylamine hydrochloride (0.10 g, 1.5 mmol) and sodium acetate (0.020, 0.24 mmol) in EtOH (8 mL). The solvent was removed *in vacuo* and the residue chromatographed [preparative layer chromatography; elution with hexane-EtOAc-MeOH (1:1:1)] to yield *{2-[1-(hydroxyimino)-3,3-*

dimethylbutyl]furan-4-yl}methyl dihydrogen phosphate **337d** as a colourless oil (87 mg, 87 %); (Found: C, 45.29; H, 6.31; N, 4.79 %. $C_{11}H_8NO_6P$ requires C, 45.36; H, 6.23; N, 4.81 %); υ/cm^{-1} 3260 (OH), 1678 (HC=N) and 1229 (P=O); δ_H/ppm (400 MHz; DMSO-d_6) 1.12 (9H, s, 3 x CH_3), 1.83 (2H, s, CH_2C=N), 2.31 (2H, s, 2 x OH), 5.09 (2H, d, J = 1.6 Hz, OCH_2), 7.17 (1H, s, 5-H), 7.32 (1H, s, 3-H) and 10.41 (1H, s, NOH); δ_C/ppm (100 MHz; DMSO-d_6) 29.0 (3 x CH_3), 32.6 (C-3'), 36.3 (C-2'), 62.3 (d, J_{P-C} = 6.6 Hz, OCH_2), 110.8 (C-3), 127.5 (C-4), 142.7 (C-5), 150.3 (C=NOH) and 152.2 (C-2).

3.5. *N*-Benzyl substituted phosphoramidic acid derivatives

Diethyl *N*-(2,2-diethoxyethyl)phosphoramidate 353 [199]

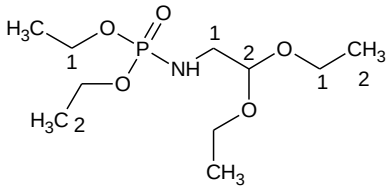

A solution of diethyl *N*-(trimethylsilyl)phosphoramidate **358** (5.00 g, 22.0 mmol) in dry benzene (30 mL) was added slowly over a period of 30 min to a stirred suspension of sodium hydride (60 % dispersion in mineral oil; 1.07 g, 26.8 mmol) in dry benzene (10 mL) under N_2. Bromoacetaldehyde diethyl acetal (3.3 mL, 22 mmol) and tetrabutylammonium bromide (0.71 g, 2.2 mmol) were then added and the resulting mixture was refluxed at 80 ^oC for 4 hours. EtOH (18 mL) was then added dropwise and the mixture was refluxed at 80 ^oC for a further 1 hour. After cooling, EtOAc (100 mL) was added and the mixture was washed with water (3 x 20 mL). The aqueous layers were combined and extracted with EtOAc (3 x 10 mL). The combined organic phases were dried (anhydr. $MgSO_4$), filtered and the solvent was evaporated *in vacuo* at 30-40 ^oC to afford diethyl *N*-(2,2-diethoxyethyl)phosphoramidate **353** as a yellow oil (4.69 g, 87 %); δ_H/ppm (400 MHz; $CDCl_3$) 1.16 (6H, t, J = 7.2 Hz, 2 x 2'-CH_3), 1.25 (6H, t, J = 7.2 Hz, 2 x 2''-CH_3), 3.94 (1H, s, NH), 3.29 (2H, d, J = 5.2 Hz, CH_2N), 3.51 and 3.62 (4H, m, 2 x 1'-OCH_2), 4.00 (4H, m, 2 x 1''-OCH_2) and 4.59 (1H, t, J = 5.4 Hz, 2-CH); δ_C/ppm (100 MHz; $CDCl_3$) 15.3 (2 x 2'-CH_3), 16.1 (d, J_{P-C} = 6.5 Hz, 2 x 2''-CH_3), 31.9 (CH_2N), 61.8 (d, J_{P-C} = 5.8 Hz, 2 x 1''-OCH_2), 62.0 (2 x 1'-OCH_2) and 101.1 (C-2).

Diethyl *N*-benzyl-*N*-(2,2-diethoxyethyl)phosphoramidate 354a

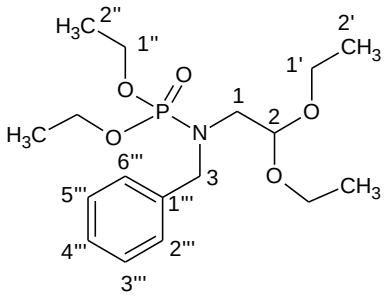

To a stirred solution of diethyl *N*-(2,2-diethoxyethyl)phosphoramidate **353** (1.00 g, 3.71 mmol) in dry THF (20 mL) under N_2 was added NaH (60 % dispersion in mineral oil; 0.20 g, 7.4 mmol) in small portions to permit controlled evolution of hydrogen. Benzyl bromide (0.44 mL, 3.7 mmol) in dry THF (5 mL) was then added and the resulting solution was stirred for at room temperature for *ca.* 24 hours. The solvent was evaporated *in vacuo* and the residue extracted with EtOAc (2 x 25 mL). The organic phase was washed sequentially with satd. aq. $NaHCO_3$ (2 × 50 mL), water (2 x 50 mL) and brine (2 × 50 mL). The aqueous washings were extracted with EtOAc (2 x 25 mL) and the combined organic layers were dried (anhydr. $MgSO_4$). The solvent was removed *in vacuo* and the residue chromatographed [on silica gel; elution with hexane-EtOAc (4:1)] to yield *diethyl* N-*benzyl*-N-*(2,2-diethoxyethyl)phosphoramidate* **354a** as a yellow oil (0.60 g, 71 %); (Found: C, 56.93; H, 8.49; N, 3.84 %. $C_{17}H_{30}NO_5P$ requires C, 56.81; H, 8.41; N, 3.90 %); υ/cm^{-1} 1232 (P=O); δ_H/ppm (400 MHz; $CDCl_3$) 1.18 (6H, t, *J* = 6.8 Hz, 2 x 2'-CH_3), 1.27 (6H, t, *J* = 7.2 Hz, 2 x 2''-CH_3), 3.32 (2H, d, *J* = 5.6 Hz, CH_2N), 3.51 and 3.64 (4H, m, 2 x 1'-OCH_2), 3.85 (2H, s, 3-CH_2), 4.03 (4H, m, 2 x 1''-OCH_2), 4.61 (1H, t, *J* = 5.2 Hz, 2-CH) and 7.29 – 7.37 (5H, m, Ar-H); δ_C/ppm (100 MHz; $CDCl_3$) 15.1 (2 x 2'-CH_3), 16.1 (d, J_{P-C} = 7.2 Hz, 2 x 2''-CH_3), 31.8 (CH_2N), 52.7 (3-CH_2), 62.4 (d, J_{P-C} = 5.5 Hz, 2 x 1''-OCH_2), 62.7 (2 x 1'-OCH_2), 101.4 (C-2), 127.3 (C-4'''), 128.3 (C-2''' and C-6'''), 128.6 (C-3''' and C-5''') and 137.4 (C-1''').

Diethyl *N*-(2,2-diethoxyethyl)-*N*-[4-(hydroxymethyl)benzyl]phosphoramidate 354b

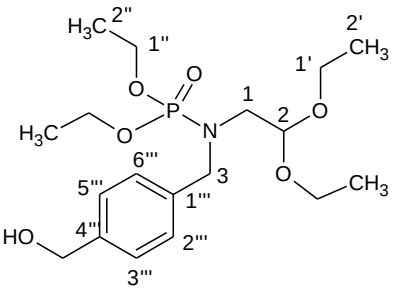

The procedure described for the synthesis of diethyl *N*-benzyl-*N*-(2,2-diethoxyethyl)-phosphoramidate **354a** was employed, using NaH (60 % dispersion in mineral oil; 0.20 g, 7.4 mmol), diethyl *N*-(2,2-diethoxyethyl)phosphoramidate **353** (1.00 g, 3.7 mmol) in dry THF (20 mL) and 4-(chloromethyl)benzyl alcohol (0.58 g, 3.7 mmol) in dry THF (5 mL). After work-up, the solvent was removed *in vacuo* and the residue chromatographed [on silica gel; elution with hexane-EtOAc (4:1)] to yield *diethyl* N-*(2,2-diethoxyethyl)*-N-*[4-(hydroxymethyl)benzyl]-phosphoramidate* **354b** as a colourless oil (0.63 g, 77 %); (Found: C, 55.60; H, 8.24; N, 3.63 %. $C_{18}H_{32}NO_6P$ requires C, 55.52; H, 8.28; N, 3.60 %); υ/cm^{-1} 3360 (OH) and 1232 (P=O); δ_H/ppm (400 MHz; $CDCl_3$) 1.16 (6H, t, *J* = 7.2 Hz, 2 x 2'-CH_3), 1.28 (6H, t, *J* = 6.8 Hz, 2 x 2''-CH_3), 2.13 (1H, s, OH), 3.27 (2H, d, *J* = 5.2 Hz, CH_2N), 3.48 and 3.61 (4H, m, 2 x 1'-OCH_2), 3.82 (2H, s, 3-CH_2), 4.05 (4H, m, 2 x 1''-OCH_2), 4.47 (1H, t, *J* = 5.2 Hz, 2-CH), 4.82 (2H, s, C*H*$_2$OH) and 7.02 – 7.10 (4H, m, Ar-H); δ_C/ppm (100 MHz; $CDCl_3$) 15.2 (2 x 2'-CH_3), 16.2 (d, J_{P-C} = 7.2 Hz, 2 x 2''-CH_3), 33.6 (CH_2N), 53.5 (3-CH_2), 62.1 (d, J_{P-C} = 6.6 Hz, 2 x 1''-OCH_2), 62.5 (2 x 1'-OCH_2), 64.2 (CH_2OH), 101.5 (C-2), 127.4 (C-2''' and C-6'''), 128.7 (C-3''' and C-5'''), 136.1 (C-1''') and 139.7 (C-4''').

Diethyl *N*-(3-aminobenzyl)-*N*-(2,2-diethoxyethyl)phosphoramidate 354c

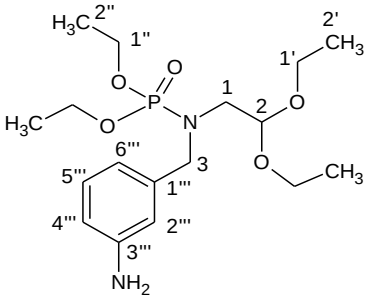

The procedure described for the synthesis of diethyl *N*-benzyl-*N*-(2,2-diethoxyethyl) phosphoramidate **354a** was employed, using NaH (60 % dispersion in mineral oil; 0.20 g, 7.4 mmol), diethyl *N*-(2,2-diethyoxyethyl)phosphoramidate **353** (1.00 g, 3.71 mmol) in dry THF (20 mL) and 3-aminobenzyl bromide (0.69 g, 3.7 mmol) in dry THF (5 mL). After work-up, the solvent was removed *in vacuo* and the residue chromatographed [on silica gel; elution with hexane-EtOAc (4:1)] to yield *diethyl* N-(*3-aminobenzyl)*-N-*(2,2-diethoxyethyl)-(phosphoramidate* **354c** as a colourless oil (0.58 g, 67 %); (Found: C, 54.67; H, 8.45; N, 7.44 %. $C_{17}H_{31}N_2O_5P$ requires C, 54.53; H, 8.35; N, 7.48 %); υ/cm^{-1} 3348 (NH_2) and 1241 (P=O); δ_H/ppm (400 MHz; $CDCl_3$) 1.18 (6H, t, *J* = 7.2 Hz, 2 x 2'-CH_3), 1.30 (6H, t, *J* = 6.8 Hz, 2 x 2''-CH_3), 2.87 (2H, d, *J* = 5.6 Hz, CH_2N), 3.47 and 3.62 (4H, m, 2 x 1'-OCH_2), 3.83 (2H, s, 3-CH_2),

3.91 (2H, s, NH_2), 4.07 (4H, m, 2 x 1''-OCH_2), 4.48 (1H, t, *J* = 5.2 Hz, 2-CH) and 6.31 – 6.87 (4H, m, Ar-H); δ_C/ppm (100 MHz; $CDCl_3$) 14.9 (2 x 2'-CH_3), 15.9 (d, J_{P-C} = 7.0 Hz, 2 x 2''-CH_3), 31.6 (CH_2N), 53.3 (3-CH_2), 62.1 (d, J_{P-C} = 5.4 Hz, 2 x 1''-OCH_2), 62.2 (2 x 1'-OCH_2), 101.2 (C-2), 114.1 (C-4'''), 114.8 (C-2'''), 118.6 (C-6'''), 129.5 (C-5'''), 138.2 (C-1''') and 147.3 (C-3''').

Diethyl *N*-(2,2-diethoxyethyl)-*N*-(3-mercaptobenzyl)phosphoramidate 354d

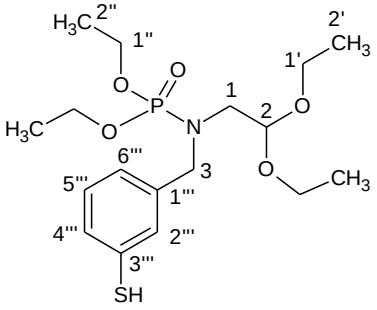

The procedure described for the synthesis of diethyl *N*-benzyl-*N*-(2,2-diethoxyethyl) phosphoramidate **354a** was employed, using NaH (60 % dispersion in mineral oil; 0.20 g, 7.4 mmol), diethyl *N*-(2,2-diethoxyethyl)phosphoramidate **353** (1.00 g, 3.71 mmol) in dry THF (20 mL) and 3-sulfanylbenzyl bromide (0.75 g, 3.7 mmol) in dry THF (5 mL). After work-up, the solvent was removed *in vacuo* and the residue chromatographed [on silica gel; elution with hexane-EtOAc (4:1)] to yield *diethyl* N-*(2,2-diethoxyethyl)*-N-*(3-mercaptobenzyl)-phosphoramidate* **354d** as a colourless oil (0.61 g, 69 %); (Found: C, 52.23; H, 7.67; N, 3.53 %. $C_{17}H_{30}NO_5PS$ requires C, 52.16; H, 7.72; N, 3.58 %); υ/cm^{-1} 2547 (SH) and 1224 (P=O); δ_H/ppm (400 MHz; $CDCl_3$) 1.20 (6H, t, *J* = 7.2 Hz, 2 x 2'-CH_3), 1.29 (6H, t, *J* = 6.8 Hz, 2 x 2''-CH_3), 2.96 (1H, s, SH), 3.34 (2H, d, *J* = 5.2 Hz, CH_2N), 3.53 and 3.66 (4H, m, 2 x 1'-OCH_2), 3.84 (2H, s, 3-CH_2), 4.05 (4H, m, 2 x 1''-OCH_2), 4.63 (1H, t, *J* = 5.6 Hz, 2-CH) and 6.89 – 7.01 (4H, m, Ar-H); δ_C/ppm (100 MHz; $CDCl_3$) 15.5 (2 x 2'-CH_3), 16.5 (d, J_{P-C} = 7.1 Hz, 2 x 2''-CH_3), 32.2 (CH_2N), 62.7 (d, J_{P-C} = 7.0 Hz, 2 x 1''-OCH_2), 62.8 (2 x 1'-OCH_2),, 69.0 (3-CH_2), 101.8 (C-2), 124.8 (C-6'''), 126.0 (C-2'''), 127.4 (C-4'''), 129.0 (C-5'''), 130.8 (C-3''') and 136.7 (C-1''').

Diethyl *N*-benzyl-*N*-(2-oxoethyl)phosphoramidate 355a

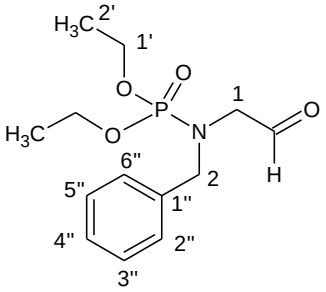

Diethyl *N*-benzyl-*N*-(2,2-diethoxyethyl)phosphoramidate **354a** (0.50 g, 1.4 mmol) and 2M-HCl (4 mL) was stirred at room temperature for *ca.* 24 hours. After completion, the reaction mixture was added to $CHCl_3$ (20 mL) and the organic phase was washed with water (3 x 20 mL). The aqueous washings were combined and extracted with $CHCl_3$ (30 mL). The organic extract was washed sequentially with satd. aq. $NaHCO_3$ (3 x 20 mL) and brine (3 x 20 mL) and then dried (anhydr. $MgSO_4$). The solvent was evaporated *in vacuo* and the residue chromatographed [on silica gel; elution with hexane-EtOAc (4:1)] to yield *diethyl* N-*benzyl*-N-*(2-oxoethyl)phosphoramidate* **355a** as a yellow oil (0.44 g, 88 %); (Found: C, 54.79; H, 7.01; N, 4.88 %. $C_{13}H_{20}NO_4P$ requires C, 54.73; H, 7.07; N, 4.91 %); υ/cm^{-1} 1698 (C=O) and 1228 (P=O); δ_H/ppm (400 MHz; $CDCl_3$) 1.33 (6H, t, *J* = 6.8 Hz, 2 x 2'-CH_3), 3.74 (2H, d, *J* = 6.0 Hz, CH_2CO), 3.83 (2H, s, CH_2Ph), 4.12 (4H, m, 2 x 1'-OCH_2), 7.31 – 7.37 (5H, m, Ar-H) and 9.82 (1H, s, CHO); δ_C/ppm (100 MHz; $CDCl_3$) 16.2 (d, J_{P-C} = 5.9 Hz, 2 x 2'-CH_3), 51.9 (d, J_{P-C} = 6.0 Hz, *C*H_2CO), 62.4 (d, J_{P-C} = 6.5 Hz, 2 x 1'-OCH_2), 67.6 (CH_2Ph), 127.6 (C-4''), 128.0 (C-2'' and C-6''), 128.1 (C-3'' and C-5''), 137.7 (C-1'') and 175.2 (C=O).

Diethyl *N*-[4-(hydroxymethyl)benzyl]-*N*-(2-oxoethyl)phosphoramidate 355b

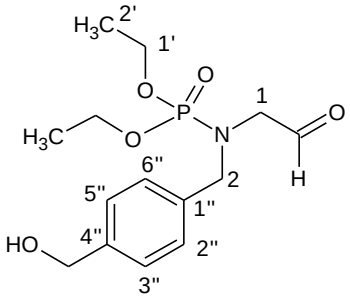

The procedure described for the synthesis of diethyl *N*-benzyl-*N*-(2-oxoethyl)phosphoramidate **355a** was employed, using diethyl *N*-(2,2-diethoxyethyl)-*N*-[4-(hydroxymethyl)benzyl]phosphoramidate **354b** (0.50 g, 1.3 mmol) and 2M-HCl (4 mL). After work-up, the solvent was removed *in vacuo* and the residue chromatographed [on silica gel; elution with hexane-EtOAc (4:1)] to yield *diethyl* N-*[4-(hydroxymethyl)benzyl]*-N-*(2-oxoethyl)phosphoramidate* **355b** as a yellow oil (0.44 g, 88 %); (Found: C, 53.51; H, 7.12; N, 4.40 %. $C_{14}H_{22}NO_5P$ requires C, 53.33; H, 7.03; N, 4.44 %); υ/cm^{-1} 3261 (OH), 1738 (C=O) and 1219 (P=O); δ_H/ppm (400 MHz; $CDCl_3$) 1.36 (6H, t, *J* = 7.2 Hz, 2 x 2'-CH_3), 2.03 (1H, s, OH), 3.72 (2H, d, *J* = 5.2 Hz, CH_2CO), 3.82 (2H, s, CH_2Ph), 4.18 (4H, m, 2 x 1'-OCH_2), 4.82 (2H, s, C*H*$_2$OH), 7.09 – 7.17 (4H, m, Ar-H) and 9.81 (1H, s, CHO); δ_C/ppm (100 MHz; $CDCl_3$) 16.3 (d,

J_{P-C} = 5.8 Hz, 2 x 2''-CH_3), 48.9 (d, J_{P-C} = 5.9 Hz, *C*H_2CO), 63.0 (d, J_{P-C} = 6.3 Hz, 2 x 1'-OCH_2), 64.9 (CH_2OH), 67.2 (CH_2Ph), 127.1 (C-2'' and C-6''), 128.2 (C-3'' and C-5''), 135.8 (C-1''), 139.8 (C-4'') and 172.8 (C=O).

Diethyl *N*-(3-aminobenzyl)-*N*-(2-oxoethyl)phosphoramidate 355c

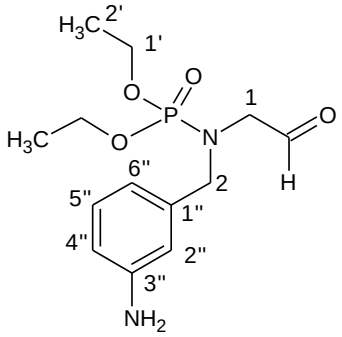

The procedure described for the synthesis of diethyl *N*-benzyl-*N*-(2-oxoethyl)phosphoramidate **355a** was employed, using diethyl *N*-(3-aminobenzyl)-*N*-(2,2-diethoxyethyl)phosphoramidate **354c** (0.50 g, 1.3 mmol) and 2M-HCl (4 mL). After work-up, the solvent was removed *in vacuo* and the residue chromatographed [on silica gel; elution with hexane-EtOAc (4:1)] to yield *diethyl* N-*(3-aminobenzyl)*-N-*(2-oxoethyl)phosphoramidate* **355c** as a yellow oil (0.46 g, 92 %); (Found: C, 52.11; H, 7.10; N, 9.29 %. $C_{13}H_{21}N_2O_4P$ requires C, 52.00; H, 7.05; N, 9.33 %); υ/cm^{-1} 3371 (NH_2), 1715 (C=O) and 1230 (P=O); δ_H/ppm (400 MHz; $CDCl_3$) 1.35 (6H, t, *J* = 6.8 Hz, 2 x 2'-CH_3), 3.24 (2H, s, NH_2), 3.71 (2H, d, *J* = 5.2 Hz, CH_2CO), 3.83 (2H, s, CH_2Ph), 4.17 (4H, m, 2 x 1'-OCH_2), 7.00 – 7.47 (4H, m, Ar-H) and 9.81 (1H, s, CHO); δ_C/ppm (100 MHz; $CDCl_3$) 16.3 (d, J_{P-C} = 6.0 Hz, 2 x 2'-CH_3), 52.8 (d, J_{P-C} = 4.9 Hz, *C*H_2CO), 61.7 (d, J_{P-C} = 6.4 Hz, 2 x 1'-OCH_2), 68.3 (CH_2Ph), 114.0 (C-4''), 114.9 (C-2''), 118.3 (C-6''), 129.8 (C-5''), 137.7 (C-1''), 147.8 (C-3'') and 174.8 (C=O).

Diethyl *N*-(3-mercaptobenzyl)-*N*-(2-oxoethyl)phosphoramidate 355d

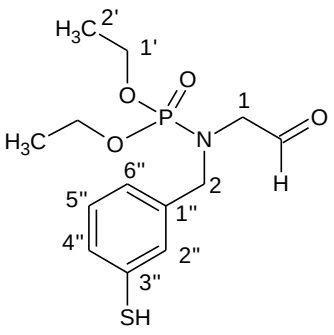

The procedure described for the synthesis of diethyl *N*-benzyl-*N*-(2-oxoethyl)-phosphoramidate **355a** was employed, using diethyl *N*-(3-mercaptobenzyl)-*N*-(2-oxoethyl)phosphoramidate **354d** (0.50 g, 1.3 mmol) and 2M-HCl (4 mL). After work-up, the solvent was removed *in vacuo* and the residue chromatographed [on silica gel; elution with hexane-EtOAc (4:1)] to yield *diethyl* N-*(3-mercaptobenzyl)*-N-*(2-oxoethyl)phosphoramidate* **355d** as a yellow oil (0.45 g, 90 %); Found: C, 49.28; H, 6.43; N, 4.47 %. $C_{13}H_{20}NO_4PS$ requires C, 49.20; H, 6.35; N, 4.41 %); υ/cm^{-1} 2567 (SH), 1692 (C=O) and 1215 (P=O); δ_H/ppm (400 MHz; $CDCl_3$) 1.36 (6H, t, *J* = 7.2 Hz, 2 x 2'-CH_3), 2.77 (1H, s, SH), 3.53 (2H, d, *J* = 6.0 Hz, CH_2CO), 3.79 (2H, s, CH_2Ph), 4.12 (4H, m, 2 x 1'-OCH_2), 6.86 – 7.40 (4H, m, Ar-H) and 9.87 (1H, s, CHO); δ_C/ppm (100 MHz; $CDCl_3$) 16.4 (d, J_{P-C} = 6.0 Hz, 2 x 2'-CH_3), 52.7 (d, J_{P-C} = 4.7 Hz, CH_2CO), 61.4 (d, J_{P-C} = 6.4 Hz, 2 x 1'-OCH_2), 68.6 (CH_2Ph), 124.6 (C-6''), 126.2 (C-2''), 127.8 (C-4''), 128.3 (C-5''), 130.4 (C-3''), 137.7 (C-1'') and 173.8 (C=O).

Diethyl *N*-benzyl-*N*-[2-(benzyloxyamino)ethyl]phosphoramidate 356a

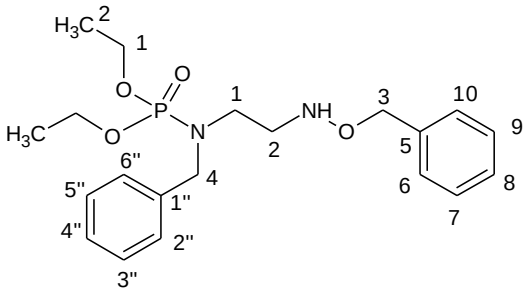

To a stirred solution of diethyl *N*-benzyl-*N*-(2-oxoethyl)phosphoramidate **355a** (0.40 g, 1.4 mmol) in MeOH (5 mL) was added a solution of *O*-benzylhydroxylamine (0.21 g, 1.8 mmol) in MeOH (8 mL). The reaction mixture was heated at 40 ^oC for 3 hours, cooled to room temperature and diluted with MeOH (50 mL). After the addition of sodium cyanoborohydride (0.27 g, 4.1 mmol), conc. HCl (1.6 mL) was added dropwise over a period of 30 min and the mixture was stirred for 1 hour. Sodium cyanoborohydride (0.10 g, 1.4 mmol) was again added and the mixture was stirred for 1 hour. The solvent was removed under reduced pressure, the residue dissolved in MeOH (30 mL) and then treated with ice-water (50 mL). The pH of the resulting mixture was adjusted to pH 10 with an aq. KOH solution and extracted with DCM (3 x 20 mL). The combined organic layers were washed with 10 % $NaHCO_3$ (50 mL) and brine (50 mL) and then dried (anhydr. $MgSO_4$). The solvent was evaporated *in vacuo* and the residual oil was purified by flash chromatography [on silica

gel; elution with hexane-EtOAc (3:1)] to yield *diethyl* N-*benzyl*-N-*[2-(benzyloxyamino)ethyl]-phosphoramidate* **356a** as a yellow oil (0.26 g, 65 %); (Found: C, 61.30; H, 7.49; N, 7.21 %. $C_{20}H_{29}N_2O_4P$ requires C, 61.21; H, 7.45; N, 7.14 %); υ/cm^{-1} 3267 (NH) and 1242 (P=O); δ_H/ppm (400 MHz; $CDCl_3$) 1.32 (6H, t, *J* = 7.2 Hz, 2 x 2'-CH_3), 2.89 (4H, m, 1-CH_2 and 2-CH_2), 3.82 (2H, s, 4-CH_2Ph), 4.10 (4H, m, 2 x 1''-OCH_2), 4.74 (2H, s, 3-CH_2Ph), 5.23 (1H, s, NH) and 7.29 – 7.37 (10H, m, Ar-H); δ_C/ppm (100 MHz; $CDCl_3$) 16.5 (d, J_{P-C} = 6.0 Hz, 2 x 2'-CH_3), 36.7 (d, J_{P-C} = 4.5 Hz, 1-CH_2), 52.1 (d, J_{P-C} = 16.7 Hz, 2-CH_2), 61.5 (d, J_{P-C} = 6.4 Hz, 2 x 1'-OCH_2), 67.3 (4-CH_2Ph), 68.3 (3-CH_2Ph), 127.6 (C-4''), 127.9 (C-8), 128.3 (C-2'' and C-6''), 128.4 (C-6 and C-10), 128.5 (C-3'' and C-5''), 128.7 (C-7 and C-9), 137.8 (C-1'') and 138.3 (C-5).

Diethyl *N*-[2-(benzyloxyamino)ethyl]-*N*-[4-(hydroxymethyl)benzyl]phosphoramidate 356b

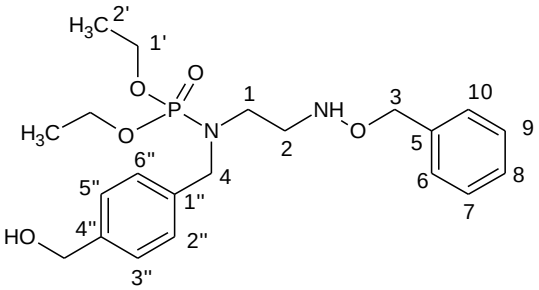

The procedure described for the synthesis of diethyl *N*-benzyl-*N*-[2-(benzyloxyamino)ethyl]-phosphoramidate **356a** was employed, using diethyl *N*-[4-(hydroxymethyl) benzyl]-*N*-(2-oxoethyl)phosphoramidate **355b** (0.42 g, 1.3 mmol), *O*-benzylhydroxylamine (0.20 g, 1.6 mmol) in MeOH (10 mL), sodium cyanoborohydride (0.24 g, 3.8 mmol), conc. HCl (1.6 mL) and further sodium cyanoborohydride (0.080 g, 1.2 mmol). After work-up, the solvent was evaporated *in vacuo* and the remaining oil was purified by flash chromatography [on silica gel; elution with hexane-EtOAc (3:1)] to yield *diethyl* N-*[2-(benzyloxyamino)ethyl]*-N-*[4-(hydroxymethyl)benzyl]phosphoramidate* **356b** as a yellow oil (0.26 g, 63 %); (Found: C, 59.86; H, 7.47; N, 6.69 %. $C_{21}H_{31}N_2O_5P$ requires C, 59.70; H, 7.40; N, 6.63 %); υ/cm^{-1} 3326 (OH), 3248 (NH) and 1223 (P=O); δ_H/ppm (400 MHz; $CDCl_3$) 1.29 (6H, t, *J* = 7.2 Hz, 2 x 2'-CH_3), 2.87 (4H, m, 1-CH_2 and 2-CH_2), 3.80 (2H, s, 4-CH_2Ph), 4.07 (4H, m, 2 x 1''-OCH_2), 4.77 (2H, s, 3-CH_2Ph), 4.86 (2H, s, C*H*$_2$OH), 7.33 – 7.42 (9H, m, Ar-H), 7.97 (1H, s, OH) and 8.11 (1H, s, NH); δ_C/ppm (100 MHz; $CDCl_3$) 16.3 (d, J_{P-C} = 6.0 Hz, 2 x 2'-CH_3), 36.4 (d, J_{P-C} = 4.8 Hz, 1-CH_2), 52.0 (d, J_{P-C} = 16.4 Hz, 2-CH_2), 61.3 (d, J_{P-C} = 6.5 Hz, 2 x 1'-OCH_2), 64.7 (CH_2OH), 67.2 (4-

CH_2Ph), 69.2 (3-CH_2Ph), 127.7 (C-2'' and C-6''), 127.8 (C-6 and C-10), 128.2 (C-8), 128.3 (C-3'' and C-5''), 128.3 (C-7 and C-9), 137.4 (C-1''), 137.8 (C-5) and 138.3 (C-4'').

Diethyl *N*-(3-aminobenzyl)-*N*-[2-(benzyloxyamino)ethyl]phosphoramidate 356c

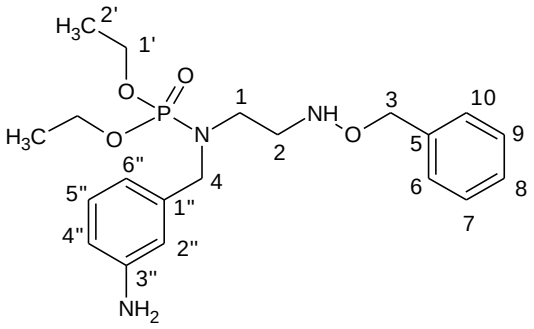

The procedure described for the synthesis of diethyl *N*-benzyl-*N*-[2-(benzyloxyamino)ethyl]-phosphoramidate **356a** was employed, using diethyl *N*-(3-aminobenzyl)-*N*-(2-oxoethyl)phosphoramidate **355c** (0.44 g, 1.5 mmol), *O*-benzylhydroxylamine (0.22 g, 1.8 mmol) in MeOH (10 mL), sodium cyanoborohydride (0.28 g, 4.4 mmol), conc. HCl (1.6 mL) and further sodium cyanoborohydride (0.090 g, 1.3 mmol). After work-up, the solvent was evaporated *in vacuo* and the remaining oil was purified by flash chromatography [on silica gel; elution with hexane-EtOAc (3:1)] to yield *diethyl* N-*(3-aminobenzyl)*-N-*[2-(benzyloxyamino)ethyl]phosphoramidate* **356c** as a yellow oil (0.30 g, 68 %); (Found: C, 59.08; H, 7.37; N, 10.33 %. $C_{20}H_{30}N_3O_4P$ requires C, 58.96; H, 7.42; N, 10.31 %); υ/cm^{-1} 3329 (NH_2), 3260 (NH) and 1232 (P=O); δ_H/ppm (400 MHz; $CDCl_3$) 1.22 (6H, t, *J* = 6.0 Hz, 2 x 2'-CH_3), 2.95 (4H, m, 1-CH_2 and 2-CH_2), 3.59 (2H, s, 4-CH_2Ph), 4.03 (4H, m, 2 x 1'-OCH_2), 4.62 (2H, s, 3-CH_2Ph), 5.55 (2H, s, NH_2), 6.59 – 6.87 (4H, m, Ar-H), 7.28-7.37 (5H, m, Ar-H) and 8.40 (1H, s, NH); δ_C/ppm (100 MHz; $CDCl_3$) 16.4 (d, $J_{P–C}$ = 6.0 Hz, 2 x 2'-CH_3), 36.5 (d, $J_{P–C}$ = 4.8 Hz, 1-CH_2), 52.0 (d, $J_{P–C}$ = 16.7 Hz, 2-CH_2), 61.5 (d, $J_{P–C}$ = 6.5 Hz, 2 x 1'-OCH_2), 67.4 (4-CH_2Ph), 69.9 (3-CH_2Ph), 113.9 (C-4''), 114.9 (C-2''), 118.3 (C-6''), 126.9 (C-6 and C-10), 127.8 (C-8), 128.3 (C-7 and C-9), 129.3 (C-5''), 136.7 (C-1''), 137.7 (C-5) and 148.3 (C-3'').

Diethyl *N*-[2-(benzyloxyamino)ethyl]-*N*-(3-mercaptobenzyl)phosphoramidate 356d

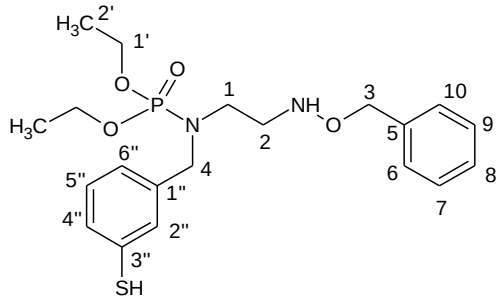

The procedure described for the synthesis of diethyl *N*-benzyl-*N*-[2-(benzyloxyamino)ethyl]-phosphoramidate **356a** was employed, using diethyl *N*-(3-mercaptobenzyl)-*N*-(2-oxoethyl)phosphoramidate **355d** (0.44 g, 1.4 mmol), *O*-benzylhydroxylamine (0.14 g, 1.1 mmol) in MeOH (10 mL), sodium cyanoborohydride (0.27 g, 4.3 mmol), conc. HCl (1.6 mL) and further sodium cyanoborohydride (0.090 g, 1.3 mmol). After work-up, the solvent was evaporated *in vacuo* and the remaining oil was purified by flash chromatography [on silica gel; elution with hexane-EtOAc (3:1)] to yield *diethyl* N-*[2-(benzyloxyamino)ethyl]*-N-*(3-mercaptobenzyl)phosphoramidate* **356d** as a yellow oil (0.29 g, 66 %); Found: C, 56.71; H, 6.95; N, 6.65 %. $C_{20}H_{29}N_2O_4PS$ requires C, 56.59; H, 6.89; N, 6.60 %); υ/cm^{-1} 3271 (NH), 2567 (SH) and 1219 (P=O); δ_H/ppm (400 MHz; $CDCl_3$) 1.28 (6H, t, *J* = 7.2 Hz, 2 x 2'-CH_3), 2.61 (4H, m, 1-CH_2 and 2-CH_2), 3.38 (1H, s, SH), 3.61 (2H, s, 4-CH_2Ph), 4.04 (4H, m, 2 x 1'-OCH_2), 4.81 (2H, s, 3-CH_2Ph), 6.75 - 7.18 (4H, m, Ar-H), 7.31 - 7.35 (5H, m, Ar-H) and 8.18 (1H, s, NH); δ_C/ppm (100 MHz; $CDCl_3$) 16.4 (d, J_{P-C} = 6.0 Hz, 2 x 2'-CH_3), 36.8 (d, J_{P-C} = 4.8 Hz, 1-CH_2), 52.1 (d, J_{P-C} = 16.7 Hz, 2-CH_2), 61.5 (d, J_{P-C} = 6.5 Hz, 2 x 1'-OCH_2), 66.7 (4-CH_2Ph), 71.2 (3-CH_2Ph), 124.6 (C-6''), 125.9 (C-2''), 127.6 (C-4''), 127.9 (C-6 and C-10), 128.0 (C-8), 128.3 (C-5''), 128.4 (C-7 and C-9), 130.6 (C-3'') and 137.8 (C-1'') and 138.0 (C-5).

Diethyl *N*-benzyl-2-[*N*-benzyloxy)acetamido]ethylphosphoramidate 357a

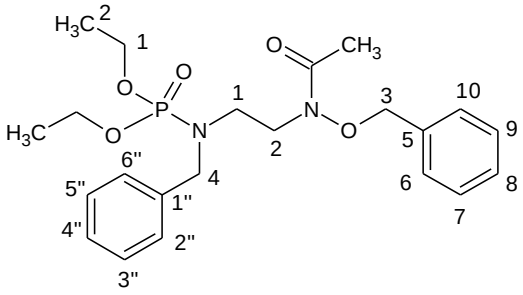

Acetyl chloride (0.12 mL, 1.3 mmol) was added dropwise to a stirred solution of diethyl *N*-benzyl-*N*-[2-(benzyloxyamino)ethyl]-phosphoramidate **356a** (0.25 g, 0.64 mmol) and triethylamine (0.13 mL, 0.96 mmol) in DCM (10 mL) under N_2 at 0 ^{o}C. The mixture was stirred at 0 ^{o}C for 1 hour, allowed to warm to room temperature and then stirred for *ca.* 24 hours. The solvent was removed under reduced pressure and the residual oil dissolved in diethyl ether (20 mL). The ethereal solution was washed sequentially with aq. K_2CO_3 solution, 0.5M-HCl and water. The organic solution was dried over anhydr. $MgSO_4$, the solvent removed *in vacuo* and the residue purified by flash chromatography [on silica gel; elution with hexane-EtOAc (7:3)] to yield *diethyl* N-*benzyl-2-[*N-*benzyloxy)acetamido]-ethylphosphoramidate* **357a** as a yellow oil (0.23 g, 83 %); (Found: C, 60.88; H, 7.23; N, 6.52 %. $C_{22}H_{31}N_2O_5P$ requires C, 60.82; H, 7.19; N, 6.45 %); υ/cm^{-1} 1683 (C=O) and 1246 (P=O); δ_H/ppm (400 MHz; $CDCl_3$) 1.29 (6H, t, *J* = 7.2 Hz, 2 x 2'-CH_3), 2.00 (3H, s, CH_3CO), 2.71 (2H, m, 1-CH_2N), 3.01 (2H, t, *J* = 6.4 Hz, 2-CH_2N), 3.67 (2H, s, 4-CH_2Ph), 4.08 (4H, m, 2 x 1''-OCH_2), 4.77 (2H, s, 3-CH_2Ph) and 7.27 - 7.39 (10H, m, Ar-H); δ_C/ppm (100 MHz; $CDCl_3$) 16.4 (d, J_{P-C} = 5.9 Hz, 2 x 2'-CH_3), 23.7 (CH_3CO), 35.4 (d, J_{P-C} = 5.4 Hz, 1-CH_2), 52.6 (d, J_{P-C} = 16.8 Hz, 2-CH_2), 62.5 (d, J_{P-C} = 6.7 Hz, 2 x 1'-OCH_2), 66.8 (4-CH_2Ph), 68.7 (3-CH_2Ph), 124.8 (C-4''), 124.9 (C-8), 127.5 (C-2'' and C-6''), 127.8 (C-6 and C-10), 128.5 (C-3'' and C-5''), 128.7 (C-7 and C-9), 138.3 (C-1'), 138.4 (C-5) and 171.6 (C=O).

Diethyl 2-[(*N*-benzyloxy)acetamido]-*N*-[4-(hydroxymethyl)benzyl]ethylphosphoramidate 357b

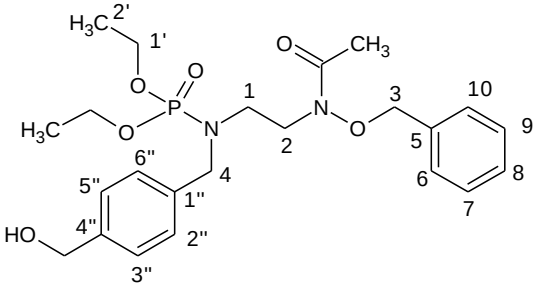

The procedure described for the synthesis of diethyl *N*-benzyl-2-[*N*-benzyloxy)acetamido]-ethylphosphoramidate **357a** was employed, using diethyl *N*-[2-(benzyloxyamino)ethyl]-*N*-[4-(hydroxymethyl)benzyl]phosphoramidate **356b** (0.25 g, 0.59 mmol), acetyl chloride (0.12 mL, 1.3 mmol) and triethylamine (0.12 mL, 0.89 mmol) in DCM (10 mL). The solvent was evaporated *in vacuo* and the residue was purified by flash chromatography [on silica gel; elution with hexane-EtOAc (7:3)] to yield *diethyl 2-[(N-benzyloxy)acetamido]-N-[4-*

(hydroxymethyl)benzyl]ethylphosphoramidate **357b** as a yellow oil (0.23 g, 85 %); (Found: C, 59.57; H, 7.23; N, 6.10 %. $C_{23}H_{33}N_2O_6P$ requires C, 59.47; H, 7.16; N, 6.03 %); υ/cm^{-1} 3243 (OH), 1687 (C=O) and 1223 (P=O); δ_H/ppm (400 MHz; $CDCl_3$) 1.32 (6H, t, *J* = 7.2 Hz, 2 x 2'-CH_3), 2.04 (3H, s, CH_3CO), 2.32 (2H, m, 1-CH_2N), 2.76 (2H, t, *J* = 6.0 Hz, 2-CH_2N), 3.71 (2H, s, 4-CH_2Ph), 4.11 (4H, m, 2 x 1''-OCH_2), 4.79 (2H, s, 3-CH_2Ph), 4.84 (2H, s, C*H*$_2$OH), 7.22 - 7.43 (9H, m, Ar-H) and 8.22 (1H, s, OH); δ_C/ppm (100 MHz; $CDCl_3$) 16.4 (d, J_{P-C} = 5.9 Hz, 2 x 2'-CH_3), 23.0 (*C*H_3CO), 36.8 (d, J_{P-C} = 4.1 Hz, 1-CH_2), 52.8 (d, J_{P-C} = 16.6 Hz, 2-CH_2), 62.3 (d, J_{P-C} = 6.6 Hz, 2 x 1'-OCH_2), 65.9 (CH_2OH), 66.6 (4-CH_2Ph), 68.7 (3-CH_2Ph), 126.3 (C-2'' and C-6''), 126.4 (C-6 and C-10), 126.8 (C-8), 127.0 (C-3'' and C-5''), 127.7 (C-7 and C-9), 137.2 (C-1''), 137.4 (C-5), 140.2 (C-4'') and 171.1 (C=O).

Diethyl *N*-(3-aminobenzyl)-2-[(*N*-benzyloxy)acetamido]ethylphosphoramidate 357c

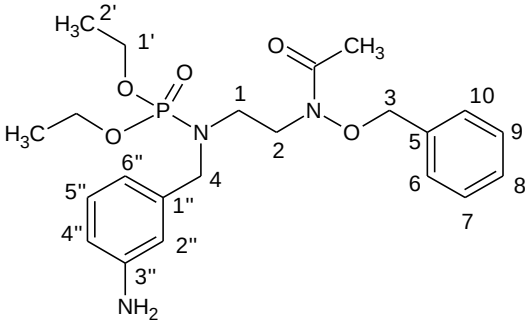

The procedure described for the synthesis of diethyl *N*-benzyl-2-[*N*-benzyloxy)acetamido]-ethylphosphoramidate **357a** was employed, using diethyl *N*-[2-(benzyloxyamino)ethyl]-*N*-(3-mercaptobenzyl)phosphoramidate **356c** (0.28 g, 0.68 mmol), acetyl chloride (0.13 mL, 1.4 mmol) and triethylamine (0.14 mL, 1.0 mmol) in DCM (10 mL). The solvent was evaporated *in vacuo* and the residue was purified by flash chromatography [on silica gel; elution with hexane-EtOAc (7:3)] to yield *diethyl* N-*(3-aminobenzyl)-2-[(*N-*benzyloxy)acetamido]-ethylphosphoramidate* **357c** as a yellow oil (0.22 g, 80 %); (Found: C, 58.86; H, 7.29; N, 9.41 %. $C_{22}H_{33}N_3O_5P$ requires C, 58.79; H, 7.18; N, 9.35 %); υ/cm^{-1} 3387 (NH_2), 1692 (C=O) and 1220 (P=O); δ_H/ppm (400 MHz; $CDCl_3$) 1.30 (6H, t, *J* = 7.2 Hz, 2 x 2'-CH_3), 2.02 (3H, s, CH_3CO), 2.81 (2H, m, 1-CH_2N), 3.23 (2H, t, *J* = 4.4 Hz, 2-CH_2N), 3.79 (2H, s, 4-CH_2Ph), 4.08 (4H, m, 2 x 1'-OCH_2), 4.52 (2H, s, NH_2), 4.81 (2H, s, 3-CH_2Ph), 6.63 - 6.78 (4H, m, Ar-H) and 7.16 - 7.19 (5H, m Ar-H); δ_C/ppm (100 MHz; $CDCl_3$) 16.4 (d, J_{P-C} = 6.6 Hz, 2 x 2'-CH_3), 23.8 (*C*H_3CO), 36.7 (d, J_{P-C} = 4.7 Hz, 1-CH_2), 52.1 (d, J_{P-C} = 16.7 Hz, 2-CH_2), 61.4 (d, J_{P-C} = 6.5 Hz, 2 x 1'-OCH_2), 68.4

(4-CH_2Ph), 69.8 (3-CH_2Ph), 114.1 (C-4''), 114.8 (C-2''), 118.6 (C-6''), 126.5 (C-6 and C-10), 127.8 (C-8), 128.3 (C-7 and C-9), 129.8 (C-5''), 137.3 (C-1''), 137.7 (C-5), 147.9 (C-3'') and 170.8 (C=O).

Diethyl 2-[(*N*-benzyloxy)acetamido]-*N*-(3-mercaptobenzyl)ethylphosphoramidate 357d

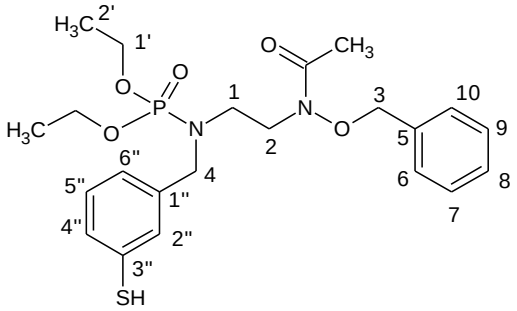

The procedure described for the synthesis of diethyl *N*-benzyl-2-[*N*-benzyloxy)acetamido]-ethylphosphoramidate **357a** was employed, using diethyl *N*-[2-(benzyloxyamino)ethyl]-*N*-(3-mercaptobenzyl)phosphoramidate **356d** (0.27 g, 0.64 mmol), acetyl chloride (0.12 mL, 1.3 mmol) and triethylamine (0.12 mL, 0.88 mmol) in DCM (10 mL). The solvent was evaporated *in vacuo* and the residue was purified by flash chromatography [on silica gel; elution with hexane-EtOAc (7:3)] to yield *diethyl 2-[(*N*-benzyloxy)acetamido]*-N-*(3-mercaptobenzyl)-ethylphosphoramidate* **357d** as a yellow oil (0.23 g, 81 %); Found: C, 56.77; H, 6.79; N, 5.92 %. $C_{22}H_{31}N_2O_5PS$ requires C, 56.64; H, 6.70; N, 6.00 %); υ/cm^{-1} 2554 (SH), 1698 (C=O) and 1217 (P=O); δ_H/ppm (400 MHz; $CDCl_3$) 1.36 (6H, t, *J* = 7.2 Hz, 2 x 2'-CH_3), 2.20 (3H, s, CH_3CO), 2.79 (2H, m, 1-CH_2N), 3.25 (2H, t, *J* = 5.6 Hz, 2-CH_2N), 3.83 (2H, s, 4-CH_2Ph), 4.19 (4H, m, 2 x 1'-OCH_2), 4.71 (2H, s, 3-CH_2Ph), 6.21 (1H, s, SH), 6.63 - 7.29 (4H, m, Ar-H) and 7.42 - 7.50 (5H, m, Ar-H); δ_C/ppm (100 MHz; $CDCl_3$) 16.4 (d, J_{P-C} = 5.9 Hz, 2 x 2'-CH_3), 24.2 (*CH_3*CO), 36.7 (d, J_{P-C} = 4.8 Hz, 1-CH_2), 52.9 (d, J_{P-C} = 16.8 Hz, 2-CH_2), 61.6 (d, J_{P-C} = 6.5 Hz, 2 x 1'-OCH_2), 68.1 (4-CH_2Ph), 70.8 (3-CH_2Ph), 124.7 (C-6''), 126.0 (C-2''), 126.2 (C-4''), 126.8 (C-6 and C-10), 128.7 (C-8), 129.1 (C-5''), 129.4 (C-7 and C-9), 130.3 (C-3''), 138.5 (C-1''), 138.8 (C-5) and 167.3 (C=O).

Diethyl *N*-(trimethylsilyl)phosphoramidate 358 [199]

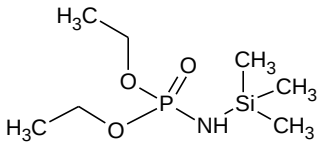

Hexamethyldisilazane (2.46 mL, 12 mmol) was added to a stirred solution of diethyl phosphoramidate **352** (3.00 g, 19.8 mmol) in dry benzene (10 mL) under N_2 and the mixture was refluxed at 80 ^oC for 3 hours. The solvent and excess hexamethyldisilazane were removed *in vacuo* at 60 ^oC for 1 hour to afford diethyl *N*-(trimethylsilyl)phosphoramidate as a brown oil, which crystallised on cooling to afford hygroscopic off-white crystals (4.69 g, 87 %); δ_H/ppm (400 MHz; $CDCl_3$) 0.19 (9H, s, 3 x CH_3Si), 1.30 (6H, t, J = 7.2 Hz, 2 x CH_3), 2.25 (1H, s, NH) and 4.04 (4H, m, 2 x OCH_2); δ_C/ppm (100 MHz; $CDCl_3$) 0.6 (d, J_{P-C} = 2.4 Hz, 3 x CH_3Si), 16.2 (d, J_{P-C} = 7.3 Hz, 2 x CH_3) and 61.9 (d, J_{P-C} = 5.3 Hz, 2 x OCH_2).

3-Aminobenzyl bromide 360c [251]

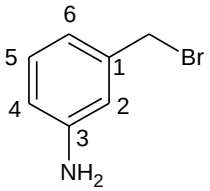

Phosphorous tribromide (0.62 mL, 6.5 mmol) was added dropwise to a stirred solution of 3-aminobenzyl alcohol (0.80 g, 6.5 mmol) in DCM (10 mL) under N_2 at 0 ^oC and the resulting mixture was stirred for 1 hour. The mixture was allowed to warm to room temperature and stirred further for *ca.* 24 hours. After the addition of satd. aq. $NaHCO_3$ (30 mL), the organic layer was separated and the aqueous layer was extracted with diethyl ether (3 x 20 mL). The organic layers were combined, dried over anhydrous $MgSO_4$ and filtered. The solvent was evaporated *in vacuo* and the residue was purified by flash chromatography [on silica gel; elution with hexane-EtOAc (4:1)] to yield 3-aminobenzyl bromide **360c** as a clear oil (0.92 g, 76 %); δ_H/ppm (400 MHz; $CDCl_3$) 2.95 (1H, s, NH_2), 4.62 (2H, s, CH_2Br), 7.43 - 7.67 (4H, m, Ar-H); δ_C/ppm (100 MHz; $CDCl_3$) 36.6 (CH_2Br), 115.5 (C-2), 116.4 (C-4), 119.9 (C-6), 129.0 (C-5), 138.0 (C-1) and 147.5 (C-3).

3-Mercaptobenzyl bromide 360d

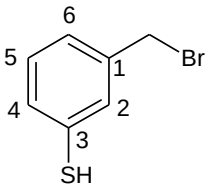

A solution of sodium nitrite (0.32 g, 4.6 mmol) in water (2 mL) was slowly added to a mixture of 3-aminobenzyl bromide **360c** (0.50 g, 2.7 mmol) in water (4 mL) and conc. HCl (1

mL) at -5 ^{o}C - 0 ^{o}C. The mixture was stirred for 1 hour, ensuring that the temperature did not exceed 0 ^{o}C. A solution of sodium sulphide (1.20 g, 4.97 mmol) and sulphur (0.16 g, 5.0 mmol) in water (15 mL) was then added dropwise during 1 hour to the cold solution of the diazonium salt and the resulting mixture was stirred at 0 ^{o}C for 1 hour. The mixture was allowed to warm to room temperature and then stirred further for 1 hour. After completion, the mixture was acidified (pH 2.5) with 2M-HCl and extracted with EtOAc (3 x 15 mL). The organic extracts were washed sequentially with 20 % aq. Na_2CO_3 (2 x 20 mL), water (2 x 20 mL) and brine (2 x 20 mL), and then dried (anhydr. $MgSO_4$). The solvent was removed *in vacuo* to give the disulphide **362**, which was used in the next step without further purification. In another flask, sodium borohydride (0.12 g, 3.2 mmol) in THF (3 mL) was added to a solution of disulphide **362** (0.25 g, 0.80 mmol) in THF (3 mL) under N_2 at 0 ^{o}C. After the addition, the mixture was allowed to warm to room temperature and stirred further for 1 hour. The reaction was quenched with water (6 mL), acidified (pH 2.5) with 2M-HCl and extracted with EtOAc (3 x 10 mL). The organic extracts were combined, washed sequentially with 20 % aq. Na_2CO_3 (3 x 10 mL) and brine (3 x 10 mL), and then dried (anhydr. $MgSO_4$). The solvent was removed *in vacuo* and the residue purified by flash chromatography [on silica gel; elution with hexane-EtOAc (4:1)] to yield 3-mercaptobenzyl bromide **360d** as a clear oil (0.92 g, 76 %); δ_H/ppm (400 MHz; $CDCl_3$) 3.35 (1H, s, SH), 4.65 (2H, s, CH_2Br), and 7.44 - 7.66 (4H, m, Ar-H); δ_C/ppm (100 MHz; $CDCl_3$) 36.4 (CH_2Br), 125.8 (C-2), 126.4 C-6), 128.3 (C-5), 130.0 (C-4), 130.2 (C-3) and 137.6 (C-1).

Diethyl *N*-benzyl-2-(*N*-hydroxyacetamido)ethylphosphoramidate 363a

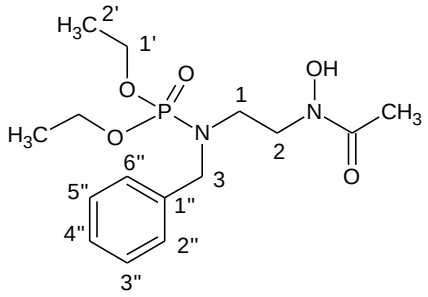

A solution of diethyl *N*-benzyl-2-[*N*-benzyloxy)acetamido]-ethylphosphoramidate **357a** (0.20 g, 0.46 mmol) in dry MeOH (2 mL) was added to a solution of Pd/C (10 %, 0.35 g) in dry MeOH (10 mL) under an H_2-atmosphere and the mixture was stirred at room temperature for 18 hours. The reaction mixture was then filtered through a celite pad, the filtrate was

evaporated *in vacuo* and the residue purified by flash chromatography [on silica gel; elution with hexane-EtOAc (3:1)] to yield *diethyl* N-*benzyl-2-(*N-*hydroxyacetamido)ethyl-phosphoramidate* **363a** as a clear oil (0.13 g, 83 %); (Found: C, 52.40; H, 7.38; N, 8.19 %. $C_{15}H_{25}N_2O_5P$ requires C, 52.32; H, 7.32; N, 8.14 %); υ/cm^{-1} 3221 (OH), 1688 (C=O) and 1238 (P=O); δ_H/ppm (400 MHz; $CDCl_3$) 1.28 (6H, t, *J* = 7.2 Hz, 2 x 2'-CH_3), 1.83 (1H, s, NOH), 2.08 (3H, s, CH_3CO), 2.89 (2H, m, 1-CH_2N), 3.21 (2H, t, *J* = 6.0 Hz, 2-CH_2N), 3.79 (2H, s, 3-CH_2Ph), 4.17 (4H, m, 2 x 1''-OCH_2) and 7.32 - 7.45 (5H, m, Ar-H); δ_C/ppm (100 MHz; $CDCl_3$) 16.1 (d, $J_{P–C}$ = 7.2 Hz, 2 x 2'-CH_3), 20.8 (*C*H_3CO), 35.8 (d, $J_{P–C}$ = 5.0 Hz, 1-CH_2), 53.6 (d, $J_{P–C}$ = 16.5 Hz, 2-CH_2), 62.3 (d, $J_{P–C}$ = 5.6 Hz, 2 x 1'-OCH_2), 67.5 (3-CH_2Ph), 127.3 (C-4''), 128.3 (C-2'' and C-6''), 128.6 (C-3'' and C-5''), 137.4 (C-1') and 167.5 (C=O).

Diethyl 2-(*N*-hydroxyacetamido)-*N*-[4-(hydroxymethyl)benzyl]ethylphosphoramidate 363b

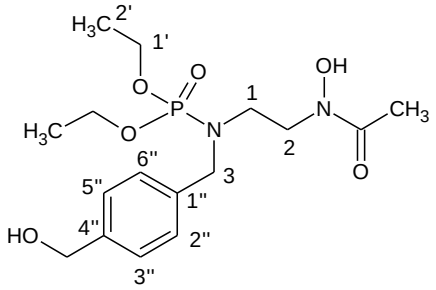

The procedure described for the synthesis of diethyl *N*-benzyl-2-(*N*-hydroxyacetamido)ethyl-phosphoramidate **363a** was employed, using diethyl 2-[(*N*-benzyloxy)acetamido]-*N*-[4-(hydroxymethyl)benzyl]ethylphosphoramidate **357b** (0.20 g, 0.43 mmol) in MeOH (2 mL) and Pd/C (10 %, 0.33 g) in MeOH (10 mL). The solvent was evaporated *in vacuo* and the residue was purified by flash chromatography [on silica gel; elution with hexane-EtOAc (3:1)] to yield *diethyl 2-(*N*-hydroxyacetamido)*-N-*[4-(hydroxymethyl)benzyl]ethylphosphoramidate* **363b** as a yellow oil (0.14 g, 84 %); (Found: C, 51.39; H, 7.22; N, 7.53 %. $C_{16}H_{27}N_2O_6P$ requires C, 51.33; H, 7.27; N, 7.48 %); υ/cm^{-1} 3313 (OH), 1695 (C=O) and 1218 (P=O); δ_H/ppm (400 MHz; $CDCl_3$) 1.32 (6H, t, *J* = 7.2 Hz, 2 x 2'-CH_3), 1.91 (1H, s, NOH), 2.12 (3H, s, CH_3CO), 2.80 (2H, m, 1-CH_2N), 3.38 (2H, t, *J* = 6.4 Hz, 2-CH_2N), 3.85 (2H, s, 3-CH_2Ph), 4.12 (4H, m, 2 x 1''-OCH_2), 5.10 (2H, s, C*H*$_2$OH), 7.25 - 7.30 (4H, m, Ar-H) and 8.02 (1H, s, CH2O*H*); δ_C/ppm (100 MHz; $CDCl_3$) 16.3 (d, $J_{P–C}$ = 6.1 Hz, 2 x 2'-CH_3), 23.4 (*CH*$_3$CO), 37.4 (d, $J_{P–C}$ = 5.2 Hz, 1-CH_2), 52.5 (d, $J_{P–C}$ = 16.5 Hz, 2-CH_2), 63.6 (d, $J_{P–C}$ = 5.8 Hz, 2 x 1'-OCH_2), 66.4 (CH_2OH), 68.8 (3-CH_2Ph), 123.4 (C-2'' and C-6''), 123.7 (C-3'' and C-5''), 136.6 (C-1''), 138.3 (C-4'') and 170.1 (C=O).

Diethyl *N*-(3-aminobenzyl)-2-(*N*-hydroxyacetamido]ethylphosphoramidate 363c

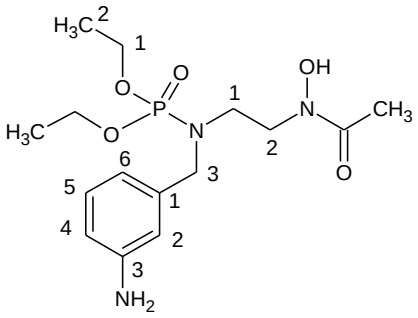

The procedure described for the synthesis of diethyl *N*-benzyl-2-(*N*-hydroxyacetamido)ethyl-phosphoramidate **363a** was employed, using diethyl *N*-(3-aminobenzyl)-2-[(*N*-benzyloxy)acetamido]-ethylphosphoramidate **357c** (0.20 g, 0.44 mmol) in MeOH (2 mL) and Pd/C (10 %, 0.33 g) in MeOH (10 mL). The solvent was evaporated *in vacuo* and the residue was purified by flash chromatography [on silica gel; elution with hexane-EtOAc (3:1)] to yield *diethyl* N-*(3-aminobenzyl)-2-(*N-*hydroxyacetamido]ethylphosphoramidate* **363c** as a yellow oil (0.12 g, 79 %); (Found: C, 50.22; H, 7.35; N, 11.67 %. $C_{15}H_{26}N_3O_5P$ requires C, 50.13; H, 7.29; N, 11.69 %); υ/cm^{-1} 3387 (OH), 3327 (NH_2), 1705 (C=O) and 1224 (P=O); δ_H/ppm (400 MHz; $CDCl_3$) 1.29 (6H, t, *J* = 6.8 Hz, 2 x 2'-CH_3), 2.14 (3H, s, CH_3CO), 2.69 (2H, m, 1-CH_2N), 3.26 (2H, t, *J* = 6.8 Hz, 2-CH_2N), 3.81 (2H, s, 3-CH_2Ph), 4.09 (4H, m, 2 x 1'-OCH_2), 4.78 (2H, s, NH_2), 5.68 (1H, s, OH) and 6.59 - 7.16 (4H, m, Ar-H); δ_C/ppm (100 MHz; $CDCl_3$) 16.3 (d, J_{P-C} = 6.2 Hz, 2 x 2'-CH_3), 21.5 (*CH_3*CO), 36.4 (d, J_{P-C} = 4.7 Hz, 1-CH_2), 53.2 (d, J_{P-C} = 16.4 Hz, 2-CH_2), 62.2 (d, J_{P-C} = 6.5 Hz, 2 x 1'-OCH_2), 68.3 (3-CH_2Ph), 114.0 (C-4''), 114.7 (C-2''), 118.6 (C-6''), 129.6 (C-5''), 136.7 (C-1''), 148.2 (C-3'') and 166.6 (C=O).

Diethyl 2-(*N*-hydroxyacetamido)-*N*-(3-mercaptobenzyl)ethylphosphoramidate 363d

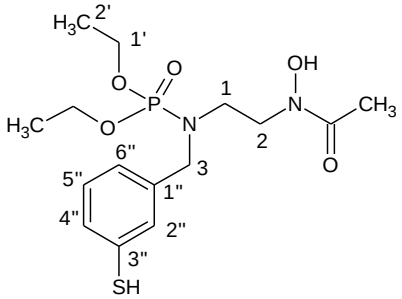

The procedure described for the synthesis of diethyl *N*-benzyl-2-(*N*-hydroxyacetamido)ethyl-phosphoramidate **363a** was employed, using diethyl 2-[(*N*-benzyloxy)acetamido]-*N*-(3-mercaptobenzyl)-ethylphosphoramidate **357d** (0.20 g, 0.43 mmol) in MeOH (2 mL) and Pd/C

(10 %, 0.33 g) in MeOH (10 mL). The solvent was evaporated *in vacuo* and the residue was purified by flash chromatography [on silica gel; elution with hexane-EtOAc (3:1)] to yield *diethyl 2-(*N*-hydroxyacetamido)*-N-*(3-mercaptobenzyl)ethylphosphoramidate* **363d** as a yellow oil (0.14 g, 88 %); Found: C, 47.93; H, 6.73; N, 7.46 %. $C_{15}H_{25}N_2O_5PS$ requires C, 47.86; H, 6.69; N, 7.44 %); υ/cm^{-1} 3219 (OH), 2534 (SH), 1693 (C=O) and 1225 (P=O); δ_H/ppm (400 MHz; $CDCl_3$) 1.30 (6H, t, *J* = 6.8 Hz, 2 x 2'-CH_3), 1.87 (1H, s, OH), 2.12 (3H, s, CH_3CO), 2.71 (2H, m, 1-CH_2N), 3.08 (1H, s, SH), 3.29 (2H, t, *J* = 6.8 Hz, 2-CH_2N), 3.83 (2H, s, 3-CH_2Ph), 4.09 (4H, m, 2 x 1'-OCH_2) and 6.61 - 7.18 (4H, m, Ar-H); δ_C/ppm (100 MHz; $CDCl_3$) 16.4 (d, J_{P-C} = 6.0 Hz, 2 x 2'-CH_3), 22.4 (*C*H_3CO), 36.4 (d, J_{P-C} = 4.8 Hz, 1-CH_2), 48.7 (d, J_{P-C} = 16.5 Hz, 2-CH_2), 61.5 (d, J_{P-C} = 6.5 Hz, 2 x 1'-OCH_2), 66.6 (3-CH_2Ph), 124.2 (C-6''), 125.0 (C-2''), 127.8 (C-4''), 128.3 (C-5''), 129.6 (C-3''), 137.2 (C-1'') and 163.0 (C=O).

_N_-Benzyl-2-(_N_-hydroxyacetamido)ethylphosphoramidic acid 351a

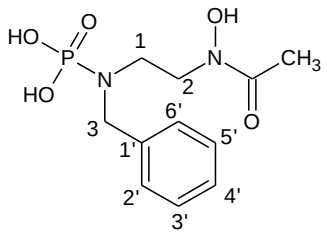

Trimethylsilyl bromide (0.15 mL, 1.0 mmol) was added dropwise to diethyl *N*-benzyl-2-(*N*-hydroxyacetamido)ethylphosphoramidate **363a** (0.12 g, 0.34 mmol) in DCM (5 mL) under N_2 at 0 ^oC and the mixture was stirred for 1 hour. The mixture was allowed to warm to room temperature, water was added (1 mL) and the resulting mixture was stirred overnight. After completion, the solvent was removed *in vacuo* and the residue chromatographed [preparative layer chromatography; elution with hexane-EtOAc-MeOH (1:1:1)] to yield N-*benzyl-2-(*N*-hydroxyacetamido)ethylphosphoramidic acid* **351a** as a colourless oil (85 mg, 87 %); (Found: C, 45.76; H, 6.01; N, 9.79 %. $C_{11}H_{17}N_2O_5P$ requires C, 45.84; H, 5.94; N, 9.72 %); υ/cm^{-1} 3245 (OH), 1653 (C=O) and 1228 (P=O); δ_H/ppm (400 MHz; DMSO-d_6) 2.09 (3H, s, CH_3CO), 2.79 (2H, m, 1-CH_2N), 3.34 (2H, t, *J* = 6.4 Hz, 2-CH_2N), 3.83 (2H, s, 3-CH_2), 5.25 (1H, s, NOH), 7.29 - 7.37 (5H, m, Ar-H) and 8.15 (2H, s, 2 x OH); δ_C/ppm (100 MHz; DMSO-d_6) 20.7 (CH_3), 42.6 (d, J_{P-C} = 4.7 Hz, 1-CH_2N), 52.3 (d, J_{P-C} = 16.9 Hz, 2-CH_2N), 67.2 (3-CH_2), 126.4 (C-4'), 128.6 (C-2' and C-6'), 129.4 (C-3' and C-5'), 139.4 (C-1') and 171.5 (C=O).

2-(*N*-Hydroxyacetamido)-*N*-[4-(hydroxymethyl)benzyl]ethylphosphoramidic acid 351b

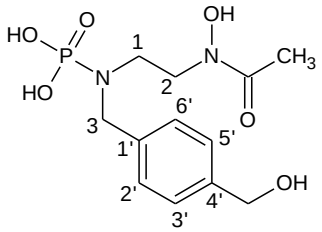

The procedure described for the synthesis of *N*-benzyl-2-(*N*-hydroxyacetamido) ethylphosphoramidic acid **351a** was employed, using diethyl 2-(*N*-hydroxyacetamido)-*N*-[4-(hydroxymethyl)benzyl]ethylphosphoramidate **363b** (0.12 g, 0.31 mmol) and TMSBr (0.12 mL, 0.93 mmol) in DCM (5 mL). The solvent was removed *in vacuo* and the residue chromatographed [preparative layer chromatography; elution with hexane-EtOAc-MeOH (1:1:0.5)] to yield *2-(*N-*Hydroxyacetamido)*-N-*[4-(hydroxymethyl)benzyl]ethylphosphoramidic acid* **351b** as a colourless oil (87 mg, 89 %); (Found: C, 45.35; H, 6.09; N, 8.73 %. $C_{12}H_{19}N_2O_6P$ requires C, 45.29; H, 6.02; N, 8.80 %); υ/cm^{-1} 3329 (OH), 1667 (C=O) and 1220 (P=O); δ_H/ppm (400 MHz; DMSO-d_6) 1.76 (1H, s, CH_2*OH*), 2.07 (3H, s, CH_3CO), 2.75 (2H, m, 1-CH_2N), 3.27 (2H, t, *J* = 6.0 Hz, 2-CH_2N), 3.82 (2H, s, 3-CH_2), 4.78 (2H, s, C*H*$_2$OH), 6.67 (1H, s, NOH), 7.09 - 7.24 (4H, m, Ar-H) and 8.92 (2H, s, 2 x OH); δ_C/ppm (100 MHz; DMSO-d_6) 20.3 (CH_3), 37.5 (d, J_{P-C} = 5.1 Hz, 1-CH_2N), 51.8 (d, J_{P-C} = 16.6 Hz, 2-CH_2N), 65.7 (CH_2OH), 68.4 (3-CH_2), 126.2 (C-3' and C-5'), 128.3 (C-2' and C-6'), 136.5 (C-1'), 139.2 (C-4') and 166.3 (C=O).

***N*-(3-Aminobenzyl)-2-(*N*-hydroxyacetamido)ethylphosphoramidic acid 351c**

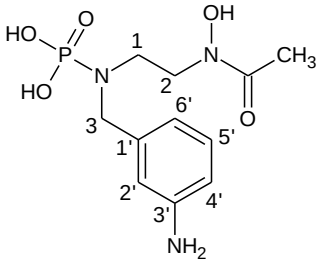

The procedure described for the synthesis of diethyl *N*-benzyl-2-(*N*-hydroxyacetamido)ethylphosphoramidate **351a** was employed, using diethyl *N*-(3-aminobenzyl)-2-(*N*-hydroxyacetamido)ethylphosphoramidate **363c** (0.10 g, 0.27 mmol) and TMSBr (0.10 mL, 0.81 mmol) in DCM (5 mL). The solvent was removed *in vacuo* and the residue chromatographed [preparative layer chromatography; elution with hexane-EtOAc-MeOH (1:1:0.5)] to yield N-*(3-aminobenzyl)-2-(*N-*hydroxyacetamido)ethylphosphoramidic*

acid **351c** as a colourless oil (71 mg, 87 %); (Found: C, 43.70; H, 5.91; N, 13.82 %. $C_{11}H_{18}N_3O_5P$ requires C, 43.57; H, 5.98; N, 13.86 %); υ/cm^{-1} 3361 (OH), 3298 (NH_2), 1684 (C=O) and 1230 (P=O); δ_H/ppm (400 MHz; DMSO-d_6) 2.08 (3H, s, CH_3CO), 2.81 (2H, m, 1-CH_2N), 3.28 (2H, t, J = 6.0 Hz, 2-CH_2N), 3.60 (2H, s, 3-CH_2), 4.66 (1H, s, NOH), 5.48 (2H, s, NH_2), 7.00 (2H, s, 2 x OH) and 7.10 - 7.29 (4H, m, Ar-H); δ_C/ppm (100 MHz; DMSO-d_6) 19.8 (CH_3), 36.7 (d, J_{P-C} = 4.9 Hz, 1-CH_2N), 53.0 (d, J_{P-C} = 16.5 Hz, 2-CH_2N), 68.1 (3-CH_2), 113.9 (C-4'), 114.7 (C-2'), 117.8 (C-6'), 128.4 (C-5'), 138.3 (C-1'), 146.5 (C-3') and 166.8 (C=0).

2-(*N*-Hydroxyacetamido)-*N*-(3-mercaptobenzyl)ethylphosphoramidic acid 351d

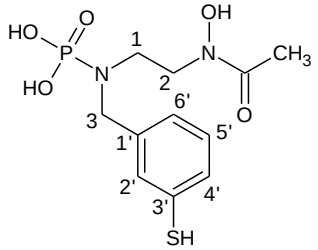

The procedure described for the synthesis of diethyl *N*-benzyl-2-(*N*-hydroxyacetamido)ethylphosphoramidate **351a** was employed, using diethyl 2-(*N*-hydroxyacetamido)-*N*-(3-mercaptobenzyl)ethylphosphoramidate **363d** (0.12 g, 0.31 mmol) and TMSBr (0.13 mL, 92 mmol) in DCM (5 mL). The solvent was removed *in vacuo* and the residue chromatographed [preparative layer chromatography; elution with hexane-EtOAc-MeOH (1:1:1)] to yield *2-(*N-*hydroxyacetamido)*-N-*(3-mercaptobenzyl)ethylphosphoramidic acid* **351d** as a colourless oil (83 mg, 84 %); (Found: C, 41.34; H, 5.41; N, 8.68 %. $C_{11}H_{17}N_2O_5PS$ requires C, 41.25; H, 5.35; N, 8.75 %); υ/cm^{-1} 3326 (OH), 2575 (SH), 1687 (C=O) and 1228 (P=O); δ_H/ppm (400 MHz; D_2O) 2.09 (3H, s, CH_3CO), 2.68 (2H, m, 1-CH_2N), 2.80 (1H, s, SH), 3.33 (2H, t, J = 6.0 Hz, 2-CH_2N), 3.84 (2H, s, 3-CH_2) and 6.85 – 7.37 (4H, m, Ar-H); δ_C/ppm (100 MHz; D_2O) 22.4 (CH_3), 40.6 (d, J_{P-C} = 4.8 Hz, 1-CH_2N), 52.7 (d, J_{P-C} = 16.5 Hz, 2-CH_2N), 68.2 (3-CH_2), 119.2 (C-6'), 123.1 (C-2'), 126.6 (C-4'), 129.4 (C-5'), 130.2 (C-3'), 138.5 (C-1') and 162.1 (C=0).

3.6. Synthesis of fosmidomycin and FR900098

Diethyl (3-oxopropyl)phosphonate 365 [118,119]

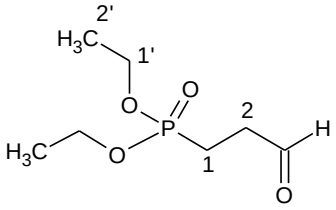

A solution of diethyl (3,3-diethoxypropyl)phosphonate **364** (2.00 g, 7.45 mmol) in 2M-HCl solution (8 mL) was stirred at room temperature for *ca.* 24 hours. The reaction mixture was then extracted with $CHCl_3$ (3 x 25 mL) and the organic layers were combined, and washed with water (2 x 25 mL). The aqueous washings were combined and extracted with $CHCl_3$ (2 x 50 mL). The combined organic extracts were washed sequentially with satd. aq. $NaHCO_3$ (2 x 50 mL) and brine (2 x 50 mL), and then dried (anhydr. $MgSO_4$). The solvent was evaporated *in vacuo* and the residue chromatographed [on silica gel; elution with hexane-EtOAc (3:1)] to yield diethyl (3-oxopropyl)phosphonate **365** as a yellow oil (1.08 g, 75 %); δ_H/ppm (400 MHz; $CDCl_3$) 1.24 (6H, t, J = 6.8 Hz, 2 x 2'-CH_3), 1.96 (2H, m, CH_2P), 2.71 (2H, m, CH_2CO), 4.03 (4H, q, J = 4.4 Hz, 2 x OCH_2) and 9.72 (1H, s, CHO); δ_C/ppm (100 MHz; $CDCl_3$) 16.2 (d, J_{P-C} = 6.3 Hz, 2 x 2'-CH_3), 20.7 (d, J_{P-C} = 143.9 Hz, CH_2P), 27.1 (d, J_{P-C} = 3.8 Hz, CH_2CO), 62.1 (d, J_{P-C} = 6.7 Hz, 2 x 1'-OCH_2) and 174.5 (d, J_{P-C} = 18.8 Hz, C=O).

Diethyl {3-[(benzyloxy)amino]propyl}phosphonate 366 [118,119]

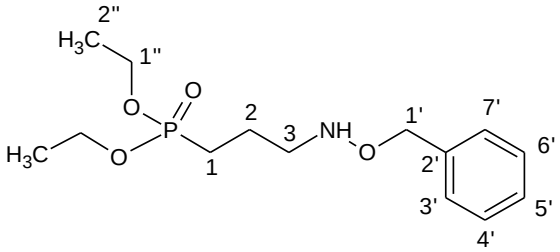

To a stirred solution of diethyl (3-oxopropyl)phosphonate **365** (0.80 g, 4.1 mmol) in MeOH (5 mL) was added a solution of *O*-benzylhydroxylamine (0.68 g, 4.9 mmol) in MeOH (15 mL). The reaction mixture was heated at 40 ^oC for 3 hours, cooled to room temperature and diluted with MeOH (80 mL). After the addition of sodium cyanoborohydride (0.80 g, 12.4 mmol), conc. HCl (4.5 mL) was added dropwise over a period of 30 min and the mixture was stirred for 1 hour. Sodium cyanoborohydride (0.27 g, 4.1 mmol) was again added and the mixture was stirred for another 1 hour. The solvent was removed under reduced pressure,

the residue dissolved in MeOH (50 mL) and then treated with ice-water (50 mL). The resulting mixture was adjusted to pH 10 with aq. KOH-solution and extracted with DCM (2 x 100 mL). The combined organic layers were washed with 10 % $NaHCO_3$ (100 mL) and brine (100 mL), and then dried (anhydr. $MgSO_4$). The solvent was evaporated *in vacuo* and the remaining oil was purified by flash chromatography [on silica gel; elution with hexane-EtOAc (3:1)] to yield diethyl {3-[(benzyloxy)amino]propyl}phosphonate **366** as a yellow oil (0.52 g, 65 %); δ_H/ppm (400 MHz; $CDCl_3$) 1.29 (6H, t, J = 6.4 Hz, 2 x 2''-CH_3), 1.82 (4H, m, 1-CH_2 and 2-CH_2), 2.93 (2H, t, J = 6.0 Hz, CH_2N), 4.08 (4H, m, 2 x 1''-OCH_2), 4.67 (2H, s, CH_2Ph), 5.58 (1H, s, NH) and 7.31 – 7.33 (5H, m, Ar-H); δ_C/ppm (100 MHz; $CDCl_3$) 16.4 (d, $J_{P–C}$ = 6.0 Hz, 2 x 2''-CH_3), 20.4 (d, $J_{P–C}$ = 4.9 Hz, C-2), 23.1 (d, $J_{P–C}$ = 141.2 Hz, CH_2P), 52.0 (d, $J_{P–C}$ = 16.7 Hz, CH_2N), 61.5 (d, $J_{P–C}$ = 6.5 Hz, 2 x 1''-OCH_2), 76.3 (CH_2Ph), 127.8 (C-5'), 128.2 (C-3' and C-7'), 128.3 (C-4' and C-6') and 137.7 (C-2').

Diethyl [3-(*N*-benzyloxy-*N*-formylamino)propyl]phosphonate 367a [118,119]

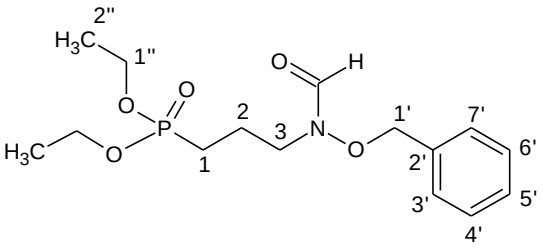

Formic acid (0.12 mL, 3.3 mmol) was added to a mixture of diethyl {3-[(benzyloxy)amino]propyl} phosphonate **366** (0.25 g, 0.85 mmol) and sodium formate (0.02 g, 0.33 mmol) in THF (10 mL) under N_2 and the resulting mixture was refluxed at 80 ^oC for 2 hours. The solvent was removed *in vacuo* and the residue dissolved in EtOAc (25 mL). The organic phase was washed with water (2 x 25 mL). The aqueous washings were combined and extracted with EtOAc (2 x 10 mL). The combined organic extracts were washed sequentially with satd. aq. $NaHCO_3$ (2 x 50 mL) and brine (2 x 50 mL), and then dried (anhydr. $MgSO_4$). The solvent was evaporated *in vacuo* and the residue chromatographed [on silica gel; elution with hexane-EtOAc (3:1)] to yield diethyl [3-(*N*-benzyloxy-*N*-formylamino)propyl]phosphonate **367a** as a yellow oil (0.16 g, 66 %); δ_H/ppm (400 MHz; $CDCl_3$) 1.32 (6H, t, J = 6.8 Hz, 2 x 2''-CH_3), 1.77 (4H, m, 1-CH_2 and 2-CH_2), 3.72 (2H, t, J = 6.4 Hz, CH_2N), 4.09 (4H, m, 2 x 1''-OCH_2), 4.84 (2H, s, CH_2Ph), 7.40 (5H, s, Ar-H) and 8.13 (1H, s, CHO); δ_C/ppm (100 MHz; $CDCl_3$) 16.3 (d, $J_{P–C}$ = 6.0 Hz, 2 x 2''-CH_3), 20.6 (d, $J_{P–C}$ = 4.9 Hz, C-2),

23.5 (d, J_{P-C} = 141.2 Hz, CH_2P), 51.7 (d, J_{P-C} = 16.8 Hz, CH_2N), 61.3 (d, J_{P-C} = 6.5 Hz, 2 x 1''-OCH_2), 76.7 (CH_2Ph), 127.7 (C-5'), 128.0 (C-3' and C-7'), 128.3 (C-4' and C-6'), 137.8 (C-2') and 165.8 (C=O).

Diethyl [3-(*N*-acetyl-*N*-benzyloxylamino)propyl]phosphonate 367b [118,119]

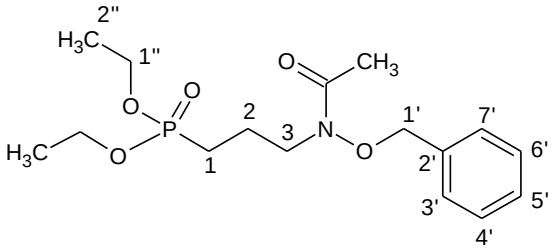

Acetyl chloride (0.08 mL, 0.96 mmol) was added dropwise to a stirred solution of diethyl {3-[(benzyloxy)amino]propyl} phosphonate **366** (0.25 g, 0.83 mmol) and triethylamine (0.13 mL, 0.99 mmol) in DCM (10 mL) under N_2 at 0 ^oC. The mixture was stirred at 0 ^oC for 1 hour, allowed to warm to room temperature and then stirred further for *ca.* 24 hours. The solvent was removed under reduced pressure and the residual oil dissolved in diethyl ether (20 mL). The solution was washed sequentially with aq. K_2CO_3 solution, 0.5M-HCl and water, and then dried over anhydrous $MgSO_4$. The solvent was removed *in vacuo* and the residue purified by flash chromatography [on silica gel; elution with hexane-EtOAc (3:1)] to yield diethyl [3-(*N*-acetyl-*N*-benzyloxylamino)propyl]phosphonate **367b** as a yellow oil (0.18 g, 73 %); δ_H/ppm (400 MHz; $CDCl_3$) 1.33 (6H, t, *J* = 6.8 Hz, 2 x 2''-CH_3), 1.82 (4H, m, 1-CH_2 and 2-CH_2), 2.06 (3H, s, CH_3CO), 3.69 (2H, t, *J* = 6.4 Hz, CH_2N), 4.11 (4H, m, 2 x 1''-OCH_2), 4.85 (2H, s, CH_2Ph) and 7.37 (5H, s, Ar-H); δ_C/ppm (100 MHz; $CDCl_3$) 16.9 (d, J_{P-C} = 6.0 Hz, 2 x 2''-CH_3), 19.7 (CH_3CO), 20.8 (d, J_{P-C} = 4.9 Hz, C-2), 23.6 (d, J_{P-C} = 141.2 Hz, CH_2P), 52.4 (d, J_{P-C} = 16.4 Hz, CH_2N), 62.0 (d, J_{P-C} = 6.5 Hz, 2 x 1''-OCH_2), 76.4 (CH_2Ph), 128.4 (C-5'), 128.3 (C-3' and C-7'), 128.9 (C-4' and C-6'), 138.0 (C-2') and 163.0 (C=O).

Diethyl [3-(*N*-hydroxyformamido)propyl]phosphonate 368a [251,252]

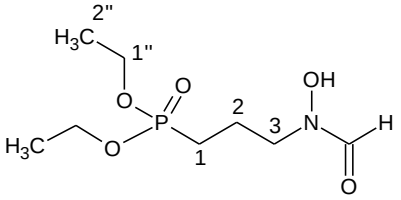

A solution of diethyl {3-[(benzyloxy)(formyl)amino]propyl}phosphonate **367a** (0.15 g, 0.46 mmol) in dry MeOH (5 mL) was added to a solution of Pd/C (10 %, 0.35 g) in dry MeOH (10

mL) under H_2 and the mixture was stirred at room temperature for 18 hours. The reaction mixture was then filtered through a celite pad, the filtrate was evaporated *in vacuo* and the residue purified by flash chromatography [on silica gel; elution with hexane-EtOAc (4:1)] to yield diethyl [3-(*N*-hydroxyformamido)propyl]phosphonate **368a** as a clear oil (0.11 g, 77 %); δ_H/ppm (400 MHz; $CDCl_3$) 1.29 (6H, t, *J* = 6.8 Hz, 2 x 2''-CH_3), 1.80 (4H, m, 1-CH_2 and 2-CH_2), 3.75 (2H, t, *J* = 6.4 Hz, CH_2N), 4.13 (4H, m, 2 x 1''-OCH_2), 5.03 (1H, s, OH) and 9.71 (1H, s, CHO); δ_C/ppm (100 MHz; $CDCl_3$) 16.3 (d, J_{P-C} = 6.0 Hz, 2 x 2''-CH_3), 20.8 (d, J_{P-C} = 4.8 Hz, C-2), 23.2 (d, J_{P-C} = 141.2 Hz, CH_2P), 51.9 (d, J_{P-C} = 16.7 Hz, CH_2N), 61.5 (d, J_{P-C} = 6.5 Hz, 2 x 1''-OCH_2) and 158.2 (C=O).

Diethyl [3-(*N*-hydroxyacetamido)propyl]phosphonate 368b [251,252]

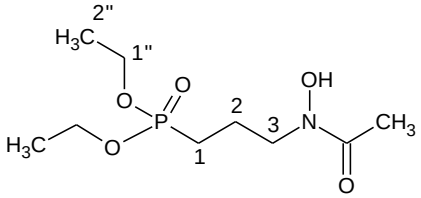

The procedure described for the synthesis of diethyl [3-(*N*-hydroxyformamido)propyl]-phosphonate **368a** was employed, using diethyl [3-(*N*-acetyl-*N*-benzyloxylamino)propyl]-phosphonate **367b** (0.15 g, 0.44 mmol) in MeOH (5 mL) and Pd/C (10 %, 0.34 g) in MeOH (10 mL). The solvent was evaporated *in vacuo* and the residue was purified by flash chromatography [on silica gel; elution with hexane-EtOAc (3:1)] to yield diethyl [3-(*N*-hydroxyacetamido)propyl]phosphonate **368b** as a yellow oil (0.12 g, 81 %); δ_H/ppm (400 MHz; $CDCl_3$) 1.33 (6H, t, *J* = 6.8 Hz, 2 x 2''-CH_3), 1.80 (4H, m, 1-CH_2 and 2-CH_2), 2.08 (3H, s, CH_3CO), 3.71 (2H, t, *J* = 6.8 Hz, CH_2N), 4.12 (4H, m, 2 x 1''-OCH_2) and 5.87 (1H, s, OH); δ_C/ppm (100 MHz; $CDCl_3$) 16.4 (d, J_{P-C} = 6.0 Hz, 2 x 2''-CH_3), 20.2 (CH_3CO), 20.7 (d, J_{P-C} = 4.8 Hz, C-2), 23.5 (d, J_{P-C} = 143.9 Hz, CH_2P), 52.6 (d, J_{P-C} = 16.4 Hz, CH_2N), 62.2 (d, J_{P-C} = 6.5 Hz, 2 x 1''-OCH_2) and 163.7 (C=O).

[3-(*N*-Hydroxyformamido)propyl]phosphonic acid 236 (Fosmidomycin) [251,252]

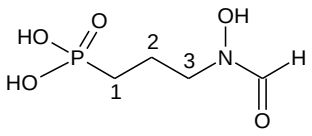

Trimethylsilyl bromide (0.17 mL, 1.3 mmol) was added dropwise to diethyl {3-[formyl(hydroxyl)amino]propyl}phosphonate **368a** (0.10 g, 0.42 mmol) in DCM (3 mL) under N_2 at 0 ^{o}C and the mixture was stirred for 1 hour. The mixture was allowed to warm to room temperature, water was added (1 mL) and the resulting mixture was stirred overnight. The solvent was removed *in vacuo* and the residue chromatographed [preparative layer chromatography; elution with hexane-EtOAc-MeOH (1:1:1)] to yield [3-(*N*-hydroxyformamido)propyl]phosphonic acid **236** as a colourless oil (66 mg, 67 %); δ_H/ppm (400 MHz; D_2O) 1.83 (4H, m, 1-CH_2 and 2-CH_2), 3.73 (2H, t, J = 6.4 Hz, CH_2N) and 9.68 (1H, s, CHO); δ_C/ppm (100 MHz; D_2O) 21.0 (d, J_{P-C} = 4.8 Hz, C-2), 23.6 (d, J_{P-C} = 141.2 Hz, CH_2P), 51.5 (d, J_{P-C} = 16.7 Hz, *CH_2*N) and 155.7 (C=O).

[3-(N-Hydroxyacetamido)propyl]phosphonic acid 237 [201,252]

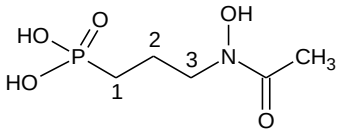

The procedure described for the synthesis of [3-(*N*-hydroxyformamido)propyl]phosphonic acid **236** was employed, using diethyl [3-(*N*-hydroxyacetamido)propyl]phosphonate **368b** (0.10 g, 0.39 mmol) and trimethylsilyl bromide (0.16 mL, 1.2 mmol) in DCM (3 mL). The solvent was removed *in vacuo* and the residue chromatographed [preparative layer chromatography; elution with hexane-EtOAc-MeOH (1:1:1)] to yield [3-(*N*-Hydroxyacetamido)propyl]phosphonic acid **237** as a colourless oil (61 mg, 64 %); δ_H/ppm (400 MHz; D_2O) 1.82 (4H, m, 1-CH_2 and 2-CH_2), 2.10 (3H, s, CH_3CO) and 3.69 (2H, t, J = 6.8 Hz, CH_2N); δ_C/ppm (100 MHz; D_2O) 20.0 (*CH_3*CO), 20.6 (d, J_{P-C} = 4.8 Hz, C-2), 23.2 (d, J_{P-C} = 143.9 Hz, CH_2P), 52.1 (d, J_{P-C} = 16.4 Hz, CH_2N) and 162.8 (C=O).

3.7. Saturation Transfer Difference (STD) NMR binding studies

The *Ec*DXR enzyme was expressed and purified, for the author, using standard protocols[115,142] by Miss Taryn Bodill in the Rhodes Centre for Chemico- and Biomedicinal Research.[211] An STD experiment was run on the different sets of ligands as follows: *Ec*DXR, stored in sodium phosphate buffer (pH 7.0), was freeze-dried and re-suspended in D_2O to make a final concentration of 20 µM. Each set of ligands was dissolved in the protein solution to give a final ligand concentration of 800 µM and thus a protein: ligand molar ratio of 1:40. The STD experiment was carried out using parameters optimized in a previous study in our group.[129] The saturating on-resonance and off-resonance pulses were set at frequencies of 0.73 ppm and 20 ppm, respectively, while cycling between the on- and off-resonance phases was used to reduce the effects of changes in temperature or magnetic field homogeneity. A 3-9-19 water suppression pulse was applied at 4.7 ppm and 6000 scans were acquired. The on- and off-resonance spectra were subtracted from each other and processed using Bruker Topspin software.

3.8. NADPH-dependent DXR inhibition assay

The bio-assay was carried out, for the author, using a reaction mixture containing 100 mM Tris–HCl (pH 7.5), 1 mM $MnCl_2$, 0.3 mM DOXP and 0.3 mM NADPH, made up to a final volume of 100 µl with assay buffer. Equal volumes of *Ec*DXR and ligand were incubated at 37 ^{o}C for 5 min and the reaction was initiated by adding 100 µL of the enzyme-ligand mixture to the rest of the assay components to make a total of 200 µL, with a final EcDXR concentration of 5 $\mu g.mL^{-1}$. The decrease in absorbance at 340 nm as a result of the reduction of NADPH (ε_{NADPH} = 6.3 x 103 $L.mol^{-1}.cm^{-1}$) was monitored at 37 ^{o}C for 10 min, using a PowerWave™ microtitre plate reader. The specific activity of the enzyme in the absence of a ligand was considered to be 100% (i.e. 0% inhibition) and the % relative inhibition of each ligand was determined in triplicate.

3.9. Modelling and simulated docking studies

The Accelrys Cerius^2 module[213] was used to construct the selected compounds *in silico* as their mono-deprotonated species. Using Gaussian 03,[214] the structure for each compound was energy-minimised at the density functional theory (DFT) B3LYP level with the 6-31G(d) base set, using (IEFPCM) solvent correction (water). Docking studies of the energy-minimised ligands were carried out using Autodock version 4.0,[215] using the crystallographically-determined enzyme structure, *Ec*DXR 2EGH,[103] which was downloaded from the Protein Data Bank (PDB; E.C. 1.1.1.267). Using Autodock 4.0, Gasteiger charges were added and the non-polar hydrogens were merged for the respective ligands and the protein model. The active-site residues Ser185, Ser221, Asn226, Lys227 and Glu230 were assigned as flexible. The AutoGrid 4.0 algorithm was employed to represent the active site with a grid box of dimensions 60 x 60 x 60 units (grid-point spacing of 0.375 Å) along the x-, y- and z-directions, and atom maps were calculated for all possible active-site residue-ligand interactions. *In silico* dockings were conducted using the Lamarckian algorithm with a population size of 150, allowing for a maximum of 27 000 generations and 2.5 x 10^6 energy evaluations. For each ligand docking experiment, ten possible docked-conformers were generated. The lowest docked-conformer for each of the ligands was selected and visualised using the Accelrys Discovery Studio Visualizer 2.0[220] software package.

4. REFERENCES

1. Sherman I. W., A Brief History of Malaria and Discovery of the Parasite's Life Cycle. In *Malaria, Parasite Biology, Pathogenesis, and Protection*; Sherman, I. W., Ed.; American Society for Microbiology, Washington, DC, 1998, pp. 3-10.

2. Webb J. L. A., An introduction to Malaria in Human History. In *Humanity's Burden, A Global History of Malaria*, Cambridge University Press, New York, 2009, pp. 1-17.

3. Webb J. L. A., Toward Global Public Health. In *Humanity's Burden, A Global History of Malaria*, Cambridge University Press, New York, 2009, pp. 127-139.

4. The Malaria site. History of Malaria. http://www.malariasite.com/malaria/history _science. htm (accessed October 12, 2010).

5. Moody A. *Clin. Microbiol. Rev.*, 2002, 15, 66-78.

6. Holt R. A., Subramanian G. M., Halpern A., Sutton G.G., Charlab R., Nusskern D.R., Wincker P., Clark A. G., Ribeiro J. M. C., Wides R., Salzber S. L., Loftus B., Yandell M., Majoros W. H., Rusch D. B., Lai Z., Kraft C. L. and Abril J. F., Anthouard V., Arensburger P., Atkinson P.W., Baden H., de Berardinis V., Baldwin D., Benes V., Biedler J., Blass C., Bolanos R., Boscus D., Barnstead M., Cai S., Center A., Chatuverdi K., Christophides G. K., Chrystal M. A., Clamp M., Cravchik A., Curwen V., Dana A., Delcher A., Dew I., Evans C. A., Flanigan M., Grundschober-Freimoser A., Friedli L., Gu Z., Guan P., Guigo R., Hillenmeyer M. E., Hladun S. L., Hogan J. R., Hong Y. S., Hoover J., Jaillon O., Ke Z., Kodira C., Kokoza E., Koutsos A., Letunic I., Levitsky A., Liang Y., Lin J., Lobo N. F., Lopez J. R., Malek J. A., McIntosh T. C., Meister S., Miller J., Mobarry C., Mongin E., Murphy S. D., O'Brochta D. A., Pfannkoch C., Qi R., Regier M. A., Remington K., Shao H., Sharakhova M. V., Sitter C. D., Shetty J., Smith T. J., Strong R., Sun J., Thomasova D., Ton L. Q., Topalis P., Tu Z., Unger M. F., Walenz B., Wang A., Wang J., Wang M., Wang X., Woodford K. J., Wortman J. R., Wu M., Yao A., Zdobnov E. M., Zhang H., Zhao Q., Zhao S., Zhu S. C., Zhimulev I., Coluzzi M., della Torre A., Roth C. W., Louis C., Kalush F., Mural R. J., Myers E. W., Adams M. D., Smith H. O., Broder S., Gardner M. J., Fraser C. M., Birney E., Bork P., Brey P. T., Venter J., Weissenbach J., Kafatos F. C., Collins F. H. and Hoffman S. L., *Science*, 2002, 298, 129-149.

7. Gardner M. J., Hall N., Fung E., White O., Berriman M., Hyman R. W., Carlton J. M., Pain A., Nelson K. E., Bowman S., Paulsen I. T., James K., Eisen J. A., Rutherford K., Salzberg S. L., Craig A., Kyes S., Chan M. S., Nene V., Shallom S. J., Suh B., Peterson J., Angiuoli S. and Pertea M., Allen J., Selengut J., Haft D., Mather M. W., Vaidya A. B., Martin D. A., Fairlamb A. H., Fraunholz M. J., Roos D. S., Ralph S. A., McFadden G. I., Cummings L. M., Subramanian G. M., Mungall C., Venter J. C., Carucci D. J., Hoffman S. L., Newbold C., Davis R. W., Fraser C. M. and Barrell B., *Nature*, 2002, 419, 498-511.

8. Singh B., Sung L. K., Matusop A., Redhakrishnan A., Shamsul S. S. G., Singh J. C., Thomas A. and Conway D. J., *The Lancet*, 2004, 363, 1017-1024.

9. Greenwood B. M., Bojang K., Whitty C. J. M. and Targett G. A. T., *The Lancet*., 2005, 365, 1487-1498.

10. Rosenthal P. J., Overview of Parasitic Infections. In *Comprehensive Medicinal Chemistry II*, vol. 7, Elsevier, 2008, New York, pp. 749-755.

11. Ayala D., Constantini C., Ose K., Kamdem G. C., Antonio-Nkondjio C., Agbor J. P., Awono-Ambene P., Fontenille D. and Simard F., *Malaria Journal*, 2009, 8, 307.

12. Coetzee M. and Fontenille D., *Insect Biochemistry and Molecular Biology*, 2004, 34, 599-605.

13. World Health Organisation, WHO Global Malaria Programme, *World Malaria Report 2010*, WHO Press, Geneva, 2010, pp. 1-60.

14. Areqawi, M.; Cibulskis, R.; Otten, M.; Williams, R.; Dye, C. World Health Organisation, *World Malaria Report 2008*, WHO Press, Geneva, 2008, pp. 1-215.

15. Hay S. I. and Snow R. W., *PLoS Medicine*, 2006, 3, 12, e473.

16. Trig P. I. and Kondrachine A. V., The Current Global Malaria Situation. In *Malaria, Parasite Biology, Pathogenesis, and Protection*; Sherman, I. W., Ed.; American Society for Microbiology, Washington, DC, 1998, pp. 11-21.

17. Ashley E., McGready R., Proux S. and Nosten F., *Travel Medicine and Infectious Disease*, 2006, 4, 159-173.

18. Muller O., Ye M., Louis R. V. and Sie A., *The Lancet*, 2009, 373, 122.

19. Ramos J. M., Reyes F. and Tesfamariam A., *J. Travel. Med.*, 2005, 12, 155-156.

20. Hemingway J. and Ranson H., *Annu. Rev. Entomol.*, 2000, 45, 371-391.

21. French N., Nakiyingi J., Lugada E., Watera C., Whitworth J. A. G. and Gilks C. F., *AIDS*, 2001, 15, 7, 899-906.

22. Whitworth J., Morgan D., Quigley M., Mayanja B., Eotu H., Omoding N., Okongo M., Malamba S. and Ojwiya A., *The Lancet*., 2000, 356, 1051-1056.

23. Van Geertruyden J. P. and D'Alessandro U., *Trends in Parasitology*, 2007, 23, 10, 465-467.

24. United Nations Millennium Development Goals. http://www.un.org/millenniumgoals/reports.shtml. (Accessed on November 2, 2010).

25. The Abuja Decleration. http://www.rollbackmalaria.org/docs/abuja_declaration.pdf. (Accessed on November 2, 2010).

26. Malaria Vaccine Initiative. http://www.malariavaccine.org/. (Accessed on November 4, 2010).

27. Multilateral Initiative on Malaria. http://www.mimalaria.org/eng/aboutmim.asp. (Accessed on November 5, 2010).

28. The Global Fund to fight HIV/AIDS, Tuberculosis and Malaria. http://www.theglobalfund. org/en/about/. (Accessed November 5, 2010).

29. World Health Organisation, *WHO Global Malaria Control and Elimination; report of a technical review*, WHO Press, Geneva, 2008.

30. Brooke B. D., Kloke G., Hunt R. H., Koekemoer L. L., Temu E. A., Taylor M. E., Small G., Hemingway J. and Coetzee M., *Bulletin of Entomological Research*, 2001, 91, 265-272.

31. Kanzok S. M. and Jacobs-Lorena M., *Trends. Parasitol.*, 2006, 22, 2, 49-51.

32. Christophides G. K., *Cell. Microbiol.*, 2005, 7, 3, 325-333.

33. Carter R., *Vaccine*, 2001, 19, 2309-2314.

34. Greenwood B. M., Fidock D. A., Kyle D. E., Kappe S. H. I., Alonso P. L., Collins F. H. and Duffy P. E., *The J. Clin. Inverst.*, 2008, 118, 1266-1276.

35. Frevert U. and Crisanti A., Invasion of Vertebrate Cells: Hepatocytes. In *Malaria, Parasite Biology, Pathogenesis, and Protection*; Sherman, I. W., Ed.; American Society for Microbiology, Washington, DC, 1998, pp. 73-92.

36. Barnwell J. W. and Galinski M. R., Invasion of Vertebrate Cells: Erythrocytes. In *Malaria, Parasite Biology, Pathogenesis, and Protection*; Sherman, I. W., Ed.; American Society for Microbiology, Washington, DC, 1998, pp. 93-107.

37. Beier J. C. and Vanderberg J. P., Sporogonic Development in the Mosquito. In *Malaria, Parasite Biology, Pathogenesis, and Protection*; Sherman, I. W., Ed.; American Society for Microbiology, Washington, DC, 1998, pp. 49-59.

38. White N. J., Malaria Pathophysiology. In *Malaria, Parasite Biology, Pathogenesis, and Protection*; Sherman, I. W., Ed.; American Society for Microbiology, Washington, DC, 1998, pp. 371-383.

39. Milhous W. K. and Kyle D. E., Introduction to the Modes of Action of and Mechanisms of Resistance to Antimalarials. In *Malaria, Parasite Biology, Pathogenesis, and Protection*; Sherman, I. W., Ed.; American Society for Microbiology, Washington, DC, 1998, pp. 303-311.

40. McMurry J., *Organic Chemistry*, 3rd ed., Brooks/Cole, California, 1992, pp. 1115-1116.

41. Clayden J., Greeves N., Warren S. and Wothers P., *Organic Chemistry*, Oxford, London, 2000, pp. 1174.

42. Dewick P., *Medicinal Natural Products: A Biosynthetic Approach*, John Wiley and Sons, New York, 1998, pp. 334-339.

43. Meshnick S. R., From Quinine to Qinghaosu: Historical Perspectives. In *Malaria, Parasite Biology, Pathogenesis, and Protection*; Sherman, I. W., Ed.; American Society for Microbiology, Washington, DC, 1998, pp. 341-349.

44. Mital A., *Curr. Med. Chem.*, 2007, 14, 759-773.

45. Muraleedharan K. M. and Avery M. A., *Advances in the Discovery of New Antimalarials. In Comprehensive Medicinal Chemistry II*, vol. 7, Elsevier, New York, 2007, pp. 765-813.

46. O'Neill P. M., Bray P. G., Hawley S. R., Ward S. A. and Park B. K., *Pharmacol. Ther.*, 1998, 77, 29-58.

47. Krogstad D. J. and De D., Chloroquine: Modes of Action and the Activity of Chloroquine Analogs. In *Malaria, Parasite Biology, Pathogenesis, and Protection*; Sherman, I. W., Ed.; American Society for Microbiology, Washington, DC, 1998, pp. 331-337.

48. Macreadie I., Ginsburg H., Sirawaraporn W. and Tilley L., *Parasitol. Today*, 2000, 16, 10, 438-444.

49. Nosten F. and White N. J., *Am. J. Trop. Med. Hyg.*, 2007, 77, 181-192.

50. Cowman A. F., The Molecular Basis of Resistance to the Sulfones, Sulfonamides, and Dihydrofolate Reductase Inhibitors. In *Malaria, Parasite Biology, Pathogenesis, and Protection*; Sherman, I. W., Ed.; American Society for Microbiology, Washington, DC, 1998, pp. 317-325.

51. Vaidya A. B., Mitochondrial Physiology as a Target for Atovaquone and Other Antimalarials. In *Malaria, Parasite Biology, Pathogenesis, and Protection*; Sherman, I. W., Ed.; American Society for Microbiology, Washington, DC, 1998, pp. 355-365.

52. Woodward R. B. and Doering W. E., *J. Am. Chem. Soc.*, 1945, 67, 860-874.

53. Stock G., Niu D., Fujimoto A., Koft E. R., Balkovec J. M., Tata J. R. and Dake G. R., *J. Am. Chem. Soc.,* 2001, 123, 3239-3242.

54. Raheem I. T., Goodman S. N. and Jacobsen E. N., *J. Am. Chem. Soc.*, 2004, 126, 706-707.

55. Igarashi J., Katsukawa M., Wang Y. G., Acharya H. P. and Kobayashi Y., *Tetrahedron Lett.*, 2004, 45, 3783-3786.

56. Surrey A. R. and Hammer H. F., *J. Am. Chem. Soc.*, 1946, 68, 113-116.

57. Johnson W. S. and Buell B. G., *J. Am. Chem. Soc.*, 1952, 74, 4513-4516.

58. Margolis B. J., Long K. A., Laird D. L. T., Ruble J. C. and Pulley S. R., *J. Org. Chem.*, 2007, 72, 2232-2235.

59. Ohnmacht C. J., Patel A. R. and Lutz R. E., *J. Med. Chem.*, 1971, 14(10), 926-928.

60. Elderfield R. C., Mertel H. E., Mitch R. T., Wempen I. M. and Werble E., *J. Am. Chem. Soc.*, 1955, 77, 4816-4819.

61. Kumar V., Mahajan A. and Chibale K., *Bioorg. Med. Chem.*, 2009, 17, 2236-2275.

62. Schmid G. and Hofheinz W., *J. Am. Chem. Soc.*, 1983, 105, 624-625.

63. Ravindranathan T., Kumar M. A., Menon R. B. and Hiremath S.V., *Tetrahedron Lett.*, 1990, 31, 5, 755-758.

64. Avery M. A., Chong W. K. M. and Jennings-White C., *J. Am. Chem. Soc.*, 1992, 114, 974-979.

65. Yadav J. S., Babu R. S. and Sabitha G., *Tetrahedron Lett.*, 2003, 44, 387-389.

66. Brossi A., Venugopalan B., Gerpe L. D., Yeh H. J. C., Flippen-Anderson J. L., Buchs P., Luo X. D., Milhous W. and Peters W., *J. Med. Chem.*, 1998, 31, 645-650.

67. Rosenthal P. J., *J. Exp. Biol.*, 2003, 206, 3735-3744.

68. Mandal S., Moudgil M. and Mandal S. K., *Eur. J. Pharamacol.,* 2009, 625, 90-100.

69. Kaschula C., Egan T. J., Hunter R., Basilico N., Parapini S., Taramelli D., Pasini E. and Monti D., *J. Med. Chem.*, 2002, 45, 3531-3539.

70. Solomon V. R., Haq W., Srivastava K., Puri S. K. and Katti S. B., *J. Med. Chem.*, 2007, 50, 394-398.

71. Ekoue-Kovi K., Yearick K., Iwaniuk D. P., Natarajan J. K., Alumasa J., de Dios A. C., Roepe P. D. and Wolf C., *Bioorg. Med. Chem.*, 2009, 17, 270-283.

72. Musonda C. C., Taylor D., Lehman J., Gut J., Rosenthal P. J. and Chibale K., *Bioorg. Med. Chem. Lett.*, 2004, 14, 3901-3905.

73. Musonda C. C., Taylor D., Lehman J., Gut J., Rosenthal P. J., Yardley V., de Souza R. C. C. and Chibale K., *Bioorg. Med. Chem. Lett.*, 2006, 14, 5605-5615.

74. Anderson M. O., Sherill J., Madrid P. B., Liou A. P., Weisman J. L., DeRisi J. L. and Guy R. K., *Bioorg. Med. Chem.*, 2006, 14, 334-343.

75. Gomes P., Araujo M. J., Rodrigues M., Vale N., Azevedo Z., Iley J., Chambel P., Morais J. and Moreira R., *Tetrahedron*, 2004, 60, 5551-5562.

76. Biot C., Glorian G., Maciejewski L. A. and Brocard J. S., *J. Med. Chem.*, 1997, 40, 3715-3718.

77. Chibale K., Moss J. R., Blackie M., van Schalkwyk D. and Smith P. J., *Tetrahedron Lett.,* 2000, 41, 6231-6235.

78. Blackie M. A. L., Beagley P., Croft S. L., Kendrick H., Moss J. R. and Chibale K., *Bioorg. Med. Chem.*, 2007, 15, 6510-6516.

79. Biot C., Pradines B., Sergeant M., Gut J., Rosenthal P. J. and Chibale K., *Bioorg. Med. Chem. Lett.*, 2007, 17, 6434-6438.

80. Hindley S., Ward S. A., Storr R. C., Searle N. L., Bray P. G., Park B. K., Davies J. and O'Neill P. M., *J. Med. Chem.*, 2002, 45, 1052-1063.

81. Nga T. T., Menage C., Begue J. P., Bonnet-Delpon D. and Gantier J. C., *J. Med. Chem.*, 1998, 41, 4101-4108.

82. O'Neill P. M., Searle N. L., Kan K. W., Storr R. C., Maggs J. L., Ward S. A., Raynes K. and Park B. K., *J. Med. Chem.*, 1999, 42, 5487-5493.

83. Ekthawatchai S., Kamchonwongpaisan S., Kongsaeree P., Tarnchompoo B., Thebataranonth Y. and Yuthavong Y., *J. Med. Chem.*, 2001, 44, 4688-4695.

84. Kouznetsov V. and Gomez-Barrio A., *Eur. J. Med. Chem.*, 2009, 44, 3091-3113.

85. Lombard M. C., N'Da D. D., Breytenbach J. C., Smith P. J. and Lategan C. A., *Bioorg. Med. Chem. Lett.*, 2010, 20, 6975-6977.

86. Kaur K., Jain M., Kau T. and Jain R., *Bioorg. Med. Chem.*, 2009, 17, 3229-3256.

87. Takeuchi Y., Azuma K., Takakura K., Abe H. and Harayama T., *Chem. Commun*., 2000, 1643-1644.

88. Bringmann G., Gampe C. M., Reichert Y., Bruhn T., Faber J. H., Mikyna M., Reichert M., Leippe M., Brun R. and Gelhaus C., *J. Med. Chem.*, 2007, 50, 6104-6115.

89. Jana S. and Paliwal J., *Int. J. Antimicrob. Agents.*, 2007, 30, 4-10.

90. Rohdich F., Bacher A. and Eisenreich W., *Biochem. Soc. Trans.,* 2005, 33, 785-791.

91. Singh N., Cheve G., Avery M. A. and McCurdy C. R., *Curr. Pharm. Des.*, 2007, 13, 1161-1177.

92. Nelson D. L. and Cox M. M., *Lehninger Principles of Biochemistry*, 4th ed., Freeman, New York, 2004, Chapter 21, pp. 787-832.

93. Wiesner J. and Jomaa H., *Curr. Drug Targets*, 2007, 8, 3-13.

94. Cassera M. B., Gozzo F. C., D'Alexandri F. L., Merino E. F., del Portillo H. A., Peres V. J., Almeida I. C., Eberlin M. N., Wunderlich G., Wiesner J., Jomaa H., Kimura E. A. and Katzin A. M., *J. Biol. Chem.*, 2004, 279, 51749-51759.

95. Wiesner J., Borrmann S. and Jomaa H., *Parasitol. Res.*, 2003, 90, S71-S76.

96. Hoeffler J. F., Tritsch D., Grosdemange-Billiard C. and Rohmer M., *Eur. J. Biochem.*, 2002, 269, 4446-4457.

97. Argyrou A. and Blanchard J. S., *Biochemistry*, 2004, 43, 4375-4384.

98. Dumas R., Biou V., Halgand F., Douce R. and Duggleby R. G., *Acc. Chem. Res.*, 2001, 34, 399-408.

99. Proteau P. J., Woo Y. H., Williamson R. T. and Phaosiri C., *Org. Lett.*, 1999, 1, 921.

100. Radykewicz T., Rohdich F., Wungsintaweekul J., Herz S., Kis K., Eisenreich W., Bacher A., Zenk M. H. and Arigoni D., *FEBS Lett.*, 2000, 465, 157-160.

101. Reuter K., Sanderbrand S., Jomaa H., Wiesner J., Steinbrecher I., Beck E., Hintz M., Klebe G. and Stubbs M. T., *J. Biol. Chem.*, 2002, 277, 5378-5384.

102. Yajima S., Nonaka T., Kuzuyama T., Seto H. and Ohsawa K., *J. Biochem.*, 2002, 131, 313-317.

103. Yajima S., Hara K., Lino D., Sasaki Y., Kuzuyama T., Ohsawa K. and Seto H., *Acta. Crystallogr. Sect. F: Struct. Biol. Cryst. Comm.*, 2007, 63, 466-470.

104. Steinbacher S., Kaiser, J., Eisenreich W., Huber R., Bacher A. and Rohdich F., *J. Biol. Chem.*, 2003, 278, 18401-18407.

105. Mac Sweeney A., Lange R., Fernandes R. P. M., Schulz, H., Dale G. E., Douangamath A., Proteau P. J. and Oefner C., *J. Mol. Biol.*, 2005, 345, 115-127.

106. Ricagno S., Grolle S., Bringer–Meyer S., Sahm H., Lindqvist Y. and Schneider G., *Biochim. Biophys. Act.,* 2004, 37-44.

107. Henriksson L. M., Unge T., Carlsson J., Aqvist J., Mowbray S. L. and Jones T. A., *J. Biol. Chem.*, 2007, 282, 19905-19916.

108. Osipiuk J., Mulligan R., Stam J., Anderson W.F. and Joachimiak A., 2002, http://www.rcsb.org/pdb/results/results.do?outformat=&qrid=43631711&tabtoshow=Current. (Accessed on January 5, 2011).

109. Takenoya M., Ohtaki A., Noguchi K., Endo K., Sasaki Y., Ohsawa K., Yajima S. and Yohda M., *J. Struct. Biol*., 2010, 170, 532-539.

110. Singh N., Cheve G., Avery M. A. and McCurdy C. R., *J. Chem. Inf. Model.*, 2006, 46, 1360-1370.

111. Goble J. L., Adendorff M. R., de Beer T. A. P., Stephens L. L. and Blatch G. L., *Protein Pept. Lett.*, 2010, 17, 109-120.

112. Kuzuyama T., Takahashi S., Takagi M. and Seto H. J., *Biol. Chem.*, 2000, 275, 19928-19932.

113. Silber K., Heidler P., Kurz T. and Klebe G., *J. Med. Chem.*, 2005, 48, 3547-3563.

114. Proteau P., *J. Bioorg. Chem.*, 2004, 32, 483-493.

115. Kuzuyama T., Shimizu T., Takahashi S. and Seto H., *Tetrahedron Lett.*, 1998, 39, 7913-7916.

116. Jomaa H., Wiesner J., Sanderbrand S., Altincicek B., Weidemeyer C., Hintz M., Turbachova I., Eberl M., Zeidler J., Lichtenthaler H. K., Soldati D. and Beck E., *Science*, 1999, 285, 1573-1576.

117. Reichenberg A., Wiesner J., Weidemeyer C., Dreiseidler E., Sanderbrand S., Altincicek B., Beck E., Schlitzer M. and Jomaa H., *Bioorg. Med. Chem. Lett.*, 2001, 11, 833-835.

118. Ortmann R., Wiesner J., Reichenberg A., Henschker D., Beck E., Jomaa H. and Schlitzer M., *Bioorg. Med. Chem. Lett.*, 2003, 13, 2163-2166.

119. Ortmann R., Wiesner J., Reichenberg A., Henschker D., Beck E., Jomaa H. and Schlitzer M., *Arch. Pharm. Chem. Life Sci.*, 2005, 338, 305−314.

120. Yajima S., Hara K., Sanders J. M., Yin F., Ohsawa K., Wiesner J., Jomaa H. and Oldfield E., *J. Am. Chem. Soc.*, 2004, 126, 35, 10824-10825.

121. Woo Y. H., Fernandes R. P. and Proteau P. J., *Bioorg. Med. Chem.*, 2006, 14, 2375-85.

122. Deng, L., Sundriyal S., Rubio V., Shi Z. and Song Y., *J. Med. Chem.*, 2009, 52, 6539-6542.

123. Devreux V., Wiesner, J., Van Der Eycken J., Jomaa H. and Van Calenbergh S., *Bioorg. Med. Chem. Lett.*, 2007, 17, 4920-4923.

124. Devreux V., Wiesner J., Jomaa H., Rozenski J., Van Der Eycken J. and Van Calenbergh S., *J. Org. Chem.*, 2007, 72, 3783-3789.

125. Devreux V., Wiesner J., Goeman J. L., Van Der Eycken J., Jomaa H. and Van Calenbergh S., *J. Med. Chem.*, 2006, 49, 2656-2660.

126. Verbrugghen T., Cos P., Maes L. and Van Calenbergh S., *J. Med. Chem.*, 2010, 53, 5342-5346.

127. Giessmann D., Heidler P., Haemers T., Van Calenbergh S., Reichenberg A., Jomaa H., Weidemeyer C., Sanderbrand S., Wiesner J. and Link A., *Chem. Biodiversity*, 2008, 5, 643-656.

128. Perruchon J., Ortmann R., Altenkamper M., Silber K., Wiesner J., Jomaa H., Klebe G. and Schlitzer M*., ChemMedChem*, 2008, 3, 1232-1241.

129. Conibear A. C., Synthesis and Evaluation of Novel Inhibitors of 1-Deoxy-D-xylulose-5-phosphate Reductoisomerase as Potential Antimalarials, MSc. Thesis, Rhodes University, Grahamstown, 2010.

130. Merckle L., de Andres-Gomez A., Dick B., Cox R. J., Godfrey C. R., *ChemBiochem*, 2005, 6, 1866-74.

131. Kuntz L., Tritsch D., Grosdemange-Billiard C., Hemmerlin A., Willem A., Bach T. J. and Rohmer M., *Biochem. J.*, 2005, 386, 127-135.

132. Kurz T., Geffken D. and Wackendorff C., *Z. Naturforsch.*, 2003, 58, 457-461.

133. Kurz, T., Geffken D. and Wackendorff C., *Z. Naturforsch.*, 2003, 58, 106-110.

134. Behrendt C.T., Kunfermann A., Illarionova V., Matheeussen A., Grawert T., Groll M., Rohdich F., Bacher A., Eisenreich W., Fischer M., Maes L. and Kurz T., *ChemMedChem*, 2010, 5, 1673-1676.

135. Hoeffler J.F., Tritsch D., Grosdemange-Billiard C. and Rohmer M., *Eur. J. Biochem.*, 2002, 269, 4446-4457.

136. Walker J.R. and Poulter C.D., *J. Org. Chem.*, 2005, 70, 9955-9959.

137. Fox D.T. and Poulter C.D., *J. Org. Chem.*, 2005, 70, 1978-1985.

138. Herforth C., Wiesner J., Heidler P., Sanderbrand S., Van Calenbergh S., Jomaa H. and Link A., *Bioorg. Med. Chem.*, 2004, 12, 755-762.

139. Salisu S. T., ATP Mimics as Glutamine Synthetase Inhibitors - an Exploratory Synthetic Study., PhD Thesis, Rhodes University, Grahamstown, 2008.

140. Gxoyiya B. S. B., Synthetic, Spectrometric and Computer Modelling Studies of Novel ATP Analogues., PhD Thesis, Rhodes University, Grahamstown, 2007.

141. Mutorwa M., Salisu S., Blatch G. L., Kenyon C., Kaye P. T., *Synth. Commun.*, 2009, 39, 2723-2736.

142. Bodill T., Conibear A. C., Blatch G. L., Lobb K. A., Kaye P. K., *Bioorg. Med. Chem.*, 2011, 19, 1321-1327.

143. Furniss B., Hannaford A., Smith P. and Tatchell A., *Vogel's Textbook of Practical Organic Chemistry*, Longman, London, 1989, pp. 926-927.

144. Smith M.B. and March J., *March's Advanced Organic Chemistry: Reactions, Mechanisms and Structure*, Wiley & Sons, New York, 2001, pp. 934-998.

145. Djerassi C., *Chem. Rev.*, 1948, 43, 271-314.

146. Arbuzov B. A., *Pure Appl. Chem.*, 1964, 9, 307–353.

147. Bhattacharya A. K. and Thyagarajan G., *Chem. Rev.*, 1981, 81, 415–430.

148. Landuer S. R. and Rydon H. N., *J. Chem. Soc.*, 1953, 2224.

149. Behrendt C.T., Kunfermann A., Illarionova V., Matheeussen A., Grawert T., Groll M., Rohdich F., Bacher A., Eisenreich W., Fischer M., Maes L. and Kurz T., *ChemMedChem,* 2010, 5, 1673-1676.

150. Haces A., Breitman T. and Driscoll J.S., *J. Med. Chem.*, 1987, 30, 405-409.

151. Solladie-Cavallo A. and Bencheqroun M., *J. Org. Chem.*, 1992, 57, 5831-5834.

152. Zradni F.Z., Hamelin J. and Derdour A., *Synth. Commun.*, 2002, 32, 3525-3531.

153. Marsh J., *Advanced Organic Chemistry*, 3rd, J. Wiley and Sons, New York, 1985, pp. 385.

154. Bruckner R., *Advanced Organic Chemistry: Reaction mechanisms*, Elsevier, New York, 2002, pp. 224-244.

155. Basha A., Lipton M. and Weinreb M., *Tetrahedron Lett.,* 1977, 48, 4171-4174.

156. Wang W. B. and Roskamp E. J., *J. Org. Chem.,* 1992, 57, 6101-6103.

157. Jang D. O., Park D. J. and Kim J., *Tetrahedron Lett.,* 1999, 40, 5323-5326.

158. Villeneuve G. B. and Chan T. H., *Tetrahedron Lett.,* 1997, 38, 6489-6492.

159. Antell M. F. In *The Chemistry of Acyl Halides.,* Patai S., Ed., InterScience, London, 1972, pp. 35-68.

160. Bruckner R., *Organic Mechanisms: Reactions, Stereochemistry and Synthesis*, Springer, Berlin, 2007, pp. 274-282.

161. Alder R. W., Bowman P. S., Steele W. R. and Winterman D. R., *J. Chem. Soc., Chem. Commun.,* 1968, 724.

162. Rose N. R., Synthesis of Novel Coumarin Derivatives as Potential Inhibitors of HIV-1 Protease., MSc. Thesis, Rhodes University, Grahamstown, 2006.

163. Izdebski J., Pachulska M. and Orowska A., *Int. J. Peptide Protein Res.,* 1994, 44, 414.

164. Moroder L., Gemeiner M., Goehring W., Jaeger E., Thamm P. and Wunsch E., *Biopolymers,* 1981, 20, 17.

165. Woodman E. K., Chaffey J. G., Hopes P. A., Hose D. R. and Gilday J. P., *Organic process Research and Development*, 2009, 13, 106-113.

166. Nakajima N. and Ikada Y., *Bioconjugate Chem.,* 1995, 6, 123-130.

167. Fatiadi A. J., *Synthesis,* 1987, 85.

168. Kolb H. C., Van Nieuwenhze M. S. and Sharpless K. B., *Chem. Rev.,* 1994, 94, 2483-2547.

169. Wilson C. V., *Org. React.*, 1950, 9, 350. b) Woodward R. B. and Brutcher F. V., *J. Am. Chem. Soc.,* 1958, 80, 209.

170. Plietker B., Niggemann M. and Pollrich A., *Org. Biomol. Chem.,* 2004, 2, 1116.

171. Plietker B. and Niggemann M., *J. Org. Chem.,* 2005, 7, 2402.

172. Plietker B., *Organic Lett.,* 2004, 6, 289-291.

173. Krise J. P. and Stella V. J., *Adv. Drug Deliv. Rev.,* 1996, 19, 287-310.

174. Salomon C. J. and Breuer E., *Tetrahedron Lett.,* 1995, 36, 6759–6760.

175. Kumar G. D., Saenz D., Lokesh G. L. and Natarajan A., *Tetrahedron Lett.,* 2006, 47, 6281-6284.

176. Tanner D. C., Over-expression, Purification and Biochemical Characterization of DOXP Reductoisomerase and The Rational Design of Novel Anti-malarial drugs., MSc. Thesis, Rhodes University, Grahamstown, 2003.

177. Belen'kii L. I., Kim T. G., Suslov I. A. and Chuvylkin N. D., *Arkivoc*, 2003, 15, 59-67.

178. Kutney J. P., Hanssen H. W. and Nair G. V., *Tetrahedron*, 1971, 27, 3323-3330.

179. Pechkin A. A., Elchaninov M. M., Lukyanov B. S. and Alekseenko Y. S., *Chemistry of Heterocyclic Compounds*, 2004, 40, 599-602.

180. Thomas A. D., Asokan J. and Asokan C. V., *Tetrahedron*, 2004, 60, 5069-5076.

181. Rai L. M. K., Musad E. A., Jagadish R. L. and Shivakumar K. N., *Synth. Commun.,* 2011, 41, 953-955.

182. Sarvari H. M. and Sharghi H., *Helv. Chim. Acta.,* 2005, 88, 2282-2287.

183. Linda P. and Marino G., *Tetrahedron,* 1967, 23, 1739-1743.

184. Ciranni G., *Tetrahedron Lett.,* 1971, 41, 3833-3836.

185. Hartough H. D. and Kosak A. I., *J. Am. Chem. Soc.,* 1947, 69, 1012.

186. Hartough H. D. and Kosak A. I., *J. Am. Chem. Soc.,* 1946, 68, 2639.

187. Pearson D. E. and Buehler C. A., *Synthesis,* 1972, 533-542.

188. Farrar M. W. and Levine R., *J. Am. Chem. Soc.,* 1950, 72, 4433-4436.

189. He F., Wu H., Chen J. and Su W., *Synth. Commun.,* 2008, 38, 255-264.

190. Clementi S., Linda P. and Vergoni M., *Tetrahedron,* 1971, 27, 4667-4672.

191. Stumpp M. C. and Schmidt R. R., *Tetrahedron,* 1986, 42, 5941-5948.

192. Pragnacharyulu P. V. and Abushanab E., *Tetrahedron Lett.,* 1995, 36, 5507-5510.

193. Nguyen C., Kasinathan G., Leal-Cortijo I., Musso-Buendia A., Kaiser M., Brun R., Ruiz-Pe´rez L. M., Johansson N. G., Gonza´lez-Pacanowska D. and Gilbert I. H., *J. Med. Chem.,* 2005, 48, 5942-5954.

194. Srinivas O., Radhika S., Bandaru N. M., Nadimpalli S. K. and Jayaraman N., *Org. Biolmol. Chem.,* 2005, 3, 4252-4257.

195. Ren R. X. and Ou W., *Tetrahedron Lett.,* 2001, 42, 8445-8446.

196. Damljanovic I., Vukicevic M. and Vukicevic R. D., *Monatsh. Fur. Chem.,* 2006, 137, 301-305.

197. Kad G.L., Bhandari M., Kaur J., Rathee R., Singh J., *Green Chem.*, 2001, 3, 275.

198. a) Barton D. H. R., Fernandez I., Richard C. S. and Zard S., *Tetrahedron,* 1987, 43, 551 b) Albanese D., Landini D. and Penso M., *Synthesis,* 1990, 333 c) Kizil M. and Murphy J. A., *Tetrahedron,* 1997, 53, 16847.

199. Zwierzak A., *Synthesis,* 1982, 11, 920-922.

200. Kuzuyama T., Shimizu T., Takahashi S. and Seto H., *Tetrahedron Lett.,* 1998, 39, 7913-7916.

201. Hemmi K., Takeno H., Hashimoto M. and Kayima T., *Chemical and Pharmaceutical Bulletin.*, 1981, 29, 646-650.

202. Fokin A. A., Yurchenko A. G., Rodionov V. N., Gunchenko P. A., Yurchenko R. I., Reichenberg A., Wiesner J., Hintz M., Jomaa H. and Schreiner P. R., *Org. Lett.,* 2007, 9, 4379-4382.

203. Brahmachari G. and Laskar S., *Tetrahedron Lett.,* 2010, 51, 2319-2322.

204. Rahman M., Kundu D., Hajra A. and Majee A., *Tetrahedron,* 2010, 51, 2896-2899.

205. Mayer M. and Meyer B., *Angew. Chem. Int. Ed.,* 1999, 38, 1784-1788.

206. Marchioro C., Davalli S., Provera S., Heller M., Ross A. and Senn H., Experiments in NMR Based Screening. In *BioNMR in Drug Research*, Zerbe O., Ed.; Wiley-VCH: Weinheim, 2003, Vol. 16, pp. 321-339.

207. Ortmann R., Wiesner J., Silber K., Klebe G., Jomaa H. and Schlitzer M., *Arch. Pharm.,* 2007, 340, 483-490.

208. Goble J. L., The Druggable Anti-malarial target 1-deoxy-D-xylulose-5-phosphate Reductoisomerase: Purification, Kinetic Characterisation and Inhibition Studies, PhD. Thesis, Rhodes University, Grahamstown, 2011. b) Umeda T., Tanaka N., Kusakabe Y., Nakanishi M., Kitade Y. and Nakamura K. T., *Scientific Reports*, 2011, 1(9), 1-9.

209. Ji, Z., Yao Z. and Liu M., *Anal. Biochem*., 2009, 385, 380-382.

210. Mayer M. and James T. L., *J. Am. Chem. Soc.,* 2002, 124, 13376-13377.

211. Bodill T., Bioassay Technician, Centre for Chemico- and Biomedicinal Research, Rhodes University, Grahamstown, 2010.

212. Wiesner J., Ortmann R., Jomaa H. and Schlitzer M., *Arch. Pharm.*, 2007, 340, 667-669.

213. *Cerius*^{2}, Version 4.10 L revision 05.0708; Accelrys Inc., Taipei Hsien, 1997.

214. *Gaussian 03*, Revision E.01, Frisch M. J., Trucks G. W., Schlegel H. B., Scuseria G. E., Robb M. A., Cheeseman J. R., Montgomery Jr. J. A., Vreven T., Kudin K. N., Burant J.C., Millam J. M., Iyengar S. S., Tomasi J., Barone V., Mennucci B., Cossi M., Scalmani G., Rega N., Petersson G. A., Nakatsuji H., Hada M., Ehara M., Toyota K., Fukuda R., Hasegawa J., Ishida M., Nakajima T., Honda Y., Kitao O., Nakai H., Klene M., Li X., Knox J. E., Hratchian H. P., Cross J. B., Bakken V., Adamo C., Jaramillo J., Gomperts R., Stratmann R. E., Yazyev O., Austin A. J., Cammi R., Pomelli C., Ochterski J. W., Ayala P.Y., Morokuma K., Voth G. A., Salvador P., Dannenberg J. J., Zakrzewski V. G., Dapprich S., Daniels A. D., Strain M. C., Farkas O., Malick D. K., Rabuck A. D., Raghavachari K., Foresman J. B., Ortiz J. V., Cui Q., Baboul A. G., Clifford S., Cioslowski J., Stefanov B.B., Liu G., Liashenko A., Piskorz P., Komaromi I., Martin R. L., Fox D. J., Keith T., Al-Laham M. A., Peng C. Y., Nanayakkara A., Challacombe M., Gill P. M. W., Johnson B., Chen W., Wong M. W., Gonzalez C., Pople J. A., Gaussian Inc.: Wallingford, CT, 2004.

215. Morris G. M., Goodsell D. S., Halliday R. S., Huey R., Hart W. E., Belew R. K. and Olson A. J., *J. Comput. Chem.,* 1998, 19, 1639-1662.

216. Tao P. and Lai L., *J. Comput.-Aided Mol. Des.*, 2001, 15, 429-446.

217. Kim R. and Skolnick J., *Journal of Computational Chemistry*, 2008, 29, 1316-1331.

218. Reynolds C. H., Tounge B. A. and Bembenek S. D., *J. Med. Chem.,* 2008, 51, 2432-2438.

219. Reynolds C. H., Tounge B. A. and Bembenek S. D., *Drug Discovery Today*, 2009, 14, 278-283.

220. *Discovery Studio Visualizer*, Release 2.0, Accelrys Software Inc., San Diego, 2007.

221. Perrin D. D. and Armarego W. L. F., *Purification of Laboratory Chemicals*, Pergamon Press, Oxford, 3rd ed., 1988.

222. Todd D., *J. Am. Chem. Soc.*, 1953, 75, 1895-1900.

223. Lee S. H., *Heterocycl. Commun.*, 2005, 11, 407-410.

224. Piffl M., Weston J. and Anders E., *Eur. J. Org. Chem.,* 2000, 2851-2859.

225. Wotiz J. H., *J. Am. Chem. Soc.*, 1953, 75, 6342-6343.

226. Snyder H. R., *J. Am. Chem. Soc.*, 1954, 76, 33-35.

227. Nitsche F., Aumann R. and Frohlich R., *J. Organomet. Chem.*, 2007, 692, 2971-2989.

228. Caramella P., Reami D., Falzoni M. and Quadrelli P., *Tetrahedron,* 1999, 55, 7027-7044.

229. Ulrich J. and Vay P. M., *Chimie Analytique.,* 1966, 48, 549-554.

230. Bocelli G., Chiusoli G. P., Costa M. and Michelotti M., *J. Chem. Soc., Perkin Trans. I.,* 1994, 1347-1357.

231. De Kimpe N., D'Hondt L. and Moens L., *Tetrahedron*, 1992, 48, 3183-3208.

232. Kubota T., Miyashita S., Kitazume T. and Ishikawa N., *J. Org. Chem.,* 1980, 45, 5052-5057.

233. Sakuma S. and Miyaura N., *J. Org. Chem.,* 2001, 66, 8944-8946.

234. Terao Y., Kametani Y., Wakui H., Satoh T., Miura M. and Nomura M., *Tetrahedron,* 2001, 57, 5967-5974.

235. Eriksson J., Aberg O. and Langstrom B., *Eur. J. Org. Chem.,* 2007, 455-461.

236. Matovic N. J., Hayes P. Y., Penman K., Lehmann R. P. and De Voss J. J., *J. Org. Chem.,* 2011, 76, 4467-4481.

237. Piffl M., Weston J. and Anders E., *Eur. J. Org. Chem.,* 2000, 2851-2859.

238. Murugesan S., Ganguly S. and Maga G., *J. Chem. Sci.*, 2010, 122, 169-176.

239. Perrone R., Berardi F., Colabufo N. A., Leopoldo M. and Tortorella V., *J. Med. Chem.,* 2000, 43, 270-277.

240. Shelke S. M., Bhosale S. H. and Mahadik K. R*., Pharma Chemica*, 2010, 2, 169-177.

241. Bang-Andersen B., Sams A. G. and Larsen K., PCT Int., Appl., WO 2009106534 (A1), 2009.

242. Gaind K. N., *J. Ind. Chem. Soc.*, 1946, 23, 9-12.

243. Meth-Cohn O., Rhouati S., Tarnowski B. and Robinson A., *J. Chem. Soc. Perkin Trans. I.,* 1981, 1537-1543.

244. Jart A. and Lundt I., *Acta. Chem. Scand.*, 1966, 19, 2404-2408.

245. Lombardo C. M., Martinez I. S., Haider S., Gabelica V., De Pauw E., Moses J. E. and Neidle S*., Chem. Commun.,* 2010, 46, 9116-9118.

246. Cziaky Z. and Sebok P*., J. Heterocycl. Chem.,* 1994, 31, 701-705.

247. Mabire D., Coupa S., Adelinet C., Poncelet A., Simonnet Y., Venet M., Wouters R., Lesage A. S. J., Van Beijsterveldt L. and Bischoff F., *J. Med. Chem.,* 2005, 48, 2134-2153.

248. Bures E., Nieman J. A., Yu S., Spinazze P. G., Bontront J. P. J., Hunt I. R., Rauk A. and Keay B. A., *J. Org. Chem.,* 1997, 62, 8750-8759.

249. Li Z. and Ganesan A., *Synlett,* 1998, 4, 405-406.

250. Takimiya K., Aso Y., Otsubo T. and Ogura F., *Chem. Express.,* 1992, 7, 865-868.

251. Kayima T., Hemmi K., Takeno H. and Hashimoto M., *Tetrahedron Lett.,* 1980, 21, 95-98.

252. Kayima T., Hemmi K., Takeno H. and Hashimoto M., US patent., US 4206156 A 1980 0603, 1980.